

AFIT/GE/ENG/91D-26

**AD-A243 635**



CHARACTERIZING THE SENSITIVITY, SELECTIVITY, AND  
REVERSIBILITY OF THE METAL-DOPED PHTHALOCYANINE  
THIN-FILMS USED WITH THE INTERDIGITATED GATE  
ELECTRODE FIELD-EFFECT TRANSISTOR (IGFET) TO  
DETECT ORGANOPHOSPHORUS COMPOUNDS  
AND NITROGEN DIOXIDE

THESIS

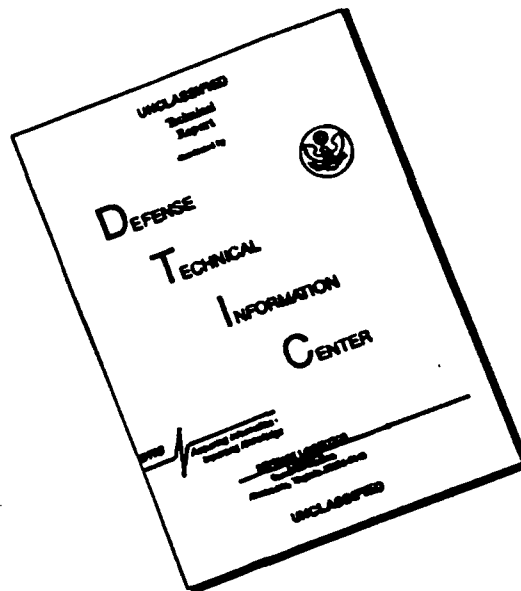
Clayton Paul Howe, Captain, USAF  
AFIT/GE/ENG/91D-26

Approved for public release; distribution unlimited

**91-19047**

**91 12 24 079**

# DISCLAIMER NOTICE



**THIS DOCUMENT IS BEST  
QUALITY AVAILABLE. THE COPY  
FURNISHED TO DTIC CONTAINED  
A SIGNIFICANT NUMBER OF  
PAGES WHICH DO NOT  
REPRODUCE LEGIBLY.**

## REPORT DOCUMENTATION PAGE

Form Approved  
OMB No. 0704-0188

Public reporting burden for this collection of information is estimated to average 1 hour per response, including the time for reviewing instructions, searching existing data sources, gathering and maintaining the data needed, and completing and reviewing the collection of information. Send comments regarding this burden estimate or any other aspect of this collection of information, including suggestions for reducing this burden, to Washington Headquarters Services, Directorate for Information Operations and Reports, 1215 Jefferson Davis Highway, Suite 1204, Arlington, VA 22202-4302, and to the Office of Management and Budget, Paperwork Reduction Project (0704-0188), Washington, DC 20503.

1. AGENCY USE ONLY (Leave blank)		2. REPORT DATE December 1991		3. REPORT TYPE AND DATES COVERED Master's Thesis	
4. TITLE AND SUBTITLE CHARACTERIZING THE SENSITIVITY, SELECTIVITY, AND REVERSIBILITY OF THE METAL-DOPED PHTHALOCYANINE THIN-FILMS USED WITH THE INTERDIGITATED GATE ELECTRODE FIELD-EFFECT TRANSISTOR TO DETECT ORGANOPHOSPHORUS COMPOUNDS AND NITROGEN DIOXIDE				5. FUNDING NUMBERS	
6. AUTHOR(S)  Clayton P. Howe, Captain, USAF					
7. PERFORMING ORGANIZATION NAME(S) AND ADDRESS(ES)  Air Force Institute of Technology, WPAFB OH 45433-6583				8. PERFORMING ORGANIZATION REPORT NUMBER  AFIT/GE/ENG/91D-26	
9. SPONSORING/MONITORING AGENCY NAME(S) AND ADDRESS(ES) Dr. Richard Burton Armstrong Aerospace Medical Research Laboratory AL/CF-CA Brooks AFB TX 78235 AVN 240-3656				10. SPONSORING/MONITORING AGENCY REPORT NUMBER	
11. SUPPLEMENTARY NOTES					
12a. DISTRIBUTION/AVAILABILITY STATEMENT  Approved for public release; distribution unlimited				12b. DISTRIBUTION CODE	
13. ABSTRACT (Maximum 200 words) This study investigated the sensitivity, reversibility, and selectivity of the thin-film coatings used on the interdigitated gate electrode field-effect transistor (IGFET) gas microsensor. These responses were quantified based on the dc resistance changes and frequency-domain responses of the microsensor. The thin-film materials included: copper phthalocyanine (CuPc), nickel phthalocyanine (NiPc), and cobalt phthalocyanine (CoPc). The challenge gases included: diisopropyl methylphosphonate (DIMP), dimethyl methylphosphonate (DMMP), nitrogen dioxide, ammonia, and boron trifluoride. Tests of the CuPc thin-films and nitrogen dioxide challenges established the primary set of test parameters expected to maximize the selectivity, sensitivity, and reversibility of the thin-film coatings. A series of experiments performed at 150°C tested the other thin-film materials, on the IGFET sensors, when challenged by listed gases. At 150°C, the nitrogen dioxide and ammonia interacted with all three film types, the boron trifluoride interacted weakly, the DIMP and DMMP show no response. All three thin-film types responded to the DIMP challenges at 90°C.					
14. SUBJECT TERMS Sensors, Integrated Sensors, CHEMFET, Detectors, Nitrogen Dioxide, Organophosphorus Compounds, IGFET				15. NUMBER OF PAGES 461	
				16. PRICE CODE	
17. SECURITY CLASSIFICATION OF REPORT Unclassified	18. SECURITY CLASSIFICATION OF THIS PAGE Unclassified	19. SECURITY CLASSIFICATION OF ABSTRACT Unclassified	20. LIMITATION OF ABSTRACT UL		

AFIT/GE/ENG/91D-26

CHARACTERIZING THE SENSITIVITY, SELECTIVITY, AND  
REVERSIBILITY OF THE METAL-DOPED PHTHALOCYANINE  
THIN-FILMS USED WITH THE INTERDIGITATED GATE  
ELECTRODE FIELD-EFFECT TRANSISTOR (IGFET)  
TO DETECT ORGANOPHOSPHORUS COMPOUNDS  
AND NITROGEN DIOXIDE

THESIS

Presented to the Faculty of the School of Engineering  
of the Air Force Institute of Technology

Air University

In Partial Fulfillment of the  
Requirements for the Degree of  
Master of Science in Electrical Engineering

Clayton Paul Howe

Captain, USAF

December 1991



Accession For	
NTIS Grant	<input checked="" type="checkbox"/>
DTIC Tab	<input type="checkbox"/>
Unapproved	<input type="checkbox"/>
Justification	<input type="checkbox"/>
By	
Distribution	
Approved for Release	
Dist	Special
A-1	

Approved for public release; distribution unlimited



## Acknowledgements

This thesis was one of the most strenuous projects I have undertaken. The help and guidance of many individuals smoothed my path along the way. I would like to first express my gratitude to my thesis advisor and mentor, Lt Col Edward Kolesar. His patient suggestions and encouragement carried me through many difficult times. I want to thank Dr. Matthew Kabrisky and Capt Thomas Jenkins for reviewing my thesis.

Capt John Wiseman and I worked closely together; I thank him for his technical insight and comradeship. I am also indebted to Capt Thomas Jenkins for his design work on the IGEFET array.

The Armstrong Aerospace Medical Research Laboratory sponsored this investigation. Their interest and support made this research possible.

I must also thank Mr. Don Smith and Mr. William Trop of the AFIT Electronics and Materials Cooperative Laboratory for their assistance with the device fabrication equipment. I want to thank Mr. Charles Price for his extraordinary help in procuring vital supplies for the research effort.

I must express my love and appreciation for my wife, Susan, and my children, Abigail and Benjamin. Their love, patience, and support made the sacrifices bearable.

## Table of Contents

Acknowledgements.....	ii
List of Figures.....	vii
List of Tables.....	xv
Abstract.....	xvii
I. Introduction.....	I-1
Background.....	I-1
Problem Statement.....	I-9
Scope.....	I-14
Limitations.....	I-18
Definitions .....	I-18
Assumptions.....	I-22
Methodology .....	I-23
Plan of Development.....	I-27
Summary.....	I-28
II. Literature Review.....	II-1
Introduction.....	II-1
Gas Detection Devices.....	II-3
Piezoelectric Devices .....	II-4
Notch Filters and Chemiresistors.....	II-9
Optical Waveguides.....	II-21
Interdigitated Gate Electrode Field-Effect Transistor (IGEFET) Microsensors.....	II-24
Conclusion.....	II-26
III. The IGEFET Microsensor Concept, Design, and Implementation .....	III-1
Introduction .....	III-1

IGEFET Microsensor Concepts.....	III-3
IGEFET Design.....	III-3
Phthalocyanine Thin-Film Coatings for the IGEFET.....	III-5
IGEFET Microsensor Design and Implementation .....	III-10
Summary .....	III-12
 IV. Experimental Methodology.....	 IV-1
Section IV-I.....	IV-1
IGEFET Device.....	IV-1
Gases Tested .....	IV-2
Thin-film Materials.....	IV-3
Problem Statement.....	IV-4
Section IV-II .....	IV-4
Methodology .....	IV-4
IGEFET Physical Measurements .....	IV-6
Thin-film Coating Deposition .....	IV-9
Testing the Device Impedance Matching Amplifier, Feedback Configurations and Bias Voltages .....	IV-15
Computer Controlled Data Gathering Using GPIB Interconnected Instrumentation .....	IV-27
Test Chamber Fabrication .....	IV-35
Gas Delivery System .....	IV-38
Experiments Designed to Limit the Range of Variables (Series I).....	IV-39
Focused Testing (Series II).....	IV-48
Series III Testing .....	IV-51
Summary .....	IV-52
 V. Experimental Results and Discussion .....	 V-1
IGEFET Device Physical Measurements.....	V-1
Visual Inspection of the IGEFET Devices .....	V-1
Determination of the IGEFET's Bias Voltages and Feedback Configurations .....	V-1
Series I Performance Evaluation .....	V-9
Thin-Film Thickness .....	V-11

IGE Structure and Thin-Film Coating Deposition	
Process.....	V-11
Results of Series II Gas Challenge Experiments .....	V-28
Diisopropyl Fluorophosphonate (DFP) Challenges.....	V-29
Dimethyl Methylphosphonate (DMMP) Challenges .....	V-30
Diisopropyl Methylphosphonate (DIMP) Challenges....	V-31
Boron Trifluoride Challenges.....	V-31
CuPc Thin-Film Response to BF <sub>3</sub> .....	V-31
CoPc Thin-Film Response to BF <sub>3</sub> .....	V-32
NiPc Thin-Film Response to BF <sub>3</sub> .....	V-33
Ammonia Challenges .....	V-33
CuPc Thin-Film Response to NH <sub>3</sub> .....	V-34
CoPc Thin-Film Response to NH <sub>3</sub> .....	V-35
NiPc Thin-Film Response to NH <sub>3</sub> .....	V-40
Nitrogen Dioxide Challenges.....	V-41
CuPc Thin-Film Response to NO <sub>2</sub> .....	V-42
CoPc Thin-Film Response to NO <sub>2</sub> .....	V-51
NiPc Thin-Film Response to NO <sub>2</sub> .....	V-54
Results of Series III Gas Challenge Experiments.....	V-63
Sensitivity and Reversibility.....	V-69
Selectivity.....	V-70
Time-Domain Responses.....	V-74
Discussion.....	V-74
VI. Conclusions and Recommendations .....	VI-1
Conclusions .....	VI-1
Recommendations.....	VI-4
Appendix A: Metal-Doped Phthalocyanine Thin-Film Deposition Process .....	A-1
Appendix B: Data Acquisition Software .....	B-1
Appendix C: Response of the CuPc Thin-Film Coatings.....	C-1
Appendix D: Response of the CoPc Thin-Film Coatings.....	D-1

Appendix E:	Response of the NiPc Thin-Film Coatings .....	E-1
Bibliography	.....	Bib-1
Vita	.....	Vita-1

## List Of Figures

Figure I-1.	Organophosphorus Chemical Warfare Nerve Agents	I-5
Figure I-2.	Interdigitated Gate-Electrode Field-Effect Transistor .....	I-7
Figure I-3	Testing Parameter Response Space .....	I-13
Figure I-4.	IGEFET-Based Microsensor Fabrication.....	I-24
Figure II-1.	Schematic Diagram of a SAW Sensor.....	II-8
Figure II-2.	General Conductimetric Device.....	II-14
Figure II-3.	General Equivalent Circuit Diagram of a Conductimetric Sensor.....	II-15
Figure II-4.	Optomechanical Interference Sensor .....	II-23
Figure III-1.	Interdigitated Gate-Electrode Field-Effect Transistor.....	III-2
Figure III-2.	Interdigitated Gate Electrode (IGE) and Impedance Matching FET Amplifier.....	III-6
Figure III-3.	Metal-Doped Phthalocyanine Molecules Showing Stacking Arrangement .....	III-8
Figure III-4.	Sketch of Interdigitated Gate-Electrode Structures, Their Impedance Matching Amplifiers and Bonding Pads.....	III-13
Figure III-5.	Overhead View of a Portion of Interdigitated Gate-Electrode and Impedance Matching Amplifier (50X).....	III-14

Figure III-6.	Overhead View of a Portion of Interdigitated Gate-Electrode and Impedance Matching Amplifier (200X).....	III-15
Figure III-7.	Overhead View Impedance Matching Amplifier (400X) .....	III-16
Figure III-8.	Overhead View of Interdigitated Gate-Electrode with CuPc Thin-Film Deposition, 3,900 Å Thick (200X) .....	III-17
Figure IV-1.	Overhead View of an Unpackaged IGE Array ...	IV-7
Figure IV-2.	SEM Photograph of IGE Structure Showing the Floating-Electrode Extending Towards the FET Gate (296X).....	IV-8
Figure IV-3.	Cross-Sectional View of an IGE Finger Supported by Silicon Dioxide Showing Undercutting Below the Edge of the IGE Finger (23,200X).....	IV-10
Figure IV-4.	Sketch of Photograph in Figure IV-3 Showing Approximate Dimensions of the Undercut .....	IV-11
Figure IV-5.	Cross-Sectional View of the IGE Finger and Interdigital Spaces After Vacuum Deposition of Copper-Phthalocyanine Thin-Film (6,600X).....	IV-12
Figure IV-6.	Cross-Sectional View of the IGE Finger and Interdigital Space After Vacuum Deposition of Copper-Phthalocyanine Thin-Film (26,300X).....	IV-13
Figure IV-7.	Sketch Emphasizing the Interdigitated Gap in the Thin-Film Depositions.....	IV-14

Figure IV-8.	Interdigitated Gate Electrode (IGE) and Impedance Matching FET Amplifier .....	IV-22
Figure IV-9.	Test Circuit Used to Measure the Performance Parameters for the Impedance Matching FET Amplifier.....	IV-24
Figure IV-10.	Test Circuit for Establishing the Effects of DC Bias at the Floating-Gate Relative to the Bandwidth of the IGEFET Impedance Matching Amplifier.....	IV-26
Figure IV-11.	Instrumentation and GPIB System Architecture..	IV-29
Figure IV-12.	DC Resistance Measurements Across the IGE.....	IV-31
Figure IV-13.	Gain and Phase Measurements of the FET Impedance Matching Amplifier.....	IV-33
Figure IV-14.	IGEFET System Gain and Phase Response Measurements .....	IV-34
Figure IV-15.	Test Cabinet and Test Chamber.....	IV-37
Figure IV-16.	Gas Generation System.....	IV-40
Figure IV-17.	Test Loop Paradigm .....	IV-53
Figure V-1.	Gain Versus Frequency. Experimental Data for FET Amplifier with $V_{bias} = -2.38$ volts.....	V-4
Figure V-2.	Output Voltage versus Input Voltage for dc Linearity Evaluation.....	V-7
Figure V-3.	Gain Changes at Various Frequencies with Sinusoidal Input Riding Superimposed Upon Several DC Offsets.....	V-8



Figure V-4.	Gain Versus Frequency Response for a 3,900 Å Thick CuPc Thin-Film.....	V-14
Figure V-5.	Gain Versus Frequency Response for a 8,800 Å Thick CuPc Thin-Film.....	V-15
Figure V-6.	Comparison of DC Resistance Measurements for Two Different Thin-film Thicknesses.....	V-17
Figure V-7.	CuPc Film (8,800 Å) Transfer Function Response to Challenge with 100 ppb Nitrogen Dioxide.....	V-18
Figure V-8.	Baseline Drift Observed with Two IGEs Coated with 30,000 Å Thick CuPc Films.....	V-19
Figure V-9.	Baseline Drift Observed with an IGE Coated with 1,200 Å Thick CuPc Film.....	V-20
Figure V-10.	Effects of Choosing Nitrogen versus Dry, Room Air as Purge Gas on Resistance Measurements for the Same CuPc Films.....	V-22
Figure V-11.	Differences in Recovery Time at Two Different Temperatures for the Same CuPc Film.....	V-24
Figure V-12.	Changes in Purge Condition Resistance Values for Three Different Thin-Film Types, Measured at Three Different Temperatures.....	V-25
Figure V-13.	Comparison of Changes in Baseline Drift Throughout Lengthy Experiments.....	V-26 and V-27
Figure V-14.	Gain Versus Frequency Response for a 1,600 Å Thick CuPc Thin-Film Exposed to Ammonia.....	V-36

Figure V-15.	Gain Versus Frequency Response for a 1,600 Å Thick CuPc Thin-Film Exposed to Ammonia ....	V-37
Figure V-16.	Phase Angle Versus Frequency Response for a 1,600 Å Thick CuPc Thin-Film Exposed to Ammonia .....	V-38
Figure V-17.	Phase Angle Versus Frequency Response for a 1,600 Å Thick CuPc Thin-Film Exposed to Ammonia .....	V-39
Figure V-18.	Percentage Change in DC Resistance Versus Time for CuPc Thin-Films Exposed to Ammonia .....	V-44
Figure V-19.	Gain Versus Frequency Response for a 3,900 Å Thick CuPc Thin-Film Exposed to Nitrogen Dioxide.....	V-46
Figure V-20.	Gain Versus Frequency Response for a 3,900 Å Thick CuPc Thin-Film Exposed to Nitrogen Dioxide.....	V-47
Figure V-21.	Gain Versus Frequency Response for a 3,900 Å Thick CuPc Thin-Film Exposed to Nitrogen Dioxide.....	V-48
Figure V-22.	Phase Angle Versus Frequency Response for a 3,900 Å Thick CuPc Thin-Film Exposed to Nitrogen Dioxide.....	V-49
Figure V-23.	Phase Angle Versus Frequency Response for a 3,900 Å Thick CuPc Thin-Film Exposed to Nitrogen Dioxide.....	V-50
Figure V-24.	Percentage Change in DC Resistance Versus Time for CoPc Thin-Films Exposed to Nitrogen Dioxide.....	V-53

Figure V-25.	Gain Versus Frequency Response for a 2,500 Å Thick CoPc Thin-Film Exposed to Nitrogen Dioxide.....	V-55
Figure V-26.	Gain Versus Frequency Response for a 2,500 Å Thick CoPc Thin-Film Exposed to Nitrogen Dioxide.....	V-56
Figure V-27.	Gain Versus Frequency Response for a 2,500 Å Thick CoPc Thin-Film Exposed to Nitrogen Dioxide.....	V-57
Figure V-28.	Phase Angle Versus Frequency Response for a 2,500 Å Thick CoPc Thin-Film Exposed to Nitrogen Dioxide.....	V-58
Figure V-29.	Phase Angle Versus Frequency Response for a 2,500 Å Thick CoPc Thin-Film Exposed to Nitrogen Dioxide .....	V-59
Figure V-30.	Phase Angle Versus Frequency Response for a 2,500 Å Thick CoPc Thin-Film Exposed to Nitrogen Dioxide .....	V-60
Figure V-31.	Percentage Change in DC Resistance Versus Time for NiPc Thin-Films Exposed to Nitrogen Dioxide .....	V-62
Figure V-32.	Gain Versus Frequency Response for a 6,200 Å Thick NiPc Thin-Film Exposed to Nitrogen Dioxide.....	V-64
Figure V-33.	Gain Versus Frequency Response for a 6,200 Å Thick NiPc Thin-Film Exposed to Nitrogen Dioxide.....	V-65

Figure V-34.	Phase Angle Versus Frequency Response for a 6,200 Å Thick NiPc Thin-Film Exposed to Nitrogen Dioxide .....	V-66
Figure V-35.	Phase Angle Versus Frequency Response for a 6,200 Å Thick NiPc Thin-Film Exposed to Nitrogen Dioxide .....	V-67
Figure V-36.	Gain Versus Frequency Response for a 12,500 Å Thick NiPc Thin-Film Exposed to Nitrogen Dioxide .....	V-68
Figure V-37.	Time-Domain Response of a 2,500 Å Thick CoPc Thin-Film Exposed to Ammonia .....	V-75
Figure V-38.	Time-Domain Response of a 2,600 Å Thick NiPc Thin-Film Exposed to Ammonia .....	V-76
Figure V-39.	Time-Domain Response of a 6,200 Å Thick NiPc Thin-Film Exposed to Nitrogen Dioxide.....	V-75
Figure C-1 to Figure C-52.	CuPc Challenged with NO <sub>2</sub> , DC Resistance Versus Time, Gain/Phase Angle Versus Frequency .....	C-2 to C-35
Figure C-53 to Figure C-69.	CuPc Challenged with NH <sub>3</sub> , DC Resistance Versus Time, Gain/Phase Angle Versus Frequency .....	C-36 to C-48
Figure C-70 to Figure C-88.	CuPc Challenged with BF <sub>3</sub> , DC Resistance Versus Time, Gain/Phase Angle Versus Frequency .....	C-49 to C-63
Figure C-89 to Figure C-94.	CuPc Challenged with DMMP and DIMP at 30°C, 90°C, and 150°C. DC Resistance Versus Time.....	C-65 to C-70

Figure D-1 to Figure D-71.	CoPc Challenged with NO <sub>2</sub> , DC Resistance Versus Time, Gain/Phase Angle Versus Frequency .....	D-2 to D-46
Figure D-72 to Figure D-86.	CoPc Challenged with NH <sub>3</sub> , DC Resistance Versus Time, Gain/Phase Angle Versus Frequency .....	D-47 to D-59
Figure D-87 to Figure D-101.	CoPc Challenged with BF <sub>3</sub> , DC Resistance Versus Time, Gain/Phase Angle Versus Frequency .....	D-60 to D-70
Figure D-102 to Figure D-107	CoPc Challenged with DMMP and DIMP at 30°C, 90°C, and 150°C. DC Resistance Versus Time.....	D-72 to D-77
Figure E-1 to Figure E-21.	NiPc Challenged with NO <sub>2</sub> , DC Resistance Versus Time, Gain/Phase Angle Versus Frequency .....	E-2 to E-18
Figure E-22 to Figure E-36.	NiPc Challenged with NH <sub>3</sub> , DC Resistance Versus Time, Gain/Phase Angle Versus Frequency .....	E-19 to E-29
Figure E-37 to Figure E-51.	NiPc Challenged with BF <sub>3</sub> , DC Resistance Versus Time, Gain/Phase Angle Versus Frequency .....	E-30 to E-40
Figure E-52 to Figure E-57.	NiPc Challenged with DMMP and DIMP at 30°C, 90°C, and 150°C. DC Resistance Versus Time.....	E-42 to E-47

## List of Tables

Table I-1.	Chemical Warfare Agents and Simulants.....	I-4
Table I-2.	Test Parameters.....	I-11
Table II-1.	Current and Projected Gas Sensor Performance Figures.....	II-10
Table II-2.	Reported Detectable Concentrations for IGE and Notch Filter Sensors .....	II-10
Table II-3.	Typical Chemiresistor Parameters for an Applied Bias of 1 - 5 Volts.....	II-20
Table III-1.	Critical Dimensions for Interdigitated Gate Electrodes.....	III-11
Table III-2.	64-Pin DIP Wirebond Contact Function Summary .....	III-18 and III-19
Table IV-1.	Conditions Used During Experimentation.....	IV-16 to IV-20
Table IV-2.	Test Parameters Used for Series II Testing.....	IV-52
Table V-1.	Non-inverting Amplifier Configuration Performance.....	V-3
Table V-2.	Test Parameters Used for Series II Testing.....	V-29
Table V-3.	DC Resistance Changes During 3 ppm DIMP Exposure .....	V-32

Table V-4.	The Average Percent Change in DC Resistance Measurements of CuPc, CoPc, and NiPc when Challenged by Nitrogen Dioxide.....	V-43
Table V-5.	The Maximum Averaged Percent Change in DC Resistance Measurements of CuPc, CoPc, and NiPc when Challenged by Nitrogen Dioxide.....	V-43
Table V-6	Sensitivity and Reversibility of the MPc Thin-Films When Exposed to Nitrogen Dioxide.....	V-71 to V-73

## *Abstract*

This study investigated the sensitivity, reversibility, and selectivity response of the thin-film coatings used on the interdigitated gate electrode, field-effect transistor (IGEFET) gas microsensor. These responses were quantified based on the dc resistance changes and frequency-domain responses of the microsensor. The thin-film materials included: copper phthalocyanine (CuPc), nickel phthalocyanine (NiPc), and cobalt phthalocyanine (CoPc). The challenge gases included: diisopropyl methlyphosphonate (DIMP), dimethyl methlyphosphonate (DMMP), nitrogen dioxide (NO<sub>2</sub>), ammonia (NH<sub>3</sub>), and boron trifluoride (BF<sub>3</sub>). Tests of CuPc thin-films and NO<sub>2</sub> challenges established the primary set of test parameters expected to maximize the selectivity, sensitivity, and reversibility of the thin-film coatings. A series of experiments performed at 150°C tested the other thin-film materials, on IGEFET sensors, when challenged by the various gases. At 150°C, the NO<sub>2</sub> and NH<sub>3</sub> interacted with all three film types, the BF<sub>3</sub> interacted weakly, the DIMP and DMMP showed no response. All three thin-film types responded to the DIMP challenges at 90°C.



CHARACTERIZING THE SENSITIVITY, SELECTIVITY,  
AND REVERSIBILITY OF THE METAL-DOPED PHTHALOCYANINE  
THIN-FILMS USED WITH THE INTERDIGITATED GATE  
ELECTRODE FIELD-EFFECT TRANSISTOR(IGFET)  
TO DETECT ORGANOPHOSPHORUS COMPOUNDS  
AND NITROGEN DIOXIDE

*I. Introduction*

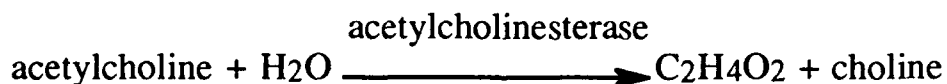
*Background*

Solid-state chemical sensors are valuable new additions to the analytical instrumentation family used to detect sub-toxic concentration levels of gaseous compounds. Selectively detecting and quantifying the concentrations of two types of gaseous contaminants is of particular interest to the Air Force. The members of one chemical compound class include the organophosphorus pesticides and their structurally-affiliated compounds. The other ensemble includes the oxides of nitrogen, particularly nitrogen dioxide ( $\text{NO}_2$ ). A third group of compounds of research interest include ammonia ( $\text{NH}_3$ ) and boron trifluoride ( $\text{BF}_3$ ).

The organophosphorus compound family includes several toxic pesticides which comprise a group of environmental contaminants that are

applied for agricultural and hygiene purposes [13]. This group is important in both the civilian and military communities. Health studies accomplished to monitor the performance of agricultural crop-dusting pilots have demonstrated a significant degradation in their flying proficiency after exposure to organophosphorus pesticides. Another group of chemically-related organophosphorus compounds comprise the chemical-warfare nerve agents. These compounds readily pass from the blood stream to the brain and other nerve synapses. Once there, they act to inhibit the activity of the acetylcholinesterase enzyme. This inhibition prevents normal neural functions, as described by Roberts *et al* [19:506] :

Nerve cells contain the molecule acetylcholine in the bound state. Stimulation of the cell releases acetylcholine, which stimulates the neighboring cell to release acetylcholine and this, in turn, its neighbor, thus transmitting the nerve impulse. Deactivation of the stimulant must be done very quickly once the impulse is transmitted. Deactivation is achieved by the enzyme acetylcholinesterase, which catalyzes the hydrolysis.



A nerve poison such as diisopropyl fluorophosphonate (DFP) forms a stable ester with the serine hydroxyl at the active site in the (*acetylcholinesterase*) enzyme, thus preventing the deactivation step from occurring.

Detecting sub-toxic concentration levels of these chemical warfare nerve agents may save lives by providing our armed forces the critical time

needed to don protective clothing. Table I-1 and Figure I-1 summarize the names and chemical structures of typical chemical warfare nerve agents and simulant compounds, respectively. This research effort focused on the detection of DMMP, DIMP, and DFP organophosphate compounds.

The other compound of primary interest in this study is nitrogen dioxide ( $\text{NO}_2$ ). Nitrogen dioxide is a gaseous pollutant generated by automobiles, diesel engines, blasting operations, industrial stacks, and when certain weapon detonators chemically-decompose during storage [5:77; 13; 14 ]. With respect to weapon detonators, nitrogen dioxide corrodes their electrical triggering mechanism, compromising their reliability.

As time permitted, other compounds of interest were included in the study. Ammonia (an electron donor) and boron trifluoride (a strong  $\sigma$ -orbital electron acceptor, in contrast to  $\text{NO}_2$ , a strong  $\pi$ -electron acceptor) were included in this study to provide additional comparisons with nitrogen dioxide and the organophosphate compounds (DMMP, DIMP and DFP).

Developing a simple, portable, rugged, solid-state detector for these compounds that could function in the field would present many advantages relative to the currently used, after-the-fact, analytical laboratory methods.

Table I-1  
Chemical Agents and Simulants (1:15).

Agent (code)	Name
GA GB GD VX EA5365 H HD L	Tabun Sarin Soman  Mustard Distilled Mustard Lewisite
Simulants	
DIMP DMMP DFP	diisopropyl methylphosphonate dimethyl methylphosphonate diisopropyl fluorophosphonate

Additionally, a solid-state detector has the potential of being mass produced at a very low cost.

The Interdigitated Gate Electrode Field-Effect Transistor (IGEFET) has shown significant promise as a solution to these detector applications [7; 22; 26]. The IGEFET is based on the conventional metal-oxide-semiconductor field-effect transistor (MOSFET); however, the IGEFET



has a unique gate-electrode structure which is coated with a chemically-active thin-film. As shown in Figure I-2, the gate-electrode structure is a broad planar expanse of interdigitated metal fingers that are supported by a high-quality silicon dioxide dielectric [7; 22; 26]. The interdigitated gate electrode (IGE) fingers are composed of two fundamental components. One component is the floating-electrode. The other component is the driven-electrode. In operation, the driven-electrode is connected to an externally applied direct current (dc) voltage, pulse, or harmonic signal source. The excitation signal is electromagnetically coupled to the floating-electrode through the chemically-active thin-film. As the charge levels change on the floating-electrode, variations in the source-to-drain MOSFET channel's conductivity are induced [14:2356]. These changes can readily be detected and amplified. The IGEFET structures become useful for detecting gaseous organophosphorus compounds and nitrogen dioxide when their interdigitated gate electrode structures are covered with a metal-doped phthalocyanine thin-film semiconducting polymer [7; 14; 22; 26].

The challenge gases used in this investigation included: diisopropyl fluorophosphonate (DFP), diisopropyl methylphosphonate (DIMP),

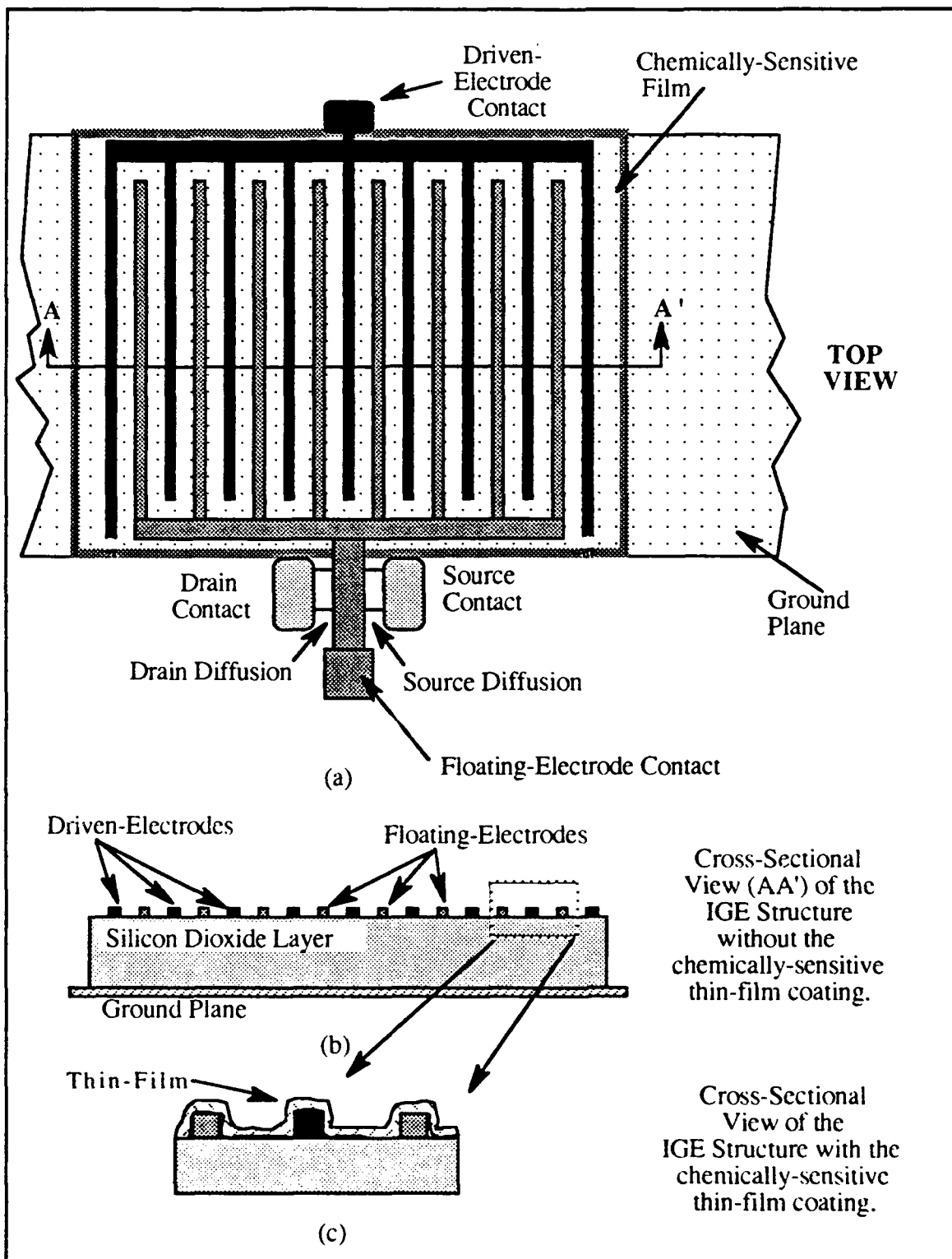


Figure I-2. Interdigitated Gate Electrode Field-Effect Transistor (IGEFET) (not to scale) [10:I-3; 13].

dimethyl methylphosphonate (DMMP), ammonia ( $\text{NH}_3$ ), boron trifluoride ( $\text{BF}_3$ ), and nitrogen dioxide ( $\text{NO}_2$ ). The DFP and DIMP challenge gases were chosen because they can be safely handled, and they are chemical analogs of the more toxic chemical warfare nerve agents.

The thin-film, metal-doped phthalocyanine polymer which covers the interdigitated gate electrode array forms a significant portion of the lossy dielectric which couples the driven- and floating-electrodes. The complex dielectric constant of the chemically-active, thin-film coating changes when certain electron acceptor or donor gases interact with it. This chemical activity is correspondingly reflected in the strength of the signal which couples the floating- and driven-electrodes as a measurable change in the drain-to-source current [7; 22; 26]. The gas-induced changes are manifested by the degree of electrical signal coupling via electrical impedance measurements, and this relationship establishes the basis for using the IGEFET as a microsensor.

Several metal-doped phthalocyanine polymers, including copper-phthalocyanine (CuPc), nickel-phthalocyanine (NiPc), and cobalt-phthalocyanine (CoPc) have demonstrated their ability to perform as IGEFET-based microsensor gas-sensitive thin-films because of their capacity to interact with the challenge gases of interest in a measurable



fashion [1; 6; 10].

### *Problem Statement*

IGEFETs coated with thin-films of copper-phthalocyanine (CuPc), nickel-phthalocyanine (NiPc), or cobalt-phthalocyanine (CoPc) may chemically interact with the challenge gases included in this investigation; specifically, diisopropyl fluorophosphonate (DFP), diisopropyl methylphosphonate (DIMP), dimethyl methylphosphonate (DMMP), ammonia (NH<sub>3</sub>), boron trifluoride (BF<sub>3</sub>), and nitrogen dioxide (NO<sub>2</sub>). The dependence of these interactions with a particular metal-doped phthalocyanine material type, its thickness, the operating temperature, relative humidity, challenge gas type, and challenge gas concentration needs to be fully quantified so that an optimal combination of these variables can be identified. In addition, procedural steps involved with sequencing the exposures affects the resultant interactions. The optimal combination of these factors is defined in this context to be the set producing the best indices of sensor sensitivity, selectivity, and reversibility. The measurement and calculation of these indices is defined in the *Definitions* section. The specific questions to be addressed for the challenge gases include:

1. Which IGEFET candidate coating and physical operating parameters produce the greatest sensitivity when exposed to the challenge gases?
2. Which IGEFET candidate coating and physical operating parameters display the best selectivity when exposed to the challenge gases?
3. Which IGEFET candidate coating and physical operating parameters exhibit the most complete degree of reversibility when exposed to the challenge gases?

The ensemble of test conditions are summarized in Table I-2. They include: thin-film type, thin-film thickness, temperature, relative humidity, challenge gas candidate, and gas concentration. If one were to try to visualize these six 'independant' factors defining a six-dimensional test condition matrix, the result might look like Figure I-3. Each of the smallest cubicles represents the response space that is expected to be

Table I-2.  
Testing Parameter Ranges.

Test Parameter	Range of Values
Challenge Gas Type	BF <sub>3</sub> , DFP, DIMP, DMMP, NH <sub>3</sub> , and NO <sub>2</sub>
Gas Concentrations	DMMP: 10 ppm DIMP : 20 ppm DFP : 1000 ppb NO <sub>2</sub> : 30, 50, 100, 500, and 1000 ppb NH <sub>3</sub> : 16, 106, 250, and 500 ppm BF <sub>3</sub> : 24, 48 and 105 ppm
Thin-film Material	Copper Phthalocyanine (CuPc) Cobalt Phthalocyanine (CoPc) Nickel Phthalocyanine (NiPc)
Thin-film Thickness	1,000 Å to 30,000 Å
Exposure and Purge Temperature	30°C, 90°C, 120°C, 150°C
Relative Humidity	0% to 30%

occupied by a unique grouping of the set,  $R_{\text{response}}$ , where:

$$R_{\text{response}} = \{\text{sensitivity}_m, \text{reversibility}_m, \text{selectivity}_m\} \quad (\text{I-1})$$

and each member of the set has the following dependence:

$$m = \{\text{thin-film type, thin-film thickness, temperature,} \\ \text{relative humidity, challenge gas type,} \\ \text{challenge gas concentration}\}. \quad (\text{I-2})$$

As reflected in Figure I-3, each of the larger boxes represents a response space sector that has been parceled into the smallest cubicles, and these smallest cubicles are distributed along the "three dimensional" axes of humidity, temperature, and challenge gas concentration. Each of the large boxes is, in turn, a subset of the "universally available" response space, as delimited and distributed along the remaining three dimensions of thin-film material type, thin-film thickness, and challenge gas type. The grouping of the six dimensional arguments was done on a purely arbitrary basis to create an aid for visualizing the response-space.

This investigation focused on several measurable IGEFET parameters including: device gain and phase relative to the excitation signal's frequency, voltage-pulse response in the time- and frequency-

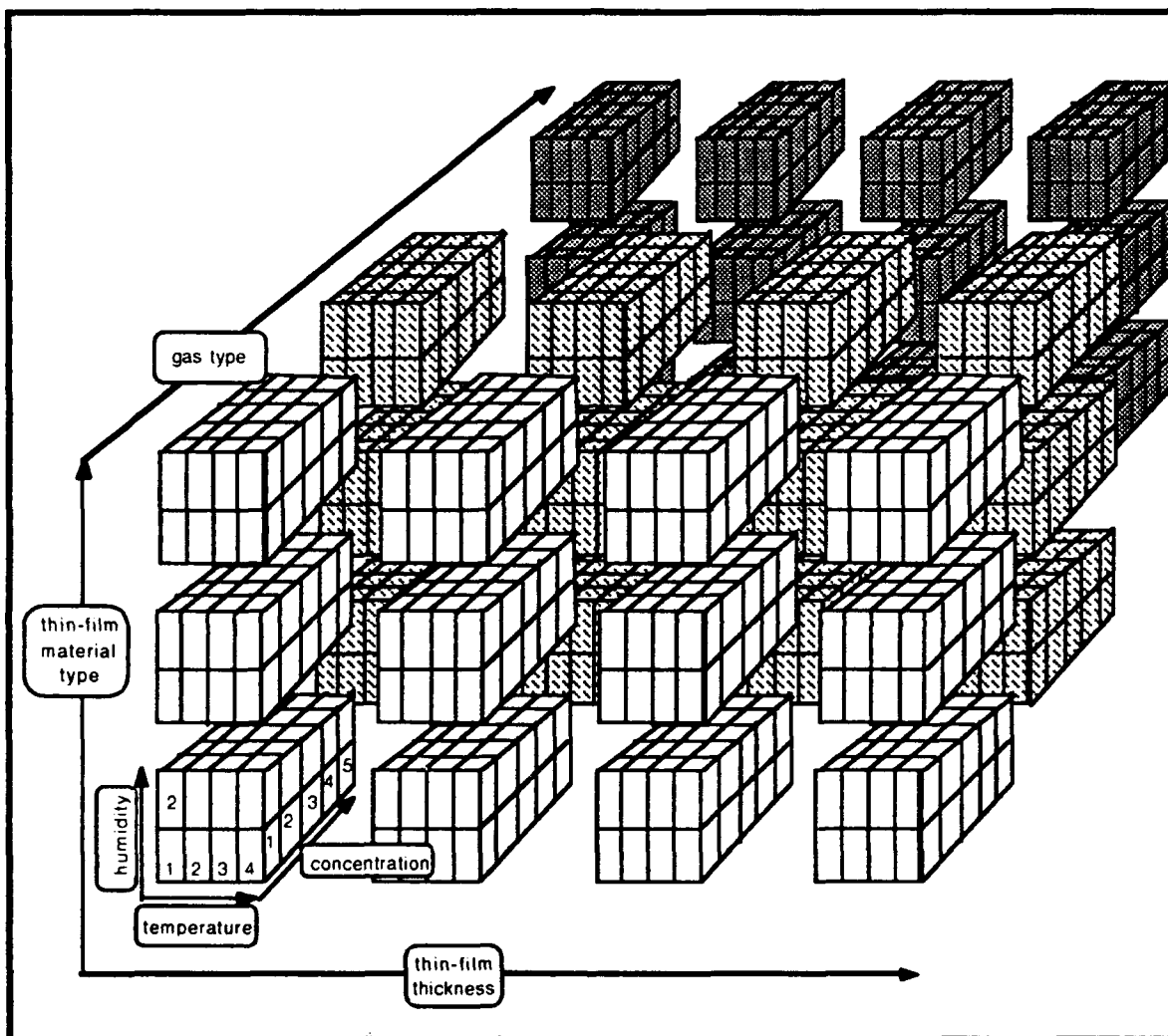


Figure I-3. Testing Parameter Response Space. Note That The Range of Values Associated with Any Particular 'Dimension' is Approximate. This Drawing is Intended to Help Readers Visualize the 6-Dimensional Parceling of the Available Response Space Containing Triplets of {Sensitivity, Reversibility, and Selectivity}.

domains, and the interdigitated gate electrode direct current (dc) resistance, as well as its alternating current (ac) impedance (magnitude and angle, as well as the real and imaginary parts). These measurements were used as input information to characterize the sensors' responses, and the measurements were mapped into the response spaces depicted in Figure I-3. The basis for recognizing the best combination of test conditions and IGEFET thin-film coating will be established relative to the sensor's numerical indices of sensitivity, selectivity, and reversibility. These indices are defined in the *Definitions* section.

### *Scope*

This thesis effort attempted to identify which particular metal-doped phthalocyanine polymeric thin-film coating and set of physical operating parameters produced the most sensitive, selective, and reversible responses relative to the BF<sub>3</sub>, DFP, DIMP, DMMP, NH<sub>3</sub> and NO<sub>2</sub> challenge gas exposures. The specific test condition parameters are summarized in Table I-2.

The initial step in the investigation was validating the IGE and metal-oxide-semiconductor field-effect transistor (MOSFET) structures on the integrated circuit die as received from the fabricator, MOSIS (Metal-Oxide-

Semiconductor Implementation System, University of California, Berkeley, California). This task was accomplished by electrically testing each of the IGEs for open and short circuits, and then measuring the gain and bandwidth of the MOSFET amplifier sections of each integrated circuit microsensors at room temperature.

Following the initial validation phase, the phthalocyanine polymeric thin-films (CuPc, CoPc, and NiPc) were deposited onto the IGE portions of the IGEFETs. The next step involved characterizing three sub-systems in each IGEFET, including: the coated IGE structure, the *in-situ* MOSFET structure, and then determining the end-to-end performance profile of the IGEFET devices with respect to the driven-electrode inputs to the MOSFET amplifier outputs while the devices were exposed to room air.

For the coated IGE structure, the initial testing focused on the dc resistance measurements between the driven- and floating-gate, with the floating-gate grounded and the driven-gate connected to a positive dc voltage source. The dc resistance was measured with seven different levels of dc voltage: +1, +2.5, +4, +5.5, +7, +8.5, and +10 volts. The driven- to floating-gate ac impedance was measured using the same voltage setpoints that were used for the dc voltages. These tests were conducted at 22°C with filtered room air at 8-10 % relative humidity.

An entire IGEFET-based microsensor system was defined to be the system extending from the driven-electrode input's and continuing through to the MOSFET differential amplifier's output. The performance baseline testing for one such system began by measuring the gain/phase transfer function versus frequency (swept from 10 Hz to 1 MHz). Based upon the results of these preliminary test trials, a set of bias and driven point voltages were identified. These voltages were used in the subsequent measurements. The time-domain response characteristics were determined by measuring the IGEFET response waveforms when the driven-gate was connected to a pulse generator. Two waveforms were used: a 5  $\mu$ s wide pulse with a 1 kHz repetition rate, and a 50 Hz square wave.

Prior to any challenge gas exposures, the first battery of performance measurements described in the previous paragraphs were used to establish a set of baseline values for the IGE and IGEFET structures. The specific tests included: impedance (dc and ac), gain and phase response, and the voltage pulse response in the time- and frequency-domains. In several experiments, the metal-doped phthalocyanine thin-film was initially exposed to a high concentration of the challenge gas and purged to minimize baseline drift between the subsequent challenge gas



exposures. In these cases, the first purge cycle after the initial high concentration preconditioning exposure was used to establish the baseline reversibility response level.

The second test battery measured the performance of the various IGEFET devices when exposed to the specific challenge gases of interest. The test parameters (temperature, humidity, film thickness, etc.) were systematically varied. These measured results were then compared to the reference (baseline) results established while the IGEFET was exposed to similar operating conditions either in the presence of room air or the purge cycle which followed the initial high concentration preconditioning exposure.

The differences between the baseline results and those gleaned from the IGEFETs while they were exposed to the challenge gases were compiled and analyzed. The investigation specifically focused on identifying the combination(s) of the parameter test matrix which produced the most significant degree of sensor sensitivity, selectivity and reversibility.

Each IGEFET was assigned an index of sensitivity, selectivity, and reversibility relative to its location in the parameter test matrix. These indices are described in detail in the *Definitions* section.

### *Limitations*

The sensor performance evaluation conditions and chemically-active coatings involved those listed in Table I-2.

### *Definitions*

For the purpose of this research, a few key terms and concepts need to be defined. They include the system physical plant, sensitivity, selectivity, and reversibility. They will be defined in terms related to the measurable IGEFET performance parameters.

The IGEFET may be viewed as an integral part of a gas detection system. It is the critical element of the system's physical plant. The inputs to the system include: challenge gas type, challenge gas concentration, operating temperature, and relative humidity. The IGEFET structure and metal-doped phthalocyanine (MPc's) coating contribute the major factors in the gas detection system's response characteristics and, for the purpose of this thesis, they will be termed the system physical plant. The measurable system response functions are reflected in the following electrical characteristics: signal gain, phase, impedance, and response to a voltage-pulse excitation (time- and frequency-domains).

Sensitivity is a relative measure of the magnitude of the physical

plant's response to a particular challenge gas at a particular location in the parameter test matrix. Beaudet *et al*, established that "the sensitivity of the sensor is the lowest concentration of agent that can be detected in the absence of background interferences with 90% confidence limits..." [1:12]. Determining the sensitivity of the sensor to a particular challenge gas is important because it facilitates comparing different sensors under reproducible conditions [1:12]. The relative sensitivities were measured relative to room air primarily because room air was used as the carrier (diluent) gas. The relative sensitivity (SenRel) is defined as the function describing the behavior of a particular thin-film type and physical system when exposed to a particular challenge gas. This measure will be quantified by calculating the mean ( $\mu$ ) of a particular response characteristic at a particular challenge gas test point. Equation I-3 describes the relationship between the mean and the discrete data values. That is,

$$\mu(x) = (1 / N) \sum_{i=1}^N x_i \quad (I-3)$$

where N is the number of test points, and  $x_i$  is a particular measured value

in the ensemble of N elements. Using the mean values and comparing the challenge gas values to the baseline values established using room air will establish the sensor's relative sensitivity. This sensitivity can be normalized with respect to the room air mean ( $\mu_{\text{air}}$ ) response as indicated in Equation I-4. That is,

$$\text{Sen}_{\text{Rel}} = \left[ \frac{(\mu_{\text{air}} - \mu_{\text{challenge gas}})}{\mu_{\text{air}}} \right]. \quad (\text{I-4})$$

Selectivity ( $\text{S}_{\text{Rel}}$ ) is a value associated with a sensor's ability to distinguish between different challenge gases in the absence of background interferences [1:13]. This metric will be a function of two (or more) gases involved in the comparison; that is,  $\text{S}_{\text{Rel}} = f(\text{gas\#1, gas\#2, ...})$ . For example, the  $\text{S}_{\text{el}}$  of a particular IGEFET measured parameter relative to challenge gas G1 in the presence of challenge gas G2 can be expressed as:

$$\text{S}_{\text{el}} (\text{G1,G2}) = \left[ \frac{(\mu(\text{G1}) - \mu(\text{G2} + \text{G1}))}{\mu(\text{G1})} \right]. \quad (\text{I-5})$$

The reversibility ( $R_{\text{gas}}$ ) of the gas detection system is a numerical function assigned to the sensor which describes the system's ability to return to a quiescent state after being exposed to a change in the challenge gas concentration ( $c_n$ ). As such, the following equation applies:

$$R_{\text{gas}} = \left[ \frac{(\mu_1(c_1, t_1) - \mu_2(c_2, t_2))}{(\mu_2(c_2, t_2) - \mu_3(c_1, t_3))} \right] \quad (\text{I-6})$$

where  $\mu_1$  is the mean value of a particular measured parameter at time  $t_1$  and quiescent concentration  $c_1$ ;  $\mu_2$  is the mean value of a particular measured parameter at time  $t_2$  and concentration  $c_2$ ; and  $\mu_3$  is the mean value of a particular measured parameter at time  $t_3$  and quiescent concentration  $c_1$ . In this investigation,  $t_1$  represents the time before the sensor is exposed to any challenge gas. At some later time, a challenge gas is introduced and a new quiescent state is achieved. At this time,  $\mu_2$  is measured. Next, the challenge gas is purged from the system and, after some interval of time, a third quiescent state is achieved. Finally,  $\mu_3$  is measured, and the reversibility can be quantified.

### *Assumptions*

This investigation assumes that the IGEFET and the thin-film chemically-active coatings will behave in a piecewise-linear, time-invariant manner while the experimental conditions are varied relative to any particular set of nominal parameter matrix test values when the sensor is exposed to a challenge gas. This assumption is not generally extended to include the regions between the test points. The linearity assumption permits the principle of superposition to be applied to the analysis at any particular region in the parameter test matrix. This initial assumption is necessary to determine if the output signals are directly proportional to the sum of the input signals.

Piecewise linearity is assumed because a real system seldom displays a continuous, linear relationship throughout its entire operational range [22:I-5]; however, real systems are often piecewise continuous and differentiable. This characteristic permits the linearity assumption to be applied over a small range of perturbations relative to a nominal reference point. In this study, each parameter test matrix setpoint is considered to be a nominal point about which the IGEFET responses will vary due to exposure to the challenge gases.

The time-invariance assumption implies that the system will not

change simply as a function of time. This feature is important for assessing the IGEFET sensitivity, selectivity, and reversibility. A time-invariant system will also attain an equilibrium response relative to a particular parameter setpoint. Experiments by earlier researchers have revealed that the reaction equilibria between the MPC's coatings and the challenge gases are likely to occur after a time period varying from a few seconds to several minutes [7; 22].

This investigation assumed from the outset that any particular measured detector system response, relative to any parameter matrix situation, will display a characteristic mean value ( $\mu$ ).

### *Methodology*

Deposition of the gas sensitive, thin-film coatings on the IGEFET sensors merits additional explanation. Figure I-4 depicts the general structure of a single IGEFET device. Each IGEFET is fabricated by depositing a thin-film coating on the interdigitated gate electrode (IGE) structure. The uncoated IGEFETs are fabricated on silicon wafers and

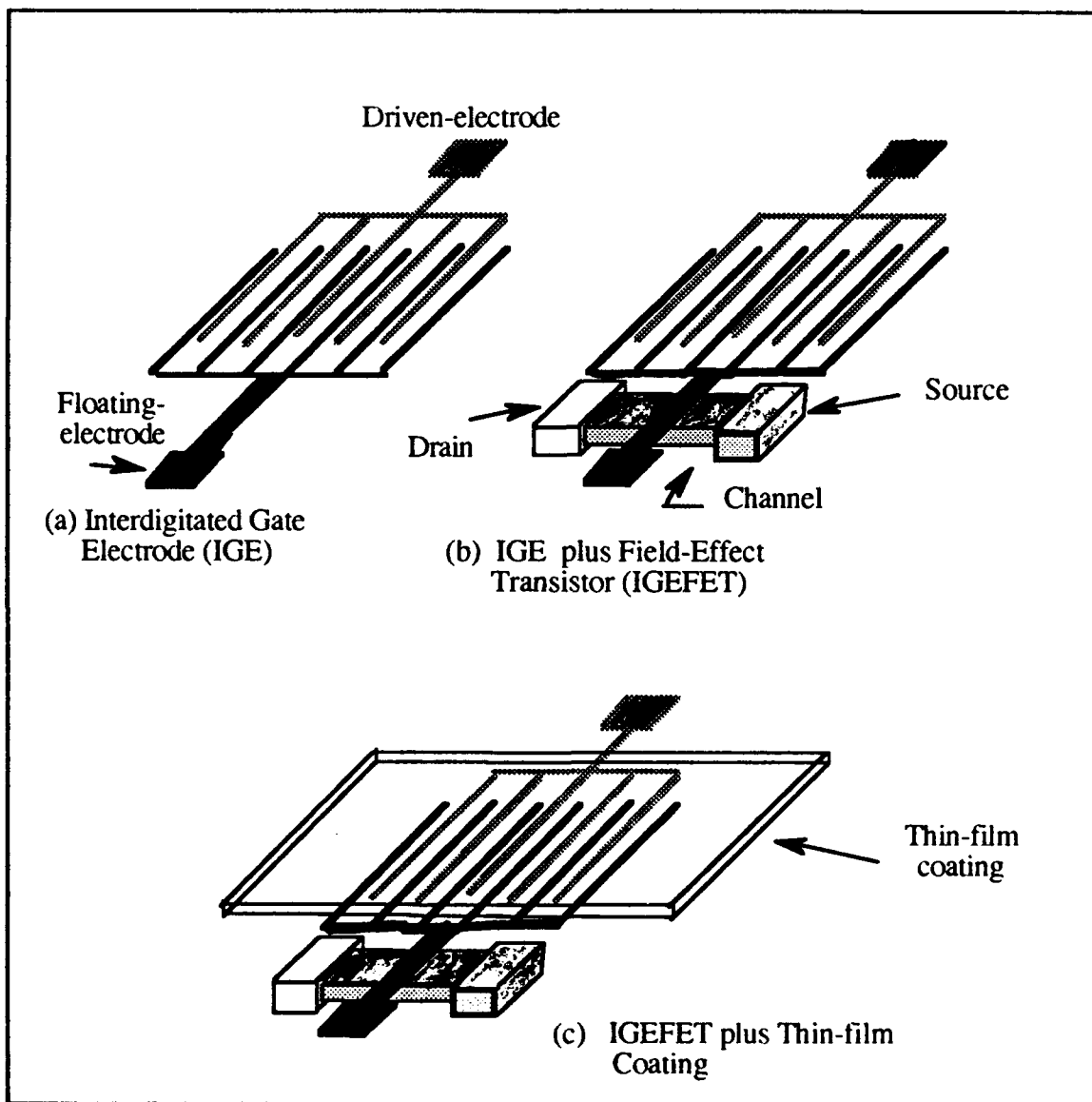


Figure I-4. IGEFET-Based Microsensor Fabrication: (a) IGE, (b) IGEFET without the Thin-Film Coating, and (c) IGEFET with the Thin-Film Coating.



packaged in dual-in-line packages (DIPs). Each DIP holds one integrated circuit die. Each integrated circuit die contains nine discrete IGEFET devices. After the chemically-active thin-film deposition process, there are nine IGEFETs in each DIP. The IGEFET design used in this study was accomplished by Captain Thomas Jenkins (GE-89D). The design was submitted to the Metal-Oxide-Semiconductor Implementation System (MOSIS) for fabrication. MOSIS fabricated the IGEFETs on silicon wafers and then packaged them in a 64-pin DIP. The DIPs were shipped from MOSIS without the chemically-sensitive thin-film coatings. The chemically-sensitive, thin films were deposited during this thesis investigation.

The IGEFET DIPs were inspected using optical microscopy as received from MOSIS to verify that they satisfied the design specifications. An electronic performance evaluation was then conducted to assess the IGEFET structure's gain and transfer function characteristics. The IGE structure's dc and ac impedances were measured. The thin-film, metal-doped phthalocyanine (MPc's) coatings were deposited on the IGE structures with an electron-beam vacuum deposition (EBVD) process following their initial electrical inspection and validation.

The thickness of a MPc's thin-film deposition was measured with a

scanning electron microscope, a stylus profilometer, and an *in situ* quartz crystal microbalance (QCM). Adjustments to the EBVD process were made as required to achieve film thicknesses to within 20% of the desired values (Table I-2).

The EBVD process was used to deposit three thicknesses of each film candidate onto individual integrated circuit die. Thus, of the nine IGE structures on each IC die, a cluster of three were coated with MPC's films having the same thickness. The chemically-active thin-films were copper phthalocyanine (CuPc), cobalt phthalocyanine (CoPc), and nickel phthalocyanine (NiPc). By covering three of the IGEFET structures with the same film thickness, redundant measurements were made simultaneously. In addition, since there were three different thicknesses of the same MPC's thin-film on each integrated circuit die, the three different thicknesses were simultaneously compared because they were operated under the same conditions.

In the final set of gas challenges involving DMMP and DIMP, the microsensor chips each had three different types of metal-doped phthalocyanine thin-films, and all the arrays were coated with a nominal thickness of 2,000 Å.

The baseline response of the IGEFETs were assessed by exposing

them to room air and systematically traversing the remainder of the parameter test matrix values. Representative samples of each IGEFET thin-film candidate and thickness were evaluated. The IGEFET response to the challenge gases was then compared to these baseline measurements.

### *Plan of Development*

Chapter I presents a concise problem statement along with the motivation and background for characterizing the sensitivity, selectivity, and reversibility of several metal-doped phthalocyanine thin-film coatings deposited on the IGEFET structures. Chapter II reviews the current literature relative to several important classes of gas phase microsensors. Chapter III focuses on the IGEFET, dealing with the physical device structures and the theoretical models used for describing their behavior. Chapter III also contains information concerning the MPC's semiconductors, the models used to describe electron transport through these structures, and the doping theories used to explain their conduction modulation by the challenge gas. Chapter IV describes the experimental methodology implemented in this thesis. Chapter V is a summary of the experimental data and interpretations of the results. Conclusions and recommendations are formulated in Chapter VI.

## *Summary*

The IGEFET sensors fabricated by depositing copper phthalocyanine (CuPc), cobalt phthalocyanine (CoPc), and nickel phthalocyanine (NiPc) thin films on their IGE structures have demonstrated significant gas sensitivity responses when exposed to trace concentrations of several organophosphorus compounds and nitrogen dioxide. The ability to detect organophosphorus compounds has military and civilian significance. Organophosphorus compounds comprise a broad class of toxic agricultural pesticides and chemical-warfare nerve agents. Nitrogen dioxide is a by-product of certain munition detonator failure modes. Since the detonator's electrical triggering mechanism can be corroded by the emitted nitrogen dioxide, sensing its evolution during weapon storage will facilitate identifying unreliable detonators.

For each of the challenge gases, this thesis attempted to identify the most sensitive, selective and reversible combination of sensor thin-film coating and operating conditions from among those in Table I-2. However, due to time constraints and the unavailability of gas generation tubes, only the 150°C temperature region was explored in depth.

## *II. Literature Review of Solid-State Sensors Used for Detecting Organophosphorus Compounds and Nitrogen Dioxide*

### *Introduction*

A number of microfabricated devices have been investigated to serve as chemical sensors [18:405]. At least four distinct technologies have been configured by investigators to detect organophosphorus compounds and nitrogen dioxide [9; 18]. These devices have successfully detected both the chemical analogs to chemical warfare nerve agents and nitrogen dioxide. The sensor technologies reviewed include: surface acoustic wave (SAW) devices, chemiresistors, optical waveguides, and interdigitated gate-electrode field-effect transistor (IGEFET) microsensors, also known as chemically-sensitive field-effect transistors (CHEMFETs).

Murray *et al* compiled a study comparing the current state of performance for these four solid-state sensor technologies, and projected their performance into the year 2000 [18]. Continuing research with these technologies seeks to improve their sensitivity and selectivity. As this research proceeds, one major feature common to all, dominates as the controlling factor concerning their ability to detect the challenge gases. That feature is the chemical coating used to transduce the presence of the

chemical moiety [18:405].

The sub-millimeter physical size of these sensing devices makes them very attractive. They are sufficiently small to be easily employed by military personnel in a deployed status; perhaps, they might even be incorporated into individual issue equipment ensembles. In addition, due to their small size, a large number of these sensors can be fabricated onto a tiny surface, yet, with each sensor element configured to be sensitive to a specific challenge gas, the summary array of sensors should be able to detect a spectrum of challenge gases from a multicomponent gas environment [1; 18:405 ]. By utilizing a multiple sensor array configuration, the possibility exists that while none of the individual sensors can be uniquely suited to detect a particular gas; nevertheless, the overall multiple sensor array response pattern may possess unique characteristics of the challenge compound [18:406]. An interesting possibility may be to use the multiple sensor array in conjunction with a computer. This would avail the user with the option of reconfiguring the system detection and identification function with specific software [1; 18: 406].

### *Gas Detection Devices.*

Six technologies are currently employed to realize the primary devices being investigated for detecting the organophosphorus and nitrogen dioxide compounds. Two of these are based upon the piezoelectronic crystal technology; the SAW device and the piezoelectric sorption detector (a bulk-wave device) [18:406; 26:2-1]. The other technologies include: the notch filter [11], the chemiresistor [18:406; 26:2-1], the optical waveguide [18:405], and the chemically-sensitive IGEFET microsensor (a. k. a. CHEMFET) [7; 18:406; 22; 26:2-1]. These microsensors are fabricated with a chemically-active thin-film coating, and they rely upon the interaction of this layer with the challenge gas. The interactions of the chemically-active layer with the challenge gases are transduced into an electronic response depending upon the sensor technology, and yield a corresponding change of a measureable parameter. For the sensors discussed in the following sections, the primary modes of interaction are adsorption of the challenge gas molecules onto the chemically-active thin-film's surface or the absorption of the gas molecules into the bulk regions of the film. The adsorption and absorption of the challenge gas molecules affect the overall physical properties of the thin-film coating. These changes are reflected in variations in the normally quantified parameters

of mass, electrical conductivity, bulk dielectric constant, and bulk permeability constant. The gas detectors reviewed in the following sections differ primarily in the mechanisms employed in detecting a change in one or more of the perturbed film properties. For example, the piezoelectric device detects changes in film mass, the chemiresistor focuses on changes in electrical resistance, etc. A description of each device is presented in the following sections.

### *Piezoelectric Devices*

The piezoelectric devices can be segregated into three basic groups, quartz microbalances (QMBs), coated piezoelectric quartz crystals, and surface acoustic wave devices (SAWs). Simple bulk-wave, coated piezoelectric quartz crystal sensors and surface acoustic wave (SAW) devices are mechanically resonant structures. These devices all rely upon the piezoelectric effect that causes a physical deformation in the crystal's shape when a voltage is applied to it. The crystal can be made to oscillate at its resonant frequency by applying an oscillating voltage at the crystal's characteristic frequency. When small changes occur in the bulk mass of the crystal due to molecular absorption on its surface, the resonant frequency will be shifted. Thus, these devices are used to detect changes in



the mass of their surface due to molecular absorption.

The simplest of the piezoelectric device structures is the quartz microbalance (QMB). In its basic form, the QMB is fabricated from a thin piezoelectric quartz wafer having attached electrodes. To produce a QMB, a quartz crystal is cut into very thin wafers, and the electrodes are deposited on both surfaces of the wafer. The QMB is frequently employed as a simple vacuum deposition film thickness monitor [17:705]. Lucklum *et al* report that the QMB can be used as a gas sensor [17:705 - 710]. They used several different QMBs, each coated with its own chemically-sensitive, thin-film layer, and then exposed the ensemble to polar and apolar organic and inorganic compounds such as CO<sub>2</sub>, CO, and NO<sub>2</sub>. They used 8.5 mm diameter, quartz crystals with a 10 MHz resonant frequency and 5 mm diameter electrodes. The chemically-sensitive thin-films were deposited onto both sides of the crystals. As the chemically-sensitive layer's mass changes due to adsorbed molecules, the resonant frequency shifts. If  $\Delta v$  is the change in the resonant frequency,  $v$ , due to a change in the crystal oscillator's mass,  $\Delta m$ , the two are related by [17:705]:

$$\Delta v = -C_f \frac{v^2}{A} \Delta m \quad (\text{II-1})$$

where A is the coating's area, and  $C_f$  is a mass sensitivity parameter [17:707].

For an AT-cut crystal vibrating in the thickness shear mode,  $C_f = 2.26 \times 10^{-10} \text{ m}^2/\text{g s}$  holds. Using 10 MHz quartz crystals, gravimetric detectors can be produced with detection limits in the nanogram level [17:705].

The QMBs were used by Lucklum *et al* to detect polar and apolar organic and inorganic compounds, such as  $\text{CO}_2$ , CO, and  $\text{NO}_2$  [17:705-710].

The piezoelectric material can be made to oscillate by applying a harmonic potential to the device's electrodes. The intensity of the oscillations becomes pronounced when the applied voltage oscillates at a frequency approaching the mechanical resonant mode of the crystal [7:2-2]. The resonant frequency can be perturbed about its nominal value with a change in the crystal's mass or by changes in the viscoelastic properties of a thin-film which has been deposited on the device's surface [9,18:406]. Schiede and Guilbault [21:1764-1768] and Roberts and Holcroft [20:56] related the frequency shift due to changes in the surface mass of the

piezoelectric quartz crystal sensor as described by Equation II-2:

$$\Delta F = (-2.3 \times 10^6 F^2)(\Delta m/A), \quad (\text{II-2})$$

where

$\Delta F$  = change in resonant frequency (Hz),

$F$  = resonant frequency (MHz),

$\Delta m$  = change in mass (gm), and

$A$  = surface area of detector (cm<sup>2</sup>).

As an example, a bulk-wave piezoelectric quartz crystal sensor with a reactive surface of 1 mm by 1 mm operated at 300 MHz, will need to undergo a mass change of  $7.24 \times 10^{-11}$  grams to produce an output frequency shift of 1500 Hz. For a DFP challenge gas (m.w. 180.2 g/mole) this implies an absorption of  $2.42 \times 10^{11}$  molecules.

The principle mode of operation for the SAW device is as a delay-line oscillator. Figure II-1, from Janta [9], depicts the general SAW device structure. The device's resonant frequency depends upon the crystal's wave velocity, the surface electrode spacing, and any thin-film coating applied to the surface of the device [18:406]. Figure II-1 shows how the central selective region modulates the waveform traversing from

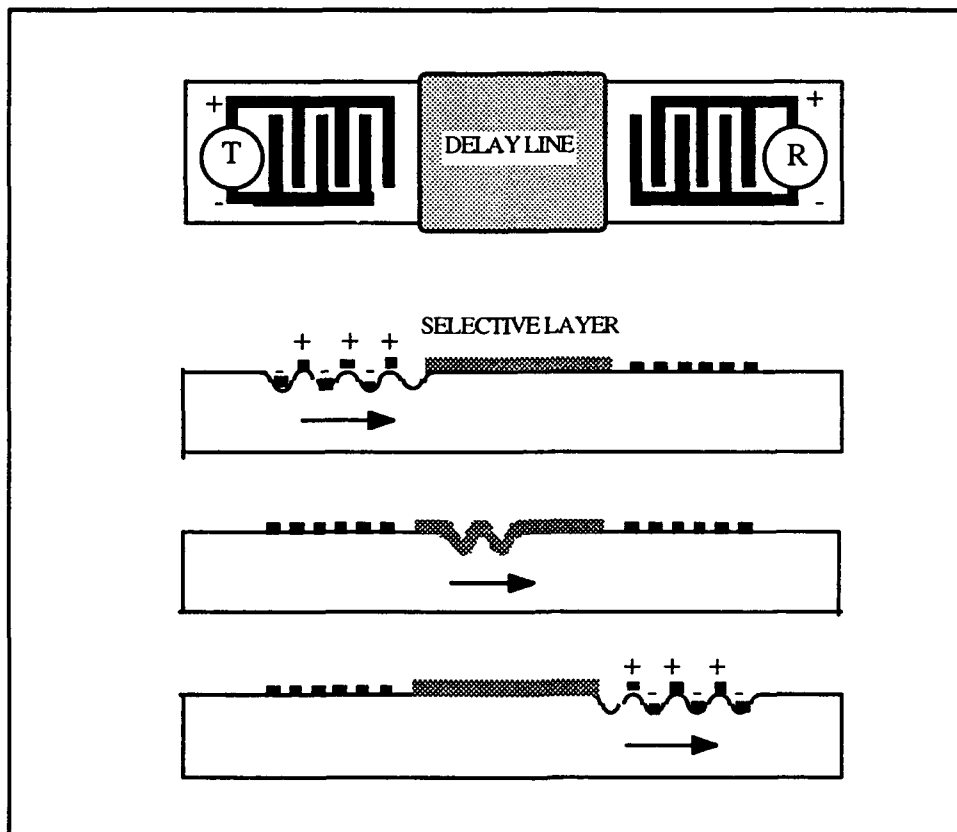


Figure II-1. Schematic diagram of a SAW sensor with transmitter, T, receiver, R, and the chemically-sensitive layer deposited on the sensor's delay line section [9:70].

end-to-end on the crystal's surface. A change in the selective layer's mass will be reflected as a change in the resonant frequency of the surface wave. The material chosen for the thin-film layer is selected for its ability to chemically-interact with the challenge gas of interest. The preferred modes of the chemical interaction are adsorption and absorption [7:2-2].

Fabrication techniques allow SAWs to be produced in sizes less than one square millimeter; however, current research is focused on SAWs with

several square millimeters of surface area. The larger areas are desired because they increase the amount of interaction between the challenge gas and the chemically active portion of the sensor. As a performance example, Murray *et al* reports a SAW with surface area of 8 mm<sup>2</sup> operating with a resonant frequency of 300 MHz which provided a frequency shift of 1500 Hz when the thin-film's mass changed by 1x10<sup>-9</sup> gm [18:406]. This device has a typical signal-to-noise ratio (SNR) of 50-to-1. These devices have detected absorbed organophosphorus compounds at concentrations below 0.1 mg/m<sup>3</sup>. Tables I-1 and II-2 summarize the current and projected performance of the SAW devices.

### *Notch Filters and Chemiresistors*

Notch filters and chemiresistors are fabricated using the same resources. The primary difference between the two sensor technologies is not in their fabrication method, but rather with the physical parameters and operational mode used to measure and detect a gas of interest. When the structure is employed to transduce a change in the dc resistance of the thin-film coating, the device is deemed a chemiresistor. When the

Table II-1.

Status of SAW, Chemiresistor, and Waveguide Vapor Sensor Technologies for the Present and the Year 2000 [17:407].

Uncoated Device Characteristics	Surface Acoustic Wave		Chemiresistor		Waveguide	
	Present	2000	Present	2000	Present	2000
Surface Area	10-1 cm <sup>2</sup>	10-4 cm <sup>2</sup>	10-1 cm <sup>2</sup>	10-4 cm <sup>2</sup>	3 cm <sup>2</sup>	10-3 cm <sup>2</sup>
System Volume	10 cm <sup>3</sup>	10-1 cm <sup>3</sup>	10 cm <sup>3</sup>	10-2 cm <sup>3</sup>	10 cm <sup>3</sup>	10-1 cm <sup>3</sup>
Power Required	1 W	10-1 W	10-2 W	10-5 W	-	-
Coated Device Characteristics						
Detection Limits mg/m <sup>3</sup> DMMP	0.05	0.001	5	0.01	100	-
Response Time (sec)	1 - 100	0.01-100	10-1000	1-100	1-100	-

Table II-2.

Reported Detectable Concentrations for IGE and Notch-Filter Technologies. [5; 3; 14].

Researcher	Thin-film Material	Device Technology	Gas Challenge	Challenge Concentration	Experiment Temp (°C)	Carrier Gas	Year
Hamann <i>et al</i> [5]	PbPc	IGE	NO <sub>2</sub>	10 ppb	50 - 120	Room Air	1991
Cranny <i>et al</i> [3]	PbPc	IGE-like	NO <sub>2</sub>	50/100 ppb	150	Room Air	1991
Kolesar [14]	Cu+CuProus Oxide	Notch-Filter	DIMP	100 ppm	90	Room Air	1990

structure is used to transduce the changes in both the thin-film resistive and reactive components, the device is being operated as a notch filter.

Kolesar designed a notch filter and reported using it for detecting organophosphorus compounds, including diisopropyl methylphosphonate (DIMP) [15:7-8]. The salient features of notch filter design, as described by Kolesar, included a chemically-active film of copper+cuprous oxide in contact with copper electrodes and isolated from a second electrode by a thin layer of non-conductive material [15:1-3]. A swept-frequency harmonic signal was injected into one electrode and the resultant signal transferred to the other electrode was measured. The transfer function is partially dependant upon the distributed dielectric properties of the cuprous oxide layer. In essence, the device acts as a distributed resistor and capacitor circuit. As the copper+cuprous oxide film interacts with the challenge gas molecules, it's dielectric function is modulated; in turn, the distributed resistance and capacitance of the thin-film reflects this modulation and the overall signal transfer function shifts by a measurable amount.

The notch filter transfer function gain is usually measured versus driving source frequency, and the resulting bandpass characteristics are recorded as accomplished by Kolesar [15:3]. When the electronic

properties of the chemically-active thin-films are perturbed by a challenge gas, the notch filter's bandpass response may acquire a new shape and center frequency. The notch filter fabricated by Kolesar was able to detect an organophosphorus compound (DIMP) at concentrations less than 10 ppm [11].

Chemiresistors are small interdigitated electrode structures coated with a chemically-active thin-film that interacts with the desired challenge gas. Chemiresistors undergo changes in their electrical resistance when they are exposed to a challenge gas. The change in the electrical conductivity is attributable to variations in the number of charge carriers made available in the thin-film coating due to the chemical interactions with the gas of interest [18:408].

Challenge gases donating, accepting, or polarizing charge carriers in the thin-film coating will produce changes in the material's bulk resistance, depending upon the efficiency of the charge or polarization transfer process and the concentration of the challenge gas.

Chemiresistors are a form of the general class of conductimetric sensors. This sensor class reports gas-sensitivity information by transducing changes in their bulk conductivity,  $G(\omega)$  [9:213]. The bulk conductance can be calculated from the following relation, where  $I(\omega)$  is



the current and  $V(\omega)$  is the potential:

$$G(\omega) = I(\omega) / V(\omega). \quad (\text{II-3})$$

The units of electrical conductance are siemens (mhos). The other relationships involved in the discussion of electrical conductivity include:

$$R = \rho L / A \quad (\text{II-4})$$

where  $R$  is the resistance in ohms,  $L$  is the conductor length,  $A$  is the conductor's cross-sectional area, and  $\rho$  is the material's resistivity. The conductivity,  $\sigma$ , is the reciprocal of  $\rho$ ; hence

$$1/\rho = \sigma = J/E = L/(AR) \quad (\text{II-5})$$

where  $\sigma$  is the ratio of the current density  $J$  ( $\text{A cm}^{-2}$ ) to the applied electric field  $E$  ( $\text{V cm}^{-1}$ ). The unit for  $\sigma$  is  $\text{siemens}^{-1} \text{ cm}^{-1}$ .

The general form of conductimetric devices, as depicted in Figure II-2, has two metal electrodes with a chemically-active material sandwiched between them [9:213]. They transduce changes in the conductivity of the selective material between the electrodes. This feature is critical to the utility of these detectors [9:213]. The dc current flow is

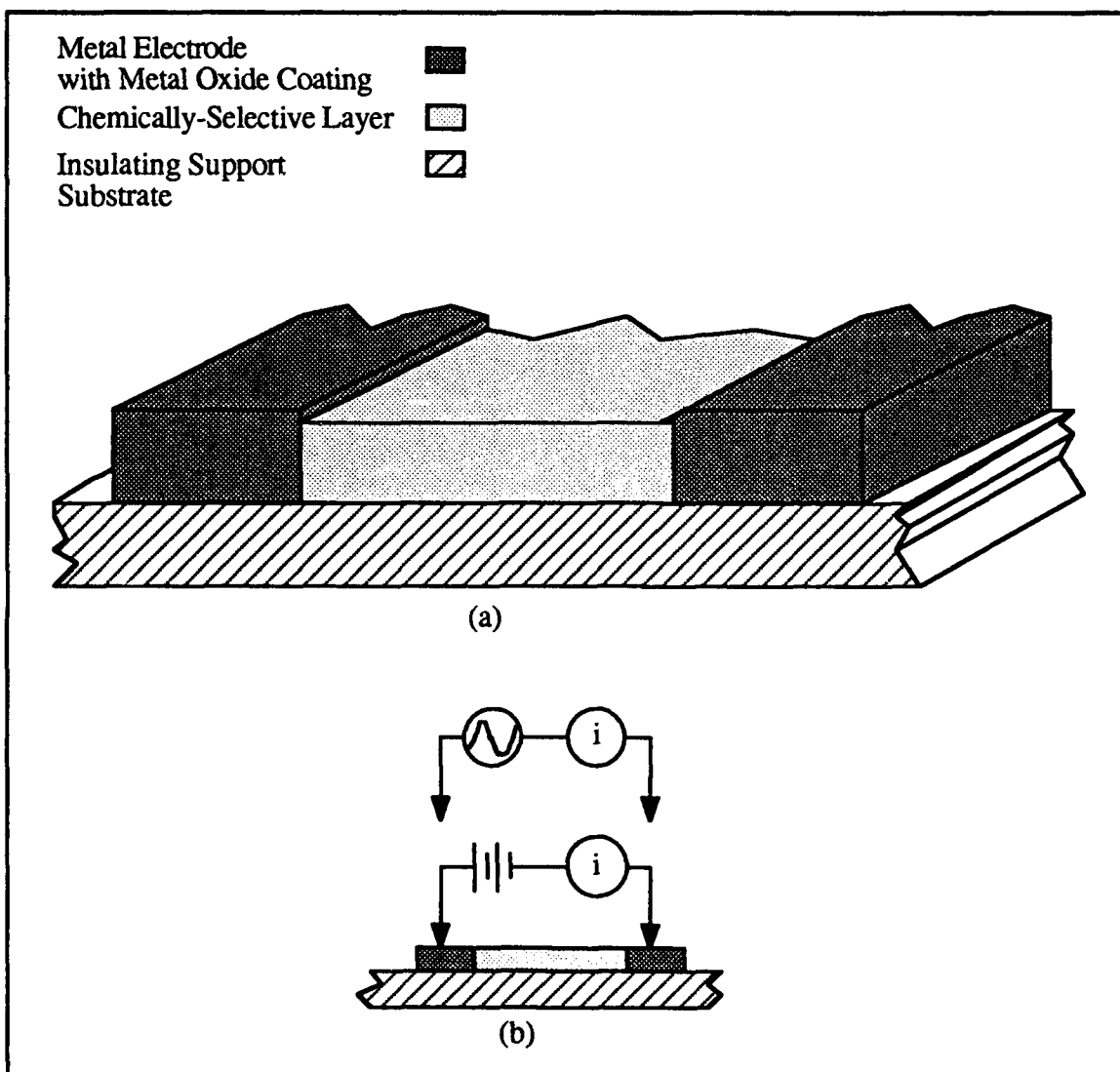


Figure II-2. General conductimetric device: (a) material configuration (b) current flow measurements.

usually the measured parameter, as depicted in Figure II-2(b). A general model for the conductimetric sensor is illustrated in Figure II-3. Focusing

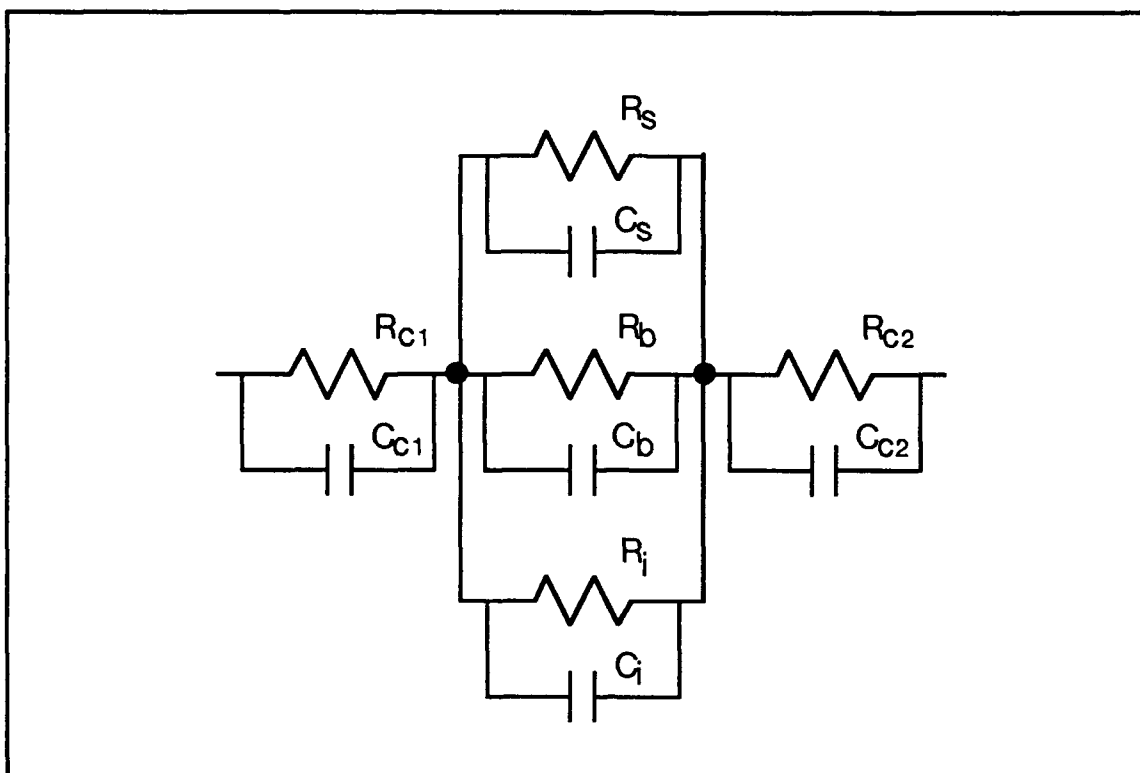


Figure II-3. General Equivalent Circuit Diagram of a Conductimetric Sensor. Subscripts c1 and c2 Refer to the Metal Oxide-to-Semiconductor Contact, s Refers to the Surface Components, b Refers to the Bulk Components, and i Refers to the Components Due to the Interface Between the Semiconductor and the Insulating Support Surface.

on the selective layer, the resistance between the contacts and the selective layer are  $R_{C1}$  and  $R_{C2}$ . The capacitance between the contacts and the selective layer are  $C_{C1}$  and  $C_{C2}$ . The resistance and capacitance of the surface of the selective layer are  $R_s$  and  $C_s$ , respectively. The resistance and capacitance of the bulk of the selective material are  $R_b$  and  $C_b$ ,

respectively [9:214]. The resistance and capacitance of the interface between the selective layer and the surface of the supporting material are  $R_i$  and  $C_i$ , respectively [9:214].

Two resistance calculations can be made: one for the contact resistance and one for the resistance of the selective layer. The contact resistance is dominated by the thin, non-conducting metal oxide generally covering the metal electrode [9:215]. The metal/metal-oxide/chemically-active thin-film junctions have a Schottky current density of:

$$J_{\text{Schottky}} = A_R T^2 \exp \left[ \frac{-q \left\{ \phi - \left( \frac{qV}{4\pi d \epsilon_i} \right)^{\frac{1}{2}} \right\}}{kT} \right] \quad (\text{II-6})$$

where  $A_R$  is Richardson's constant, and

$$A_R = 4\pi m q k^2 / h^3 \quad (\text{II-7})$$

with  $T$  the temperature in degrees Kelvin,  $q$ , the fundamental unit of electron charge,  $\phi$ , the average barrier height,  $d$ , the insulator thickness,  $h$ , Planck's constant,  $m$ , the electron's effective mass,  $V$ , the applied voltage and,  $\epsilon_i$ , the dielectric constant [9:215]. The dielectric constant,  $\epsilon_i$ , is equal

to  $\epsilon_0\epsilon_r$  where  $\epsilon_0$  is the free space dielectric constant, and  $\epsilon_r$  is the material's relative dielectric constant. For a time-varying excitation, the capacitance of the equivalent circuit model must be considered along with its resistance.

The resistance of the chemically-active selective layer can be viewed as the parallel combination of the bulk conductivity ( $\sigma_{\text{bulk}}$ ) and the surface conductivity ( $\sigma_{\text{surface}}$ ) [9:216].

The bulk conductivity depends upon the charge carrier concentrations and mobilities [9:216]. The general conductivity relationship for the semiconductor bulk material can be expressed as [9:216; 9:222]:

$$\sigma_{\text{bulk}} = q[\mu_p p + \mu_n n] \quad (\text{II-8})$$

and

$$G_b = n_b q \mu_b Wd/L \quad (\text{II-9})$$

where

$G_b$  = bulk conductance,

$\sigma_{\text{bulk}}$  = bulk conductivity (mhos/m),

$\mu_p$  = hole mobility ( $\text{m}^2$  per volt-second),

$\mu_n$  = electron mobility ( $\text{m}^2$  per volt-second),

$\mu_b$  = bulk carrier mobility ( $\text{m}^2$  per volt-second),

$n_b$  = bulk carrier density ( $\text{m}^{-3}$ ),

$q$  = electron charge,

$W$ ,  $d$ , and  $L$  = width, depth and length of the material being measured (m), and

$p$ ,  $n$  = density of holes and electrons ( $\text{m}^{-3}$ ), respectively.

The current density can be expressed as [4:70]:

$$J = Eq[\mu_p p + \mu_n n] \quad (\text{II-10})$$

where  $E$  is the applied electric field.

These relations account for the contribution of the transported holes ( $p$ ) and the electrons ( $n$ ). Modulation of the  $\sigma_{\text{bulk}}$  conductivity depends upon the ability of the modulating compound (gas to be sensed) to actually enter into a charge carrier donating, accepting, or polarizing equilibrium that is translated into the bulk of the chemically-sensitive thin-film [9:216].

The chemical modulation of the surface layer conductivity depends upon the ability of the challenge gas molecules to donate, accept, or polarize the charge carriers at the surface of the semiconductor material [9:221]. For n-type semiconductors this can be expressed as Equation II-11 [9:221]; that is,

$$\Delta\sigma_s = q\mu_s\Delta n_s \quad (\text{II-11})$$

where the change in the surface conductivity  $\Delta\sigma_s$  is due to the change of the surface electron density,  $\Delta n_s$ , and the surface electron mobility,  $\mu_s$ .

For a layer of thickness of  $d$ , then [9:222]:

$$\Delta n_s = \int_0^d [n(z) - n_b] dz \quad (\text{II-12})$$

and the corresponding change in surface conductance,  $\Delta G_s$  is:

$$\Delta G_s = \Delta\sigma_s W/L. \quad (\text{II-13})$$

Assuming that  $\mu_b$  approximately equals  $\mu_s$ , Equations II-12, and II-13 can be used to create [9:222] a relative index of surface-to-bulk conductivity,  $\Delta G_s/G_b$ . That is,

$$\Delta G_s/G_b = \Delta n_s/n_b d \quad . \quad (II-14)$$

For thin-film coatings deposited on a chemiresistor, the principle source of chemical modulation is the surface layer [9:218].

The fabrication of chemiresistors is frequently accomplished by evaporation, Langmuir-Blodgett techniques, or spin coating [9:219].

Typical device parameters are listed in Table II-3.

Table II-3.

Typical Chemiresistor Parameters for 1 - 5 Volts Applied [8:219].

Electrode Spacing	10 - 100 $\mu\text{m}$
Total Electrode Area	0.1 - 1 $\text{cm}^2$
Thin-Film Thickness	0.01 - 1 $\mu\text{m}$
Typical Current Flow	nA range
Inter-Electrode Resistance	$10^8 - 10^{11}$ ohms

Chemiresistor devices using metal/phthalocyanine (1000Å)/metal configurations are reported by Janta [9:219] to function with the Schottky-conductivity type behavior.

Janta reports that surface conductivity changes were attributed to the signal changes when using a Pb-phthalocyanine chemiresistor [9:220]. This behavior represents an order-of-magnitude greater sensitivity than



demonstrated with current SAW technology [18]. Using a Pb thin-film coating for selectively detecting DMMP has been demonstrated at a level of less than 5 mg/m<sup>3</sup> [18]. Estimates of the chemiresistor performance are shown in Table II-2.

### *Optical Waveguides*

Optical waveguides coated with chemically-sensitive and optically-active films have been used to detect gases. The methods used for low concentration gas phase studies include refractometry and interferometry [9; 18:409]. Using an optical detection method presents an opportunity to exploit the advantages of remote sensing, and the method's inherent imperviousness to electromagnetic interference [18]. The disadvantages of this technology include susceptibility to stray light and possible photo-degradation of the chemically-active coating materials. The waveguide detectors also have a limited dynamic range [18].

The physical property exploited for the optical waveguide detectors is the critical angle of light reflection when traversing a medium with a higher index of refraction relative to a medium with a lower index of refraction. As reported by Murday [18], photorefractometry has been used to measure changes in the refractive index on the order of 1 part-per-

million.

Detecting various challenge gases using waveguides coated with polymers has been shown to be sensitive to the challenge gases at parts-per-million concentrations; however, the underlying processes have not been modeled sufficiently well to project ultimate sensitivities.

Another approach for using optical waveguides is coating the guide with a material which will change its dimensions under the influence of an external challenge gas. Murday [18] reports that Butler [2] has demonstrated that this concept will work for gas-phase detectors of H<sub>2</sub> at concentration levels of 1 to 10<sup>4</sup> ppm, while using a Pt-coated waveguide. Janta [8:280] describes an optomechanical sensor which has a sensitive coating capable of physically stretching the length of the optical waveguide it encases.

Figure II-4 depicts the arrangement of an optical sensor coated with Pd. The coherent light beam emitted from the HeNe laser source is split, and the resultant beams are propagated along two separate paths. One path is through an uncoated waveguide. The other path is through a waveguide coated with Pd. The beams are then recombined, and the resulting interference pattern is established before a challenge gas is introduced into the system. This mode defines the sensor's baseline interference response

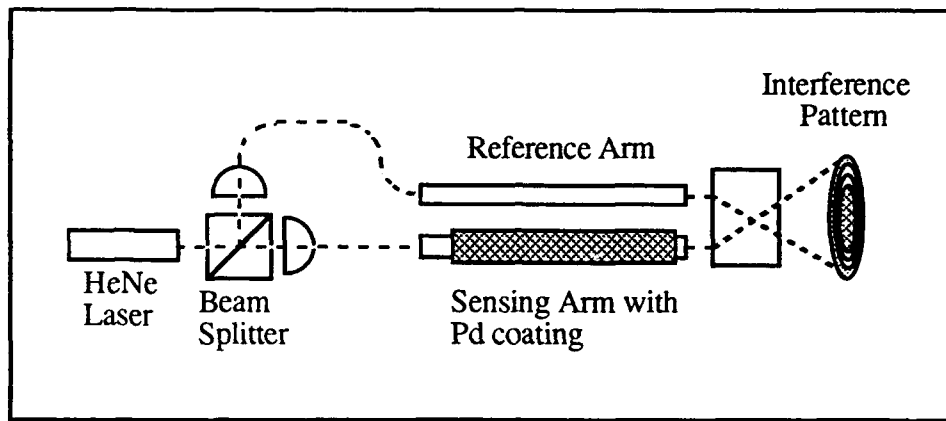


Figure II-4. Optomechanical Interference Sensor Technology (9:280).

pattern. When a challenge gas is introduced,  $H_2$  in this case, the challenge gas interacts with the waveguide coating and expands the lattice constant of the Pb. The relative change,  $\Delta a_0$ , in the lattice constant,  $a_0$ , (atom spacing) is proportional to the amount of palladium hydride,  $CPdH$ , formed, which is proportional to the partial pressure of the  $H_2$  [9:280]. That is;

$$\frac{\Delta a_0}{a_0} = 0.026 \Delta C_{PdH}. \quad (II-15)$$

The changing Pd lattice structure, in turn, stretches the waveguide longitudinally. The changing waveguide length modulates the optical

interference pattern. When used to measure H<sub>2</sub>, the dynamic range of the sensor spans 1 to 10<sup>4</sup> ppm [9:281].

### *Interdigitated Gate-Electrode Field-Effect Transistor (IGEFET)*

#### *Microsensors*

The IGEFET microsensor is the primary technology of interest in this thesis. Chapter III is devoted to a detailed description of the models dealing with the microsensor's components, including: the thin-film semiconductor coating material, the interdigitated electrode structure, the MOSFET structure, and the system-level IGEFET microsensor device. This microsensor has shown significant promise as a solution to the organophosphorus compound and NO<sub>2</sub> detection applications [7; 22; 26]. This sensor technology is based on the conventional metal-oxide-semiconductor field-effect transistor (MOSFET), but the IGEFET sensor has a unique gate-electrode structure which is coated with a chemically-active film. The gate-electrode is a broad expanse of interdigitated metal fingers which are supported by a high-quality, silicon dioxide dielectric [7; 22; 26]. A metal-oxide-semiconductor field-effect transistor with an interdigitated gate electrode structure is also called an interdigitated gate-

electrode field-effect transistor (IGEFET) [14]. The gate electrode fingers are composed of two fundamental components. One component of the interdigitated gate electrode structure is the floating-electrode; the other component is the driven-electrode. In operation, the driven-electrode is excited with an externally generated signal; typically a pulse or swept-frequency sine wave. The excitation signal is electromagnetically coupled to the floating-electrode via the chemically-active film coating. As the charge levels change on the floating-electrode, variations in the source-to-drain MOSFET channel's conductivity are induced [14:2356]. These changes can be detected and amplified. The IGEFET microsensor becomes useful for detecting gaseous organophosphorus compounds and nitrogen dioxide when its interdigitated electrode is covered with a semiconducting, metal-doped phthalocyanine polymer thin-film [7; 14; 22; 26].

The sensitivity of the IGEFET microsensor (a.k.a. CHEMFET) depends upon the transconductance of the system-level device, and the altered potential resulting from a change in the thin-film coating impedance [18:410].

NO<sub>2</sub> sensor studies have been conducted by Temofonte and Schoch using NiPc and PbPc thin-films on IGE structures [24:1350-1355]. They

deposited their gas-sensitive films with a thickness on the order of 0.15  $\mu\text{m}$ . They used a vacuum sublimation technique for their depositions. Following the depositions, the typical interelectrode resistance, before exposure to the  $\text{NO}_2$  challenge gas, spanned  $1 \times 10^{16}$  to  $4 \times 10^{16}$  ohms. After exposing the devices to  $\text{NO}_2$  concentrations of 25 ppb, 1.2 ppm, and 60 ppm, the resistance values changed to final values on the order of  $10^{15}$ ,  $10^{12}$ , and  $10^9$  ohms, respectively [24]. They report, "The organic semiconductor thin-film (MPc) gas sensor having ultra high sensitivity ( $\leq 25\text{ppb}$ ) and a very fast response time ( $\leq 60$  s) has been demonstrated" [22:1355].

### *Conclusions*

Murray [18] states that the SAW sensor is the most advanced technology at this time. The chemiresistor and the optical waveguide may get similar results based upon theoretical projections. That is, "The CHEMFET is still further behind and struggling with microfabrication and passivation problems" [18:410; 24:1355]. Temofonte and Schoch express, "Future work to optimize sensor characteristics is needed, and low-noise IC compatible FET device structures have been designed and fabricated for

this purpose" [24:1355].

The purpose of this thesis is to advance the understanding and applicability of the IGEFET microsensor to selectively detect and identify organophosphorus compounds and NO<sub>2</sub>.

### *III. The IGEFET Microsensor Concept, Design, and Implementation*

#### *Introduction*

The microsensors used for this investigation are similar to those used by previous researchers [ 7; 14; 22; 26]. The microsensors were designed using an interdigitated gate-electrode field-effect transistor (IGEFET) structure. Figure III-1(a) shows the fundamental configuration of the IGEFET microsensor.

The fundamental IGEFET-based microsensor structure used in this investigation is very similar to the integrated circuit (IC) devices used in previous investigations at AFIT [ 7; 14; 22; 26]. The organization and functionality of the multi-sensor array and IC die has been modified for this research effort. When contrasted with the design used by Shin [22], the following revisions can be observed: the analog signal multiplexer/decoder was deleted from the design, only nine sensor arrays were fabricated on each IC die, no feedback resistors were fabricated on the IC die, each IGEFET microsensor is an integral part of its own impedance matching differential input amplifier, and no reference amplifier is employed on the IC die.



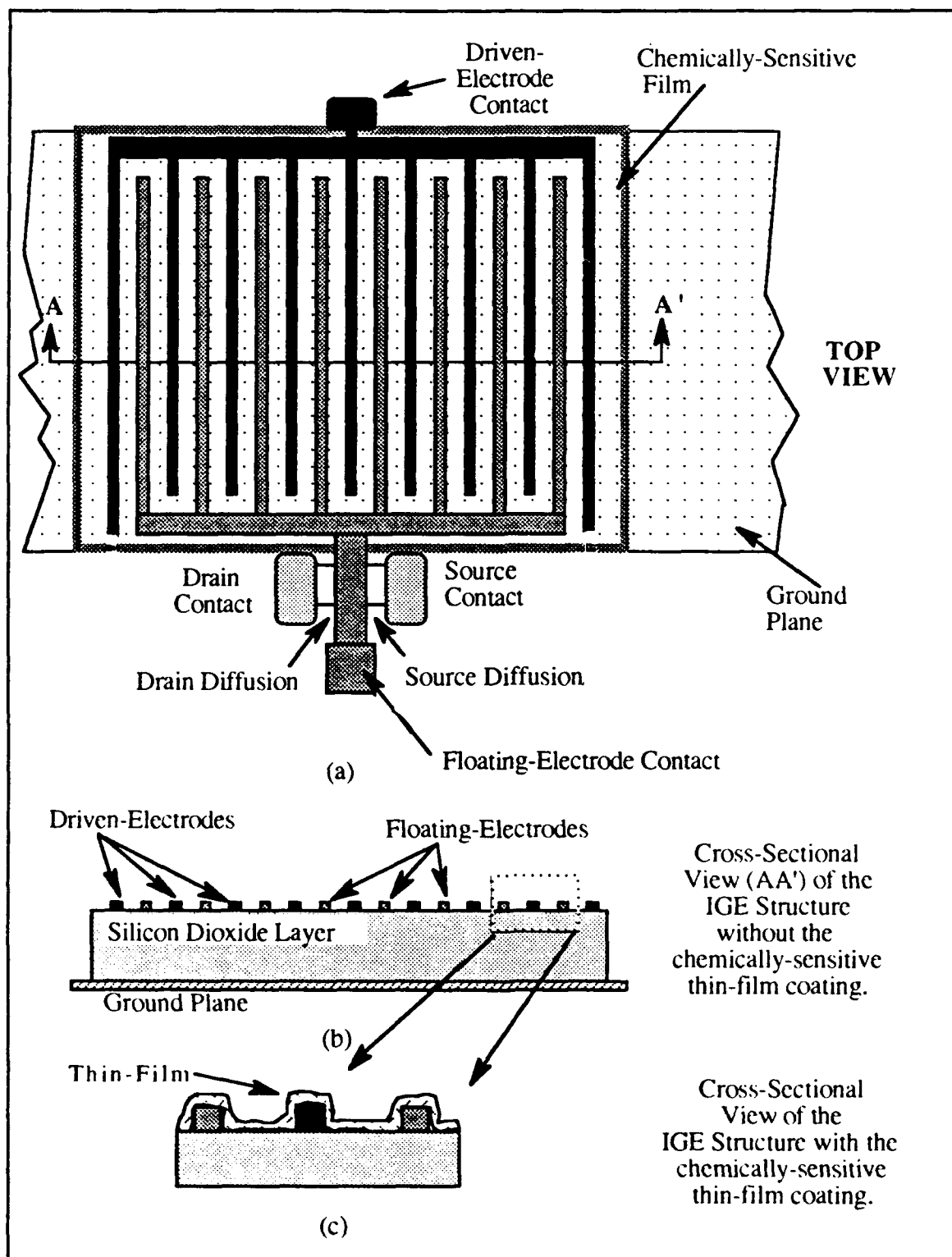


Figure III-1. Interdigitated Gate Electrode Field-Effect Transistor (IGEFET) (not to scale) [12; 26:I-3].

These revisions were made primarily due to the difficulties encountered by previous researchers while attempting to achieve adequate performance from the analog signal multiplexer and amplifier. Since these difficulties at the IC die organization level detracted from the investigation of the IGEFET microsensor, a decision was made to remove the analog signal multiplexer and its associated amplifier from the multi-sensor design. The new IC design had nine impedance matching amplifiers, one for each of the nine IGE structures, all fabricated on the same IC die.

### *IGEFET Microsensor Concept*

The IGEFET microsensor used in this research is a device that can transduce variations in the impedance of its chemically-active, thin-film by modulating its output current. The thin-film's impedance can be modulated by exposing it to various challenge gases. The changes result from interactions of the gas molecules with the semiconducting, thin-film surface and bulk material.

### *IGEFET Design*

As depicted in Figure III-1(a) and (b), the basic structural

components of the IGEFET can be discerned. During fabrication, the interdigitated driven- and floating-electrodes are fabricated from photolithographically patterned aluminum. The interdigitated driven- and floating-electrodes form a structure called the interdigitated gate-electrode (IGE). The chemically active thin-film is deposited on the IGE structure, partially covering the surface of the fingers and filling a portion of the space between them.

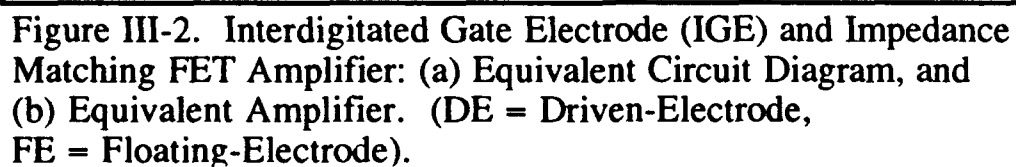
The IGE is composed of two components, the driven-electrode and the floating-electrode. Usually, an input signal is applied to the driven-electrode, and it is electromagnetically coupled primarily through the intervening space filled with the thin-film coating to the floating-electrode. The magnitude and phase of the signal coupled to the floating-electrode is dependent, in part, upon the impedance of the thin-film. The floating-electrode serves two purposes. The first is to be an electrical contact point for the signal coupled through the thin-film from the driven-electrode. (The IGE with the deposited thin-film structure is analogous to two parallel plates separated by a bulk material). The second purpose served by a portion of the floating-electrode is to function as the gate electrode for the sensor's *in situ* metal-oxide-semiconductor field-effect transistor (MOSFET). In this role, it modulates the current flow between the

MOSFET's drain and source electrodes. The *in situ* MOSFET design was selected because its high input impedance would not excessively load the IGE structure, and noise due to interconnecting lead lengths could be minimized.

To provide gain to the modulated signal without sacrificing the sensor's isolation, each IGEFET was designed as the non-inverting input to a differential amplifier. This feature can be observed schematically in Figure III-2. In Figure III-2(a), the IGE structure with its driven-electrode (DE) and floating-electrode (FE) is shown connected to transistor Q4. In fact, the floating-electrode modulates the drain-to-source current flow for transistor Q4. Transistor Q4 is the FET portion of the IGEFET sensor. Transistor Q4 is also the non-inverting input for the differential transistor pair formed by Q4 and Q5. Transistors Q6 and Q7 are functionally current-limiting resistors. Transistors Q1 and Q2 establish the quiescent current flows which are dependent upon the relative level of  $V_{bias}$ . Transistor Q5 drives the output ( $V_{out}$ ).

#### *Phthalocyanine Thin-Film Coatings for the IGEFET*

A critical aspect of the microsensor is the chemically active thin-film used to modulate the signal coupled between the driven-electrode and the



floating-electrode. Metal-doped phthalocyanines were used in this investigation because their semiconducting properties can be modulated by the absorption, adsorption, and desorption of various gas molecules [16:345]. The changes in electrical conductivity are believed to occur as a result of the electron donor-acceptor complexes formed between the phthalocyanine and the challenge gas. This interaction is believed to be driven, in part, by the partial pressure of the challenge gas [16:347].

The semiconducting phthalocyanines are available as either metal-free or metal-doped compounds. The metal-doped phthalocyanine structures have a centrally located metal atom as depicted in Figure III-3. For this research, phthalocyanines doped with either copper, cobalt, or nickel were used. In addition, the phthalocyanine ring structure may have one or more groups substituted onto it at a peripheral location. Chemically-active thin-films have been fabricated using either substituted or unsubstituted phthalocyanines [16:368].

Deposition of the phthalocyanines to the IGE structure is usually accomplished via one of two techniques, Langmuir-Blodgett (L-B) or vacuum sublimation. The only method available for this investigation was the sublimation process which was implemented using an electron-beam vacuum deposition system (Denton Vacuum Corp; Model DV-602).

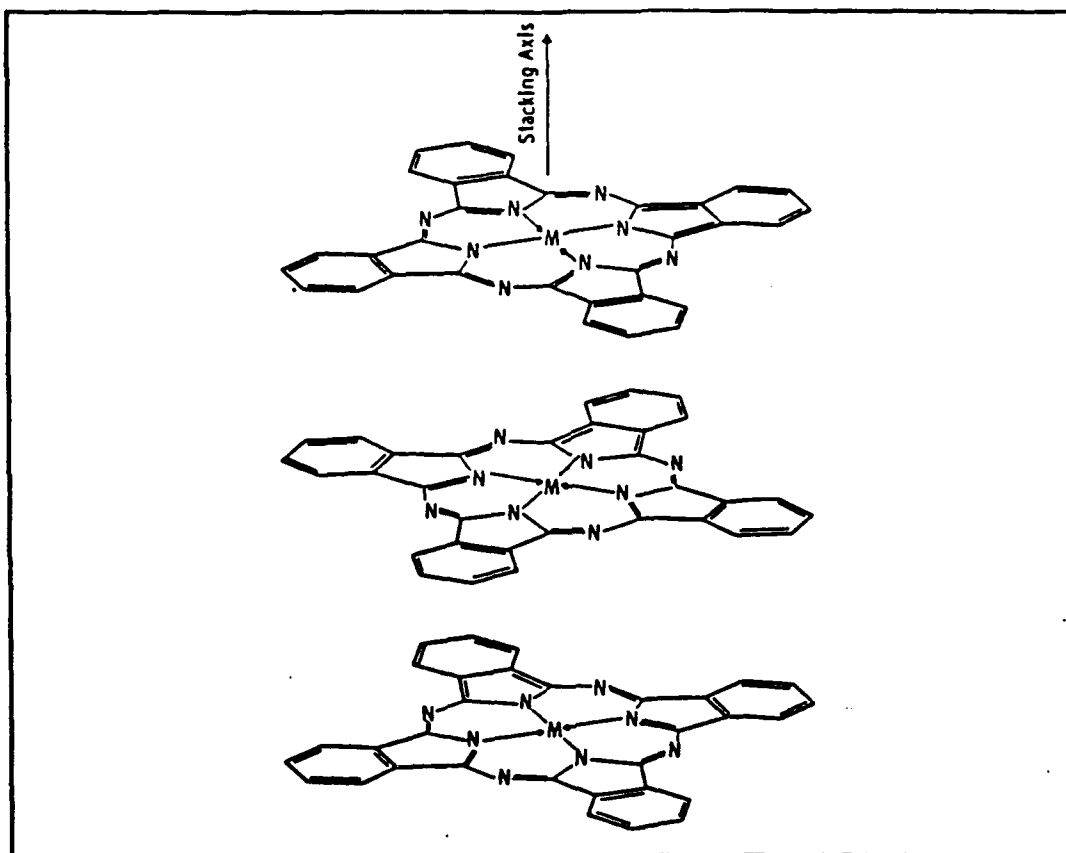


Figure III-3. Metal-Doped Phthalocyanine Molecules Showing Their Stacking Arrangement [24:1350].

The metal-doped phthalocyanine (MPc) thin-film morphology significantly influences its response to a challenge gas. The charge-transfer mechanism occurring during the challenge gas complex formation with the thin-film material is best facilitated on the planar face of the MPc ring. The charge-transfer mechanism is favorably facilitated along the axis perpendicular to the face of the stacked MPc rings [16:351].

The metal-doped phthalocyanines are classified as a p-type semiconductor material based upon the material's response to exposures of electron donor and acceptor complexes. That is, the electrical conductivity of MPc is enhanced when it is exposed to electron-acceptor gases such as oxygen and nitrogen dioxide. Additionally, the MPc's electrical conductance has been observed to decrease upon exposure to ammonia, an electron donor [16:347]. The degree of acceptor-donor electron localization appears to influence the magnitude of the conductance change. Nitrogen dioxide, a  $\pi$ -electron acceptor, forms a delocalized hole structure within the MPc. This mechanism facilitates charge carrier transport. Boron trifluoride, a  $\sigma$ -electron acceptor, forms a more localized hole structure in the MPc, which acts to retard charge carrier transport [16:349].



### *IGEFET Microsensor Design and Implementation*

The design of the IGEFET microsensor has evolved through several iterations at the Air Force Institute of Technology (AFIT). The design version used in this investigation was finalized by Captain Thomas Jenkins and submitted to MOSIS (Metal Oxide Semiconductor Implementation System) for fabrication. This particular iteration of the IGEFET microsensor's evolution focused upon enhancing the inter-lead signal isolation and reducing the complexity of the IC die analog signal paths. The latter was accomplished by removing the analog multiplexing circuitry and fabricating an amplifier section for each individual IGEFET.

Nine IGEFET microsensor systems were fabricated on each IC die. The IGE fingers were fabricated with second-level aluminum. The critical dimensions for the IGE structure are shown in Table III-1. The fabrication method employed by MOSIS was a scalable 2-micron, double-metal, double-polysilicon, p-well technology [8]. The level-one metal was used in part to form the ground plane as shown in Figure III-1. The second-level metal was used to form the IGE floating - and driven-gate elements. The general layout of the nine IGE arrays on a IC die is sketched in Figure III-4. The outside dimensions of each IGE array are 1370  $\mu\text{m}$  by 1370  $\mu\text{m}$ . Figures III-5, III-6, III-7, and III-8 show

additional features of typical interdigitated gate electrode structures and their MOSFET amplifiers. Figure III-5 is the lowest magnification, and so

Table III-1.

Critical Dimensions of the Interdigitated Gate Electrode.

Number of Driven-Electrode Fingers	35
Number of Floating-Electrode Fingers	34
Driven-Electrode Area ( $\mu\text{m}^2$ )	483,100
Floating-Electrode Area ( $\mu\text{m}^2$ )	468,900
Finger Width ( $\mu\text{m}$ )	10
Finger Separation ( $\mu\text{m}$ )	10
Overall Array Length ( $\mu\text{m}$ )	1370
Overall Array Width ( $\mu\text{m}$ )	1370

shows a large portion of an IGE. Figure III-6 depicts a higher level of magnification, showing the metal strip of the floating-electrode extending over the input of the MOSFET's channel. Figure III-7 shows a closer view of the amplifier section. Figure III-8 shows a thin-film coating

(~5,000 Å thick) deposited onto a typical IGE.

Capt Thomas Jenkins performed SPICE simulation on the MOSFET segment of the overall design [8]. The IC die was designed to reduced the parasitic effects caused by having numerous lengthy metal conductors routing signals on the IC die. To do this, only a single layer of metal was used for signal pathways (excluding the IGEs), thus eliminating any vertically spaced crossings between conductor runs [8]. Also, each array is serviced by its own bondwires, thus reducing unintentional cross-talk and providing a redundancy of function for those cases where an element may fail.

The dies were packaged in 64-pin DIPs. The wirebond contact functions are detailed in Table III-2.

### *Summary*

The IGEFET microsensor is a well developed technology. The device used in this study was designed by Capt Thomas Jenkins, and fabricated by MOSIS. The devices delivered by MOSIS were inspected, and metal-doped phthalocyanine thin-films deposited onto the IGE structures using a vacuum deposition process. The IGEFET microsensors were subsequently investigated as described in Chapter IV.

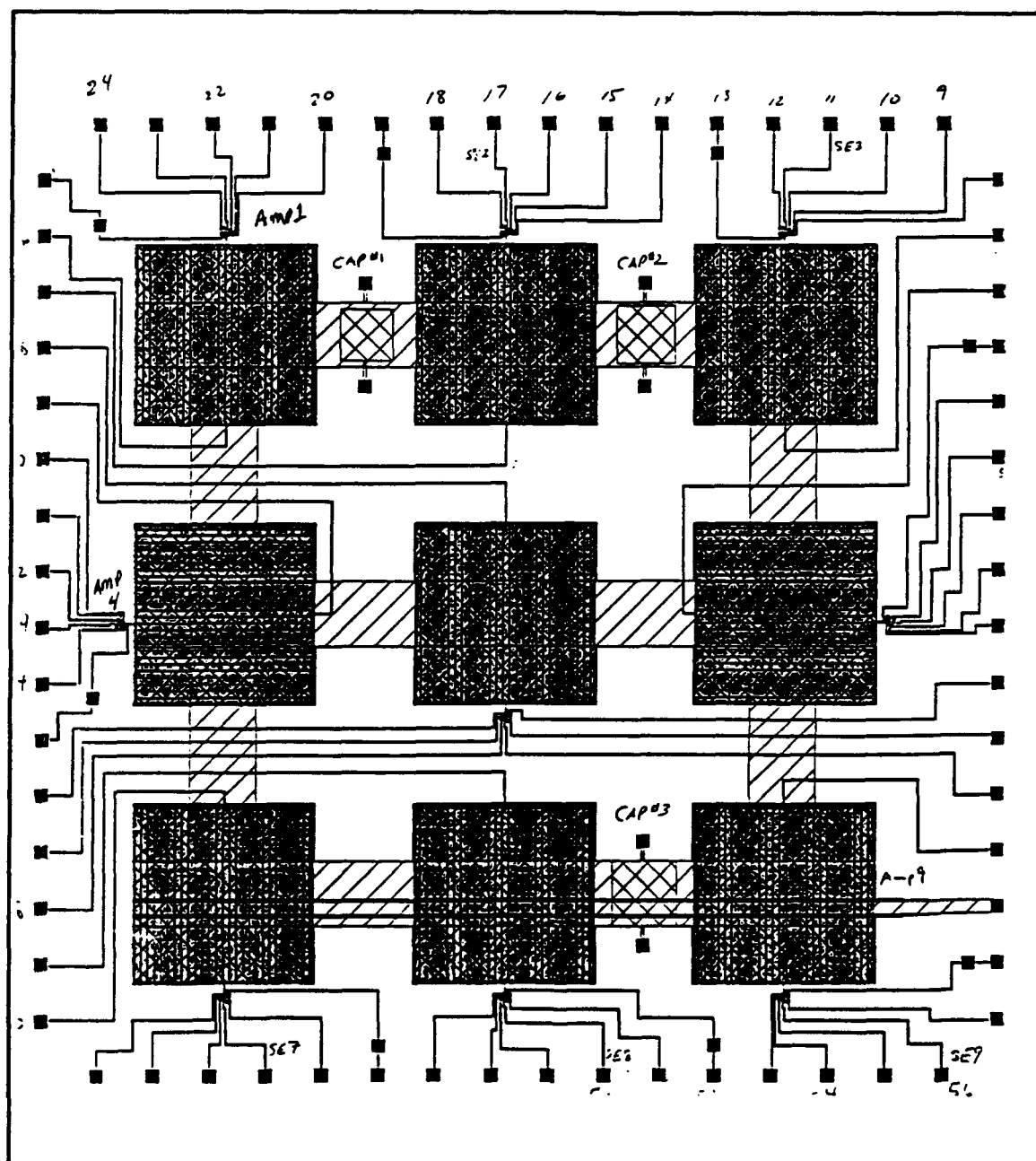


Figure III-4. Sketch of Nine Interdigitated Gate-Electrode Structures, Their Impedance Matching Amplifiers, and Wire Bonding Pads [8].

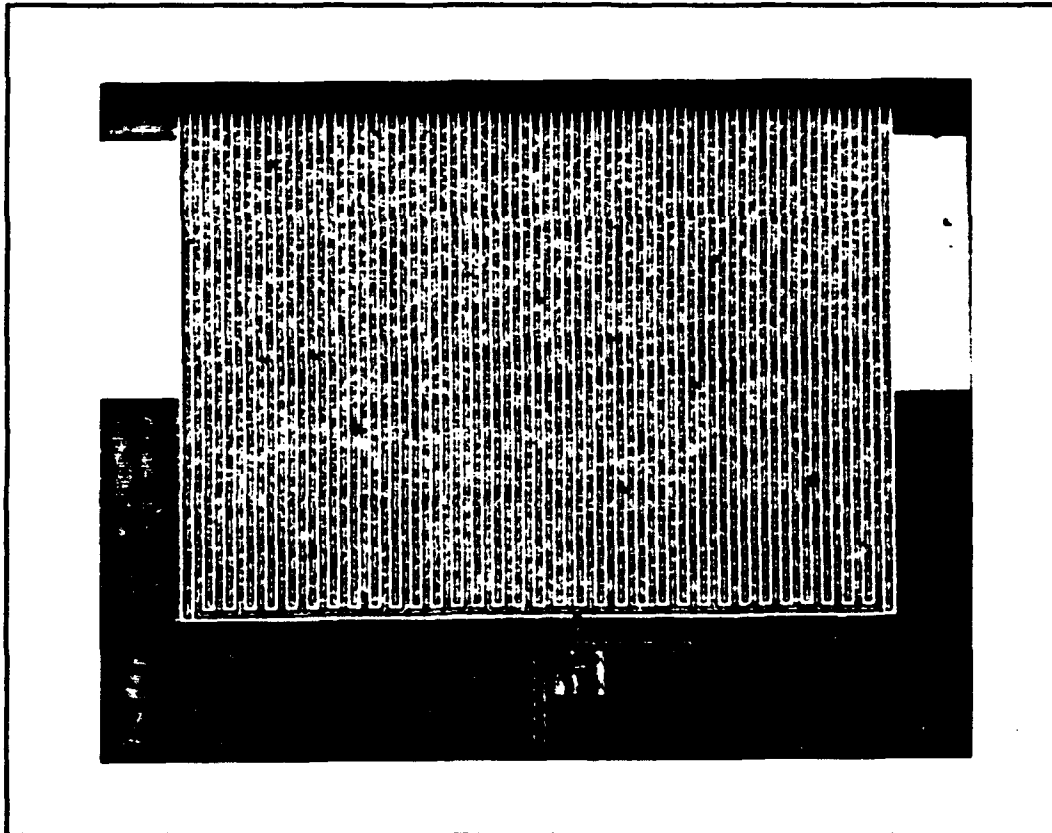


Figure III-5. Overhead View of a Portion of Interdigitated Gate Electrode and Impedance Matching Amplifier (50X).

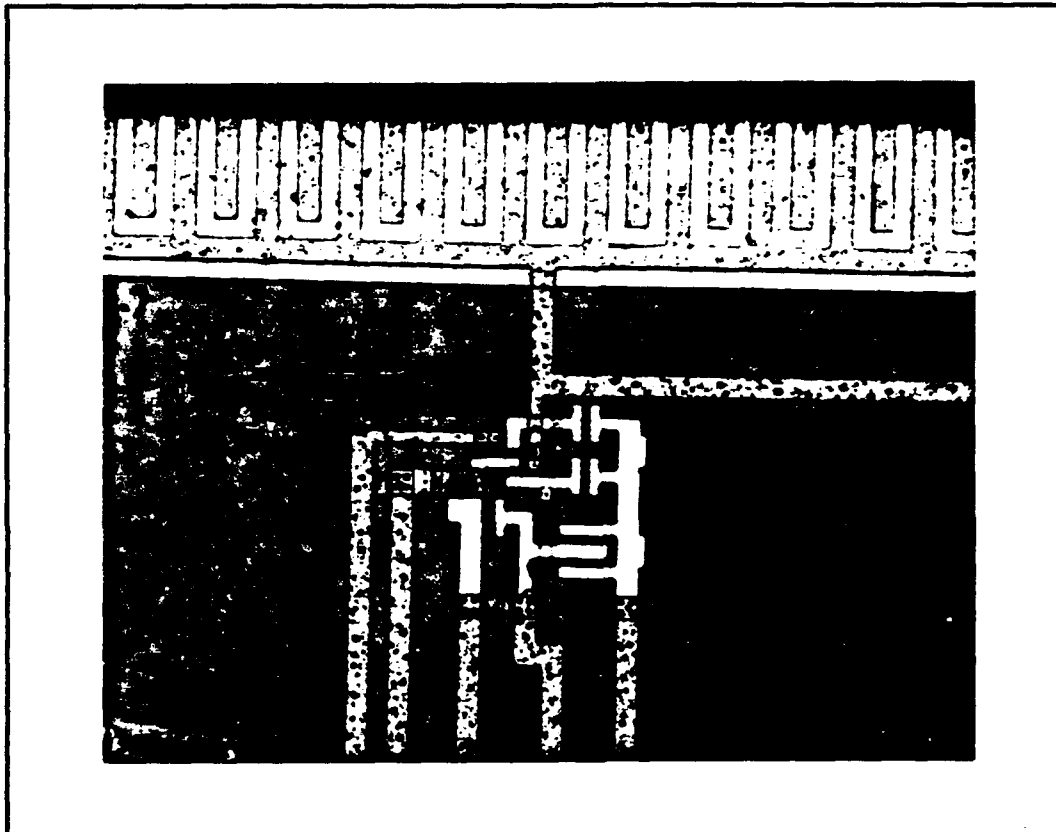


Figure III-6. Overhead View of a Portion of Interdigitated Gate Electrode and Impedance Matching Amplifier (200X).

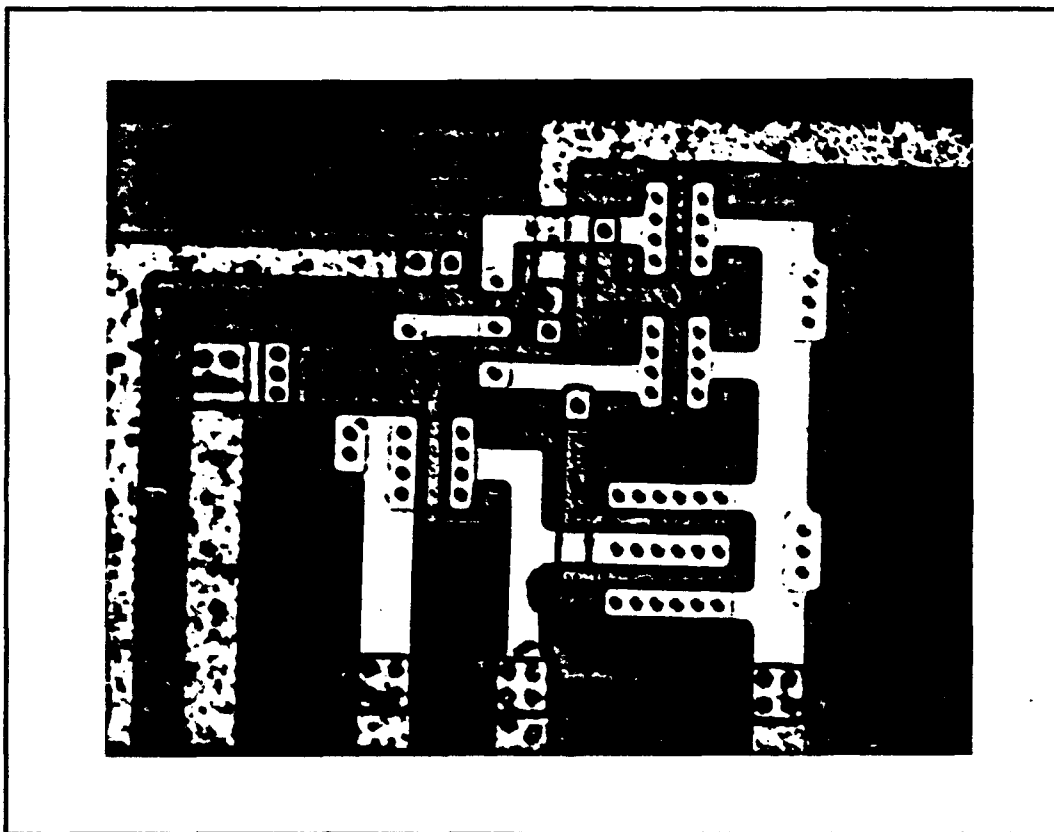


Figure III-7. Overhead View of the Impedance Matching Amplifier (400X).

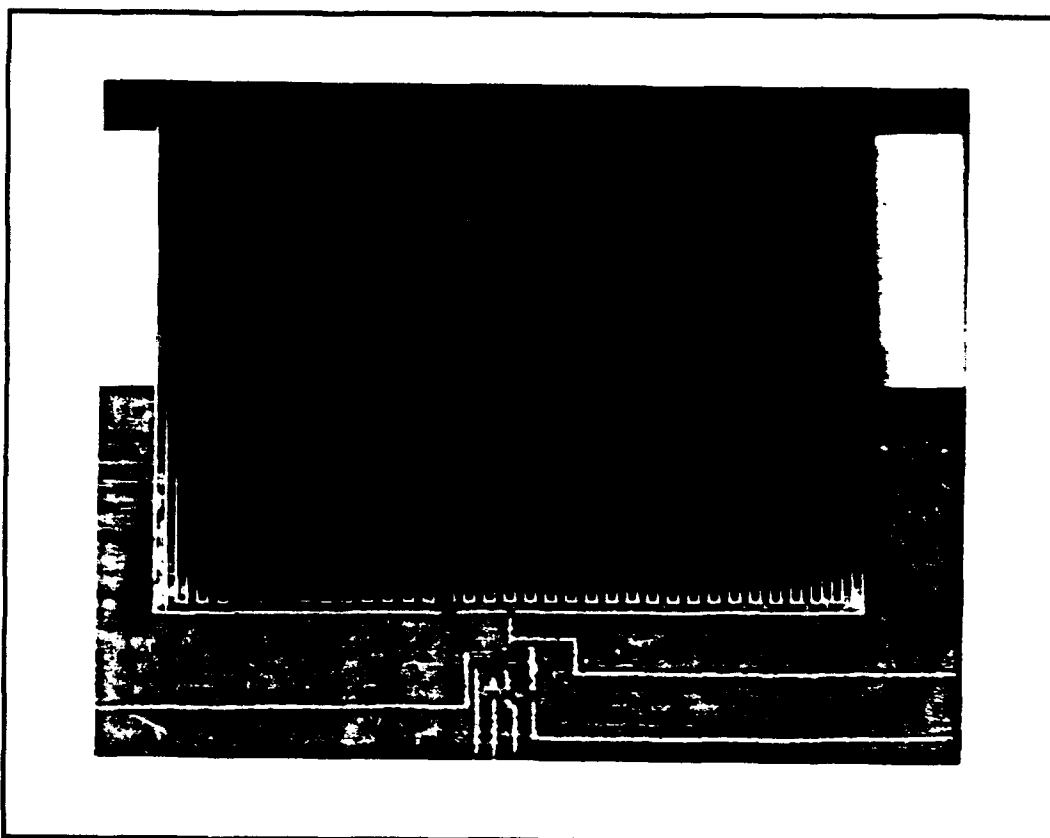


Figure III-8. Overhead View of the Interdigitated Gate Electrode Structure with a 3,900 Å Thick CuPc Deposition (400X).



Table III-2.

64-Pin DIP Wirebond Contact Function Summary (Continued on the next page).

Pad Number	Signal Name and Associated Microsensor	
1	V <sub>bias</sub>	IGE #6
2	V <sub>ss</sub>	IGE #6
3	V <sub>out</sub>	IGE #6
4	V <sub>dd</sub>	IGE #6
5	Floating-Gate	IGE #6
6	Driven-Gate	IGE #6
7	Driven-Gate	IGE #3
8	V <sub>off</sub>	IGE #3
9	V <sub>bias</sub>	IGE #3
10	V <sub>ss</sub>	IGE #3
11	V <sub>out</sub>	IGE #3
12	V <sub>dd</sub>	IGE #3
13	Floating-Gate	IGE #3
14	V <sub>off</sub>	IGE #2
15	V <sub>bias</sub>	IGE #2
16	V <sub>ss</sub>	IGE #2
17	V <sub>out</sub>	IGE #2
18	V <sub>dd</sub>	IGE #2
19	Floating-Gate	IGE #2
20	V <sub>off</sub>	IGE #1
21	V <sub>bias</sub>	IGE #1
22	V <sub>ss</sub>	IGE #1
23	V <sub>out</sub>	IGE #1
24	V <sub>dd</sub>	IGE #1
25	Floating-Gate	IGE #1
26	Driven-Gate	IGE #1
27	Driven-Gate	IGE #2
28	Driven-Gate	IGE #5
29	Driven-Gate	IGE #4
30	V <sub>off</sub>	IGE #4
31	V <sub>bias</sub>	IGE #4
32	V <sub>ss</sub>	IGE #4
33	V <sub>out</sub>	IGE #4
34	V <sub>dd</sub>	IGE #4
35	Floating-Gate	IGE #4
36	V <sub>off</sub>	IGE #5

Table III-2.

## 64-Pin DIP Wirebond Function Summary (Continuation from Previous Page).

Pad Number	Signal Name and Associated Microsensor	
37	V <sub>bias</sub>	IGE #5
38	V <sub>ss</sub>	IGE #5
39	Driven-Gate	IGE #8
40	Driven-Gate	IGE #7
41	V <sub>off</sub>	IGE #7
42	V <sub>bias</sub>	IGE #7
43	V <sub>ss</sub>	IGE #7
44	V <sub>out</sub>	IGE #7
45	V <sub>dd</sub>	IGE #7
46	Floating-Gate	IGE #7
47	V <sub>off</sub>	IGE #8
48	V <sub>bias</sub>	IGE #8
49	V <sub>ss</sub>	IGE #8
50	V <sub>out</sub>	IGE #8
51	V <sub>dd</sub>	IGE #8
52	Floating-Gate	IGE #8
53	V <sub>off</sub>	IGE #9
54	V <sub>bias</sub>	IGE #9
55	V <sub>ss</sub>	IGE #9
56	V <sub>out</sub>	IGE #9
57	V <sub>dd</sub>	IGE #9
58	Floating-Gate	IGE #9
59	Ground Plane	
60	Driven-Gate	IGE #9
61	V <sub>out</sub>	IGE #5
62	V <sub>dd</sub>	IGE #5
63	Floating-Gate	IGE #5
64	V <sub>off</sub>	IGE #6

#### *IV. Experimental Methodology*

The discussion of experimental methodology is divided into two sections. Section IV-I discusses the basic microelectronic sensor device studied, the specific questions to be answered, and the primary issues addressed during the investigation. Section IV-II describes the tasks which were accomplished during the investigation to provide the data required for resolving the questions posed.

##### *Section IV-I.*

*IGEFET Device.* Coating the interdigitated gate electrode (IGE) structure of the interdigitated gate electrode field-effect transistor (IGEFET) with a metal-doped phthalocyanine thin-film results in a gas detector which has shown significant promise for sensing organophosphorus compounds and NO<sub>2</sub>. The IGEFET is based on the conventional metal-oxide-semiconductor field-effect transistor (MOSFET). The interdigitated gate electrode (IGE) structure is composed of two fundamental components. One component is the floating -electrode. The other is the driven-electrode. In operation, the driven-electrode may be excited with an external dc voltage, a voltage pulse, or a

harmonic signal. The excitation signal is electromagnetically coupled to the floating-electrode. As the charge levels change on the floating-electrode, variations in the MOSFET source-to-drain channel's conductivity are induced [14:2356]. These changes can be readily detected and amplified. The IGEFET structures become useful for detecting gaseous organophosphorus compounds and nitrogen dioxide when their interdigitated gates are covered with a thin-film of a metal-doped phthalocyanine semiconducting polymer [7; 14; 22; 26].

*Gases Tested.* The challenge gases used in this investigation included: ammonia ( $\text{NH}_3$ ), boron trifluoride ( $\text{BF}_3$ ), diisopropyl fluorophosphonate (DFP), diisopropyl methylphosphonate (DIMP), dimethyl methylphosphonate (DMMP), and nitrogen dioxide ( $\text{NO}_2$ ).

Ammonia was selected for study because of its highly polar nature and the fact that the nitrogen portion of the molecule acts as an electron donor [23:473]. The anticipated action of the ammonia would be to increase the resistance of the p-type semiconductor metal-doped phthalocyanine thin-films. Boron trifluoride, a strong  $\sigma$ -electron acceptor, was included for comparison with nitrogen dioxide, a strong  $\pi$ -electron acceptor. The organophosphorus compound challenge gases, DFP, DIMP, and DMMP, were chosen because they can be safely handled under a chemical hood,

and they are chemical analogs of the more toxic chemical warfare nerve agents. Characterizing the interaction of these challenge gases with the p-type semiconductor MPc thin-films when individually exposed under controlled conditions was the purpose of this research.

*Thin-Film Materials.* Several metal-doped phthalocyanine polymers, including cobalt-phthalocyanine (CoPc), copper-phthalocyanine (CuPc), and nickel-phthalocyanine (NiPc) have demonstrated their ability to perform as IGEFET gas-sensitive thin-films because of their capacity to interact with the challenge gases of interest in a measurable fashion [7; 22; 26]. The thin-film, metal-doped phthalocyanine polymer which covers the interdigitated gate electrode array forms a significant portion of the lossy dielectric which couples the floating- and driven-electrodes. The complex dielectric constant of the chemically-active, thin-film coating changes when certain gaseous compounds interact with it. This chemical activity is correspondingly reflected in the strength of the signal which couples the floating- and driven-electrodes as a measurable change in the MOSFET's drain-to-source current [7; 22; 26]. Measuring the gas-induced changes manifested by the degree of signal coupling via the electrical impedance establishes the basis for using the IGEFET with a chemically-active thin-film coating as a gas sensor.

*Problem Statement.* IGEFETs coated with thin-films of cobalt-phthalocyanine (CoPc), copper-phthalocyanine (CuPc), and nickel-phthalocyanine (NiPc) are known to interact with the challenge gases included in this investigation; specifically, ammonia (NH<sub>3</sub>), boron trifluoride (BF<sub>3</sub>), diisopropyl fluorophosphonate (DFP), diisopropyl methylphosphonate (DIMP), dimethyl methylphosphonate (DMMP), and nitrogen dioxide (NO<sub>2</sub>). The question to be answered is what are the dependencies of these interactions upon the polymeric thin-film material type, its thickness, the operating temperature, the relative humidity, and the challenge gas concentration. The optimal combination is defined in this context to be the set producing the best indices of sensor sensitivity, selectivity, and reversibility. The calculation of these indices is defined in the Definitions section of Chapter I.

#### *Section IV-II*

*Methodology.* This investigation began by delineating the specific physical and electrical characteristics to be measured and the parameters to be varied during the gas sensor evaluation. This portion of the investigation was carried forward by reviewing the current literature,

prior theses, and discussions with Captain Wiseman and Lt Colonel Kolesar. Using this background, the situations most likely to yield favorable IGEFET performance measurements were established as shown in Chapter I, Table I-2. The physical issues included cross-sectional photography and dimensional measurements of the IGE structure; both with and without the MPc thin-films. To further narrow the field of potential test parameters, a short series of experiments was performed to identify the appropriate bias voltages and a favorable configuration for running the *in situ* impedance matching amplifiers which served as the interdigitated gate electrodes on each IC die. Another series of tests were arranged to further limit the region of the test matrix most likely to contain the optimal combination of factors including the thin-film thickness, temperature, and the exposure and purge cycle durations. Time also permitted the pursuit of a short, third series of tests which focused on the IGEFET responses to DIMP and DMMP at 30°C, 90°C, and 150°C.

The measurements chosen to characterize the solid-state performance of the IGE structure included the direct current resistance, gain and phase angle versus frequency, ac impedance versus frequency, and the time-domain response. These measurements were made using independent instruments instead of simply computing the redundant

parameter. The test instrument configuration provided a degree of internal measurement verification. While these measurements were being established, the initial fabrication and physical characterization (dimension measurements) were accomplished.

*IGEFET Physical Measurements.* The visual inspection and microphotography of the IGE and IGEFET structures were accomplished to assess the physical characteristics of the electrodes and the physical structure that the thin-film would have when it was applied to an IGE. The acceptance criteria for the devices in this step was no observable open or short circuits in the IGE structure, and no breaks in the bond wires.

Figure IV-1 is a drawing depicting an unpackaged array of nine individual IGEFET elements. An unpackaged IGEFET array was sacrificed to facilitate taking scanning electron microscopy (SEM) photographs of its surface features. Figure IV-2 depicts an overhead view of a portion of the IGE structure. After taking these views, the IC die was broken to permit a cross-sectional perspective of the IGE structure with the SEM (Figure IV-3). Figure IV-3 depicts a cross-sectional view of a single electrode finger supported on a silicon dioxide layer. Below



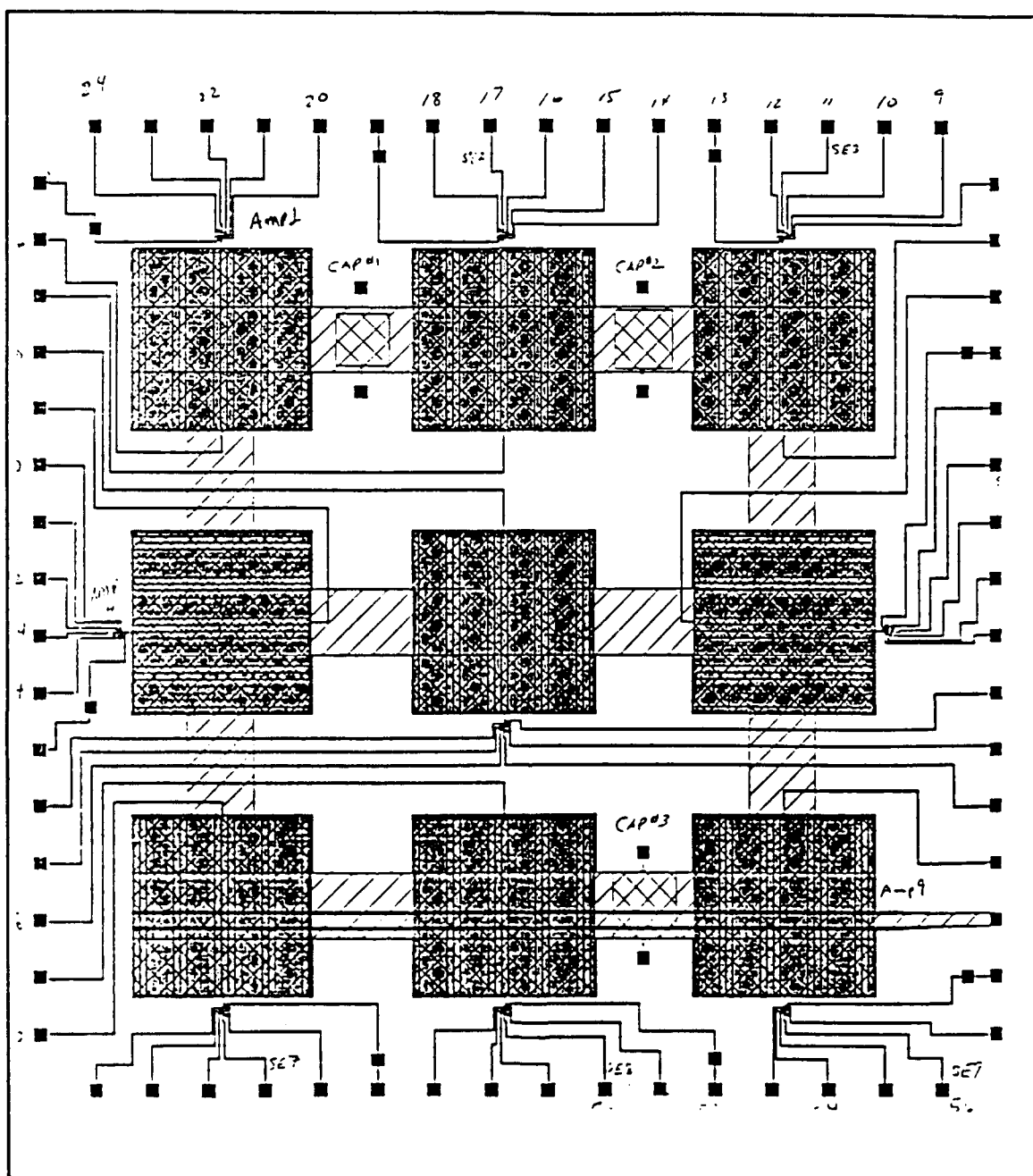


Figure IV-1. Sketch of Nine Interdigitated Gate-Electrode Structures. Their Impedance Matching Amplifiers, and Wire Bonding Pads [8].

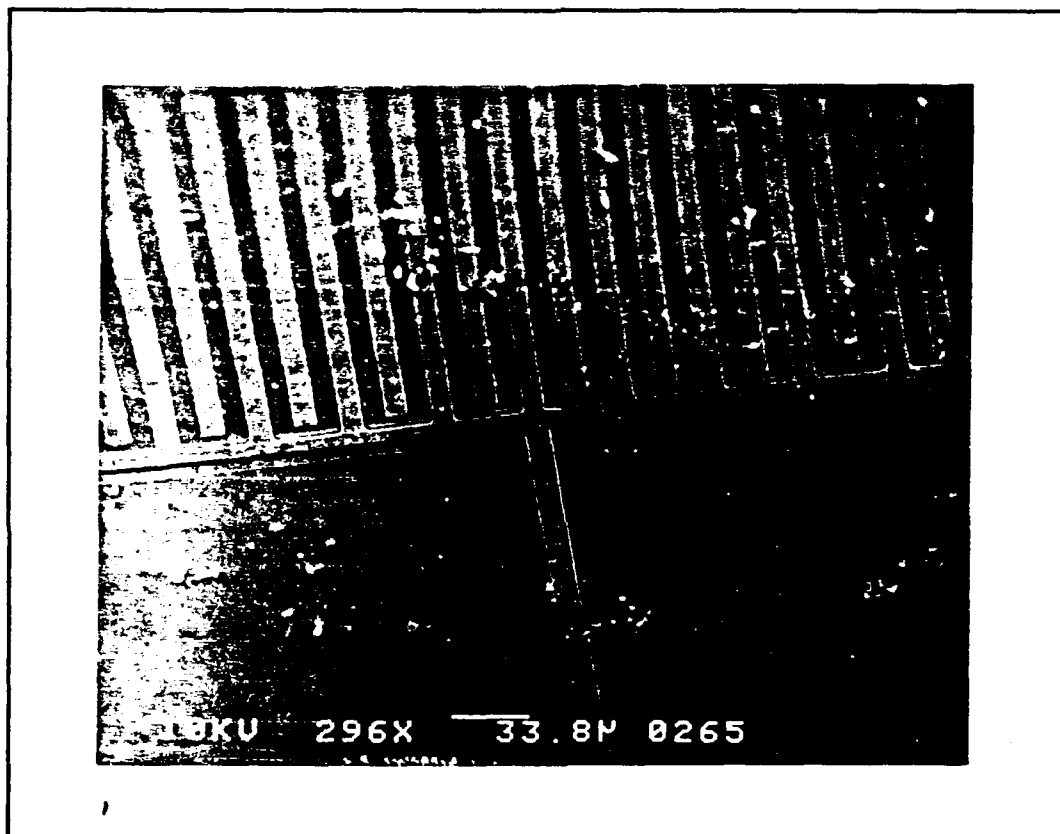


Figure IV-2. Overhead View of the IGE Structure Showing the Floating-Electrode Extending Towards the MOSFET Gate Contact. (296x magnification).

these two features is a metal ground plane which is supported by a thick silicon dioxide layer. Approximate dimensions for these layers are labeled in Figure IV-4. The MOSIS etch process used to remove the silicon dioxide from the region between the metal electrodes produced significant undercuts below the edges of the metal electrodes. The silicon dioxide layer between the electrodes was etched to a level slightly below the lower edge of the metal electrode. The deviations from the 'desired' structure were not significant enough to preclude further testing. SEM photographs were made of an IGE coated with a thin-film of CuPc (Figures IV-5 and IV-6). These figures show that the CuPc thin-film does not extend between the metal electrodes as a continuous layer. That is, air gaps exist at the fringes of the interdigitated, space-filling CuPc thin-film. This situation is depicted in Figure IV-7.

*Thin-Film Coating Deposition.* The chemically-sensitive thin-film coatings were applied to each of the nine IGE structures on each of the mounted IC die in the 64-pin DIPs. These coatings were applied using a vacuum deposition system (Denton Vacuum Corp., Model DV-602) via the process described in Appendix A. The phthalocyanine based compounds were deposited at thicknesses ranging from 1,000 Å to 30,000 Å, depending upon the objective of the associated experiment. Three

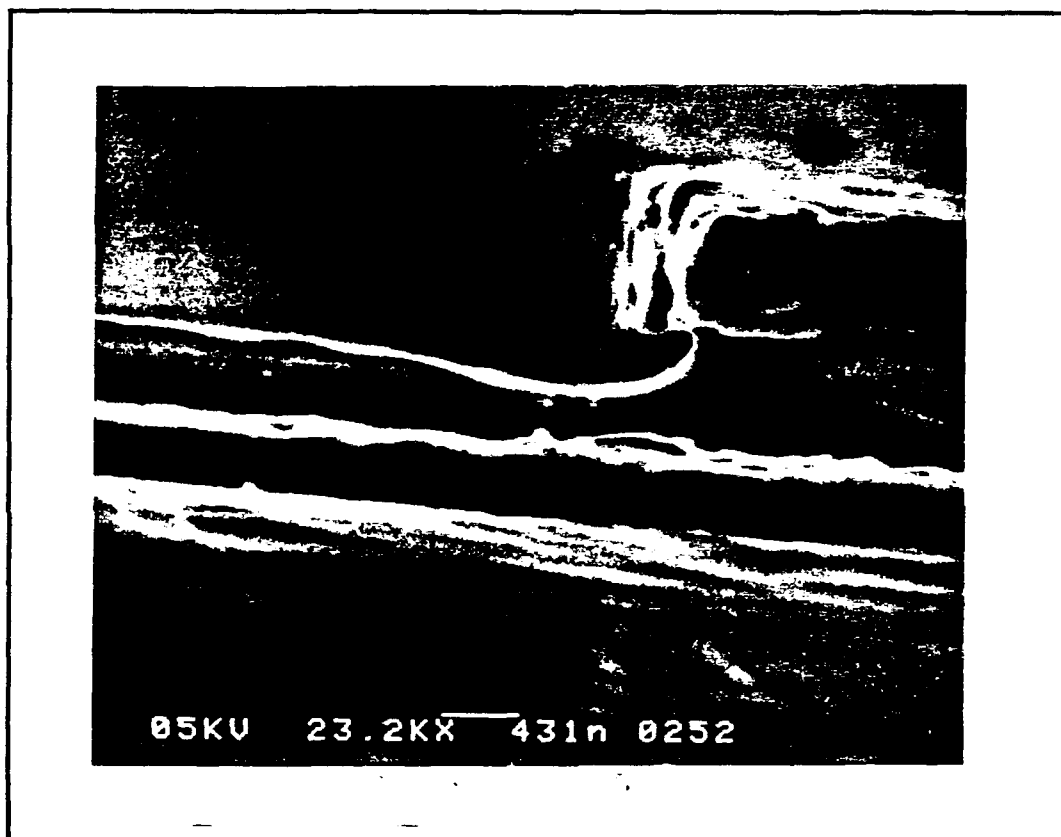


Figure IV-3. Cross-Sectional View of an IGE Finger Supported by Silicon Dioxide Showing the Undercut Below the Edge of the IGE Finger. (23,200x magnification).

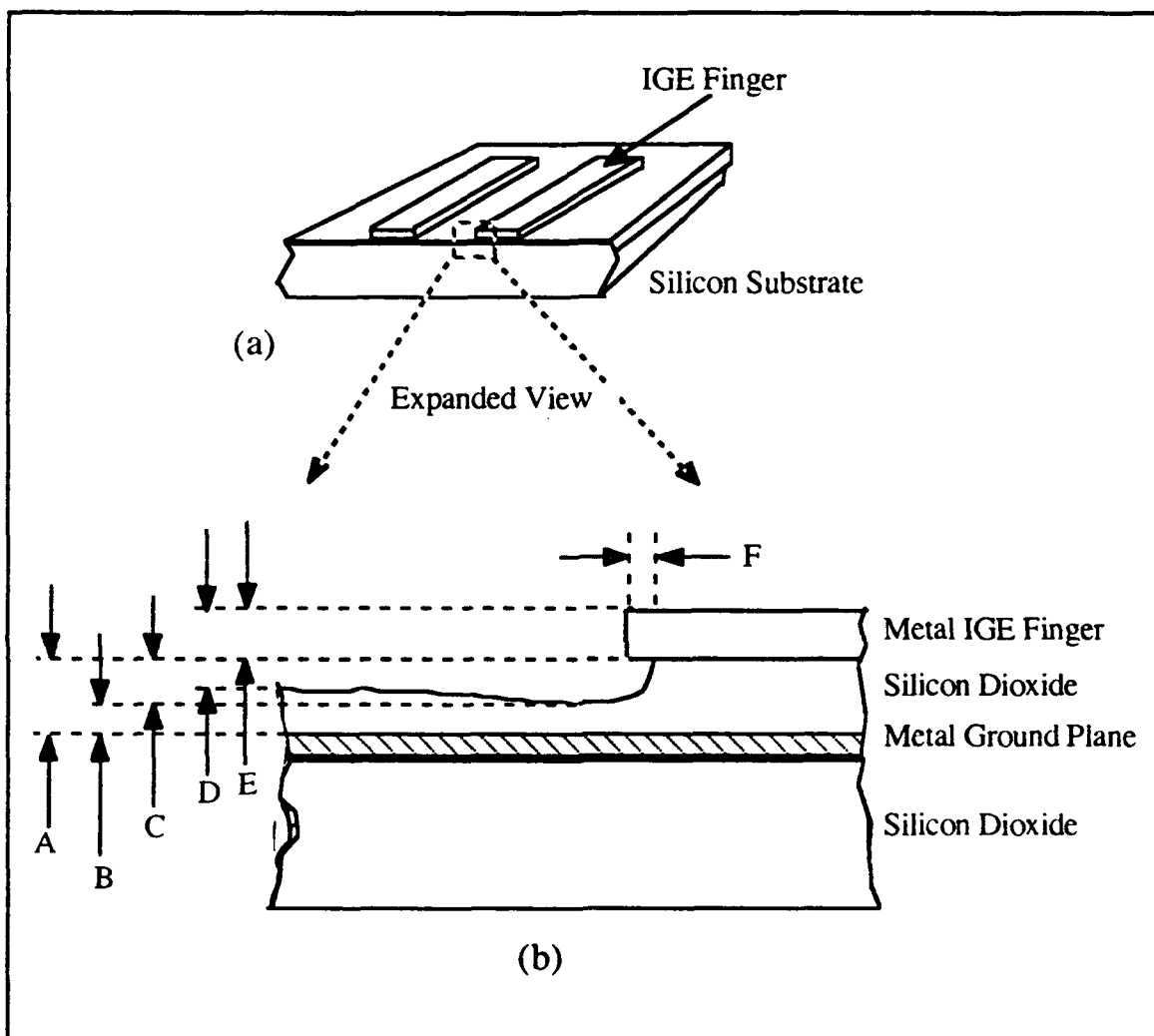


Figure IV-4. Sketch of the Photograph in Figure IV-3. Cross-Sectional View of the Etch Induced Undercut Below an IGE Finger: (a) Cross-Sectional View Orientation of (b) Undercut Structure. Approximate Measurements: A = 587 nm, B = 313 nm, C = 352 nm, D = 1097 nm, E = 789 nm, and F = 195 nm.

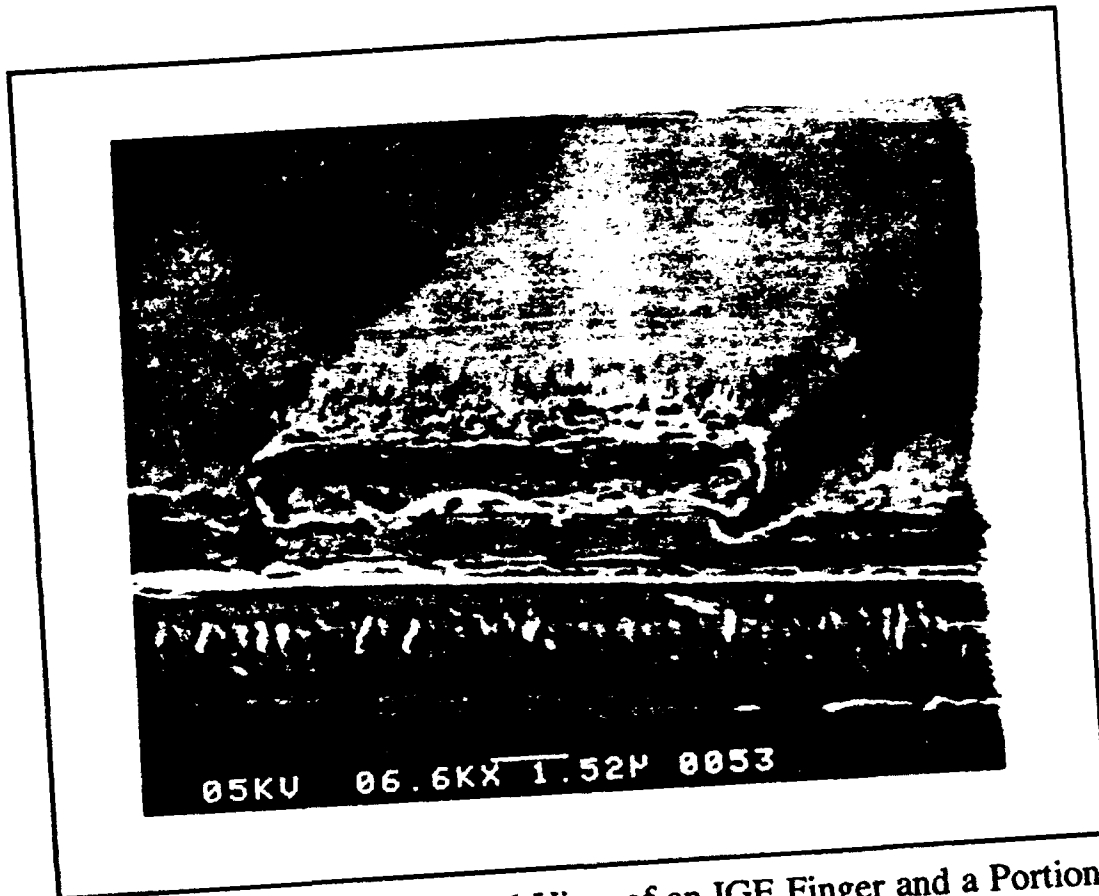


Figure IV-5. Cross-Sectional View of an IGE Finger and a Portion of the Spaces Between IGE Fingers After Vacuum Deposition of Copper-Phthalocyanine (CuPc) Thin-Film. The Discontinuity in the CuPc Thin-Film Between the Side of the Metal Finger and the Interdigital CuPc can be Observed.(6,600x magnification).

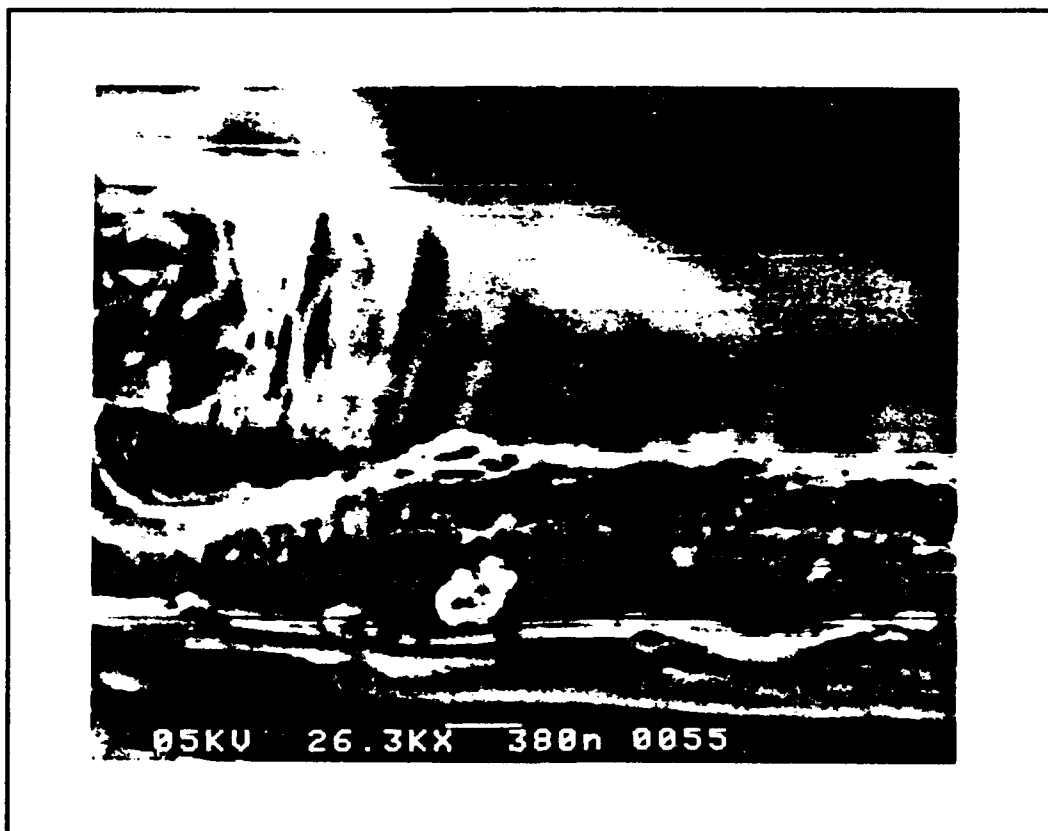


Figure IV-6. Higher Magnification of an IGE Finger's Cross-Sectional View. The Tapering of the Copper-Phthalocyanine Layer (CuPc) and Discontinuity Between the Interdigitated CuPc and the CuPc Deposited Upon the Metal Finger can be Observed(26,300x magnification).

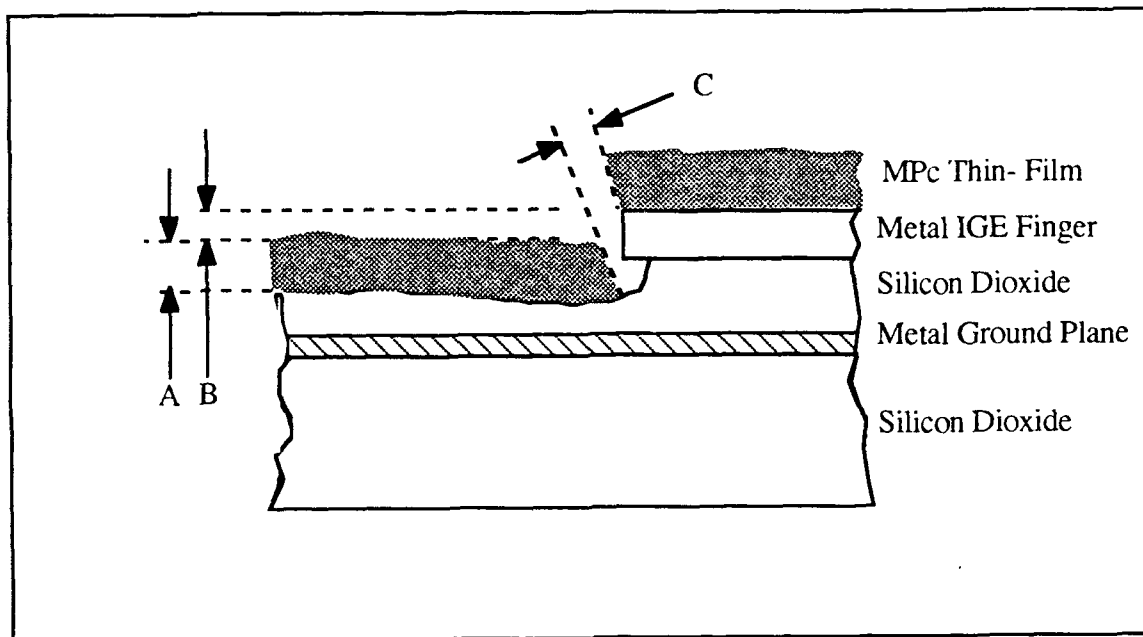


Figure IV-7. Cross-Sectional View of an IGE Finger Depicting the Gaps Present Between the Metal-Phthalocyanine (MPc) Thin-Film and the IGE Fingers with Devices Fabricated by Vacuum Deposition.

A = the Film-Thickness. B = the Vertical Distance Between Top of Thin-Film and Top of Electrode Finger. C = the Gap Between Side-wall of an Electrode Finger and the Side of the Thin-Film Deposited in the Interdigitated Space.

thicknesses (2,000 Å, 5,000 Å, and 10,000 Å) were chosen for the coatings applied to the majority of the devices used in the experimental gas exposure measurements. Information concerning the thin-film coatings applied to particular IGE structures tested is in Table IV-2.

Thickness measurements of the thin-films were made using a stylus profilometer (Sloan Technology Corp., Model Dek-Tak 900051). These



measurements were implemented on thin-films deposited onto blank silicon wafers co-located with the IGEFET DIPs while they were being coated. Prior to taking the thickness measurements, the test wafers were coated with approximately 200 Å of gold to prevent scratching the MPc coatings with the profilometer, as reported by Capt Thomas Jenkins [7:C-9]. The gold coatings were applied with a sputter coating device (Structure Probe Inc., Model 13131). The film thicknesses provided by the profilometer were averaged to arrive at the thicknesses listed in Table IV-1.

*Testing the Device Impedance Matching Amplifier, Feedback Configurations, and Bias Voltages.* Figure IV-8 shows the circuit diagram for the basic IGEFET device; it is composed of the IGE and its associated impedance matching amplifier.

The basic performance of the *in situ* impedance matching amplifier was evaluated to determine a set of voltage levels for the supply sources, the inverting input gate configuration, and the bias current limiter.

Table IV-1.

Summary Listing of Conditions used During Experimentation  
(Continued on Next Page).

CuPc Films					
Experiment Number	3 and 5	6 and 7	4	8	9
Film Thickness (Angstroms)	6000	6000	2000	1600	1600
	12000	12000	50000	3900	3900
	30000	30000	60000	8800	8800
Temperature (°C)	90	90	90	90	30/90 *
Carrier Gas	Room Air	N2	Room Air	N2	N2
Challenge Gas	NO2	NO2	NO2	NO2	NO2
Gas Concentrations (ppb)	100	100	20	100	100
			50		
			100		
			500		
			1000		
Time-Domain Signal	50 Hz Sq	50 Hz Sq	50 Hz Sq	50 Hz Sq	50 Hz Sq
CuPc Films					
Experiment Number	10	11	12	13	14
Film Thickness (Angstroms)	1600	1600	1600	1600	2400
	3900	3900	3900	3900	27000
	8800	8800	8800	8800	56000
Temperature (°C)	90/120 **	120	120	120	120
Carrier Gas	N2	N2	N2	Room Air	N2
Challenge Gas	NO2	NO2	Room Air	NO2	NO2
Gas Concentrations (ppb)	100	100	@ 100 %	100 ppb	100 ppb
Time-Domain Signal	50 Hz Sq	50 Hz Sq	50 Hz Sq	50 Hz Sq	50 Hz Sq
* = Challenged at 30°C, Purged at 90 °C.					
** = Challenged at 90°C, Purged at 120 °C.					

Table IV-1.

Summary Listing of Conditions used During Experimentation  
(Continued on Next Page).

CuPc Films					
Experiment Number	15	16	17	18 and 24	21
Film Thickness (Angstroms)	2400	1600 (B-phase	2000	2000	1600
	27000	3900 (B-phase	10000	5200	3900
	56000	8800 (B-phase	14800	9900	8800
Temperature (°C)	150	150	150	150	150
Carrier Gas	Room Air	Room Air	Room Air	Room Air	Room Air
Challenge Gas	NO <sub>2</sub>	NO <sub>2</sub>	NO <sub>2</sub>	DMMP	NO <sub>2</sub>
Gas Concentrations (ppb)	100 ppb	100	30	200	1000 ***
			50	400	30
			100	800	50
			500	1600	100
			1000	3200	500
					1000
Time-Domain Signal	50 Hz Sq	50 Hz Sq	50 Hz Sq	50 Hz Sq	50 Hz Sq
CuPc Films					
Experiment Number	27	31	34	35	
Film Thickness (Angstroms)	2100	2100	3200	3200	
	8200	8200			
	16000	16000			
Temperature (°C)	150	150	150	150	
Carrier Gas	Room Air	Room Air	Room Air	Room Air	
Challenge Gas	NH <sub>3</sub>	BF <sub>3</sub>	DMMP	DIMP	
Gas Concentrations (ppb) unless otherwise noted	500 ppm ***	105 ppm	10 ppm	3 ppm	
	16 ppm	24 ppm			
	106 ppm	105 ppm			
	250 ppm				
	500 ppm				
Time-Domain Signal	50 Hz Sq	50 Hz Sq	50 Hz Sq	50 Hz Sq	

\*\*\* = Preconditioning Exposure for 1.25 Hours.

Table IV-1.

Summary Listing of Conditions used During Experimentation  
(Continued on Next Page).

CuPc Films		
Experiment Number	37	38
Film Thickness (Angstroms)	3200	3200
Temperature (°C)	150/90/30	150/90/30
Carrier Gas	Room Air	Room Air
Challenge Gas	DMMP	DIMP
Gas Concentrations (ppb) unless otherwise noted	10 ppm	3 ppm
Time-Domain Signal	50 Hz Sq	50 Hz Sq
*** = Preconditioning Exposure for 1.25 Hours.		

Table IV-1.

Summary Listing of Conditions used During Experimentation  
(Continued on Next Page).

CoPc Films					
Experiment Number	19	20	26	28	34
Film Thickness (Angstroms)	2500	2500	2500	2500	5200
	5400	5400	5400	5400	
	10500	10500	10500	10500	
Temperature (°C)	150	150	150	150	150
Carrier Gas	Room Air	Room Air	Room Air	Room Air	Room Air
Challenge Gas	NO <sub>2</sub>	NO <sub>2</sub>	BF <sub>3</sub>	NH <sub>3</sub>	DMMP
Gas Concentrations (ppb)	30	1000 ***	24 ppm	500 ppm ***	10 ppm
	50	30	48 ppm	16 ppm	
	100	50		106 ppm	
	500	100		250 ppm	
	1000	500		500 ppm	
		1000			
Time-Domain Signal	50 Hz Sq	50 Hz Sq	50 Hz Sq	50 Hz Sq	50 Hz Sq
CoPc Films					
Experiment Number	34	37	38		
Film Thickness (Angstroms)	5200	5200	5200		
Temperature (°C)	150	150/90/30	150/90/30		
Carrier Gas	Room Air	Room Air	Room Air		
Challenge Gas	DIMP	DMMP	DIMP		
Gas Concentrations (ppb)	3 ppm	10 ppm	3 ppm		
Time-Domain Signal	50 Hz Sq	50 Hz Sq	50 Hz Sq		
*** = Preconditioning Exposure for 1.25 Hours.					

Table IV-1.

Summary Listing of Conditions used During Experimentation  
(Continued from Previous Page).

NiPc Films					
Experiment Number	22	23	25	29,32 and 33	30
Film Thickness (Angstroms)	2600	2600	2600	2600	2600
	6200	6200	6200	6200	6200
	12500	12500	12500	12500	12500
Temperature (°C)	150	150	150	150	150
Carrier Gas	Room Air	Room Air	Room Air	Room Air	Room Air
Challenge Gas	NO <sub>2</sub>	DMMP	DFP	NH <sub>3</sub>	BF <sub>3</sub>
Gas Concentrations (ppb) unless otherwise noted	1000 ***	3200 ***	1000	500 ppm ***	24 ppm
	30	200		16 ppm	105 ppm
	50	400		106 ppm	
	100	800		250 ppm	
	500	1600		500 ppm	
	1000	3200			
Time-Domain Signal	50 Hz Sq	50 Hz Sq	50 Hz Sq	50 Hz Sq	50 Hz Sq
NiPc Films					
Experiment Number	34	35	37	38	
Film Thickness (Angstroms)	6800	6800	6800	6800	
Temperature (°C)	150	150	150/90/30	150/90/30	
Carrier Gas	Room Air	Room Air	Room Air	Room Air	
Challenge Gas	DMMP	DIMP	DMMP	DIMP	
Gas Concentrations (ppb) unless otherwise noted	10 ppm	3 ppm	10 ppm	3 ppm	
Time-Domain Signal	50 Hz Sq	50 Hz Sq	50 Hz Sq	50 Hz Sq	
*** = Preconditioning Exposure for 1.25 Hours.					

The intent was to use these voltages throughout the remainder of the challenge gas test matrix.

The first evaluation (determination of  $V_{bias}$  for operation) was conducted to determine a favorable value for  $V_{bias}$  and to check the gain/bandwidth of the MOSFET amplifier. A non-inverting input configuration was chosen. Using the circuit shown in Figure IV-9, the  $V_{bias}$  level was varied by adjusting the potentiometer (P1) until  $V_{out}$  was zero volts with no input signal. The supply voltages for the IGEFET amplifiers,  $V_{dd}$  and  $V_{ss}$ , were chosen to be + 5 volts and - 5 volts, respectively. The  $V_{out}$  offset was minimized with a  $V_{bias} = -2.88$  volts measured with a VOM (B&K Precision Test Bench, Model 388-HD). A basic feedback configuration was tested using the circuit shown in Figure IV-9. The input sinusoidal test voltage was applied directly to the floating-gate (FG) using a signal generator (Wavetek Corp., Model 186). The voltage at the metal-oxide-semiconductor field-effect transistor (MOSFET) differential amplifier output was measured with an oscilloscope (B&K Instruments, Model 1570A).

The gain/bandwidth data was intended to verify the gain stability of

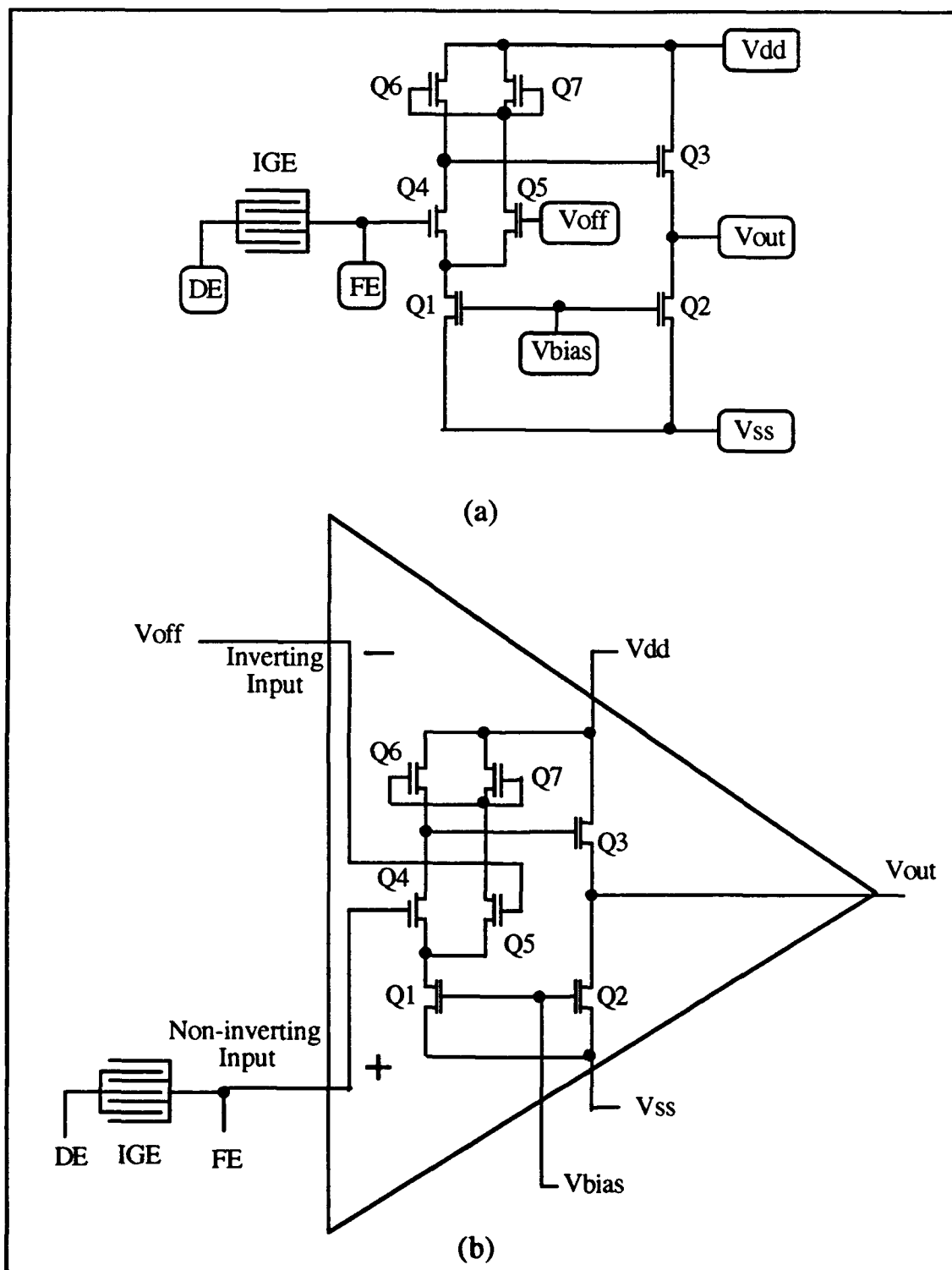


Figure IV-8. Interdigitated Gate Electrode (IGE) and Impedance Matching FET Amplifier: (a) Equivalent Circuit Diagram, and (b) Equivalent Amplifier. (DE = Driven-Electrode, FE = Floating-Electrode).



the MOSFET amplifier when used in the non-inverting feedback mode.

The second experiment was designed to investigate the amount of dc voltage drift that could be tolerated on the floating-electrode before the output voltage of the MOSFET operational amplifier would saturate.

Since there is no convenient method for removing the dc voltage from the floating-electrode while the device is being exposed to challenge gases, any large drift might limit the dynamic range of the IGEFET system. Figure IV-10 shows the circuit used to investigate the possible effects of large voltage drift on the floating-electrode with respect to the dynamic range of the IGEFET system with the amplifier configured as a voltage-follower. This voltage-follower displayed a uniform gain versus frequency response. The circuit is similar to ones depicted by Hufault [6:88-89].

Amplifier A1 in Figure IV-10 is configured as a summing amplifier. It sums the  $V_{dc}$  and  $V_{ac}$  inputs at the inverting input through resistors R1 and R2. Resistor R3 provides a feedback path to establish the inverted gain of amplifier A1, which is set near zero dB. The impedance matching amplifier A2 was configured as a voltage follower because it was a straightforward configuration to implement with the current IGEFET integrated circuit. The 10 kohm resistor (R4) provided a uniform load

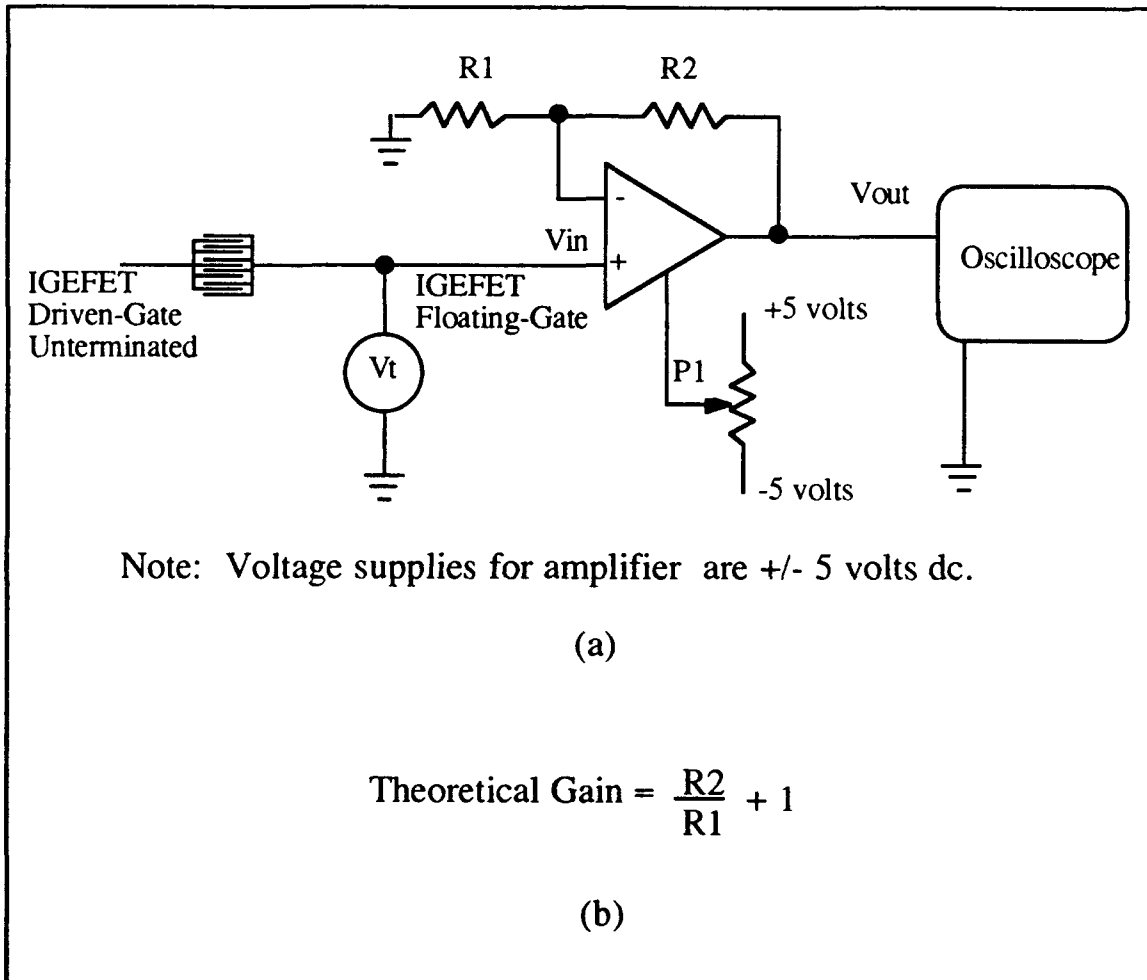


Figure IV-9. Operational Amplifier Performance Evaluation: (a) Circuit for Checking the Gain, Bandwidth and  $V_{bias}$  Level, and (b) Calculation of Theoretical Gain.

for amplifier A2 while it was connected to the high impedance input of the dual-channel oscilloscope (B&K Instruments, Model 1570A). The signal generator for  $V_{ac}$  (Wavetek Corp., Model 186) provided a sine wave that was manually swept through selected frequencies ranging from 10 Hz to 5 MHz. The signal generator for  $V_{dc}$  (Hewlett-Packard, Model-6236B) provided a dc voltage level that was set at the following voltage levels: -3.80, -3.03, -1.00, 0 , +1.00, +2.00, and +3.80 volts. In addition,  $V_{bias}$  for amplifier A2 was set at -2.87 volts dc as measured with a voltmeter (B&K Instruments, Model 388-HD).

The dc voltage,  $V_{dc}$ , was set at one of the selected levels while the frequency of the ac signal was varied. The outputs of the summing amplifier A1 and the voltage follower amplifier A2 were ac coupled to the oscilloscope inputs. These output voltages were recorded and compared at each frequency of interest.

The dc resistance measurements across the IGE's driven- and floating-electrodes were performed using the procedure recommended by the electrometer manufacturer (Keithley Instruments, Inc., Model 617) [10]. In particular, the electrometer was used in the voltage/ampere (V/I) mode. This operational mode permits the

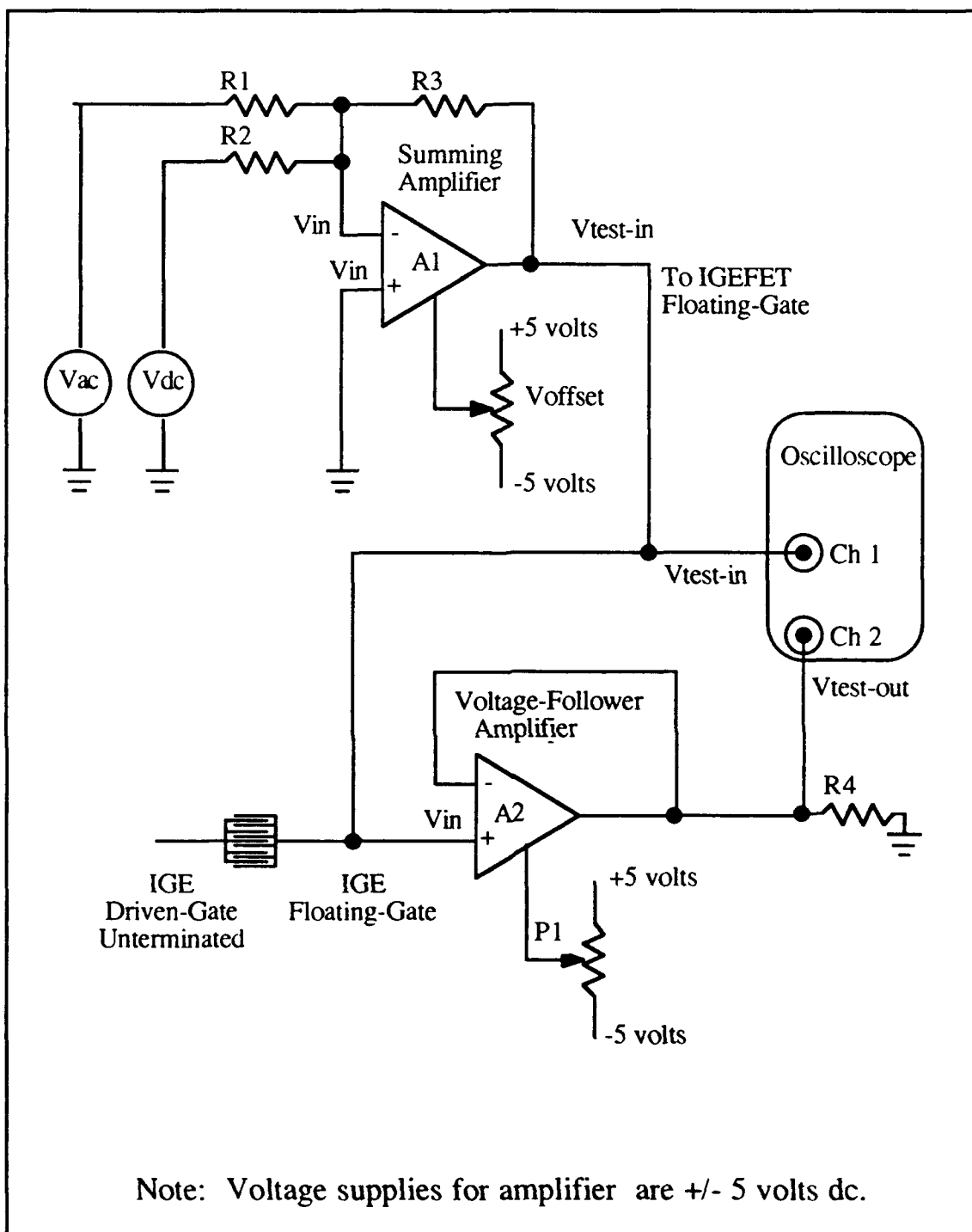


Figure IV-10. Test Circuit for Establishing the Effects of dc Bias on Floating-Gate Upon the Gain and Bandwidth of IGEFET Impedance Matching Amplifier with the Voltage-Follower Configuration:  $R1 = 10.22 \text{ kohm}$ ,  $R2 = 10.26 \text{ kohm}$ ,  $R3 = 10.25 \text{ kohm}$ ,  $R4 = 10.19 \text{ kohm}$ ,  $A1 = 1/2 \text{ UA747CN}$ , and  $A2 = \text{IGE FET Impedance Matching Amplifier}$ .

measurement of resistances on the order of  $10^{16}$  ohms [10:2-19]. Using this mode minimizes the effects of the leakage resistances and distributed capacitance [ 10:2-19, 26:4-30]. When operated in this mode, the electrometer uses a bias voltage to drive a current through the device under test (DUT). For this investigation, the level of bias voltage was selected to be in a region where the DUT would be expected to behave in a linear fashion. The dc bias voltage used in conjunction with the electrometer for the dc resistance measurements across the interdigitated floating- and driven-electrodes was established by reviewing the previous research accomplished by Jenkins [7:5-13,15], Shin [22:IV-7] and Hamann [5:77]. This bias level is a 'best pick' choice for attaining a region of voltage versus resistance which closely approximates linearity for the CuPc, CoPc, and NiPc materials.

#### *Computer Controlled Data Gathering Using the GPIB*

*Interconnected Instrumentation.* One of the prime objectives of this thesis was to collect data from five instruments, on a minute-by-minute basis, for periods of time extending exceeding one day in duration. A reasonable method of accomplishing this objective was to utilize the General Purpose Instrumentation Bus (GPIB) available on all of the primary measuring instruments. The GPIB bus was controlled with a

Zenith 248 personal computer equipped with a GPIB interface card (Capital Equipment, Model PC<>488).

The general layout of the GPIB controller, instrumentation, and the devices under test are depicted in Figure IV-11. Detailed signal flow and wiring diagrams are available in Appendix I. The software to control the GPIB instrumentation was originally written in BASIC, and then translated into PASCAL. The PASCAL package was modified as changes arose in the requirements for the software's performance.

The software performed several functions while controlling the GPIB system shown in Figure IV-11. The software reset, initialized, and triggered the instrumentation, and then stored the data on magnetic media. Simultaneously, the software sequenced the opening and closure of the signal line switching relays which routed the signal line pathways from the instrumentation to each of the nine IGEFET microsensors in chamber #1 and chamber #2, so that measurements could be made on all the elements of both of the microsensor arrays in rapid succession.

Each test chamber contained a single, 64-pin DIP which held a single IC fabricated with nine individual IGEFET systems. Each IGEFET system was composed of an interdigitated gate electrode (IGE) and an impedance matching amplifier with one input (a MOSFET gate)

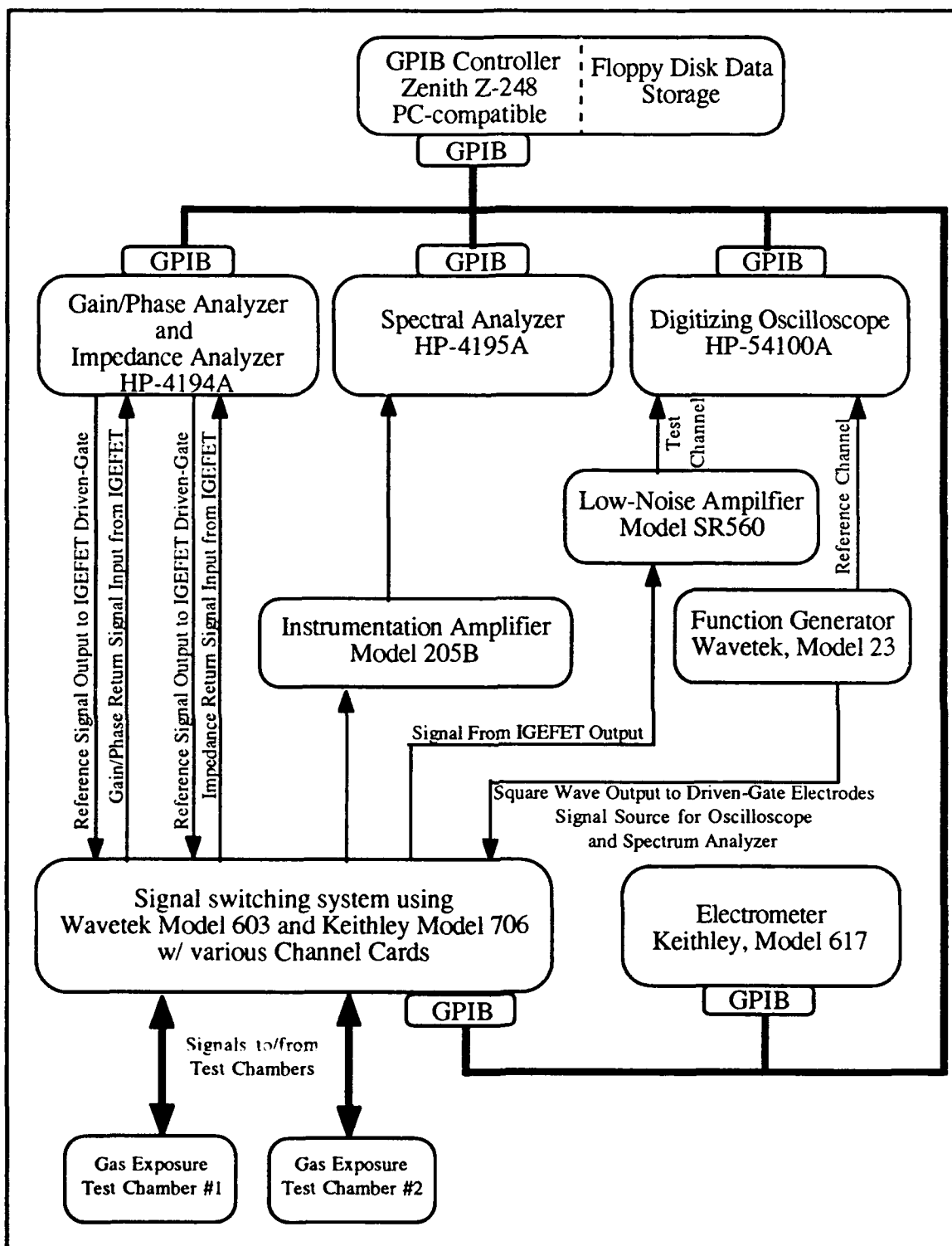


**Figure IV-11. Instrumentation and GPIB System Architecture.**

connected to the floating-electrode. The IGEFET DIP in test chamber #1 was used to study the IGE structure's dc resistance and impedance values. The IGEFET DIP in test chamber #2 was used to study the IGEFET system's response, including the overall system's gain/phase, time- and frequency-domain response to 50 Hz square waves at 2 volts peak-to-peak.

Two relay scanner frames (Wavetek Corp., Model 603, and Keithley Instruments Inc., Model 706) formed the switching matrix providing signal paths between the instruments and the integrated circuits.

In test chamber #1, either dc resistance measurements or impedance measurements were collected, but not simultaneously. That is, when in the dc resistance mode, a measurement (Keithley Instruments Inc., Model 617) was taken every 20 to 30 seconds on one of the IGE structures. This meant that each individual array element was assayed approximately every 4 minutes. Figure IV-12 depicts the test wiring diagram for the dc resistance measurements across the IGE. When this chamber was used in the impedance mode (Hewlett-Packard Co., Model HP-4194A), measurements were taken on each individual array element approximately every 15 minutes.

In test chamber #2, three individual IGEFET systems were always



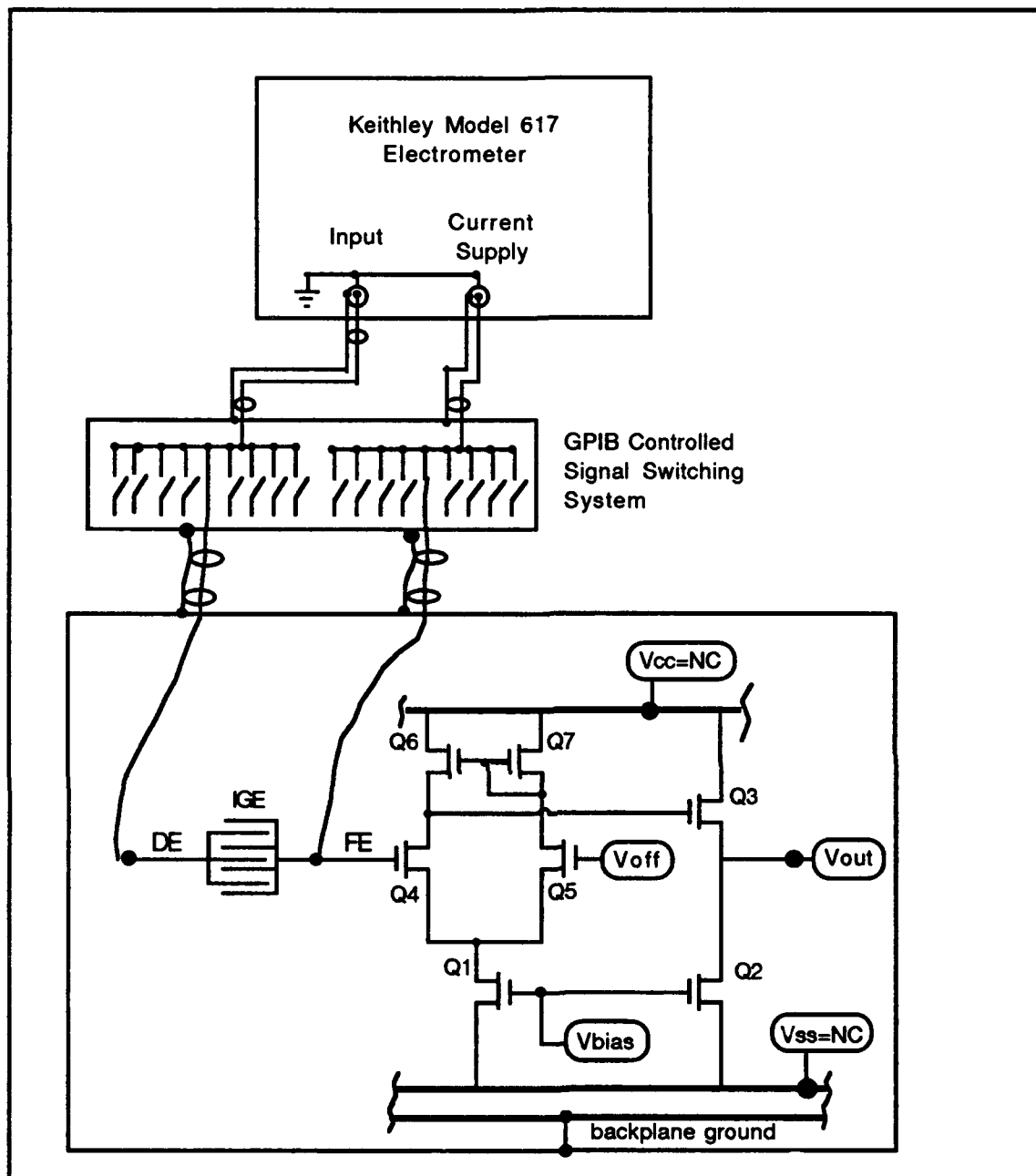


Figure IV-12. DC Resistance Measurements. (DE = Driven-Electrode, FE = Floating-Electrode, Voff, Vcc, Vss, Vbias, and Vout are Not Connected (NC)).

being measured at any one time. While the gain/phase response of one IGEFET system was being measured (Hewlett-Packard Co., Model HP-4194A), the spectrum response of a second IGEFET system was being gathered (Hewlett-Packard Co., Model 4195A), and the time-domain response of a third IGEFET system was being collected (Hewlett-Packard Co., Model HP-54100A). The function generator (Wavetek Corp., Model 23) provided a 50 Hz, 50 % duty cycle square wave with a 2 volt<sub>pk-to-pk</sub> signal amplitude which served to excite the microsensor's driven-electrode. Figure IV-13 depicts the gain and phase angle measurement scheme for the IGE's impedance matching differential amplifier system response. Figure IV-14 depicts the gain-phase measurement scheme for accomplishing the response measurements for the impedance amplifier only.

The impedance matching amplifiers in the IGEFET systems were configured as voltage followers (unity-gain). The low-noise amplifier (Stanford Research Systems, Model SR560) was used with unity gain and a -3 dB rolloff at 1 MHz to provide optimal ac coupling to the oscilloscope.

The output of the impedance matching amplifiers of the IGEFET systems were ac coupled through an amplifier (Trig-Tek Instrumentation, Model 205B) before being passed to the spectrum analyzer.

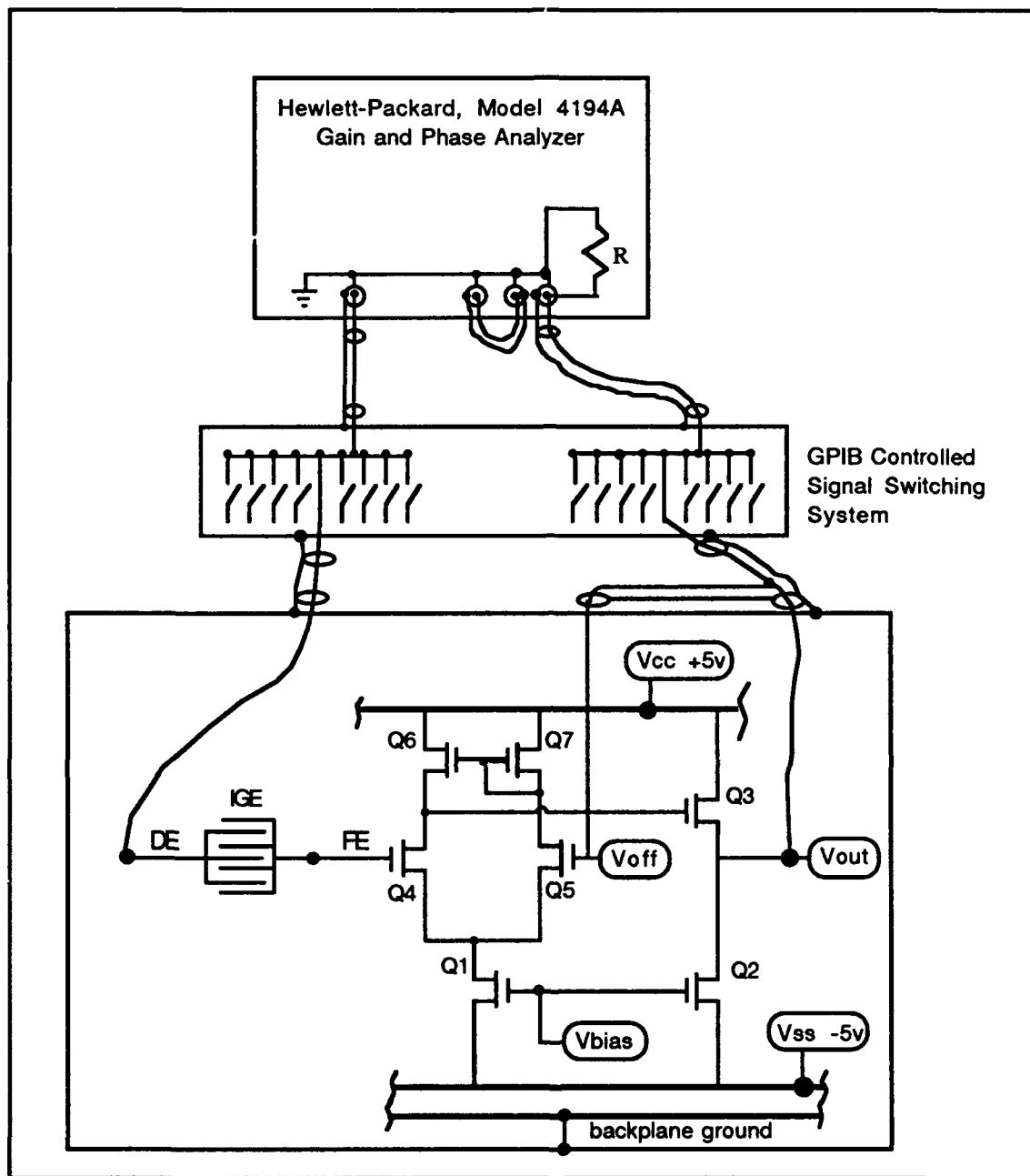


Figure IV-13. IGEFET System Gain and Phase Angle Response Measurements. (The Floating-Electrode (FE) Bond Wire is Disconnected During Testing. DE = Driven-Electrode. IGE = Interdigitated Gate Electrode. The Amplifier is Formed by Q1 through Q7. R = 10 kohm).

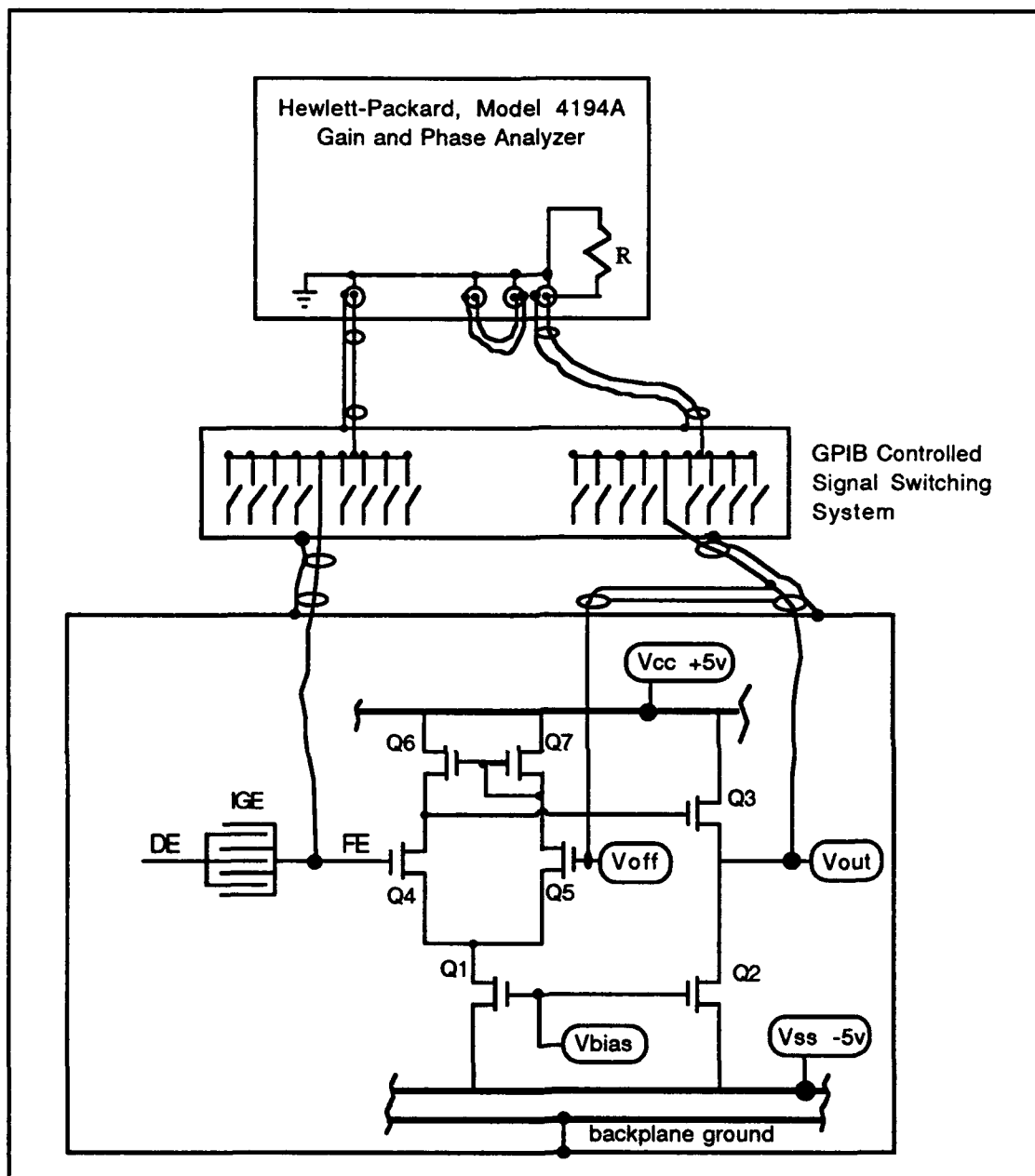


Figure IV-14. Gain and Phase Angle Characterization of the MOSFET Impedance Matching Amplifier. (DE = Driven-Electrode, FE = Floating-Electrode, IGE = Interdigitated Gate Electrode, Q1 through Q7 Form the Amplifier, R = 10 kohms).

A 64-pin DIP header was constructed with known resistor values soldered between the pins that matched the floating-gate and driven-gate pairs on the IGEFET DIP. A similar header was constructed with known resistor values soldered between the pins that matched the driven-gate and impedance matching amplifier pairs on the IGEFET DIP. These headers were used during the test and development of the software and hardware reflected in the Figure IV-11 architecture. The resistor header values were measured by the various instruments and recorded on a floppy disk for storage. The values recorded were checked against those actually in the headers. The software/hardware was cycled relative to known checkpoints to verify the proper opening and closing of the signal switching relays.

To check the overall bandpass and attenuation of the signal switching system, a 20-dB attenuation standard (Pomona Electronics, 4108-20 dB, 50 ohms) was inserted at test cabinet #2, between the input/output cable pair that would normally be connected to the driven-electrode and impedance matching amplifier's output for IGEFET array #1. The measured attenuation was -19.9 dB.

*Test Chamber Fabrication.* The test chambers and test-lead cabinets used for the gas exposure experiments were designed and built at AFTT.

These chambers were modified by replacing the original zero-insertion-force sockets (ZIFs) with more robust versions capable of withstanding temperatures up to 200°C (3M Corporation, Textool PNs 264-4493-39-240 and 264-4493-00-2422).

The test chamber is a rectangular box with all but the bottom made of stainless steel. The bottom of the box is a printed circuit board with a 64-pin ZIF receptacle mounted upon it. In addition, leads for the dc power supply for the internal heater strip and leads for a thermocouple entered the test chamber through the printed circuit board. All of the openings were sealed with a flexible, high-temperature adhesive. The internal heater strip was sandwiched between the ZIFs and the 64-pin DIP during testing to establish and control the temperature of the DIP. The DIP's surface temperature was measured with a thermocouple attached to the top of the DIP.

The test chamber was mounted on an aluminum cabinet. Individual 50-ohm coaxial test leads were connected to each of the 64 pins of the ZIF, and they pass directly from the bottom of the test chamber into the interior of the aluminum cabinet. The cable shields are tied together and terminated on the body of the test cabinet. The test lead center conductors are terminated on BNC bulkhead connectors mounted on the

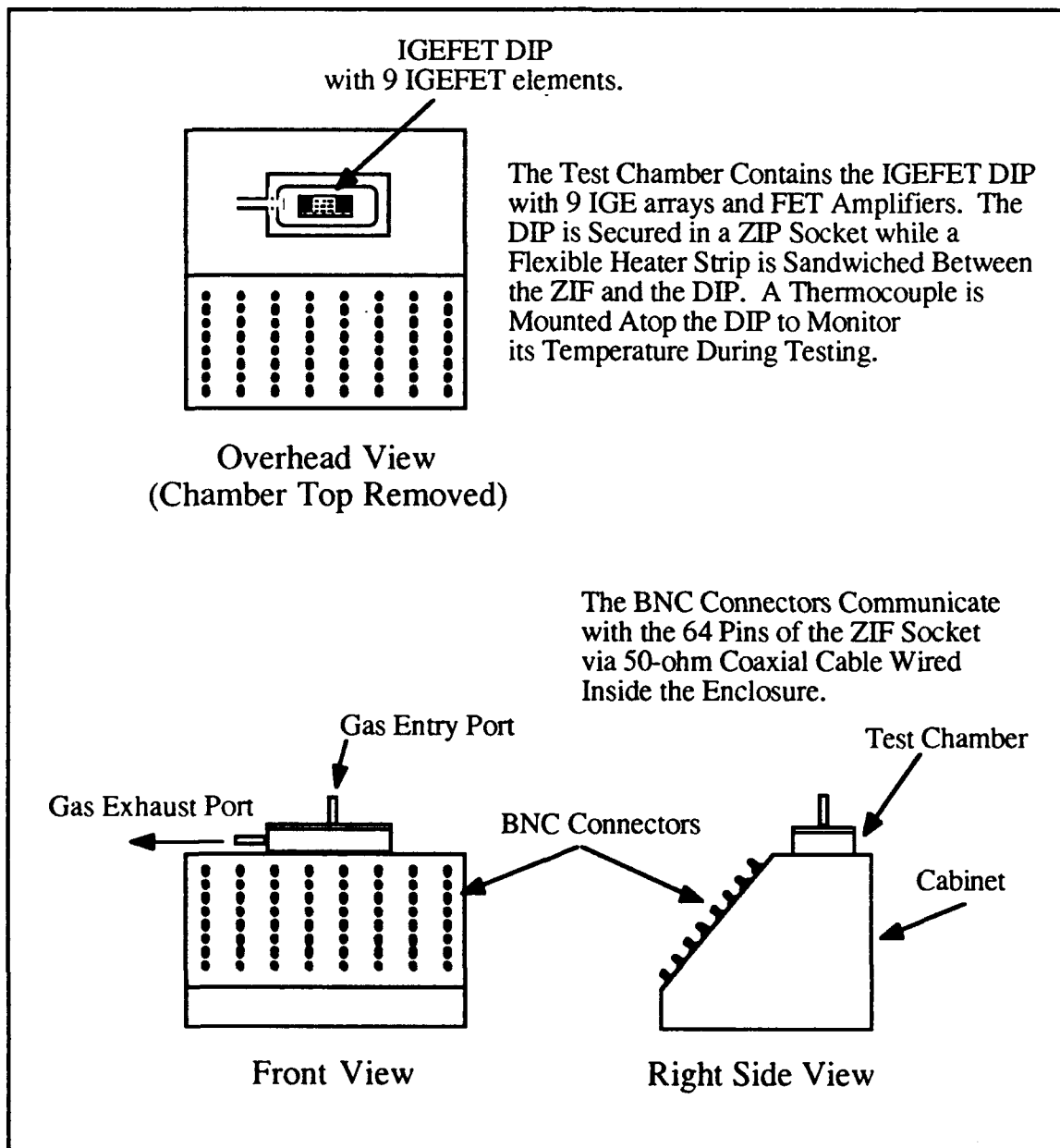


Figure IV-15. Test Cabinet and Test Chamber.

front panel of the aluminum cabinet. During the test measurements, the cabinet and the interior shields were tied to the signal path grounds which isolated them from the power supply ground paths.

*Gas Delivery System.* The gas delivery system controlled the concentrations and volume flow rates of the carrier (purge and diluent functions) and challenge gases. These gases are delivered to the test chambers, as depicted in Figure IV-16.

The carrier gases used in the experiments were either dehumidified room air or pure N<sub>2</sub>. The room air was dehumidified using a desiccant vessel, and then passed through an activated charcoal filter to remove organic contaminants. This process was monitored with a hygrometer.

The gas generation system provided flow control of the carrier and challenge gases. Provision was made to mix these gases prior to their entry into the test chamber.

The test gases were generated from gas permeation tubes (G-Cal Permeation Devices, GC Industries, Chatsworth, California) containing the particular gas molecules of interest. The permeation tubes release the gas of interest at a predetermined rate which depends upon the tube's temperature while it is situated in a heating bath (NesLab, Model RTE-8DD). The actual concentration of the challenge gas generated is then



established by controlling the volume flow of the carrier gas across the throat of the tube. The flow rate of all the gases entering the test chamber was controlled by using calibrated glass-bead flow meters (Gilmont Instruments, Inc., Great Neck, New York). With the exception of the glass walls and teflon fittings of the flow meters, the gas pathways were stainless-steel tubing.

*Experiments Designed to Limit the Range of Variables (Series I).* A series of experiments (Series I) was conducted with the purpose of establishing coarse boundaries on the ranges of five experimental variables. One variable was the temperature to be used for the gas exposures. Another variable was the range of film-thicknesses expected to bracket a 'best' thickness at a fixed exposure temperature. The third was the choice of carrier and purge gas. The fourth variable was the length of time the thin-films would be exposed to the challenge gases. The fifth was the length of any 'preconditioning' or 'curing' exposure associated with the challenge gases.

This series of experiments was conducted using the GPIB system shown in Figure IV-11. The gas delivery system is depicted in Figure IV-16. Details of the experimental results are presented in Chapter V.

Based upon the preliminary test data conducted to evaluate the

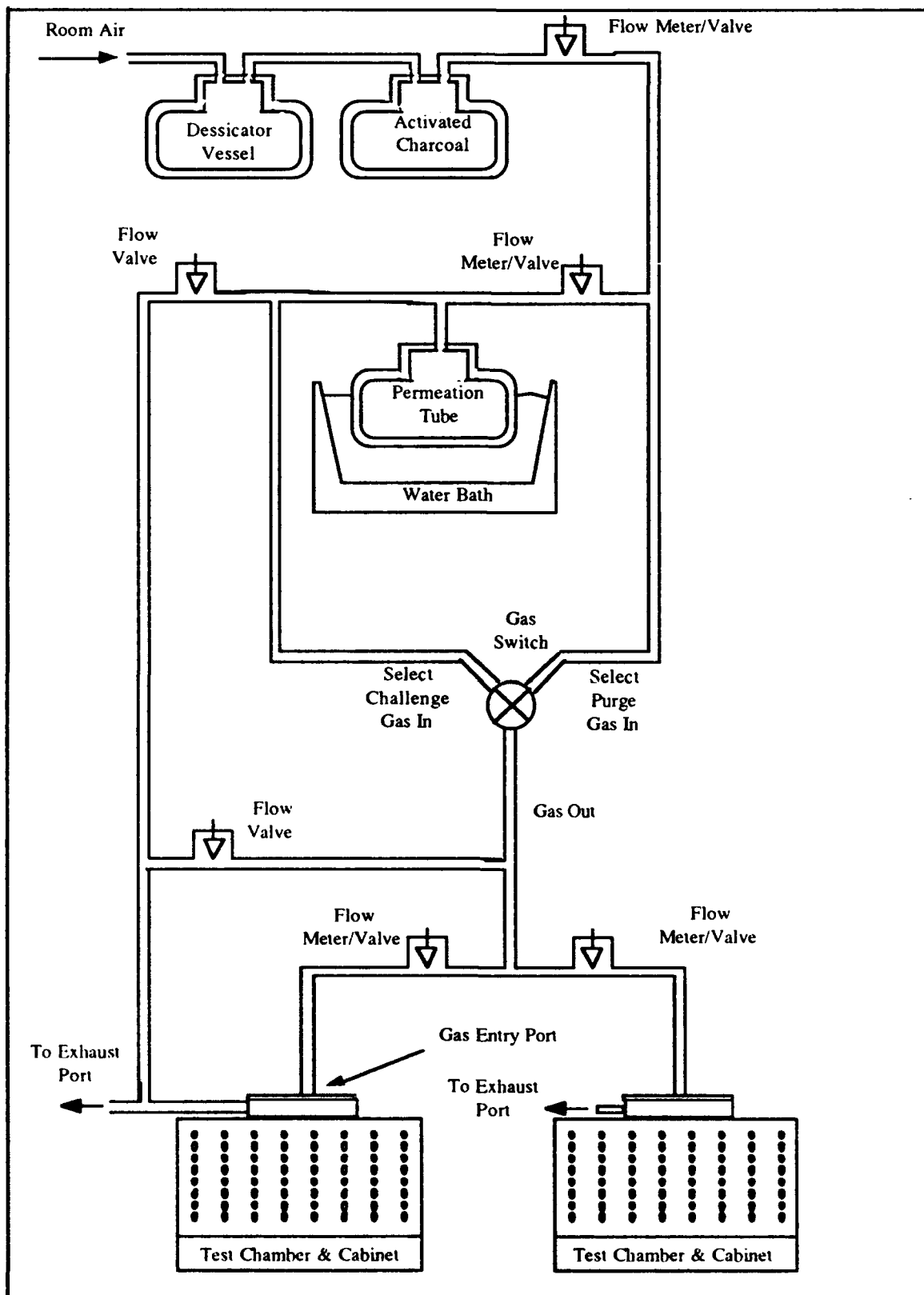


Figure IV-16. Gas Generation System.

IGFET operational amplifier's bandwidth and gain as the dc level on the floating-electrode was varied from +3.8 to -3.8 volts dc, the basic operational configuration for the gain/phase, spectral and pulse measurements were conducted with the MOSFET amplifiers operated as unity-gain devices with a bias voltage at 0 volts dc. This configuration manifested good stability and bandwidth.

The Series I experiments were conducted with the IGFETs coated with CuPc thin-films of various thicknesses and NO<sub>2</sub> as the challenge gas. This combination was selected because previous investigators [7, 26] reported achieving reproducible responses relative to the challenge gas concentrations that could be produced with the gas generation system.

Using the CuPc thin-films and the NO<sub>2</sub> challenge gas as a routine parameter pair, the effects of temperature were investigated. Identifying a single operational temperature for the exposure and purge cycles was of primary interest. The goal was to establish a temperature which manifested acceptable sensitivity and reversibility in a time frame less than 60 minutes. The upper limit of the temperatures investigated was bounded by the components used in the construction of the test chamber; a maximum excursion of 200°C. Thus, a series of gas exposure and purge responses at 30°C, 90°C, 120°C, and 150°C were investigated. One test

was accomplished at 30°C for the entire test, with the exception of a one-hour long trial at 90°C during the post-exposure purge cycle. Another test trial was accomplished using 90°C for the entire test with the exception of a one-hour duration trial at 120°C during the post-exposure purge cycle. The temperature chosen as the 'best' temperature tested was 150 °C. This choice was reinforced by work performed on lead-phthalocyanine thin-films conducted by Cranny and Atkinson [3:172]. The 150°C operating temperature reduced the apparent influence attributed to oxygen and water vapor, and it also dramatically shortened the PbPc recovery time [3:172]. The 150°C temperature was used for the majority of all subsequent Series II challenge gas exposure and purge trials.

Determining a range of film-thicknesses to be used for the investigation was difficult. As a preliminary step, scanning-electron microscopy photographs of coated and uncoated IGE structures were analyzed. There appeared to be an air-gap between the metal fingers of the IGE and the MPc material deposited between, and upon, the fingers. In addition, a significant undercut below the edges of the metal IGE finger's at the interface between the metallic fingers and the supporting silicon dioxide. This undercut appeared to be an artifact of the IGEFET fabrication process. Initially, MPc film thicknesses were considered that

would provide three different levels of overlap between the top of the MPc film and the edges of the metal fingers. For the initial studies, the chosen thicknesses were 2,000 Å, 12,000 Å, and 30,000 Å. Figure IV-7 depicts the relation between the top of the MPc and the IGE fingers. The first thickness was intended to provide a small overlap of the top of the MPc film with the lower edge of the metal finger. The 12,000 Å thick film established the top of the MPc film between the top and bottom edges of the metal finger edges. The third thickness (30,000 Å) resulted in the top edge of the MPc layer extending past the upper edge of the metal fingers. After testing these thicknesses, an assessment was made regarding their ability to sense a challenge gas and then subsequently revert to the pre-exposure condition. Based upon these results, a second set of film thicknesses was identified (2,000 Å, 5,000 Å and 10,000 Å). These thicknesses were used for the bulk of the remaining Series I and Series II tests.

The selection of a carrier and purge gas was determined by examining the merits of using N<sub>2</sub> or dehumidified room air as diluent and purge gas. N<sub>2</sub> was attractive because the number of gas components in the system during the purges would be limited to one, and the number during challenges would be two. This situation contrasted the multicomponent system resulting from the use of room air as the carrier and purge gas. To

assess the affect of N<sub>2</sub> versus dehumidified room air as a purge gas, a seven-hour long test was conducted at 120°C. During the first three hours of the test, N<sub>2</sub> was used in the test chambers. Room air at 8 % relative humidity was utilized for the next hour, followed by an N<sub>2</sub> purge lasting three hours.

The decision to use room air as the purge and carrier gas was made based upon the desire to test the devices under conditions in which they would likely be exposed to in practical applications, namely room air, not a pure N<sub>2</sub> atmosphere.

The choice of the type of signal waveform for the time domain analysis was influenced by the early findings in the frequency-domain response data gathered during the Series I tests. Initially, the waveform used was a voltage pulse with a repetition rate of 1,000 Hz. These early tests were examined for changes in the frequency- and time-domain content upon exposure to the challenge gas. The pulse waveform contained significant power in only the higher harmonics of the 1,000 Hz fundamental. Since we found the overall IGEFET system response similar to a low-pass filter with the transfer function shape modulated by the challenge gas exposure, much of the low frequency information regarding

the modulation was lost when using the pulse wave described above. In order to gather more information in the lower frequency region, a waveform with a much lower fundamental harmonic frequency content was desired. In addition, a symmetric, square wave was chosen to reduce any dc voltage charge-induced buildup at the driven- and floating-electrodes. A square wave with a 50 Hz repetition rate, 50 % duty cycle, and 2 volt<sub>pk-to-pk</sub> amplitude was chosen for the remainder of the Series I, and subsequent Series II tests.

Establishing the exposure duration for the challenge cycles was motivated by the desire to operate near equilibrium, but not to the point of saturation. During the initial experiments in the Series I exposures, the trials were one-hour long. In most cases, this time duration was much longer than needed for the resistance values to attain equilibrium. Usually, approximately 15 minutes was sufficient to attain a near-equilibrium response.

Another related issue was the question of whether or not to 'pre-condition' (or 'cure') the films by exposing them to a 'very high' concentration of the challenge gas (larger than would normally be expected in the environment) for a 'very long period of time', at the start of each new test. Results reported by Wilson *et al* [25] while working with PbPc

thin-films exposed to NO<sub>2</sub> supports the concept of preconditioning. That is;

Essentially, to attain reproducibility the sensor must be operated with a constant residual value, which we call the baseline, of strongly bound NO<sub>2</sub> on the surface. Further, reversal of the sensor response in clean air to remove less strongly bound NO<sub>2</sub> must not be allowed to continue too long, otherwise a proportion of the strongly bound NO<sub>2</sub> will desorb, change the fractional surface coverage, and hence modify the response kinetics. Typically, the behavior of a fresh film exhibits an initialization effect whereby the sensor shows little response to the presence of NO<sub>2</sub> over a period of several hours. This is attributed to population of the various adsorption sites by NO<sub>2</sub> and desorption of bound oxygen. On subsequent exposures to NO<sub>2</sub> the response increases until reproducible kinetics are obtained.... If the sensor is reversed in clean air, a certain base surface coverage will remain, giving a measurable response on subsequent exposures. If, however, the sensor is fully reversed, for example by heating... the initialization process is observed again. [25:500].

A Series I test was conducted with a one hour long exposure prior to exposures at lower concentrations to provide data to evaluate the impact of the preconditioning process. The resistance values from this test were compared to the results obtained with the same concentrations of gases, but without the preconditioning exposure. The comparison focused on the effects noted in the overall baseline drift throughout the entire test's duration.



Based upon the initial Series I tests, it was decided that an hour long preconditioning exposure to the highest concentration to be used during the test would provide a more stable baseline for calculating sensitivity and reversibility. A one hour duration preconditioning exposure was incorporated in all the Series II tests.

Although no testing of the effects of relative humidity were accomplished during this research effort, a fixed level of relative humidity used during this investigation was established based upon the work of prior investigators [5:76]. The desired level of relative humidity (RHAPSODY) in the purge and carrier gases passing through the test chamber during the experiments was controlled to a level spanning 0 to 10 %. The RH was limited because H<sub>2</sub>O molecules are known to compete for absorption sites on the thin-films [5:76]. The humidity of the room air carrier gas was reduced to an acceptable level by passing it through an absorbent material prior to routing it to the gas metering and challenge gas generation apparatus. Additionally, the temperature of an IGEFET sensor under test was thermostated at 150°C ± 2°C. At this high temperature, any absorbed H<sub>2</sub>O molecules would be evolved from the thin-film surface with the added effect of desorbing weakly bound O<sub>2</sub> [3:172]. An additional impetus for

drying the air was the possibility that the challenge gases might interact with the H<sub>2</sub>O. As an example, the NO<sub>2</sub> challenge gas may react to form nitric acid [5:76]. That is;



To summarize, the series I tests were used as a basis for identifying the basic test parameter boundaries that were used during the Series II tests. The parameter boundaries used for the Series II tests included: film types (CoPc, CuPc and NiPc); nominal film thicknesses of 2,000 Å, 5,000 Å, 10,000 Å; temperature for challenge and purge cycles thermostated at 150°C; the gas for the carrier and purge cycles (dehumidified, filtered room air); the time-domain signal input was a 50 Hz, 50 % duty cycle square wave with a 2 volt<sub>pk-to-pk</sub> amplitude; and a one-hour duration preconditioning challenge gas exposure.

*Focused Testing (Series II).* At the end of the preliminary test phase, a set of particularly promising test variable ranges and test conditions had been defined. This led to the structured test and evaluation paradigm depicted in Figure IV-17. The following nominal test

parameters were applied to the paradigm:  $\text{BF}_3$ ,  $\text{NO}_2$ , DMMP, DIMP, and  $\text{NH}_3$  for the challenge gases; CoPc, CuPc, and NiPc as the thin-film materials with 0.2, 0.5, and 1.0  $\mu\text{m}$  as their thicknesses; 150° C as the sensor's temperature; and two to five different challenge gas concentrations would be utilized. The test cycle manifesting the best performance was chosen with a preconditioning, high concentration challenge gas exposure with the intent of curing the thin-films and reducing the amount of baseline drift with respect to time.

The time phasing of the purge and challenge gas merits an explanation. At least two hours prior to activating the data collection instrumentation, the IGEFETs to be tested were placed in their respective test chambers. In the time period prior to the data collection process, the DIPs were brought up to the 150°C test temperature with room air purge gas flowing over them. After this 2-hour stabilization process, the data collection process was initiated. For fifteen minutes, the purge process was continued to collect the baseline data. Next, the DIPs were challenged with a high concentration of challenge gas for 1.25 hour. This process established the preconditioning phase. This event was followed with an hour long purge. The remainder of the test cycle consisted of serially challenging the DIPs for fifteen minutes, and then purging them for one

hour. These challenge/purge cycles were repeated four times at each concentration of the challenge gas. Each challenge gas was typically tested using two to five different concentration levels. This meant that the data collection for a particular type of film, for a particular challenge gas, could consume nearly 30 hours.

The test paradigm used to capture the test variable ranges was established as a nested loop structure. Figure IV-17 depicts the nested structures. The central loop represents the test features that were iterated most frequently, namely, the specific IGE device or IGEFET microsensor system selected from the DIP's 3 x 3 array. Two, nine-element array DIPs were tested at the same time; one in test chamber #1 and the other in test chamber #2. One nine element array was used for dc resistance measurements, while simultaneously, the other array had its ac parameters measured. Moving outward in the nested loop, the various items iterated upon are shown, until finally, the last item iterated upon is the type of gas being used to challenge the coated IGEFETs.

One of the primary concerns in the test sequence was establishing the amount of time needed for the IGEFETs to respond during a challenge gas exposure and attain equilibrium. Based upon previous experiments conducted on similar devices, the choice was made to use a single, one

hour preconditioning exposure of the challenge gas, followed by a purge/challenge cycle described in the previous paragraph. This was the basis for the 'Test Cycle' loop in the nests.

A recap of the specific test parameters derived from the Series I tests and used in the Series II tests is given in Table IV-2.

*Series III Testing.* A short series of tests were conducted to assess the impact of lowering the purge and exposure temperature relative to the response of the IGEs and IGEFET sensors to DIMP and DMMP at low concentrations (3 ppm and 10 ppm, respectively). These tests were conducted with a modified 'purge and expose' paradigm with three different temperature phases. In the first phase, the temperature was equilibrated at 150°C for 1.25 hours with the purge gas, followed by 1.25 hours of challenge gas exposure at the same temperature. At the beginning of the second phase, the purge gas was selected, and the temperature was lowered to 90°C. After 1.25 hours of purge, the second challenge was accomplished at 90°C. The third phase purge and exposure temperature was 30°C. At the end of the third challenge, the purge gas was selected, and the temperature was increased to 150°C for 15 minutes.

Table IV-2.

## Test Parameters Used for Series II Testing.

Thin-Film Materials	CuPc, NiPc, CoPc
Nominal Film Thicknesses	2,000 Å, 5,000 Å, 10,000Å
Challenge Gases and Concentrations	NO <sub>2</sub> : 30, 50, 100, 500, 1,000 ppb NH <sub>3</sub> : 16, 106, 250, 500 ppm BF <sub>3</sub> : 24, 105 ppm DMMP: 0.2, 0.4, 0.8, 1.6, 3.2, 10 ppm DIMP : 3 ppm
Test Temperature	Constant 150 ° C $\pm$ 2 ° C
Carrier/Purge Gas	Filtered room air (0 - 10% RH)
V <sub>dd</sub> and V <sub>ss</sub>	+5 volts dc & -5 volts dc, respectively
V <sub>bias</sub>	0 volts dc relative to V <sub>ss</sub>
Impedance Matching Amplifiers in a Unity-Gain Configuration and a Constant 10 kohm Load Resistor on the Outputs.	

*Summary.*

In summary, the investigation process began with the visual and electronic qualification of the uncoated IGEFET arrays received from the MOSIS IC fabricator. The inspections continued with the SEM

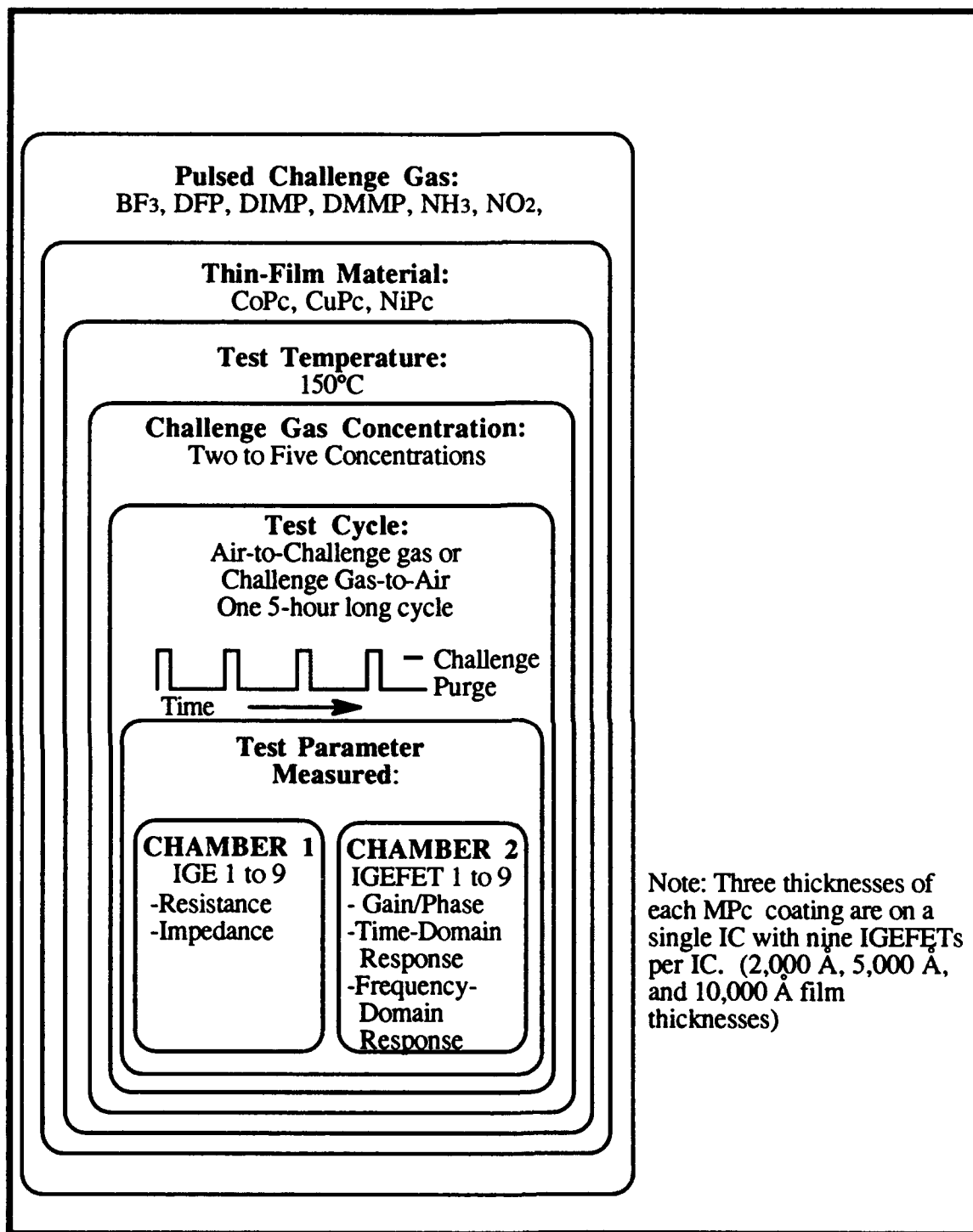


Figure IV-17. Test Loop Relationships for Each of the Challenge Gases ( BF<sub>3</sub>, DFP, DIMP, DMMP, NO<sub>2</sub>, and NH<sub>3</sub>).

photographs of the bare IGE structure and the thin-film coated IGE structures. The deposition of the thin-films was accomplished using vacuum sublimation, and the film's thickness was established using stylus profilometry. The material's deposited included the polymeric semiconductors CoPc, CuPc, and NiPc. Once the devices were fabricated, they were again checked for adequate performance prior to being exposed to the challenge gases. An automated test and data collection system was designed and constructed utilizing a GPIB instrument controller and a GPIB-controlled signal pathway switching matrix which linked the test equipment and the devices under test. Two test chambers were modified to facilitate test temperatures as high as 200°C. They were also modified to accommodate an entry port for the challenge gases so that they were delivered above the thin-film coated IGEs. A gas generation system was used to provide delivery of the purge and challenge gases to the device test chambers. Two series of tests were performed to determine the sensitivity and reversibility of the fabricated devices. Test Series I identified the basic boundaries of the test parameters that promised to provide useful information. The Series II tests accomplished an in-depth data gathering effort as the test parameters were varied through their respective limited ranges. The Series III investigation utilized a modified testing paradigm



to investigate the affects of lower exposure and purge temperatures relative to the response of DIMP and DMMP at low concentrations (3 ppm and 10 ppm, respectively).

## *V. Experimental Results and Discussion.*

### *IGEFET Device Physical Measurements.*

*Visual Inspection of the IGEFET Devices.* A complete and detailed macroscopic visual inspection of the devices and their packages did not reveal any obvious defects or significant deviations relative to the physical specifications sent to MOSIS for implementing the fabrication process. Microscopic inspection of the IGEFET devices proved to be less impressive. Specifically, the etching process used to remove the metallic conductor material between the interdigitated gate-electrode (IGE) fingers also removed much more material than anticipated, thereby reducing the thickness of the insulating layer between the metal ground plane and the region which supports the chemically-active thin-film material. The etching process also severely undercut the material supporting the IGE metal fingers. This defect is shown pictorially in Figures IV-3 and IV-4.

### *Determination of the IGEFET's Bias Voltages and Feedback*

*Configuration.* Before evaluating the thin-film responses to the challenge gas, the IGEFET's operational parameters for the *in situ* MOSFET amplifier section established. The primary goal of this effort was to establish a complete operational system configuration which would be very

stable throughout the duration of the challenge gas exposure trials, and which would not require a significant amount of operator intervention while the experiments were being conducted. A fundamental issue requiring resolution was whether the MOSFET amplifier would perform as designed and simulated using the SPICE® software tool [8].

The initial MOSFET amplifier measurements focused on determining the  $V_{bias}$  levels. Figure IV-9 shows the instrumentation arrangement used to investigate the effects of varying the bias voltage, along with the necessary components for configuring the amplifier's feedback. By using resistive feedback components, the overall gain of the amplifier could be readily established. This mode prevented the gain from being dominated by the electrical nature of the amplifier itself, with its inherent susceptibility to thermal effects and local noise sources. Additionally, since the primary function of the MOSFET amplifier was to provide isolation of the IGE structure from the loading effects imposed by the test instrumentation, its utility in a stable operational mode was desirable. Basically, the MOSFET amplifier acts as an impedance matching device by providing maximum signal transfer with minimal loading to the IGE structure. In the non-inverting mode, with gain, the least amount of signal clipping was observed to occur when the amplifier

was operated with an applied  $V_{bias}$  of -2.88 volts.

During this experiment, the gain/bandwidth information demonstrated the stability and linearity of the MOSFET amplifier. Table V-1 provides a comparison of the theoretical gains with those obtained by direct measurement. The resistors, R1 and R2, are those shown in Figure IV-8. The measured -3 dB bandwidth also is shown on Table V-1.

Table V-1

Non-Inverting Amplifier Configuration Performance.

R1 (ohms)	R2 (kohms)	Theoretical Gain (dB)	Actual Gain (dB)	-3dB Frequency (kHz)
1030	2,260	66.8	55.7	20
1030	114.7	40.93	39.6	200
10.7	114.7	20.6	20.4	700

The theoretical gain for the non-inverting MOSFET amplifier configuration matched the actual gains up to the apparent open-loop circuit limit near 55 dB. The gain-bandwidth plots in Figure V-1 depict the measured data collected during this experiment. Curve "A" resulted when R1 and R2 were 1,030 ohms and  $2.26 \times 10^6$  ohms, respectively. The

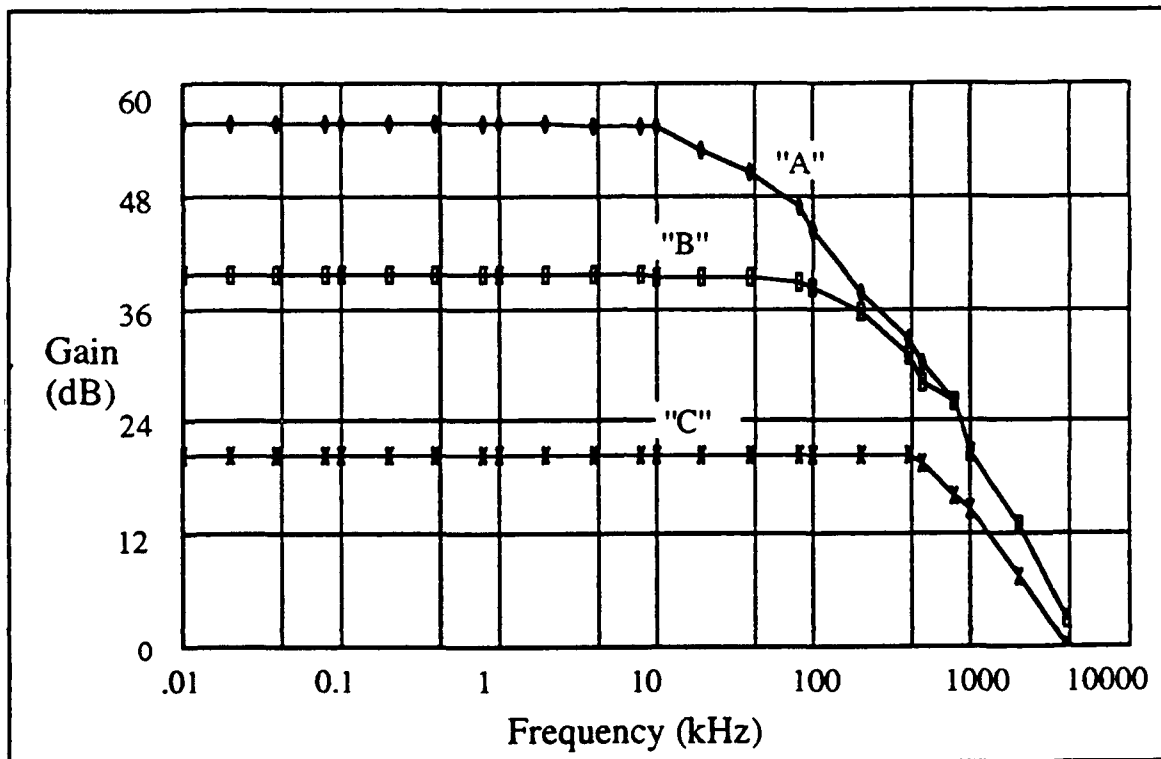


Figure V-1. Gain versus Frequency. Experimental Results of the MOSFET Amplifier with  $V_{bias} = -2.88$  volts. (Plot A is for  $R2/R1 = 2,260/1.030$ . Plot B is for  $R2/R1 = 114.7/1.030$ . Plot C is for  $R2/R1 = 114.7/10.7$ ).

theoretical gain of 66 dB was not achieved, and it is apparently bounded by the limitations of the MOSFET amplifier's own open-loop gain. Curves "B" and "C" were dominated by the resistive elements in the feedback loop, as should be the case. This experiment provided sufficient information to justify using the MOSFET amplifier in a feedback configuration with a constant applied  $V_{bias}$  level. These initial experiments demonstrated the feasibility of operating the MOSFET amplifier (a.k.a. impedance matching amplifier or IMA) in a non-inverting feedback configuration with a constant  $V_{bias}$ .

Since it was prudent to limit the magnitude of the output signal levels from the system combinations of the IGEFETs and their impedance matching amplifiers (IGEFET-IMAs), the feasibility of using the IGEFET-IMAs in a voltage-follower configuration was investigated. This configuration required fewer resistors compared to the non-inverting feedback design, and it also simplified the signal path connections. Figure IV-10 depicts the configuration used while evaluating the voltage-follower configuration for the IGEFET-IMA.

This next set of measurements validated the linearity of the IGEFET-IMA when operated in a voltage-follower configuration. For inputs levels spanning + 4 volts to - 4 volts, the gain linearity is shown in Figure V-2.

This voltage range is far more broad than the range of voltages expected to be impressed on the floating-electrode portion of the MOSFET gate-electrode driving the input of the IGEFET-IMAs. Another important issue addressed during this experiment was the ability of the voltage-follower IGEFET-IMA configuration to provide a linear output as the dc voltage level of the non-inverting input (the floating-gate electrode) drifted due to positive or negative charge accumulations. The maximum expected dc voltage drift was anticipated to be well within  $\pm 3$  volts. The effects of the change in voltage gain due to the floating-gate dc voltage drift by  $\pm 3$  volts while the IGEFET-IMA was configured as a voltage-follower, are shown in Figure V-3 for representative dc levels of interest. Within the frequency range less than 1 MHz, no significant signal clipping occurred.

In summary, the IGEFET-IMA was shown to possess stable, linear operation when configured as a voltage-follower with a 10 kohm load resistor applied to its output; supply voltages in the range of  $\pm 5$  volts and an applied  $V_{\text{bias}}$  level of -2.88 volts. The 10 kohm resistor provided a constant, stable load to the operational amplifier's output.

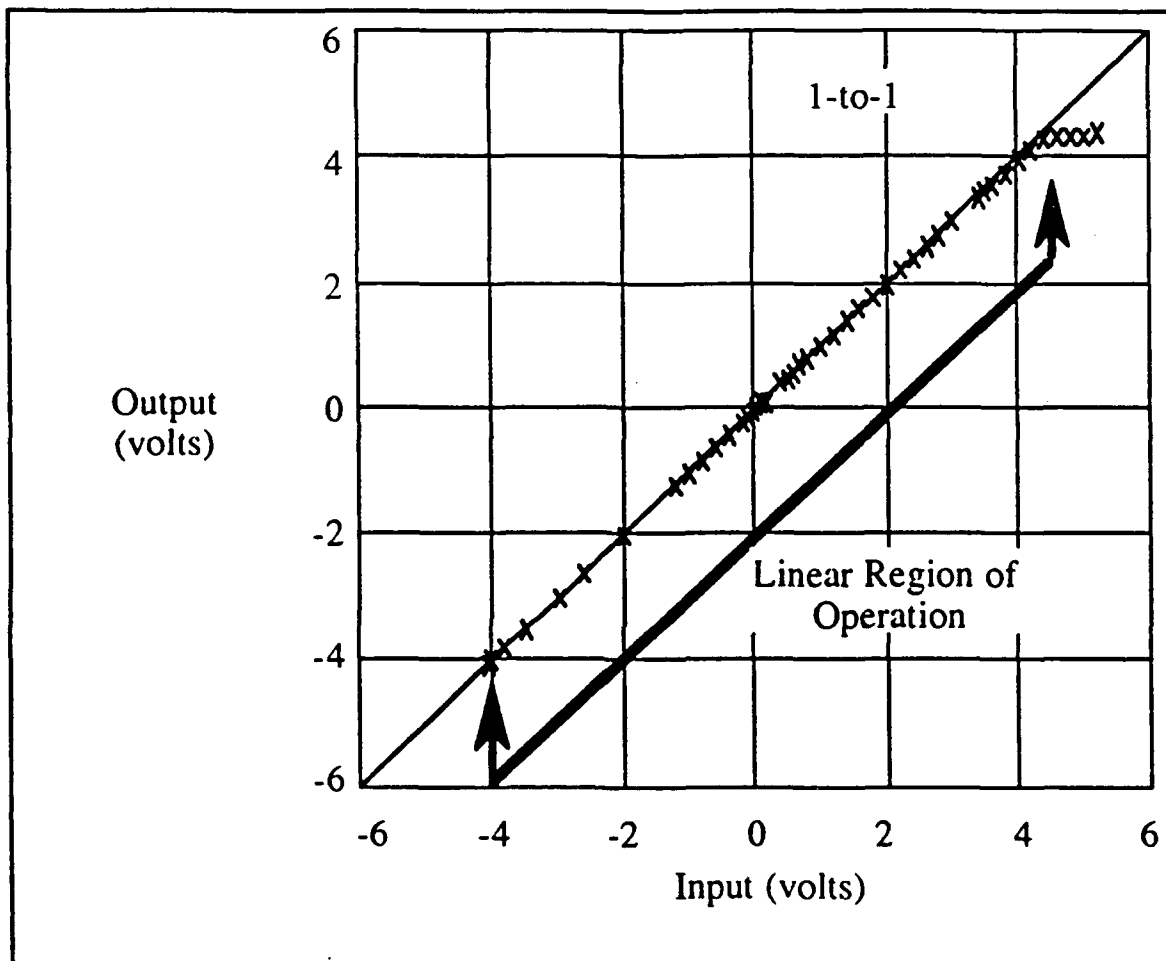


Figure V-2. Output Voltage versus Input Voltage for dc Linearity Evaluation of the IGEFET Operational Amplifier in Voltage-Follower Configuration. (The X's indicate the Measured Values).



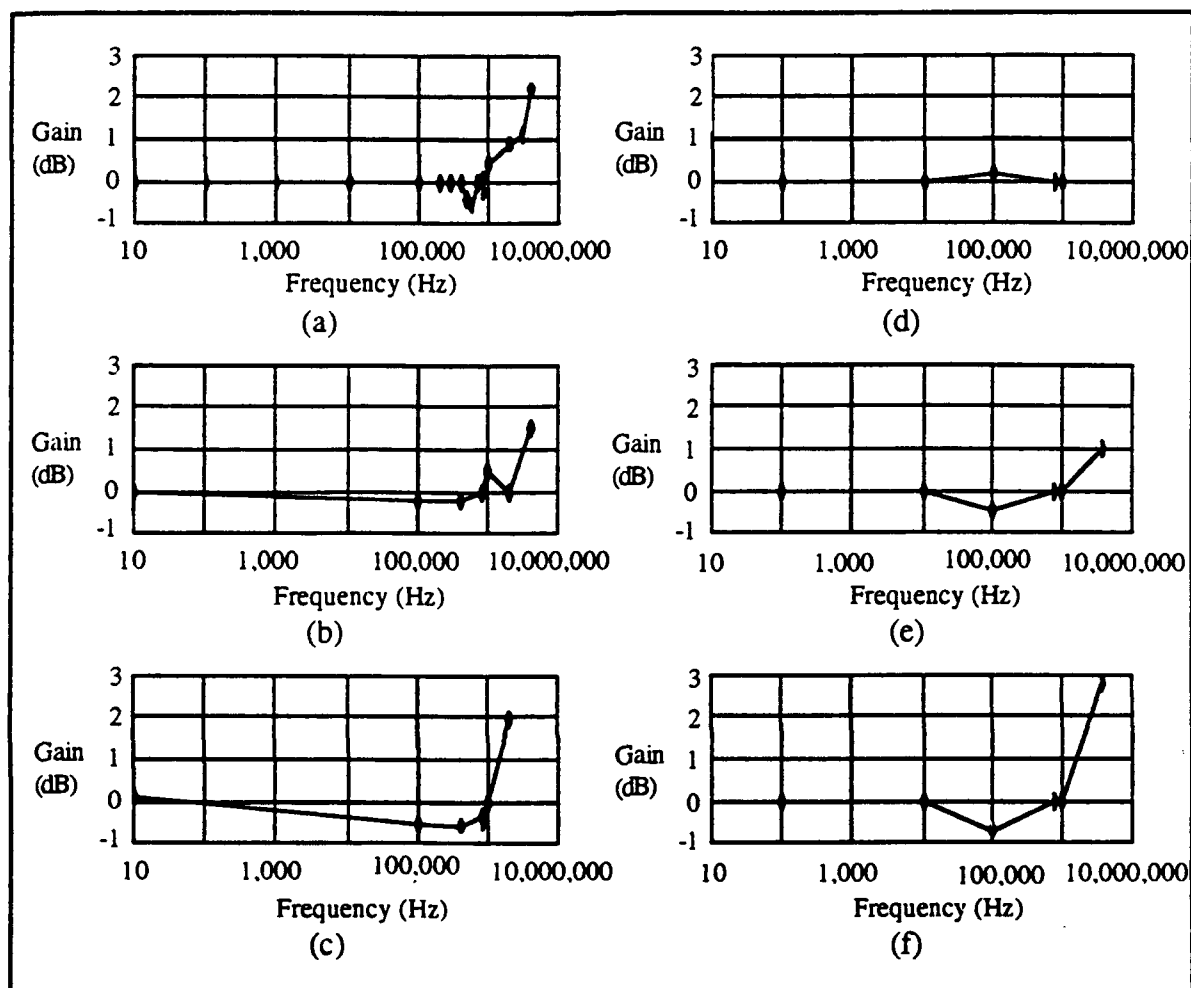


Figure V-3. Gain versus Frequency for the Sinusoidal Modulation of the DC Input Offset Values of: (a) +1.00 volt, (b) +2.00 volts, (c) +3.81 volts, (d) -1.00 volt, (e) -3.03 volts, and (f) -3.80 volts.

Choosing to configure the IGEFET-IMAs as voltage followers proved to be a very good decision. Changes in the overall IGEFET-microsensor's system response that might have been attributed to the MOSFET-IMAs were reduced, and thus, the focus shifted towards interpreting those changes induced by the thin-film's interaction with the challenge gases.

### *Series I Performance Evaluation*

The Series I performance evaluations focused on defining an envelope of physical parameters which would provide an opportunity to observe the interactions between the respective challenge gases and the chemically-active thin-film coatings. The list of physical parameters included, but was not limited to, the following: thin-film type, thin-film thickness, challenge gas type, challenge gas concentration, operating temperature, relative humidity, and carrier gas type. Additionally, the procedural steps employed while conducting these experiments had a direct impact on the overall system's response to the challenge gases.

The initial thesis plan of attack proposed to reduce the physical test parameter domain to a set of three operational temperatures, three thin-film types, three thin-film thicknesses, two relative humidities, three or

four challenge gas types, three or four concentrations of each type of gas, and each challenge gas concentration exposure was to be repeated three times. The initial experiments revealed that, for the CuPc thin-film material to achieve a psuedo-equilibrium during each phase of a purge-challenge-purge gas exposure cycle, a minimum of approximately two hours was required. Once this tentative time requirement was established, a projection for the total experimental manhours was computed. Due to the scope of the testing, this detailed projection of the required manhours revealed that more than three months of continuous testing would be needed to finish these tests. This quantity was deemed untenable, given the length of time permitted to complete this thesis investigation. Based upon this manpower estimate, the Series I performance evaluation was used to establish a basis for simultaneously reducing the physical test parameter envelope to include a single temperature and a single relative humidity level, thereby reducing the manhours required to achieve a level of approximately three weeks of continuous testing.

The combination of CuPc thin-films and the NO<sub>2</sub> challenge gas was used in the Series I performance evaluations. This combination represented a viable ensemble based upon the previous work by other investigators [7; 14; 22; 26]. The first two parameters investigated

included the effects of the thin-film thickness and the operating temperature relative to the sensor's sensitivity and reversibility with the CuPc and NO<sub>2</sub> ensemble.

*Thin-Film Thickness.* One important aspect of the thin-film thickness concerned the amount of overlap anticipated between the interdigital layer of CuPc thin-film and the edges of the IGE fingers. Prior to the gas exposure experiments, a microscopic examination of several IGEs with thin-film coatings was conducted. The results revealed that the deposited CuPc thin-films had very distinct gaps at the interface between the IGE finger's vertical side walls and the interdigital, dielectric supported regions. There was no visually discernible physical contact between these two regions. The following paragraphs include further observations concerning the physical architecture of the IGE and thin-film CuPc structure.

*IGE Structure and Thin-Film Coating Deposition Process.* Etching the IGE structure during the MOSIS fabrication process had a dramatic impact on the thin-film's structure. Instead of a single, uniform, continuous, chemically-active layer deposited on the IGE elements when the thin-film MPc materials were deposited, many discontinuities were formed along the junction between each IGE finger and the dielectric

support material. These gaps are depicted in Figures IV-5 and IV-6. In addition, the over-etched interdigital dielectric support material made it very difficult to predict the relationship between the top of the thin-film material and the top, and vertical edges of the IGE fingers. One of the goals of the thin-film deposition process was to produce three distinct thicknesses of thin-film material on different sets of IGE array elements, with one thickness just barely contacting the lower vertical side wall of the IGE, a second thickness that was near the mid-point of the IGE finger's side wall, and a third thickness level reaching the top surface of the IGE fingers. These thicknesses were selected to (hopefully) span a region with electrical impedance characteristics which would include a 'good' region of selectivity and reversibility for each of the challenge gas types. The basic idea was to vary the amount of physical contact between the thin-film and the IGE fingers.

Monitoring the thin-film thicknesses produced in the vacuum deposition system was accomplished with an *in situ* quartz crystal microbalance (QCM) and a stylus profilometer. As described by Capt Jenkins, the stylus profilometer scratches the fragile MPc films, and thus, it reveals only an approximation of the actual thickness with a significant bias error [7]. The QCM and the stylus profilometer thickness measurements

were generally within 20% of each other. The stylus profilometer measurements were used to report the thicknesses.

Several of the initial experiments dealt with determining the triad of thickness values to be used in the Series II experiments. The transfer functions for a typical experiment are shown in Figures V-4 and V-5. The thicker film requires more time to return to its equilibrium level after a challenge gas exposure. Even though this experiment was conducted at 90°C, similar observations were made at higher temperatures; that is, the thicker films tend to require more time to revert to their pre-challenge values, and they were more likely to not reverse as completely as the thinner films. Figure V-6 clearly supports this implication. In Figure V-6, two thin-films differing in thickness by an order of magnitude (1,600 Å versus 30,000 Å) show marked differences in response speed to the same challenge gas exposure concentrations, as well as the rate of reversal toward achieving a post-challenge purge equilibrium resistance. Another example of the reversal delay can be observed in Figure V-7 for a film that is 8,800 Å thickness at a constant 120°C temperature.

Another phenomenon observed while investigating the thin-film thickness effects was the downward drifting of the 'baseline' resistance values; this lasted for many hours. This behavior is shown in Figure V-8

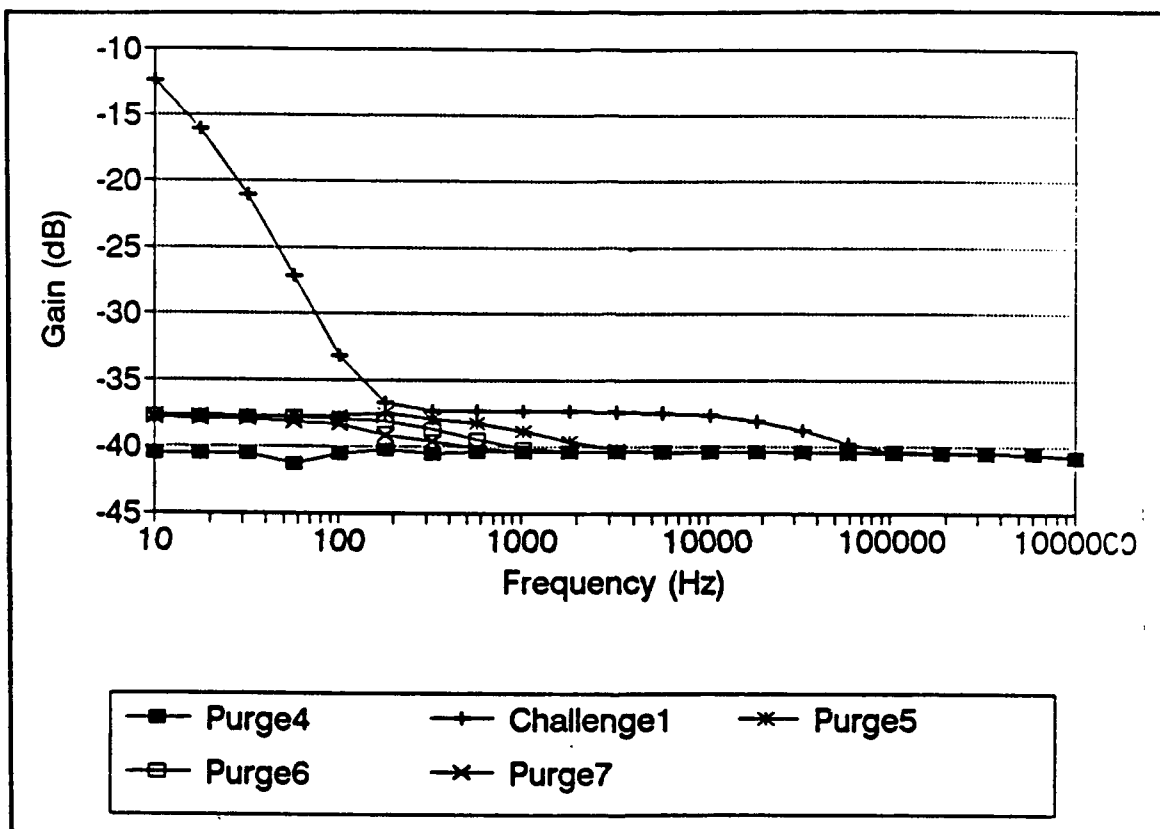


Figure V-4. Gain Versus Frequency Response for a 3,900 Angstroms Thick CuPc Thin-Film. Purge 4 Occurred Just Prior to 100 ppb Nitrogen Dioxide Challenge. Purges 5, 6, and 7 Followed the Challenge. The Time Between Purges is Approximately 10 Minutes.

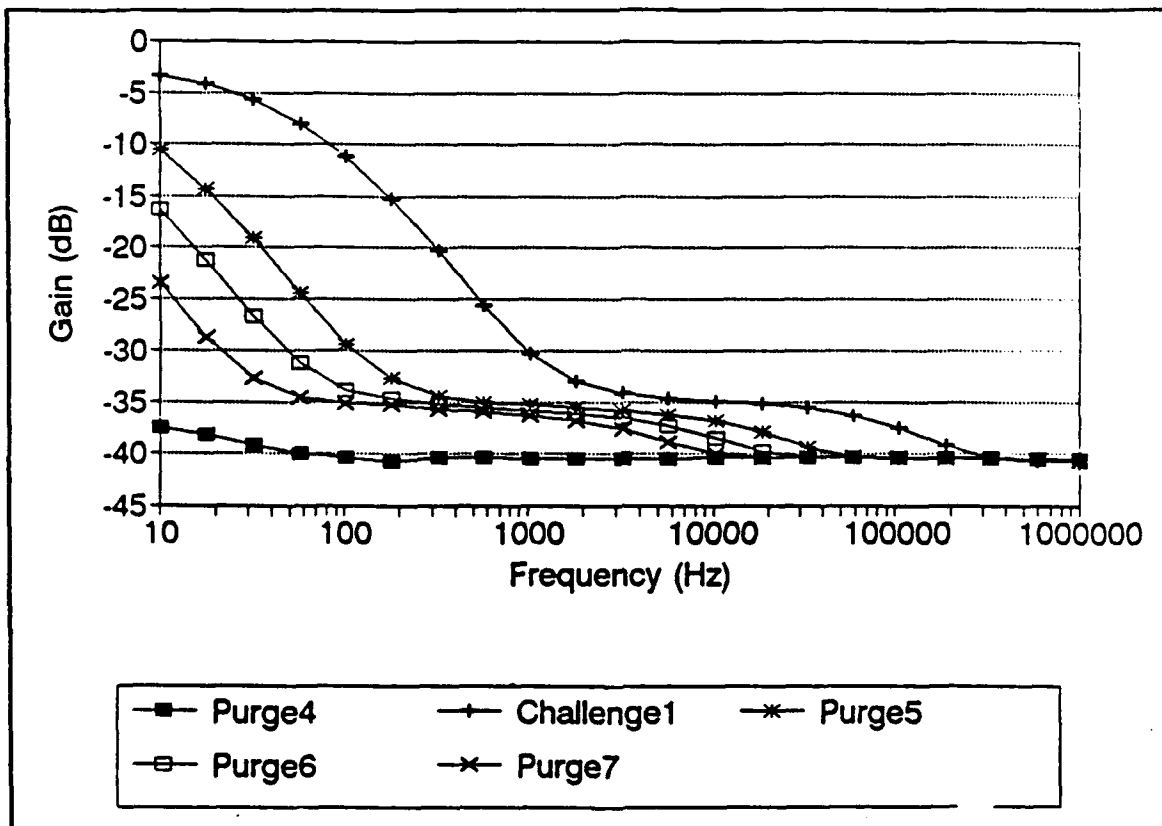


Figure V-5. Gain Versus Frequency Response for an 8,800 Angstrom Thick CuPc Thin-Film. Purge 4 Occurred Just Prior to the 100 ppb Nitrogen Dioxide Challenge. Purges 5, 6, and 7 Followed the Challenge. The Time Between Purges is Approximately 10 Minutes.



where the resistance versus time values for two 30,000 Å thick CuPc films are shown. The continuous downward drift in resistance during the entire experiment can be observed, and it is most noticeable during the first few hours. Much less drift was observed with the thinner films. Figure V-9 shows an example of this behavior for a 1,200 Å thick CuPc film. Based upon repeated observations similar to those mentioned in the previous paragraphs, a decision was made to use a nominal film thickness triad of 2,000 Å, 5,000 Å, and 10,000 Å for the remaining experiments.

During the early stages of the Series I performance evaluations, the issue concerning an appropriate purge and carrier gas for the experimental investigation was considered. Both N<sub>2</sub> and dehumidified room air were available. An experiment was conducted to determine the difference in the thin-film's dc resistance when exposed to an N<sub>2</sub> purge gas versus a dehumidified room air purge. The results are shown in Figure V-10. The change from N<sub>2</sub> to dehumidified, room air manifested itself as a decrease in the measured resistance by a factor of approximately 3 for the 8,800 Å thick CuPc thin-film when measured at 120°C. The effect on the 1,600 Å thick film was not as pronounced. Dehumidified room air was

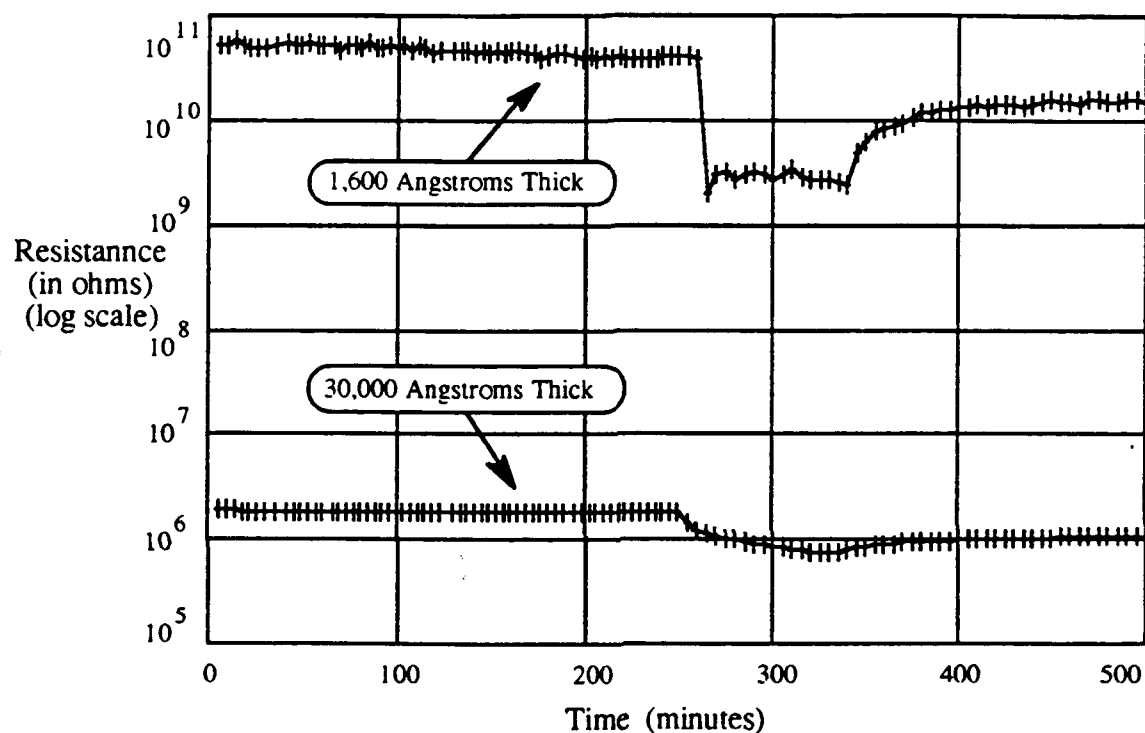


Figure V-6. Comparison of the dc Resistance Measurements for Two Different Thin-Film Thicknesses. Test Conditions: CuPc Thin-films (Thicknesses as Indicated); Temperature of 90 Degrees Centigrade; 100 ppb Nitrogen Dioxide Challenge Gas; Nitrogen Carrier/Purge Gas; Test Protocol Implemented was a Four Hour Purge Followed by a Single, One Hour Long Challenge, Followed by Purge Until the End of the Experiment.

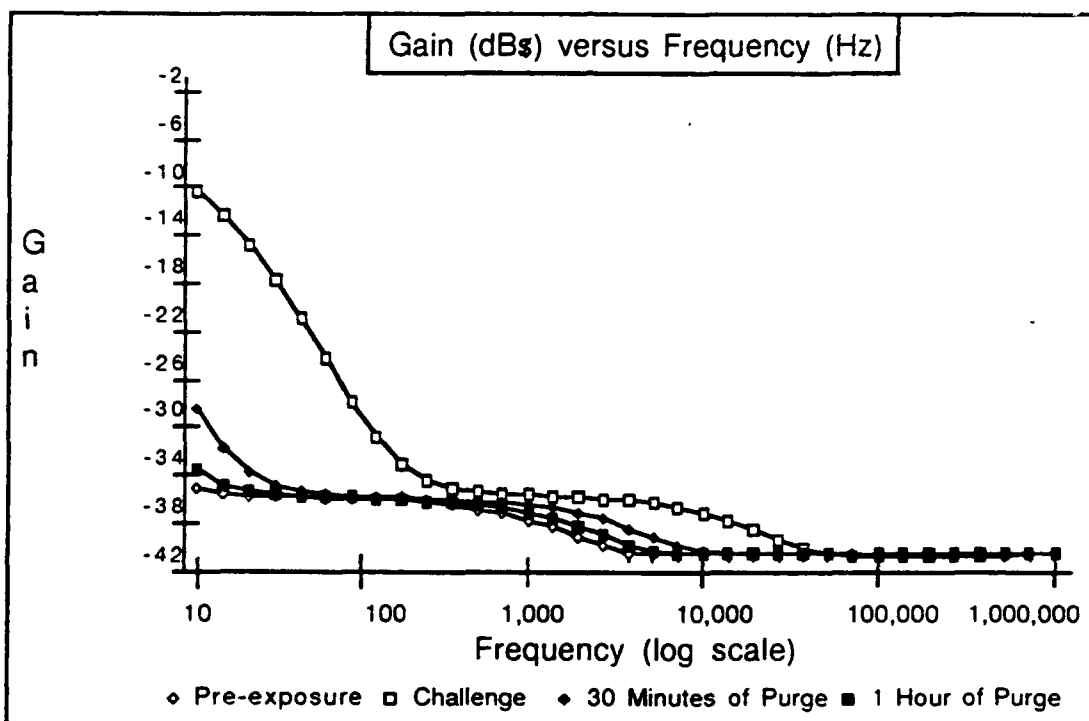


Figure V-7. CuPc Thin-Film (8,800 Å Thick) Transfer Function Response to a 100 ppb Nitrogen Dioxide Challenge at 120°C.

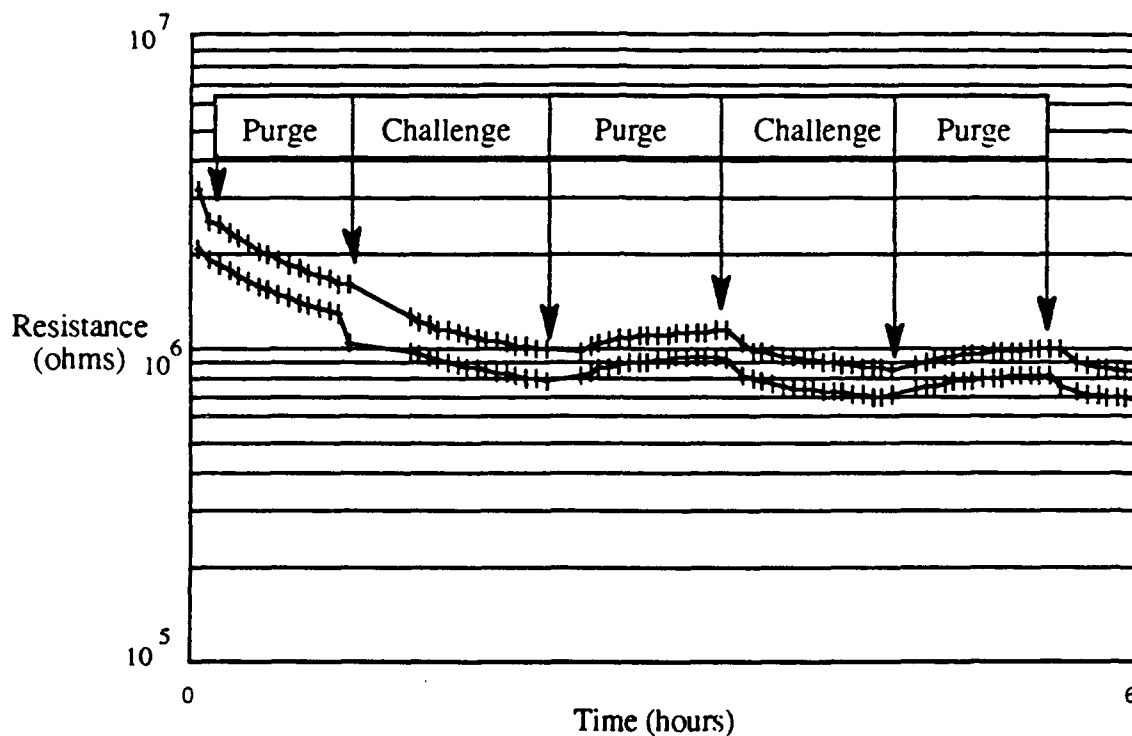


Figure V-8. Baseline Drift Observed with Two IGEs Coated with 30,000 Å Thick CuPc Films. Test Conditions: CuPc Thin-films; Temperature of 90 Degrees Centigrade; 100 ppb Nitrogen Dioxide Challenge Gas Concentration; Room Air Carrier/Purge Gas; Test Sequence as Indicated on the Plot.

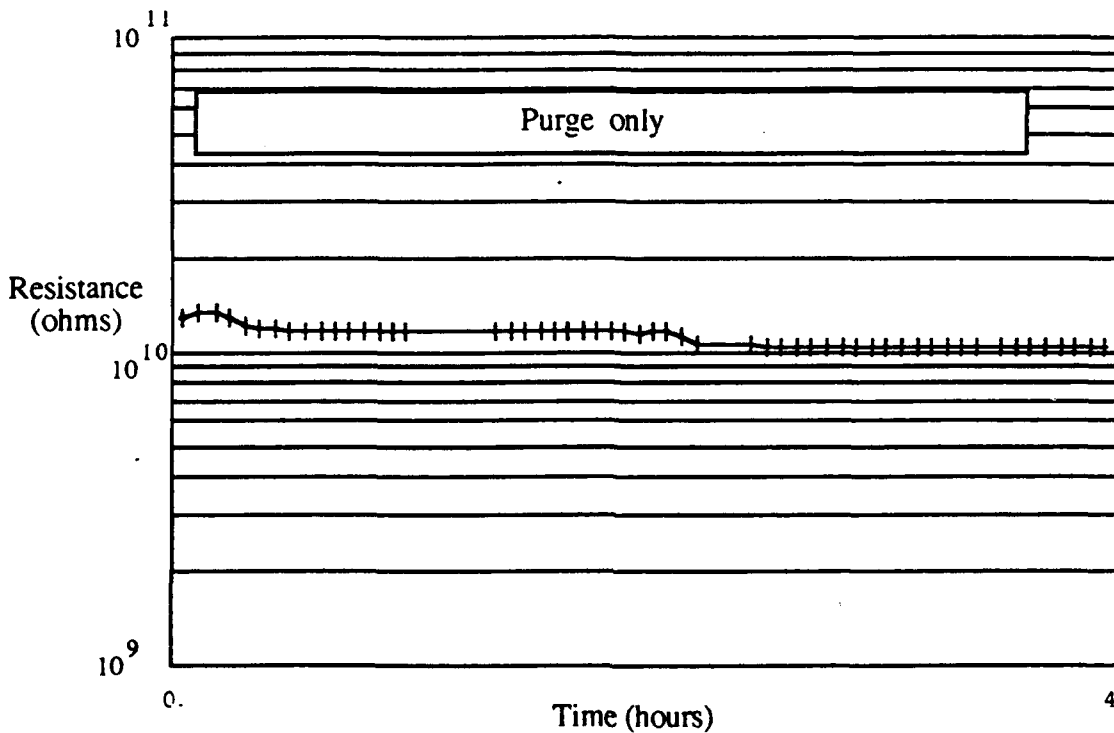


Figure V-9. Baseline Drift Observed with an IGE Coated with a 1,200 Å Thick CuPc Film. Test Conditions: CuPc Thin-Film; Temperature of 90 Degrees Centigrade; 100 ppb Nitrogen Dioxide Challenge Gas Concentration; Nitrogen Carrier/Purge Gas; Test Sequence as Indicated on the Plot.

selected as the purge and carrier gas for the Series II experiments because this would test the IGEFET-microsensor under conditions more akin to those in a practical application.

Determining the operating temperature for the Series II experiments was very difficult for several reasons. During the first set of experiments, the electrical sockets inside the test chamber were not rated above 150°C; hence, the restriction to the maximum temperature of 120°C. Later in the course of the experiments, new sockets rated at 200°C were acquired and installed into the test chambers. This change permitted investigations to be conducted at 150°C, while retaining a fair margin of safety to compensate for any localized 'hot spots' in the heater strips.

The results of two experiments conducted with temperature as the variable are shown in Figure V-11. The upper trace was measured at 90°C, while the lower plot was measured at 120°C. Two observations are noteworthy. First, the temperature affected the initial purge resistance by decreasing the resistance nearly an order of magnitude with the corresponding temperature increase. Second, the recovery time for the lower temperature is longer. The purge resistance's temperature

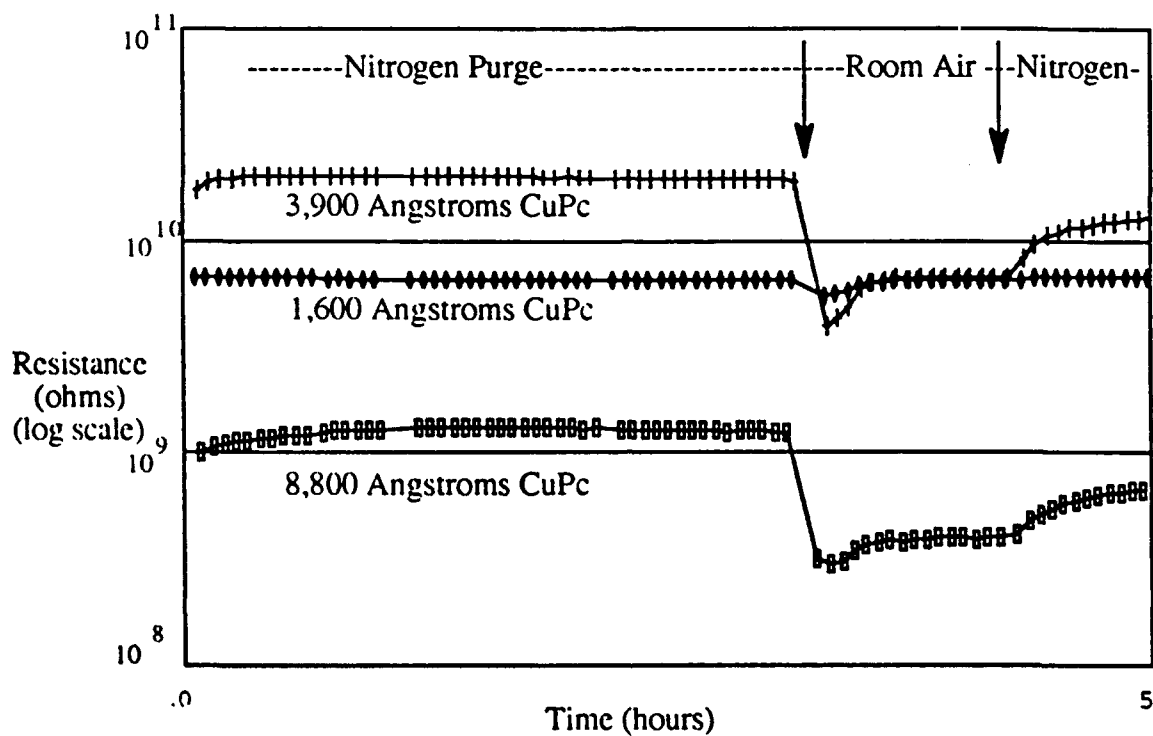


Figure V-10. Effect of Choosing Nitrogen versus Dehumidified, Room Air as a Purge Gas on the Resistance Measurements for the Same CuPc Films. Test Conditions: CuPc Thin-films (1,600, 3,900, and 8,800 Å Thick); Temperature of 120 Degrees Centigrade; Test Sequence as Indicated on the Plot.

dependence was confirmed in a subsequent experiment where a device was purged and challenged (with DMMP) at three temperatures, starting at 150°C, then at 90°C, and finally at 30°C. Figure V-12 displays the purge and challenge resistance values. Since it was desirable to reduce the overall time required for each purge-challenge-purge cycle, the temperature was increased to 150°C with a trade-off being made to reduce the purge equilibration and the reversal times at the expense of possibly lowering the rate of challenge gas interaction with the MPc films. The 150°C temperature was subsequently used throughout the Series II tests.

The next experimental parameter established was the procedure for challenging the IGEFETs with each test gas used in each Series II test. The first scheme utilized three sequential challenges at each concentration of interest, with monotonically increasing concentrations. The results of a CuPc and NO<sub>2</sub> experiment are shown in Figure V-13. Figure V-13(a) shows that drift occurred in the purge resistance baseline as the experiment progressed. In order to reduce the amount of baseline drift, a preconditioning phase was integrated into the procedure. The results of this procedural change are demonstrated in the Figure V-13(b). The drift is only reduced, not eliminated. The preconditioning phase was adopted for the subsequent tests.



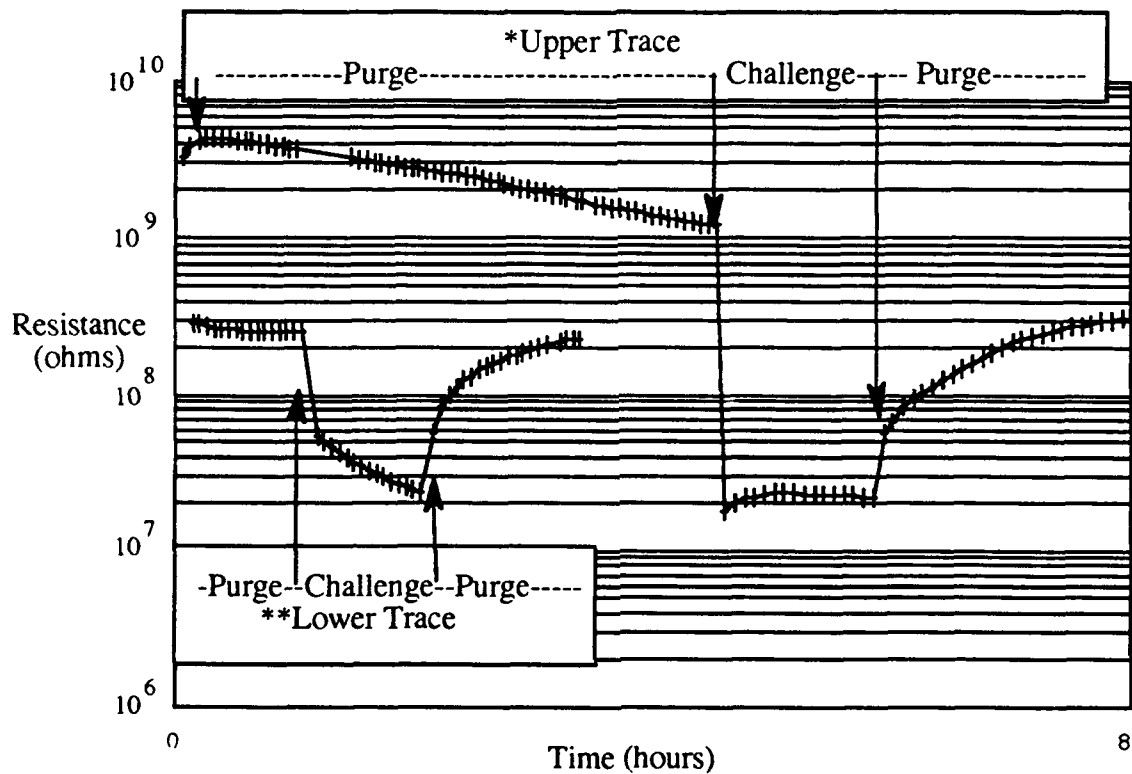


Figure V-11. Differences in Recovery Time At Two Different Temperatures for the Same CuPc Film. Test Conditions: CuPc Thin-film (8,800 Å Thick); Upper Trace Temperature of 90 Degrees Centigrade, Lower Trace At 120 Degrees Centigrade; 100 ppb Nitrogen Dioxide Challenge Gas Concentration; Nitrogen Carrier/Purge Gas; Test Sequence as Indicated on the Plot.

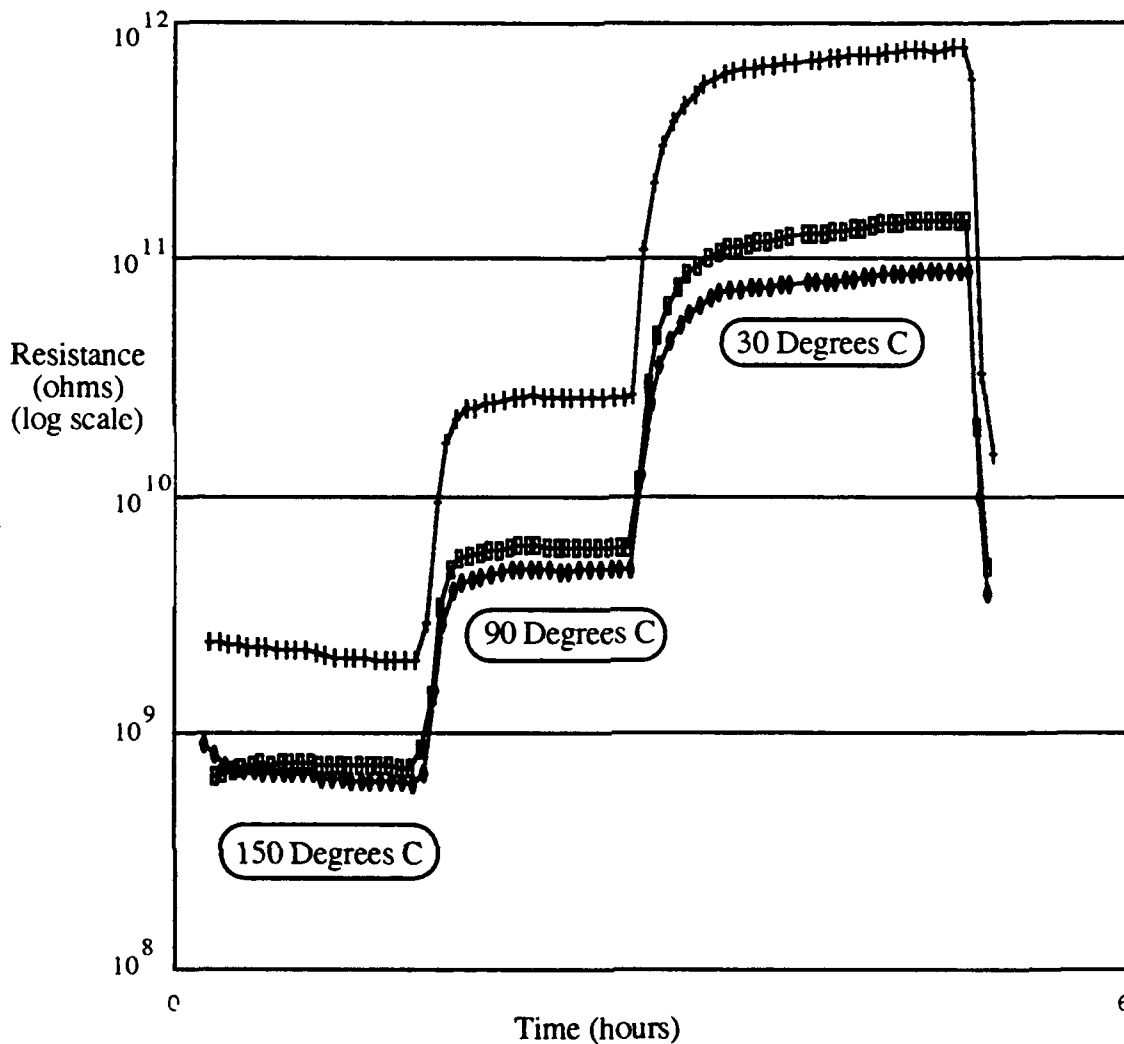


Figure V-12 Changes in Purge Condition Resistance Values for Three Different Thin-film Types Measured at Three Different Temperatures. Diamond Markers are for a 3,200 Å Thick CuPc Thin-film. Cross Markers are for a 5,200 Å Thick CoPc Thin-Film. Rectangle Markers are for a 6,800 Å Thick NiPc Thin-Film. Test Conditions: Three Temperatures (150, 90, and 30 Degrees Centigrade); 10 ppm DMMP Challenge Gas Concentration; Room Air Carrier/Purge Gas; Test Sequence was 45 Minute Purge Followed by a 45 Minute Challenge at each Temperature.

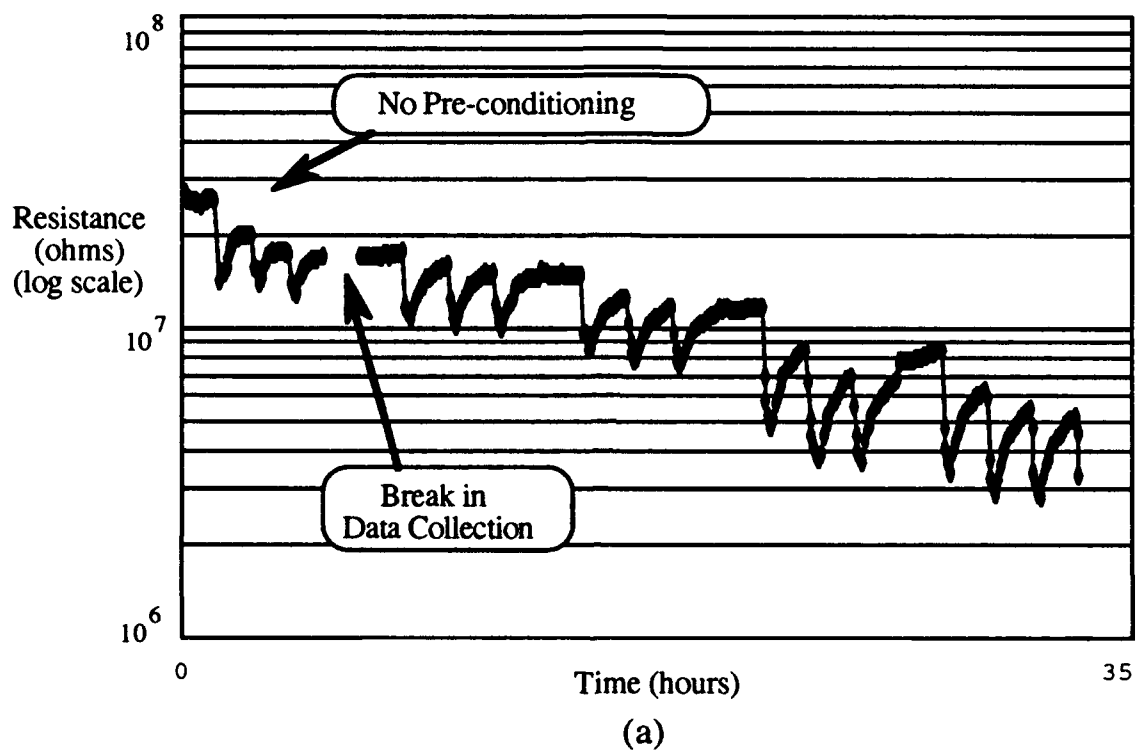


Figure V-13. Comparison of Changes in the Baseline Drift Throughout a Lengthy Experiment. (continued on next page).

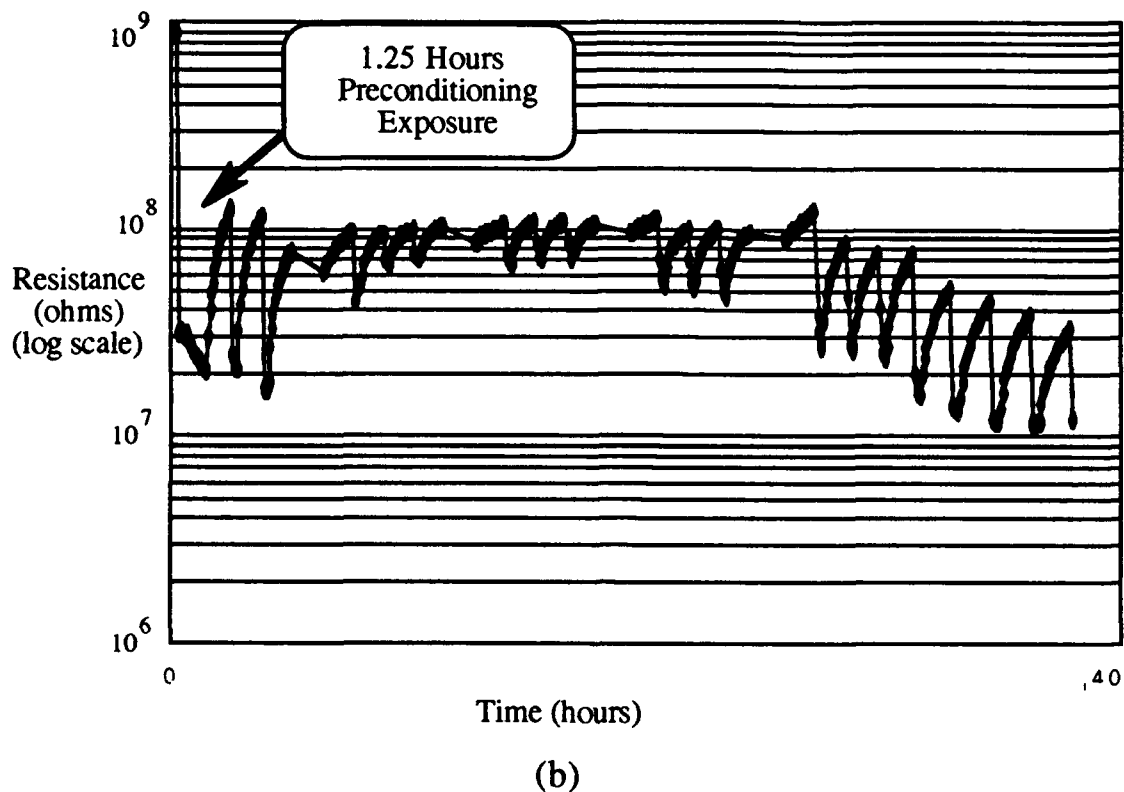


Figure V-13. Comparison of the Changes in the Baseline Drift Throughout a Lengthy Experiment. (a) 10,000 Å Thick CuPc Film with No Preconditioning Phase. This Test Series was Conducted Using Three Exposures each at 30 ppb, 50 ppb, 100 ppb, 500 ppb and 1000 ppb. (b) Behavior of a 8,800 Å Thick CuPc Film with a Preconditioning Phase. This Test Series was for Three Exposures each at 1000 ppb, 30 ppb, 50 ppb, 100 ppb, 500 ppb and 1000 ppb. Test Conditions: Temperatures (150 °C); Nitrogen Dioxide Challenge Gas; Room Air for Carrier/Purge.

At this point, the test parameters for the Series II tests had been established. Specifically they included: temperature of 150°C; nominal thin-film thicknesses of 2,000 Å, 5,000 Å, and 10,000 Å; dehumidified room air carrier and purge gas; preconditioning the thin-films with a 1.25 hour duration exposure to a high concentration of the challenge gas; subsequent challenge exposures repeated in triplicate with each exposure lasting 15 minutes and each intermediate purge lasting approximately 1 hour.

The specific concentrations of the challenge gas used depended upon the physical limitations of the gas generation system, and the available rates of gas release from the permeation tubes in the laboratory stock. The test parameter envelope developed from the Series I tests, and the other experimental limitations discussed are summarized in Table V-2.

#### *Results of the Series II Gas Challenge Experiments.*

This portion of the results discussion is organized by the specific challenge gas used for the exposures. The test conditions used in the Series II tests are summarized in Table V-2. Detailed experimental results for the CuPc, CoPc, and NiPc films are summarized in Appendix C, Appendix D, and Appendix E, respectively.

Table V-2.

## Test Parameter Ranges for the Series II Tests.

Test Parameter	Range of Values
Challenge Gas Type	BF <sub>3</sub> , DFP, DIMP, DMMP, NH <sub>3</sub> , and NO <sub>2</sub>
Gas Concentrations	DMMP: 10 ppm DIMP : 20 ppm DFP : 1000 ppb NO <sub>2</sub> : 30, 50, 100, 500, and 1000 ppb NH <sub>3</sub> : 16, 106, 250, and 500 ppm BF <sub>3</sub> : 24, 48 and 105 ppm
Thin-Film Material	Copper Phthalocyanine (CuPc) Cobalt Phthalocyanine (CoPc) Nickel Phthalocyanine (NiPc)
Thin-Film Thickness	2,000 Å, 5,000 Å, and 10,000 Å (nominal)
Exposure and Purge Temperature	150°C
Relative Humidity	2-5% nominal

*Diisopropylfluorophosphonate (DFP) Challenges.* The DFP permeation tube contained a liquid in its upper chamber, and so, its ability to provide a reliable flow of gas was questioned. A replacement tube could not be requisitioned in time to be included in this investigation.

*Dimethyl Methylphosphonate (DMMP) Challenges.* The first test with DMMP was interesting because the response with the CuPc thin-films was so strong. However, the reliability of this first set of responses was suspect for two reasons: first, an attempt to repeat the experiment yielded only a negligible response; second, a close inspection of the DMMP gas permeation tube revealed a clear liquid in its upper chamber. There was no simple way to determine if the integrity of the permeation tube standard was still intact. Perhaps the tube had been dispensing more than the expected rate of DMMP during the first experiment. Perhaps the tubes wall had been breached and it was not dispensing DMMP during the second confirmation test. The most viable option was acquiring a new permeation tube and repeating the experiment a third time. This action was subsequently accomplished. The resulting dc resistance values showed that no significant changes occurred during exposures to DMMP at concentrations of 10 ppm at 150°C. This behavior was true for CoPc with a 5,200 Å thickness, CuPc with a 3,200 Å thickness, and NiPc with a 6,800 Å thickness. The conclusion was that, under Series II conditions, the three film types were not responsive to the DMMP challenges at 10 ppm. Plots of the dc resistance values versus time during purge and exposures for each film type are documented in their respective

appendices.

*Diisopropyl Methylphosphonate (DIMP) Challenges.* The maximum DIMP concentration that could be produced by the challenge gas generation apparatus was 3 ppm. A single, one hour duration challenge was accomplished with the 3 ppm challenge, at 150°C. The resulting changes in dc resistance are noted in Table V-3. At this temperature, the changes are not very strong.

*Boron Trifluoride Challenges.* Generally, all three film types responded very weakly to the repeated BF<sub>3</sub> challenges. Plots of the dc resistance versus the purge and challenge cycles for CuPc, CoPc, and NiPc are summarized in Appendices C, D, and E, respectively.

*CuPc Thin-Film Response to BF<sub>3</sub>.* The dc resistance measurements of the CuPc Thin-films increased slightly upon initial exposure to BF<sub>3</sub>, with the activity more prominent in the thicker films. During the 1.25 hour duration preconditioning phase with 24 ppm of BF<sub>3</sub>, the dc resistance of a CuPc (16,000 Å thick) thin-film increased from  $2.2 \times 10^7$  to  $2.8 \times 10^7$  ohms. During the same period, the signal transfer gain



Table V-3.

DC Resistance Changes During the 3 ppm DIMP Exposure.

Thin-film Type	Resistance Values (ohms)	Change (%)
CuPc (3,200 Å)	$5 \times 10^8$ to $4.6 \times 10^8$	-8
CoPc (5,200 Å)	$0.8 \times 10^9$ to $0.7 \times 10^9$	-14
NiPc (6,800 Å)	$4.8 \times 10^8$ to $4.5 \times 10^8$	-6

at 10 Hz increased by almost 4 dB. However, subsequent 15-minute long exposures produced gain changes on the order of +0.5 dB. The phase angle response during the same exposure changed by nearly +9 degrees at 10 Hz. This response change also diminished after the initial exposure. At these low levels of response, the degree of reversibility is difficult to interpret reliably.

*CoPc Thin-Film Response to BF<sub>3</sub>.* The dc resistance measurements decreased slightly upon exposure to the BF<sub>3</sub> challenges with the activity fairly uniform among the similar film samples. During the 1.25 hour long preconditioning phase with the 24 ppm BF<sub>3</sub> challenges, the dc resistance of the CoPc (5,400 Å thick) thin-film's resistance decreased from  $7 \times 10^9$  to  $1.3 \times 10^9$  ohms. During the same period, the signal

transfer gain at 10 Hz increased by nearly +18 dB. The phase angle response during the same exposure changed by more than -9 degrees at 10 Hz, and -30 degrees at approximately 100 Hz. However, subsequent 15 minutes duration exposures produced gain changes on the order of less than +0.5 dB and phase angle changes less than 1 degrees. This level of response also decreased after the initial conditioning exposure. At these low levels of response, changes in the degree of reversibility were difficult to interpret.

*NiPc Thin-Film Response to BF<sub>3</sub>.* The dc resistance increased slightly upon exposure to BF<sub>3</sub>, with the activity slightly more pronounced with the thicker films. During the 1.25 hour long preconditioning phase with 24 ppm of BF<sub>3</sub>, the dc resistance of an NiPc (12,500 Å thick) thin-film increased from  $6.0 \times 10^8$  to  $6.5 \times 10^8$  ohms. During this same period, the gain at 10 Hz decreased by 0.5 dB. The phase angle response did not change over the 10 Hz to 1 MHz range. Subsequent 15 minutes duration exposures produced even less gain and phase angle changes. At these low response levels, the degree of reversibility was difficult to interpret reliably.

*Ammonia Challenges.* Generally, the CuPc and CoPc film types

responded to the  $\text{NH}_3$  challenges more strongly compared to the NiPc thin-film. With all three film types, the observed changes included increases in the sensor's dc resistance and modulation of the transfer function reflected in the gain and phase angle versus frequency plots. Detailed experimental results for the CuPc, CoPc, and NiPc films are summarized in Appendix C, Appendix D, and Appendix E, respectively.

*CuPc Thin-Film Response to  $\text{NH}_3$ .* The dc resistance increased slightly upon exposure to the  $\text{NH}_3$ , with the activity being more prominent in the thicker films. During the 1.25 hour duration preconditioning phase with 500 ppm of  $\text{NH}_3$ , the dc resistance of a CuPc (2,100 Å thick) thin-film increased from  $2.5 \times 10^8$  to  $8 \times 10^8$  ohms. In the first fifteen minute challenge cycle, the same IGE's dc resistance increased from  $4 \times 10^8$  to  $5.2 \times 10^8$  ohms, a 28 % resistance increase. During the same time period, the signal transfer gain at 10 Hz changed by approximately -4 dB. The phase angle response during the same exposure changed by nearly +9 degrees at 10 Hz. However, subsequent 15 minutes duration exposures produced smaller gain changes, on the order of -2 dB. The dc resistance reversal at the end of the hour long purge cycles was within 5 % of the original resistance value for the 500 ppm exposures.

The frequency domain responses, in the form of gain and phase angle versus frequency for CuPc are presented in Figures V-14 through V-17. They clearly show the increase in impedance due to exposures to NH<sub>3</sub> at concentrations of ammonia between 100 ppm and 500 ppm.

*CoPc Thin-Film Response to NH<sub>3</sub>.* The dc resistance measurements increased slightly upon exposure to the NH<sub>3</sub> challenges, with the activity fairly uniform among the different thicknesses of films. During the 1.25 hour long preconditioning phase with the 500 ppm NH<sub>3</sub> challenges, the dc resistance of a CoPc (5,400 Å thick) thin-film increased from  $1.3 \times 10^8$  to  $2.4 \times 10^8$  ohms. During the same period, the signal transfer gain at 10 Hz changed by almost -3 dB. The phase angle response during the same exposure changed by more than -10 degrees at 10 Hz. However, subsequent 15 minutes duration exposures produced gain changes on the order of less than -0.5 dB, and phase angle changes less than 2 degrees. This response change also diminished after the initial exposure.

For a CoPc (5,400 Å thick) thin-film, plots of the change in gain versus frequency revealed that the greatest changes occurred near 200 Hz; on the order of a -5 dB change relative to the preconditioning purge value. The magnitude of the change is not repeated for subsequent 500 ppm

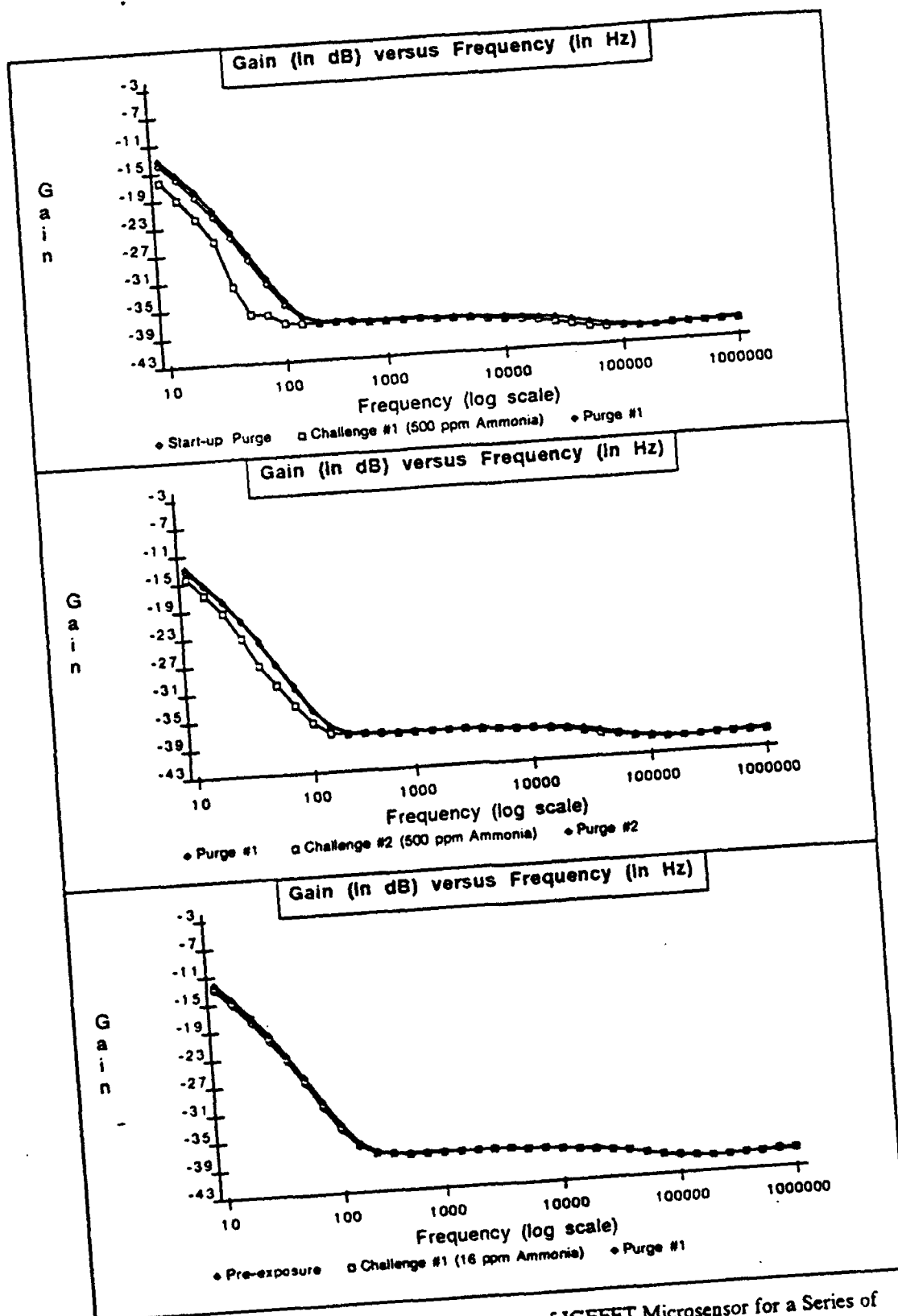


Figure V-14. Gain versus Frequency Response of IGEFET Microsensor for a Series of Room Air Purges and Challenge Gas Exposures. Testing Conditions: IGE Microsensor Number 1: CuPc Thin-film (1,600 Angstroms Thick); Temperature of 150 degrees Centigrade; Ammonia Challenge Gas (Order of Exposures: 500 ppm, 16 ppm, 106 ppm, 250 ppm, 500 ppm).

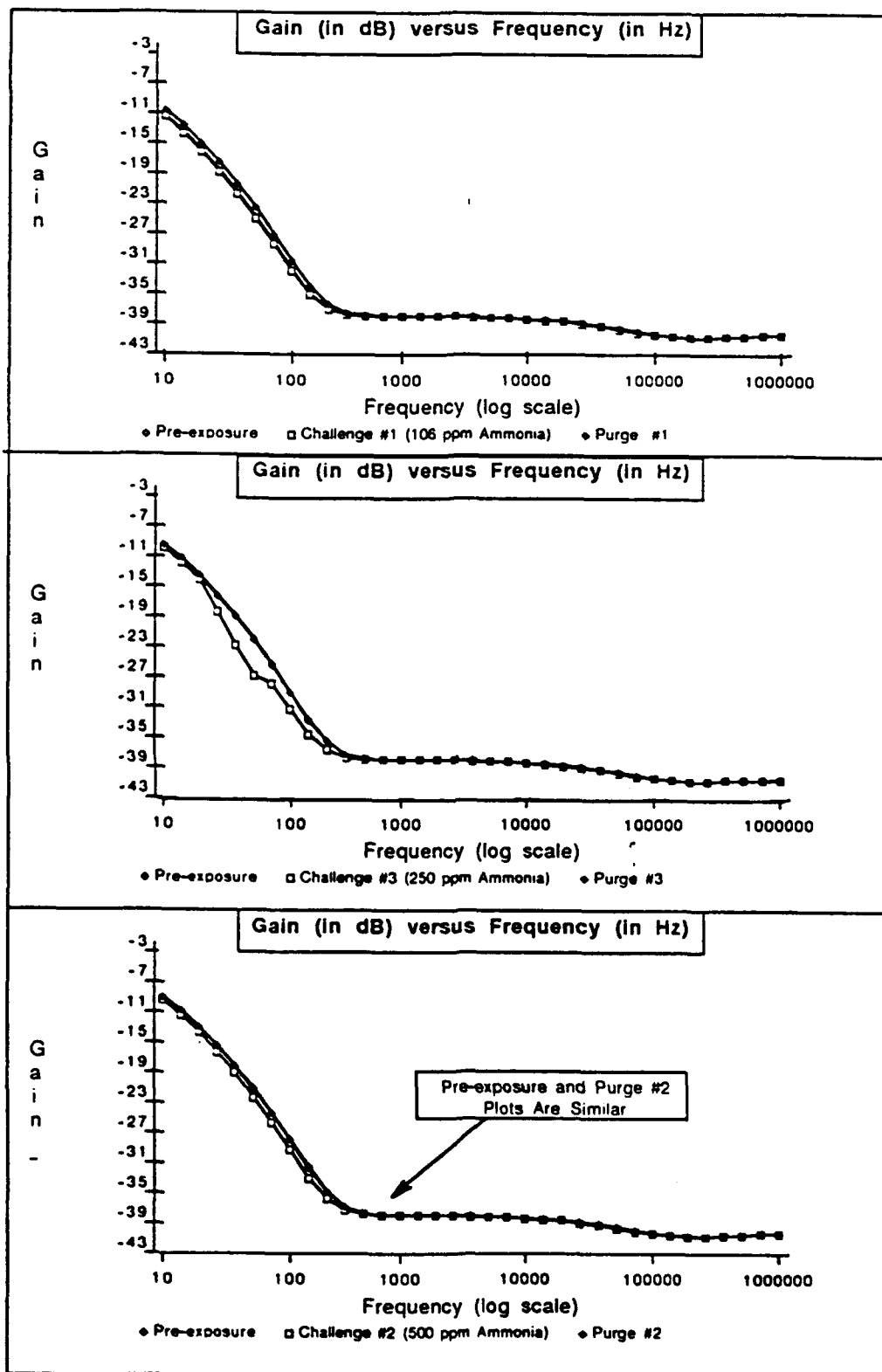


Figure V-15. Gain versus Frequency Response of IGEFET Microsensor for a Series of Room Air Purges and Challenge Gas Exposures. Testing Conditions: IGE Microsensor Number 1; CuPc Thin-film (1,600 Angstroms Thick); Temperature of 150 degrees Centigrade; Ammonia Challenge Gas (Order of Exposures: 500 ppm, 16 ppm, 106 ppm, 250 ppm, 500 ppm).

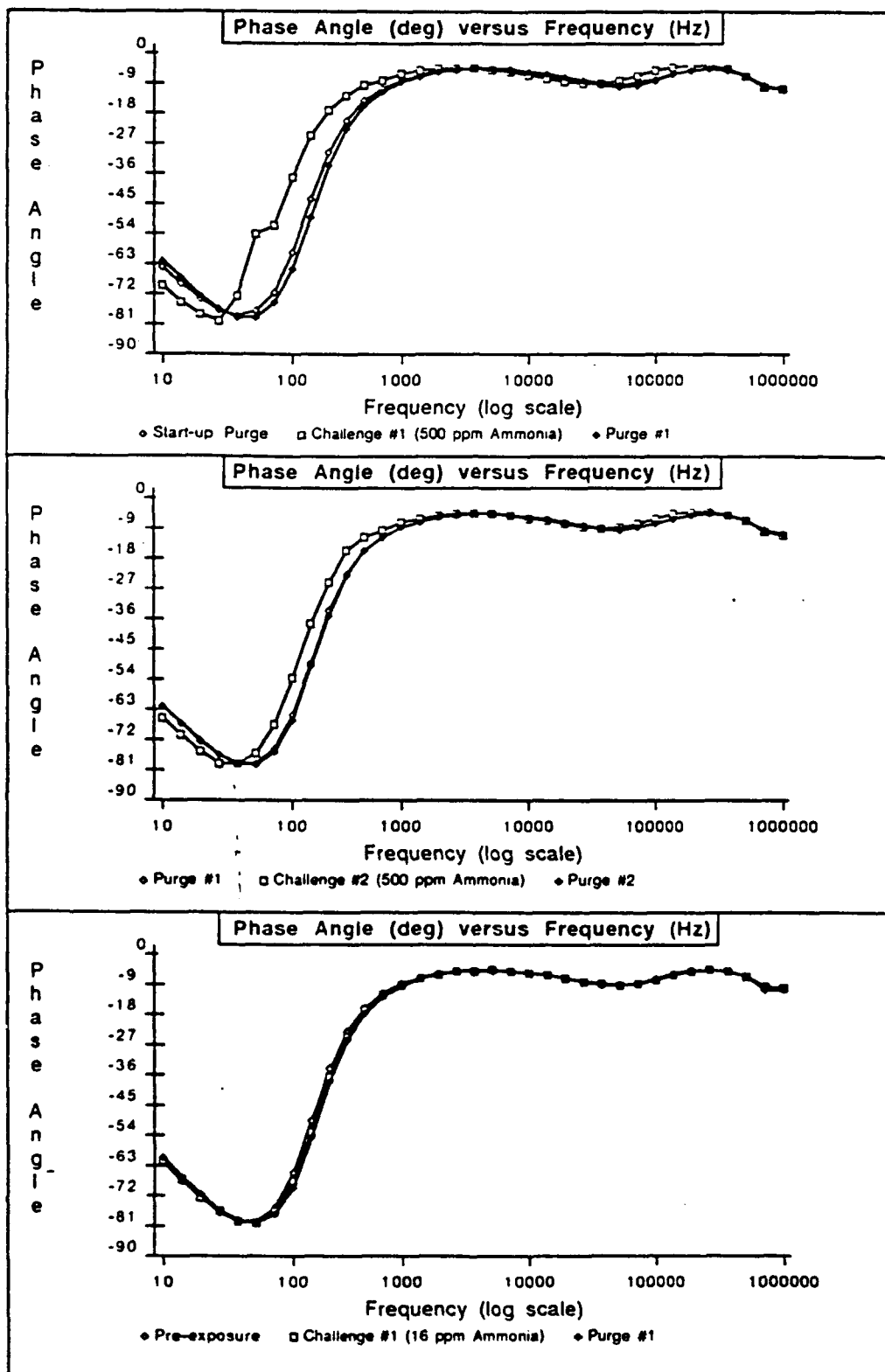


Figure V-16. Phase Angle versus Frequency Response of IGEFET Microsensor for a Series of Room Air Purges and Challenge Gas Exposures. Testing Conditions: IGE Microsensor Number 1; CuPc Thin-film (1.600 Angstroms Thick); Temperature of 150 degrees Centigrade; Ammonia Challenge Gas (Order of Exposures: 500 ppm, 16 ppm, 106 ppm, 250 ppm, 500 ppm).

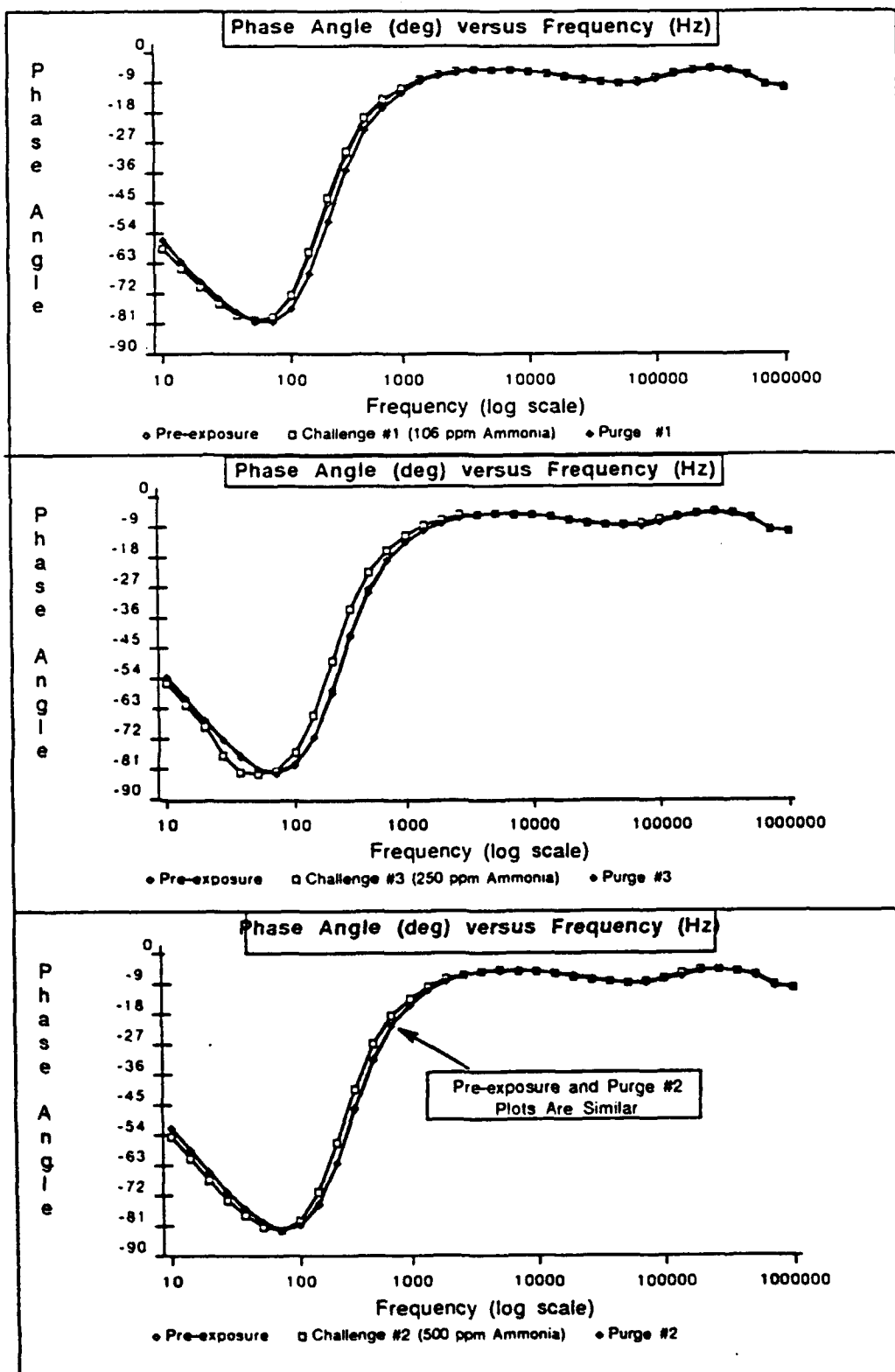


Figure V-17 Phase Angle versus Frequency Response of IGEFET Microsensor for a Series of Room Air Purges and Challenge Gas Exposures. Testing Conditions: IGE Microsensor Number 1; CuPc Thin-film (1,600 Angstroms Thick); Temperature of 150 degrees Centigrade; Ammonia Challenge Gas (Order of Exposures: 500 ppm, 16 ppm, 106 ppm, 250 ppm, 500 ppm).



exposures, decreasing to about -2.5 dB at 100 Hz. The peak change in the phase angle for the conditioning exposure is +18 degrees at 500 Hz. Again, upon subsequent 15 minutes duration exposures at 500 ppm, the magnitude of the change in phase is not as pronounced, peaking at approximately +3 degrees at 400 Hz.

*NiPc Thin-Film Response to NH<sub>3</sub>.* The dc resistance measurements increased slightly upon exposure to the NH<sub>3</sub>, with the activity slightly more pronounced with the thicker films. During the 1.25 hour duration preconditioning phase with the 500 ppm NH<sub>3</sub> challenge, the dc resistance of an NiPc (12,500 Å thick) thin-film increased from  $4.2 \times 10^8$  to  $5.6 \times 10^8$  ohms. During the same period, the signal transfer gain at 10 Hz changed by -1.8 dB. The phase angle response changed by -13 degrees at 10 Hz. However, subsequent 15 minutes duration exposures at 500 ppm produced gain changes on the order of less than -0.2 dB, and phase angle changes less than -1 degrees.

For an NiPc (12,500 Å thick) thin-film, plots of the change in gain versus frequency reveal the greatest change occurring near 40 Hz; nearly -2.4 dB below the preconditioning purge values. The magnitude of the change is not repeated for subsequent 500 ppm exposures, changing to

approximately -0.1 dB at 40 Hz. The peak change in the phase angle for the conditioning exposure is +9 degrees at 120 Hz. A subsequent 15 minutes duration exposure at 500 ppm, the magnitude of the change in phase was not as pronounced, peaking at approximately +1 degrees at 100 Hz.

*Nitrogen Dioxide Challenges.* The NO<sub>2</sub> challenges produced the most dramatic changes in the measured parameters relative to the other challenge gases at their respective concentrations. Generally, the CuPc and NiPc film types responded to the NO<sub>2</sub> challenges more strongly than the CoPc film. With all three film types, the observed changes included decreases in the sensor's dc resistance, and modulation of the transfer function was reflected in the gain and phase angle versus frequency plots. Table V-4 and V-5 summarize the resultant percentage changes in resistance for the three thin-film types when they were exposed to the NO<sub>2</sub> challenge gas. From these tables, the observation may be made that the CuPc changes the most when exposed to the NO<sub>2</sub> challenge under the Series II test conditions, followed by the NiPc thin-film. The CoPc thin-film is the least active. Detailed experimental results for the CuPc, CoPc, and NiPc films are summarized in Appendix C, Appendix D, and Appendix E,

respectively.

*CuPc Thin-Film Response to NO<sub>2</sub>.* The dc resistance measurements decreased during exposure to the NO<sub>2</sub> challenge, with the activity more prominent in the mid-range and thickest films. Detailed figures showing the dc resistance changes versus time while the sensors were exposed to NO<sub>2</sub> are presented in Appendix C. Figure V-18 shows the percent change in the dc resistance of three different thickness of CuPc thin-film for four concentrations of the NO<sub>2</sub> challenge. The sensor parameter changes were averaged, they are posted on Table V-4 and V-5. From these visual aids, the most active thin-film types and thicknesses can be identified. For the CuPc material, the most active thickness was the 3,900 Å (the medium thickness). A review of the data in Appendix C revealed several other items of interest.

During the 1.25 hour long preconditioning phase with a 1,000 ppb NO<sub>2</sub> challenge, the dc resistance of the CuPc (1,600 Å thick) thin-film decreased from  $2.2 \times 10^9$  to  $9.5 \times 10^8$  ohms (a -57% change relative to the preconditioning purge value). In comparison, a 3,900 Å thick CuPc film decreased from  $4 \times 10^9$  to  $8 \times 10^7$  ohms (a -98% change relative to the preconditioning purge value) while a 8,800 Å thick film's dc resistance

Table V-4

Average Percent Change in the DC Resistance Measurements of CuPc, CoPc, and NiPc Thin-Films at Three Different Thicknesses when Challenged with Nitrogen Dioxide.

CuPc Thickness(Å)	Percent Change in Resistance Due to a Nitrogen Dioxide Challenge at:				
	30 ppb	50 ppb	100 ppb	500 ppb	1000 ppb
1,600	13.1	8.2	19.6	52.9	67.8
<b>3,900</b>	<b>47.1</b>	<b>50.0</b>	<b>69.7</b>	<b>86.7</b>	<b>90.9</b>
8,800	39.3	38.2	54.6	74.3	83.8

CoPc Thickness(Å)	Percent Change in Resistance Due to a Nitrogen Dioxide Challenge at:				
	30 ppb	50 ppb	100 ppb	500 ppb	1000 ppb
<b>2,500</b>	<b>18.4</b>	<b>24.2</b>	<b>29.8</b>	<b>37.9</b>	<b>55.7</b>
5,400	15.1	14.4	24.1	32.0	50.6
10,500	7.0	19.1	27.4	34.2	50.1

NiPc Thickness(Å)	Percent Change in Resistance Due to a Nitrogen Dioxide Challenge at:				
	30 ppb	50 ppb	100 ppb	500 ppb	1000 ppb
2,600	48.3	52.4	58.1	68.1	<b>85.2</b>
<b>6,200</b>	<b>50.1</b>	<b>56.2</b>	<b>65.4</b>	<b>73.9</b>	84.9
12,500	23.5	52.0	62.5	70.8	81.6

Boldface Numbers Highlight the Greatest Changes.

Table V-5

Maximum Percent Changes in the DC Resistance Measurements of the CuPc, CoPc, and NiPc Thin-Films when Challenged with Nitrogen Dioxide.

Thin-Film Type and Thickness(Å)	Percent Change in Resistance Due to Nitrogen Dioxide Challenge at:				
	30 ppb	50 ppb	100 ppb	500 ppb	1000 ppb
CuPc 3,900	47.1	50.0	<b>69.7</b>	<b>86.7</b>	<b>90.9</b>
CoPc 2,500	18.4	24.2	29.8	37.9	55.7
NiPc 6,200	<b>50.1</b>	<b>56.2</b>	65.4	73.9	84.9

Boldface Numbers Highlight the Greatest Changes.

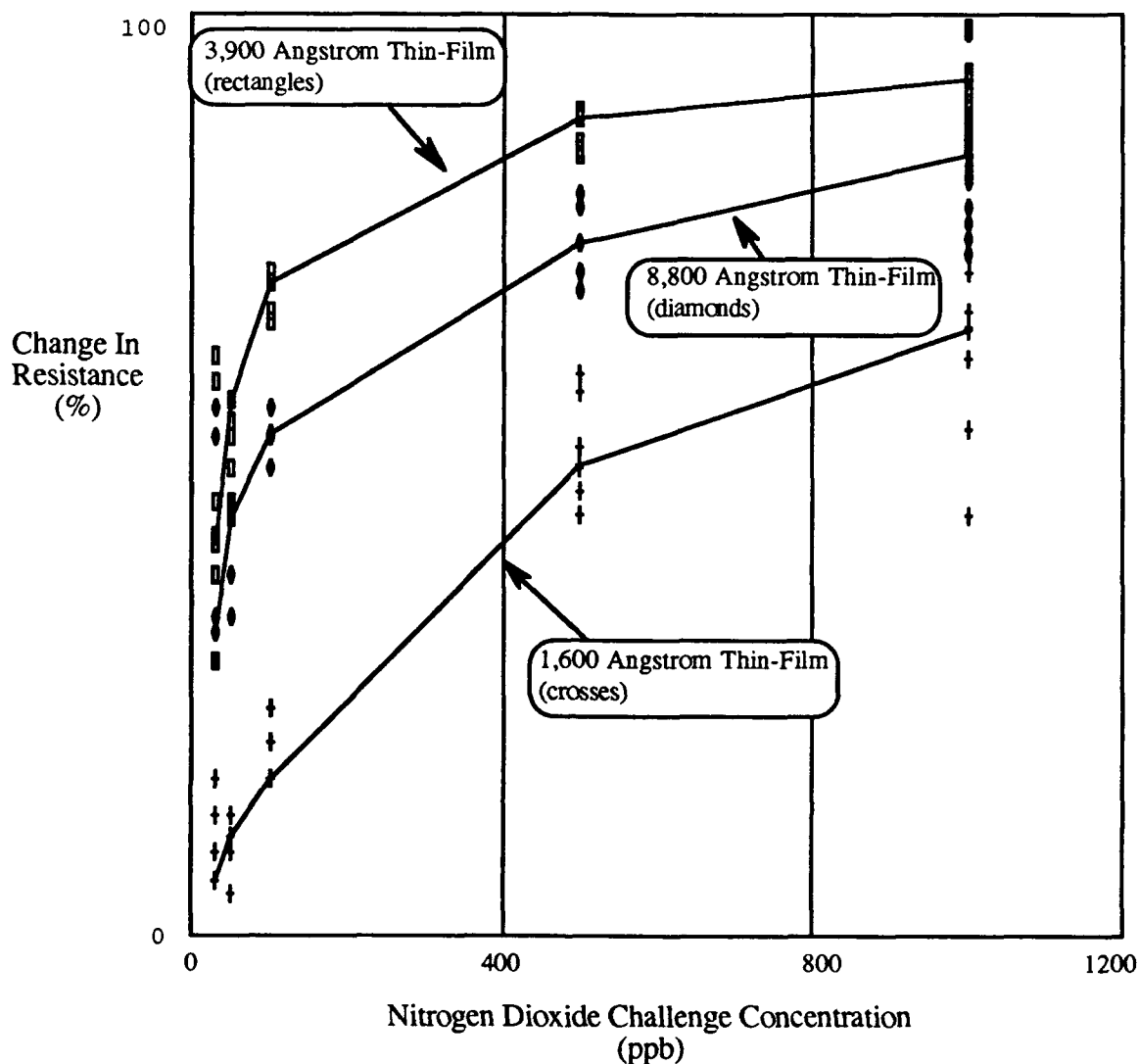


Figure V-18. Percentage Changes in CuPc DC Resistance Due to the Nitrogen Dioxide Challenge Gas Exposures, for Three Different Film Thicknesses. Test Conditions: CuPc Thin-Film Material (1,600 Å, 3,900 Å, and 8,800 Å Thick); Temperature of 150°C; Nitrogen Dioxide Challenge Gas (30 ppb, 50 ppb, 100 ppb, 500 ppb, and 1000 ppb). The Plotted Lines are Primarily a Visual Aid, Connecting Points Calculated from a Polynomial Curve Fit at the Five Challenge Concentrations for Each of the Film Thicknesses.

decreased from  $6 \times 10^8$  to  $1.4 \times 10^7$  ohms (a -98% change relative to the preconditioning purge). During the same period, the gain for the 1,600 Å thick film, at 10 Hz, increased approximately +30 dB. The phase angle response for the same exposure changed by nearly -60 degrees at 10 Hz. Subsequent 15 minutes duration exposures at 1,000 ppb continued to yield gain and phase angle changes at 10 Hz on the order of +30 dB and -54 degrees, respectively, for the 1,600 Å thick film.

A very dramatic contrast in the reversibility of the thinner (1,600 Å thick) versus the thicker (3,900 Å and 8,800 Å thick) films was observed. The resistance versus time plots in Appendix C readily show that the 1,600 Å thick film attains its purge equilibrium value in approximately 15 minutes after the cessation of a 1,000 ppb challenge. In contrast, the reversal of the thicker films was incomplete, even after a full hour of purge.

The frequency domain responses, in the form of gain and phase angle versus frequency for CuPc are presented in Figures V-19 to V-23. They clearly show the decrease in impedance due to the exposures with NO<sub>2</sub> at concentrations of 50 ppb and 1000 ppb.

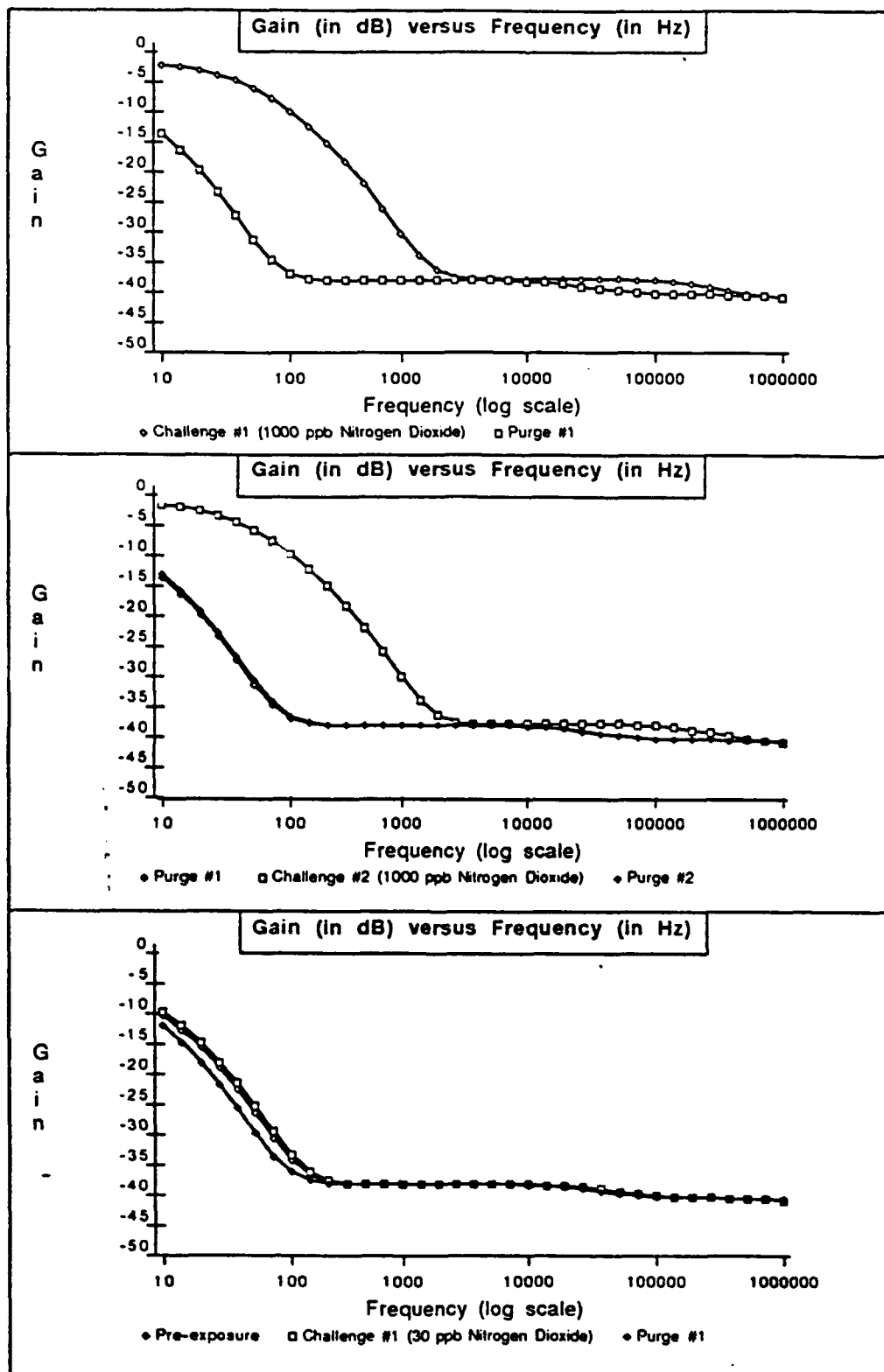


Figure V-19.. Gain versus Frequency Response of IGEFET Microsensor for a Series of Room Air Purges and Challenge Gas Exposures. Testing Conditions: IGE Microsensor Number 4; CuPc Thin-film (3,900 Angstroms Thick); Temperature of 150 degrees Centigrade; Nitrogen Dioxide Challenge Gas (Order of Exposures:1000 ppb, 30 ppb, 50

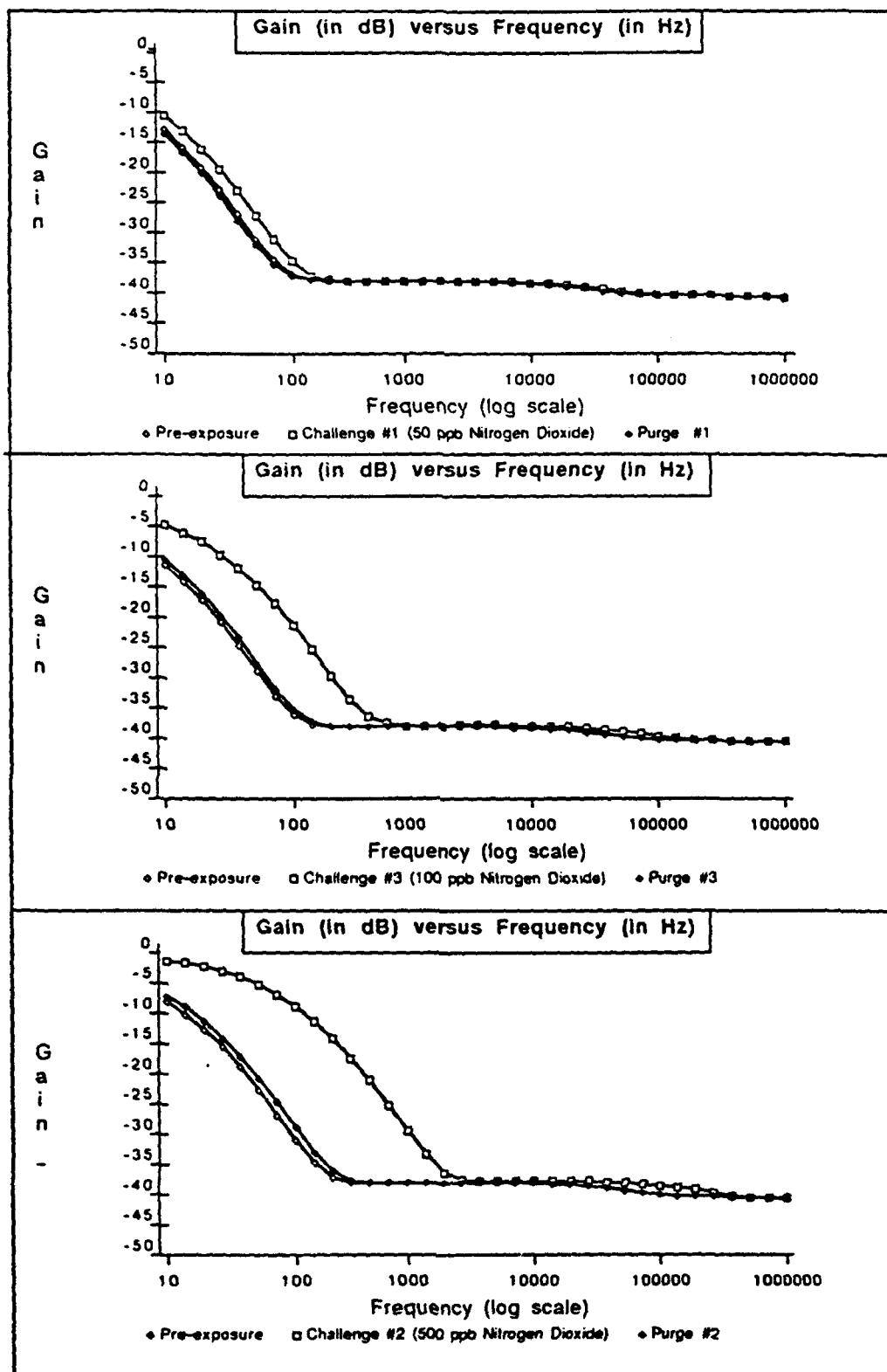


Figure V-20. Gain versus Frequency Response of IGEFET Microsensor for a Series of Room Air Purges and Challenge Gas Exposures. Testing Conditions: IGE Microsensor Number 4; CuPc Thin-film (3,900 Angstroms Thick); Temperature of 150 degrees Centigrade; Nitrogen Dioxide Challenge Gas (Order of Exposures: 1000 ppb, 30 ppb, 50 ppb, 100 ppb, 500 ppb, 1000 ppb).



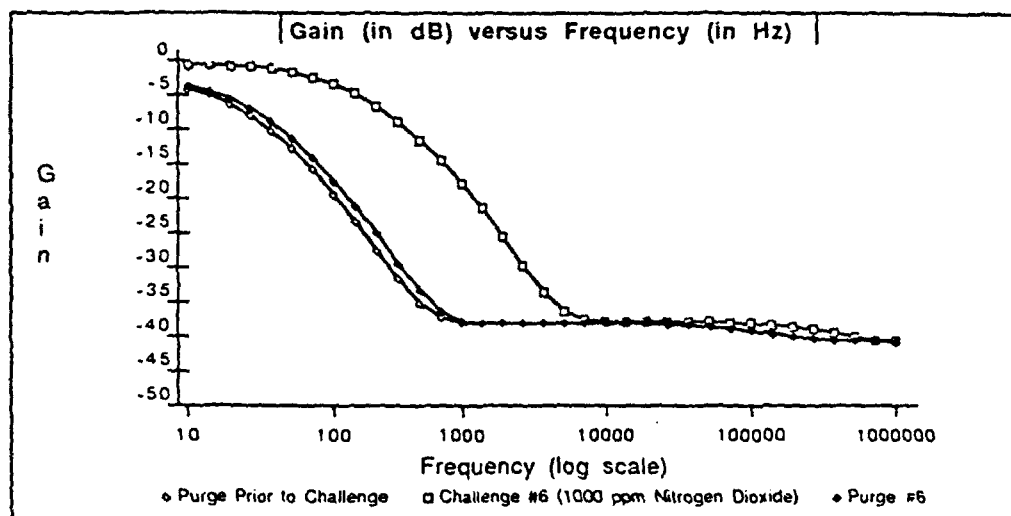


Figure V-21. Gain versus Frequency Response of IGEFET Microsensor for a Series of Room Air Purges and Challenge Gas Exposures. Testing Conditions: IGE Microsensor Number 4; CuPc Thin-film (3,900 Angstroms Thick); Temperature of 150 degrees Centigrade; Nitrogen Dioxide Challenge Gas (Order of Exposures: 1000 ppb, 30 ppb, 50 ppb, 100 ppb, 500 ppb, 1000 ppb).

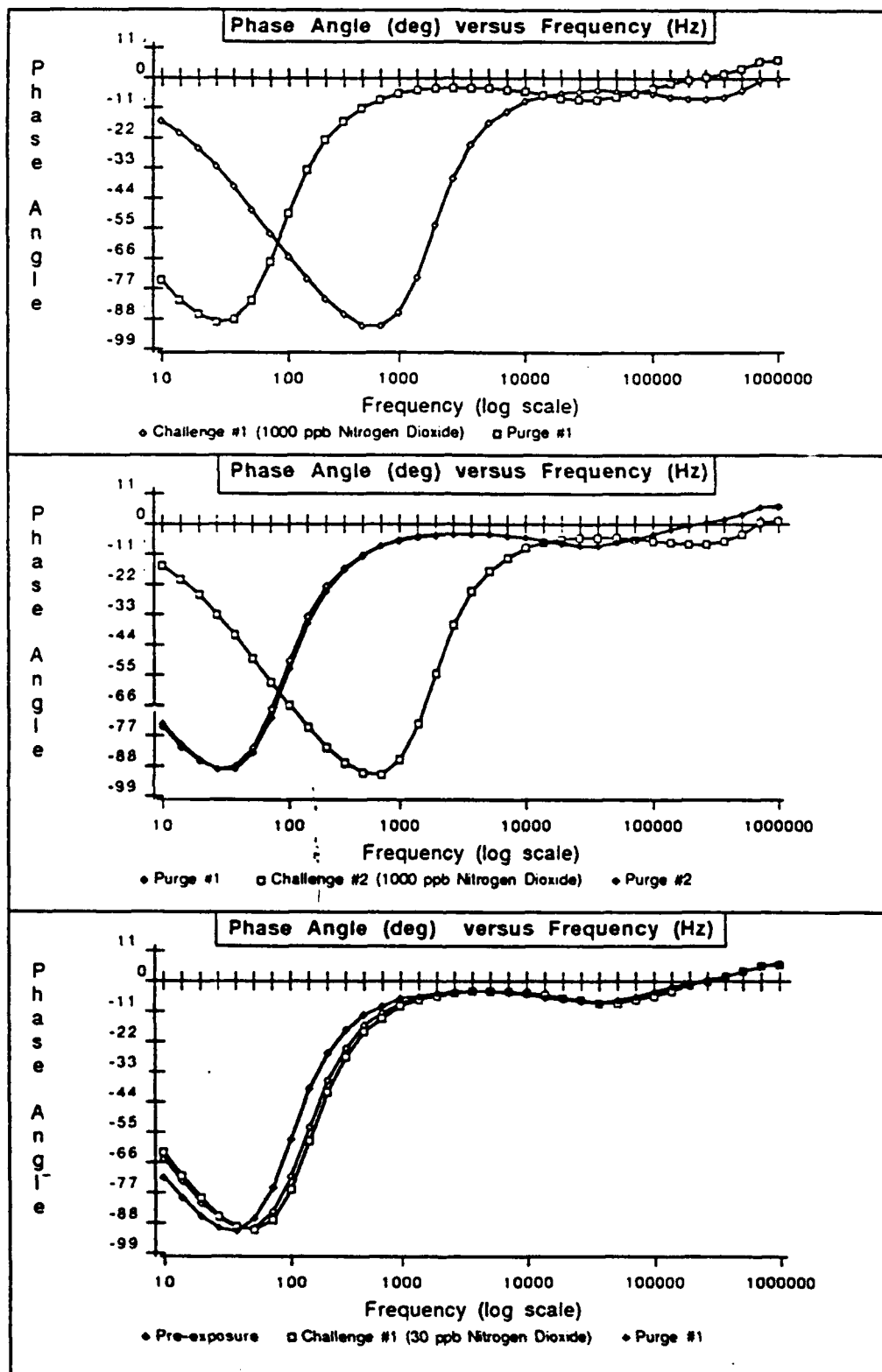


Figure V-22. Phase Angle versus Frequency Response of IGEFET Microsensor for a Series of Room Air Purges and Challenge Gas Exposures. Testing Conditions: IGE Microsensor Number 4; CuPc Thin-film (3,900 Angstroms Thick); Temperature of 150 degrees Centigrade; Nitrogen Dioxide Challenge Gas (Order of Exposures: 1000 ppb, 30 ppb, 50 ppb, 100 ppb, 500 ppb, 1000 ppb).

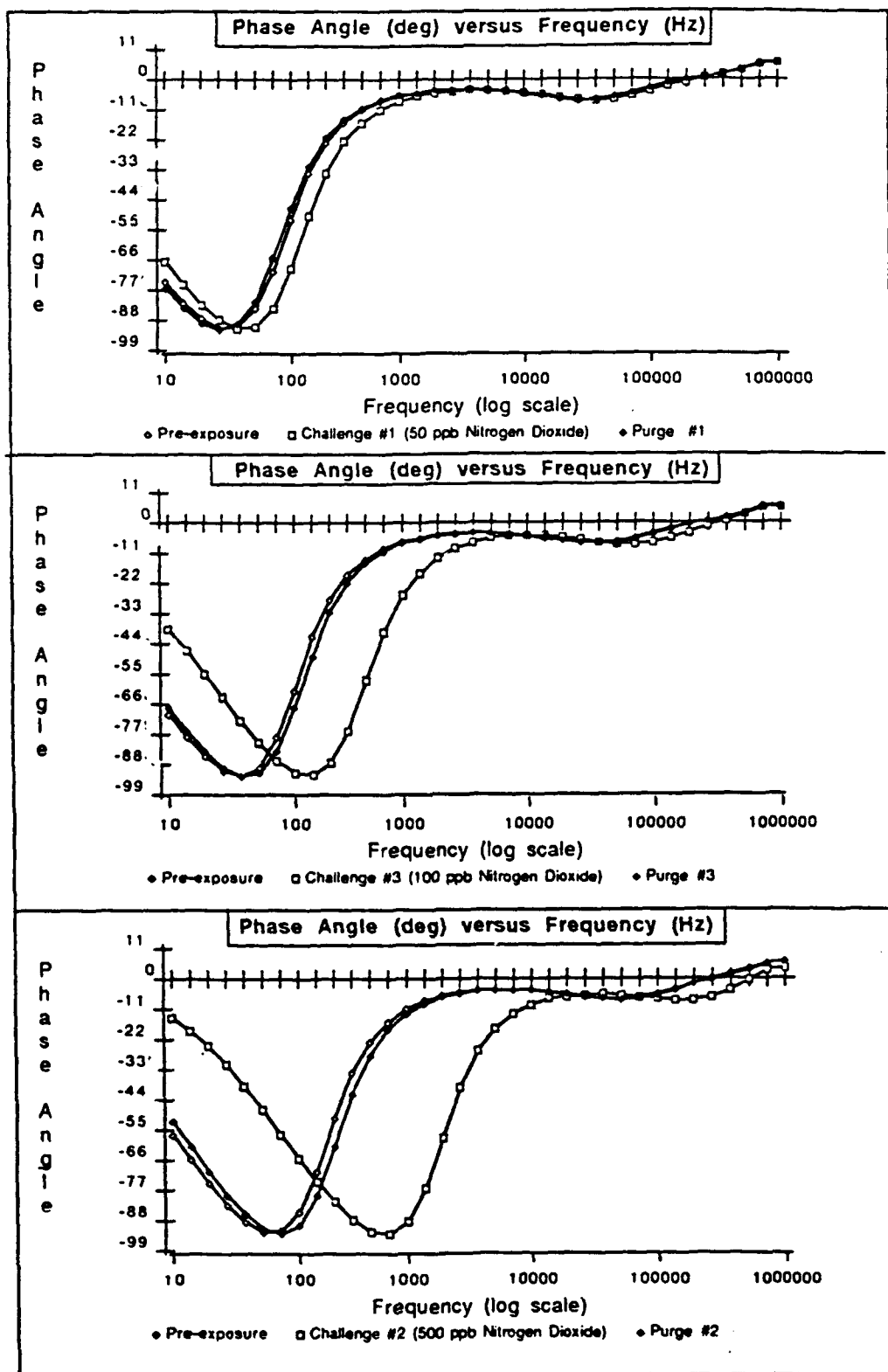


Figure V-23. Phase Angle versus Frequency Response of IGEFET Microsensor for a Series of Room Air Purges and Challenge Gas Exposures. Testing Conditions: IGE Microsensor Number 4; CuPc Thin-film (3,900 Angstroms Thick); Temperature of 150 degrees Centigrade; Nitrogen Dioxide Challenge Gas (Order of Exposures: 1000 ppb, 30 ppb, 50 ppb, 100 ppb, 500 ppb, 1000 ppb).

*CoPc Thin-Film Response to NO<sub>2</sub>.* The dc resistance measurements decreased during exposure to the NO<sub>2</sub>, with the activity being essentially uniform among the three film thicknesses. Detailed figures showing the dc resistance change versus time while the sensors were exposed to NO<sub>2</sub> are presented in Appendix C. Figure V-15 reveals that the percent change in the dc resistance of three different thicknesses of CoPc for the four concentrations of the NO<sub>2</sub> challenge. The sensors' dc resistance changes were averaged and are posted in Table V-4 and V-5. From these visual aids, the most active thin-film types and thicknesses can be identified. For the CoPc material, the most active thickness was the 2,500 Å thick film (the least thick). Review of the data in Appendix D revealed several other items of interest.

During the 1.25 hour duration preconditioning phase with the 1,000 ppb NO<sub>2</sub> challenge, the dc resistance the 2,500 Å thick CoPc thin-film decreased from  $2.8 \times 10^8$  to  $8 \times 10^7$  ohms (a -72% change relative to the preconditioning purge value). By comparison, the 5,400 Å thick CoPc film's dc resistance decreased from  $1.8 \times 10^7$  to  $6.0 \times 10^6$  ohms (a -67% change relative to the preconditioning purge value) while the 10,500 Å

thick CoPc film changed from  $1.6 \times 10^7$  to  $5.2 \times 10^6$  ohms (a -68% change relative to the preconditioning purge). During the same period, the signal transfer gain for the 2,500 Å thick CoPc thin-film at 10 Hz increased by +2.5 dB. The phase angle response during the same exposure changed by nearly +15 degrees at 10 Hz. Subsequent 15 minutes duration exposures at 1,000 ppb continued to yield gain and phase angle changes at 10 Hz on the order of +2.0 dB and +11 degrees, respectively, for the 2,500 Å thick CoPc thin-film.

The peak change in the gain for the 2,500 Å thick CoPc thin-film occurred at 700 Hz with a value of +10 dB as measured relative to the preconditioning purge. The peak phase angle change of -4 degrees occurred at 2000 Hz. For subsequent exposures at 1,000 ppb, the magnitudes of the changes decreased, but the frequency where the peak change occurred remained the same. For the 1,000 ppb exposures of the 5,400 Å thick films, the gain and phase angle frequencies associated with the peak changes were 7,000 Hz and 1,000 Hz, respectively. The peak change frequencies for the 10,500 Å thick films, under the same test conditions were 10,700 Hz and 2,200 Hz, respectively.

The dramatic contrast in the reversibility of the CoPc thin films versus the thicker CoPc films was not observed. The resistance versus time

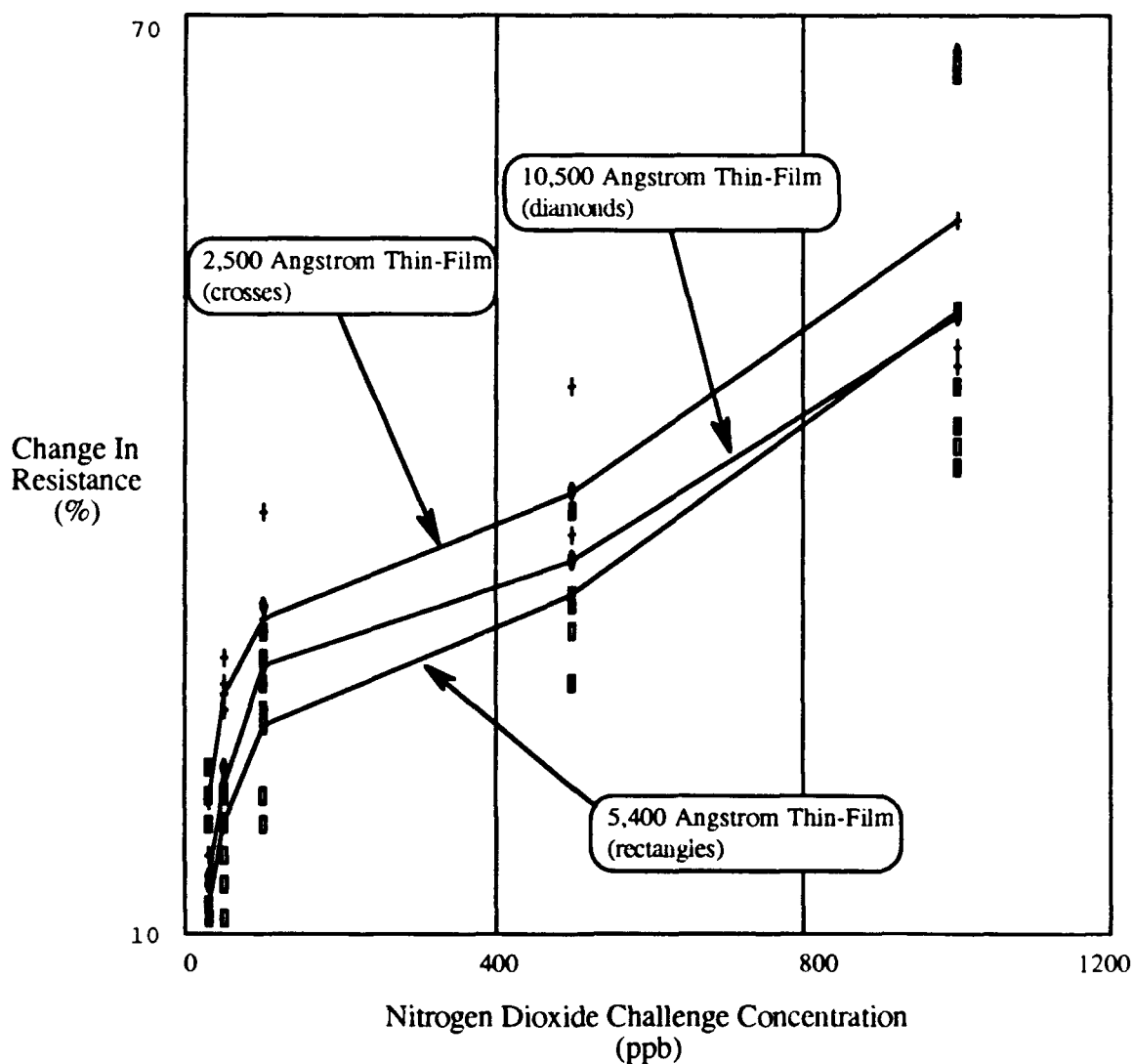


Figure V-24. Percentage Change in CoPc DC Resistance Due to the Nitrogen Dioxide Challenge Gas Exposures, for Three Different Film Thicknesses. Test Conditions: CoPc Thin-Film Material (2,500 Å, 5,400 Å, and 10,500 Å Thick); Temperature of 150°C; Nitrogen Dioxide Challenge Gas (30 ppb, 50 ppb, 100 ppb, 500 ppb, and 1000 ppb). The Plotted Lines are Primarily a Visual Aid, Connecting Points Calculated from a Polynomial Curve Fit at the Five Challenge Concentrations for Each of the Film Thicknesses.

plots in Appendix D readily show that the reversals of the three films are incomplete, even after one full hour of purge.

The frequency domain responses, in the form of gain and phase angle versus frequency for CoPc thin-film are presented in Figures V-25 to V-30. They clearly show the decrease in impedance due to the exposures with NO<sub>2</sub> at concentrations of 50 ppb and 1000 ppb.

*NiPc Thin-Film Response to NO<sub>2</sub>.* The dc resistance measurements decreased during exposure to the NO<sub>2</sub>, with the activity more pronounced in the thicker films. Detailed figures showing the dc resistance change versus time while the sensors were exposed to NO<sub>2</sub> are presented in Appendix C. Figure V-31 shows the percent change in the dc resistance of three different thicknesses of NiPc thin-films relative to the four concentrations of the NO<sub>2</sub> challenge. The sensors' dc resistance changes were averaged, and they are presented on Tables V-4 and V-5. From these visual aids, the most active thin-film types and thicknesses can be identified. For the NiPc material, the most active thickness was the 6,200 Å thin-film (the medium thickness). A review of the material in Appendix E revealed several other items of interest.

During the 1.25 hour duration preconditioning phase with 1,000 ppb

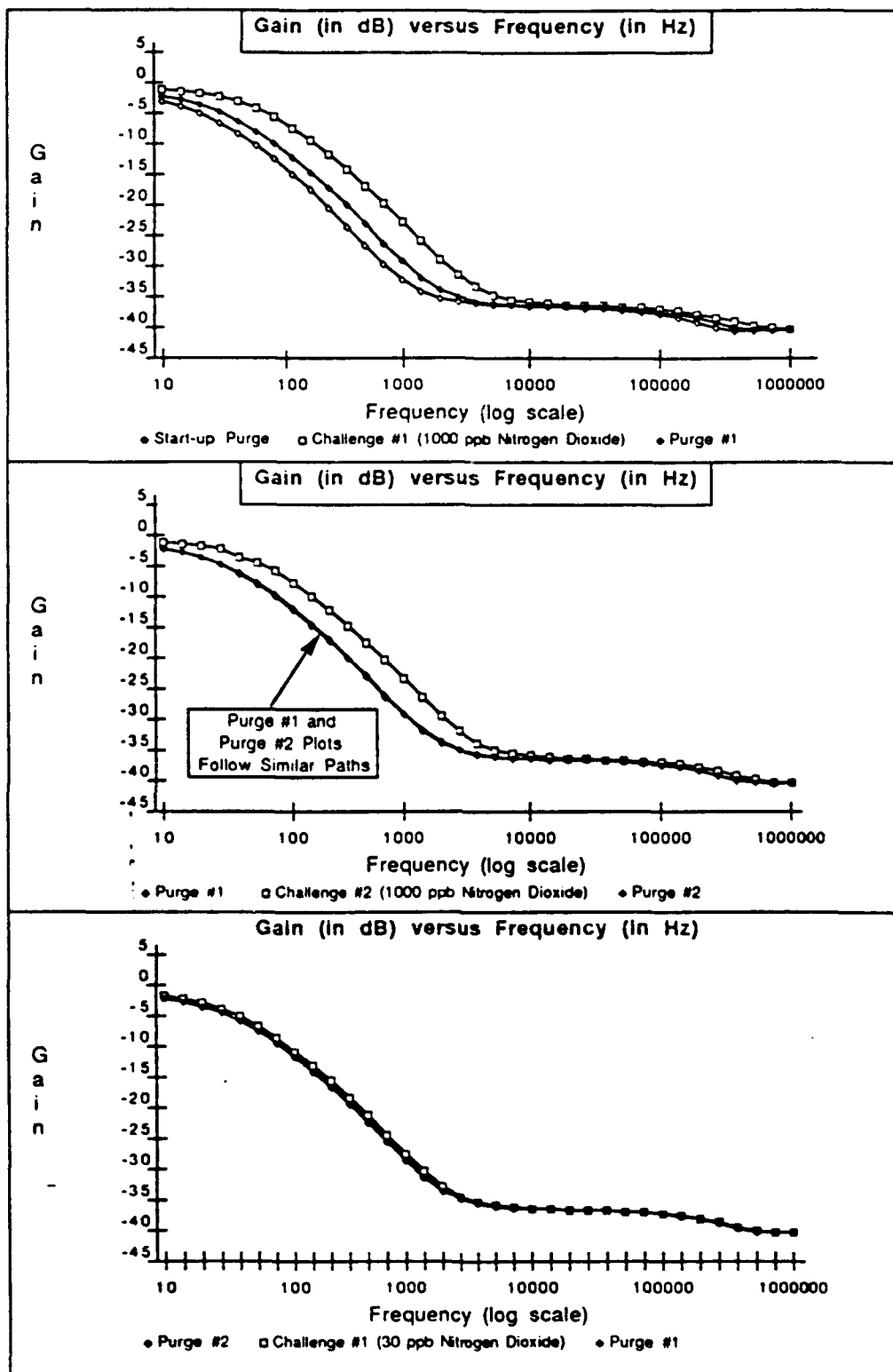


Figure V-25. Gain versus Frequency Response of IGEFET Microsensor for a Series of Room Air Purges and Challenge Gas Exposures. Testing Conditions: IGE Microsensor Number 1; CoPc Thin-film (2,500 Angstroms Thick); Temperature of 150 degrees Centigrade; Nitrogen Dioxide Challenge Gas (Order of Exposures: 1000 ppb, 30 ppb, 50 ppb, 100 ppb, 500 ppb, 1000 ppb).



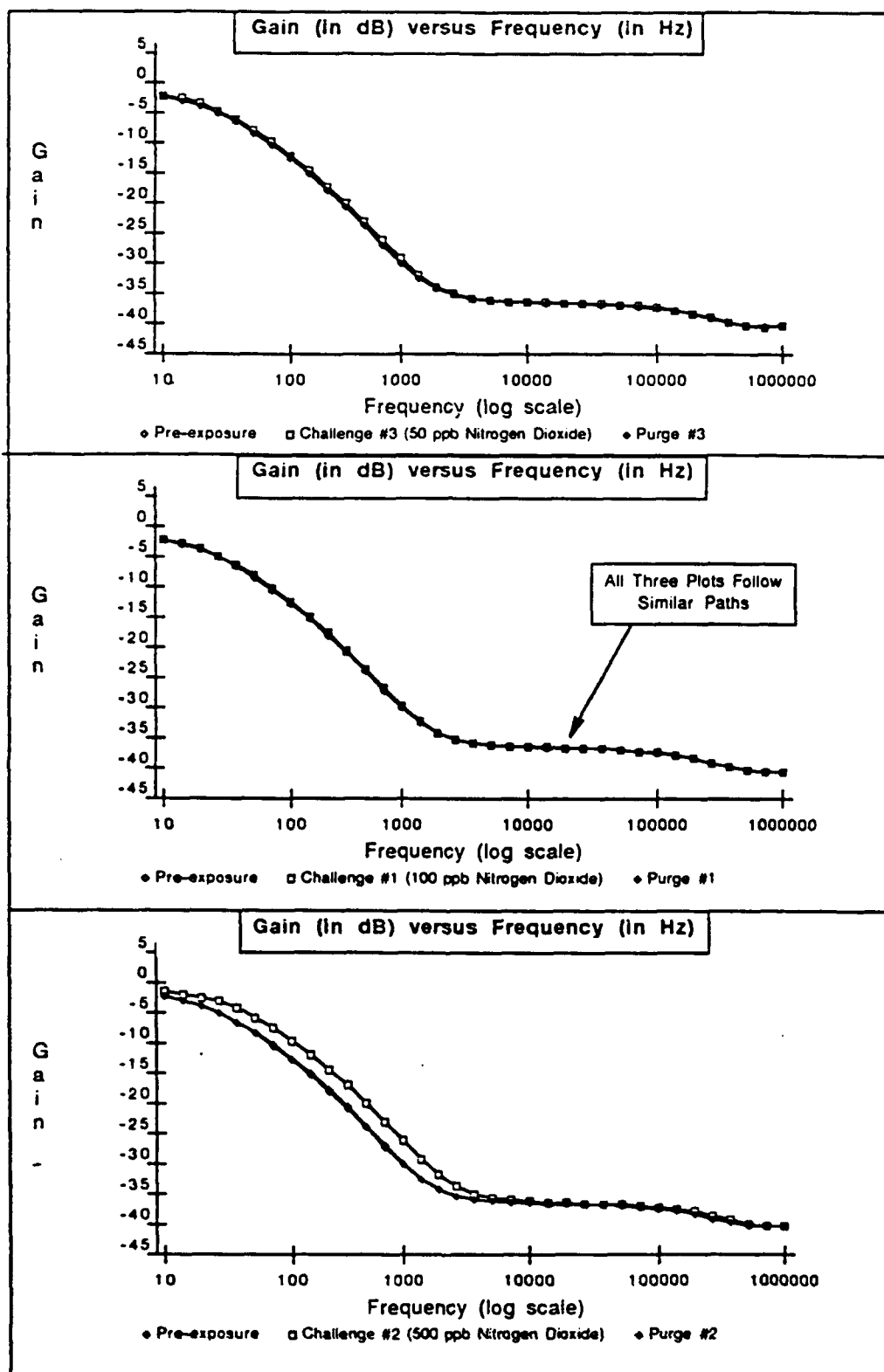


Figure V-26. Gain versus Frequency Response of IGEFET Microsensor for a Series of Room Air Purges and Challenge Gas Exposures. Testing Conditions: IGE Microsensor Number 1; CoPc Thin-film (2,500 Angstroms Thick); Temperature of 150 degrees Centigrade; Nitrogen Dioxide Challenge Gas (Order of Exposures: 1000 ppb, 30 ppb, 100 ppb, 500 ppb, 1000 ppb).

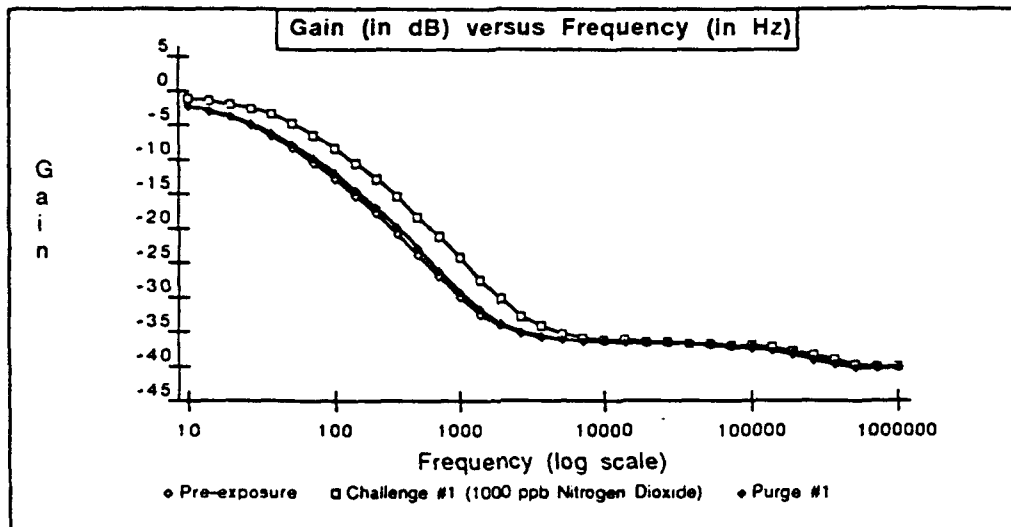


Figure V-27. . Gain versus Frequency Response of IGEFET Microsensor for a Series of Room Air Purges and Challenge Gas Exposures. Testing Conditions: IGE Microsensor Number 1; CoPc Thin-film (2,500 Angstroms Thick); Temperature of 150 degrees Centigrade; Nitrogen Dioxide Challenge Gas (Order of Exposures: 1000 ppb, 30 ppb, 100 ppb, 500 ppb, 1000 ppb).

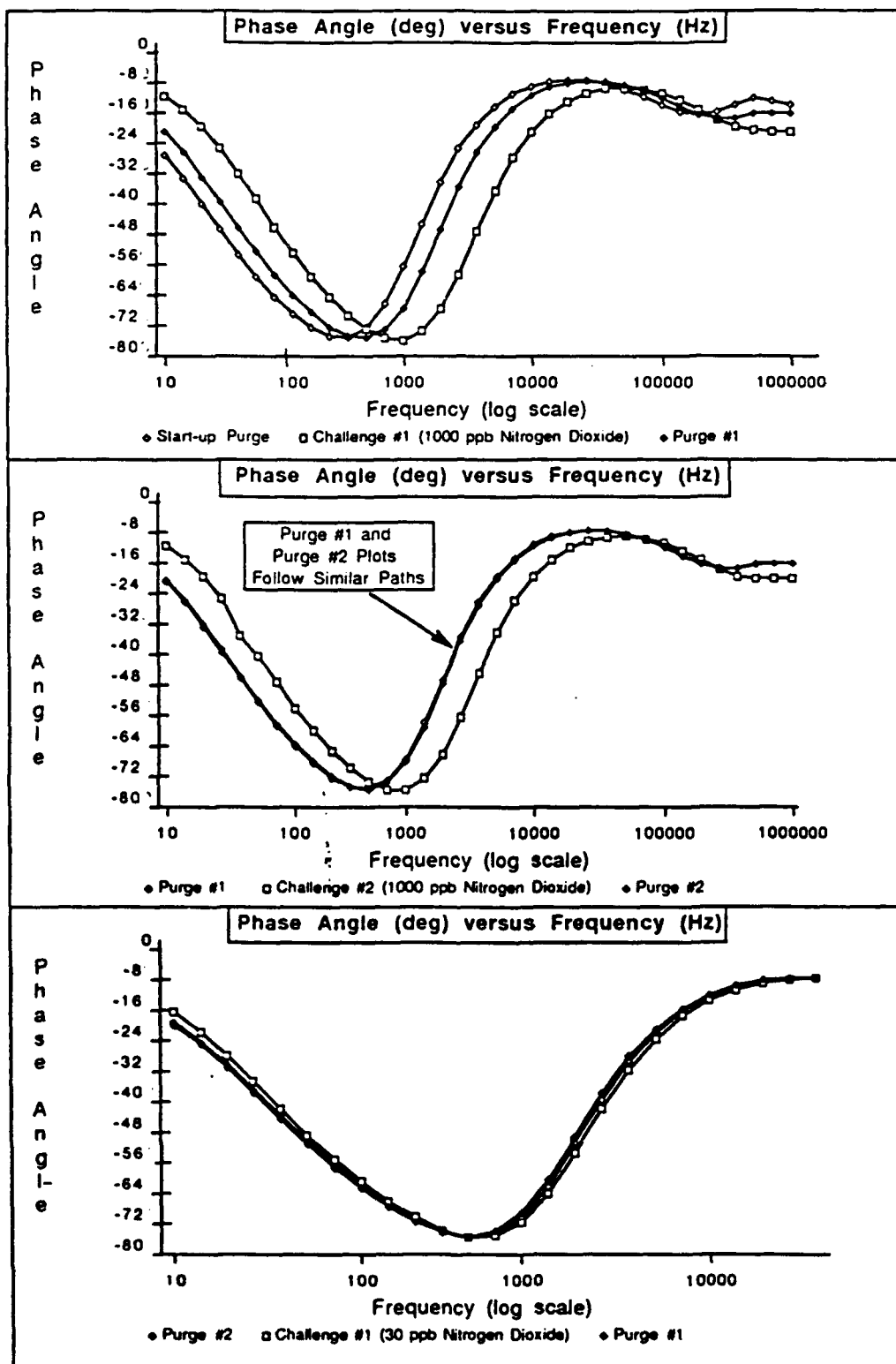


Figure V-28. . Phase Angle versus Frequency Response of IGFET Microsensor for a Series of Room Air Purges and Challenge Gas Exposures. Testing Conditions: IGE Microsensor Number 1: CoPc Thin-film (2,500 Angstroms Thick); Temperature of 150 degrees Centigrade; Nitrogen Dioxide Challenge Gas (Order of Exposures: 1000 ppb, 30 ppb, 50 ppb, 100 ppb, 500 ppb, 1000 ppb).

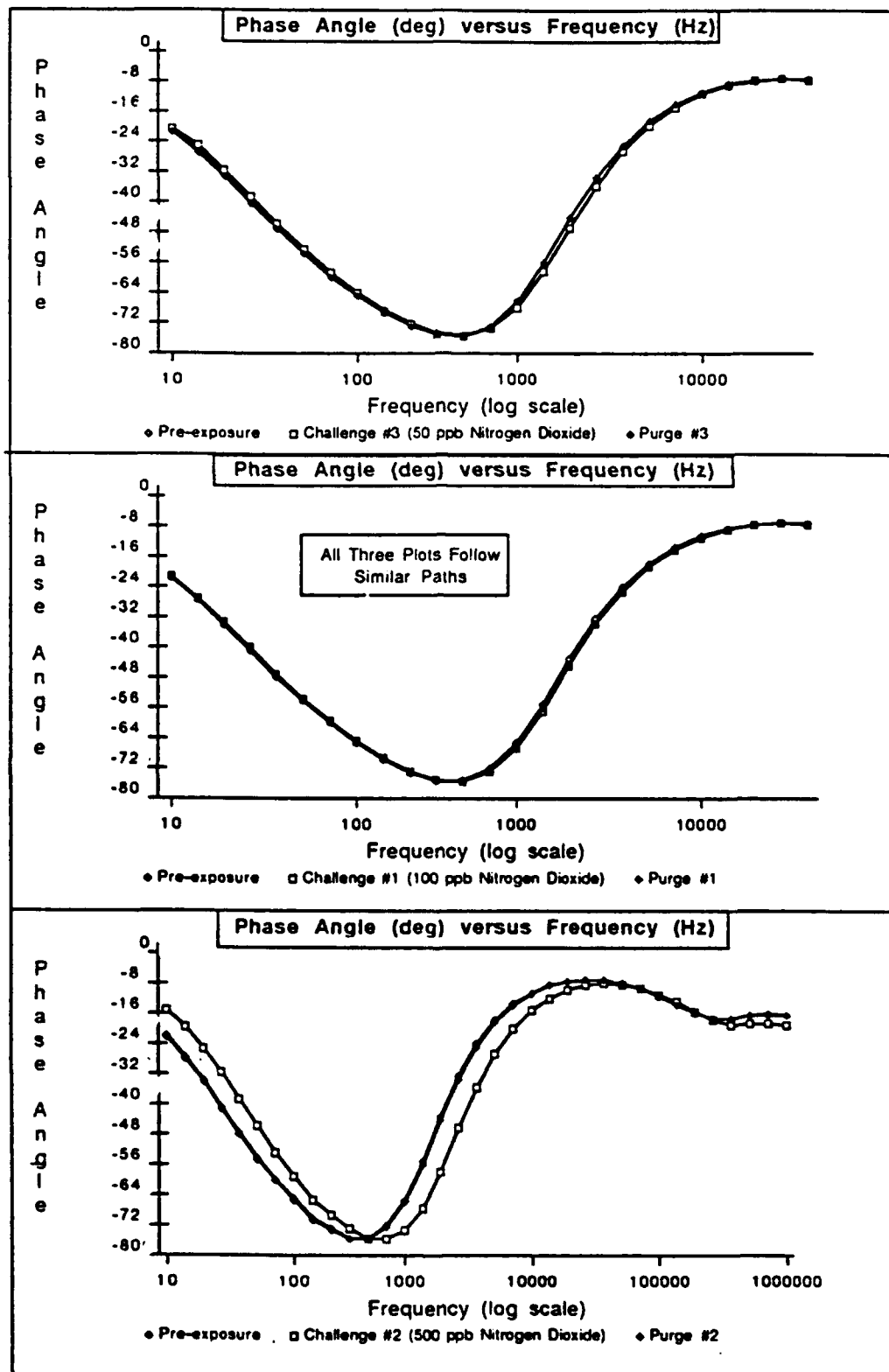


Figure V-29. . Phase Angle versus Frequency Response of IGEFET Microsensor for a Series of Room Air Purges and Challenge Gas Exposures. Testing Conditions: IGE Microsensor Number 1; CoPc Thin-film (2,500 Angstroms Thick); Temperature of 150 degrees Centigrade; Nitrogen Dioxide Challenge Gas (Order of Exposures: 1000 ppb, 30 ppb, 100 ppb, 500 ppb, 1000 ppb).

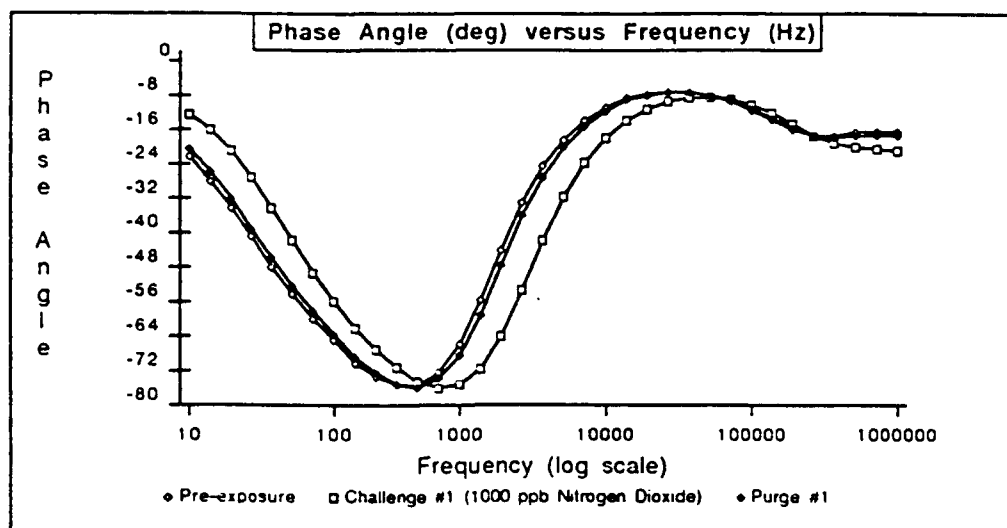


Figure V-30. . Phase Angle versus Frequency Response of IGEFET Microsensor for a Series of Room Air Purges and Challenge Gas Exposures. Testing Conditions: IGE Microsensor Number 1; CoPc Thin-film (2,500 Angstroms Thick); Temperature of 150 degrees Centigrade; Nitrogen Dioxide Challenge Gas (Order of Exposures: 1000 ppb, 30 ppb, 100 ppb, 500 ppb, 1000 ppb).

of NO<sub>2</sub>, the dc resistance of the 2,600 Å thick film decreased from  $3 \times 10^9$  to  $3 \times 10^8$  ohms (a -90% change relative to the preconditioning purge value). By comparison, a 6,200 Å thick NiPc film decreased from  $1.8 \times 10^9$  to  $4.0 \times 10^7$  ohms (a -98% change relative to the preconditioning purge value) while a 12,500 Å thick film decreased from  $1.2 \times 10^9$  to  $2.9 \times 10^7$  ohms (a -98% change relative to the preconditioning purge). During the same period the gain for the 2,600 Å thick film at 10 Hz changed by +33 dB. The phase angle response during the same exposure changed by more than -50 degrees at 10 Hz. Subsequent 15 minutes duration exposures at 1,000 ppb continued to yield gain and phase angle changes at 10 Hz on the order of +22 dB and +45 degrees, respectively, for the 2,600 Å thick film. The peak change in the gain relative to the preconditioning purge for the 2,600 Å thick film occurred slightly less than 10 Hz. That is, the peak phase angle change of -75 degrees occurred at 90 Hz. For subsequent exposures at 1,000 ppb, the magnitudes of these changes decreased, and the peak frequencies also shifted. That is, the peak gain change occurred at 30 Hz, and the peak phase angle change occurred at 150 Hz. For the 1,000 ppb exposures of the 6,200 Å thick NiPc films, the gain and phase angle peak frequencies were 100 Hz and 800 Hz, respectively.

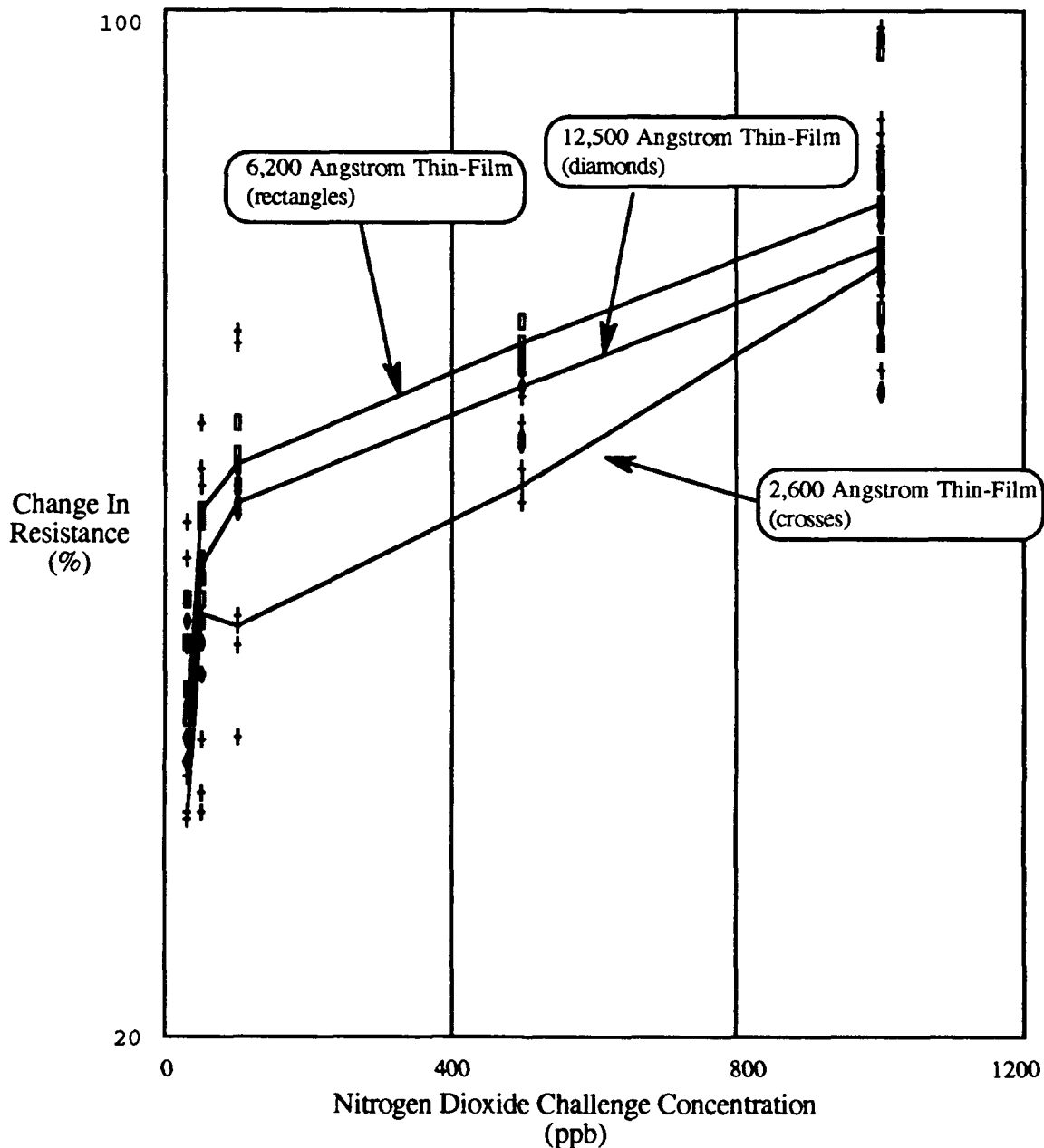


Figure V-31. Percentage Change in NiPc DC Resistance Due to the Nitrogen Dioxide Challenge Gas Exposures for Three Different Film Thicknesses. Test Conditions: NiPc Thin-Film Material (2,600 Å, 6,200 Å, and 12,500 Å Thick); Temperature of 150°C; Nitrogen Dioxide Challenge Gas (30 ppb, 50 ppb, 100 ppb, 500 ppb, and 1000 ppb). The Plotted Lines are Primarily a Visual Aid, Connecting Points Calculated from a Polynomial Curve Fit at the Five Challenge Concentrations for Each of the Film Thicknesses.

The peak frequencies for the 12,500 Å thick film under the same test conditions were 800 Hz and 2,000 Hz, respectively.

The frequency domain responses, in the form of gain and phase angle versus frequency for the NiPc thin-film are presented in Figures V-32 to V-36. They clearly show the decreases in impedance due to exposures to NO<sub>2</sub> at concentrations of 50 ppb and 1000 ppb.

The contrast in the degree of reversibility of the thin films versus the thicker films that was noted with the CuPc material was manifested in the NiPc films, but not with the same level of contrast. The resistance versus time plots in Appendix E readily show that the thinnest film is more nearly equilibrated at the end of the one hour duration purges compared to either of the thicker films. The thicker films never achieve a purge equilibrium response, even after one hour of purge.

#### *Results of the Series III Gas Challenge Experiments.*

After completing the Series II tests, the effect of changing the thin-film temperature on the modulation of the thin-films by DMMP and DIMP was accomplished. The maximum concentrations of the respective gases that the permeation tubes could generate were utilized. The results for the CuPc, CoPc, and NiPc thin-films are in Appendices C, D, and E, respectively. The test series began with a lengthy room air purge at 150°C.





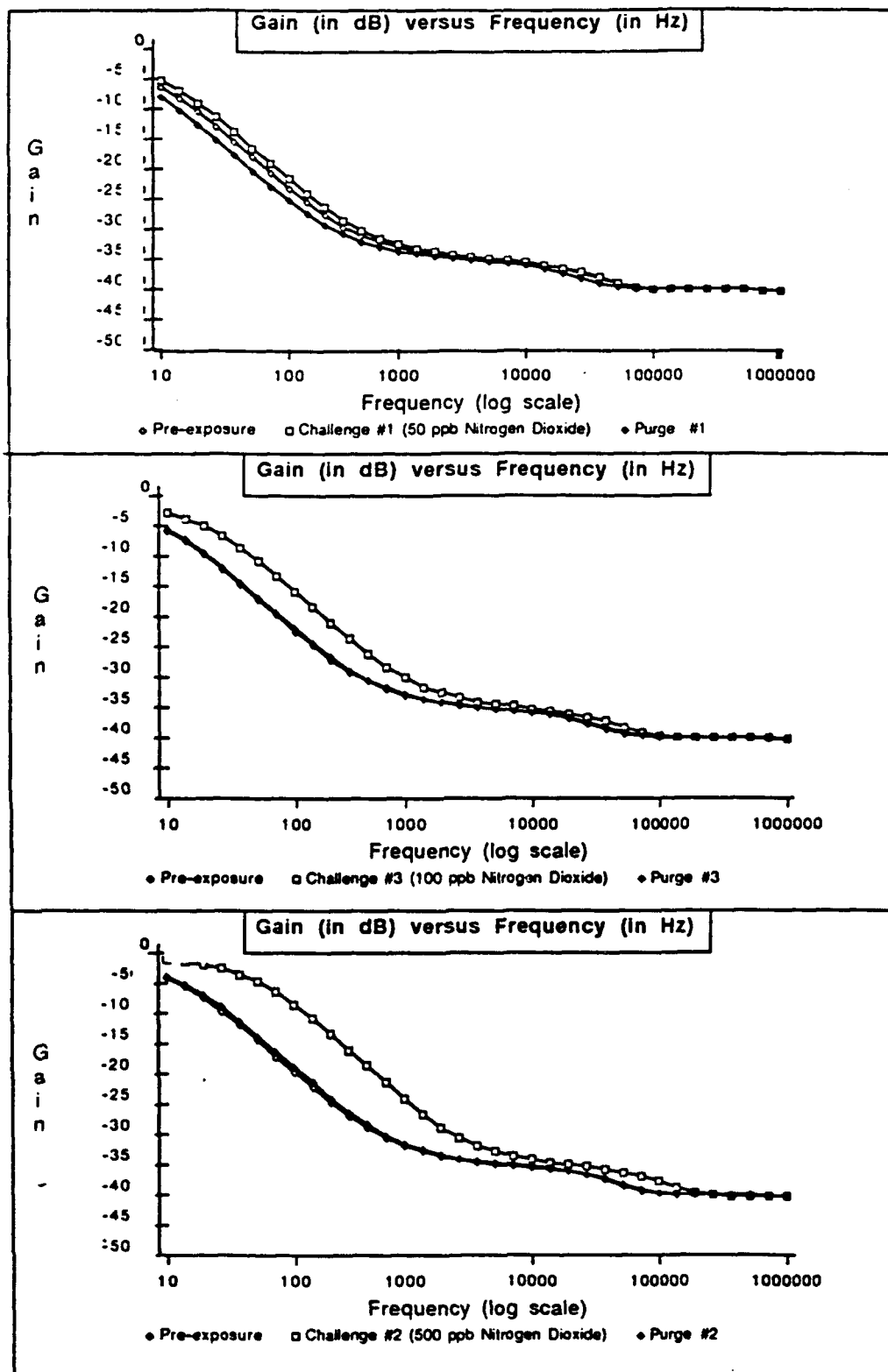


Figure V-33. Gain versus Frequency Response of IGEFET Microsensor for a Series of Room Air Purges and Challenge Gas Exposures. Testing Conditions: IGE Microsensor Number 4; NiPc Thin-film (6,200 Angstroms Thick); Temperature of 150 degrees Centigrade; Nitrogen Dioxide Challenge Gas (Order of Exposures: 1000 ppb, 30 ppb, 50 ppb, 100 ppb, 500 ppb, 1000 ppb).

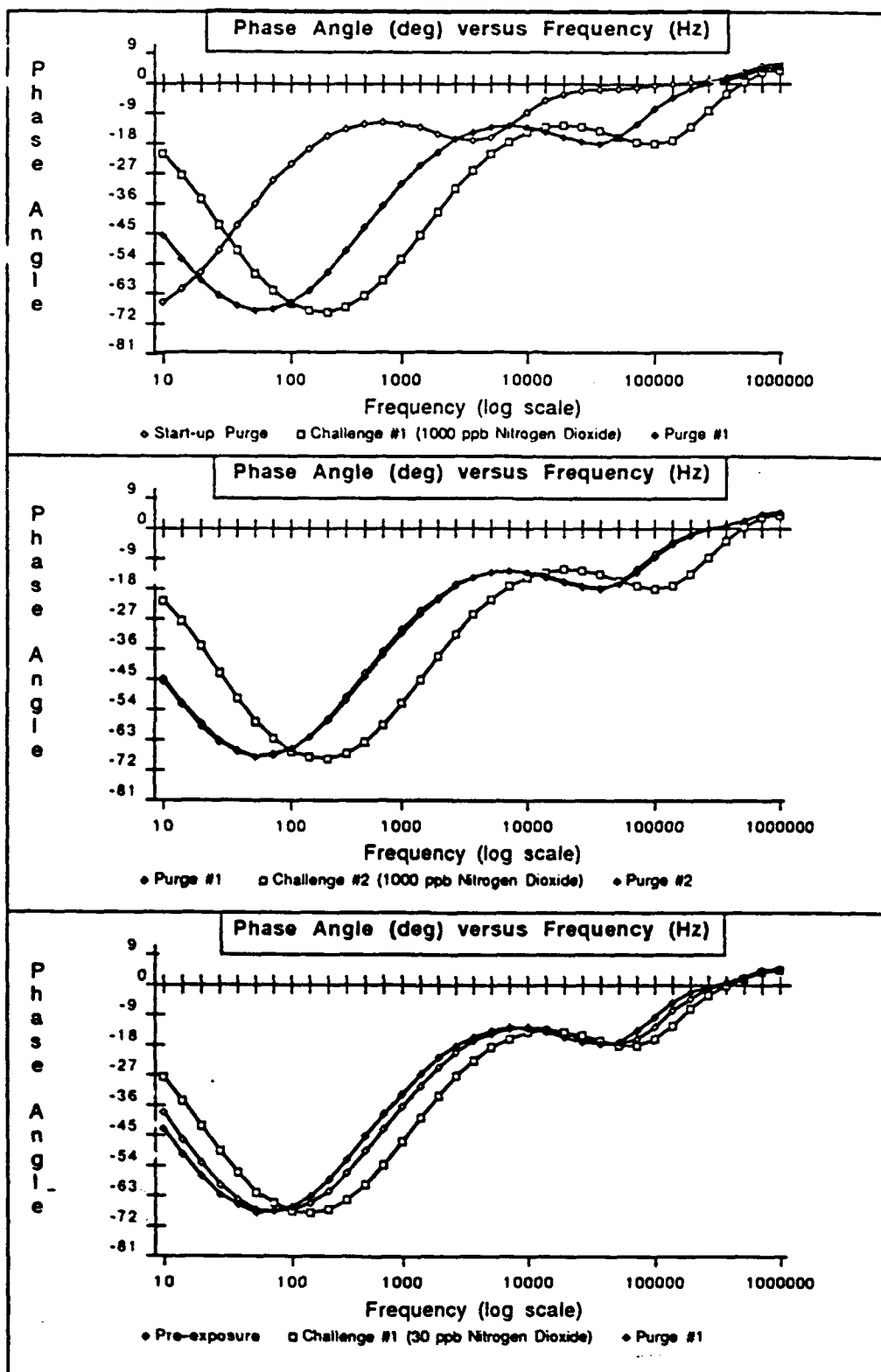


Figure V-34. Phase Angle versus Frequency Response of IGEFET Microsensor for a Series of Room Air Purges and Challenge Gas Exposures. Testing Conditions: IGE Microsensor Number 4; NiPc Thin-film (6,200 Angstroms Thick); Temperature of 150 degrees Centigrade; Nitrogen Dioxide Challenge Gas (Order of Exposures: 1000 ppb, 30 ppb, 50 ppb, 100 ppb, 500 ppb, 1000 ppb).

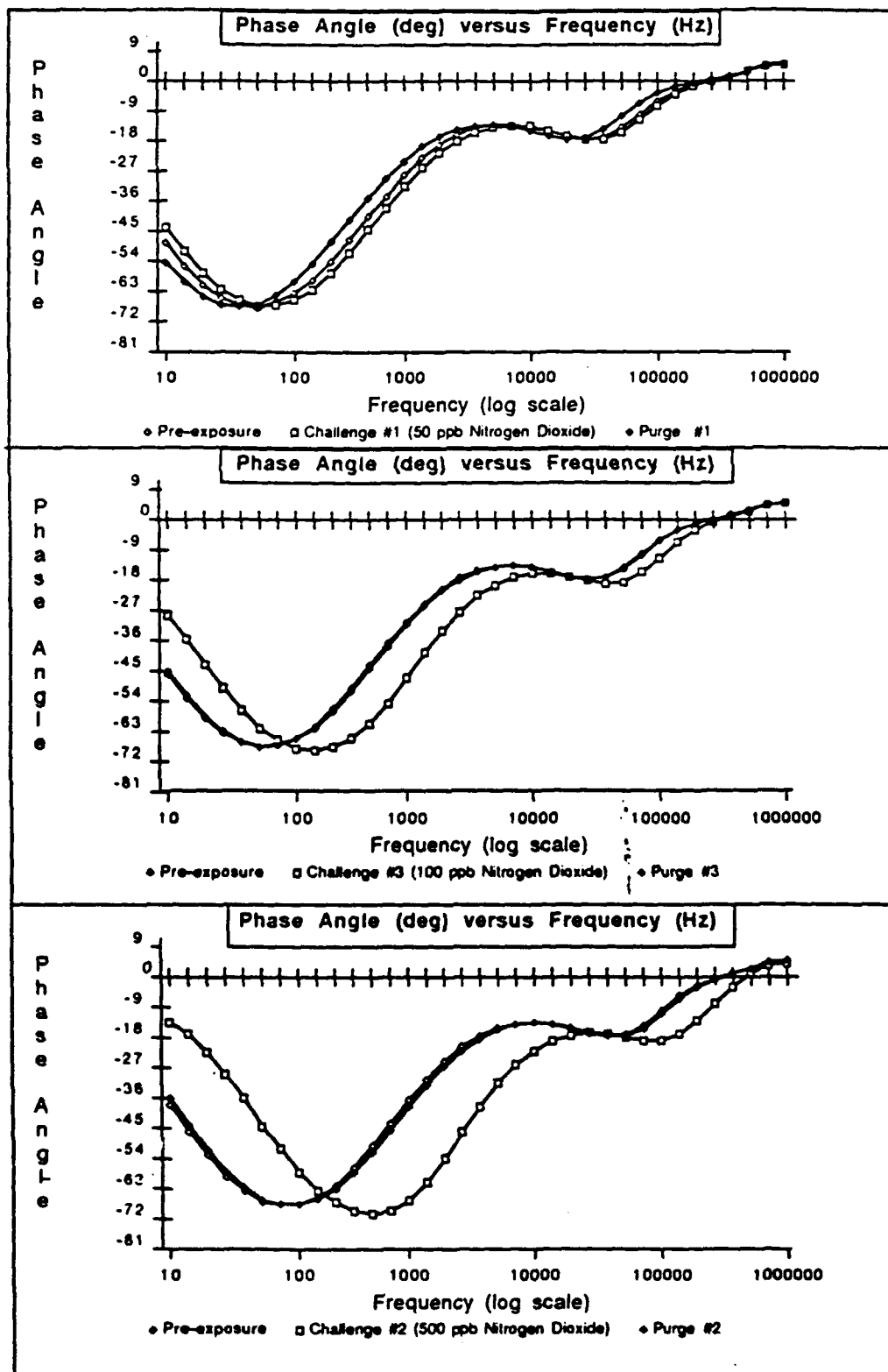


Figure V-35. Phase Angle versus Frequency Response of IGEFET Microsensor for a Series of Room Air Purges and Challenge Gas Exposures. Testing Conditions: IGE Microsensor Number 4; NiPc Thin-film (6,200 Angstroms Thick); Temperature of 150 degrees Centigrade; Nitrogen Dioxide Challenge Gas (Order of Exposures: 1000 ppb, 30 ppb, 50 ppb, 100 ppb, 500 ppb, 1000 ppb).

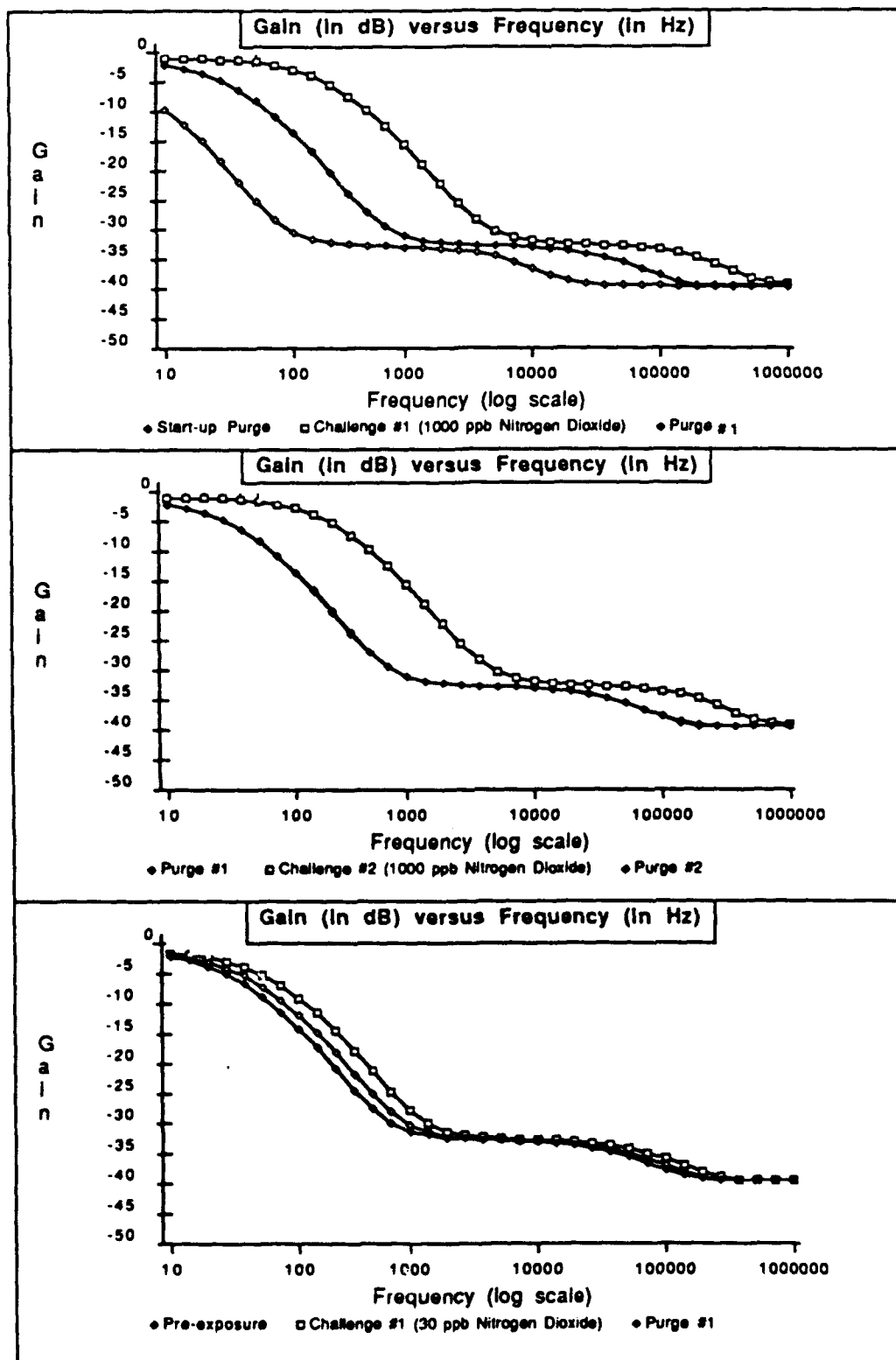


Figure V-36. Gain versus Frequency Response of IGEFET Microsensor for a Series of Room Air Purges and Challenge Gas Exposures. Testing Conditions: IGE Microsensor Number 9; NiPc Thin-film (12,500 Angstroms Thick); Temperature of 150 degrees Centigrade; Nitrogen Dioxide Challenge Gas (Order of Exposures: 1000 ppb, 30 ppb, 50 ppb, 100 ppb, 500 ppb, 1000 ppb).

The device responses were recorded for one hour with the room air purge; then the DMMP (or DIMP) was introduced for one hour. The next step was another one hour purge while simultaneously establishing the temperature at 90°C. After the purge was completed a one hour long challenge was performed with DMMP (or DIMP) at 90°C. This overall process was repeated again after establishing an operating temperature of 30°C.

The DMMP activity at 120°C and 30°C mimicked that observed in the Series II tests. The DIMP activity was more noteworthy at the 120°C temperature with the 3 ppm challenge concentration. The dc resistance of the 3,200 Å thick CuPc film decreased from  $9.0 \times 10^9$  to  $5.0 \times 10^9$  ohms (a -44% change relative to the purge resistance). The dc resistance of the 5,200 Å thick CoPc film decreased from  $6.4 \times 10^{10}$  to  $2.9 \times 10^{10}$  ohms (a -55% change relative to the purge resistance). The dc resistance of the 6,800 Å thick NiPc film decreased from  $8.0 \times 10^9$  to  $3.9 \times 10^9$  ohms (a -51% change relative to the purge resistance).

#### *Sensitivity and Reversibility*

Table V-6 presents the sensitivity and reversibility indices generated by applying the respective algorithms to the gain and phase angle data

collected during the Series II experiments. Figures V-36 to V-38 show the sensitivity and reversibility versus frequency for a CoPc thin-film (5,400 Å thickness) exposed to NO<sub>2</sub>. Similar graphs can be found for the other MPc materials in Appendices C and D. The NO<sub>2</sub> interactions with all three film types is presented in Table V-6 (the extraction of these indices from the other challenge gas data sets has not been accomplished). The information for each thin-film type and thickness is arranged in the order that the exposures were accomplished. Based on the information in Table V-6, and the sensitivity and reversibility plots in Appendices C, D, and E, the 30 ppb challenge data shows a residual effect that may have been caused by the 1000 ppb preconditioning and challenge cycles. This influence appears to cause the gain and phase angle baselines to drift, resulting in several reversibility indices for the 30 ppb challenge which are seemingly inconsistent with the remaining concentrations.

### *Selectivity*

Calculations of the selectivity indices require measuring the microsensor's responses to simultaneous exposure to at least two different challenge gases. Time limitations prevented these experiments from being conducted; thus, no selectivity indices were calculated for any MPc.

Table V-6.  
Sensitivity and Reversibility of MPC Thin-Films When Exposed to  
Nitrogen Dioxide Challenges. (Continued on the Next Page).

Thin-Film Type and Thickness (Angstrom)	Challenge Gas Concentration (ppb)	Maximum Gain Change (dB)	Frequency (kHz)	Maximum Phase Change (degree)	Frequency (kHz)
CuPc; 1,600	1000 pre	30.7	0.01	-90	0.04
	1000	30	0.01	-90	0.04
	30	1.2	0.01	-25	0.01
	50	18.5	0.01	-86	0.02
	100	27.5	0.01	-85	0.03
	500	35.6	0.14	-93	0.23
CuPc; 3,900	1000 pre	35.6	0.03	-55	0.46
	1000	27.1	0.08	-80	0.91
	50	3.4	0.06	-17	0.11
	100	24.1	0.16	-76	0.91
	500	na	na	na	na
CuPc; 8,800	1000 pre	30	0.16	-76	1.83
	1000	20.6	0.46	-59	2.58
	30	1	0.32	-5	0.64
	50	2.2	0.32	-11	0.64
	100	11.3	0.46	-43	1.29
	500	15.9	0.91	-60	2.58
		'na' indicates measurement not used.		'pre' indicates pre-conditioning exposure.	



Table V-6.  
Sensitivity and Reversibility of MPC Thin-Films When Exposed to  
Nitrogen Dioxide Challenges. (Continued on the Next Page).

Thin-Film Type and Thickness (Angstrom)	Challenge Gas Concentration (ppb)	Maximum Gain Change (dB)	Frequency (kHz)	Maximum Phase Change (degree)	Frequency (kHz)	Minimum Gain Reversal (dB)	Frequency (kHz)	Minimum Phase Reversal (degree)	Frequency (kHz)
CoPc; 2,500	1000 pre	10	0.65	-33	2.58	na	na	na	na
	1000	5.7	0.65	-21	2.58	na	na	na	na
	30	0.7	0.91	-2	1.83	na	na	na	na
	50	0.5	0.02	1	0.14	na	na	na	na
	100	0.6	0.64	-2	1.83	na	na	na	na
	500	4.1	0.64	-15	1.83	na	na	na	na
CoPc; 5,400	1000 pre	16.5	7.32	-28	29.33	3.2	7.32	-10	20.73
	1000	5	10.35	-16	29.33	0.1	7.32	-3	20.73
	30	-0.6	10.35	2	29.33	-0.7	7.32	2	20.73
	50	-0.6	7.32	-4	20.73	0.8	7.32	-2	20.73
	100	1.3	7.32	-4	20.73	0.4	5.17	-2	20.73
	500	2.7	10.35	-8	29.33	0.2	10.32	-1	20.73
CoPc; 10,500	1000 pre	7.9	14.65	19	1.83	1.5	10.35	4	1.29
	1000	5.7	14.65	14	1.83	1.4	10.35	4	1.29
	30	-0.9	14.65	-3	1.83	-0.8	10.35	-2	1.29
	50	<0.1	na	na	na	<0.5	na	1	14.65
	100	0.62	20.73	na	na	<0.5	na	2	83.09
	500	3.2	20.73	7	2.58	<0.5	na	0	41.50
'na' indicates measurement not used. 'pre' indicates pre-conditioning exposure.									

Table V-6.  
Sensitivity and Reversibility of MPC Thin-Films When Exposed to  
Nitrogen Dioxide Challenges. (Continued from Previous Page).

Thin-Film Type and Thickness (Angstrom)	Challenge Gas Concentration (ppb)	Maximum Gain Change (dB)	Frequency (kHz)	Maximum Phase Change (degree)	Frequency (kHz)	Minimum Gain Reversal (dB)	Frequency (kHz)	Minimum Phase Reversal (degree)	Frequency (kHz)
NiPc; 2,600	1000 pre	33.2	0.01	-80	0.08	11.5	0.01	-68	0.01
	1000	25	0.02	-55	0.16	-0.5	0.01	2	0.03
	30	11	0.01	-34	0.04	-3.7	0.01	12	0.03
	50	7.3	0.01	-27	0.03	-2.7	0.01	13	0.01
	100	16.5	0.01	-58	0.06	0.4	0.01	-2	0.02
	500	22.1	0.02	-68	0.11	0.8	0.01	-3	0.03
NiPc; 6,200	1000 pre	24	0.03	-53	0.32	26.3	0.02	-43	0.16
	1000	13.1	0.08	24	0.01	<0.1	na	1	0.46
	30	4.9	0.08	11	0.01	-1.8	0.06	5	0.46
	50	2.2	0.08	4	0.01	-2.3	0.04	-6	0.32
	100	9.9	0.11	16	0.01	0.4	0.08	-1	0.46
	500	17	0.23	30	0.02	0.7	0.08	-2	0.91
NiPc; 12,500	1000 pre	28	0.16	-71	1.29	17.2	0.91	-57	3.65
	1000	16.6	0.46	-55	1.83	-3.2	3.65	12	0.46
	30	4.1	0.32	-15	0.91	<0.1	na	<0.1	na
	50	2.6	0.23	-10	0.46	-3.0	1.83	11	0.46
	100	8.8	0.32	-31	0.91	0.3	1.83	-1	0.46
	500	14	0.46	-48	1.29	1.4	0.32	-5	0.64
		'na' indicates measurement not used.		'pre' indicates pre-conditioning exposure.					

### *Time-Domain Responses*

The time-domain response of several IGEFET microsensors that were exposed to the challenge gases are shown in Figures V-37 through V-39. The waveform used to drive the IGEFET microsensors' was a 2 V<sub>pk-to-pk</sub> 50 Hz square wave with a 50 % duty cycle. Figure V-37 clearly shows the change in waveforms for a NiPc thin-film (2,600 Å thickness) when exposed to NO<sub>2</sub> at a concentration of 1000 ppb; the overall output signal level increases due to the enhanced electron conductivity of the gas sensitive thin-film. Figure V-38 depicts the response for a thicker NiPc film (6,200 Å thickness). The thicker material demonstrates a more significant response to the same challenge gas concentration. This behavior agrees with the observed dc resistance measurements discussed previously. Figure V-39 depicts the effect of the ammonia challenge gas upon a CoPc film (2,500 Å thickness). With the ammonia challenge, the impedance increases and the resulting output waveform's amplitude is decreased relative to the purge envelope. This behavior also reflects the changes observed in the dc resistance measurements.

### *Discussion*

The thrust of this investigation was to identify the physical conditions which would result in the greatest sensitivity, reversibility, and selectivity

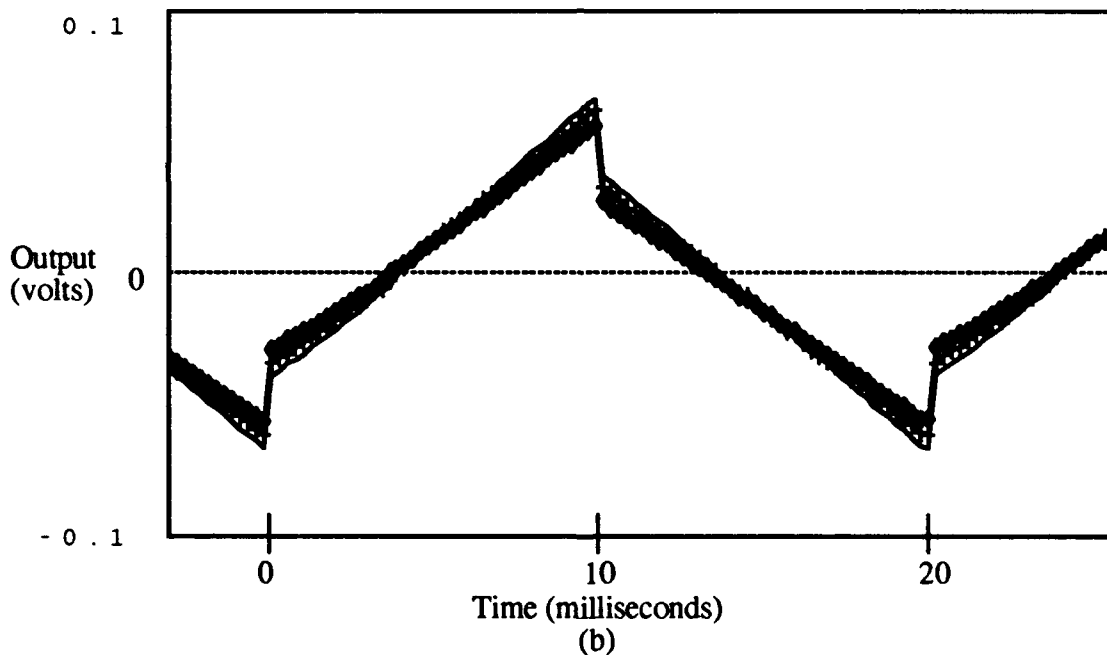
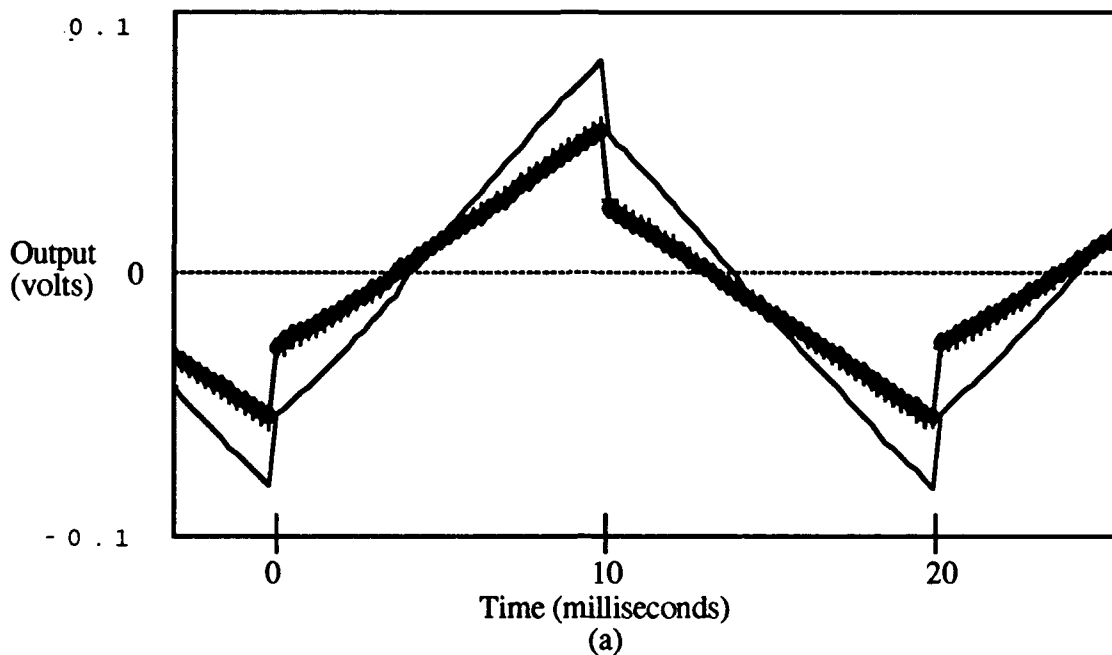


Figure V-37. Time-Domain Response of CoPc Thin-Film (2,600 Å Thick) to Ammonia Challenge Gas. Solid Line is Pre-Challenge; Diamonds Denote the Gas Challenge; Crosses are the Purge Values. (a) Plots for 1.25 Hour Duration Challenge, (b) Plots for Subsequent 15 Minute Challenge. Test Conditions Included: CoPc Thin-Film (2,500 Angstroms Thick); Temperature at 150 Degrees Centigrade; Challenge Gas was Ammonia at 500 ppm; Input Signal was 50 Hz Squarewave, 2 volts peak-to-peak; Dehumidified Room Air for Purge and Carrier Gas.

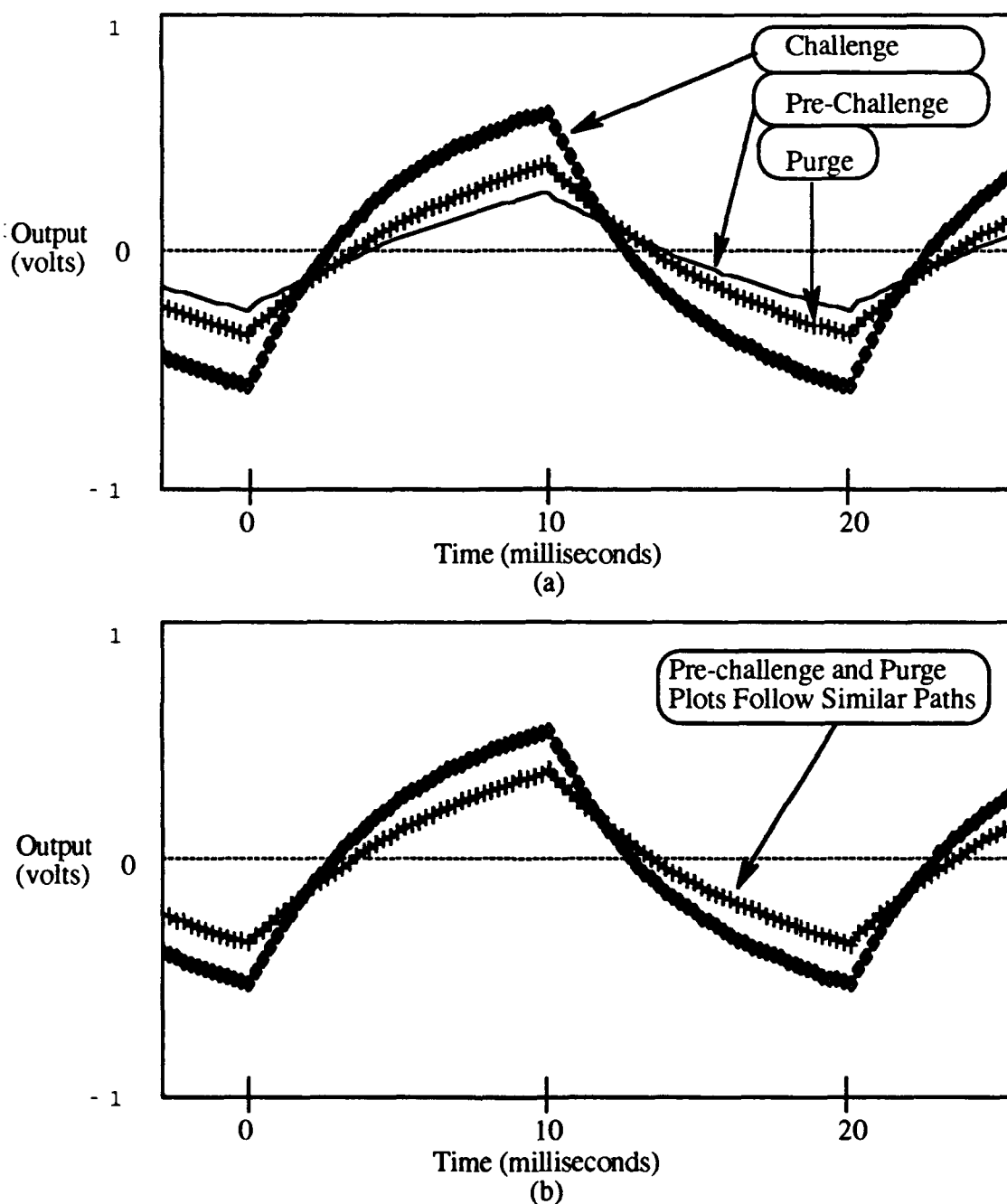
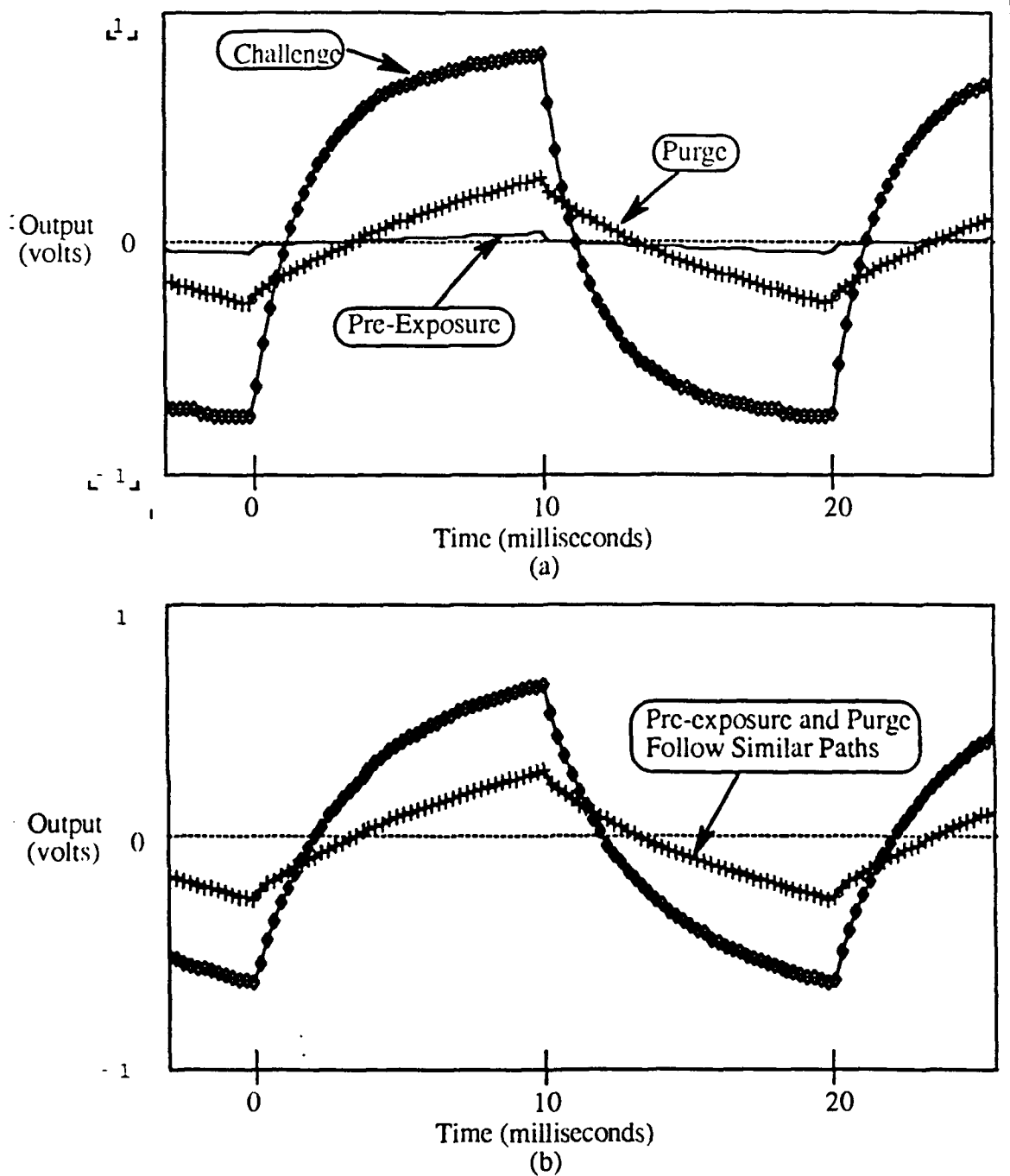


Figure V-38. Time-Domain Response of the NiPc (2,600 Å Thick) Thin-Film to Nitrogen Dioxide Challenge Gas Exposures. Solid Line is Pre-Challenge; Diamonds Denote the Gas Challenge; Crosses are Purge Values. (a) 1.25 Hour Duration Challenge, (b) Subsequent 15 Minute Challenge. Test Conditions Included: NiPc Thin-Film (2,600 Angstroms Thick); Temperature at 150 Degrees Centigrade; Challenge Gas was Nitrogen Dioxide at 1000 ppb; Input Signal was a 50 Hz Squarewave, 2 volt peak-to-peak; Dehumidified Room Air for Purge and Carrier Gas.



**Figure V-39.** Time-Domain Response to Challenge Gas. Solid Line is Pre-Challenge; Diamonds are during Gas Challenge; Crosses are Purge Values. (a) Plots for 1.25 Hour Duration Challenge, (b) Plots for Subsequent 15 Minute Challenge. Test Conditions Included: NiPc Thin-Film (6,200 Angstroms Thick); Temperature at 150 Degrees Centigrade; Challenge Gas was Nitrogen Dioxide at 1000 ppb; Input Signal was 50 Hz Squarewave, 2 volts peak-to-peak; Dehumidified Room Air for Purge and Carrier Gas.

when using CoPc, CuPc, and NiPc chemically-active thin-film materials with IGEFET microsensor. The conditions included, but were not limited to, temperature, thin-film type, thin-film thickness, challenge gas type, challenge gas concentration, and relative humidity. The sensitivity, reversibility, and selectivity indices are primary figures of merit (FOMs) established to assess the IGEFET microsensor's performance.

During the course of this investigation, sensitivity and reversibility indices were calculated for many pairwise combinations of metal-doped phthalocyanines (MPc) and challenge gases. Time limitations did not permit any testing of microsensors when exposed to two, or more, challenge gas types. This meant that the selectivity indices were not calculated for any MPc.

Not all of the desired variations of the experimental parameters and conditions were able to be explored due to time restraints. Instead, the combination of CuPc thin-films exposed to NO<sub>2</sub> challenge gas was used as a testbed (during the Series I tests) to narrow the field of temperatures to a single value, identify viable film thicknesses, and formulate a repeatable experimental protocol for use in the Series II tests. The results of pursuing this course of action were mixed, partly because of the limited span of several critical parameters; especially since only a single temperature was

more fully investigated. The 150°C temperature was adequate for the CuPc/NO<sub>2</sub> combination, but may have been too high for the organophosphorus compounds and the BF<sub>3</sub> challenge gas.

Given the 150°C test chamber temperature and the preconditioning protocol employed for the Series II tests, the measurements were used to calculate the figures of merit (FOMs) for the various thin-films. Detailed plots of these FOMs versus frequency for the CuPc, CoPc, and NiPc thin-films are in Appendices C, D, and E, respectively.



## VI. Conclusions and Recommendations

### *Conclusions.*

Chemically-active, metal-doped phthalocyanine (MPc) thin-films were deposited onto a microsensor that was capable of detecting parts-per-million levels of gaseous nitrogen dioxide, ammonia, boron trifluoride, and diisopropyl methylphosphonate (DIMP). The microsensor design was based upon the interdigitated gate electrode, field-effect transistor (IGEFET) technology. Thin-films of chemically-active material were deposited onto the interdigitated gate structures. Changes in the chemical nature of the p-type semiconducting MPc thin-films due to interactions with the challenge gases were inferred through measurements of the films' time- and frequency-domain responses.

The *in situ* MOSFET portion of each sensor element functioned as the inverting input into a dedicated differential amplifier. Each sensor's amplifier served to isolate the very high impedance, small capacitance IGE structure from the loading effects of the measurement instrumentation. Further stabilization was achieved by using the *in situ* amplifier in a voltage follower configuration. In this configuration, the FET-differential amplifier's gain transfer function was flat, extending from dc to a -3 dB

point near 5 MHz. The overall IGEFET-microsensor's transfer function was greatly attenuated when the thin-film coated IGE was included in the overall transfer function analysis. Exposing the thin-films to the challenge gases modulated the overall IGEFET-microsensor transfer function.

A nine-element array of IGEFET structures was fabricated using the monolithic silicon integrated circuit technology and packaged in a 64-pin DIP package. These devices were visually inspected for gross defects and electrically sampled short circuits and MOSFET amplifier functionality. Thin-films of copper phthalocyanine (CuPc), cobalt phthalocyanine (CoPc), and nickel phthalocyanine (NiPc) were deposited at various thicknesses unto the interdigitated portion of each sensor element via vacuum sublimation.

The IGEFET-sensors with the MPc thin-films of several thicknesses were subjected to a variety of test conditions including temperature, challenge gas type and concentration, and the gas used for purges and the challenge gas diluent. Two experimental procedural formats were investigated; one with a 'preconditioning' phase (which meant a long exposure to a high concentration of a particular challenge gas at the outset of the experiment), and one without any preconditioning. The preconditioning methodology was employed for the majority of the tests

because it resulted in less severe baseline drift throughout the duration of the experiments.

Once the test parameter envelope was explored using CuPc and NO<sub>2</sub> as a testbed, a set of test conditions were selected to implement the additional investigations of the MPc thin-film interactions with the various challenge gases. This test set included: nominal thin-film thicknesses of 2,000 Å, 5,000 Å, and 10,000 Å; temperature of 150°C; preconditioning exposure for 1.25 hours; gas challenges that were 15 minutes duration followed by dry, room air purges for one hour. Using these test conditions, the thinnest CuPc films exposed to nitrogen dioxide or ammonia produced the best overall blend of sensitivity and reversibility; the CoPc films were intermediate with respect to sensitivity and reversibility, while the NiPc films were the least sensitive.

In conclusion, the IGEFET microsensor technology has repeatedly demonstrated its viability as a detector for nitrogen dioxide and ammonia. This behavior was clearly demonstrated. The elevated temperature proved to be a wise choice for sensing nitrogen dioxide and ammonia when sensitivity and reversibility are the critical performance issues. At the elevated (150°C) temperature, the sensor was not able to clearly detect DMMP or DIMP at the concentrations generated during our tests;

although, at 90°C the sensor was able to detect the DIMP. At the elevated (150°C) temperature, the sensor was able to detect boron trifluoride at the concentrations generated during our tests, but demonstrated poor overall reversibility. Using the MOSFET portion of the IGEFET as the input to a voltage follower differential amplifier was a wise choice, providing a stable configuration while allowing the research to remain focused upon the activities occurring in the IGE structures coated with the gas-sensitive thin-films.

#### *Recommendations.*

This research effort has clearly demonstrated the high level of sensitivity and reversibility with which the IGEFET microsensor can detect nitrogen dioxide and ammonia in an environment of dry, room air at 150°C. Future work should focus on uncovering a set of good test parameters for the detecting DMMP and DIMP. The long range goal should be the development of a multi-element, IGEFET microsensor array with several chemically-active thin-films with the intention of detecting and identifying a number of different gas types and concentrations. Specific recommendations for future studies include:

1. The voltage follower configuration works well -- continue to use

it. Reconfiguration of the amplifier portion of the IGEFET microsensor to include the signal paths necessary for an 'on chip' voltage follower configuration should be accomplished. This will reduce the number of wirebonds and the amount of cabling required 'off chip'.

2. The response data from the IGEFET microsensor arrays should be subjected to pattern recognition techniques to see how effective this discipline is for discerning challenge gas types and concentrations. This should be an effort focused as a pattern recognition investigation with intended goals of formulating a method for parceling the available measurement data into a recognition pattern.

3. Evaluate the sensitivity and reversibility of other semiconducting thin-films of metal-substituted phthalocyanines including lead and iron phthalocyanine when challenged by nitrogen dioxide, ammonia, DIMP, and DMMP.

4. Limit the amount of redundant data collected. Too many data sources networked onto a single channel GPIB bus can produce a bottleneck, resulting in greater time sampling periods between measurements and coarse data set resolution.

5. Conduct data analysis concurrently with the experimentation. Don't wait until the 'end' before trying to extract and analyze the majority

of the data.

6. Establish an easily reproduced standard of comparison for indexing response qualities for the investigations done at AFIT. For example, use a 2,000 Å thick CuPc film exposed to 100 ppb of nitrogen dioxide at 90°C to establish reference indices of sensitivity and reversibility for the dc resistance. This will make comparisons among other exposure parameters more meaningful.

## *Appendix A: Metal-Doped Phthalocyanine Thin-Film Deposition onto Interdigitated Gate Electrode (IGE) Structures*

The deposition of metal-doped phthalocyanine material onto the IGE structures was accomplished at the AFIT Cooperative Electronics and Materials Processing Laboratory at Wright-Patterson AFB. This appendix describes the techniques used to accomplish that task.

### *IGEFET Validation*

Each 64-pin dual-in-line package (DIP) contained a single integrated circuit (IC) die which had a nine element array of interdigitated gate electrode field-effect transistor (IGEFET) microsensors built onto it. Prior to the deposition of any metal-doped phthalocyanine (MPc) compounds onto the IGE structures, they were visually and electronically checked for apparent open and short circuits. The metal-oxide -semiconductor field-effect transistor amplifiers were checked for gain and frequency bandwidth while in a voltage follower configuration.

### *Deposition Mask Preparation*

A mask was prepared from thin copper sheets (approximately

2 cm x 5 cm) for use in controlling the deposition of the MPc material onto each of the IGE structures of each DIP-mounted IC. The mask was fabricated by punching nine square holes (each 1370  $\mu\text{m}$  x 1370  $\mu\text{m}$ ) into the copper sheet in a pattern matching the 3 x 3 matrix of IGEs on each die. Several strips (approximately 3 mm x 20 mm) of copper sheet metal were also fabricated. These strips were used as necessary to occlude groups of three of the square holes in the mask.

When in use, this mask suspended slightly above the IC die, resting on the DIP package, and was visually aligned over the nine IGEs. The mask was then secured into place using adhesive tape. Sections of the mask were occluded as necessary by securing one, or more, of the copper metal strips atop of the mask.

### *Thin-Film Deposition*

The first step in preparing the DIPs for the MPc deposition was to wrap their pins in conducting aluminum foil to reduce the risk of static electricity damaging the IC. Once this was accomplished, a mask was secured above the IGE array as described in the previous section. The aluminum foil was extended to cover any remaining exposed DIP surfaces to prevent undesirable MPc deposits. Once the DIPs were masked and



wrapped, they were ready to be processed in the vacuum deposition system (Denton Vacuum Corp., Model DV-602, Cherry Hill, NJ). They were positioned inside the vacuum chamber above the boat which contained the particular MPc chosen for deposition. In addition to the DIP(s), a blank silicon wafer was positioned near the DIP(s) to aid in assessing the thickness of the deposited MPc.

After the vacuum chamber had been sealed and a vacuum of  $10^{-5}$  atmosphere had been achieved, the MPc was heated by passing approximately 145 amperes through the metal boat it was resting in. This caused the sublimation of the MPc; in particular, the sublimed molecules impacted upon the unmasked portions of the DIP. The vacuum chamber also contained a quartz microbalance (QMB) used to monitor the rate of sublimation of the MPc. This deposition process was used for all three MPc types deposited during this investigation: Copper Phthalocyanine (Fluka Chemical Corp., Stock 61215, Ronkonkoma, NY), Cobalt Phthalocyanine (Fluka Chemical Corp., Stock 60855, Ronkonkoma, NY), and Nickel Phthalocyanine (Fluka Chemical Corp., Stock 72265, Ronkonkoma, NY). The masks were occluded when necessary to limit the depositions on certain IGEs by using the copper metal strips.

### *Determining Thin-Film Thickness*

The thickness of the MPc films deposited onto the IGEs was inferred through two measurements; the thickness calculated from the QMB rate measurements, and the thickness of the layers deposited onto the blank silicon wafers positioned near the DIPs during the deposition process. The QMB reading was read directly while the deposition process was ongoing. After each deposition was complete, the thickness of the MPc deposit on the silicon blank was measured by first coating the MPc film with a 300 Å thick, gold metal coat (Structure Probe Inc., SPI Sputterer, Model 13131, West Chester, PA) . As described by Capt Thomas Jenkins [7], this step helps reduce mechanical errors caused by using the profilometer ( Sloan Technology Corp., Dek-Tak Model 900051, Santa Barbara, CA) for the second estimate of the film thickness.

### *Summary*

The vacuum sublimation process used in this research for thin-film deposition was performed at the AFIT Cooperative Electronics and Materials Processing Laboratory. This method provided an adequate avenue for fabricating MPc thin-films onto the IGE structures of the IGEFET microsensors used in this research.

## *Appendix B: Data Acquisition Software*

This appendix contains copies of the software written for gathering data records, storing the data onto magnetic media, and extracting data from the record files for display and analysis. The data was gathered from the instrumentation via a computer controlled general purpose instrumentation bus (GPIB). The software in this appendix includes:

1. WAM1.BAS, a GPIB controller program written in BASIC,
2. GPIB, a GPIB controller program written in PASCAL,
3. OSTRX.PAS, a program for extracting oscilloscope sweep data from the GPIB generated data records,
4. IGRGPTRX.PAS, a program for extracting gain/phase angle analyzer sweep data from the GPIB generated data records,
5. IGRRSTRX.PAS, a program for extracting electrometer generated dc resistance data from the GPIB generated data records, and
6. SSENSITIVITY\_REVERSIBILITY\_MATH\_ENGINE, a program written for generating sensitivity and reversibility analysis graphs from the IGRGPTRX.PAS generated gain/phase angle data files.

```

151
152 INSTRUMENT:ID=HPCAINPHASE:BUTTONS="GET1":GOSUB 1200:BUTTONS="AOFF1":GOSUB 1
200:BUTTONS="BOFF1":GOSUB 1200:
    'SET OFFSET VALID, SELECT GAIN PHAS
153 INSTRUMENT:ID=HPCAINPHASE:BUTTONS="CLOSEAVE":GOSUB 1200:GOSUB 1200 'CLOSE SWITCH
    'SET OFFSET VALID, SELECT GAIN PHAS
154 INSTRUMENT:ID=HPCAINPHASE:BUTTONS="CLOSEKEITH":GOSUB 1200:GOSUB 1200 'CLOSE SWITCHES
    'SET OFFSET VALID, SELECT GAIN PHAS
155 INSTRUMENT:ID=HPCAINPHASE:BUTTONS="CLOSEKEITH":GOSUB 1200:GOSUB 1200 'CLOSE SWITCHES
    'SET OFFSET VALID, SELECT GAIN PHAS
156 CURRENT=8
157 NO INTERRUPT:FLAGS="N"
158 ***** DONE WITH SET-UP FOR MAIN SEGMENT 1
159 ***** MAIN SEGMENT 1
160 FOR MAIN = 1 TO 9:PRINT "***** MAIN 1 AT *MAIN
161 'START SWEEP OF O'SCOPE ANALYZER
162 'START SWEEP OF SPECTRAL ANALYZER
163 'START SWEEP OF GAIN/PHASE ANALYZER
164
165 GOSUB 5300
166 'WAIT FOR END OF O'SCOPE SWEEP
167 'O-SCOPE SWEEP DOWNLOAD FILE
168 GOSUB 5320
169 'WAIT FOR END OF GAIN/PHASE SWEEP
170 'WAIT FOR END OF SPECTRAL SWEEP
171
172 GOSUB 6000:GOSUB 6030 'OPEN/CLOSE SWITCHING CHANNEL
173 GOSUB 6320 'GAIN/PHASE SWEEP DOWNLOAD FILE
174 GOSUB 6420 'SPECTRAL ANALYSIS DOWNLOAD FILE
175
176 IF (MAIN MOD 18)=0 THEN GOSUB 700 'DATA DISK NEEDS REPLACING
177 NEXT MAIN
178 ***** END OF MAIN SEGMENT 1
179 ***** MAIN SEGMENT 2
180 ***** SET UP FOR MAIN SEGMENT 2
181 *****
182
183 INSTRUMENT:ID=HPCAINPHASE:BUTTONS="GET2":GOSUB 1200:BUTTONS="OPM1":GOSUB 1
200:BUTTONS="BOFF1":GOSUB 1200:
    'SET OFFSET VALID, SELECT IMPEDANCE MEASUR
201
202 INSTRUMENT:ID=HPCAINPHASE:BUTTONS="OPENHVE":GOSUB 1200:GOSUB 1200 'OPEN SWITCHES 0
    'IMP MEASUREMENTS
203
204 INSTRUMENT:ID=HPCAINPHASE:BUTTONS="OPENHVE":GOSUB 1200:GOSUB 1200 'OPEN SWITCH
    'IMP MEASUREMENTS
205
206 CURRENT=4:GOSUB 9330
207 'RESET CURRENT FOR THE SWITCHING BATCHSET ROUTINE
208 T-TIMER=TIMER:UNTIL T+5 > T-TIMER:VEND 'DELAY TO LET IGEFTS SETTLE AFTER CLOSURE
209 'TIMER OFF: NO INTERRUPT:FLAGS="N"
210 ***** DONE WITH SET-UP FOR MAIN SEGMENT 2
211 ***** MAIN SEGMENT 1
212 FOR MAIN = 1 TO 9:PRINT "***** MAIN 2 AT *MAIN
213 'START SWEEP OF IMPEDANCE ANALYZER
214 'START SWEEP OF SPECTRAL ANALYZER
215 'START SWEEP OF O'SCOPE ANALYZER
216
217 GOSUB 5300
218 'WAIT FOR END OF O'SCOPE SWEEP
219 'O-SCOPE ANALYSIS DOWNLOAD FILE
220 GOSUB 5320
221 'WAIT FOR END OF IMPEDANCE SWEEP
222 'WAIT FOR END OF SPECTRAL SWEEP
223
224 GOSUB 6000:GOSUB 6030 'OPEN/CLOSE SWITCHING CHANNEL
225 GOSUB 6320 'GAIN/PHASE SWEEP DOWNLOAD FILE
226 GOSUB 6420 'SPECTRAL ANALYSIS DOWNLOAD FILE
227
228 ***** SET UP FOR MAIN SEGMENT 1
229 *****
230
231
232
233
234
235
236
237
238
239
240
241
242
243
244
245
246
247
248
249
250
251
252
253
254
255
256
257
258
259
260
261
262
263
264
265
266
267
268
269
270
271
272
273
274
275
276
277
278
279
280
281
282
283
284
285
286
287
288
289
290
291
292
293
294

```

```

1
2
3
4
5
6
7
8
9
10
11
12
13
14
15
16
17
18
19
20
21
22
23
24
25
26
27
28
29
30
31
32
33
34
35
36
37
38
39
40
41
42
43
44
45
46
47
48
49
50
51
52
53
54
55
56
57
58
59
60
61
62
63
64
65
66
67
68
69
70
71
72
73
74
75
76
77
78
79
80
81
82
83
84
85
86
87
88
89
90
91
92
93
94
95
96
97
98
99
100
101
102
103
104
105
106
107
108
109
110
111
112
113
114
115
116
117
118
119
120
121
122
123
124
125
126
127
128
129
130
131
132
133
134
135
136
137
138
139
140
141
142
143
144
145
146
147
148
149
150
151
152
153
154
155
156
157
158
159
160
161
162
163
164
165
166
167
168
169
170
171
172
173
174
175
176
177
178
179
180
181
182
183
184
185
186
187
188
189
190
191
192
193
194
195
196
197
198
199
200
201
202
203
204
205
206
207
208
209
210
211
212
213
214
215
216
217
218
219
220
221
222
223
224
225
226
227
228
229
230
231
232
233
234
235
236
237
238
239
240
241
242
243
244
245
246
247
248
249
250
251
252
253
254
255
256
257
258
259
260
261
262
263
264
265
266
267
268
269
270
271
272
273
274
275
276
277
278
279
280
281
282
283
284
285
286
287
288
289
290
291
292
293
294
295
296
297
298
299
300
301
302
303
304
305
306
307
308
309
310
311
312
313
314
315
316
317
318
319
320
321
322
323
324
325
326
327
328
329
330
331
332
333
334
335
336
337
338
339
340
341
342
343
344
345
346
347
348
349
350
351
352
353
354
355
356
357
358
359
360
361
362
363
364
365
366
367
368
369
370
371
372
373
374
375
376
377
378
379
380
381
382
383
384
385
386
387
388
389
390
391
392
393
394
395
396
397
398
399
400
401
402
403
404
405
406
407
408
409
410
411
412
413
414
415
416
417
418
419
420
421
422
423
424
425
426
427
428
429
430
431
432
433
434
435
436
437
438
439
440
441
442
443
444
445
446
447
448
449
450
451
452
453
454
455
456
457
458
459
460
461
462
463
464
465
466
467
468
469
470
471
472
473
474
475
476
477
478
479
480
481
482
483
484
485
486
487
488
489
490
491
492
493
494
495
496
497
498
499
500
501
502
503
504
505
506
507
508
509
510
511
512
513
514
515
516
517
518
519
520
521
522
523
524
525
526
527
528
529
530
531
532
533
534
535
536
537
538
539
540
541
542
543
544
545
546
547
548
549
550
551
552
553
554
555
556
557
558
559
560
561
562
563
564
565
566
567
568
569
570
571
572
573
574
575
576
577
578
579
580
581
582
583
584
585
586
587
588
589
590
591
592
593
594
595
596
597
598
599
600
601
602
603
604
605
606
607
608
609
610
611
612
613
614
615
616
617
618
619
620
621
622
623
624
625
626
627
628
629
630
631
632
633
634
635
636
637
638
639
640
641
642
643
644
645
646
647
648
649
650
651
652
653
654
655
656
657
658
659
660
661
662
663
664
665
666
667
668
669
670
671
672
673
674
675
676
677
678
679
680
681
682
683
684
685
686
687
688
689
690
691
692
693
694
695
696
697
698
699
700
701
702
703
704
705
706
707
708
709
710
711
712
713
714
715
716
717
718
719
720
721
722
723
724
725
726
727
728
729
730
731
732
733
734
735
736
737
738
739
740
741
742
743
744
745
746
747
748
749
750
751
752
753
754
755
756
757
758
759
760
761
762
763
764
765
766
767
768
769
770
771
772
773
774
775
776
777
778
779
780
781
782
783
784
785
786
787
788
789
790
791
792
793
794
795
796
797
798
799
800
801
802
803
804
805
806
807
808
809
810
811
812
813
814
815
816
817
818
819
820
821
822
823
824
825
826
827
828
829
830
831
832
833
834
835
836
837
838
839
840
841
842
843
844
845
846
847
848
849
850
851
852
853
854
855
856
857
858
859
860
861
862
863
864
865
866
867
868
869
870
871
872
873
874
875
876
877
878
879
880
881
882
883
884
885
886
887
888
889
890
891
892
893
894
895
896
897
898
899
900
901
902
903
904
905
906
907
908
909
910
911
912
913
914
915
916
917
918
919
920
921
922
923
924
925
926
927
928
929
930
931
932
933
934
935
936
937
938
939
940
941
942
943
944
945
946
947
948
949
950
951
952
953
954
955
956
957
958
959
960
961
962
963
964
965
966
967
968
969
970
971
972
973
974
975
976
977
978
979
980
981
982
983
984
985
986
987
988
989
990
991
992
993
994
995
996
997
998
999
1000

```



```

698 ..... END OF DISPLAY CURRENT FILE HEADER .....
699 .....
700 .....
701 ..... PUT NEW DATA DISK INTO DRIVE B ..... YOU BOZD .....
710 PRINT "***** PUT A DATA DISK INTO DRIVE B ..... YOU BOZD ..... *****"
715 PRINT "***** Press 'RETURN' when you're done. ...."
720 AS-INVENTS-BEEP: IF AS="" THEN GOTO 720 ..... WAIT FOR DISK TO BE PUT IN
730 RETURN ..... PRINT FILE HEADERS ON NEW DISK
740 RETURN ..... GO BACK TO SPOT WHERE INTERRUPT OCCUR'D
750 .....
76 .....
77 .....
78 .....
79 .....
80 .....
81 ..... INQUIRE OPERATOR'S WISHES FOR MORE .....
82 INPUT "DO YOU WANT TO DO ANOTHER EXPERIMENTAL RUN (Y/N) ?" ANSW
83 IF LEFT$(ANS,1) <> "Y" THEN END
84 RETURN
85 .....
86 ..... END OF INQUIRY .....
87 .....
88 .....
89 .....
90 .....
91 .....
92 .....
93 .....
94 .....
95 .....
96 .....
97 .....
98 .....
99 .....
100 .....
101 ..... RESET EXPERIMENT TIMER TO ZERO .....
102 .....
103 .....
104 TIMES="00:00:00" ..... USED TO FORMAT PRINTOUT
105 RETURN
106 .....
107 .....
108 .....
109 .....
110 .....
111 .....
112 .....
113 .....
114 .....
115 .....
116 .....
117 .....
118 .....
119 .....
120 .....
121 .....
122 .....
123 .....
124 .....
125 .....
126 .....
127 .....
128 .....
129 .....
130 .....
131 .....
132 .....
133 .....
134 .....
135 .....
136 .....
137 .....
138 .....
139 .....
140 .....
141 .....
142 .....
143 .....
144 .....
145 .....
146 .....
147 .....
148 .....
149 .....
150 .....
151 .....
152 .....
153 .....
154 .....
155 .....
156 .....
157 .....
158 .....
159 .....
160 .....
161 .....
162 .....
163 .....
164 .....
165 .....
166 .....
167 .....
168 .....
169 .....
170 .....
171 .....
172 .....
173 .....
174 .....
175 .....
176 .....
177 .....
178 .....
179 .....
180 .....
181 .....
182 .....
183 .....
184 .....
185 .....
186 .....
187 .....
188 .....
189 .....
190 .....
191 .....
192 .....
193 .....
194 .....
195 .....
196 .....
197 .....
198 .....
199 .....
200 .....
201 .....
202 .....
203 .....
204 .....
205 .....
206 .....
207 .....
208 .....
209 .....
210 .....
211 .....
212 .....
213 .....
214 .....
215 .....
216 .....
217 .....
218 .....
219 .....
220 .....
221 .....
222 .....
223 .....
224 .....
225 .....
226 .....
227 .....
228 .....
229 .....
230 .....
231 .....
232 .....
233 .....
234 .....
235 .....
236 .....
237 .....
238 .....
239 .....
240 .....
241 .....
242 .....
243 .....
244 .....
245 .....
246 .....
247 .....
248 .....
249 .....
250 .....
251 .....
252 .....
253 .....
254 .....
255 .....
256 .....
257 .....
258 .....
259 .....
260 .....
261 .....
262 .....
263 .....
264 .....
265 .....
266 .....
267 .....
268 .....
269 .....
270 .....
271 .....
272 .....
273 .....
274 .....
275 .....
276 .....
277 .....
278 .....
279 .....
280 .....
281 .....
282 .....
283 .....
284 .....
285 .....
286 .....
287 .....
288 .....
289 .....
290 .....
291 .....
292 .....
293 .....
294 .....
295 .....
296 .....
297 .....
298 .....
299 .....
300 .....
301 .....
302 .....
303 .....
304 .....
305 .....
306 .....
307 .....
308 .....
309 .....
310 .....
311 .....
312 .....
313 .....
314 .....
315 .....
316 .....
317 .....
318 .....
319 .....
320 .....
321 .....
322 .....
323 .....
324 .....
325 .....
326 .....
327 .....
328 .....
329 .....
330 .....
331 .....
332 .....
333 .....
334 .....
335 .....
336 .....
337 .....
338 .....
339 .....
340 .....
341 .....
342 .....
343 .....
344 .....
345 .....
346 .....
347 .....
348 .....
349 .....
350 .....
351 .....
352 .....
353 .....
354 .....
355 .....
356 .....
357 .....
358 .....
359 .....
360 .....
361 .....
362 .....
363 .....
364 .....
365 .....
366 .....
367 .....
368 .....
369 .....
370 .....
371 .....
372 .....
373 .....
374 .....
375 .....
376 .....
377 .....
378 .....
379 .....
380 .....
381 .....
382 .....
383 .....
384 .....
385 .....
386 .....
387 .....
388 .....
389 .....
390 .....
391 .....
392 .....
393 .....
394 .....
395 .....
396 .....
397 .....
398 .....
399 .....
400 .....
401 .....
402 .....
403 .....
404 .....
405 .....
406 .....
407 .....
408 .....
409 .....
410 .....
411 .....
412 .....
413 .....
414 .....
415 .....
416 .....
417 .....
418 .....
419 .....
420 .....
421 .....
422 .....
423 .....
424 .....
425 .....
426 .....
427 .....
428 .....
429 .....
430 .....
431 .....
432 .....
433 .....
434 .....
435 .....
436 .....
437 .....
438 .....
439 .....
440 .....
441 .....
442 .....
443 .....
444 .....
445 .....
446 .....
447 .....
448 .....
449 .....
450 .....
451 .....
452 .....
453 .....
454 .....
455 .....
456 .....
457 .....
458 .....
459 .....
460 .....
461 .....
462 .....
463 .....
464 .....
465 .....
466 .....
467 .....
468 .....
469 .....
470 .....
471 .....
472 .....
473 .....
474 .....
475 .....
476 .....
477 .....
478 .....
479 .....
480 .....
481 .....
482 .....
483 .....
484 .....
485 .....
486 .....
487 .....
488 .....
489 .....
490 .....
491 .....
492 .....
493 .....
494 .....
495 .....
496 .....
497 .....
498 .....
499 .....
500 .....
501 .....
502 .....
503 .....
504 .....
505 .....
506 .....
507 .....
508 .....
509 .....
510 .....
511 .....
512 .....
513 .....
514 .....
515 .....
516 .....
517 .....
518 .....
519 .....
520 .....
521 .....
522 .....
523 .....
524 .....
525 .....
526 .....
527 .....
528 .....
529 .....
530 .....
531 .....
532 .....
533 .....
534 .....
535 .....
536 .....
537 .....
538 .....
539 .....
540 .....
541 .....
542 .....
543 .....
544 .....
545 .....
546 .....
547 .....
548 .....
549 .....
550 .....
551 .....
552 .....
553 .....
554 .....
555 .....
556 .....
557 .....
558 .....
559 .....
560 .....
561 .....
562 .....
563 .....
564 .....
565 .....
566 .....
567 .....
568 .....
569 .....
570 .....
571 .....
572 .....
573 .....
574 .....
575 .....
576 .....
577 .....
578 .....
579 .....
580 .....
581 .....
582 .....
583 .....
584 .....
585 .....
586 .....
587 .....
588 .....
589 .....
590 .....
591 .....
592 .....
593 .....
594 .....
595 .....
596 .....
597 .....
598 .....
599 .....
600 .....
601 .....
602 .....
603 .....
604 .....
605 .....
606 .....
607 .....
608 .....
609 .....
610 .....
611 .....
612 .....
613 .....
614 .....
615 .....
616 .....
617 .....
618 .....
619 .....
620 .....
621 .....
622 .....
623 .....
624 .....
625 .....
626 .....
627 .....
628 .....
629 .....
630 .....
631 .....
632 .....
633 .....
634 .....
635 .....
636 .....
637 .....
638 .....
639 .....
640 .....
641 .....
642 .....
643 .....
644 .....
645 .....
646 .....
647 .....
648 .....
649 .....
650 .....
651 .....
652 .....
653 .....
654 .....
655 .....
656 .....
657 .....
658 .....
659 .....
660 .....
661 .....
662 .....
663 .....
664 .....
665 .....
666 .....
667 .....
668 .....
669 .....
670 .....
671 .....
672 .....
673 .....
674 .....
675 .....
676 .....
677 .....
678 .....
679 .....
680 .....
681 .....
682 .....
683 .....
684 .....
685 .....
686 .....
687 .....
688 .....
689 .....
690 .....
691 .....
692 .....
693 .....
694 .....
695 .....
696 .....
697 .....
698 .....
699 .....
700 .....
701 .....
702 .....
703 .....
704 .....
705 .....
706 .....
707 .....
708 .....
709 .....
710 .....
711 .....
712 .....
713 .....
714 .....
715 .....
716 .....
717 .....
718 .....
719 .....
720 .....
721 .....
722 .....
723 .....
724 .....
725 .....
726 .....
727 .....
728 .....
729 .....
730 .....
731 .....
732 .....
733 .....
734 .....
735 .....
736 .....
737 .....
738 .....
739 .....
740 .....
741 .....
742 .....
743 .....
744 .....
745 .....
746 .....
747 .....
748 .....
749 .....
750 .....
751 .....
752 .....
753 .....
754 .....
755 .....
756 .....
757 .....
758 .....
759 .....
760 .....
761 .....
762 .....
763 .....
764 .....
765 .....
766 .....
767 .....
768 .....
769 .....
770 .....
771 .....
772 .....
773 .....
774 .....
775 .....
776 .....
777 .....
778 .....
779 .....
780 .....
781 .....
782 .....
783 .....
784 .....
785 .....
786 .....
787 .....
788 .....
789 .....
790 .....
791 .....
792 .....
793 .....
794 .....
795 .....
796 .....
797 .....
798 .....
799 .....
800 .....
801 .....
802 .....
803 .....
804 .....
805 .....
806 .....
807 .....
808 .....
809 .....
810 .....
811 .....
812 .....
813 .....
814 .....
815 .....
816 .....
817 .....
818 .....
819 .....
820 .....
821 .....
822 .....
823 .....
824 .....
825 .....
826 .....
827 .....
828 .....
829 .....
830 .....
831 .....
832 .....
833 .....
834 .....
835 .....
836 .....
837 .....
838 .....
839 .....
840 .....
841 .....
842 .....
843 .....
844 .....
845 .....
846 .....
847 .....
848 .....
849 .....
850 .....
851 .....
852 .....
853 .....
854 .....
855 .....
856 .....
857 .....
858 .....
859 .....
860 .....
861 .....
862 .....
863 .....
864 .....
865 .....
866 .....
867 .....
868 .....
869 .....
870 .....
871 .....
872 .....
873 .....
874 .....
875 .....
876 .....
877 .....
878 .....
879 .....
880 .....
881 .....
882 .....
883 .....
884 .....
885 .....
886 .....
887 .....
888 .....
889 .....
890 .....
891 .....
892 .....
893 .....
894 .....
895 .....
896 .....
897 .....
898 .....
899 .....
900 .....
901 .....
902 .....
903 .....
904 .....
905 .....
906 .....
907 .....
908 .....
909 .....
910 .....
911 .....
912 .....
913 .....
914 .....
915 .....
916 .....
917 .....
918 .....
919 .....
920 .....
921 .....
922 .....
923 .....
924 .....
925 .....
926 .....
927 .....
928 .....
929 .....
930 .....
931 .....
932 .....
933 .....
934 .....
935 .....
936 .....
937 .....
938 .....
939 .....
940 .....
941 .....
942 .....
943 .....
944 .....
945 .....
946 .....
947 .....
948 .....
949 .....
950 .....
951 .....
952 .....
953 .....
954 .....
955 .....
956 .....
957 .....
958 .....
959 .....
960 .....
961 .....
962 .....
963 .....
964 .....
965 .....
966 .....
967 .....
968 .....
969 .....
970 .....
971 .....
972 .....
973 .....
974 .....
975 .....
976 .....
977 .....
978 .....
979 .....
980 .....
981 .....
982 .....
983 .....
984 .....
985 .....
986 .....
987 .....
988 .....
989 .....
990 .....
991 .....
992 .....
993 .....
994 .....
995 .....
996 .....
997 .....
998 .....
999 .....
1000 .....

```



```

4029 BUTTIONS=FNC2: GOSUB 1200 'SELECT SPECTRUM FUNCTION
4040 BUTTIONS=START-14KHZ: GOSUB 1200 'FREQUENCY SWEEP START POINT
4042 BUTTIONS=STOP-100KHZ: GOSUB 1200 'FREQUENCY SWEEP END POINT
4044 BUTTIONS=RAW-100KHZ: GOSUB 1200 'RESOLUTION BANDWIDTH
4045 BUTTIONS=SUM2: GOSUB 1200 'SELECT SINGLE SWEEP MODE
4048 PRINT ***** SENT COMPENSATION SETTINGS TO HP-4155A SPECTRUM
4060 'RUN COMPENSATION SWEEP
4061 BUTTIONS=CLS: GOSUB 1200: BUTTIONS=SUM2: GOSUB 1200 'CLEAR STATUS
4062 BUTTIONS=SWTRG:
4064 GOSUB 1200
4066 'BEGIN SERIAL POLLING THE HP SPECTRUM FOR END OF SWEEP
4067 PRINT ***** WAITING FOR END OF GAIN/PHASE COMPENSATION SWEEP
4068 'THE VARIABLE 'POLLS' CONTAINS THE STATUS BYTE FROM THE HP SPECTRUM
4070 CALL SPOLLA(INSTRUMENT ID#,POLLS STATUS)
4071 IF STATUS=0 THEN PRINT "ERROR STATUS DURING HP G/P POLLING IS BAD"
4072 PRINT "SPOLL=": POLLS
4076 IF POLLS AND 2 THEN GOTO 4080
4078 T=TIMER: WHILE T>1: T=TIMER: WEND: GOTO 4070 'DELAY ROUTINE
4080 PRINT: PRINT ***** SPECTRUM BASELINE SWEEP COMPLETE *****
4081 BUTTIONS=ATRI-008: GOSUB 1200 'SELECT ODB ATTENUATOR
4084 PRINT ***** STEP 2: REMOVE RMC JUMPER FROM DG#2 AND AMP OUTPUT#2
4086 INPUT "PRESS 'RETURN' WHEN DONE": NULLS
4106 CLS: PRINT ***** THE HP SPECTRUM BASELINES SWEEP IS NOW COMPLETE.
4110 RETURN
4120 ..... END OF HP-SPECTRUM BASELINE ROUTINE IS DONE..
4122 .....
4200 .....
4201 ..... START A SWEEP. SPECTRUM ANALYZER MEASUREMENT.
4210 'START A NEW SWEEP OF HP-SPECTRUM ANALYZER.
4211 PRINT ***** START A NEW SWEEP OF HP-SPECTRUM ANALYZER
4214 INSTRUMENT ID#-HP SPECTRUM
4218 BUTTIONS=CLS: GOSUB 1200 'CLEAR STATUS
4220 BUTTIONS=SWTRG: GOSUB 1200 'START SWEEP
4295 RETURN
4296 ..... END OF SPECTRUM MEASUREMENT SWEEP
4298 .....
4299 ..... WAIT FOR SPECTRAL COMPLETION AND
4300 ..... AND DOWNLOAD DATA TO DISK
4301 PRINT ***** WAITING FOR SPECTRAL SWEEP TO END
4304 IF NO INTERRUPT FLAG="Y" THEN GOTO 4306
4305 TIMER ON: TIMER STOP
4306 KEY(2) ON: KEY(1) ON: KEY(4) ON: KEY(5) ON
4307 KEY(2) STOP: KEY(1) STOP: KEY(4) STOP: KEY(5) STOP
4310 INSTRUMENT ID#-HP SPECTRUM: TYP=SPE
4311 PRINT "SPE " : T=TIMER: WHILE T>1: T=TIMER: WEND: 'A DELAY LOOP
4312 CALL SPOLLA(INSTRUMENT ID#,POLLS STATUS)
4316 IF POLLS AND 2 THEN GOTO 4317
4318 GOTO 4304
4319 BUTTIONS=AUTO: GOSUB 1200: GOSUB 1100 'AUTOSCALE AND UPDATE TIMER
4319 PRINT "DONE WITH SPECTRAL SWEEP"
4319 RETURN
4320 ***** NOW ATTEMPTING TO GET DATA FROM HP-SPECTRAL ANALYZER
4321 INSTRUMENT ID#-HP SPECTRUM: TYP=SPE: TIMEDEX=((ICEPTR+8) MOD 9)
4322 PRINT ***** NOW ATTEMPTING TO GET DATA FROM HP-SPECTRAL ANALYZER
4323 PRINT "ELAPSED TIME " : ELAPSED TIME ICES(TYP,TIMEDEX)
4328 OPEN IMPFILES*.SPE FOR APPEND AS #4 'SET UP OUTPUT FILE
4334 BUTTIONS=147
4350 GOSUB 1200
4352 BUTTIONS=HLA TALK 18: GOSUB 1250 'TRANSMIT TO SPECTRUM

```

```

4353 PRINT #4: ELAPSED TIME ICES(TYP,TIMEDEX)
4354 FOR I=0 TO 40
4356 TEMPS=SPACES(110): GOSUB 1360 'RECEIVE DATA FROM HP-P
4357 GAINS=TEMPS
4360 PRINT #4: GAINS
4364 NEXT I
4374 BUTTIONS=XY*
4380 GOSUB 1200 'READ SPECTRUM ABRAY OVER GP18
4381 BUTTIONS=HLA TALK 18: GOSUB 1250 'TRANSMIT TO SPECTRUM
4382 PRINT #4: ELAPSED TIME ICES(TYP,ICEDEX)
4384 FOR I=0 TO 40
4386 TEMPS=SPACES(130): GOSUB 1360 'RECEIVE DATA FROM HP-P
4387 GAINS=TEMPS
4390 PRINT #4: GAINS
4392 NEXT I
4392 CLS: PRINT ***** DONE WITH SPECTRAL DATA DOWNLOAD
4393 RETURN
4396 ..... END OF WAITING AND DOWNLOAD FOR HP-SPECTRUM ANALYZER
4398 .....
4399 .....
5001 ..... INITIALIZE THE O-SCOPE HP-54100A
5010 PRINT ***** BEGIN INITIALIZATION OF HP-54100A O-SCOPE
5012 PRINT ***** the HP-54100A O-Scope is being initialized now.
5026 INSTRUMENT ID#-HPSCOPE: GOSUB 1200 'SET UP READY MASK
5027 BUTTIONS=REQUEST 3074: GOSUB 1200 'DISPLAY SELECTION
5028 BUTTIONS=DISP: GOSUB 1200 'GRID SELECTION
5029 BUTTIONS=GRATICULE GRID: GOSUB 1200 'TRIGGER MENU SELECT
5030 BUTTIONS=TRIGGER: GOSUB 1200 'TRIGGER LEVEL SET TO 1V
5031 BUTTIONS=LEVEL 1: GOSUB 1200 'SELECT TIMEBASE MODE TO AUTO
5032 BUTTIONS=SOURCE CHANNEL: GOSUB 1200 'SELECT TIMEBASE MODE TO AUTO
5034 BUTTIONS=TIMEBASE: GOSUB 1200 'TIMEBASE MENU SELECTION
5035 BUTTIONS=MODE AUTO: GOSUB 1200 'SELECT TIMEBASE MODE TO AUTO
5036 BUTTIONS=SENSITIVITY 2E-6: GOSUB 1200 'LEFT BORDER FOR TIME REFERENCE
5037 BUTTIONS=REFERENCE LEFT: GOSUB 1200 'LEFT BORDER FOR TIME REFERENCE
5038 BUTTIONS=DELAY -4E-6: GOSUB 1200 'DELAY TIME SWEEP BY 4 USEC
5040 BUTTIONS=CHANNEL 1: GOSUB 1200 'CHANNEL 1 MENU
5042 BUTTIONS=SENSITIVITY 100E-3: GOSUB 1200 '100mV/DIV FOR CHANNEL 1
5043 BUTTIONS=OFFSET 200E-3: GOSUB 1200 'SET CHANNEL 1 OFFSET TO 200mV
5046 BUTTIONS=CHANNEL 2: GOSUB 1200 'CHANNEL 2 MENU
5047 BUTTIONS=SENSITIVITY 20E-3: GOSUB 1200 '20mV/DIV FOR CHANNEL 2
5048 BUTTIONS=OFFSET 30E-3: GOSUB 1200 'SET CHANNEL 2 OFFSET TO 30mV
5050 'ADJUST THE PULSE GENERATOR
5054 BEEP: PRINT: PRINT ***** Now please adjust the pulse generator.....
5056 INPUT ***** Press 'RETURN' when this is done. **: NULLS
5062 BUTTIONS=ACQUIRE: GOSUB 1200 'ENTER DIGITALIZATION ACQUIRE METHOD
5064 BUTTIONS=COMPLETE 95: GOSUB 1200 '95% OF BUCKETS FILLED BEFORE DUMP
5066 BUTTIONS=TYPE AVERAGE: GOSUB 1200 'SELECT AVERAGING MODE
5068 BUTTIONS=PTS 500: GOSUB 1200 'COLLECT 500 DATA POINTS
5070 BUTTIONS=COUNT 50: GOSUB 1200 'COLLECT 500 POINTS AT EACH TIME
5090 PRINT ***** O-SCOPE INITIALIZATION COMPLETE *****
5096 RETURN
5098 ..... END OF HP-O-SCOPE INITIALIZATION
5099 .....
5200 ..... START A SWEEP. O-SCOPE MEASUREMENT
5201 .....
5210 'START A NEW SWEEP OF HP-O-SCOPE
5211 PRINT ***** START A NEW SWEEP OF HP-O-SCOPE
5214 INSTRUMENT ID#-HPSCOPE
5218 BUTTIONS=DIGITIZE CHANNEL 1,2: GOSUB 1200 'START DIGITIZED DATA COLLECTION

```





**B-8**





```

begin
  Number_of_Points:=0;PntCtr:=1;
  while PntCtr < 500 do
    begin (R2)
      If Pnts_Skipped > 0
      then PntCtr:=PntCtr+Pnts_Skipped
      else Inc(PntCtr);
      Inc(Number_of_Points);
    end; (Begin R2)
    (While PntCtr)
    (While Number_of_Extracted_Points)
  end; (End Number_of_Extracted_Points)

  procedure Check_Flag; (check for I/O errors and
  begin
    procedure transpose_files;
    begin
      Number_of_Extracted_Points;
      for I := 1 to 9 do
        begin
          TestColor(I);
          Writing_Transposing file number 'I', 'new.';
          reset(OP1A(I));
          for R1 := 1 to Disk_Count*3 do
            begin (R1)
              for CC := 1 to Number_of_Points do
                begin
                  read(OP1A(I),Tachn_Array[R1,CC]);
                  read(OP2A(I),Refcn_Array[R1,CC]);
                end; (for CC)
              end; (for R1)
            end; (for R1)
            reset(OP1A(I));
            reset(OP2A(I));
            for CC := 1 to Number_of_Points do
              begin
                for R1 := 1 to Disk_Count*3 do
                  begin
                    write(OP1A(I),Tachn_Array[R1,CC]:$,' ');
                    write(OP2A(I),Refcn_Array[R1,CC]:$,' ');
                  end; (for R1)
                write(OP1A(I));write(OP2A(I));
              end; (for CC)
            close(OP1A(I));
            close(OP2A(I));
          end; (End of I do loop)
        end; (End Transpose_files)
      end;

  procedure Scope;
  begin
    assign(OP1A,DriveExpInfo.FileName+'.PLS');
    (
      If (Query in ['N','n']) then
        begin
          WriteLn('Beginning Scope extraction NOW, Believe You Me !!');
          append(OP1); (writing out the file of timeline sample points);
          close(OP1); (done writing baseline frequency file)
        end; (End if Query)
      )
  end;

```

```

for I := 1 to 9 do
begin
  Record_Index:=0;
  repeat
    reset(OSFile);
    IO_Flag := IOResult;
    Check_Flag;
    until IO_Flag = 0;

    append(OP1A(I));
    append(OP2A(I));
    append(OP3A(I));
    TestColor(I);
    WriteLn('beginning to get data from records',I);
    while not EOF(OSFile) do
      begin
        repeat
          read(OSFile,OSRec);
          IO_Flag := IOResult;
          Check_Flag;
          until IO_Flag = 0;

          if OSRec.LENUM = 1 then
            begin
              Inc(Record_Index);
              if Record_Index in (Slot(1),Slot(2),Slot(3)) then
                begin
                  (next decompose the o'scope preamble string into numbers)
                  N:=1;Temp_String:= ''; (index for the Value array)
                  Preamble_String:=OSRec.OSR preamble;
                  repeat (R3)
                    Temp_Char:= copy(Preamble_String,1,1);
                    delete(Preamble_String,1,1);
                    if Temp_Char < ' ' then
                      Temp_String :=Temp_String + Temp_Char;
                    if Temp_Char = ' ' then
                      begin
                        Val(Temp_String, Value[N], code);
                        Inc(N);
                        Temp_String:= '';
                      end;
                    until Preamble_String = ''; (repeat R3)
                  end;
                  PntCtr:=1; (PntCtr indexes the individual raw dat point)
                  while PntCtr < 500 do
                    begin (R2)
                      Y_Value:=OSRec.OSRData(PntCtr);(raw datum)
                      Y_Ref :=Value[10]; (y-axis reference)
                      Y_Inc :=Value[8]; (voltage per y-axis increment)
                      Y_Orig :=Value[9]; (y-axis origin offset)
                      X_Inc :=Value[5]; (x-axis time increment)
                      Y_Act :=(Y_Value-Y_Ref)*Y_Inc + Y_Orig; (calculate y-value)
                      write(OP1A(I),Y_Act:10:3,' ');
                      if Pnts_Skipped=0
                        then PntCtr:=PntCtr+Pnts_Skipped
                        else PntCtr:= PntCtr+1;
                    end; (while R2)
                  end; (while PntCtr)
                end;
              write(OP1A(I));
            end; (if Record_Index)
          end; (if OSRec.LENUM)
          if I = 1 then Number_of_Records := Number_of_Records + 1;
        end; (while not EOF(OSRec))
      end;

```





```

procedure ETimer(Typ: TTimerIndex; GECTR:IGET);
var
  Hours, Minutes, Seconds, Hundredths : word;
  CurrentTime, CurrentHours : single;
begin
  GetTime(Hours, Minutes, Seconds, Hundredths);
  CurrentHours := Hours;
  CurrentTime := 3600*CurrentHours + Minutes*60 + Seconds;
  If ElapsedTime > CurrentTime then ElapsedTime := 24*5600-CurrentTime
  else ElapsedTime:=CurrentTime;
  Elapsed_Time_IGET(Typ, GECTR) := ElapsedTime;
end; ETimer);

function Timer :single;
begin
  Timer:=ETimer(TIB, 1);
  Timer:=ElapsedTime;
end; (Timer)

```

```

procedure SendMail(Obj: Integer; ComStr: string);
begin
  Command:=ComStr;
  ComStr:=int-length(Command);
  ComStr:=address := obj(Command)+1;
  send (Obj, ComStr, stat);
  If stat=0 then begin
    FastColor(Stat=12);
    WriteLn('Status Error Sending to @18 bus');
    FastColor(Cyan);
  end;
end;

procedure TransMail(ComStr: string);
begin
  Command:=ComStr;
  ComStr:=int-length(Command);
  ComStr:=address := obj(Command)+1;
  TransMail(ComStr, stat);
  If stat=0 then begin
    FastColor(Stat=12);
    WriteLn('Status Error Writing to @18 bus');
    FastColor(Cyan);
  end;
end;

procedure RecvMail(var RecvStr: string; Len: Integer);
begin
  ComStr:=int-Len;
  ComStr:=address := obj(RecvStr)+1;
  RecvStr:=ComStr, stat;
  If stat=0 then WriteLn(' @18 bus = Receiving from @18 bus ');
  RecvStr(0):=Char(StatLen);
  RecvStr:=RecvStr;
end;

procedure EnterMail(Device : Integer; var RecvStr: string; Len: Integer);
begin
  ComStr:=int-Len;
  ComStr:=address := obj(RecvStr)+1;
  Enter (ComStr, StatLen, Device, stat);
  If stat=0 then WriteLn(' @18 bus = Entering from @18 bus ');
  RecvStr(0):=Char(StatLen);
  RecvStr:=RecvStr;
end;

```

```

procedure ValInt(S: string; var I: Integer);
var
  Code: Integer;
begin
  Val(I, Code);
  If Code=0 then WriteLn('Error in value conversion');
end;

procedure ValReal(S: string; var R: Real);
var
  Code: Integer;
begin
  Val(R, Code);
  If Code=0 then WriteLn('Error in value conversion');
end;

procedure ValSingle(S: string; var S1: Single);
var
  Code: Integer;
begin
  Val(S1, Code);
  If Code=0 then WriteLn('Error in value conversion');
end;

```



```

TestColor(Green);
write(' Error Estimate: ');
if ErrorEst<0.3 then TestColor(128+Red) else TestColor(Cyan);
ErrorEst:=ErrorEst*100;
writeln(ErrorEst:6:3, '%');
TestColor(White);
end; (CLR)

begin
  ( PName:=ParamStr(1);
  for i:=1 to length(PName) do PName[i]:=upCase(PName[i]);
  SendMail(hp145, 'GT ' + PName + '...', status);
  write('Save hp145 data on drive A: ok?');
  readln(PName);
  for i:=1 to 2 do begin
    ReadDataSet(i);
    end;
    if PName<>'' then begin
      TestColor(Green);writeln('Saving as ', PName);
      sendMail(hp145, 'GT-' + PName);
      if i=1 then begin
        if iORresult=0 then writeln ('Error writing to A:')
        else begin
          for j:=1 to NumPoints do
            writeln(Offset, DataSet(1, j), PDataSet(2, j));
          end;
          close(Offset);
          if iORresult=0 then (Clear iORresult)
          end;
          qtr;
          TestColor(White);
          writeln('Done');
        end;
      end;
    end;
  end;
end;

```

```

procedure MinInterrupt;
const
  VolTags:=array [1..20] of string(20)='V1', 'V2';
  NumPoints:=512;
  type
    string13=string(13);
  var
    i,
    S:integer; string;
    PName: string;
    Offset: text;
    DataSet: array [1..2, 1..NumPoints] of string13;

  procedure ReadDataSet(Src:integer);
  var i:integer; iORresult:string;
  begin
    writeln(hp145, 'get', S);
    TransMail(hp145, 'UM, UM');
    SendMail(hp145, 'RC');
    SendMail(hp145, 'NO ' + VolTags[Src] + '...');
    TransMail(hp145, 'MA, TALK 2');
    TestColor(Green);
    writeln('Retrieving '); TestColor(LightRed);
    writeln(VolTags[Src]);
    for i:=1 to NumPoints do begin
      ReadMail(hp145, 13);
      DataSet(Src, i):=Copy(hp145, 2, 11);
      if (i mod 100)=0 then writeln(' ');
    end;
    writeln('TestColor(Green);
    TransMail(hp145, 'UM, UM');
    end;
  end;

```

```

procedure qtr;
const m:=12;
var Ch:char;
i:integer;
i, j:real;
code:integer;
Slope, Intercept:real;
NumInteger;
Srv, Sv, Sy, Sx, Sg, SgInt:real;
Err, ErrorEst:real;

```

```

begin
  Num:=0;
  Srv:=0; Sv:=0; Sy:=0; Sx:=0; Sg:=0; SgInt:=0;
  for Num:=1 to n do begin
    Val(DataSet(1, Num), Y, Code);
    Val(DataSet(2, Num), X, Code);
    Srv:=Srv+Y;
    Sv:=Sv+Y*Y;
    Sx:=Sx+X;
    Sg:=Sg+X*Y;
    SgInt:=SgInt+X*X;
    end;
    Slope:=(Srv-Sy*(Sx/Sv))/(Sg-Sx*SgInt/Sv);
    Intercept:=Sy/Num-Slope*Sx/Num;
    TestColor(Green); writeln('Slope: ');
    TestColor(Cyan); writeln(Slope:6:4);
    TestColor(Green); writeln('Intercept: ');
    TestColor(Cyan); writeln(Intercept:6:4);
    Err:=0;
    for Num:=1 to n do begin
      Val(DataSet(1, Num), Y, Code);
      Val(DataSet(2, Num), X, Code);
      Err:=Err+Abs(Y-(Intercept+Slope*X));
    end;
    ErrorEst:=Sqrt(Err/n-2));
  end;
end;

```



[illegible]



```

TransmitData('MMA TALE 17');
for i=1 to 200 do begin
    WriteLn(i);
    Wait(temp,15);
    wait(SECCounter+1,6),GPIOut.indata(DI);
end;
SendMsg(WPInPhase,'SAVE!');      (Save G/P Configuration)

Send(GPIConfig)

procedure GPIrig;
begin
    tntcolor(lgblblue);
    writeln('~~~~~ Starting a New HP G/P Swap ~~~~~');
    SendMsg(WPInPhase,'START!');
    Delay(1000);
    SendMsg(WPInPhase,'START!');
    wait(WPInPhase,Poll,Sec);
    if Sec=0 then writeln('ERROR = Status During HP G/P Pollin');
end;

procedure GPAlt;
begin
    tntcolor(white);
    writeln('~~~~~ Waiting for Gdn/Phase Swap to End ~~~~~');
    tntcolor(green);
    repeat
        ChkRdy:=Timer then RCHistance;
        writeLn(DI);
        Delay(1000);
        SetPin(WPInPhase,Poll,Sec);
        wait(Poll and 2nd);
        ETime(S,P,SECCounter(1));
        SendMsg(WPInPhase,AUTON; AUTOB;
    tntcolor(white);
    writeln('~~~~~ Done with Gdn/Phase Swap ~~~~~');
    tntcolor(green);
end; (GPAlt)

procedure GPHup;
var
    GPhas: GPInlet;
    X1, I, J : integer;
    temp : string;
    tempval : real;
begin
    tntcolor(white);
    writeln('~~~~~ Getting Data from WPInPhase ~~~~~');
    writeln('Elapsed Time = ', Elapsed_Time, 'prev(SECCounter(1)):8.0');
    writeln;
    GPhas.Gdanc := Gdanc;
    GPhas.ElapsedTime:= Elapsed_Time, SEC_P, prev(SECCounter(1));
    GPhas.IDASH := prev(SECCounter(1));
    for I:=1 to 2 do begin
        for J:=1 to 2 do begin
            Temp:=GetPin(WPInPhase,'A?') else SendMsg(WPInPhase,'B?');
            Transmit(Tale,Tale,17);
            for K:=0 to 10 do begin
                ReadLn(temp,139);
                ReadLn(temp,9,9 do begin
                    Value:=copy(temp,'*',13)+'.12',tempval);
                    if I then GPhas.Dln((X1*10)+J+1):= round(tempval*100)
                        else GPhas.Phase((X1*10)+J+1):= round(tempval*10);
                end; (J)
            end; (K)
        end; (I)
    end; (I)
    tntcolor(green);

assign(GPFile,ExpInfo.FilerPrefix+'.g.p');
reset(GPFile);
seek(GPFile, filEnd(GPFile));

```



```

end; (end if Query)

(* ----- just together an array of row x cols with each column
representing a selected set of the swept gain or phases
at a given time during experiment. Each row represents a
set of gains at a particular frequency vs time. ----- *)

reset(OPfile);
for I := 1 to 9 do
begin
  Number_of_Records(I) := 0;
end; (for I loop)
TextColor(3);
writeln('beginning to get data from records ');
while not EOF(OPfile) do
begin
  read(OPfile, OPrec);
  Index := 0;
  IGE_Number := OPrec.IGENUM;
  FreqCtr := 1; (starting to dissect a record)
  Inc(NumberOf_Records(IGE_Number));
  writeln('Number of Records is ', NumberOf_Records(IGE_Number));
  while FreqCtr <= 200 do
  begin
    Inc(Index);
    Gain_Array[IGE_Number, Number_of_Records(IGE_Number), Index] := OPrec
      .Gain(FreqCtr);
    Phase_Array[IGE_Number, Number_of_Records(IGE_Number), Index] := OPrec
      .Phase(FreqCtr);
    If FreqCtr = 200
    then FreqCtr := FreqCtr + 1
    else FreqCtr := FreqCtr + 1;
  end; (while FreqCtr loop)
  Time_Array[Index, Number_of_Records(IGE_Number)] :=
    OPrec.Time(FreqCtr);
  Gain_Array[Index, Number_of_Records(IGE_Number), Index+1] := OPrec
    .Gain(200);
  Phase_Array[Index, Number_of_Records(IGE_Number), Index+1] := OPrec
    .Phase(200);
end; (while not EOF(OPrec))

for I := 1 to 9 do
begin
  writeln('I is ', I);
  append(OP1A(I));
  append(OP2A(I));
  append(OP3A(I));
  for IR := 1 to Number_of_Records(I) do
  begin
    writeln('number of records are ', IR);
    for CC := 1 to Number_of_Frequencies do
    begin
      write(OP1A(I), Gain_Array[I, IR, CC]:10, ' ');
      write(OP2A(I), Phase_Array[I, IR, CC]:10, ' ');
    end; (end CC)

    writeln(OP1A(I));
    writeln(OP2A(I));
    write(OP3A(I), Time_Array[I, IR]:10);
  end; (end IR)
  writeln(OP3A(I));
  close(OP1A(I));
  close(OP2A(I));
  close(OP3A(I));
end; (for I loop)

```

```

(* ----- Main program body begins here ----- *)

begin (Main)
  clrscr; Query := 'N'; Disk_Count := 0;
  writeln('You have begun to transform raw data into (Q20 & MathCAD form);
  write('Enter drive with SOURCE data '); readln(SDrive);
  write('Enter DESTINATION drive for transformed files '); readln(DDrive);
  Get Base Data;
  create file hierarchy; (* setting up file structure *)
  write('You may data should be skipped between selected points (0-200)?');
  readln(FreqCtr);
  repeat (RT)
  GainPhase;
  repeat (G2)
    TextColor(7);
    Sound(447);
    Delay(200);
    Sound(230);
    Delay(230);
    Sound(690);
    Delay(150);
  resound;
  Inc(Disk_Count); (Index of number of disks read)
  writeln('You have translated ', Disk_Count, ' disks');
  write('Shall we transform another disk to the DMR side ? (Y/N):');
  readln(QUERY);
  until (Query in ['Y', 'N', 'y', 'n']); (G2)
  until (Query in ['N', 'n']); (RT)

  TextColor(12);
  write('US DIME for now --press return');
  readln(QUERY);
  clrscr(' ');
end. (Main)

```

File Structure for LOGPLOT.PAS files

-688	-482	-81	-85	-74	-105
-683	-514	-83	-84	-78	-105
-682	-520	-85	-82	-82	-105
-684	-563	-87	-81	-87	-104
-641	-585	-93	-80	-89	-106
-631	-597	-94	-87	-19	-72
-624	-60	-91	-76	-17	-65
-344	-55	-83	-70	-16	-63
-386	-59	-64	-74	-16	-64
-422	-61	-64	-77	-17	-64
-267	-64	-88	-20	-13	-54
-37	-67	-55	-4	-10	-37
-33	-74	-39	-5	-10	-35
-32	-75	-34	-4	-9	-34
-36	-80	-33	-3	-9	-35
-35	-81	-33	-5	-9	-34
-34	-81	-29	-3	-9	-35
-34	-82	-30	-4	-9	-34
-34	-86	-27	-4	-9	-33

(Filename: Phase1.dat each row is a freq sweep)







```

close(OP1A1));
end; (for i loop) (done extracting from raw data files)
close(SCache1);
write(OP1);
for L := 1 to 9 do
begin
write(OP1, Ctrl(L):10, L:10); (print raw value count, array number)
end; (end for L loop)
close(OP1);
end; (DCResistance)

```

```

(* ----- Procedure to transpose data files into ICR format ----- *)

```

```

procedure transpose_files;
begin
for i := 1 to 9 do
begin
TestColor(14);
write('Transposing file number ', i, ' mm. ');
reset(OP1A1);
for R := 1 to Ctrl(i) do (Ctrl i is set during data writing)
begin
read(OP1A1, Time_Batr_Array[R], i, Time_Batr_Array[R], 2);
end; (for R)
reset(OP1A1);
for R := 1 to Ctrl(i) do
begin
write(OP1A1, Time_Batr_Array[R], i, 10:5, ' ');
end; (for R)
write(OP1A1);
close(OP1A1);
end; (end of i do loop)
end; (end Transpose_files)

```

```

(* ----- Main program body begins here ----- *)

```

```

begin (Main)
clear; Query:=1; Disk_Count:=0;
for L:=1 to 9 do
begin
Ctrl(L):=0; Old_Time(L):=0; New_Time(L):=0;
write('You have begun to transform raw data into ICR & MathCAD form');
write('Enter drive with source data '); readln(Drive);
write('Enter DESTINATION drive for transformed files '); readln(Drive);
Get Base Data;
create_files_hierarchy; (* setting up file structure *)
repeat (R)
DCResistance;
repeat (R2)
TestColor(7);
Sound(447);
Delay(200);
Sound(230);
Delay(230);
Sound(600);
Delay(150);
resound;
Inc(Disk_Count); (index of number of disks read)
write('You have translated ', Disk_Count, ' disks');
write('Shall we transform another disk to the ICR side ? (Y/N): ');
readln(QUERY);

```

```

until (Query in ('Y', 'y', 'Y')); (R2)
until (Query in ('N', 'n', 'N')); (R)
transpose_files;
TestColor(14);
write('YOU are DONE for NOW follow hit return');
readln(QUERY);
Close('1..');
end; (ICRstr.pas)

```

# file structure for ICRSTR.PAS file

File names: ICRSTR1.DAT, two continuous rows of serial values. The first row contains the resistance values while the second row contains the times at which the resistances were measured.

Resistance Values (in ohms)

2934.799872	.00000	2940.401728	.00000	2927.800064	.00000	2915.200000	.00000	2899.699968	.00000	966360000	.00000
764729984	.00000	666979968	.00000	621740032	.00000	572560000	.00000	530300000	.00000	504260000	.00000
462310016	.00000	449970016	.00000	438430016	.00000	419669984	.00000	402540000	.00000	384440000	.00000
358929984	.00000	345720000	.00000	339620000	.00000	329670016	.00000	326100000	.00000	3086169984	.00000
1188320000	.00000	1312870016	.00000	1462769952	.00000	1699629952	.00000	1875609984	.00000	1627350016	.00000
1686769952	.00000	1728039956	.00000	1781539968	.00000	1827500032	.00000	1858950016	.00000	1901200000	.00000
1929209984	.00000	1969510016	.00000	429160000	.00000	369340000	.00000	348270016	.00000	336340000	.00000
776609984	.00000	1009230016	.00000	1172339968	.00000	1299129984	.00000	1393030016	.00000	1486440000	.00000
1558540032	.00000	1622380032	.00000	1674790016	.00000	1726600064	.00000	1772150016	.00000	1793340032	.00000
1832380032	.00000	1860699968	.00000	1893740032	.00000	1911570048	.00000				

Measurement Times (in seconds)

38	.00000	278	.00000	508	.00000	751	.00000	984	.00000	1203	.00000
1452	.00000	1687	.00000	1917	.00000	2164	.00000	2390	.00000	2627	.00000
2859	.00000	3089	.00000	3311	.00000	3552	.00000	3784	.00000	4014	.00000
4261	.00000	4504	.00000	4762	.00000	5002	.00000	5265	.00000	5493	.00000
5726	.00000	5969	.00000	6216	.00000	6450	.00000	6693	.00000	6918	.00000
7180	.00000	7410	.00000	7643	.00000	7868	.00000	8122	.00000	8341	.00000
8580	.00000	8808	.00000	9056	.00000	9285	.00000	9538	.00000	9843	.00000
10096	.00000	10363	.00000	10583	.00000	10828	.00000	11069	.00000	11327	.00000
11571	.00000	11806	.00000	12057	.00000	12310	.00000	12550	.00000	12791	.00000
13037	.00000	13263	.00000	13517	.00000	13754	.00000	13984	.00000	14204	.00000
14441	.00000										

File names: Ranges.DAT, an array of the number of resistance measurements versus the ICR number.

61	1
61	2
61	3
61	4
60	5
60	6
60	7
60	8
60	9

The following procedures read in the triad: response data matrices for an individual ICEFT-microsensor element. The filenames of the data files are associated with the variables inside the brackets

```
Gain file := READPRN [gainx dat] Phase file := READPRN [phasex dat]

Frequencies := READPRN [freq dat]

Times file := READPRN [times dat]
```

The individual ROWs of the data matrices represent a set of sampled data values obtained during given timeframe while the measuring device swept through the frequencies of interest (10 Hz to 1 MHz). These ROWs of swept frequency values may be grouped into triad associations where the first member of the triad contains the transfer function values obtained prior to exposing the thin-film to a challenge gas ('Pre-exposure'), the second member of the triad contains a representative transfer function obtained during the thin-film exposure to a challenge gas ('Challenge'), and the third member of the triad contains the transfer function values measured after the challenge gas has been purged ('Purge') from the test chamber holding the device under test.

In order for this software to be able to extract representative triad sets from the data matrices, these matrices were manually scanned and associated with the testing time and event logs. The pertinent sets (Pre-exposure, Challenge, Purge) of triads were identified. A mapping matrix was composed which maps the software to the data set. This mapping matrix is called 'Triad'. Each row of Triad holds a triad set for a particular challenge at a particular gas concentration (Pre-exposure, Challenge, Purge). Each row of Triad maps to three rows of the measurement matrices (gainx.dat, phasex.dat, timesx.dat).

	1	7	11
	11	12	16
	31	32	36
Triad :=	45	47	50
	66	67	70
	91	93	96

number\_of\_traces := 6  
 number of traces refers to the number of concentrations to be analyzed

Filename: Sensitivity Reversibility Math\_Engines  
 Location: Math engines Disk  
 Requires: MathCAD with the data files resident in same file as the MathCAD application (unless user reallocates the file associations)

The purpose of this software file is to calculate the sensitivity and reversibility indices for the chemically-active thin-film materials used for coating the sensor portion of each ICEFT-microsensor element tested during the course of this investigation. Nine such microsensor elements are arrayed on to each device package under test.

Each of the indices are calculated from the signal transfer response functions measured across the individual sensor elements using an MP Gain and Phase Angle measurement test set. This data was downloaded from the MP analyser and stored on disk for later analysis.

The data set for each individual ICEFT-microsensor element was segregated into triplets of separate data files. For each element, a file holding gain versus frequency data was made along with a file holding the phase angle versus frequency information; the third file of the triplet held the times at which each frequency sweep commenced, relative to the start time of the entire experimental run.

Within the gain data files ('gainx.dat' files) the data is arranged in an matrix structure. Each element of the matrix represents a gain value. The ROWs of the matrix represent gain values sampled at specific frequencies. The left to right each row of gain values is arranged in order of increasing frequency. Each member of the gain data set is a four-digit integer with a leading sign entry. The four digits represent the dB value of the transfer function times 100 (dB x 100). This format was used to speed data file transfer and reduce disk file size.

The phase angle files ('phasex.dat' files) are similarly arranged, with the individual values being four-digit signed integers representing angles in degrees.

j := 1 number\_of\_traces 'j' is the ROW number index

i := 1 : 35 'i' is the ROW ELEMENT index

To calculate the difference ( in dba or degrees) between a pre-exposure and the challenge gas exposure transfer response, the following are evaluated (one set per IGEPET-microsensor element). Each row of the data matrices holds 35 elements. The 'j' subscripts references to the ROW NUMBER of the Triad matrix, mapping to a ROW NUMBER of the data matrix. The 'i' subscript references the individual ROW ELEMENTS of the referenced ROW.

$$\begin{aligned}
 GCng_{j,1} &:= \frac{\text{Gain\_file}_{Triad,j,1} - \text{Gain\_file}_{Triad,j,1}}{100} \\
 PCng_{j,1} &:= \frac{\text{Phase\_file}_{Triad,j,1} - \text{Phase\_file}_{Triad,j,1}}{100} \\
 ARng_{j,1} &:= \frac{\text{Gain\_file}_{Triad,j,1} - \text{Gain\_file}_{Triad,j,1}}{100} \\
 ARvp_{j,1} &:= \frac{\text{Phase\_file}_{Triad,j,1} - \text{Phase\_file}_{Triad,j,1}}{100}
 \end{aligned}$$

# SENSITIVITY CALCULATIONS

The sensitivity calculations are based upon the following:

$$Sensitivity = (G2 - G1)/G1,$$

where G1 is the output voltage during the pre-challenge purge cycle, and G2 is the output during the challenge gas exposure. This relationship is used for both the gain and phase angle sensitivity calculations; however, care must be taken to convert the gain data from dba to voltage prior to using the above equation.

In the following, 'SensG' is the gain sensitivity in percent.

$$SensG_{j,1} := 100 \cdot \frac{\left[ \frac{\text{Gain\_file}_{Triad,j,1} - \text{Gain\_file}_{Triad,j,1}}{2000} \right] - \left[ \frac{\text{Gain\_file}_{Triad,j,1} - \text{Gain\_file}_{Triad,j,1}}{2000} \right]}{10}$$

In the following, 'SensP' is the phase angle sensitivity in percent.

$$SensP_{j,1} := 100 \cdot \frac{\left[ \frac{\text{Phase\_file}_{Triad,j,1} - \text{Phase\_file}_{Triad,j,1}}{2000} \right] - \left[ \frac{\text{Phase\_file}_{Triad,j,1} - \text{Phase\_file}_{Triad,j,1}}{2000} \right]}{10}$$

The reversibility indices are calculated by a two step process. First the pre-exposure transfer response values are subtracted from the purge response values. This result is normalized by dividing it by the pre-exposure values. If the material completely reverses, this result would be zero. Secondly, the normalized value is subtracted from one, and the result reported in percent. A final value of one would indicate complete reversibility. Values other than one indicate an incomplete reversal.

$$RevC_{j,i} := 100 - \frac{\left[ \frac{Gain\_file\_Tried_{j,i}}{2000} - \frac{Gain\_file\_Tried_{j,i}}{2000} \right]}{10} + 1$$

$$RevP_{j,i} := 100 - \frac{\left[ \frac{Phase\_file\_Tried_{j,i}}{2000} - \frac{Phase\_file\_Tried_{j,i}}{2000} \right]}{10} + 1$$

## *Appendix C: Response of CuPc Thin-Film Coatings.*

This appendix presents a portion of the significant responses to the challenge gas for the CuPc thin-films evaluated during this investigation. The appendix is divided into two sections: Section 1 deals with the responses to challenge gases at 150°C (referred to as the Series II tests in the thesis body); Section 2 presents information concerning DMMP and DIMP challenges to CuPc at temperatures of 150°C, 90°C, and 30°C.

### *Section 1*

Resistance and gain and phase angle transfer function responses for the challenge and purge cycles are provided as:

- CuPc challenged with NO<sub>2</sub> (Figures C-1 to C-52),
  - dc resistance measurements versus time,
  - gain and phase angle measurements versus frequency,
  - sensitivity, and reversibility calculations versus frequency,
- CuPc challenged with NH<sub>3</sub> (Figures C-53 to C- 69),
  - dc resistance measurements versus time,
  - gain and phase angle measurements versus frequency,
- CuPc challenged with BF<sub>3</sub> (Figures C-70 to C-88),
  - dc resistance measurements versus time,
  - gain and phase angle measurements versus frequency,

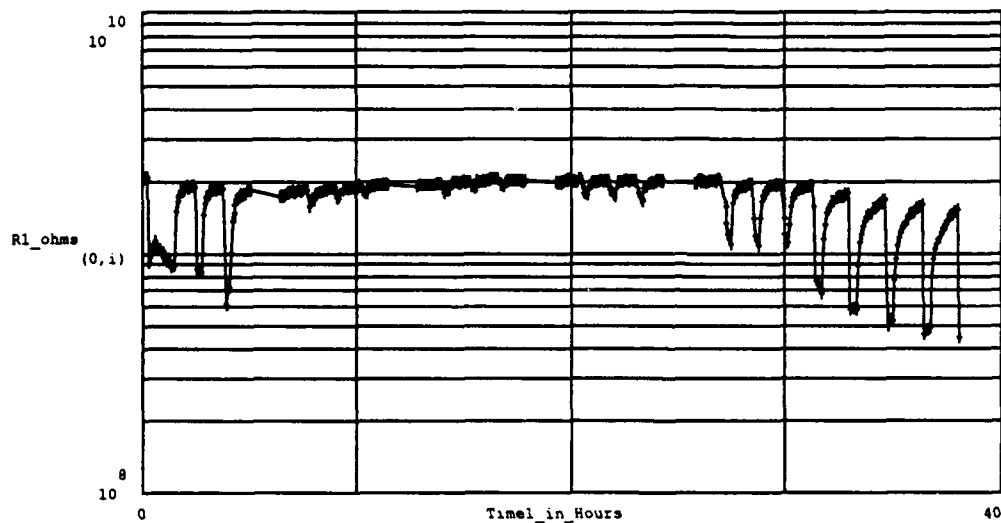


Figure C-1. . DC Resistance Measured Between the Driven-Electrode and Floating-Electrode of the IGE Array, During Series of Purges and Challenge Gas Exposures. The Number of Measurements (at crosses) is 479. The Testing Conditions Included the Following:

IGE Array Number : 1,	Thin-film Material : Copper Phthalocyanine,
Thin-film Thickness : 1,600 Angstroms	Test Temperature(s) : Purge & Challenge at 150°C
Purge Gas : Room Air,	Challenge Gas : Nitrogen Dioxide,
Challenge Gas Concentration(s) (in order run) : 1000 ppb, 30 ppb, 50 ppb, 100 ppb, 500 ppb, 1000 ppb.	

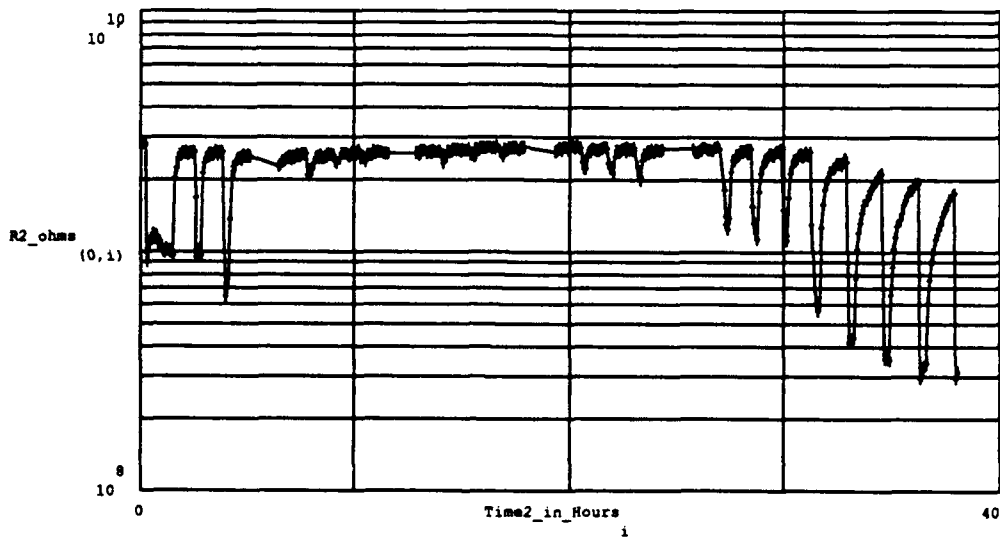


Figure C-2. . DC Resistance Measured Between the Driven-Electrode and Floating-Electrode of the IGE Array, During Series of Purges and Challenge Gas Exposures. The Number of Measurements (at crosses) is 479. The Testing Conditions Included the Following:

IGE Array Number : 2,	Thin-film Material : Copper Phthalocyanine,
Thin-film Thickness : 1,600 Angstroms	Test Temperature(s) : Purge & Challenge at 150°C
Purge Gas : Room Air,	Challenge Gas : Nitrogen Dioxide,
Challenge Gas Concentration(s) (in order run) : 1000 ppb, 30 ppb, 50 ppb, 100 ppb, 500 ppb, 1000 ppb.	

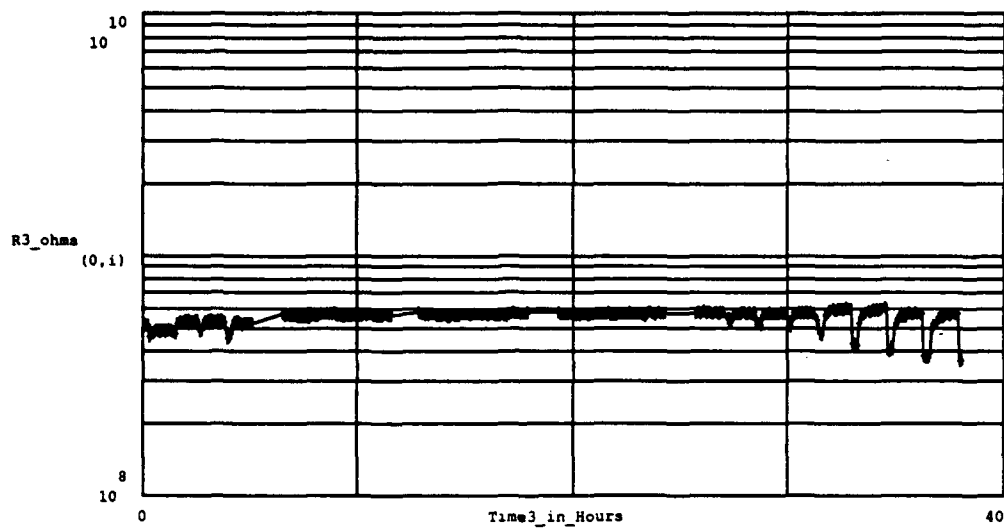


Figure C-3. . DC Resistance Measured Between the Driven-Electrode and Floating-Elec rode of the IGE Array, During Series of Purges and Challenge Gas Exposures. The Number of Measurements (at crosses) is 479. The Testing Conditions Included the Following:

IGE Array Number : 3,	Thin-film Material : Copper Phthalocyanine,
Thin-film Thickness : 1,600 Angstroms	Test Temperature(s) : Purge & Challenge at 150°C
Purge Gas : Room Air,	Challenge Gas : Nitrogen Dioxide,
Challenge Gas Concentration(s) (in order run) : 1000 ppb, 30 ppb, 50 ppb, 100 ppb, 500 ppb, 1000 ppb.	

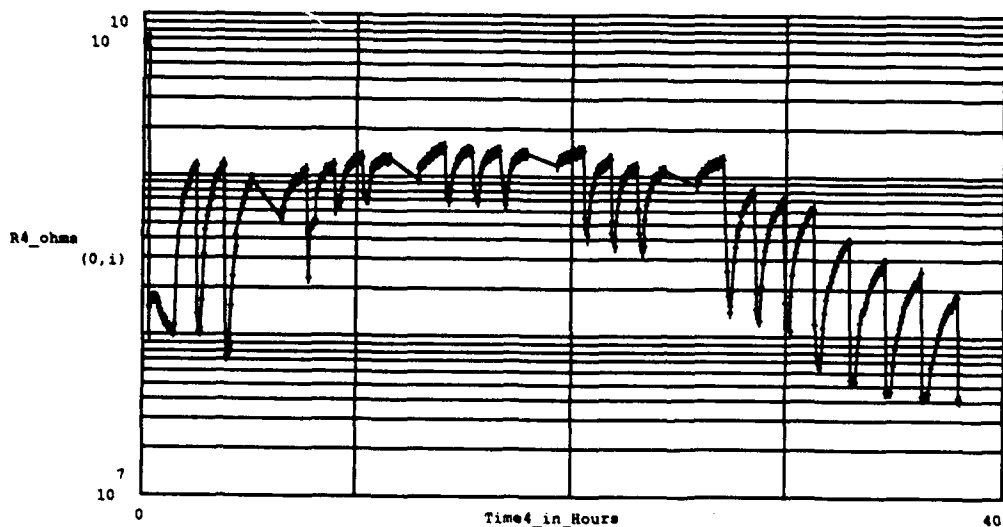


Figure C-4. . DC Resistance Measured Between the Driven-Electrode and Floating-Electrode of the IGE Array, During Series of Purges and Challenge Gas Exposures. The Number of Measurements (at crosses) is 479. The Testing Conditions Included the Following:

IGE Array Number : 4,	Thin-film Material : Copper Phthalocyanine,
Thin-film Thickness : 3,900 Angstroms	Test Temperature(s) : Purge & Challenge at 150°C
Purge Gas : Room Air,	Challenge Gas : Nitrogen Dioxide,
Challenge Gas Concentration(s) (in order run) : 1000 ppb, 30 ppb, 50 ppb, 100 ppb, 500 ppb, 1000 ppb.	



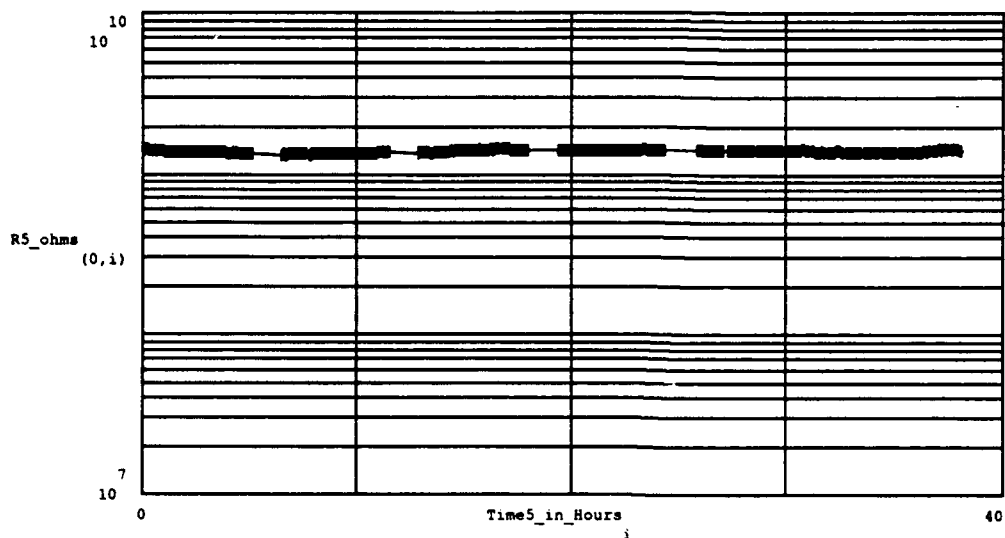


Figure C-5. . This IGE Microsensor Malfunctioned. DC Resistance Measured Between the Driven-Electrode and Floating-Electrode of the IGE Array, During Series of Purges and Challenge Gas Exposures. The Number of Measurements (at crosses) is 479. The Testing Conditions Included the Following:

IGE Array Number : 5,	Thin-film Material : Copper Phthalocyanine,
Thin-film Thickness : 3,900 Angstroms	Test Temperature(s) : Purge & Challenge at 150°C
Purge Gas : Room Air,	Challenge Gas : Nitrogen Dioxide,
Challenge Gas Concentration(s) (in order run) : 1000 ppb, 30 ppb, 50 ppb, 100 ppb, 500 ppb, 1000 ppb.	

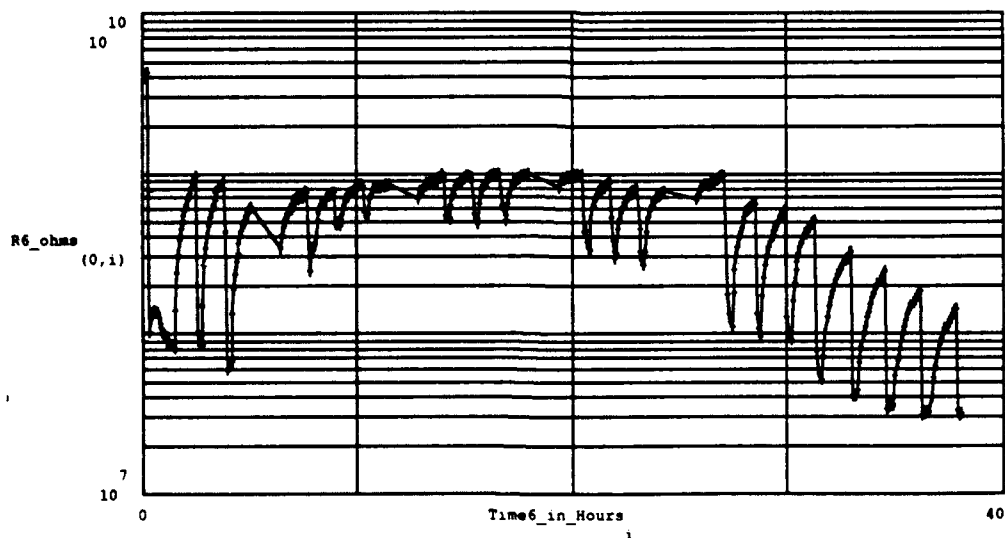


Figure C-6. . DC Resistance Measured Between the Driven-Electrode and Floating-Electrode of the IGE Array, During Series of Purges and Challenge Gas Exposures. The Number of Measurements (at crosses) is 479. The Testing Conditions Included the Following:

IGE Array Number : 6,	Thin-film Material : Copper Phthalocyanine,
Thin-film Thickness : 3,900 Angstroms	Test Temperature(s) : Purge & Challenge at 150°C
Purge Gas : Room Air,	Challenge Gas : Nitrogen Dioxide,
Challenge Gas Concentration(s) (in order run) : 1000 ppb, 30 ppb, 50 ppb, 100 ppb, 500 ppb, 1000 ppb.	

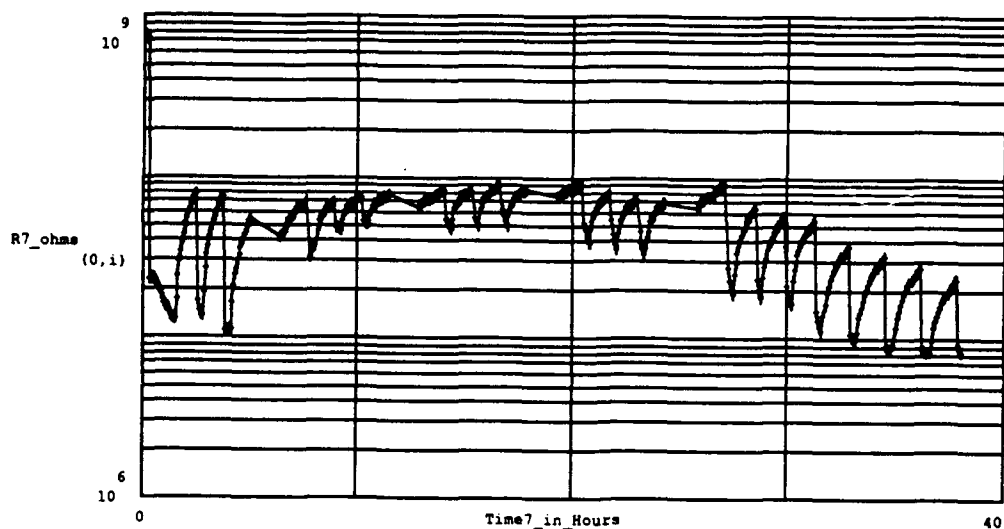


Figure C-7. . DC Resistance Measured Between the Driven-Electrode and Floating-Electrode of the IGE Array, During Series of Purges and Challenge Gas Exposures. The Number of Measurements (at crosses) is 479. The Testing Conditions Included the Following:

IGE Array Number : 7,	Thin-film Material : Copper Phthalocyanine,
Thin-film Thickness : 8,800 Angstroms	Test Temperature(s) : Purge & Challenge at 150°C
Purge Gas : Room Air,	Challenge Gas : Nitrogen Dioxide,
Challenge Gas Concentration(s) (in order run) : 1000 ppb, 30 ppb, 50 ppb, 100 ppb, 500 ppb, 1000 ppb.	

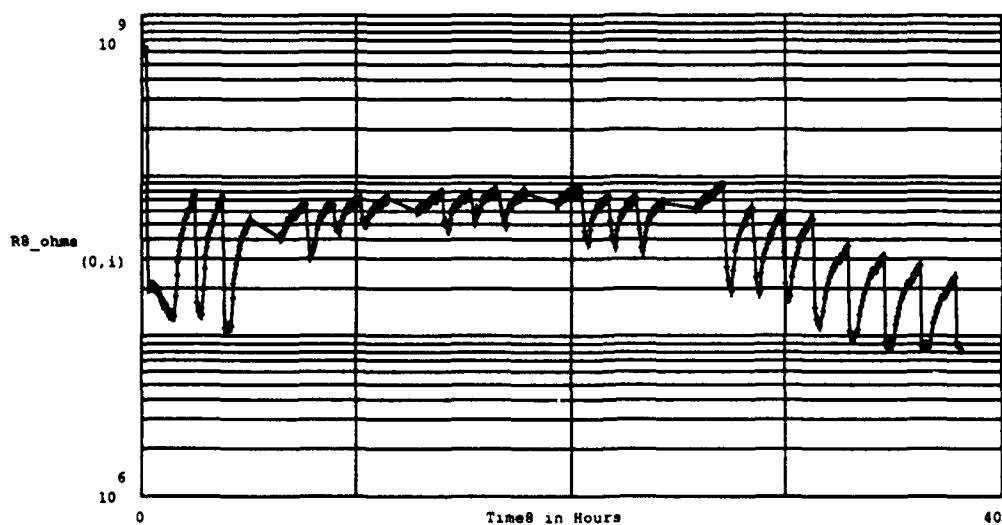


Figure C-8. . DC Resistance Measured Between the Driven-Electrode and Floating-Electrode of the IGE Array, During Series of Purges and Challenge Gas Exposures. The Number of Measurements (at crosses) is 479. The Testing Conditions Included the Following:

IGE Array Number : 8,	Thin-film Material : Copper Phthalocyanine,
Thin-film Thickness : 8,800 Angstroms	Test Temperature(s) : Purge & Challenge at 150°C
Purge Gas : Room Air,	Challenge Gas : Nitrogen Dioxide,
Challenge Gas Concentration(s) (in order run) : 1000 ppb, 30 ppb, 50 ppb, 100 ppb, 500 ppb, 1000 ppb.	

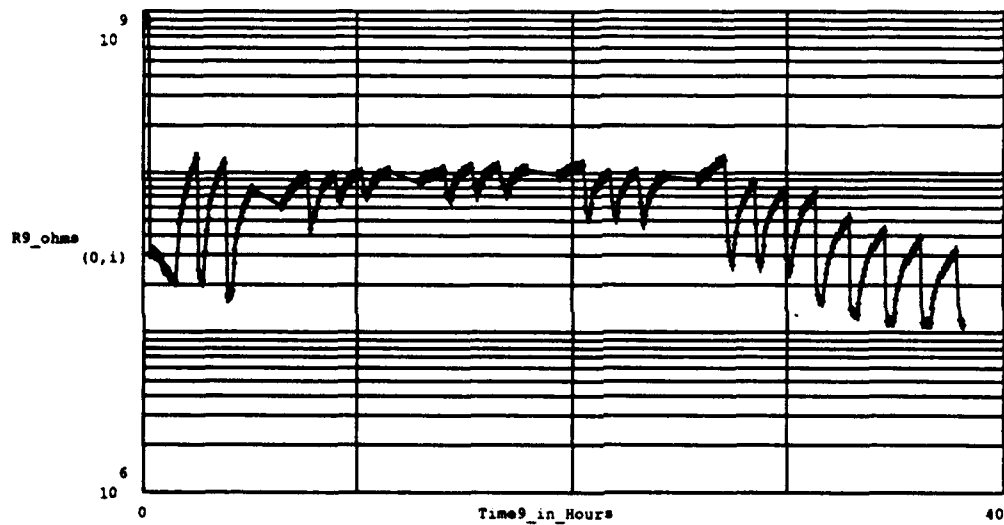


Figure C- 9. . DC Resistance Measured Between the Driven-Electrode and Floating-Electrode of the IGE Array, During Series of Purges and Challenge Gas Exposures. The Number of Measurements (at crosses) is 479. The Testing Conditions Included the Following:

IGE Array Number : 9,	Thin-film Material : Copper Phthalocyanine.
Thin-film Thickness : 8,800 Angstroms	Test Temperature(s) : Purge & Challenge at 150°C
Purge Gas : Room Air,	Challenge Gas : Nitrogen Dioxide.
Challenge Gas Concentration(s) (in order run) : 1000 ppb, 30 ppb, 50 ppb, 100 ppb, 500 ppb, 1000 ppb.	

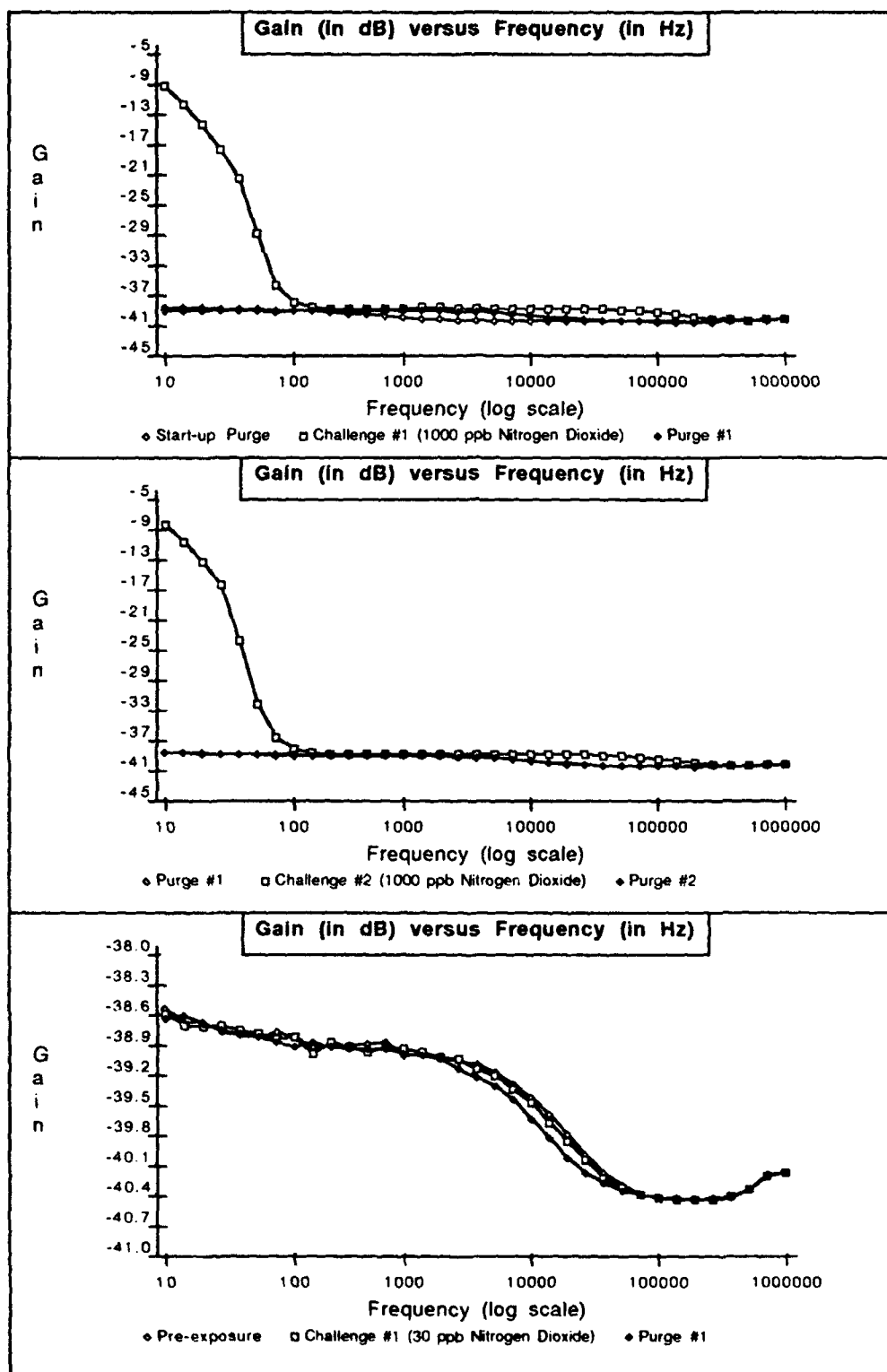


Figure C-10 . Gain versus Frequency Response of IGEFET Microsensor for a Series of Room Air Purges and Challenge Gas Exposures. Testing Conditions: IGE Microsensor Number 1; CuPc Thin-film (1,600 Angstroms Thick); Temperature of 150 degrees Centigrade; Nitrogen Dioxide Challenge Gas (Order of Exposures:1000 ppb, 30 ppb, 50 ppb, 100 ppb, 500 ppb, 1000 ppb).

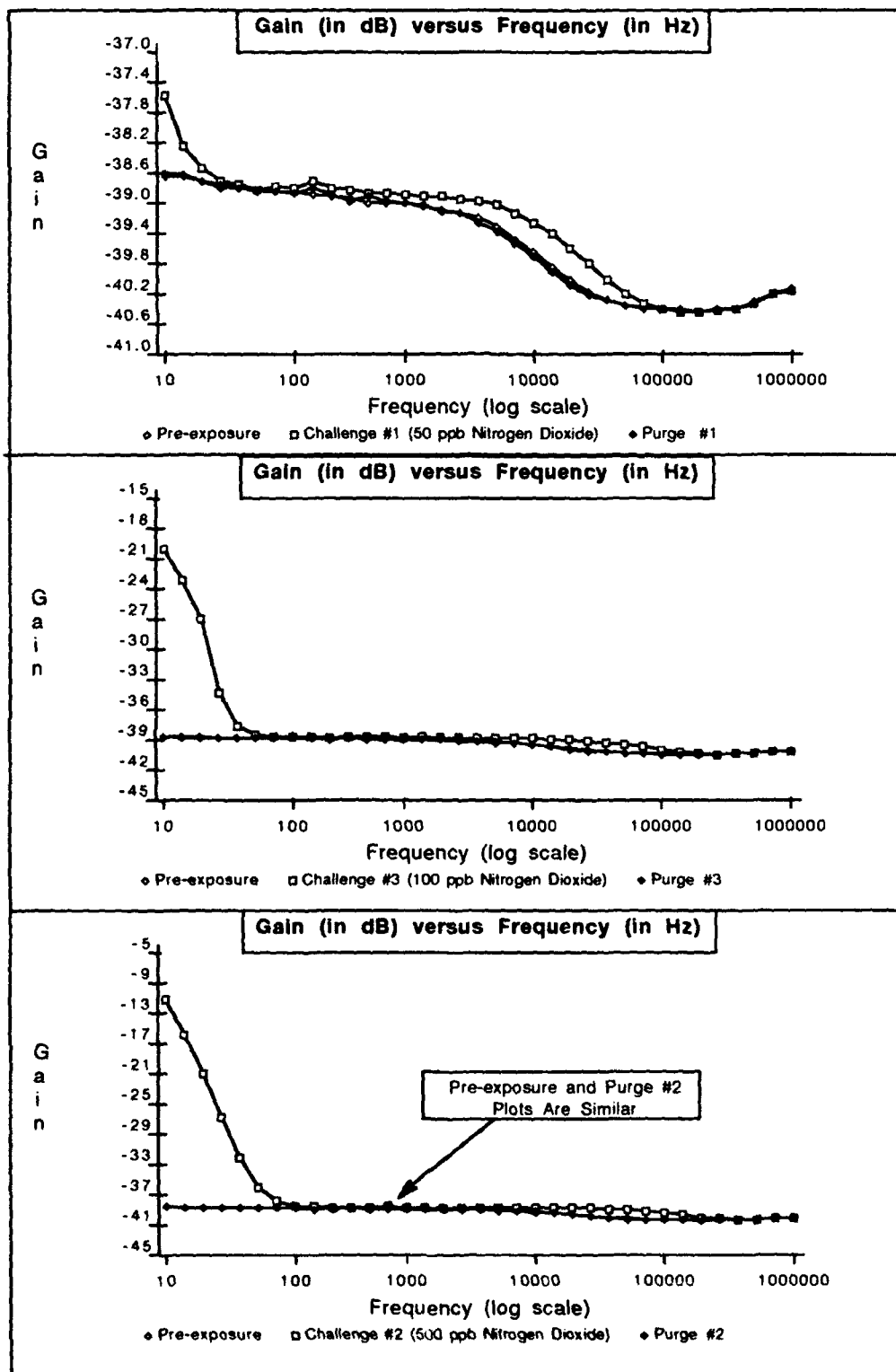


Figure C-11. Gain versus Frequency Response of IGEFET Microsensor for a Series of Room Air Purges and Challenge Gas Exposures. Testing Conditions: IGE Microsensor Number 1; CuPc Thin-film (1,600 Angstroms Thick); Temperature of 150 degrees Centigrade; Nitrogen Dioxide Challenge Gas (Order of Exposures: 1000 ppb, 30 ppb, 50 ppb, 100 ppb, 500 ppb, 1000 ppb).

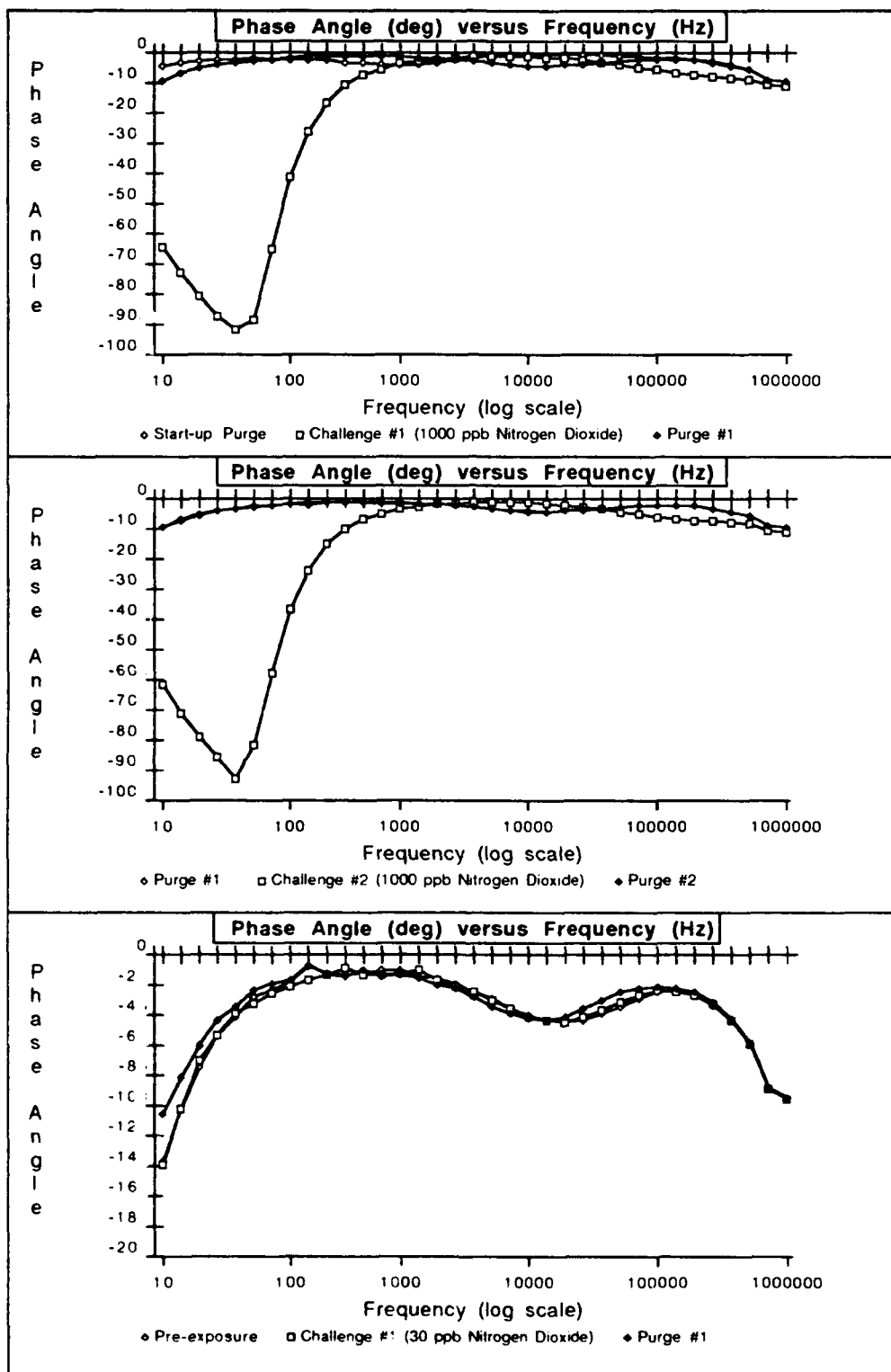


Figure C-12. Phase Angle versus Frequency Response of IGEFET Microsensor for a Series of Room Air Purges and Challenge Gas Exposures. Testing Conditions: IGE Microsensor Number 1; CuPc Thin-film (1,600 Angstroms Thick); Temperature of 150 degrees Centigrade; Nitrogen Dioxide Challenge Gas (Order of Exposures: 1000 ppb, 30 ppb, 50 ppb, 100 ppb, 500 ppb, 1000 ppb).

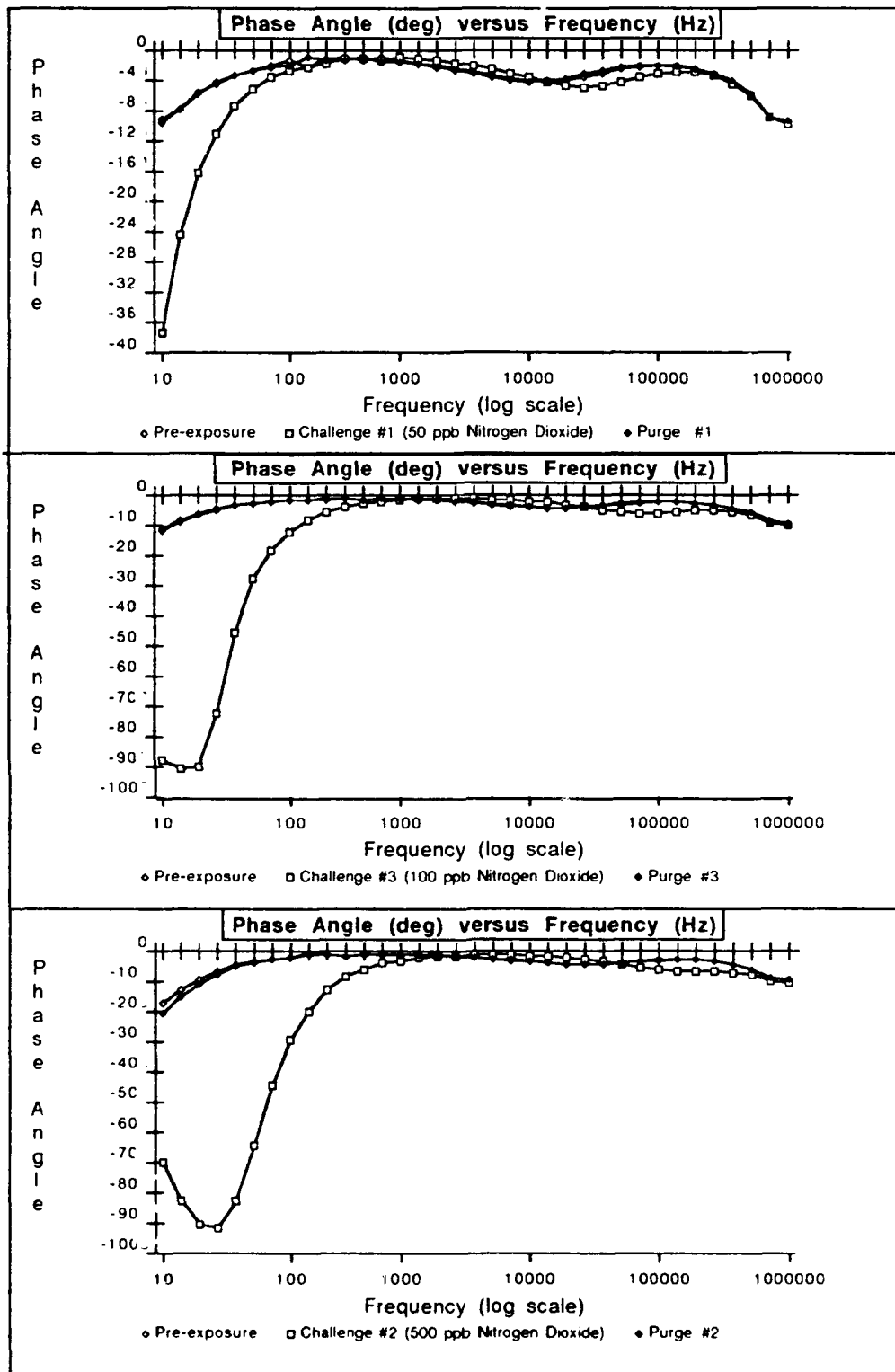


Figure C-13 . Phase Angle versus Frequency Response of IGEFET Microsensor for a Series of Room Air Purges and Challenge Gas Exposures. Testing Conditions: IGE Microsensor Number 1; CuPc Thin-film (1,600 Angstroms Thick); Temperature of 150 degrees Centigrade; Nitrogen Dioxide Challenge Gas (Order of Exposures: 1000 ppb, 30 ppb, 50 ppb, 100 ppb, 500 ppb, 1000 ppb).

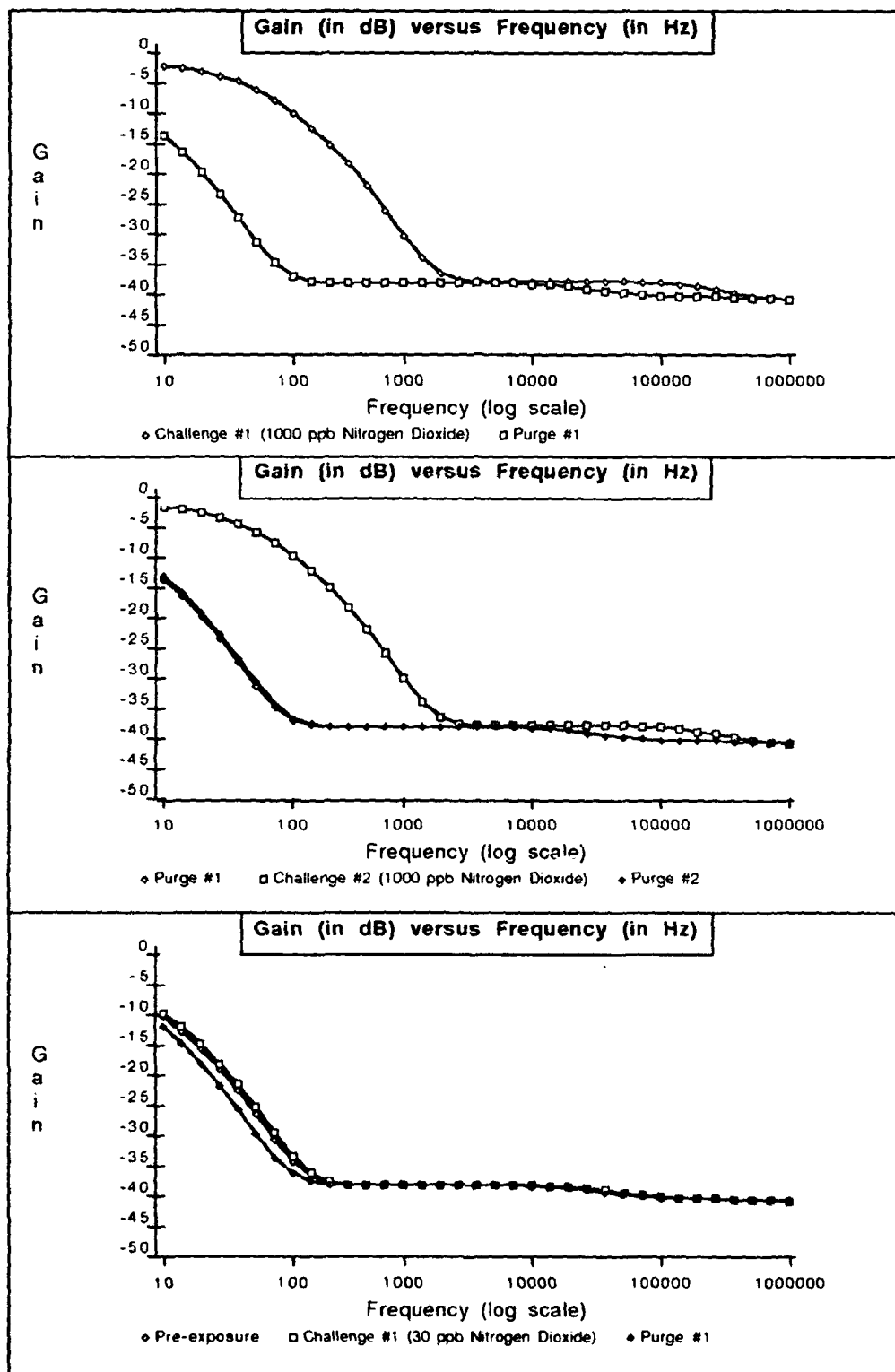


Figure C-14 . Gain versus Frequency Response of IGEFET Microsensor for a Series of Room Air Purges and Challenge Gas Exposures. Testing Conditions: IGE Microsensor Number 4; CuPc Thin-film (3,900 Angstroms Thick); Temperature of 150 degrees Centigrade; Nitrogen Dioxide Challenge Gas (Order of Exposures: 1000 ppb, 30 ppb, 50 ppb, 100 ppb, 500 ppb, 1000 ppb).



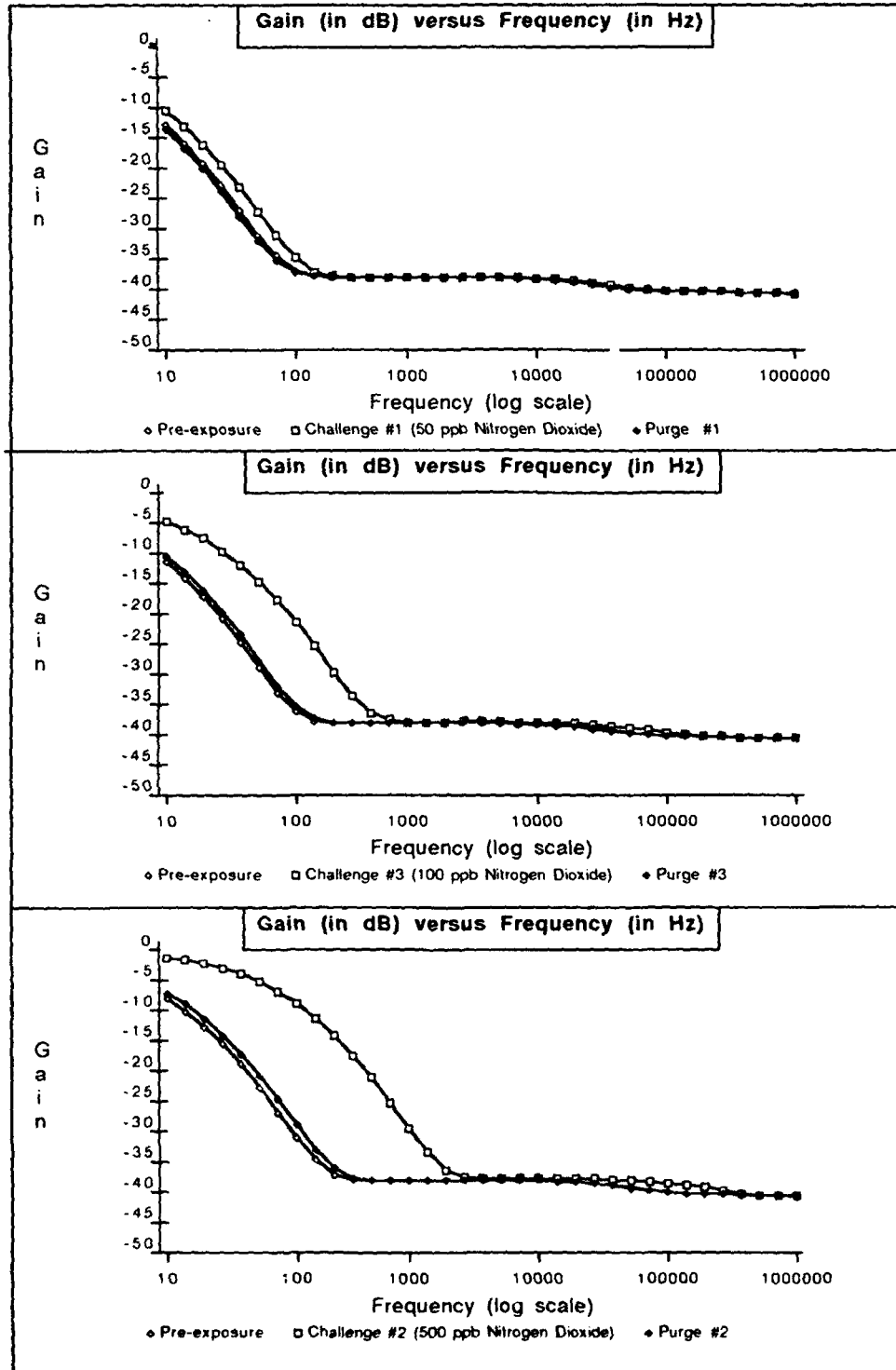


Figure C-15. Gain versus Frequency Response of IGEFET Microsensor for a Series of Room Air Purges and Challenge Gas Exposures. Testing Conditions: IGE Microsensor Number 4: CuPc Thin-film (3,900 Angstroms Thick); Temperature of 150 degrees Centigrade; Nitrogen Dioxide Challenge Gas (Order of Exposures: 1000 ppb, 30 ppb, 50 ppb, 100 ppb, 500 ppb, 1000 ppb).

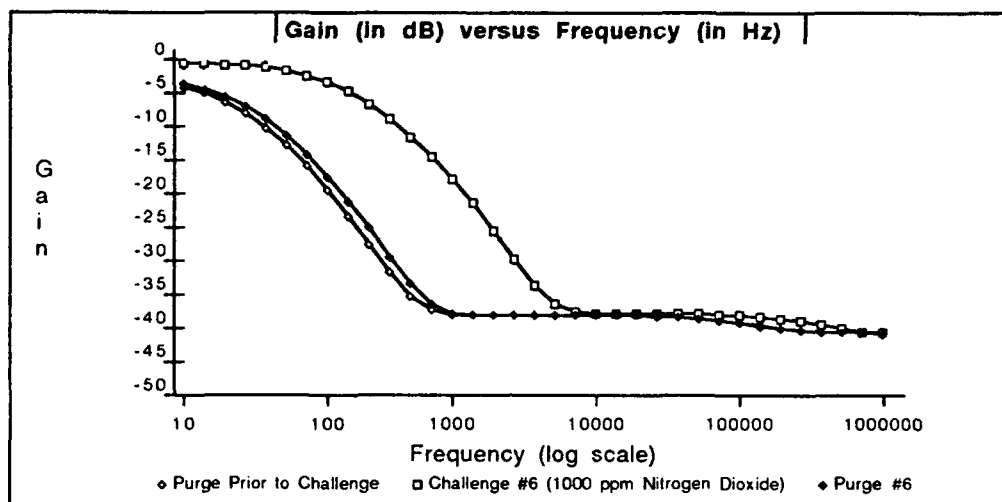


Figure C-16 . Gain versus Frequency Response of IGEFET Microsensor for a Series of Room Air Purges and Challenge Gas Exposures. Testing Conditions: IGE Microsensor Number 4; CuPc Thin-film (3,900 Angstroms Thick); Temperature of 150 degrees Centigrade; Nitrogen Dioxide Challenge Gas (Order of Exposures: 1000 ppb, 30 ppb, 50 ppb, 100 ppb, 500 ppb, 1000 ppb).

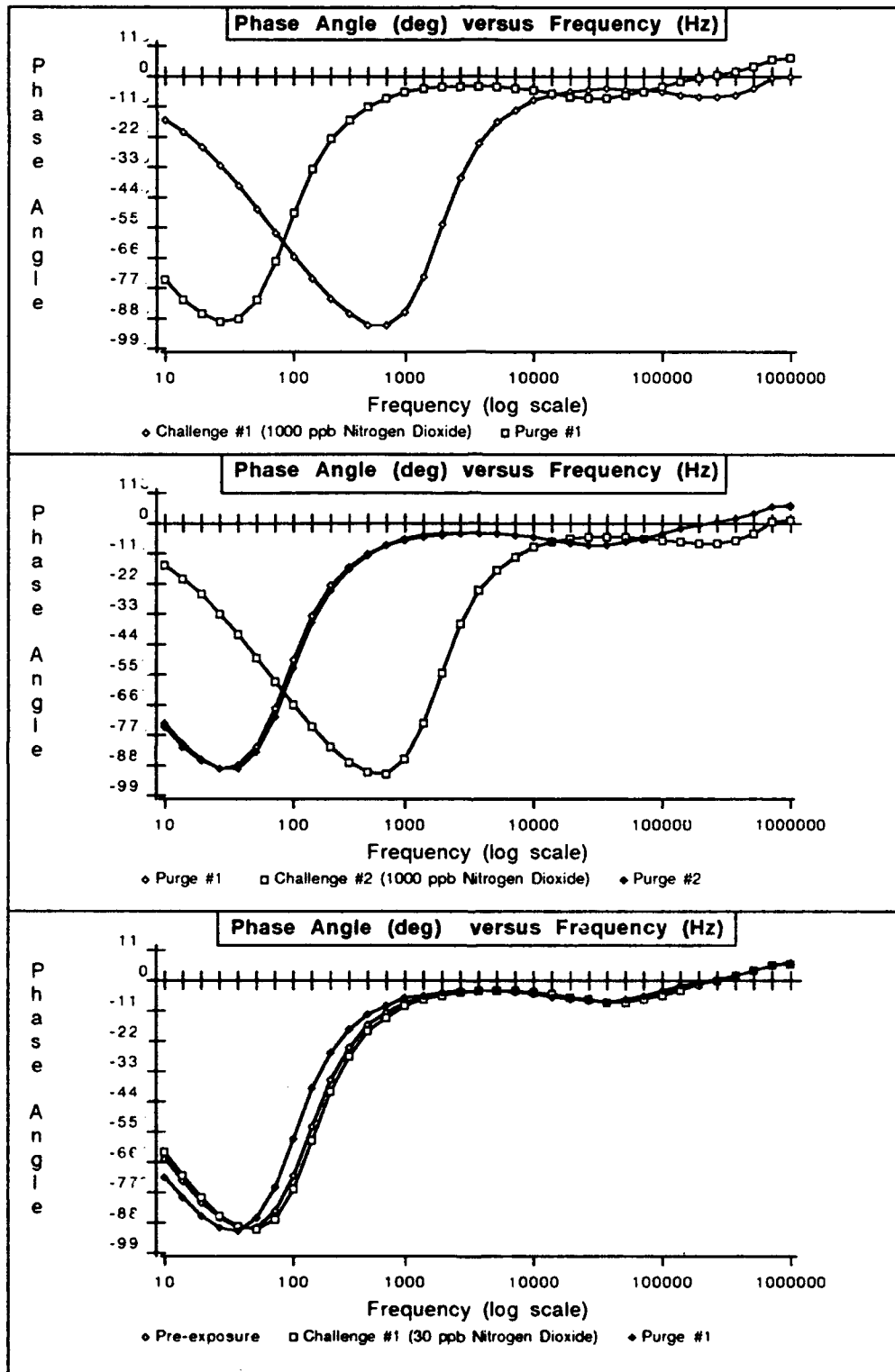


Figure C-17 . Phase Angle versus Frequency Response of IGEFET Microsensor for a Series of Room Air Purges and Challenge Gas Exposures. Testing Conditions: IGE Microsensor Number 4; CuPc Thin-film (3,900 Angstroms Thick); Temperature of 150 degrees Centigrade; Nitrogen Dioxide Challenge Gas (Order of Exposures: 1000 ppb, 30 ppb, 50 ppb, 100 ppb, 500 ppb, 1000 ppb).

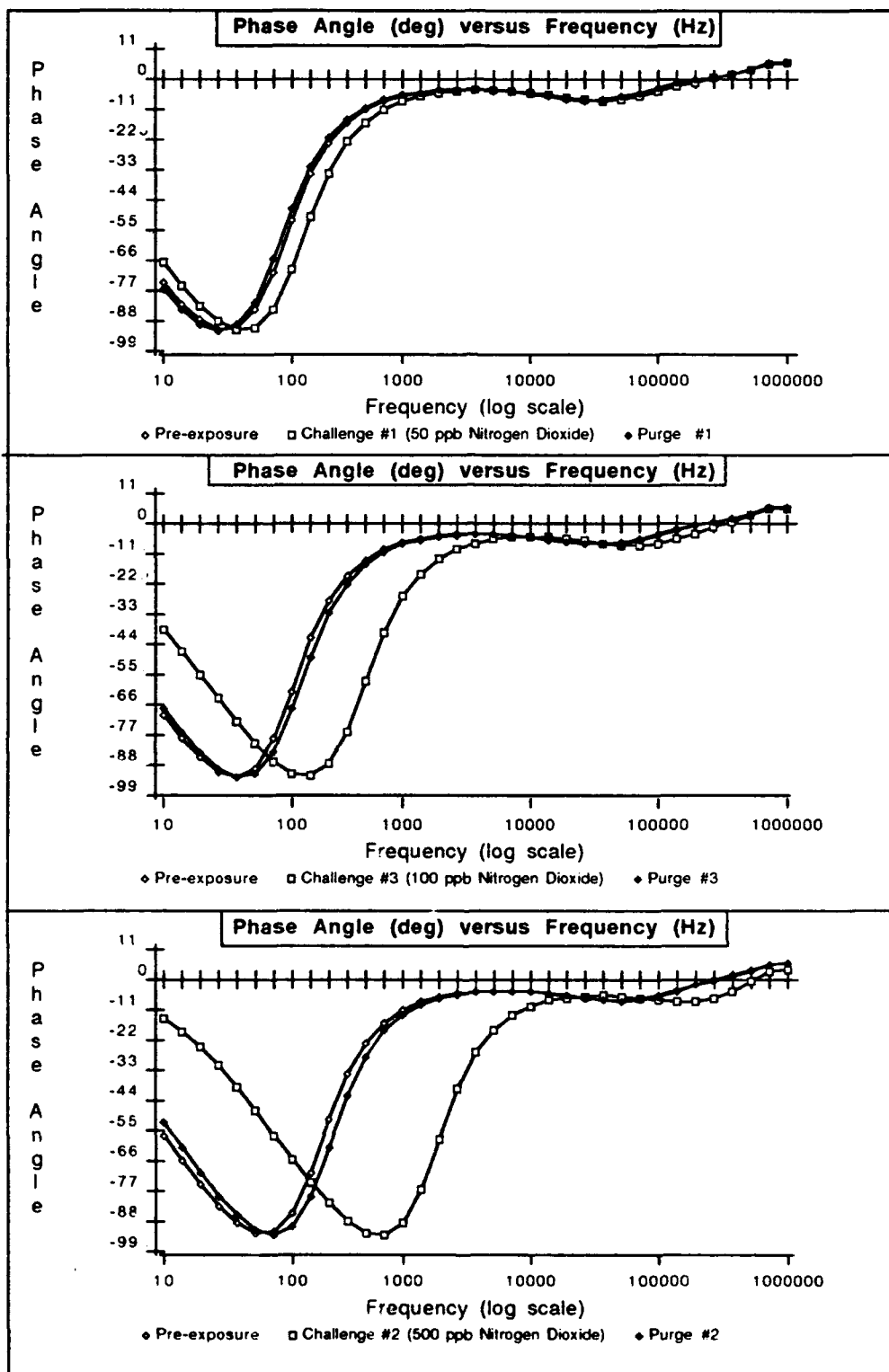


Figure C-18. Phase Angle versus Frequency Response of IGEFET Microsensor for a Series of Room Air Purges and Challenge Gas Exposures. Testing Conditions: IGE Microsensor Number 4; CuPc Thin-film (3,900 Angstroms Thick); Temperature of 150 degrees Centigrade; Nitrogen Dioxide Challenge Gas (Order of Exposures: 1000 ppb, 30 ppb, 50 ppb, 100 ppb, 500 ppb, 1000 ppb).

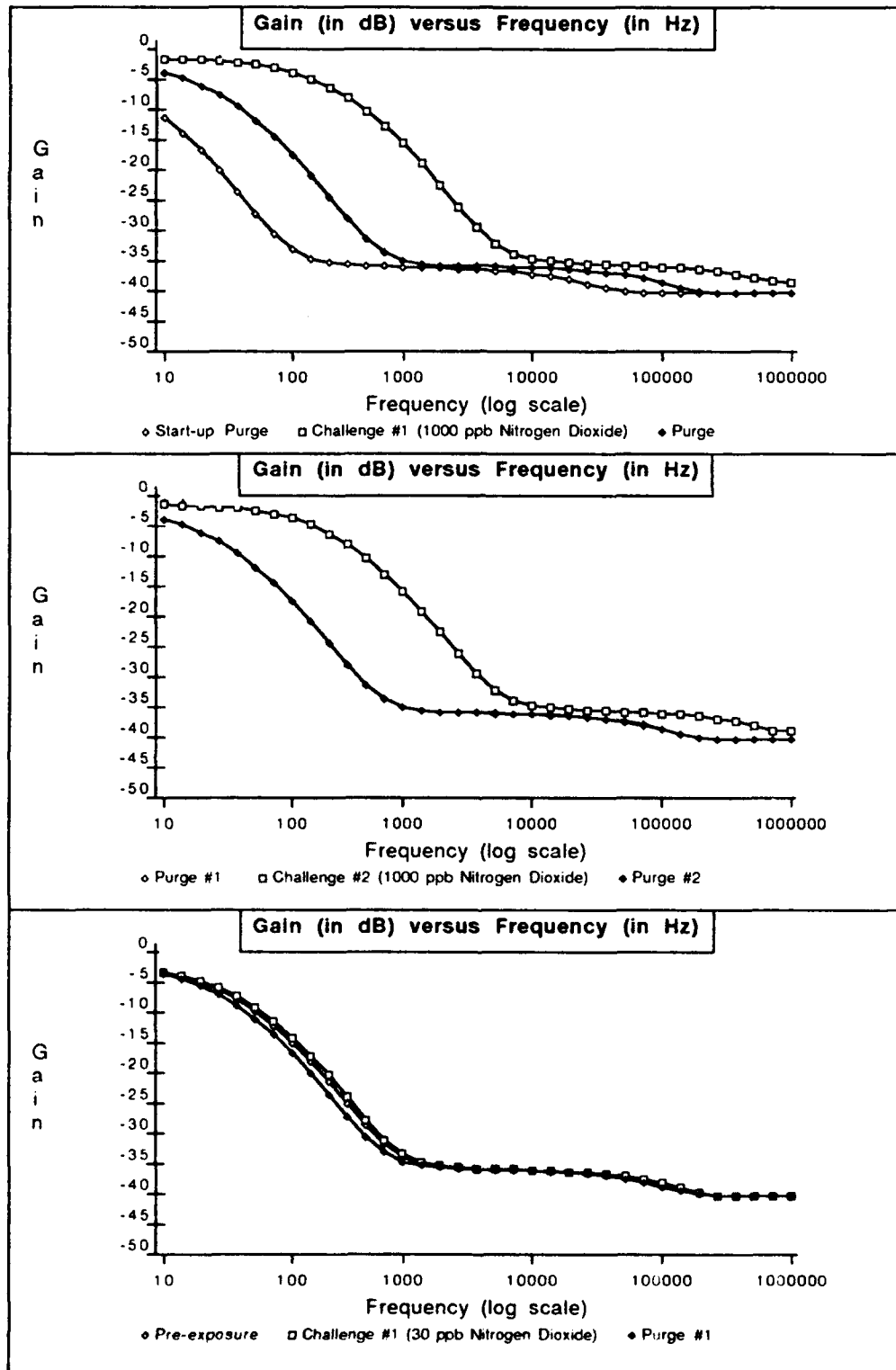


Figure C-19.. Gain versus Frequency Response of IGEFET Microsensor for a Series of Room Air Purges and Challenge Gas Exposures. Testing Conditions: IGE Microsensor Number 9; CuPc Thin-film (8,800 Angstroms Thick); Temperature of 150 degrees Centigrade; Nitrogen Dioxide Challenge Gas (Order of Exposures: 1000 ppb, 30 ppb, 50 ppb, 100 ppb, 500 ppb, 1000 ppb).

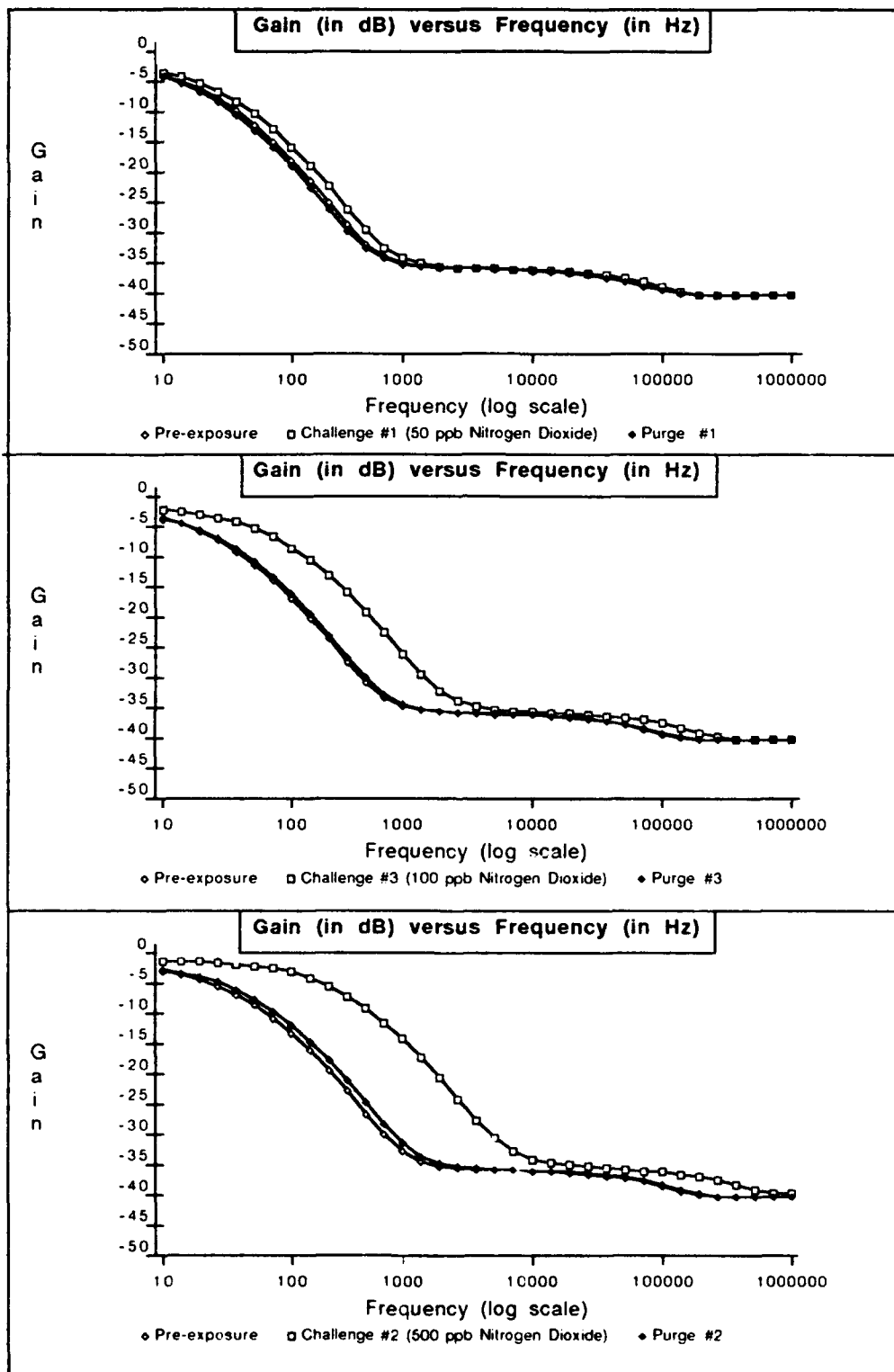


Figure C-20 . Gain versus Frequency Response of IGEFET Microsensor for a Series of Room Air Purges and Challenge Gas Exposures. Testing Conditions: IGE Microsensor Number 9; CuPc Thin-film (8,800 Angstroms Thick); Temperature of 150 degrees Centigrade; Nitrogen Dioxide Challenge Gas (Order of Exposures: 1000 ppb, 30 ppb, 50 ppb, 100 ppb, 500 ppb, 1000 ppb).

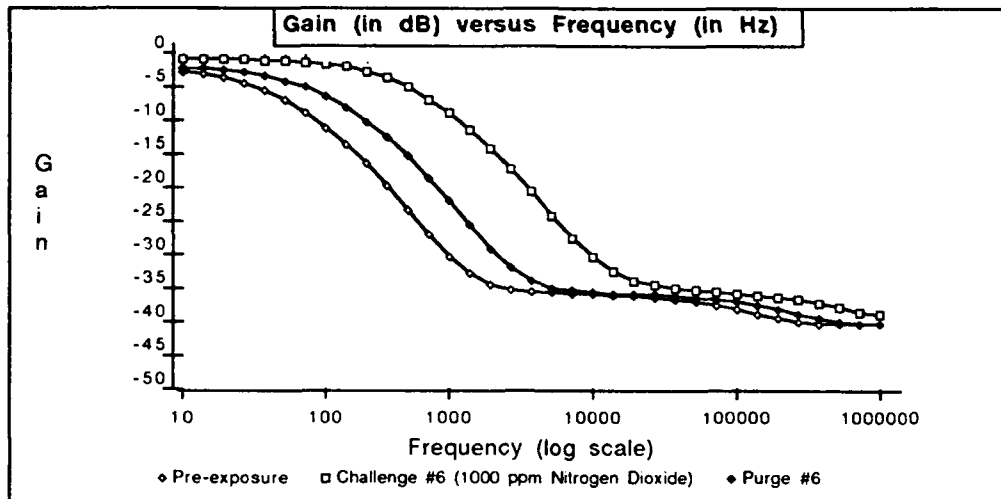


Figure C-21. Gain versus Frequency Response of IGEFET Microsensor for a Series of Room Air Purges and Challenge Gas Exposures. Testing Conditions: IGE Microsensor Number 9; CuPc Thin-film (8,800 Angstroms Thick); Temperature of 150 degrees Centigrade; Nitrogen Dioxide Challenge Gas (Order of Exposures: 1000 ppb, 30 ppb, 50 ppb, 100 ppb, 500 ppb, 1000 ppb).

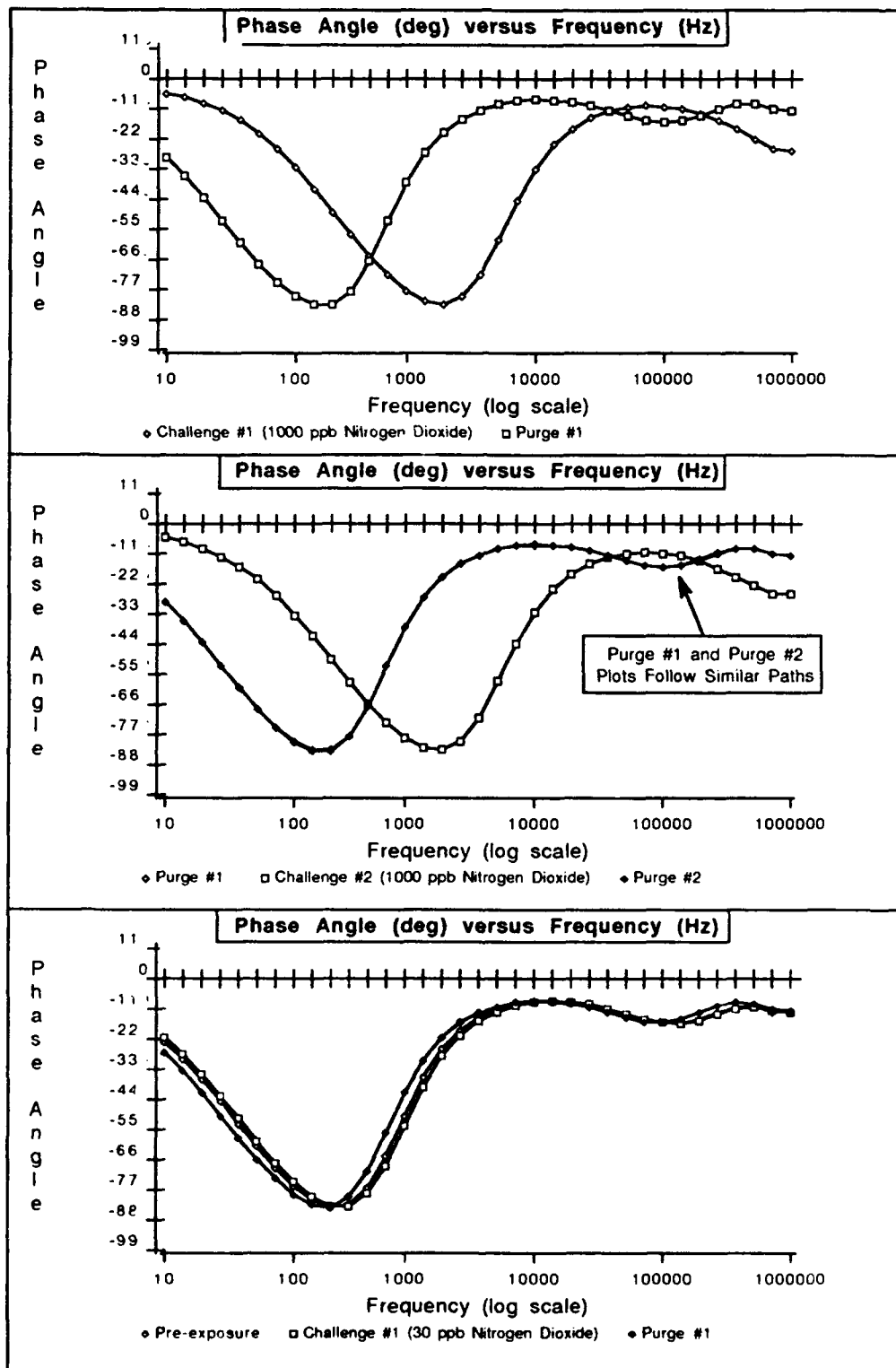


Figure C-22. . Phase Angle versus Frequency Response of IGEFET Microsensor for a Series of Room Air Purges and Challenge Gas Exposures. Testing Conditions: IGE Microsensor Number 9; CuPc Thin-film (8,800 Angstroms Thick); Temperature of 150 degrees Centigrade; Nitrogen Dioxide Challenge Gas (Order of Exposures: 1000 ppb, 30 ppb, 50 ppb, 100 ppb, 500 ppb, 1000 ppb).



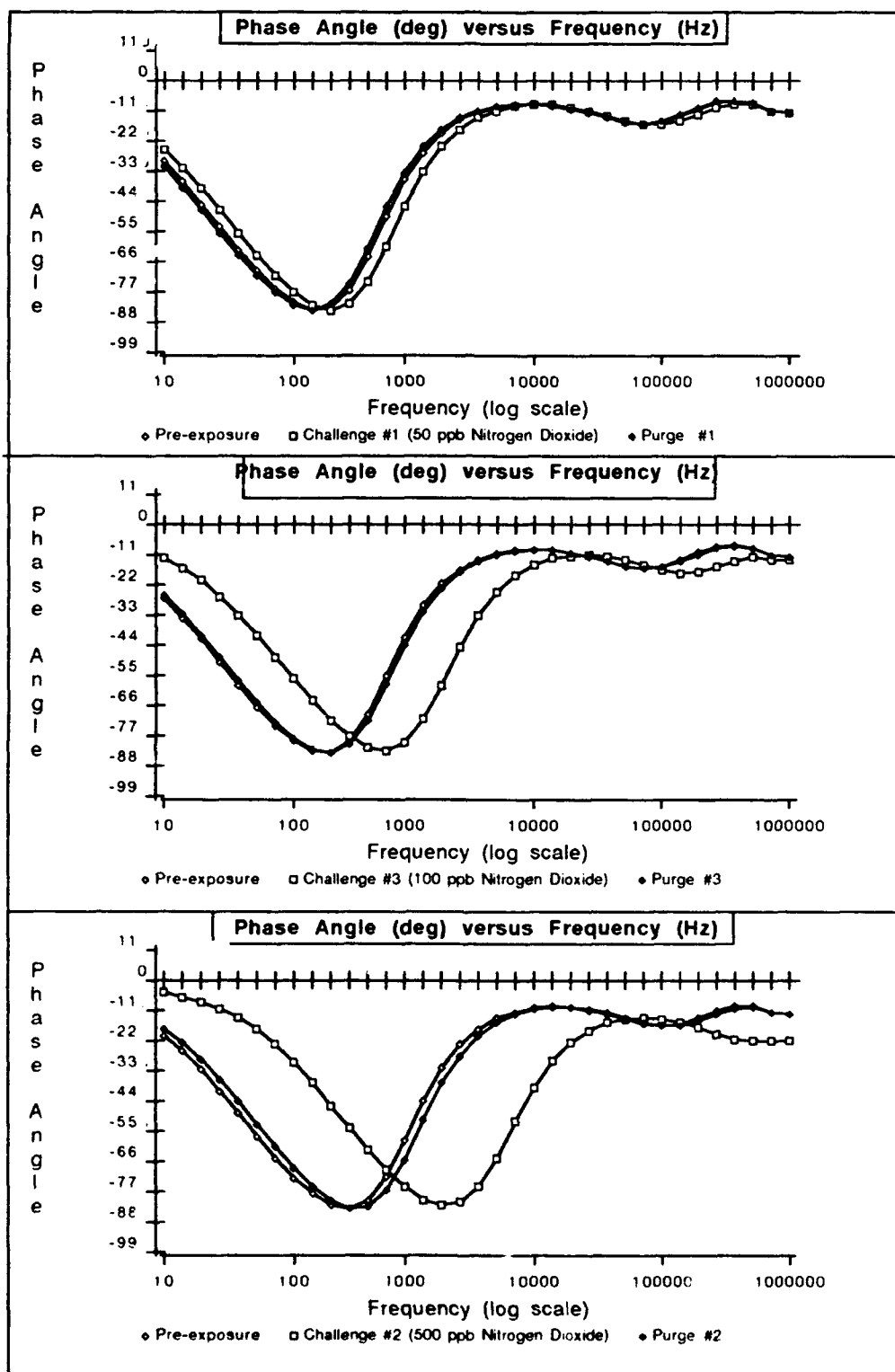


Figure C-23. Phase Angle versus Frequency Response of IGEFET Microsensor for a Series of Room Air Purges and Challenge Gas Exposures. Testing Conditions: IGE Microsensor Number 9; CuPc Thin-film (8,800 Angstroms Thick); Temperature of 150 degrees Centigrade; Nitrogen Dioxide Challenge Gas (Order of Exposures: 1000 ppb, 30 ppb, 50 ppb, 100 ppb, 500 ppb, 1000 ppb).

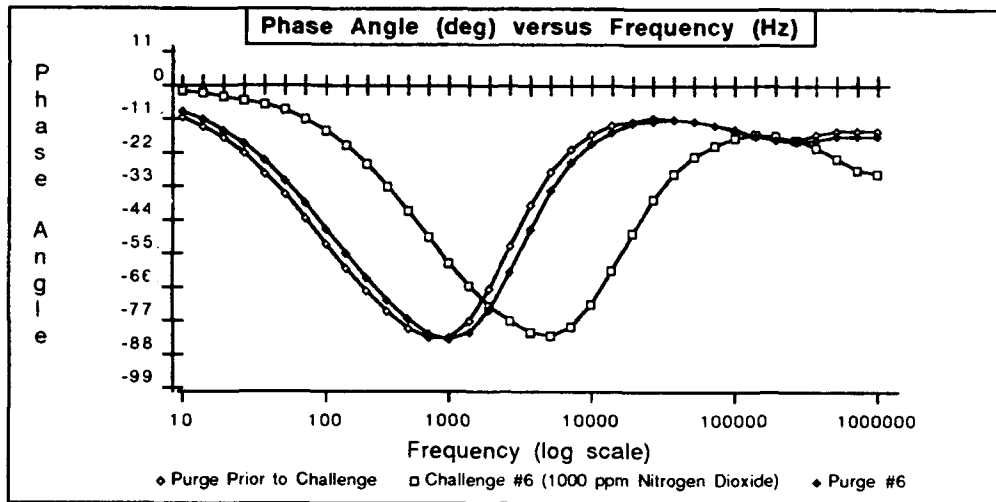


Figure C-24 . Phase Angle versus Frequency Response of IGEFET Microsensor for a Series of Room Air Purges and Challenge Gas Exposures. Testing Conditions: IGE Microsensor Number 9; CuPc Thin-film (8,800 Angstroms Thick); Temperature of 150 degrees Centigrade; Nitrogen Dioxide Challenge Gas (Order of Exposures: 1000 ppb, 30 ppb, 50 ppb, 100 ppb, 500 ppb, 1000 ppb).

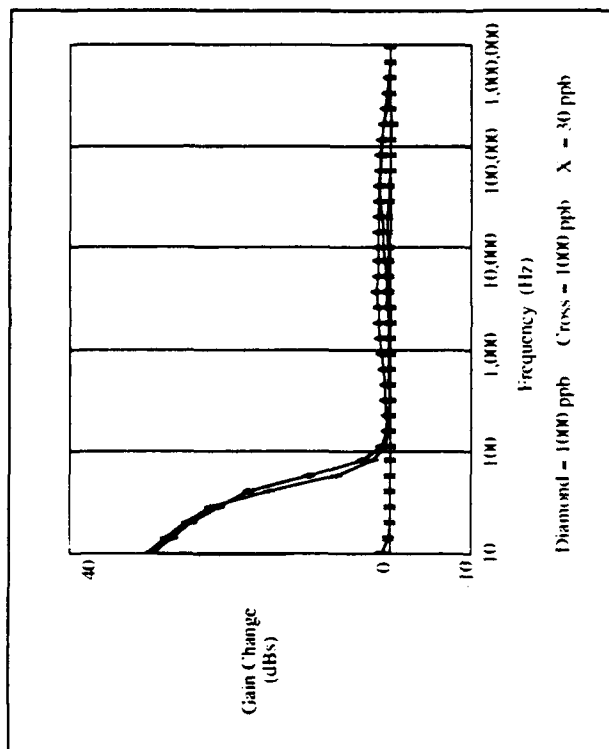


Figure C-25 Change in Gain Transfer Response versus Frequency for CuPc Exposed to Nitrogen Dioxide. The Diamond Plot is the Change from the Start-Up Purge to the End of the 1000 ppb Pre-conditioning Cycle. The Cross Plot is the Change from the Next Purge Cycle to the Second 1000 ppb Exposure. The 'X' Plot is the Change from Purge to 30 ppb Exposure. Testing Conditions: IGE Microsensor Number 1; CuPc Thin-film (1,600 Angstroms Thick); Temperature of 150 Degrees Centigrade; Nitrogen Dioxide Challenge Gas.

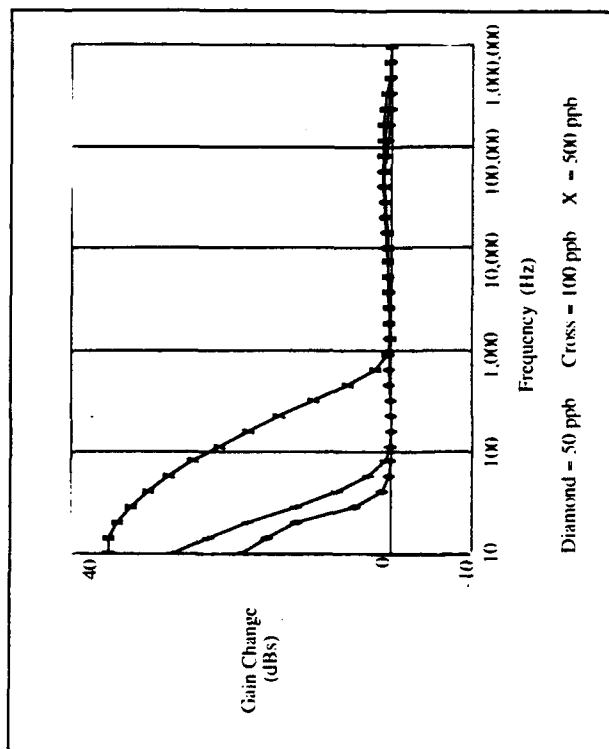


Figure C-26 Change in Gain Transfer Response versus Frequency for CuPc Exposed to Nitrogen Dioxide. The Diamond Plot is the Change from Purge to the End of the 50 ppb Exposure. The Cross Plot is the Change from the Next Purge Cycle to 100 ppb Exposure. The 'X' Plot is the Change from Purge to 500 ppb Exposure. Testing Conditions: IGE Microsensor Number 1; CuPc Thin-film (1,600 Angstroms Thick); Temperature of 150 Degrees Centigrade; Nitrogen Dioxide Challenge Gas.

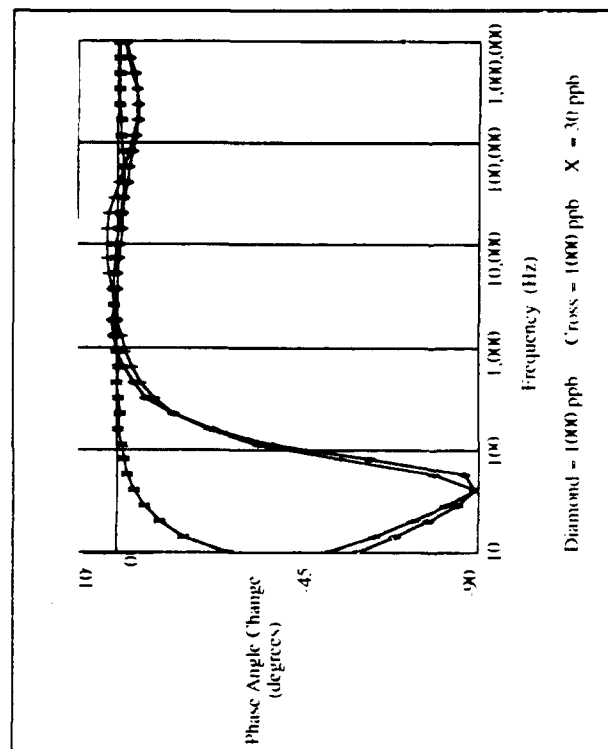


Figure C-27 Change in Phase Angle Transfer Response versus Frequency for CuPc Exposed to Nitrogen Dioxide. The Diamond Plot is the Change from the Start-Up Purge to the End of the 1000 ppb Pre-conditioning Cycle. The Cross Plot is the Change from the Next Purge Cycle to the Second 1000 ppb Exposure. The 'X' Plot is the Change from Purge to 30 ppb Exposure. Testing Conditions: IGF; Microsensor Number 1; CuPc Thin-film (1.600 Angstroms Thick); Temperature of 150 Degree Centigrade; Nitrogen Dioxide Challenge Gas.

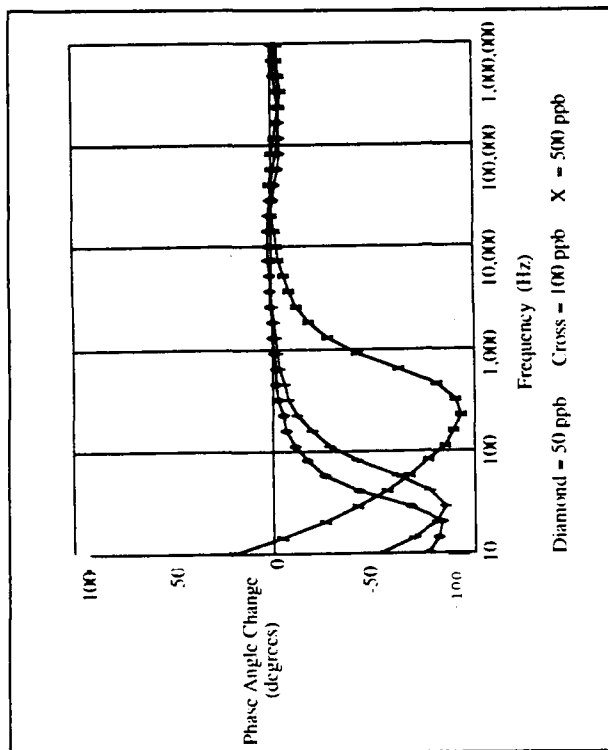


Figure C-28 Change in Phase Angle Transfer Response versus Frequency for CuPc Exposed to Nitrogen Dioxide. The Diamond Plot is the Change from Purge to the End of the 50 ppb Exposure. The Cross Plot is the Change from the Next Purge Cycle to 100 ppb Exposure. The 'X' Plot is the Change from Purge to 500 ppb Exposure. Testing Conditions: IGF; Microsensor Number 1; CuPc Thin-film (1.600 Angstroms Thick); Temperature of 150 Degree Centigrade; Nitrogen Dioxide Challenge Gas.

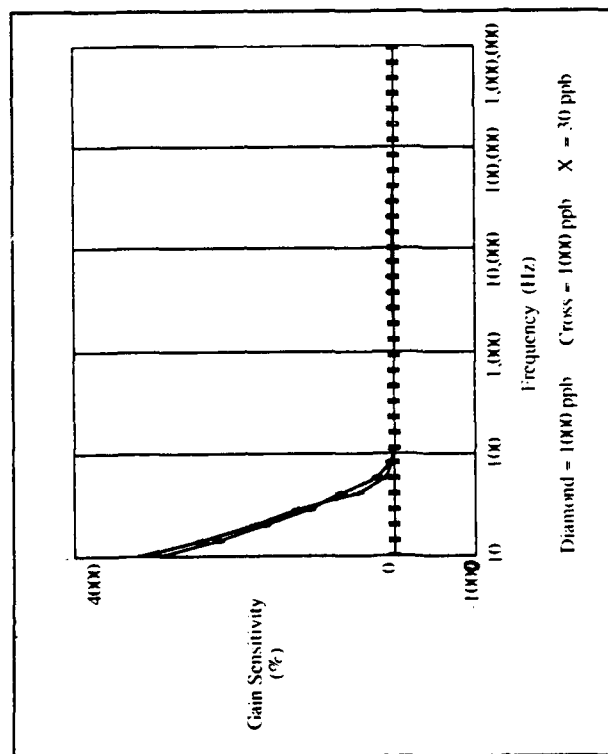


Figure C-20. Percent Change in Gain Transfer Response versus Frequency for CuPc Exposed to Nitrogen Dioxide. The Diamond Plot is the Change from the Start-Up Purge to the End of the 1000 ppb Pre-conditioning Cycle. The Cross Plot is the Change from the Next Purge Cycle to the Second 1000 ppb Exposure. The 'X' Plot is the Change from Purge to 30 ppb Exposure. Testing Conditions: IGE; Microsensor Number 1; CuPc Thin-film (1,600 Angstroms Thick); Nitrogen Dioxide Challenge Gas.

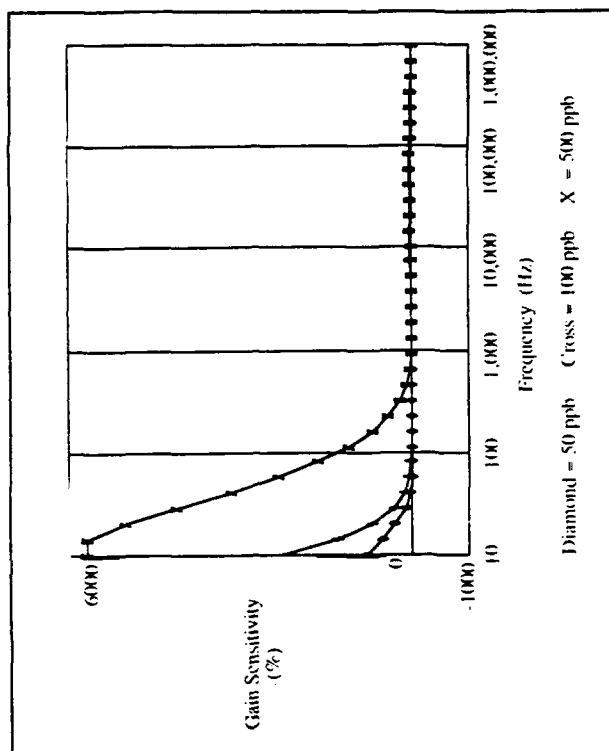


Figure C-30. Percent Change in Gain Transfer Response versus Frequency for CuPc Exposed to Nitrogen Dioxide. The Diamond Plot is the Change from Purge to the End of the 50 ppb Exposure. The Cross Plot is the Change from the Next Purge Cycle to 100 ppb Exposure. The 'X' Plot is the Change from Purge to 500 ppb Exposure. Testing Conditions: IGE; Microsensor Number 1; CuPc Thin-film (1,600 Angstroms Thick); Temperature of 150 Degree Centigrade; Nitrogen Dioxide Challenge Gas.

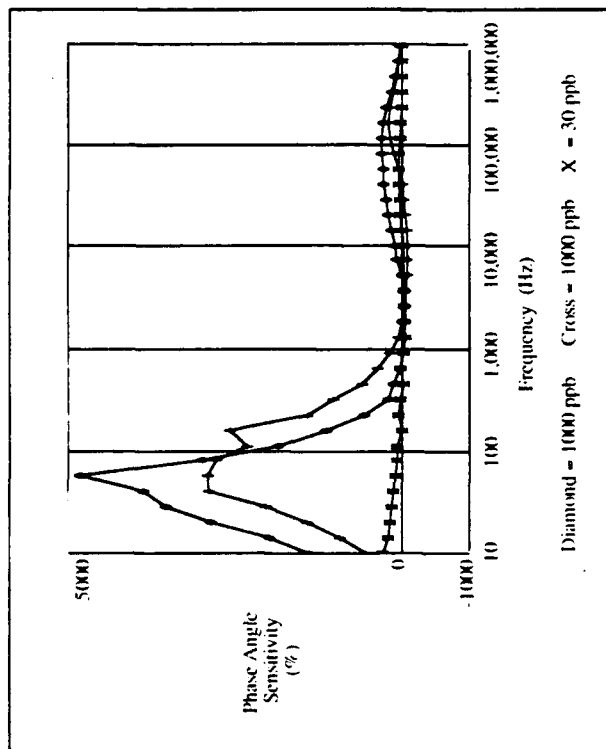


Figure C-31. Percent Change in Phase Angle Transfer Response versus Frequency for Cu/Pc Exposed to Nitrogen Dioxide. The Diamond Plot is the Change from the Start-Up Purge to the End of the 1000 ppb Pre-conditioning Cycle. The Cross Plot is the Change from the Next Purge Cycle to the Second 1000 ppb Exposure. The 'X' Plot is the Change from Purge to 30 ppb Exposure. Testing Conditions: IGI; Microsensor Number 1; Cu/Pc Thin-film (1,600 Angstroms Thick); Temperature of 150 Degree Centigrade; Nitrogen Dioxide Challenge Gas.

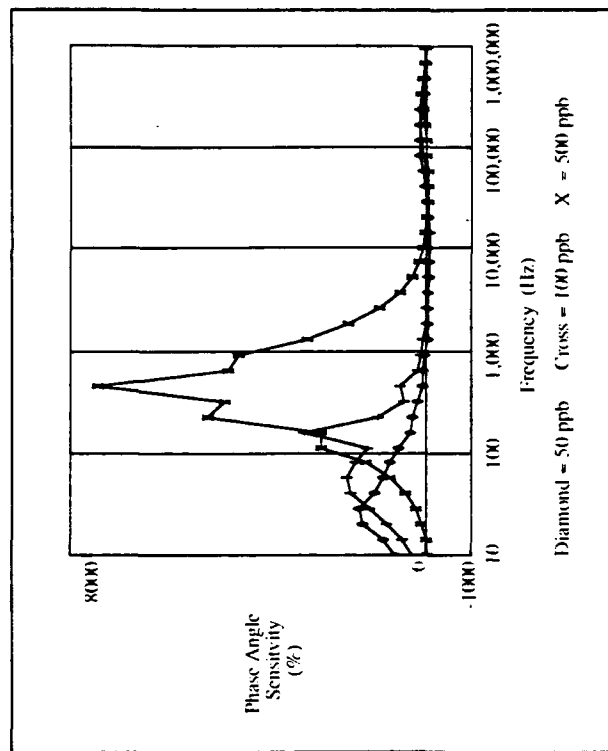


Figure C-32. Percent Change in Phase Angle Transfer Response versus Frequency for Cu/Pc Exposed to Nitrogen Dioxide. The Diamond Plot is the Change from Purge to the End of the 50 ppb Exposure. The Cross Plot is the Change from the Next Purge Cycle to 100 ppb Exposure. The 'X' Plot is the Change from Purge to 500 ppb Exposure. Testing Conditions: IGI; Microsensor Number 1; Cu/Pc Thin-film (1,600 Angstroms Thick); Temperature of 150 Degree Centigrade; Nitrogen Dioxide Challenge Gas.

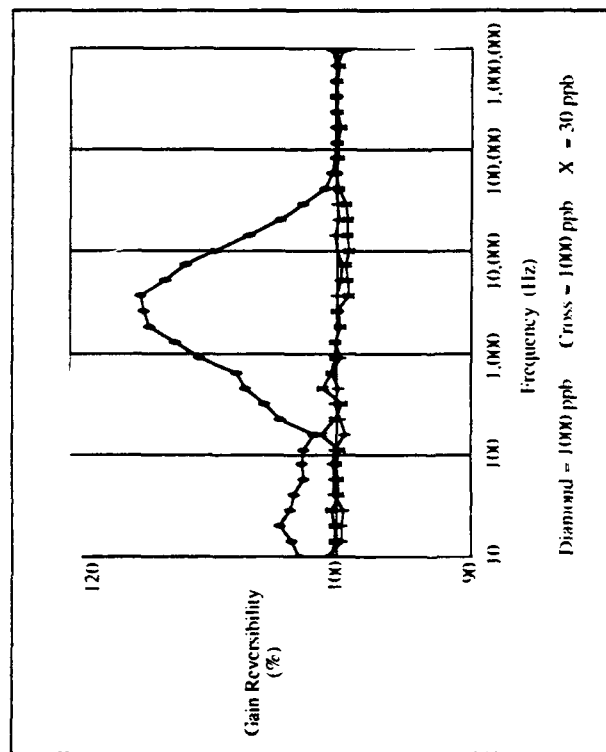


Figure C-33. Reversibility of Gain Transfer Response (Relative to Pre-exposure Purge) versus Frequency for CuPc Exposed to Nitrogen Dioxide. The Diamond Plot is the Change from the Start-Up Purge to the Purge Following the 1000 ppb Pre-conditioning Cycle. The Cross Plot is the Change from the Next Purge Cycle to the Purge Following the Second 1000 ppb Exposure. The 'X' Plot is the Change Between the Purges Before and After a 30 ppb Exposure. Testing Conditions: IGE; Microsensor Number 1; CuPc Thin-film (1,600 Angstroms Thick); Temperature of 150 Degrees Centigrade; Nitrogen Dioxide Challenge Gas.

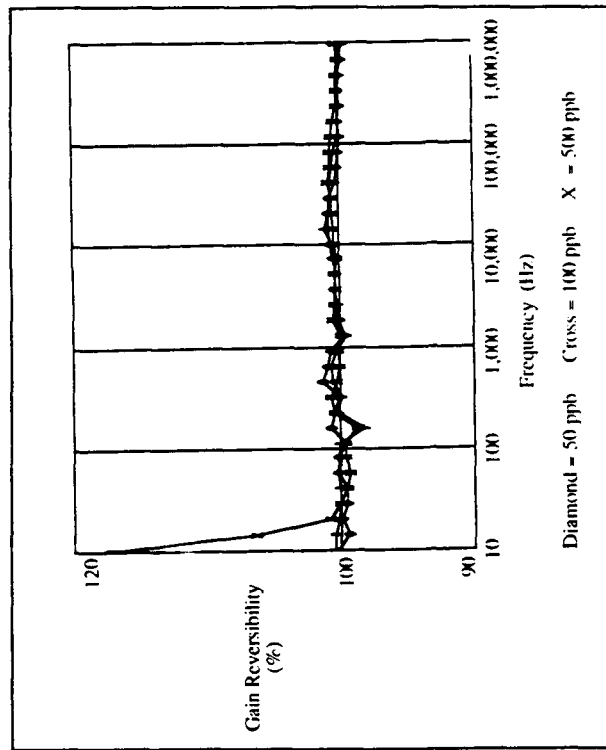


Figure C-34. Reversibility of Gain Transfer Response (Relative to Pre-exposure Purge) versus Frequency for CuPc Exposed to Nitrogen Dioxide. The Diamond Plot is the Change Between the Purges Before and After a 50 ppb Exposure. The Cross Plot is the Change from the Next Purge Cycle to the Purge Following the a 100 ppb Exposure. The 'X' Plot is the Change Between the Purges Before and After a 500 ppb Exposure. Testing Conditions: IGE; Microsensor Number 1; CuPc Thin-film (1,600 Angstroms Thick); Temperature of 150 Degree Centigrade; Nitrogen Dioxide Challenge Gas.

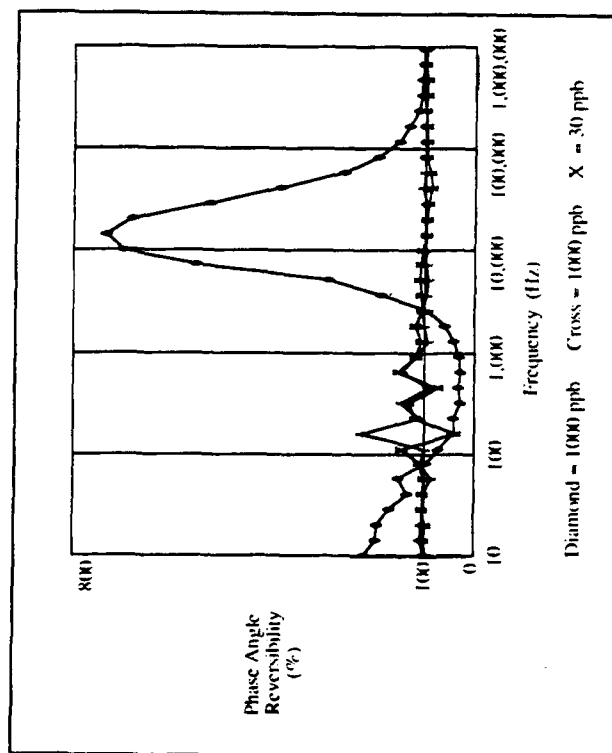


Figure C-35. Reversibility of Phase Angle/Transfer Response (Relative to Pre-exposure Purge) versus Frequency for CuPe Exposed to Nitrogen Dioxide. The Diamond Plot is the Change from the Start-Up Purge to the Purge Following the 1000 ppb Pre-conditioning Cycle. The Cross Plot is the Change from the Next Purge Cycle to the Purge Following the Second 1000 ppb Exposure. The 'X' Plot is the Change Between the Purges Before and After a 30 ppb Exposure. Testing Conditions: IGE; Microsensor Number 1; CuPe Thin-film (1,600 Angstroms Thick); Temperature of 150 Degree Centigrade; Nitrogen Dioxide Challenge Gas.

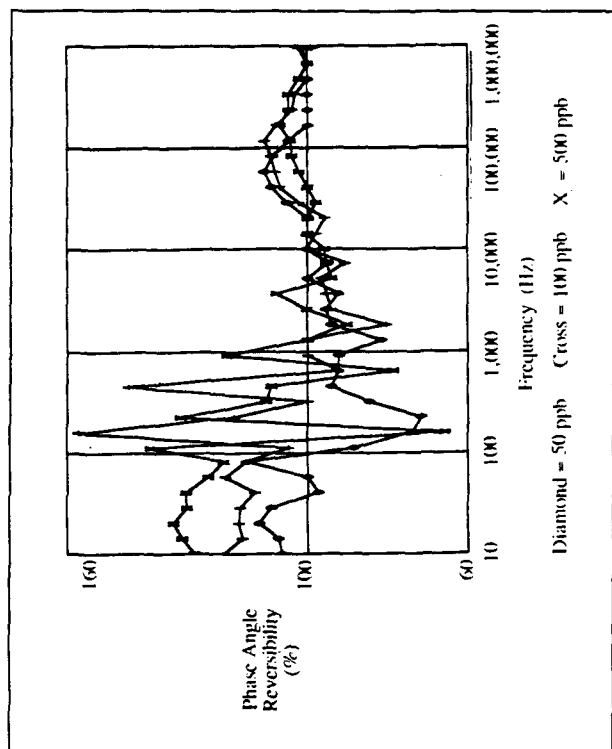


Figure C-36. Reversibility of Phase Angle/Transfer Response (Relative to Pre-exposure Purge) versus Frequency for CuPe Exposed to Nitrogen Dioxide. The Diamond Plot is the Change Between the Purges Before and After a 50 ppb Exposure. The Cross Plot is the Change from the Next Purge Cycle to the Purge Following the a 100 ppb Exposure. The 'X' Plot is the Change Between the Purges Before and After a 500 ppb Exposure. Testing Conditions: IGE; Microsensor Number 1; CuPe Thin-film (1,600 Angstroms Thick); Temperature of 150 Degree Centigrade; Nitrogen Dioxide Challenge Gas.



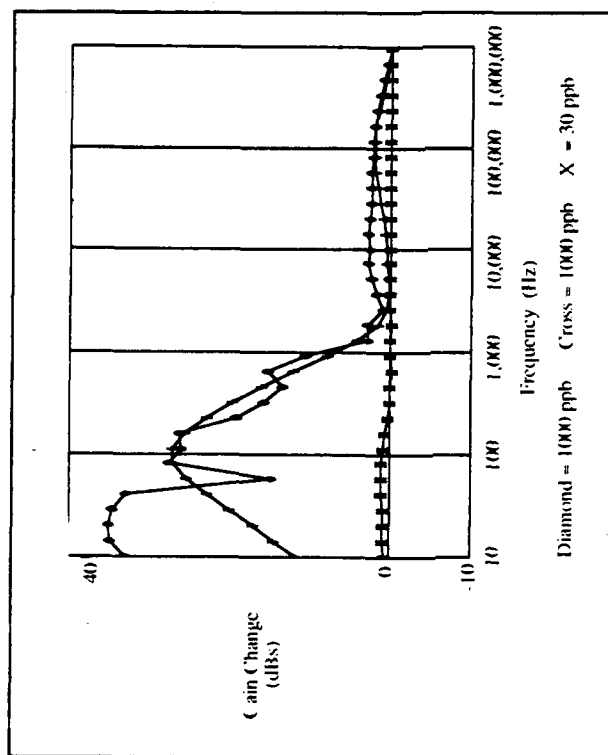


Figure C-37. Change in Gain Transfer Response versus Frequency for CuPc Exposed to Nitrogen Dioxide. The Diamond Plot is the Change from the Start-Up Purge to the End of the 1000 ppb Pre-conditioning Cycle. The Cross Plot is the Change from the Next Purge Cycle to the Second 1000 ppb Exposure. The 'X' Plot is the Change from Purge to 30 ppb Exposure. Testing Conditions: IGI; Microsensor Number 4; CuPc Thin-film (3,900 Angstroms Thick); Temperature of 150 Degree Centigrade; Nitrogen Dioxide Challenge Gas.

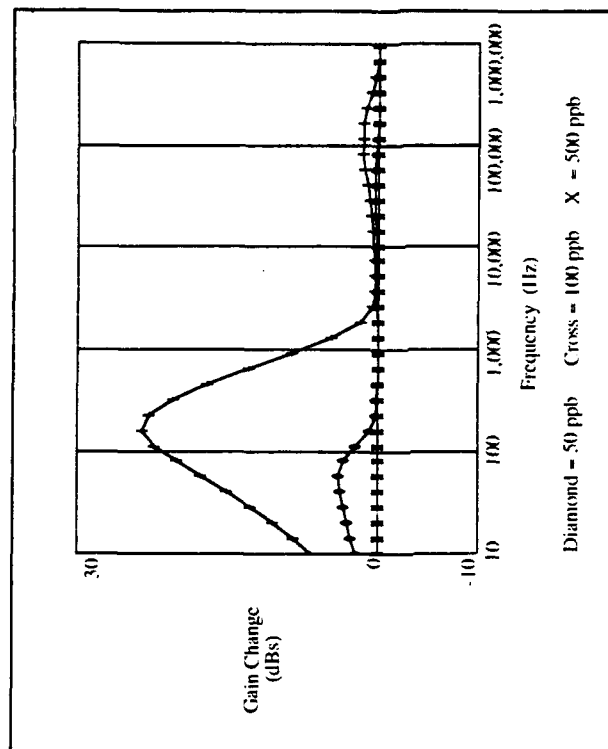


Figure C-38. Change in Gain Transfer Response versus Frequency for CuPc Exposed to Nitrogen Dioxide. The Diamond Plot is the Change from Purge to the End of the 50 ppb Exposure. The Cross Plot is the Change from the Next Purge Cycle to 100 ppb Exposure. The 'X' Plot is the Change from Purge to 500 ppb Exposure. Testing Conditions: IGI; Microsensor Number 4; CuPc Thin-film (3,900 Angstroms Thick); Temperature of 150 Degree Centigrade; Nitrogen Dioxide Challenge Gas.

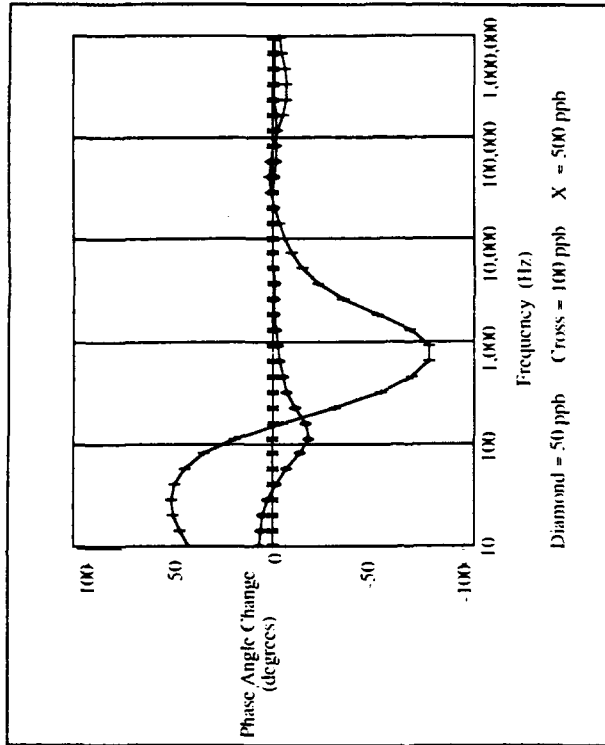


Figure C-40. Change in Phase Angle Transfer Response versus Frequency for CuPc Exposed to Nitrogen Dioxide. The Diamond Plot is the Change from Purge to the End of the 50 ppb Exposure. The Cross Plot is the Change from the Next Purge Cycle to 100 ppb Exposure. The 'X' Plot is the Change from Purge to 500 ppb Exposure. Testing Conditions: IGI; Microsensor Number 4; CuPc Thin-film (3,900 Angstroms Thick); Temperature of 150 Degree Centigrade; Nitrogen Dioxide Challenge Gas.

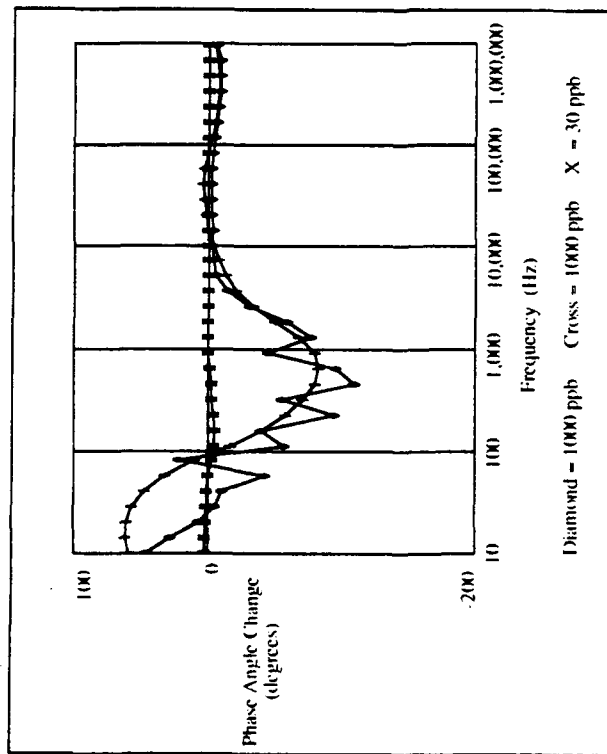


Figure C-39. Change in Phase Angle Transfer Response versus Frequency for CuPc Exposed to Nitrogen Dioxide. The Diamond Plot is the Change from the Start-Up Purge to the End of the 1000 ppb Pre-conditioning Cycle. The Cross Plot is the Change from the Next Purge Cycle to the Second 1000 ppb Exposure. The 'X' Plot is the Change from Purge to 30 ppb Exposure. Testing Conditions: IGI; Microsensor Number 4; CuPc Thin-film (3,900 Angstroms Thick); Temperature of 150 Degree Centigrade; Nitrogen Dioxide Challenge Gas.

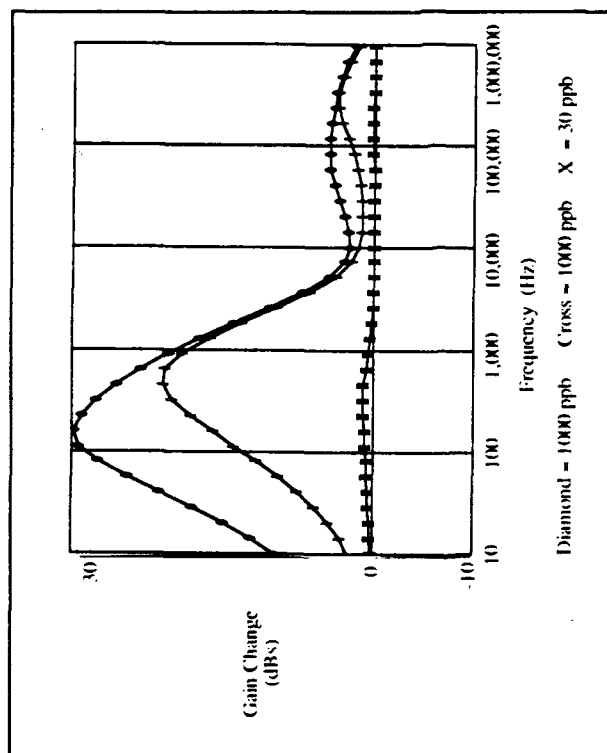


Figure C-41. Change in Gain Transfer Response versus Frequency for CuPc Exposed to Nitrogen Dioxide. The Diamond Plot is the Change from the Start-Up Purge to the End of the 1000 ppb Pre-conditioning Cycle. The Cross Plot is the Change from the Next Purge Cycle to the Second 1000 ppb Exposure. The 'X' Plot is the Change from Purge to 30 ppb exposure. Testing Conditions: IGIE Microsensor Number 9; CuPc Thin-film (8,800 Angstroms Thick); Temperature of 150 Degree Centigrade; Nitrogen Dioxide Challenge Gas.

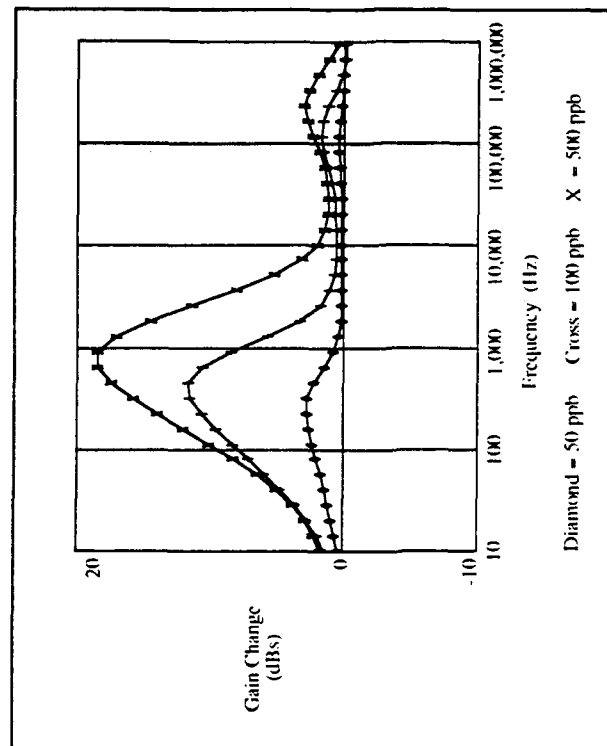


Figure C-42. Change in Gain Transfer Response versus Frequency for CuPc Exposed to Nitrogen Dioxide. The Diamond Plot is the Change from Purge to the End of the 50 ppb Exposure. The Cross Plot is the Change from the Next Purge Cycle to 100 ppb Exposure. The 'X' Plot is the Change from Purge to 500 ppb Exposure. Testing Conditions: IGIE Microsensor Number 9; CuPc Thin-film (8,800 Angstroms Thick); Temperature of 150 Degree Centigrade; Nitrogen Dioxide Challenge Gas.

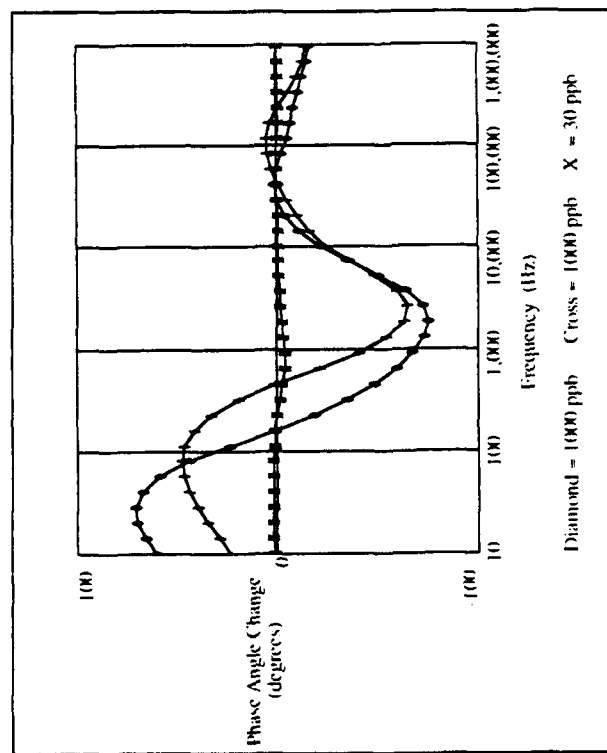


Figure C-43. Change in Phase Angle Transfer Response versus Frequency for CuPc Exposed to Nitrogen Dioxide. The Diamond Plot is the Change from the Start-Up Purge to the End of the 1000 ppb Pre-conditioning Cycle. The Cross Plot is the Change from the Next Purge Cycle to the Second 1000 ppb Exposure. The 'X' Plot is the Change from Purge to 30 ppb Exposure. Testing Conditions: IGE; Microsensor Number 9; CuPc Thin-film (8,800 Angstroms Thick); Temperature of 150 Degree Centigrade; Nitrogen Dioxide Challenge Gas.

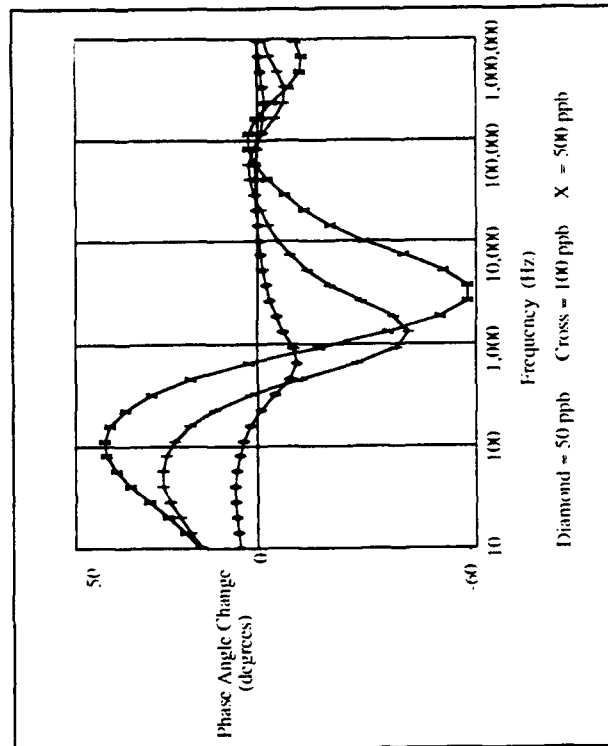


Figure C-44. Change in Phase Angle Transfer Response versus Frequency for CuPc Exposed to Nitrogen Dioxide. The Diamond Plot is the Change from Purge to the End of the 50 ppb Exposure. The Cross Plot is the Change from the Next Purge Cycle to 100 ppb Exposure. The 'X' Plot is the Change from Purge to 500 ppb Exposure. Testing Conditions: IGE; Microsensor Number 9; CuPc Thin-film (8,800 Angstroms Thick); Temperature of 150 Degree Centigrade; Nitrogen Dioxide Challenge Gas.

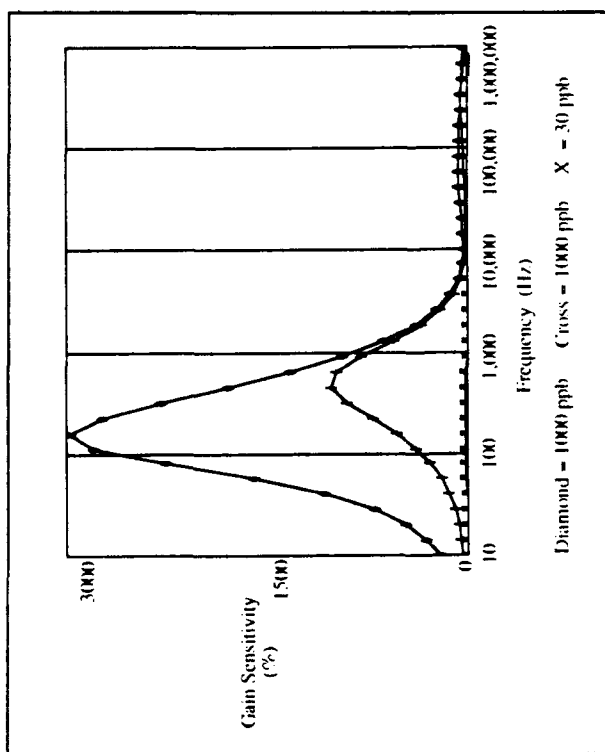


Figure C-45. Percent Change in Gain Transfer Response versus Frequency for CuPe Exposed to Nitrogen Dioxide. The Diamond Plot is the Change from the Start-Up Purge to the End of the 1000 ppb Pre-conditioning Cycle. The Cross Plot is the Change from the Next Purge Cycle to the Second 1000 ppb Exposure. The 'X' Plot is the Change from Purge to 30 ppb Exposure. Testing Conditions: ICI; Microsensor Number 9; CuPe Thin-film (8,800 Angstroms Thick); Temperature of 150 Degree Centigrade; Nitrogen Dioxide Challenge Gas.

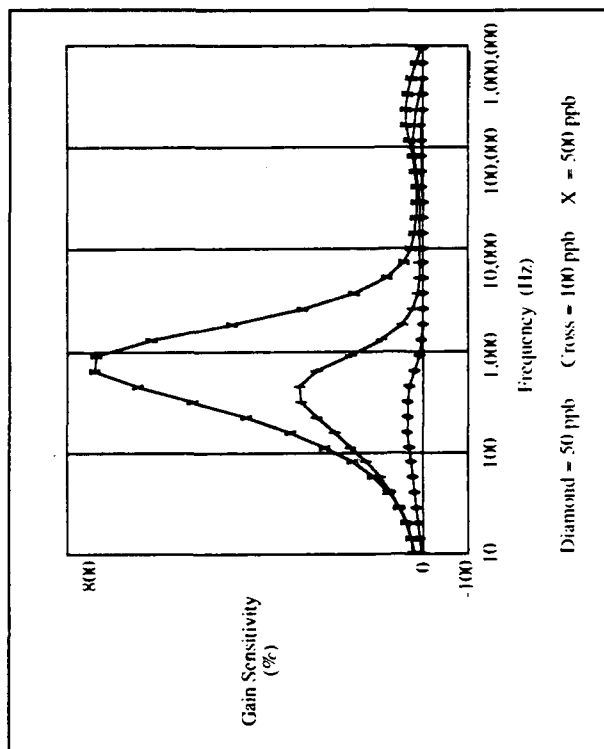


Figure C-46. Percent Change in Gain Transfer Response versus Frequency for CuPe Exposed to Nitrogen Dioxide. The Diamond Plot is the Change from Purge to the End of the 50 ppb Exposure. The Cross Plot is the Change from the Next Purge Cycle to 100 ppb Exposure. The 'X' Plot is the Change from Purge to 500 ppb Exposure. Testing Conditions: ICI; Microsensor Number 9; CuPe Thin-film (8,800 Angstroms Thick); Temperature of 150 Degree Centigrade; Nitrogen Dioxide Challenge Gas.

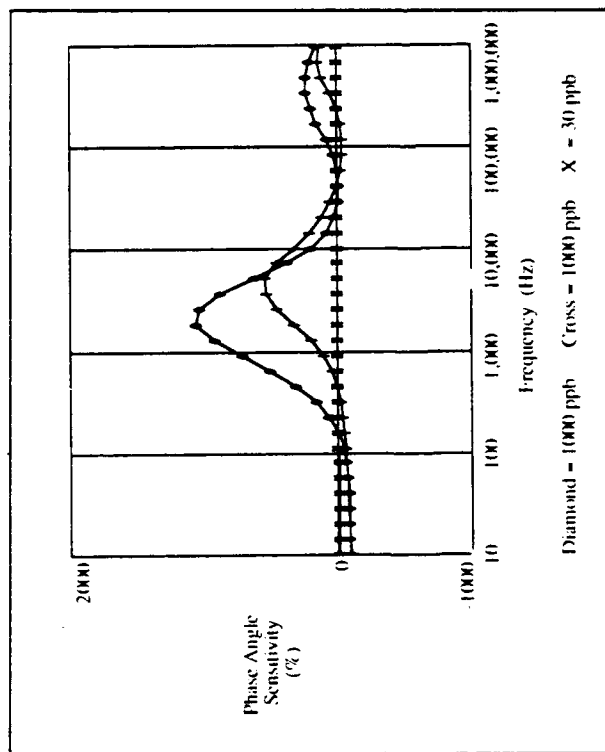


Figure C-47. Percent Change in Phase Angle Transfer Response versus Frequency for CuPc Exposed to Nitrogen Dioxide. The Diamond Plot is the Change from the Start-Up Purge to the End of the 10000 ppb Pre-conditioning Cycle. The Cross Plot is the Change from the Next Purge Cycle to the Second 10000 ppb Exposure. The 'X' Plot is the Change from Purge to 30 ppb Exposure. Testing Conditions: IGF; Microsensor Number 9; CuPc Thin-film (8,800 Angstroms Thick); Temperature of 150 Degree Centigrade; Nitrogen Dioxide Challenge Gas.

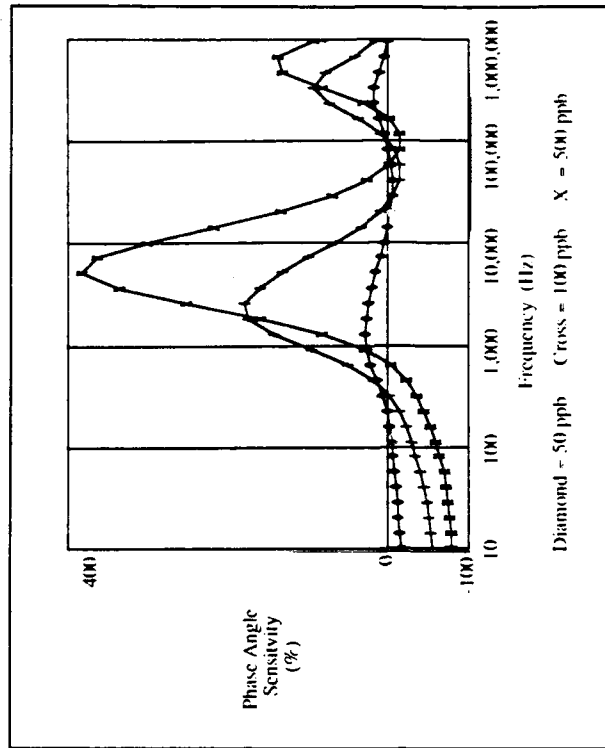


Figure C-48. Percent Change in Phase Angle Transfer Response versus Frequency for CuPc Exposed to Nitrogen Dioxide. The Diamond Plot is the Change from Purge to the End of the 50 ppb Exposure. The Cross Plot is the Change from the Next Purge Cycle to 100 ppb Exposure. The 'X' Plot is the Change from Purge to 500 ppb Exposure. Testing Conditions: IGF; Microsensor Number 9; CuPc Thin-film (3,300 Angstroms Thick); Temperature of 150 Degree Centigrade; Nitrogen Dioxide Challenge Gas.

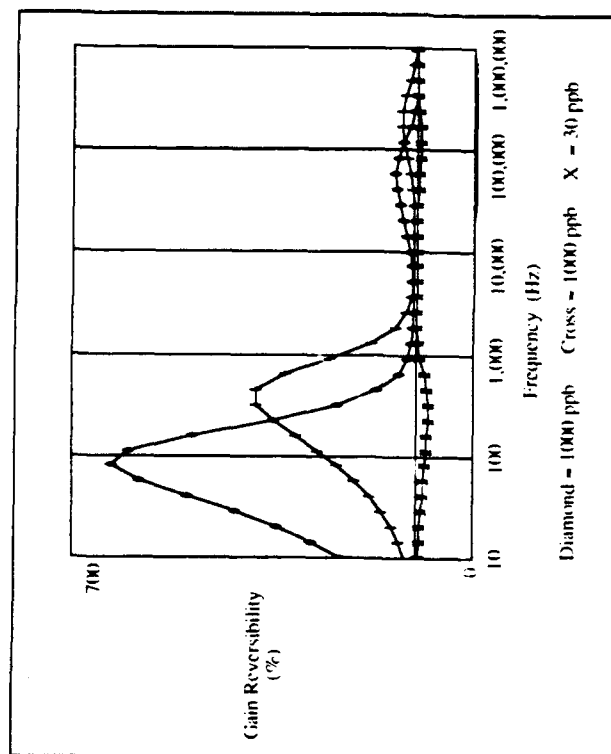


Figure C-49. Reversibility of Gain Transfer Response (Relative to Pre-exposure Purge) versus Frequency for CuPc Exposed to Nitrogen Dioxide. The Diamond Plot is the Change from the Start-Up Purge to the Purge Following the 1000 ppb Pre-conditioning Cycle. The Cross Plot is the Change from the Next Purge Cycle to the Purge Following the Second 1000 ppb exposure. The 'X' Plot is the Change Between the Purges Before and After a 30 ppb Exposure. Testing Conditions: IGL; Microsensor Number 9; CuPc Thin-film (8,800 Angstroms Thick); Temperature of 150 Degree Centigrade; Nitrogen Dioxide Challenge Gas.

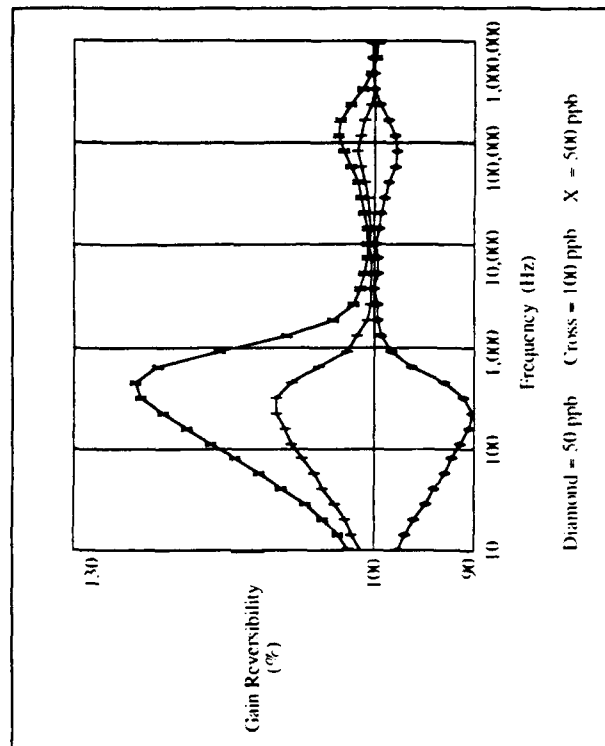


Figure C-50. Reversibility of Gain Transfer Response (Relative to Pre-exposure Purge) versus Frequency for CuPc Exposed to Nitrogen Dioxide. The Diamond Plot is the Change Between the Purges Before and After a 50 ppb Exposure. The Cross Plot is the Change from the Next Purge Cycle to the Purge Following the a 100 ppb Exposure. The 'X' Plot is the Change Between the Purges Before and After a 500 ppb Exposure. Testing Conditions: IGL; Microsensor Number 9; CuPc Thin-film (8,800 Angstroms Thick); Temperature of 150 Degree Centigrade; Nitrogen Dioxide Challenge Gas.

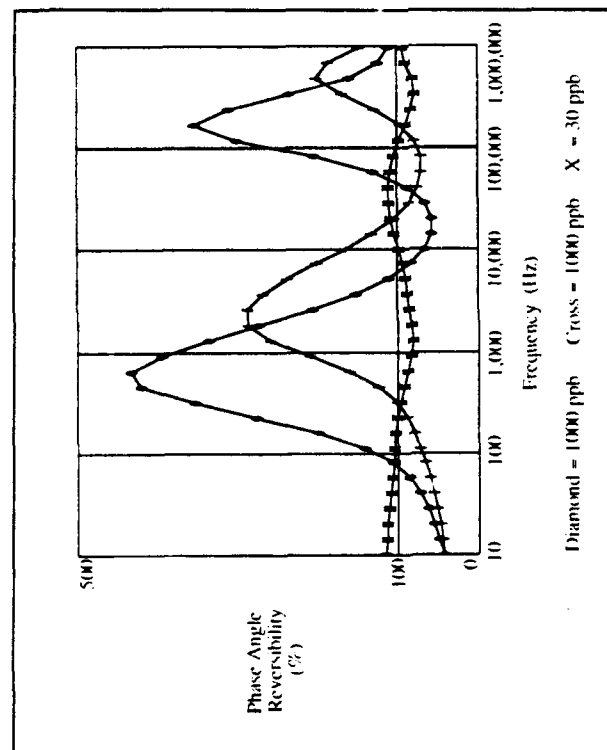


Figure G-51. Reversibility of Phase Angle Transfer Response (Relative to Pre-exposure Purge) versus Frequency for CuPc Exposed to Nitrogen Dioxide. The Diamond Plot is the Change from the Start-Up Purge to the Purge Following the 1000 ppb Pre-conditioning Cycle. The Cross Plot is the Change from the Next Purge Cycle to the Purge Following the Second 1000 ppb Exposure. The 'X' Plot is the Change Between the Purges Before and After a 30 ppb Exposure. Testing Conditions: IGE Microsensor Number 9; CuPc Thin-film (8,800 Angstroms Thick); Temperature of 150 Degree Centigrade; Nitrogen Dioxide Challenge Gas.

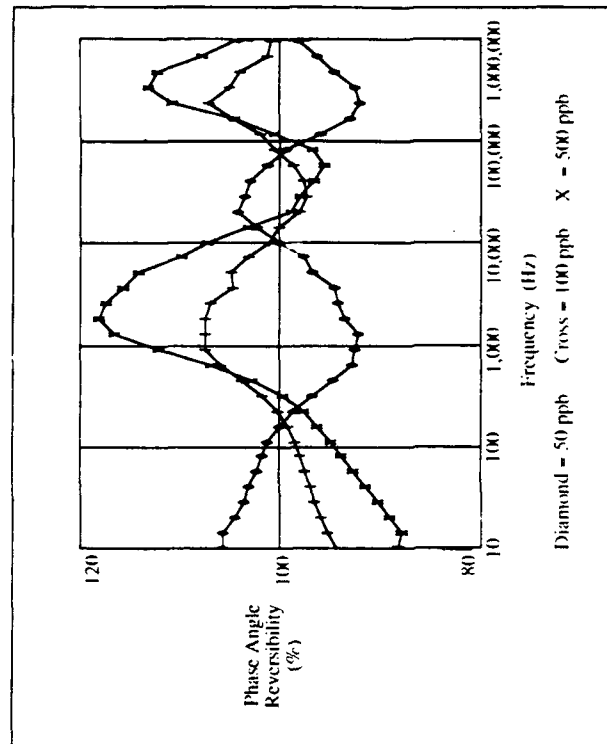


Figure G-52. Reversibility of Phase Angle Transfer Response (Relative to Pre-exposure Purge) versus Frequency for CuPc Exposed to Nitrogen Dioxide. The Diamond Plot is the Change Between the Purges Before and After a 50 ppb Exposure. The Cross Plot is the Change from the Next Purge Cycle to the Purge Following the 100 ppb Exposure. The 'X' Plot is the Change Between the Purges Before and After a 500 ppb Exposure. Testing Conditions: IGE Microsensor Number 9; CuPc Thin-film (8,800 Angstroms Thick); Temperature of 150 Degree Centigrade; Nitrogen Dioxide Challenge Gas.



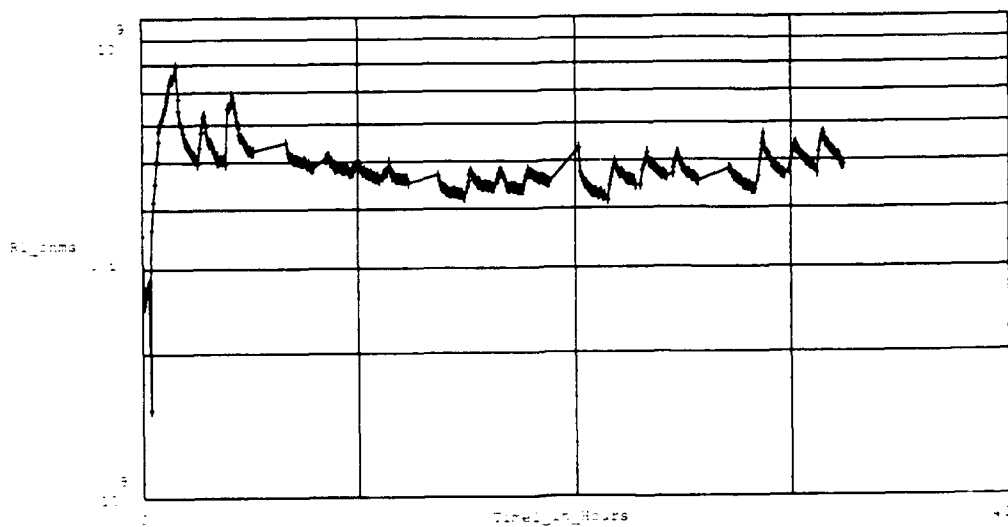


Figure C-53 . DC Resistance Measured Between the Driven-Electrode and Floating-Electrode of the IGE Array, During Series of Purges and Challenge Gas Exposures. The Number of Measurements (at crosses) is 398. The Testing Conditions Included the Following:

IGE Array Number . . . 1.	Thin-film Material . . . Copper Phthalocyanine.
Thin-film Thickness . . . 2,100 Angstroms	Test Temperature(s) . . . Purge & Challenge at 150°C
Purge Gas . . . Room Air.	Challenge Gas . . . Ammonia.
Challenge Gas Concentration(s) (in order run) : 500 ppm, 16 ppm, 106 ppm, 250 ppm, 500 ppm.	

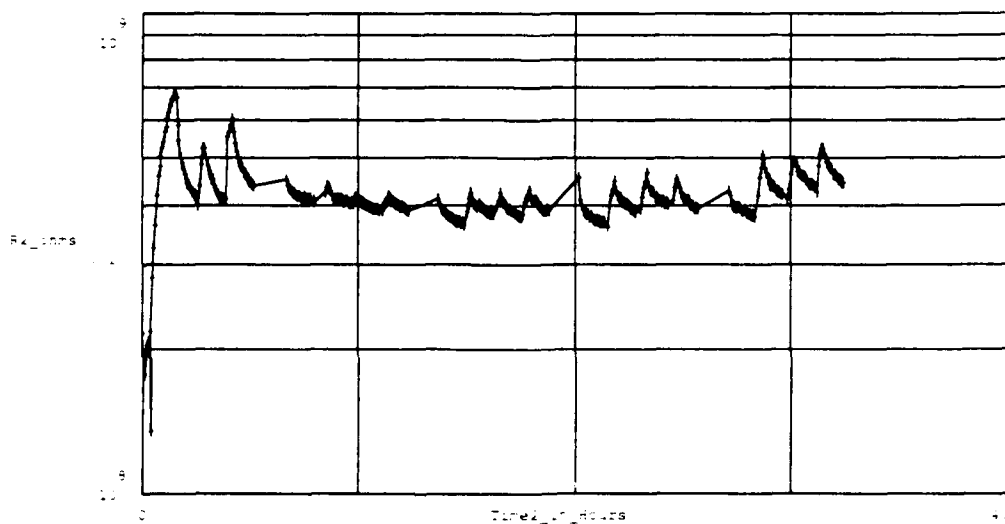


Figure C-54 . DC Resistance Measured Between the Driven-Electrode and Floating-Electrode of the IGE Array, During Series of Purges and Challenge Gas Exposures. The Number of Measurements (at crosses) is 398. The Testing Conditions Included the Following

IGE Array Number . . . 2.	Thin-film Material . . . Copper Phthalocyanine.
Thin-film Thickness . . . 2,100 Angstroms	Test Temperature(s) . . . Purge & Challenge at 150°C
Purge Gas . . . Room Air.	Challenge Gas . . . Ammonia.
Challenge Gas Concentration(s) (in order run) : 500 ppm, 16 ppm, 106 ppm, 250 ppm, 500 ppm.	

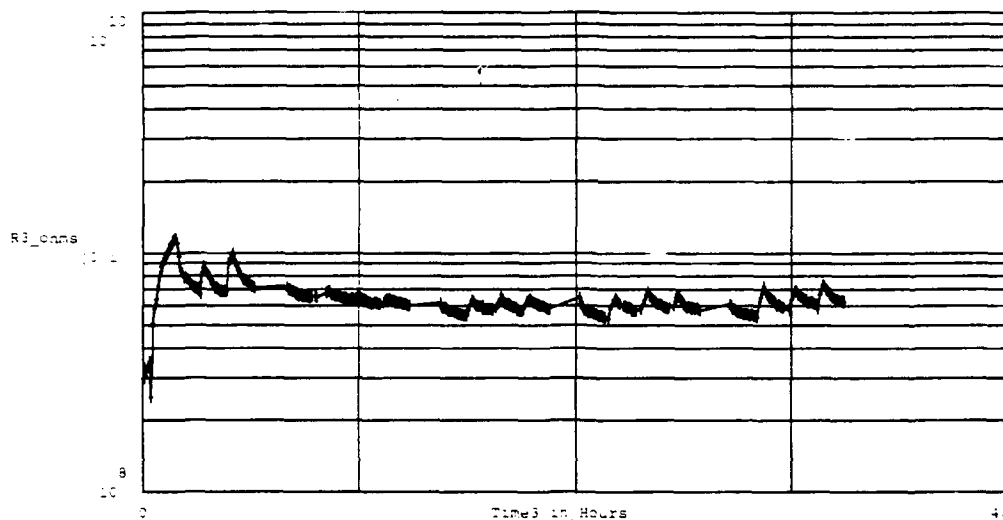


Figure C- 55 . DC Resistance Measured Between the Driven-Electrode and Floating-Electrode of the IGE Array, During Series of Purges and Challenge Gas Exposures. The Number of Measurements (at crosses) is 398. The Testing Conditions Included the Following:

IGE Array Number : 3,	Thin-film Material : Copper Phthalocyanine,
Thin-film Thickness : 2.100 Angstroms	Test Temperature(s) : Purge & Challenge at 150°C
Purge Gas : Room Air.	Challenge Gas : Ammonia.
Challenge Gas Concentration(s) (in order run) : 500 ppm, 16 ppm, 106 ppm, 250 ppm, 500 ppm.	

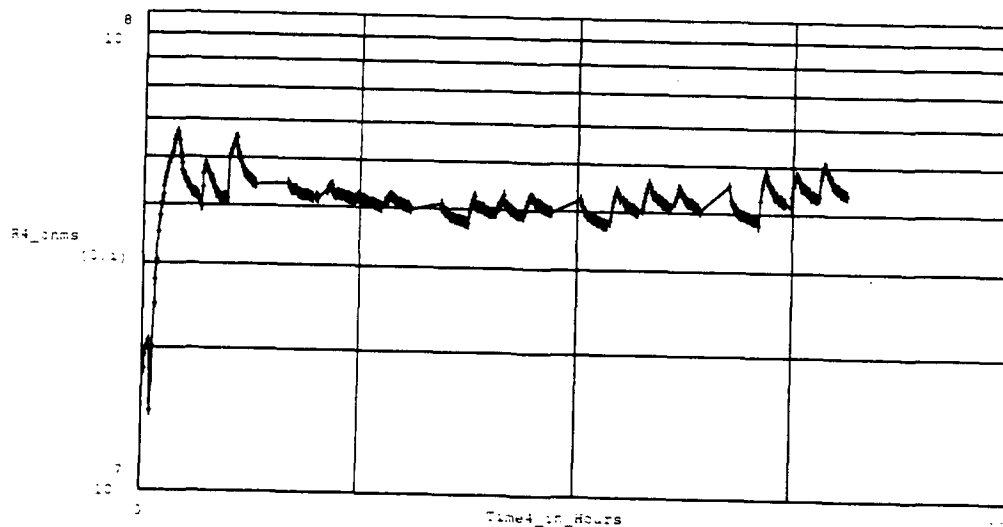


Figure C- 56 . DC Resistance Measured Between the Driven-Electrode and Floating-Electrode of the IGE Array, During Series of Purges and Challenge Gas Exposures. The Number of Measurements (at crosses) is 398. The Testing Conditions Included the Following:

IGE Array Number : 4,	Thin-film Material : Copper Phthalocyanine,
Thin-film Thickness : 8.200 Angstroms	Test Temperature(s) : Purge & Challenge at 150°C
Purge Gas : Room Air.	Challenge Gas : Ammonia.
Challenge Gas Concentration(s) (in order run) : 500 ppm, 16 ppm, 106 ppm, 250 ppm, 500 ppm.	

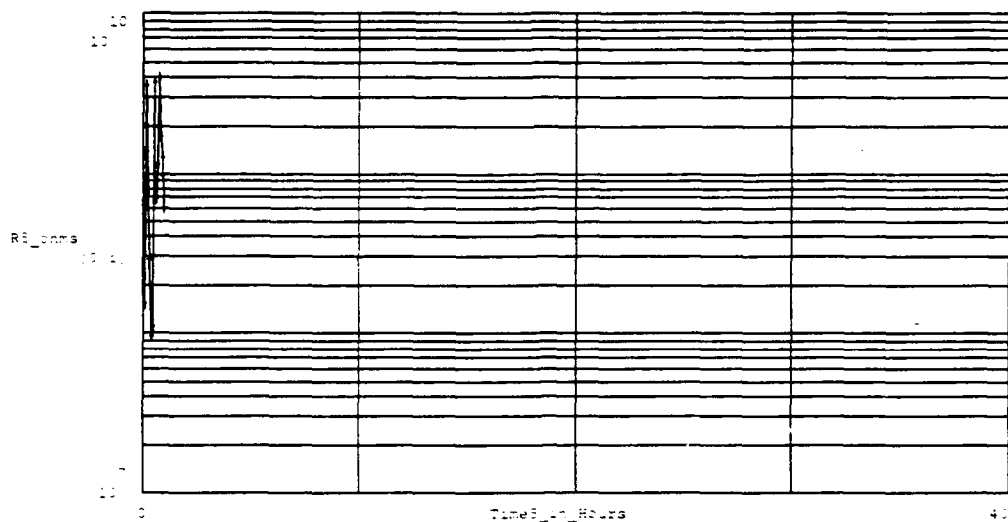


Figure C- 57 . **This IGE Microsensor Malfunctioned.** DC Resistance Measured Between the Driven-Electrode and Floating-Electrode of the IGE Array, During Series of Purges and Challenge Gas Exposures. The Number of Measurements (at crosses) is 398. The Testing Conditions Included the Following:

IGE Array Number : 5,	Thin-film Material : Copper Phthalocyanine,
Thin-film Thickness : 8,200 Angstroms	Test Temperature(s) : Purge & Challenge at 150°C
Purge Gas : Room Air,	Challenge Gas : Ammonia,
Challenge Gas Concentration(s) (in order run) : 500 ppm, 16 ppm, 106 ppm, 250 ppm, 500 ppm.	

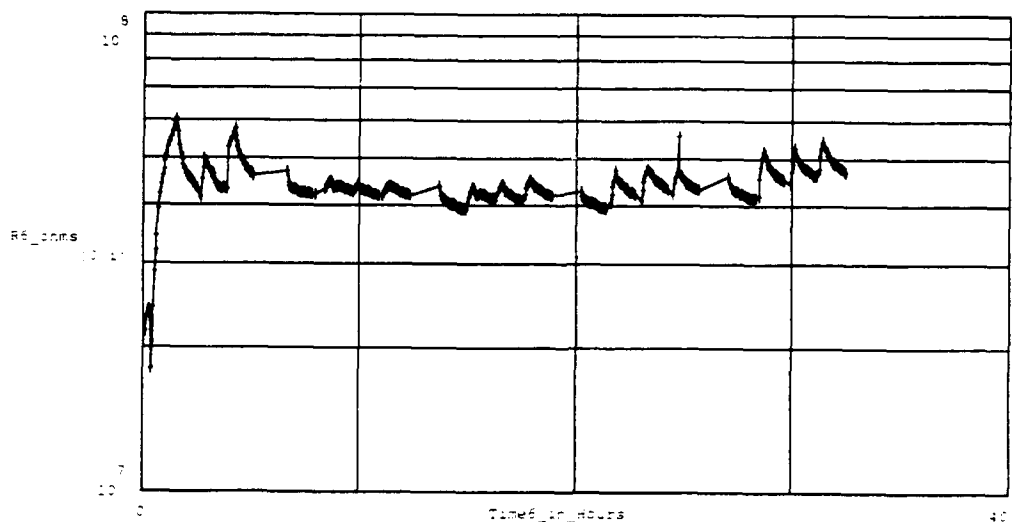


Figure C- 58 . DC Resistance Measured Between the Driven-Electrode and Floating-Electrode of the IGE Array, During Series of Purges and Challenge Gas Exposures. The Number of Measurements (at crosses) is 398. The Testing Conditions Included the Following:

IGE Array Number : 6,	Thin-film Material : Copper Phthalocyanine,
Thin-film Thickness : 8,200 Angstroms	Test Temperature(s) : Purge & Challenge at 150°C
Purge Gas : Room Air,	Challenge Gas : Ammonia
Challenge Gas Concentration(s) (in order run) : 500 ppm, 16 ppm, 106 ppm, 250 ppm, 500 ppm.	

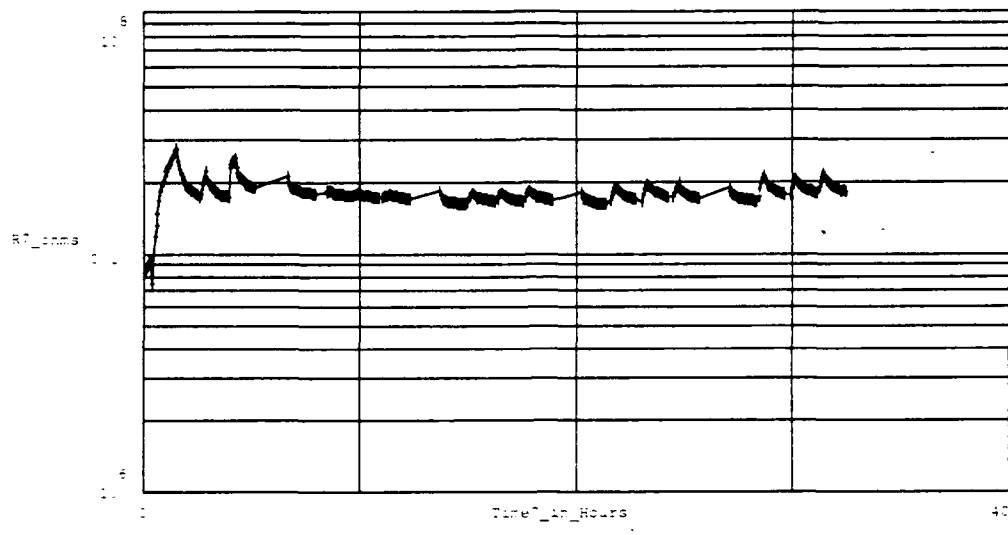


Figure C- 59 . DC Resistance Measured Between the Driven-Electrode and Floating-Electrode of the IGE Array. During Series of Purges and Challenge Gas Exposures. The Number of Measurements (at crosses) is 398. The Testing Conditions Included the Following:

IGE Array Number : 7.	Thin-film Material : Copper Phthalocyanine.
Thin-film Thickness : 16,000 Angstroms	Test Temperature(s) : Purge & Challenge at 150°C
Purge Gas : Room Air.	Challenge Gas : Ammonia.
Challenge Gas Concentration(s) (in order run) : 500 ppm, 16 ppm, 106 ppm, 250 ppm, 500 ppm.	

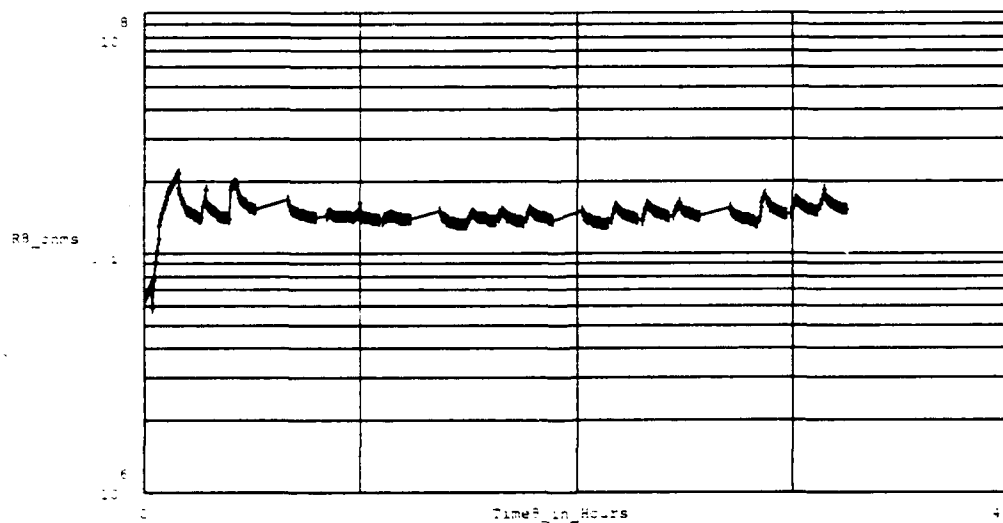


Figure C- 60 . DC Resistance Measured Between the Driven-Electrode and Floating-Electrode of the IGE Array. During Series of Purges and Challenge Gas Exposures. The Number of Measurements (at crosses) is 398. The Testing Conditions Included the Following:

IGE Array Number : 8.	Thin-film Material : Copper Phthalocyanine.
Thin-film Thickness : 16,000 Angstroms	Test Temperature(s) : Purge & Challenge at 150°C
Purge Gas : Room Air.	Challenge Gas : Ammonia.
Challenge Gas Concentration(s) (in order run) : 500 ppm, 16 ppm, 106 ppm, 250 ppm, 500 ppm.	

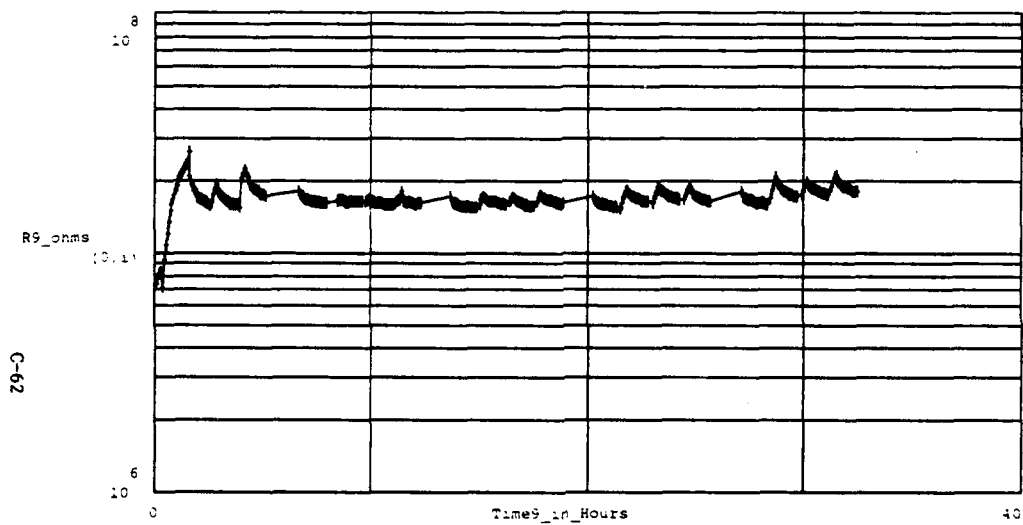


Figure C- 61 . DC Resistance Measured Between the Driven-Electrode and Floating-Electrode of the IGE Array, During Series of Purges and Challenge Gas Exposures. The Number of Measurements (at crosses) is 398. The Testing Conditions Included the Following:

IGE Array Number : 9,	Thin-film Material : Copper Phthalocyanine,
Thin-film Thickness : 16,000 Angstroms	Test Temperature(s) : Purge & Challenge at 150°C
Purge Gas : Room Air,	Challenge Gas : Ammonia,
Challenge Gas Concentration(s) (in order run) : 500 ppm, 16 ppm, 106 ppm, 250 ppm, 500 ppm.	

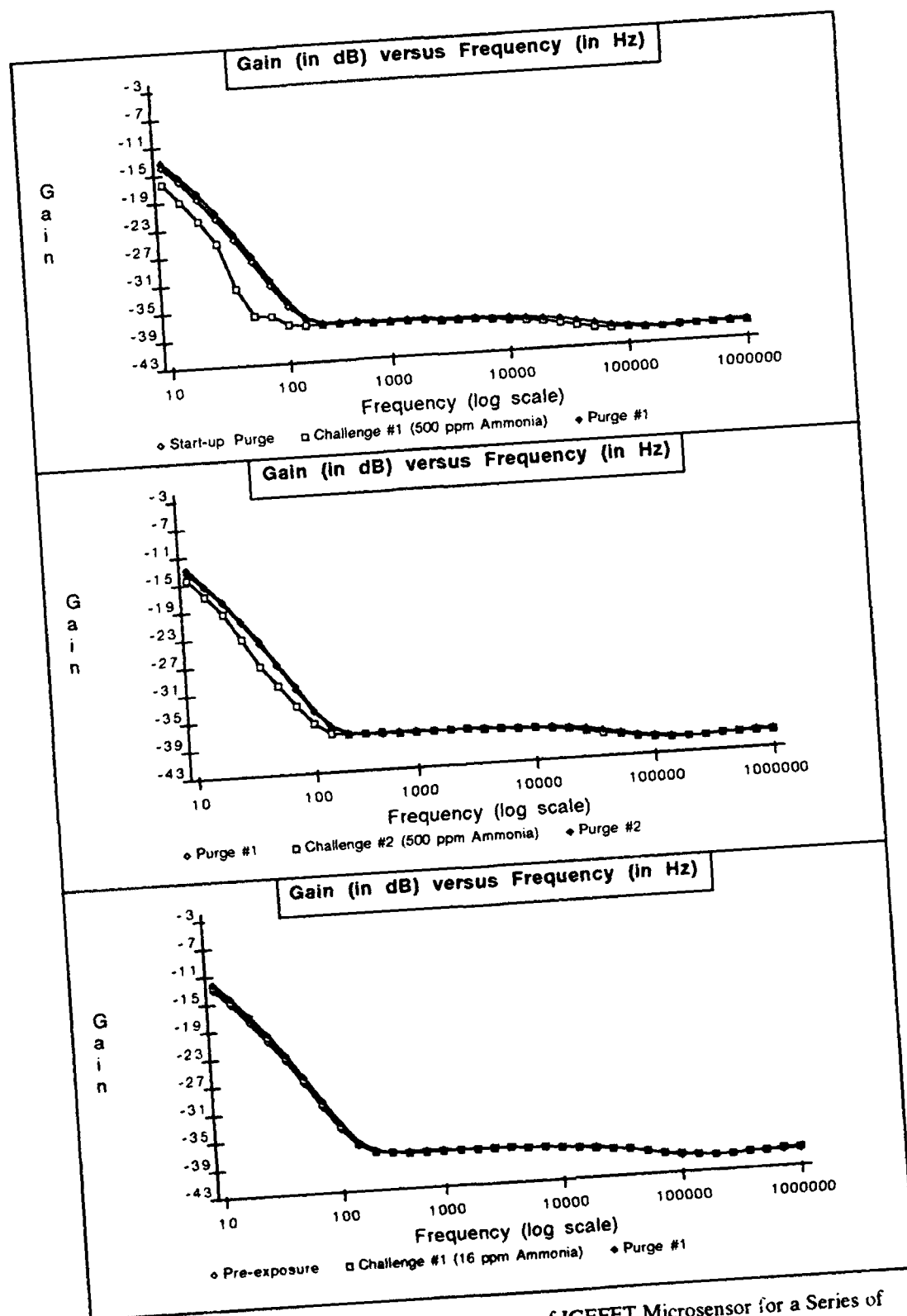


Figure C-62 . Gain versus Frequency Response of IGEFET Microsensor for a Series of Room Air Purges and Challenge Gas Exposures. Testing Conditions: IGE Microsensor Number 1; CuPc Thin-film (1,600 Angstroms Thick); Temperature of 150 degrees Centigrade: Ammonia Challenge Gas (Order of Exposures: 500 ppm, 16 ppm, 106 ppm, 250 ppm, 500 ppm).

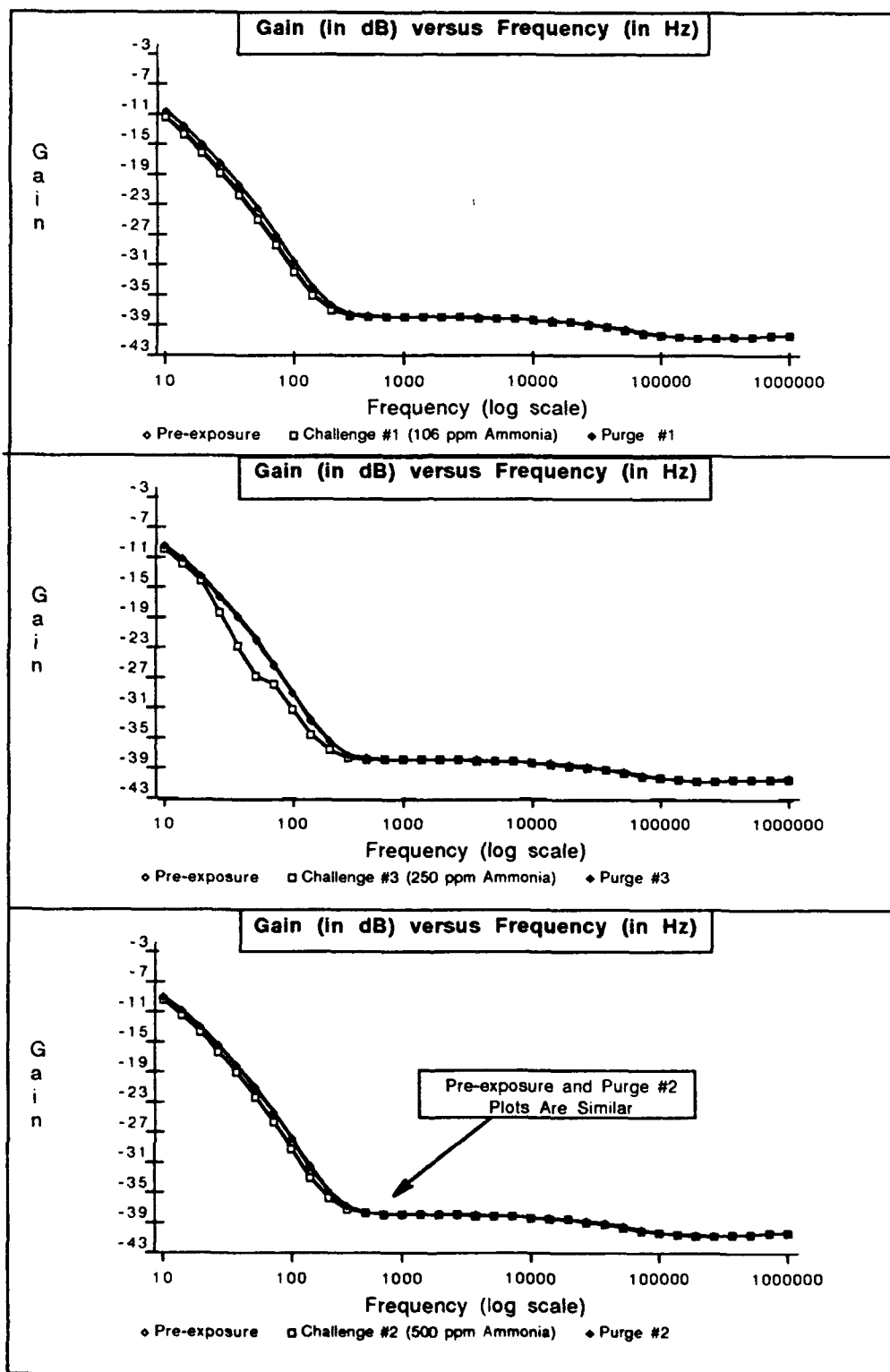


Figure C-63. Gain versus Frequency Response of IGEFET Microsensor for a Series of Room Air Purges and Challenge Gas Exposures. Testing Conditions: IGE Microsensor Number 1; CuPc Thin-film (1,600 Angstroms Thick); Temperature of 150 degrees Centigrade: Ammonia Challenge Gas (Order of Exposures: 500 ppm, 16 ppm, 106 ppm, 250 ppm, 500 ppm).

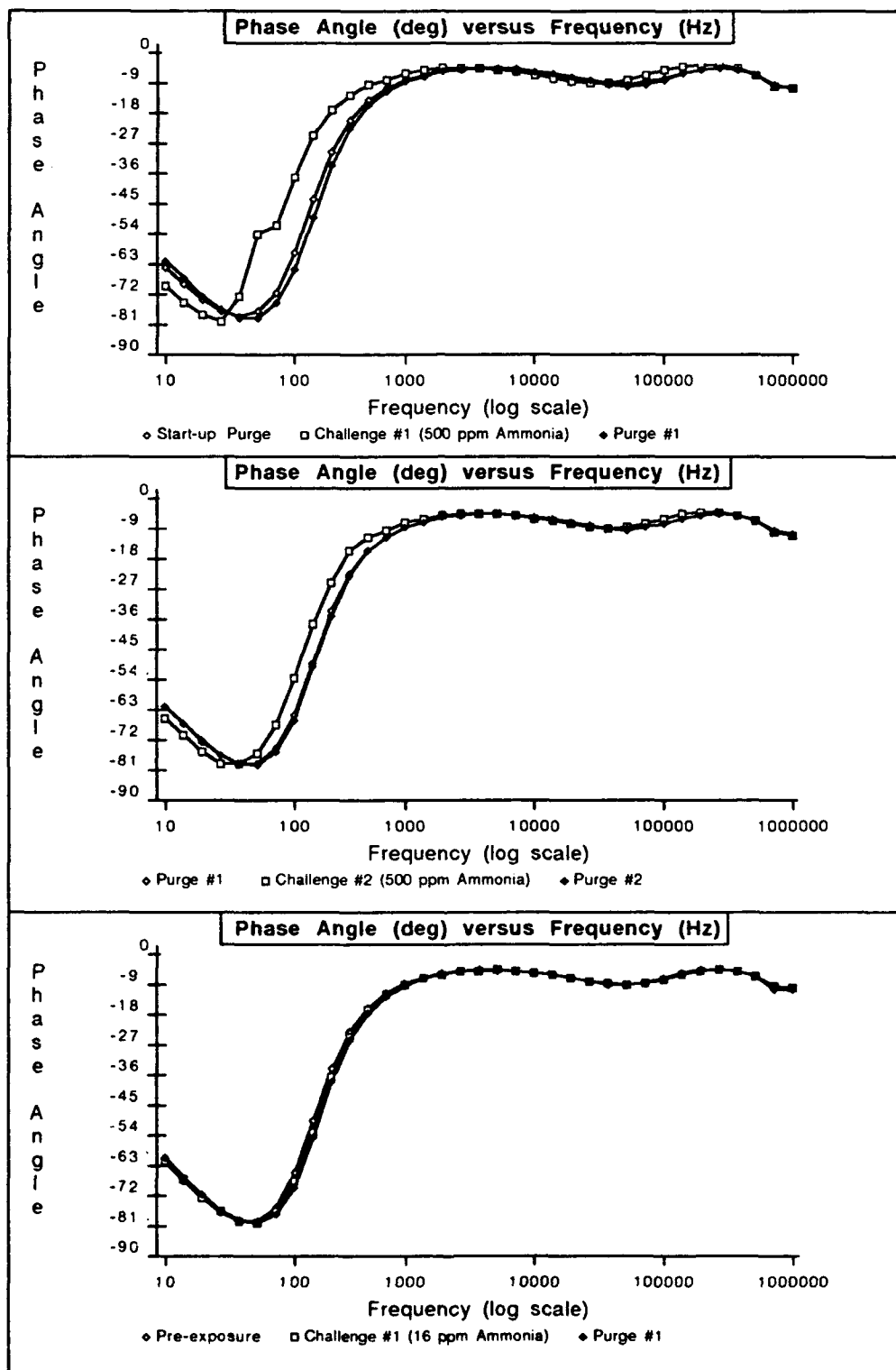


Figure C-64. Phase Angle versus Frequency Response of IGEFET Microsensor for a Series of Room Air Purges and Challenge Gas Exposures. Testing Conditions: IGE Microsensor Number 1; CuPc Thin-film (1,600 Angstroms Thick); Temperature of 150 degrees Centigrade; Ammonia Challenge Gas (Order of Exposures: 500 ppm, 16 ppm, 106 ppm, 250 ppm, 500 ppm).



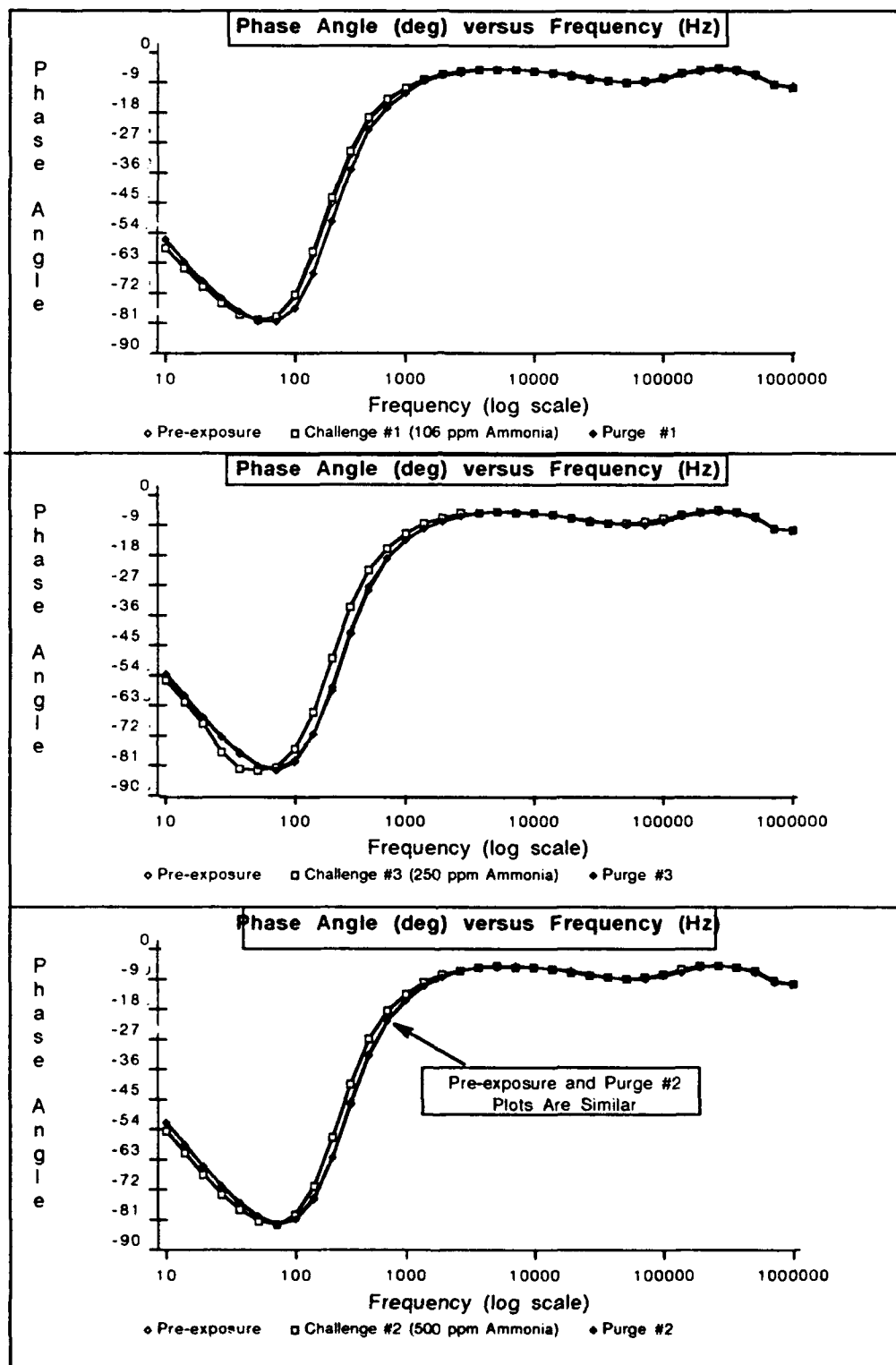


Figure C-65. Phase Angle versus Frequency Response of IGEFET Microsensor for a Series of Room Air Purges and Challenge Gas Exposures. Testing Conditions: IGE Microsensor Number 1; CuPc Thin-film (1,600 Angstroms Thick); Temperature of 150 degrees Centigrade; Ammonia Challenge Gas (Order of Exposures: 500 ppm, 16 ppm, 106 ppm, 250 ppm, 500 ppm).

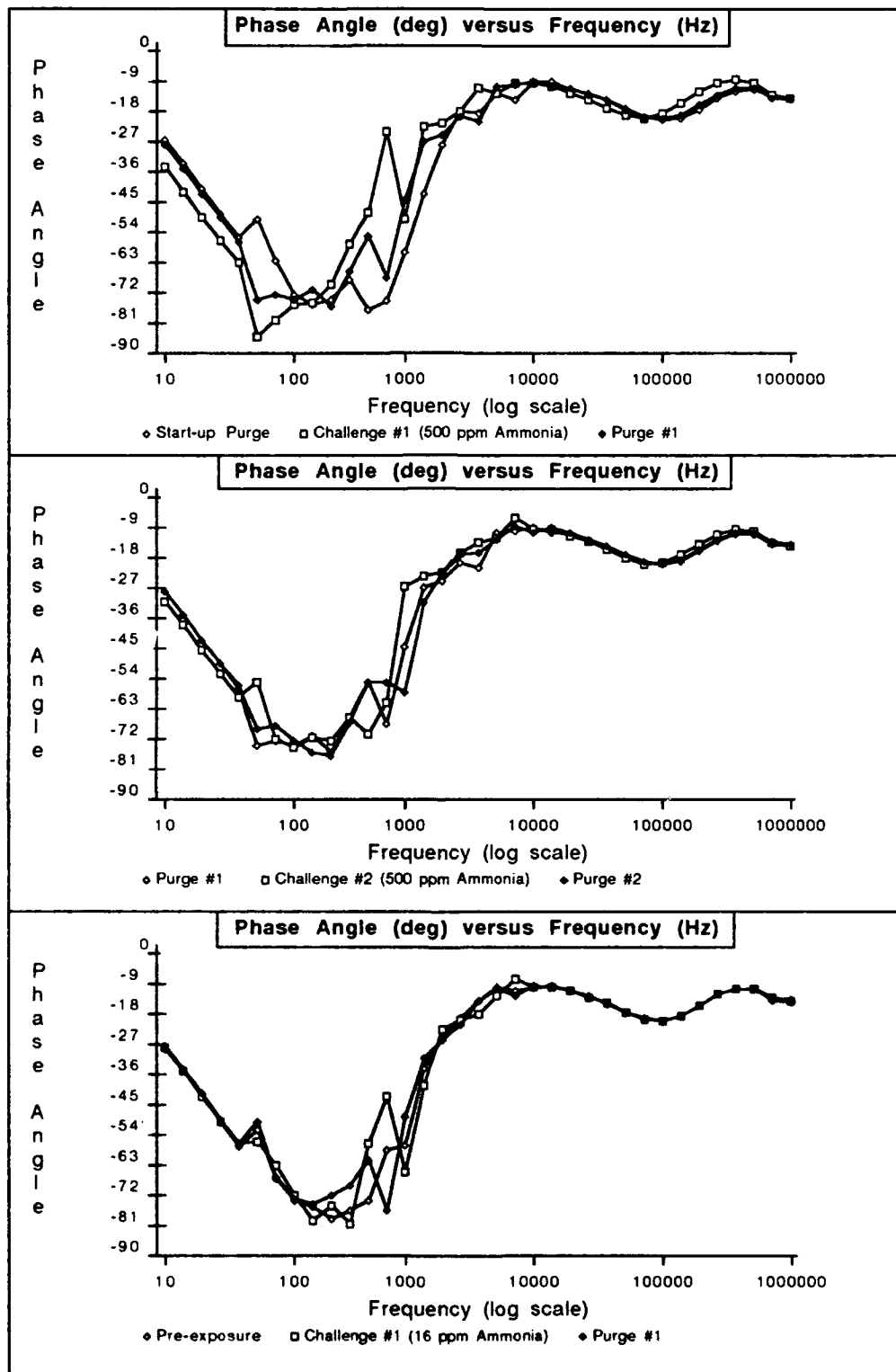


Figure C-66 Phase Angle versus Frequency Response of IGEFET Microsensor for a Series of Room Air Purges and Challenge Gas Exposures. Testing Conditions: IGE Microsensor Number 5; CuPc Thin-film (3,900 Angstroms Thick); Temperature of 150 degrees Centigrade; Ammonia Challenge Gas (Order of Exposures: 500 ppm, 16 ppm, 106 ppm, 250 ppm, 500 ppm).

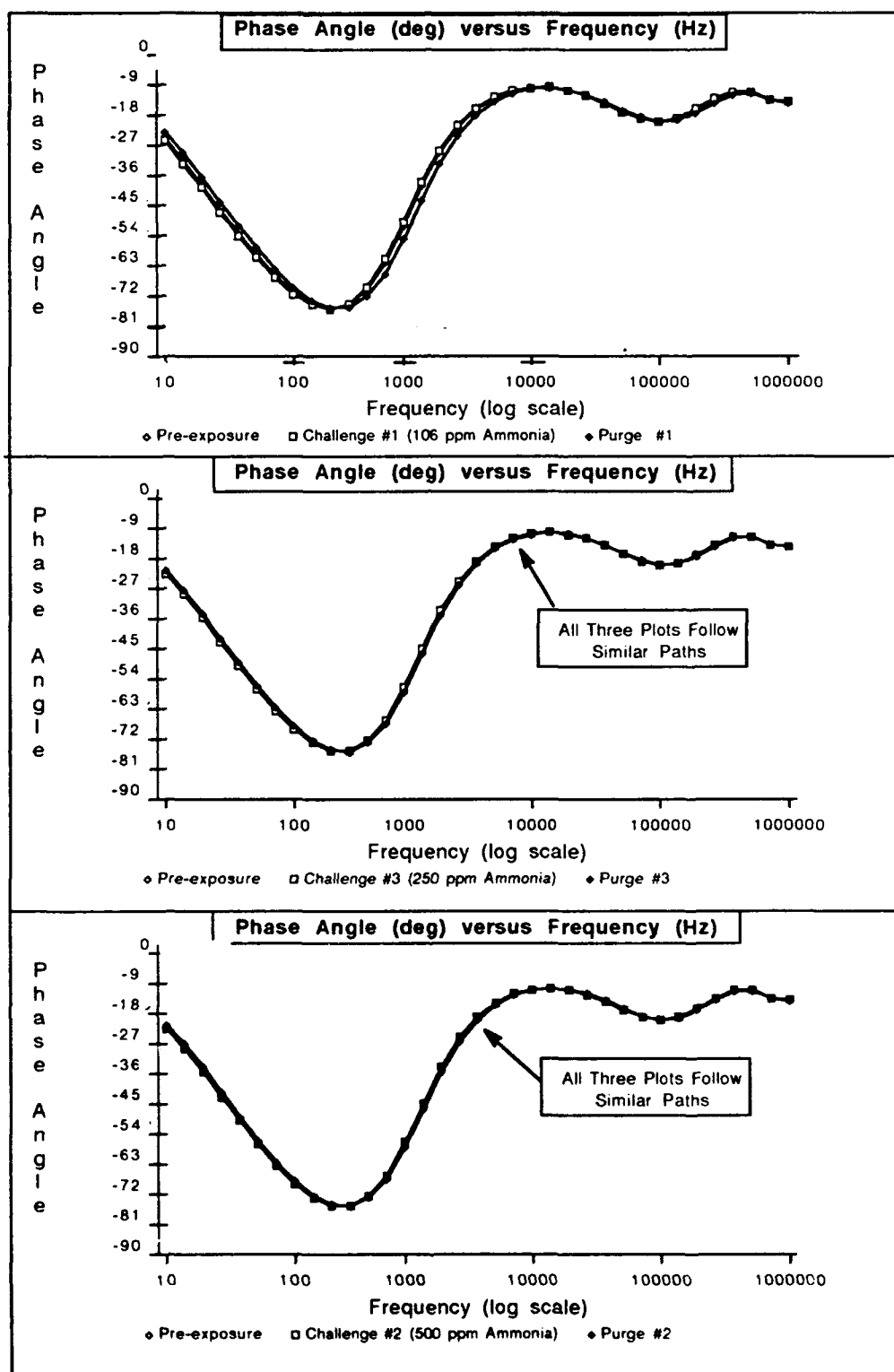


Figure C-67 . Phase Angle versus Frequency Response of IGEFET Microsensor for a Series of Room Air Purges and Challenge Gas Exposures. Testing Conditions: IGE Microsensor Number 5; CuPc Thin-film (3,900 Angstroms Thick); Temperature of 150 degrees Centigrade; Ammonia Challenge Gas (Order of Exposures: 500 ppm, 16 ppm, 106 ppm, 250 ppm, 500 ppm).

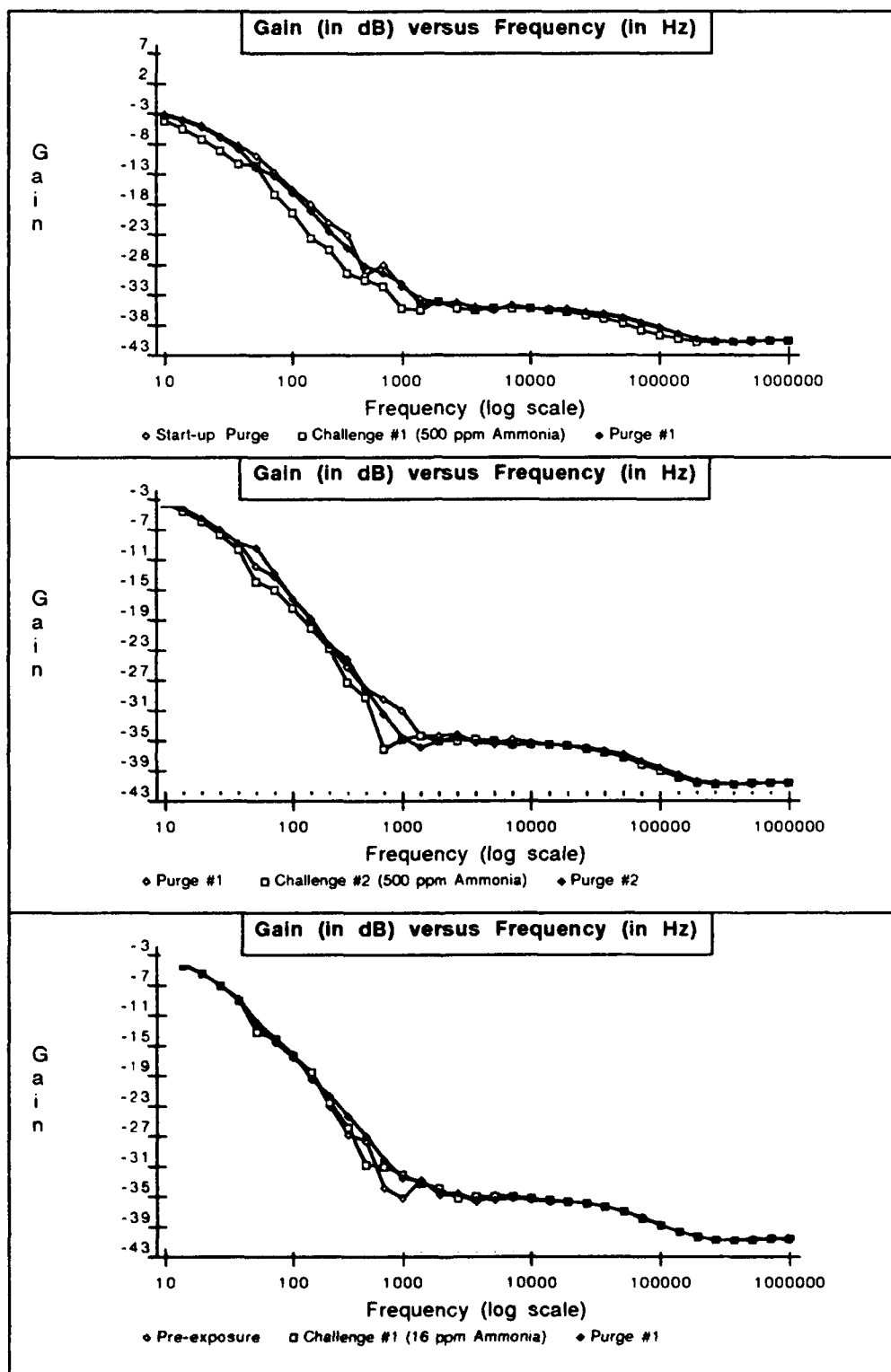


Figure C-68 . Gain versus Frequency Response of IGEFET Microsensor for a Series of Room Air Purges and Challenge Gas Exposures. Testing Conditions: IGE Microsensor Number 5; CuPc Thin-film (3,900 Angstroms Thick); Temperature of 150 degrees Centigrade; Ammonia Challenge Gas (Order of Exposures:500 ppm, 16 ppm, 106 ppm, 250 ppm, 500 ppm).

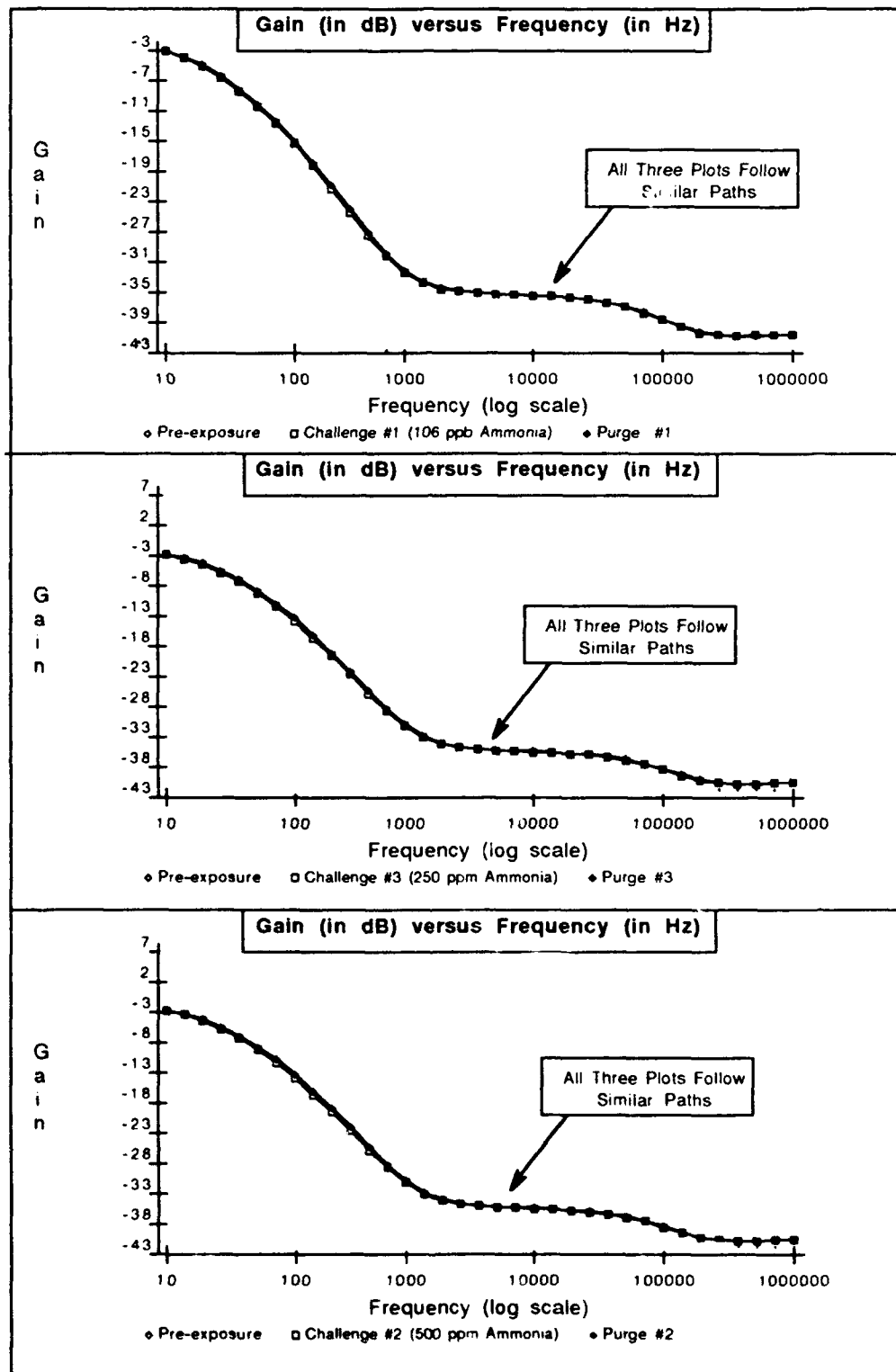


Figure C-69. Gain versus Frequency Response of IGEFET Microsensor for a Series of Room Air Purges and Challenge Gas Exposures. Testing Conditions: IGE Microsensor Number 5; CuPc Thin-film (3,900 Angstroms Thick); Temperature of 150 degrees Centigrade; Ammonia Challenge Gas (Order of Exposures: 500 ppm, 16 ppm, 106 ppm, 250 ppm, 500 ppm).

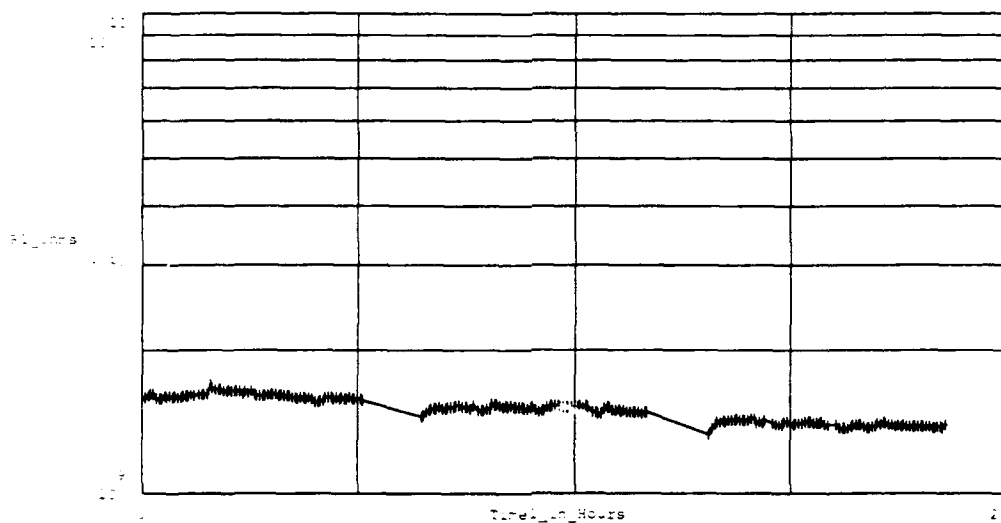


Figure C-70 : DC Resistance Measured Between the Driven-Electrode and Floating-Electrode of the IGE Array, During Series of Purges and Challenge Gas Exposures. The Number of Measurements (at crosses) is 244. The Testing Conditions Included the Following:

IGE Array Number : 1.	Thin-film Material : Copper Phthalocyanine.
Thin-film Thickness : 2,100 Angstroms	Test Temperature(s) : Purge & Challenge at 150°C
Purge Gas : Room Air.	Challenge Gas : Boron Trifluoride.
Challenge Gas Concentration(s) (in order run) : 105 ppm, 24 ppm, 105 ppm.	

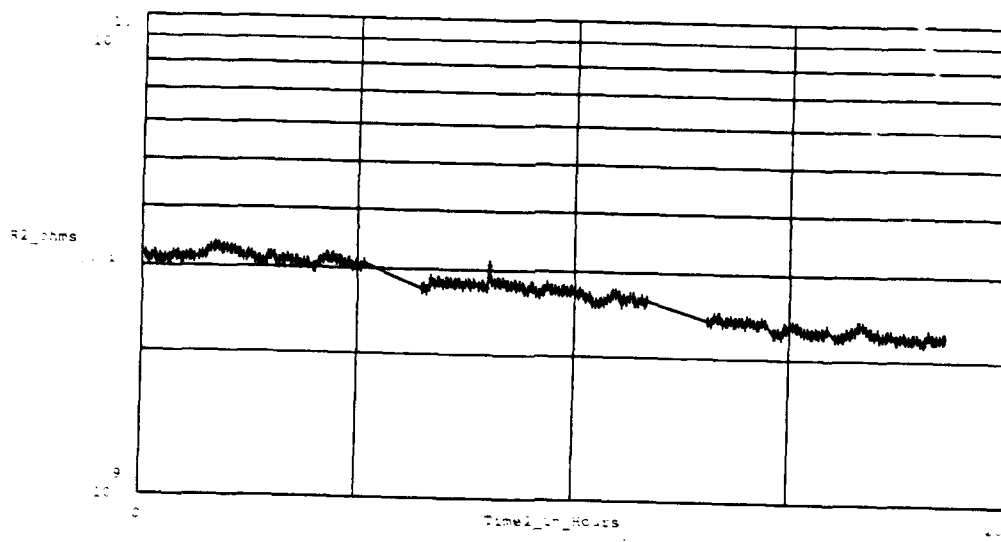


Figure C-71 : DC Resistance Measured Between the Driven-Electrode and Floating-Electrode of the IGE Array, During Series of Purges and Challenge Gas Exposures. The Number of Measurements (at crosses) is 244. The Testing Conditions Included the Following:

IGE Array Number : 2.	Thin-film Material : Copper Phthalocyanine.
Thin-film Thickness : 2,100 Angstroms	Test Temperature(s) : Purge & Challenge at 150°C
Purge Gas : Room Air.	Challenge Gas : Boron Trifluoride.
Challenge Gas Concentration(s) (in order run) : 105 ppm, 24 ppm, 105 ppm.	

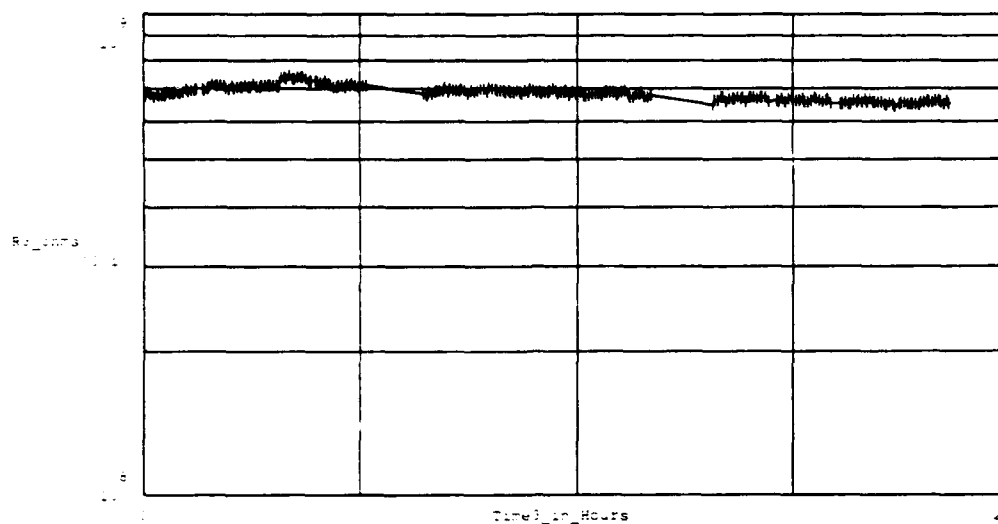


Figure C-72 : DC Resistance Measured Between the Driven-Electrode and Floating-Electrode of the IGE Array, During Series of Purges and Challenge Gas Exposures. The Number of Measurements (at crosses) is 244. The Testing Conditions Included the Following:

IGE Array Number : 3,	Thin-film Material : Copper Phthalocyanine,
Thin-film Thickness : 2,100 Angstroms	Test Temperature(s) : Purge & Challenge at 150°C
Purge Gas : Room Air,	Challenge Gas : Boron Trifluoride,
Challenge Gas Concentration(s) (in order run) : 105 ppm, 24 ppm, 105 ppm.	

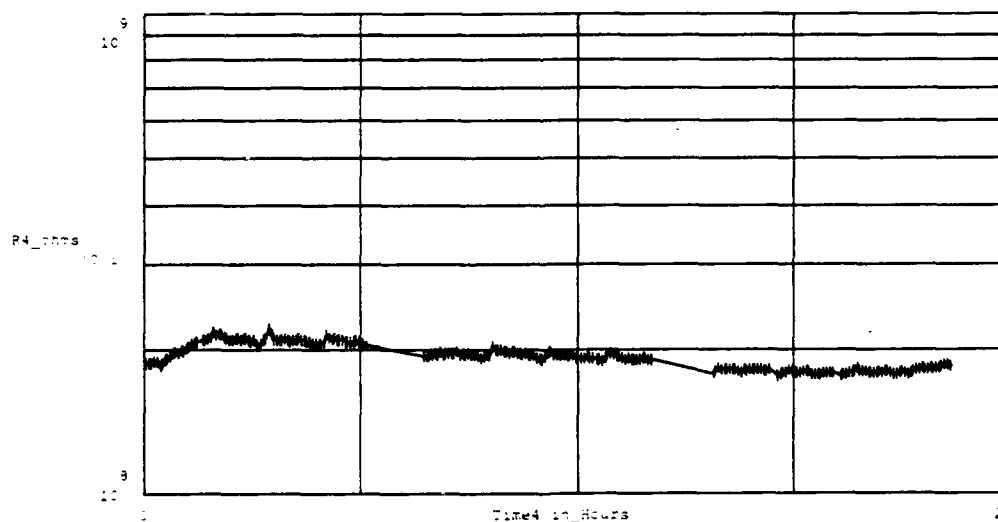


Figure C-73 : DC Resistance Measured Between the Driven-Electrode and Floating-Electrode of the IGE Array, During Series of Purges and Challenge Gas Exposures. The Number of Measurements (at crosses) is 244. The Testing Conditions Included the Following:

IGE Array Number : 4,	Thin-film Material : Copper Phthalocyanine,
Thin-film Thickness : 8,200 Angstroms	Test Temperature(s) : Purge & Challenge at 150°C
Purge Gas : Room Air,	Challenge Gas : Boron Trifluoride,
Challenge Gas Concentration(s) (in order run) : 105 ppm, 24 ppm, 105 ppm.	

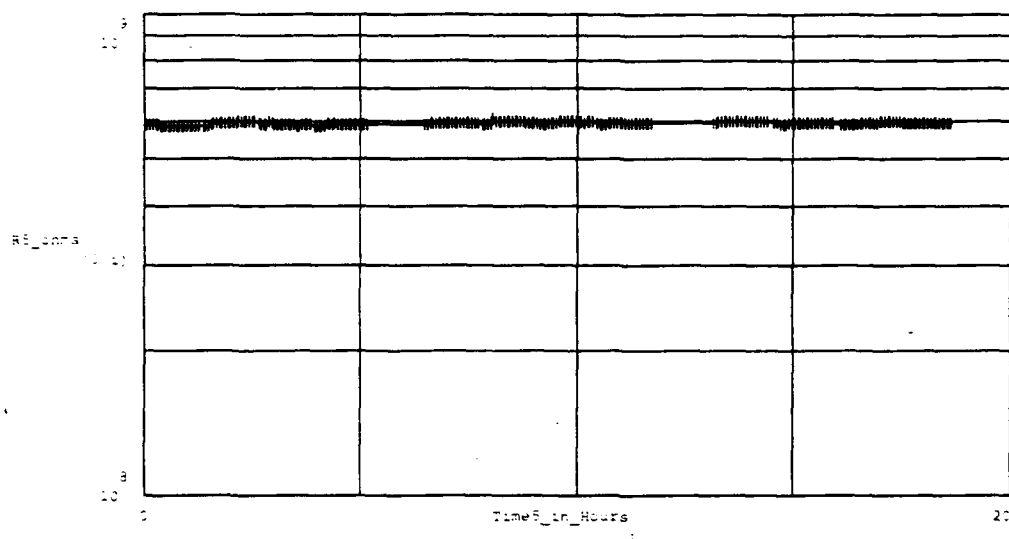


Figure C- 74 . DC Resistance Measured Between the Driven-Electrode and Floating-Electrode of the IGE Array, During Series of Purges and Challenge Gas Exposures. The Number of Measurements (at crosses) is 244. The Testing Conditions Included the Following:

IGE Array Number : 5, Thin-film Material : Copper Phthalocyanine,  
 Thin-film Thickness : 8,200 Angstroms Test Temperature(s) : Purge & Challenge at 150°C  
 Purge Gas : Room Air, Challenge Gas : Boron Trifluoride,  
 Challenge Gas Concentration(s) (in order run) : 105 ppm, 24 ppm, 105 ppm.

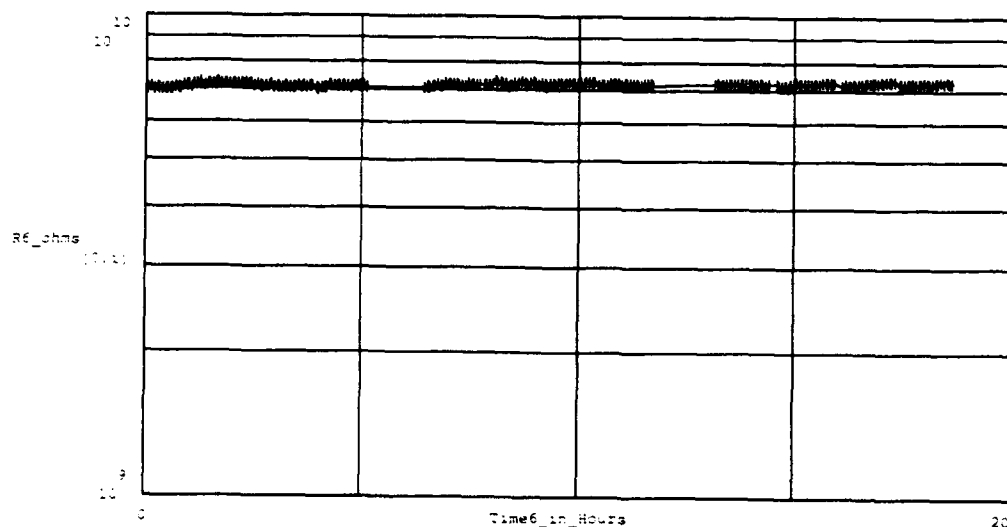


Figure C- 75. DC Resistance Measured Between the Driven-Electrode and Floating-Electrode of the IGE Array, During Series of Purges and Challenge Gas Exposures. The Number of Measurements (at crosses) is 244. The Testing Conditions Included the Following:

IGE Array Number : 6, Thin-film Material : Copper Phthalocyanine,  
 Thin-film Thickness : 8,200 Angstroms Test Temperature(s) : Purge & Challenge at 150°C  
 Purge Gas : Room Air, Challenge Gas : Boron Trifluoride,  
 Challenge Gas Concentration(s) (in order run) : 105 ppm, 24 ppm, 105 ppm.



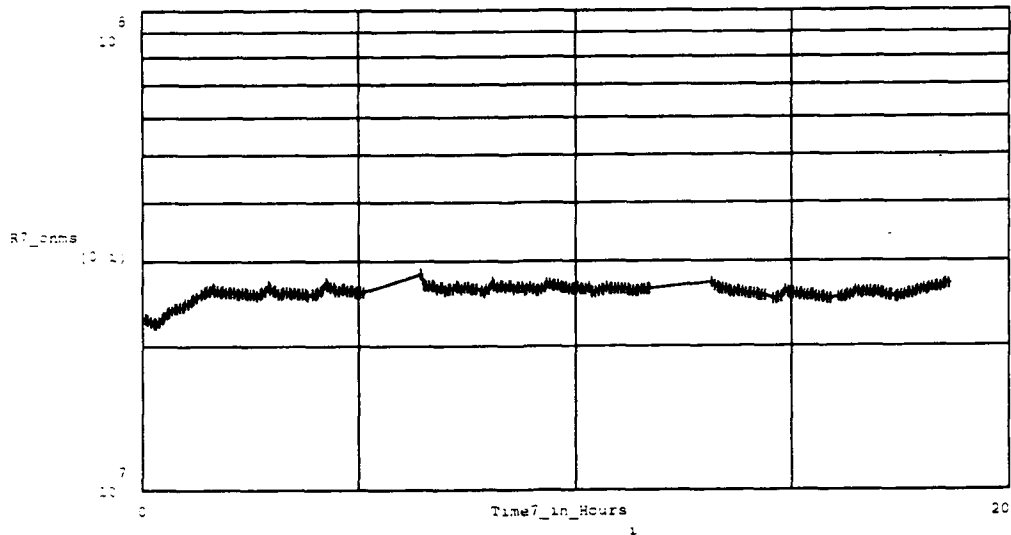


Figure C-76 . DC Resistance Measured Between the Driven-Electrode and Floating-Electrode of the IGE Array. During Series of Purges and Challenge Gas Exposures. The Number of Measurements (at crosses) is 244. The Testing Conditions Included the Following:

IGE Array Number : 7.	Thin-film Material : Copper Phthalocyanine.
Thin-film Thickness : 16,000 Angstroms	Test Temperature(s) : Purge & Challenge at 150°C
Purge Gas : Room Air.	Challenge Gas : Boron Trifluoride.
Challenge Gas Concentration(s) (in order run) : 105 ppm, 24 ppm, 105 ppm.	

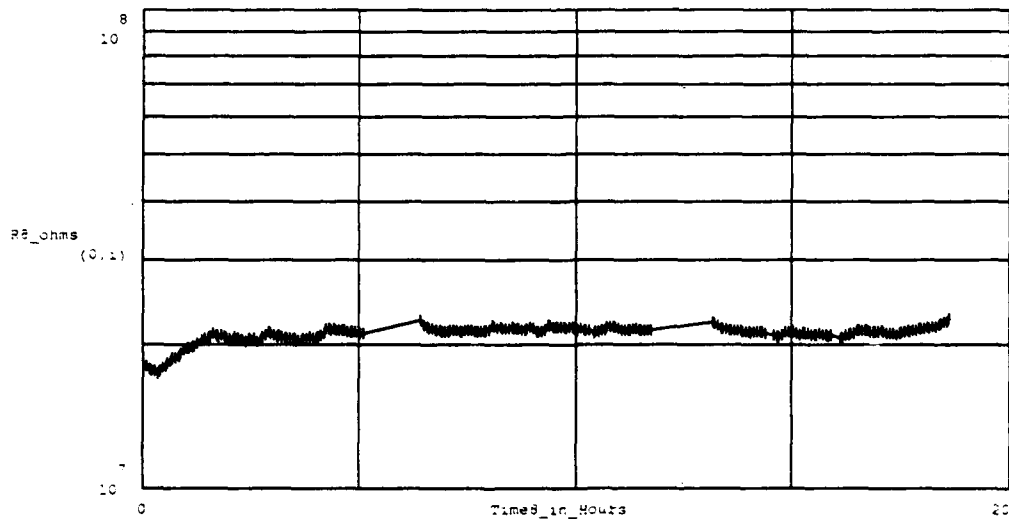


Figure C-77 . DC Resistance Measured Between the Driven-Electrode and Floating-Electrode of the IGE Array. During Series of Purges and Challenge Gas Exposures. The Number of Measurements (at crosses) is 244. The Testing Conditions Included the Following:

IGE Array Number : 8.	Thin-film Material : Copper Phthalocyanine.
Thin-film Thickness : 16,000 Angstroms	Test Temperature(s) : Purge & Challenge at 150°C
Purge Gas : Room Air.	Challenge Gas : Boron Trifluoride.
Challenge Gas Concentration(s) (in order run) : 105 ppm, 24 ppm, 105 ppm.	

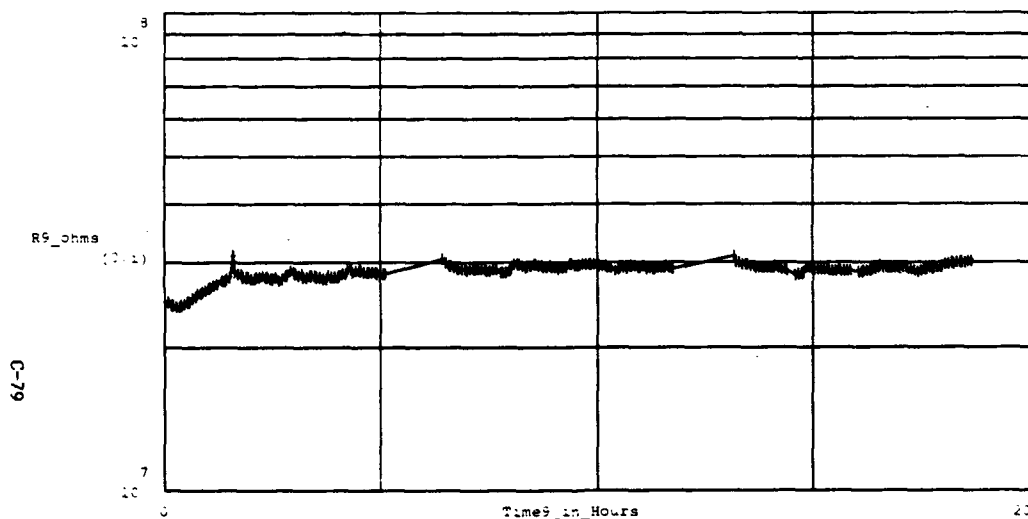


Figure C- 78 . DC Resistance Measured Between the Driven-Electrode and Floating-Electrode of the IGE Array. During Series of Purges and Challenge Gas Exposures. The Number of Measurements (at crosses) is 244. The Testing Conditions Included the Following:

IGE Array Number : 9.	Thin-film Material : Copper Phthalocyanine.
Thin-film Thickness : 16,000 Angstroms	Test Temperature(s) : Purge & Challenge at 150°C
Purge Gas : Room Air.	Challenge Gas : Boron Trifluoride.
Challenge Gas Concentration(s) (in order run) : 105 ppm, 24 ppm, 105 ppm.	

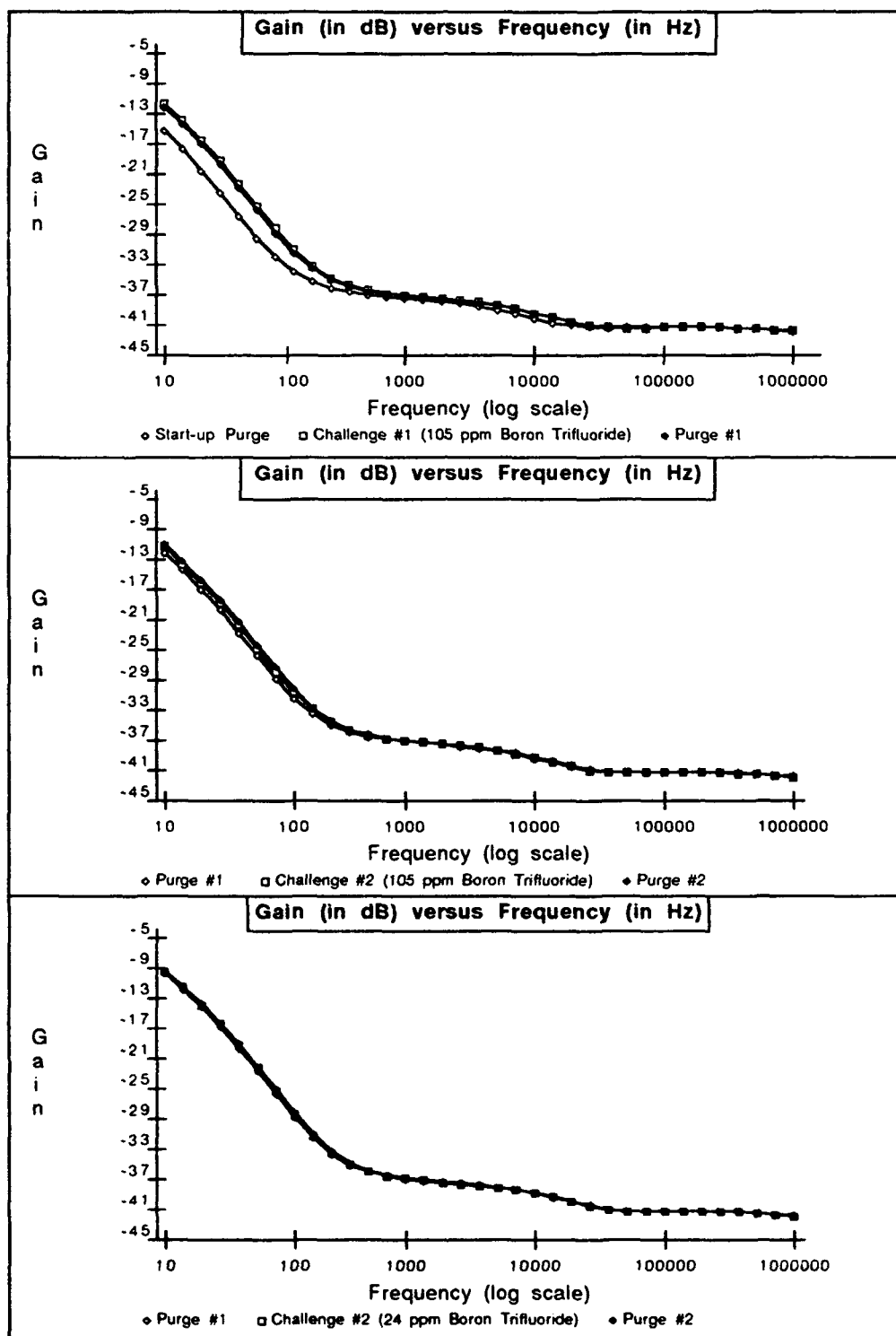


Figure C-79. Gain versus Frequency Response of IGEFET Microsensor for a Series of Room Air Purges and Challenge Gas Exposures. Testing Conditions: IGE Microsensor Number 3; CuPc Thin-film (2,100 Angstroms Thick); Temperature of 150 degrees Centigrade; Boron Trifluoride Challenge Gas (Order of Exposures: 105 ppm, 24 ppm, 105 ppm).

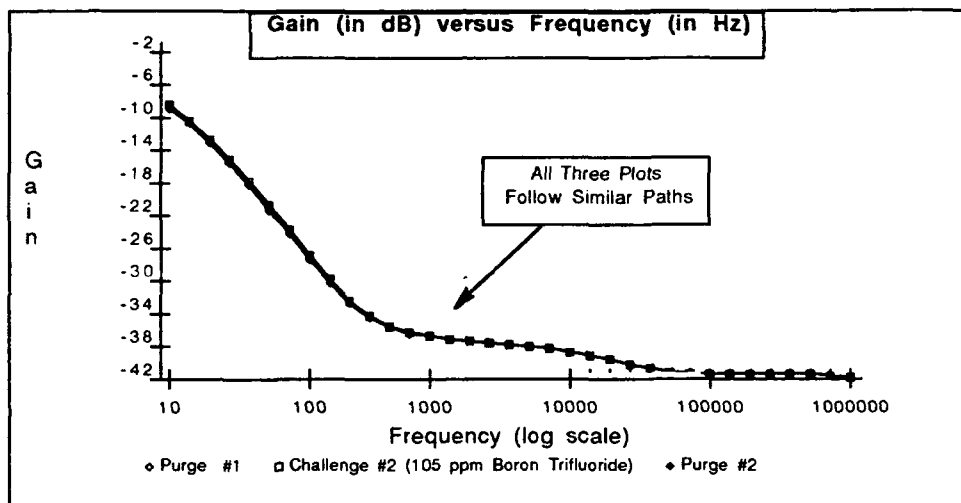


Figure C-80. Gain versus Frequency Response of IGEFET Microsensor for a Series of Room Air Purges and Challenge Gas Exposures. Testing Conditions: IGE Microsensor Number 3; CuPc Thin-film (2,100 Angstroms Thick); Temperature of 150 degrees Centigrade; Boron Trifluoride Challenge Gas (Order of Exposures: 105 ppm, 24 ppm, 105 ppm).

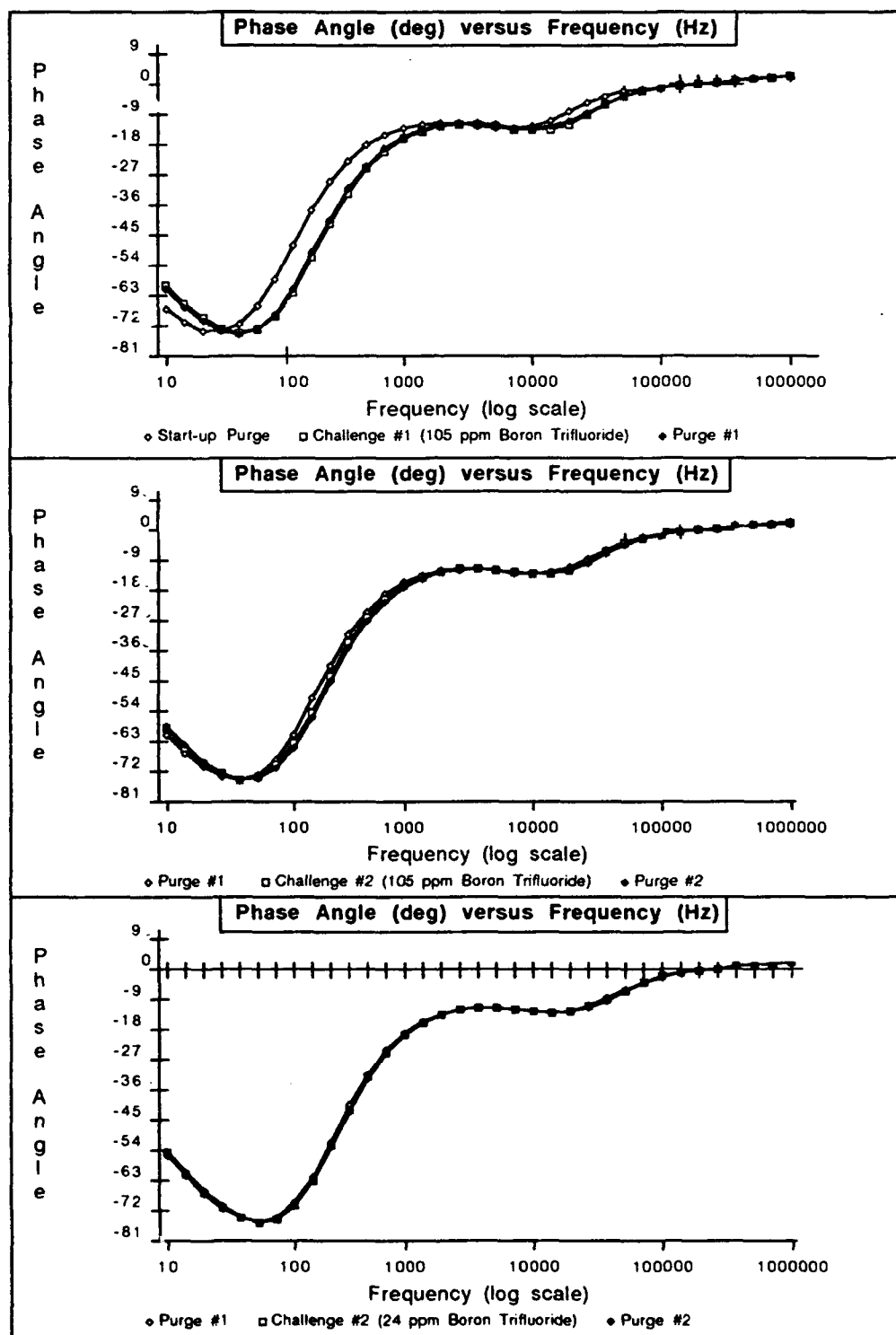


Figure C-81 . Phase Angle versus Frequency Response of IGEFET Microsensor for a Series of Room Air Purges and Challenge Gas Exposures. Testing Conditions: IGE Microsensor Number 3; CuPc Thin-film (2,100 Angstroms Thick); Temperature of 150 degrees Centigrade; Boron Trifluoride Challenge Gas (Order of Exposures: 105 ppm, 24 ppm, 105 ppm).

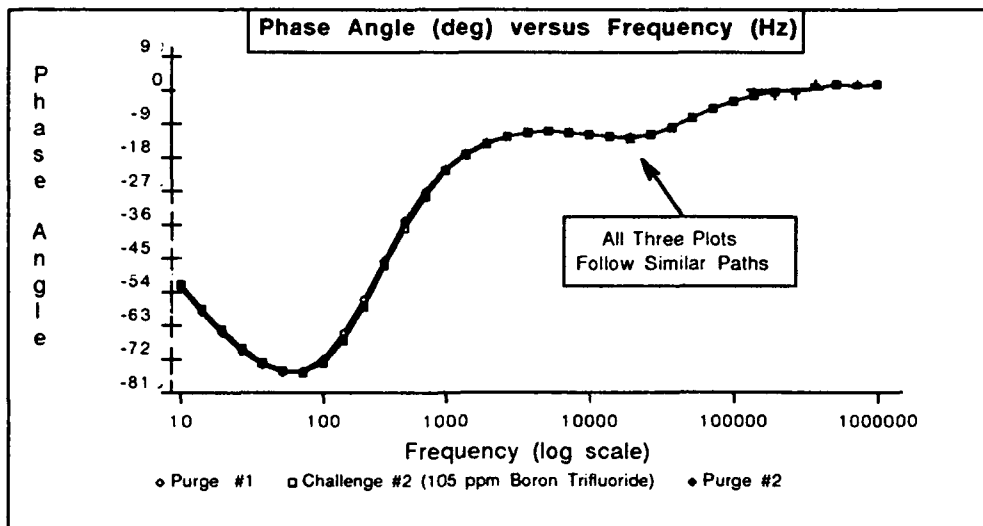


Figure C-82 . Phase Angle versus Frequency Response of IGEFET Microsensor for a Series of Room Air Purges and Challenge Gas Exposures. Testing Conditions: IGE Microsensor Number 3; CuPc Thin-film (2,100 Angstroms Thick); Temperature of 150 degrees Centigrade; Boron Trifluoride Challenge Gas (Order of Exposures: 105 ppm, 24 ppm, 105 ppm).

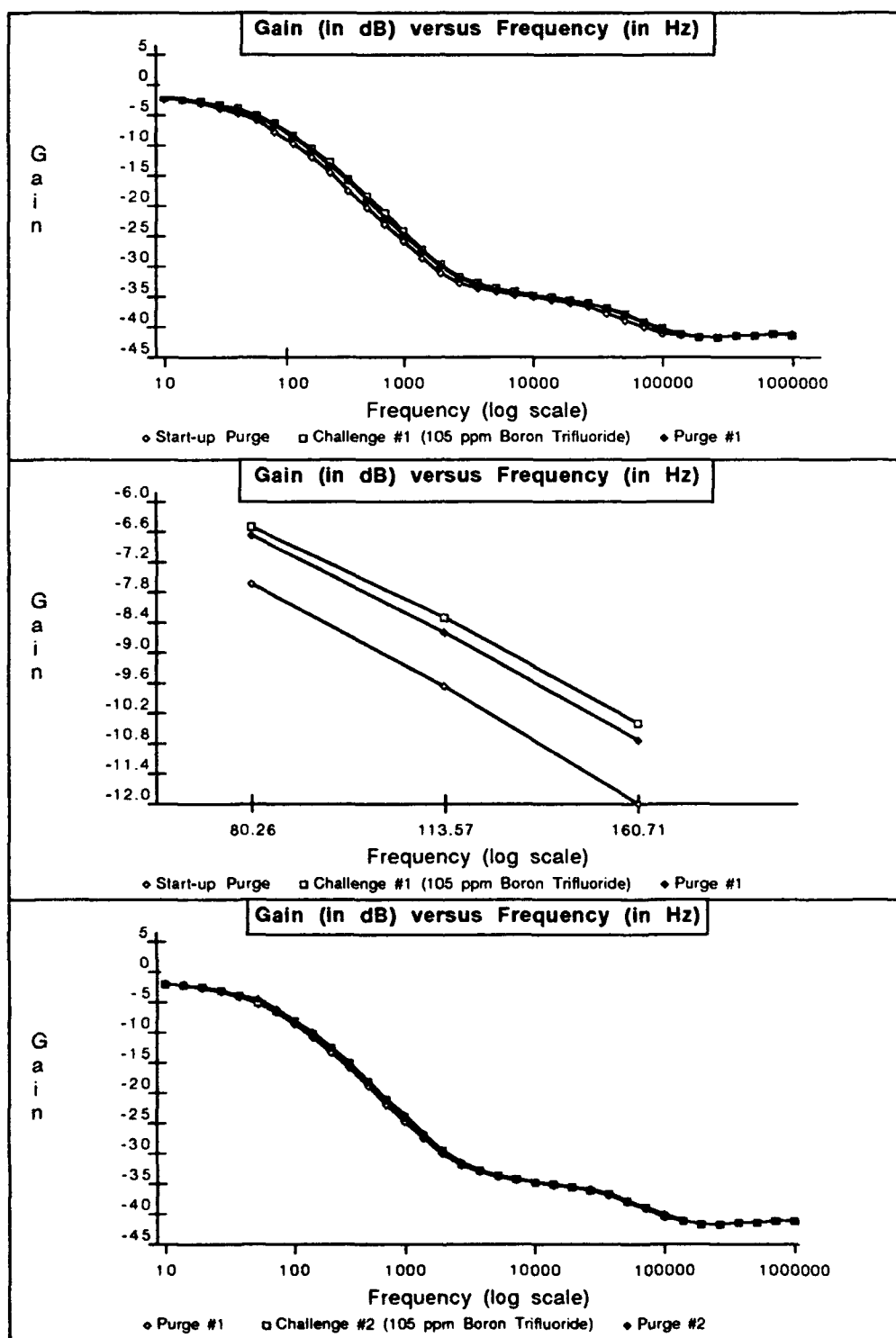


Figure C-83 . Gain versus Frequency Response of IGEFET Microsensor for a Series of Room Air Purges and Challenge Gas Exposures. Testing Conditions: IGE Microsensor Number 5; CuPc Thin-film (8,200 Angstroms Thick); Temperature of 150 degrees Centigrade; Boron Trifluoride Challenge Gas (Order of Exposures: 105 ppm, 24 ppm, 105 ppm).

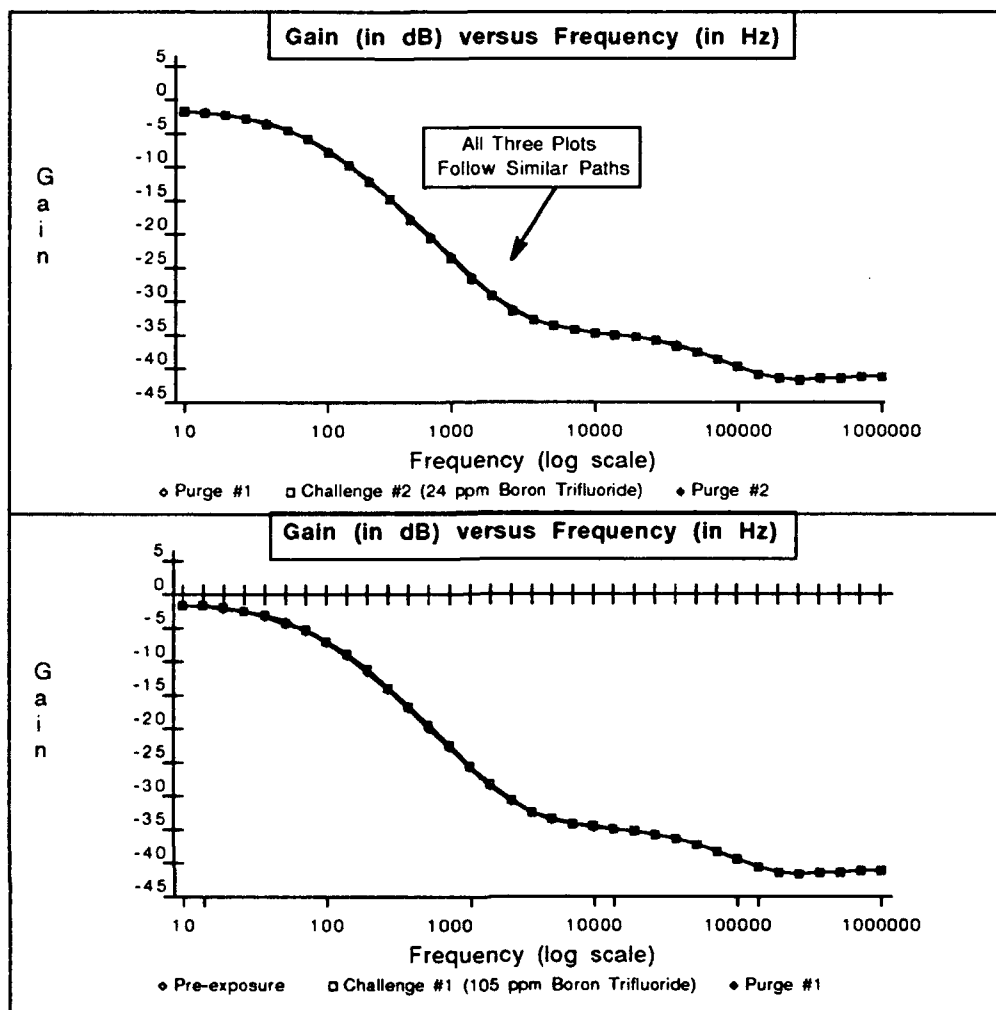


Figure C-84. Gain versus Frequency Response of IGEFET Microsensor for a Series of Room Air Purges and Challenge Gas Exposures. Testing Conditions: IGE Microsensor Number 5; CuPc Thin-film (8,200 Angstroms Thick); Temperature of 150 degrees Centigrade; Boron Trifluoride Challenge Gas (Order of Exposures: 105 ppm, 24 ppm, 105 ppm).



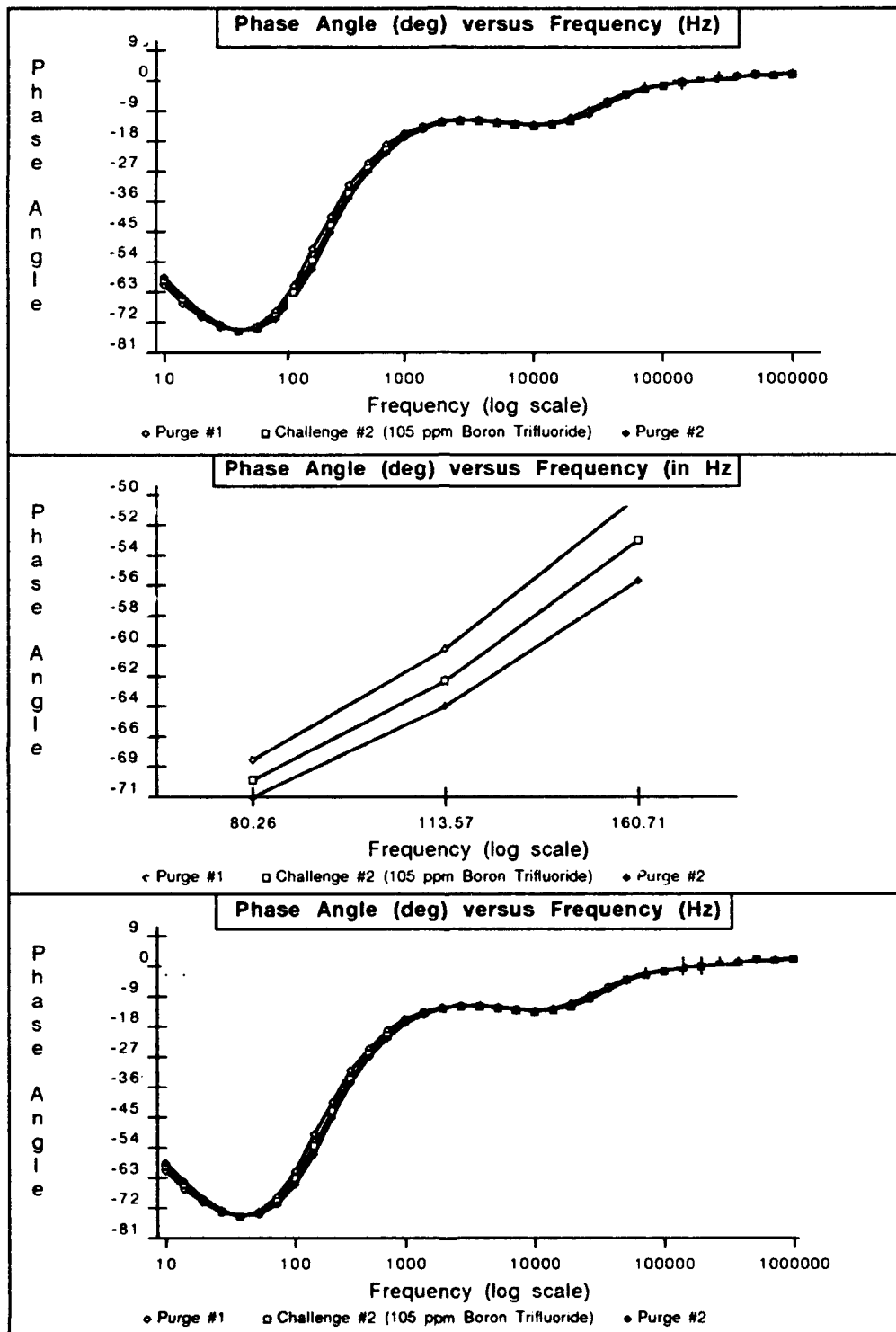


Figure C-85. Phase Angle versus Frequency Response of IGEFET Microsensor for a Series of Room Air Purges and Challenge Gas Exposures. Testing Conditions: IGE Microsensor Number 5; CuPc Thin-film (8,200 Angstroms Thick); Temperature of 150 degrees Centigrade; Boron Trifluoride Challenge Gas (Order of Exposures: 105 ppm, 24 ppm, 105 ppm).

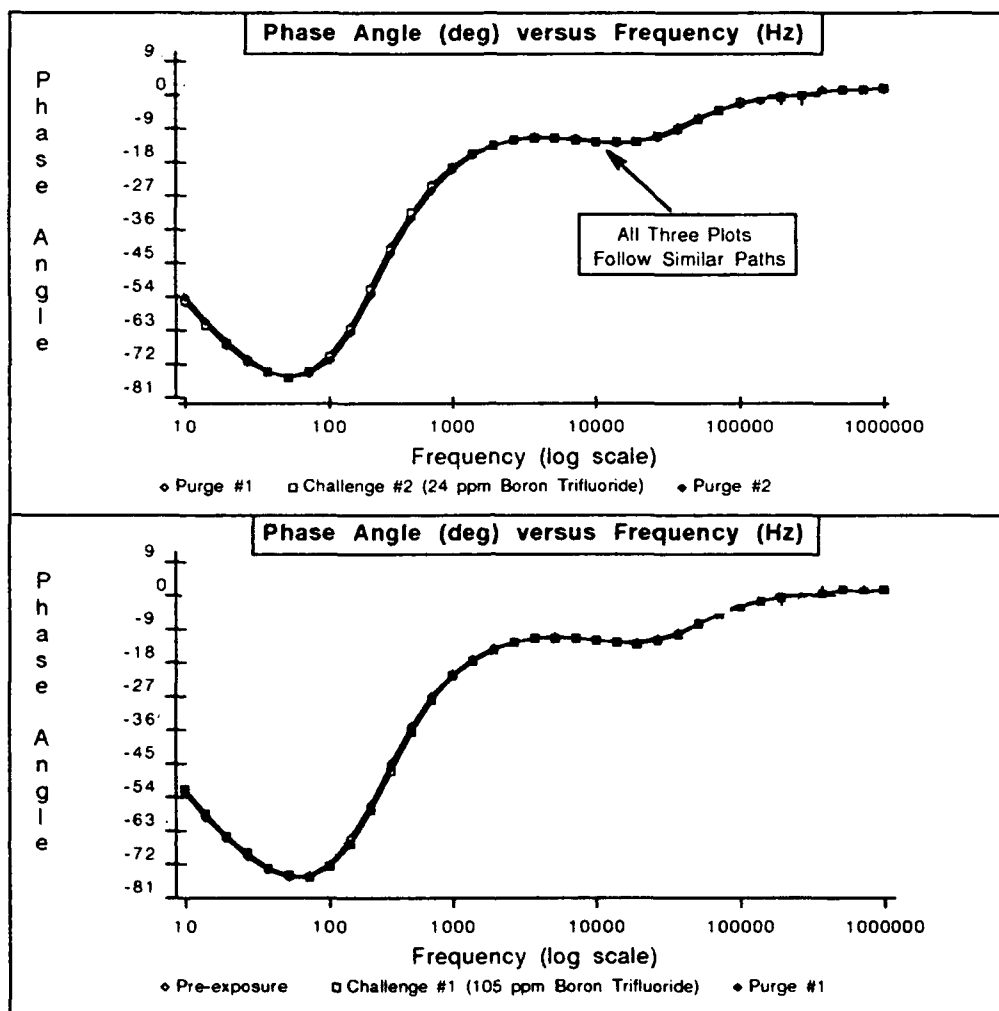


Figure C-86. Phase Angle versus Frequency Response of IGEFET Microsensor for a Series of Room Air Purges and Challenge Gas Exposures. Testing Conditions: IGE Microsensor Number 5; CuPc Thin-film (8,200 Angstroms Thick); Temperature of 150 degrees Centigrade; Boron Trifluoride Challenge Gas (Order of Exposures: 105 ppm, 24 ppm, 105 ppm).

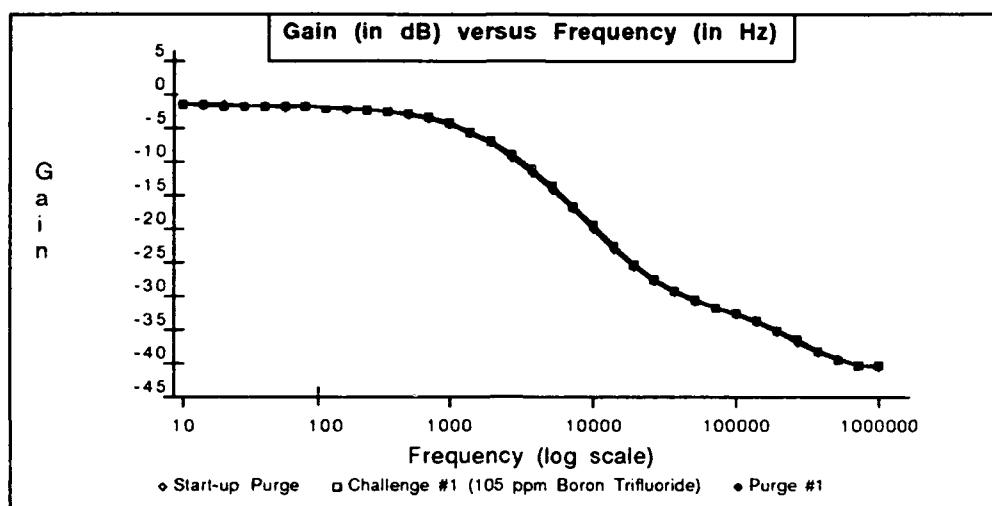


Figure C-87 . Gain versus Frequency Response of IGEFET Microsensor for a Series of Room Air Purges and Challenge Gas Exposures. Testing Conditions: IGE Microsensor Number 8; CuPc Thin-film (16,000 Angstroms Thick); Temperature of 150 degrees Centigrade; Boron Trifluoride Challenge Gas (Order of Exposures: 105 ppm, 24 ppm, 105 ppm).

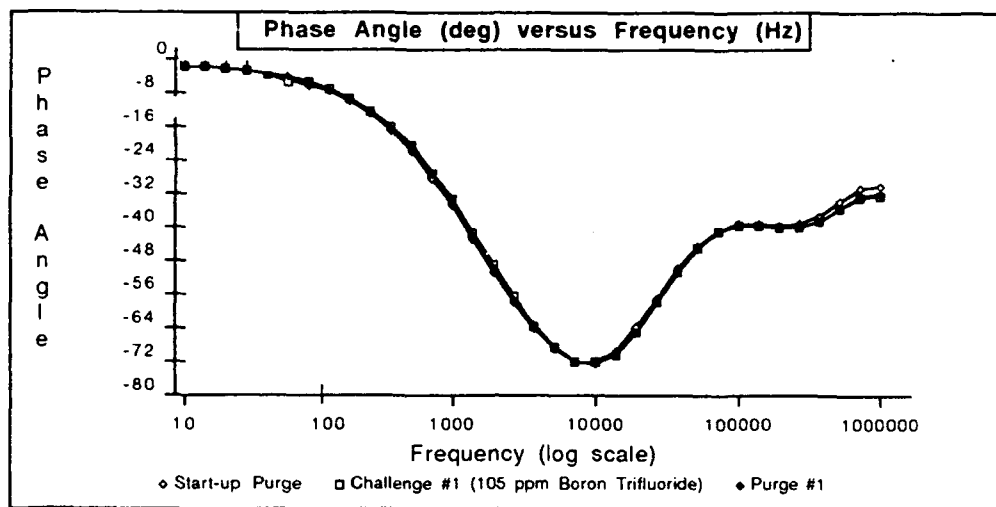


Figure C-88.. Phase Angle versus Frequency Response of IGEFET Microsensor for a Series of Room Air Purges and Challenge Gas Exposures. Testing Conditions: IGE Microsensor Number 8; CuPc Thin-film (16,000 Angstroms Thick); Temperature of 150 degrees Centigrade; Boron Trifluoride Challenge Gas (Order of Exposures: 105 ppm, 24 ppm, 105 ppm).

## *Section 2*

This section summarizes the dc resistance versus time plots for the CuPc films exposed separately to DMMP (Figures C-89 to C-91) and DIMP (Figures C-92 to C-94) at three temperatures: 150°C, 90°C, and 30°C.

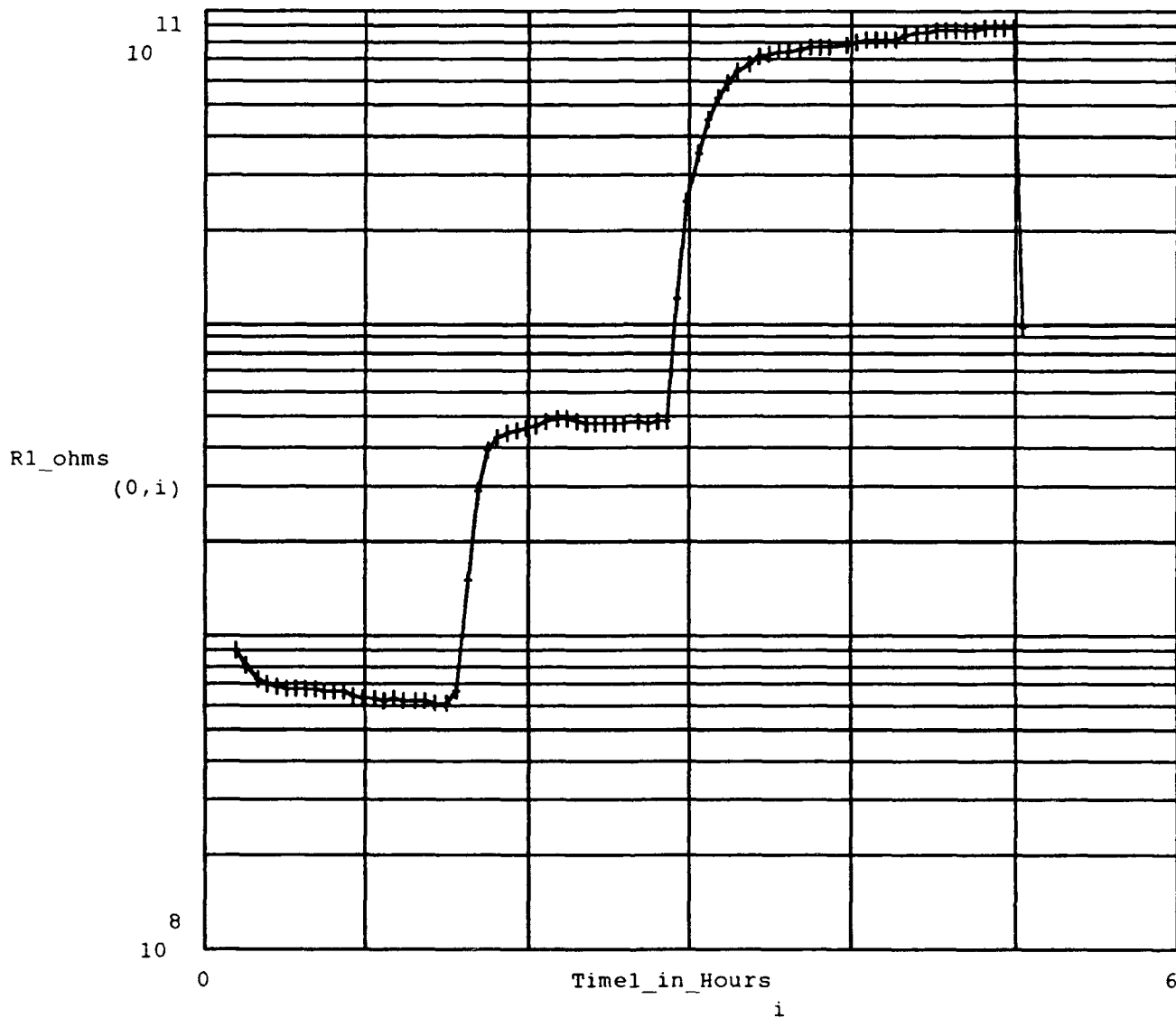


Figure C-89 . DC Resistance Measured Between the Driven-Electrode and Floating-Electrode of the IGE Array, During Series of Purges and Challenge Gas Exposures. The Testing Conditions Included the Following:

IGE Array Number : 1,  
 Thin-film Material : Copper Phthalocyanine,  
 Thin-film Thickness : 3200 Angstroms  
 Test Temperature(s) : Initial Purge & Challenge at 150°C, Second Purge  
 & Challenge at 90°C, Third Purge and Challenge at 30°C,  
 Purge Gas : Room Air,  
 Challenge Gas : DMMP,  
 Challenge Gas Concentration(s) (in order run) : 10 ppm.

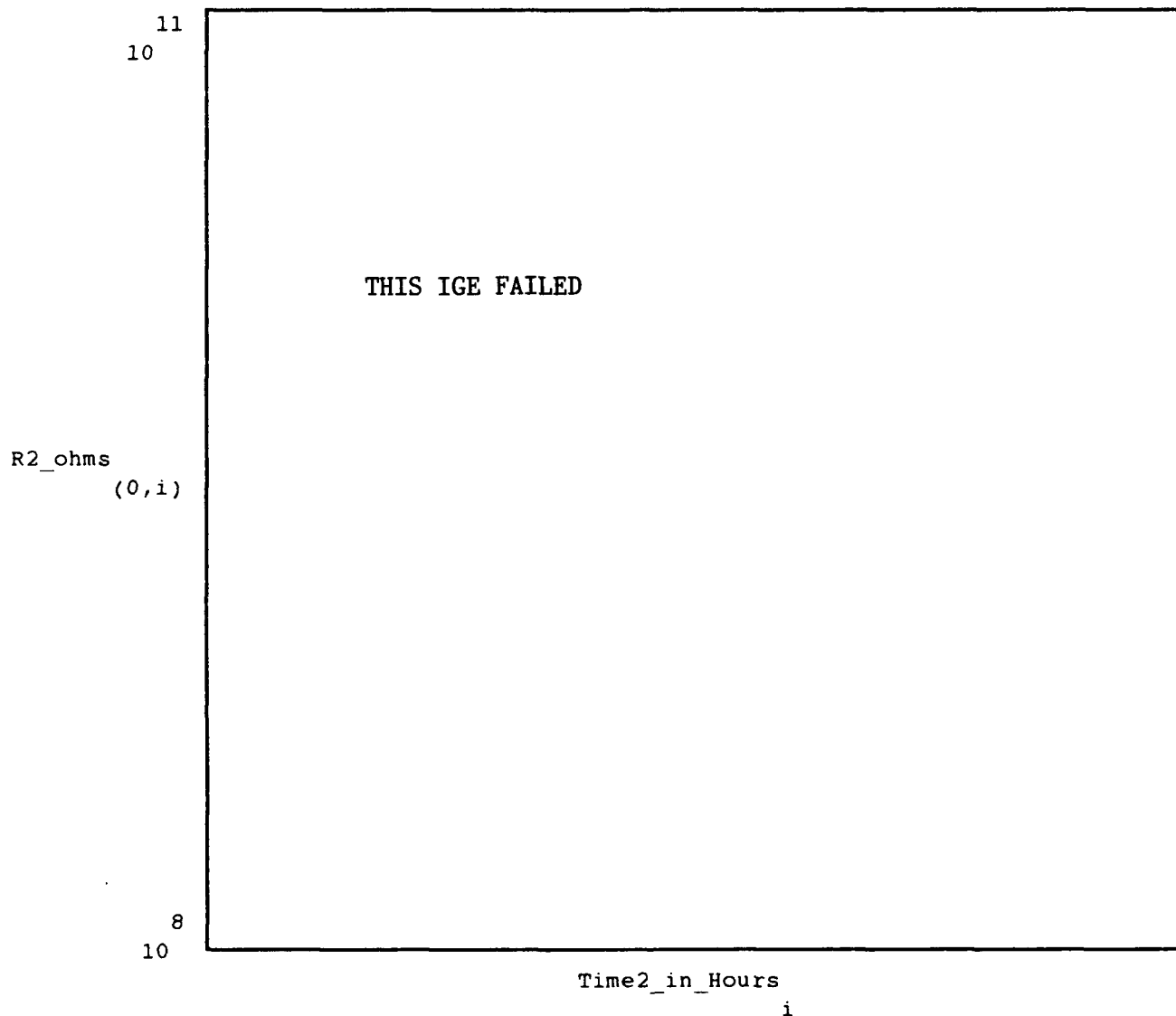


Figure C- 90 . DC Resistance Measured Between the Driven-Electrode and Floating-Electrode of the IGE Array. During Series of Purges and Challenge Gas Exposures. The Testing Conditions Included the Following:

IGE Array Number : 2,  
 Thin-film Material : Copper Phthalocyanine,  
 Thin-film Thickness : 3200 Angstroms  
 Test Temperature(s) : Initial Purge & Challenge at 150°C, Second Purge  
 & Challenge at 90°C, Third Purge and Challenge at 30°C,  
 Purge Gas : Room Air,  
 Challenge Gas : DMMP,  
 Challenge Gas Concentration(s) (in order run) : 10 ppm.

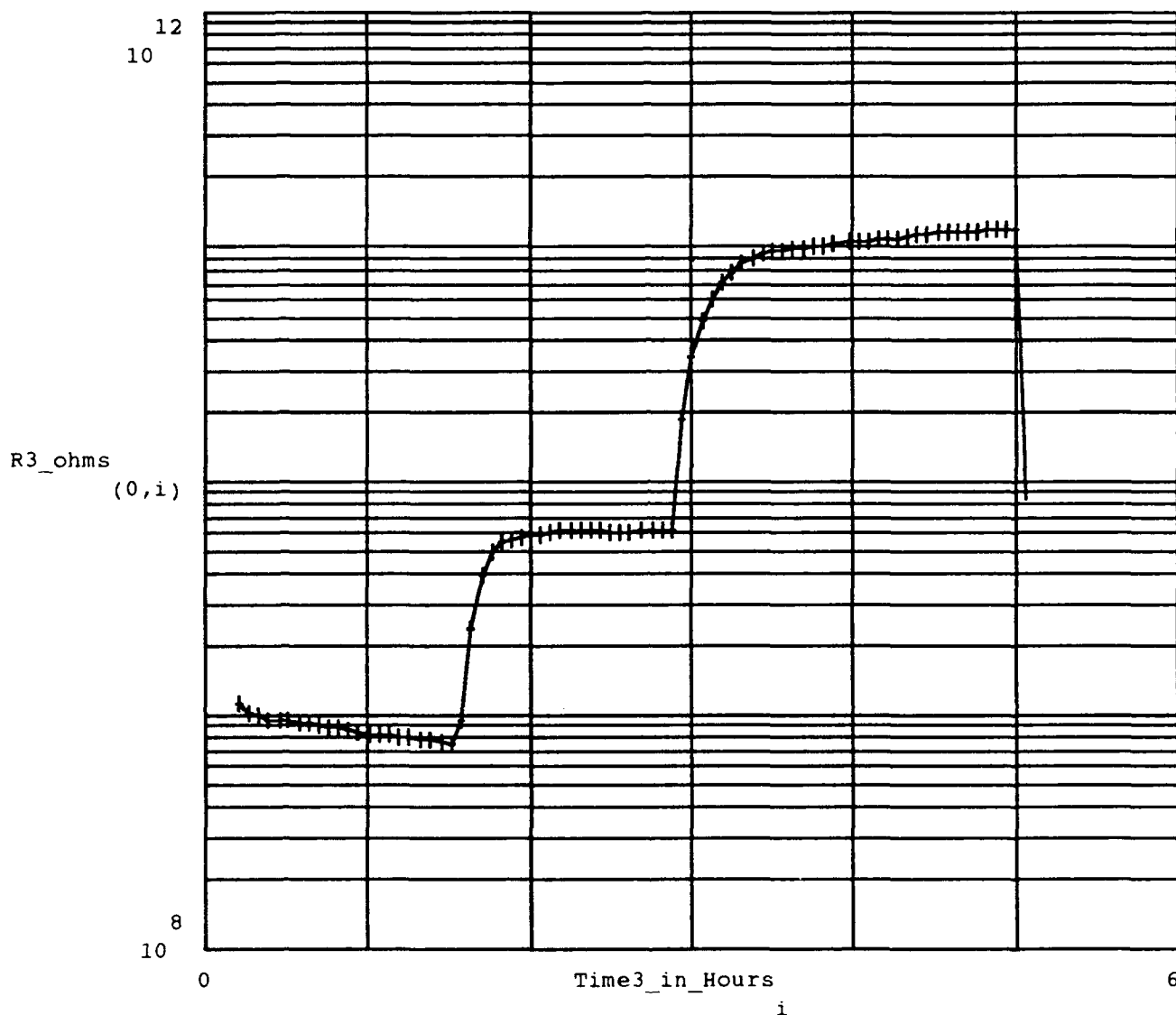


Figure C- 91 . DC Resistance Measured Between the Driven-Electrode and Floating-Electrode of the IGE Array, During Series of Purges and Challenge Gas Exposures. The Testing Conditions Included the Following:

IGE Array Number : 3,  
 Thin-film Material : Copper Phthalocyanine,  
 Thin-film Thickness : 3200 Angstroms  
 Test Temperature(s) : Initial Purge & Challenge at 150°C, Second Purge  
 & Challenge at 90°C, Third Purge and Challenge at 30°C,  
 Purge Gas : Room Air,  
 Challenge Gas : DMMP,  
 Challenge Gas Concentration(s) (in order run) : 10 ppm.



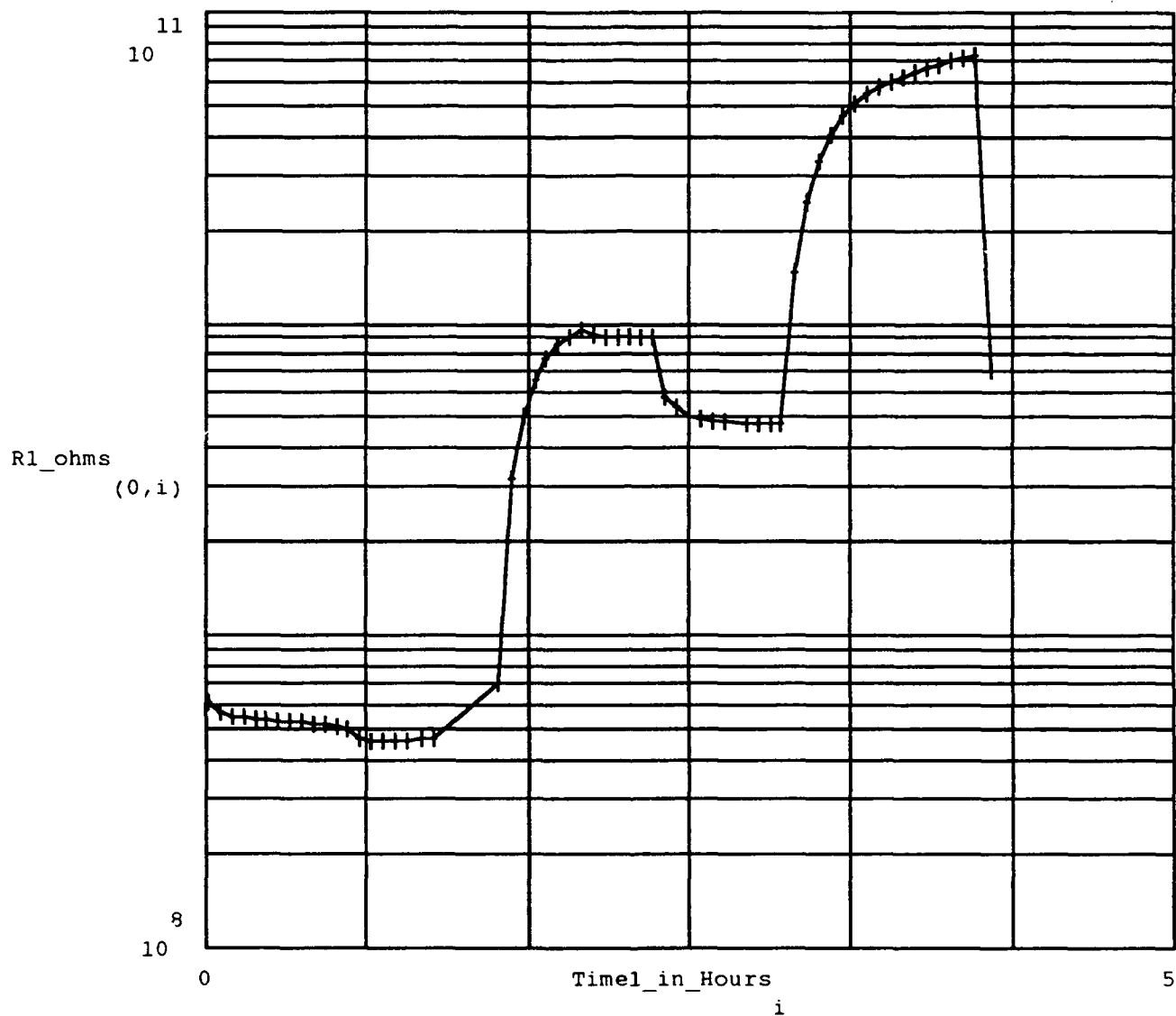


Figure C- 92 . DC Resistance Measured Between the Driven-Electrode and Floating-Electrode of the IGE Array, During Series of Purges and Challenge Gas Exposures. The Testing Conditions Included the Following:

IGE Array Number : 1,  
 Thin-film Material : Copper Phthalocyanine,  
 Thin-film Thickness : 3200 Angstroms  
 Test Temperature(s) : Initial Purge & Challenge at 150°C, Second Purge  
 & Challenge at 90°C, Third Purge and Challenge at 30°C,  
 Purge Gas : Room Air,  
 Challenge Gas : DIMP,  
 Challenge Gas Concentration(s) (in order run) : 3 , ppm.

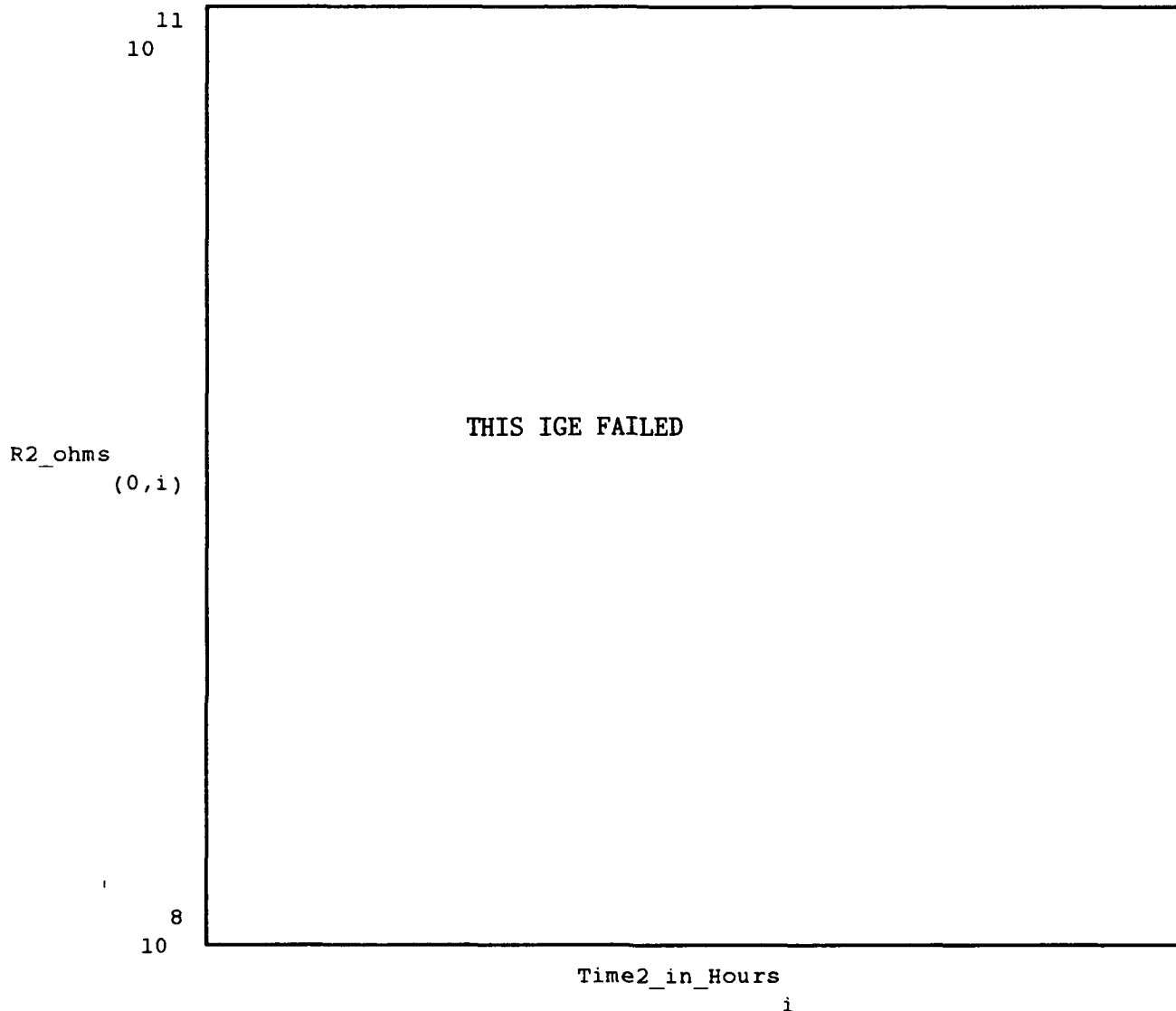


Figure C- 93 : DC Resistance Measured Between the Driven-Electrode and Floating-Electrode of the IGE Array, During Series of Purges and Challenge Gas Exposures. The Testing Conditions Included the Following:

IGE Array Number : 2,  
 Thin-film Material : Copper Phthalocyanine,  
 Thin-film Thickness : 3200 Angstroms  
 Test Temperature(s) : Initial Purge & Challenge at 150°C, Second Purge  
 & Challenge at 90°C, Third Purge and Challenge at 30°C,  
 Purge Gas : Room Air,  
 Challenge Gas : DIMP,  
 Challenge Gas Concentration(s) (in order run) : ppm.

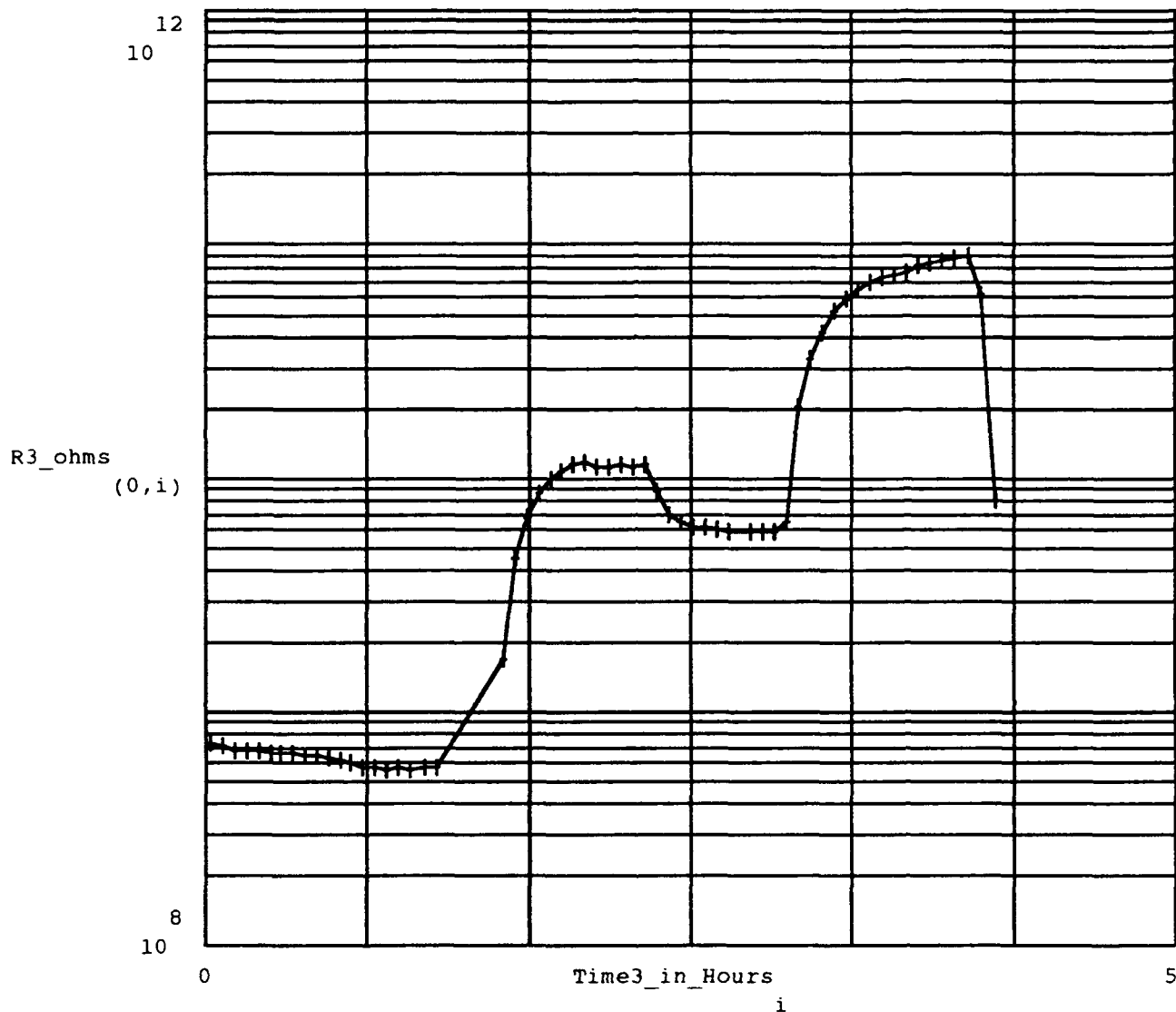


Figure C- 94 . DC Resistance Measured Between the Driven-Electrode and Floating-Electrode of the IGE Array, During Series of Purges and Challenge Gas Exposures. The Testing Conditions Included the Following:

IGE Array Number : 3,  
 Thin-film Material : Copper Phthalocyanine,  
 Thin-film Thickness : 3200 Angstroms  
 Test Temperature(s) : Initial Purge & Challenge at 150°C. Second Purge  
 & Challenge at 90°C, Third Purge and Challenge at 30°C,  
 Purge Gas : Room Air,  
 Challenge Gas : DIMP,  
 Challenge Gas Concentration(s) (in order run) : 3 ppm.

## *Appendix D: Response of CoPc Thin-Film Coatings.*

This appendix presents a portion of the significant responses to the challenge gases for the CoPc thin-films evaluated during this investigation. The appendix is divided into two sections: Section 1 deals with the responses to challenge gases at 150°C (referred to as the Series II tests in the thesis body); Section 2 presents information concerning DMMP and DIMP challenges to CoPc at temperatures of 150°C, 90°C, and 30°C.

### *Section 1*

Resistance and gain and phase angle transfer function responses for the challenge and purge cycles are provided as:

- CoPc challenged with NO<sub>2</sub> (Figures D-1 to D-71),
  - dc resistance measurements versus time,
  - gain and phase angle measurements versus frequency,
  - sensitivity, and reversibility calculations versus frequency,
- CoPc challenged with NH<sub>3</sub> (Figures D-72 to D-86),
  - dc resistance measurements versus time,
  - gain and phase angle measurements versus frequency,
- CoPc challenged with BF<sub>3</sub> (Figures D-87 to D-101),
  - dc resistance measurements versus time,
  - gain and phase angle measurements versus frequency,

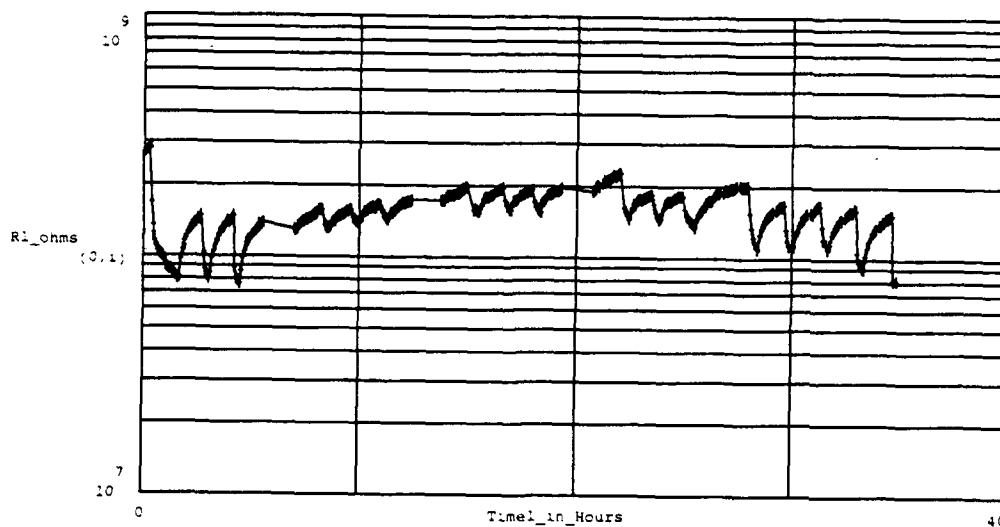


Figure D-1 . DC Resistance Measured Between the Driven-Electrode and Floating-Electrode of the IGE Array. During Series of Purges and Challenge Gas Exposures. The Number of Measurements (at crosses) is 420. The Testing Conditions Included the Following:

IGE Array Number : 1,	Thin-film Material : Cobalt Phthalocyanine,
Thin-film Thickness : 2,500 Angstroms	Test Temperature(s) : Purge & Challenge at 150°C
Purge Gas : Room Air.	Challenge Gas : Nitrogen Dioxide.
Challenge Gas Concentration(s) (in order run) : 1000 ppb, 30 ppb, 50 ppb, 100 ppb, 500 ppb, 1000 ppb.	

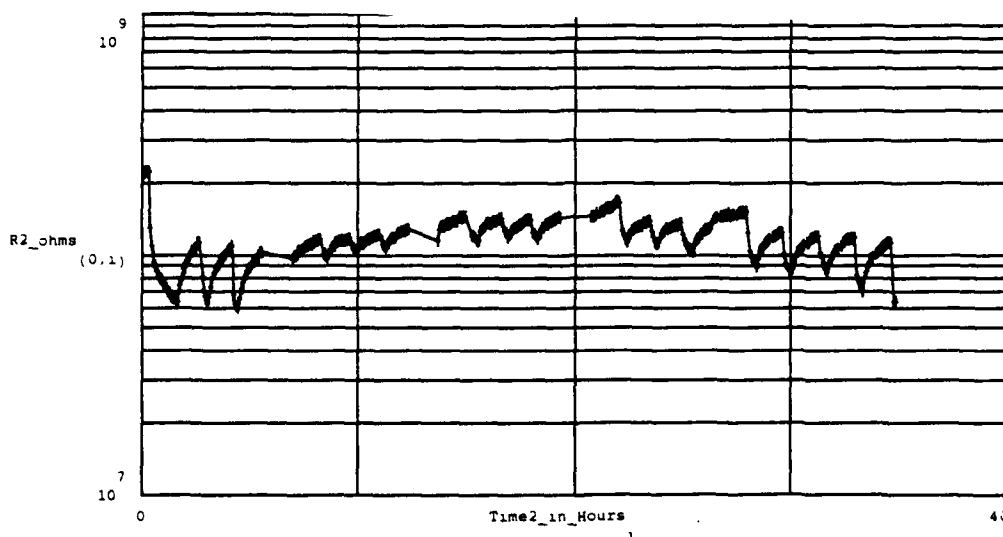


Figure D-2 . DC Resistance Measured Between the Driven-Electrode and Floating-Electrode of the IGE Array. During Series of Purges and Challenge Gas Exposures. The Number of Measurements (at crosses) is 420. The Testing Conditions Included the Following:

IGE Array Number : 2,	Thin-film Material : Cobalt Phthalocyanine,
Thin-film Thickness : 2,500 Angstroms	Test Temperature(s) : Purge & Challenge at 150°C
Purge Gas : Room Air.	Challenge Gas : Nitrogen Dioxide.
Challenge Gas Concentration(s) (in order run) : 1000 ppb, 30 ppb, 50 ppb, 100 ppb, 500 ppb, 1000 ppb.	

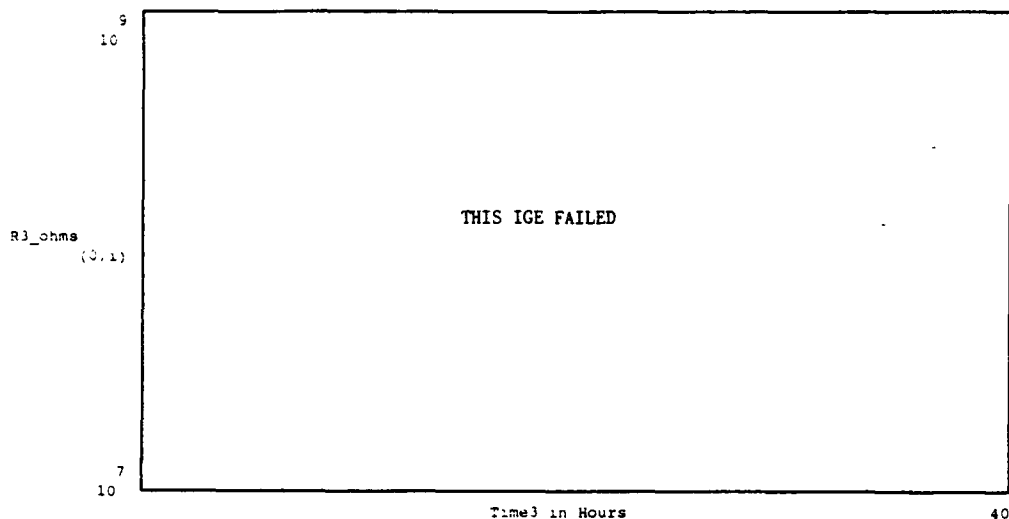


Figure D-3 . This Device Malfunctioned. DC Resistance Measured Between the Driven-Electrode and Floating-Electrode of the IGE Array, During Series of Purges and Challenge Gas Exposures. The Number of Measurements (at crosses) is 420. The Testing Conditions Included the Following:

IGE Array Number : 3,	Thin-film Material : Cobalt Phthalocyanine,
Thin-film Thickness : 2,500 Angstroms	Test Temperature(s) : Purge & Challenge at 150°C
Purge Gas : Room Air,	Challenge Gas : Nitrogen Dioxide,
Challenge Gas Concentration(s) (in order run) : 1000 ppb, 30 ppb, 50 ppb, 100 ppb, 500 ppb, 1000 ppb.	

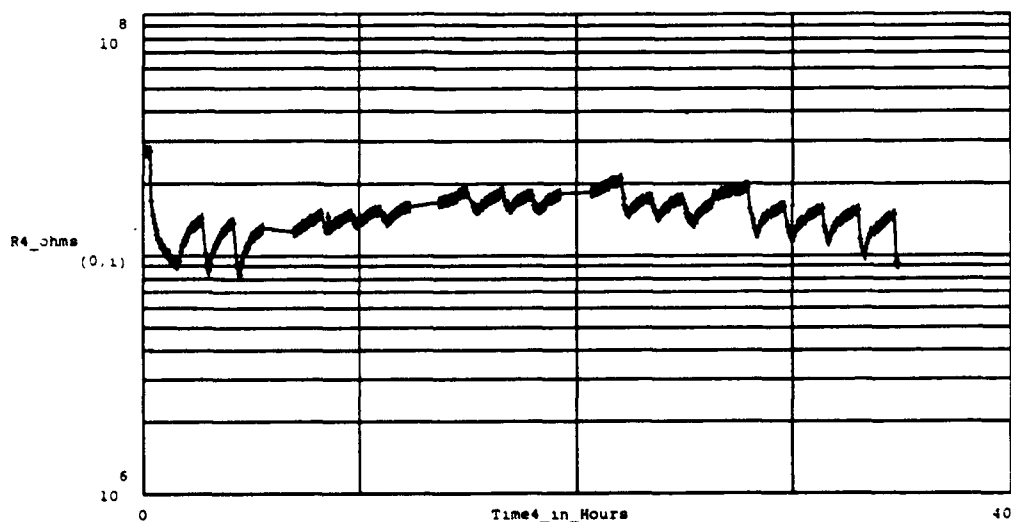


Figure D-4 . DC Resistance Measured Between the Driven-Electrode and Floating-Electrode of the IGE Array, During Series of Purges and Challenge Gas Exposures. The Number of Measurements (at crosses) is 420. The Testing Conditions Included the Following:

IGE Array Number : 4,	Thin-film Material : Cobalt Phthalocyanine,
Thin-film Thickness : 5,400 Angstroms	Test Temperature(s) : Purge & Challenge at 150°C
Purge Gas : Room Air,	Challenge Gas : Nitrogen Dioxide,
Challenge Gas Concentration(s) (in order run) : 1000 ppb, 30 ppb, 50 ppb, 100 ppb, 500 ppb, 1000 ppb.	

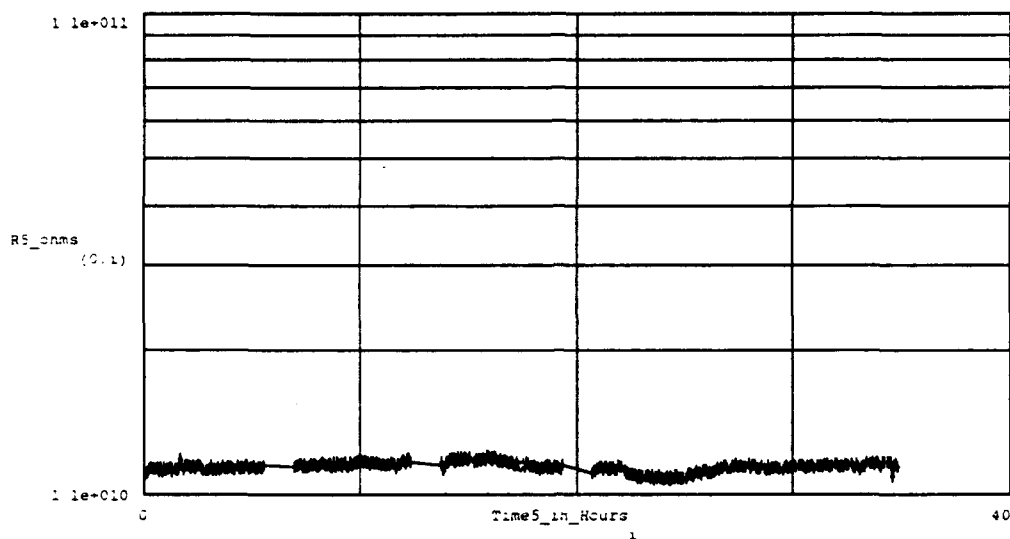


Figure D-5 . This Device Malfunctioned. DC Resistance Measured Between the Driven-Electrode and Floating-Electrode of the IGE Array, During Series of Purges and Challenge Gas Exposures. The Number of Measurements (at crosses) is 420. The Testing Conditions Included the Following:

IGE Array Number : 5.	Thin-film Material : Cobalt Phthalocyanine.
Thin-film Thickness : 5,400 Angstroms	Test Temperature(s) : Purge & Challenge at 150°C
Purge Gas : Room Air.	Challenge Gas : Nitrogen Dioxide.
Challenge Gas Concentration(s) (in order run) : 1000 ppb, 30 ppb, 50 ppb, 100 ppb, 500 ppb, 1000 ppb.	

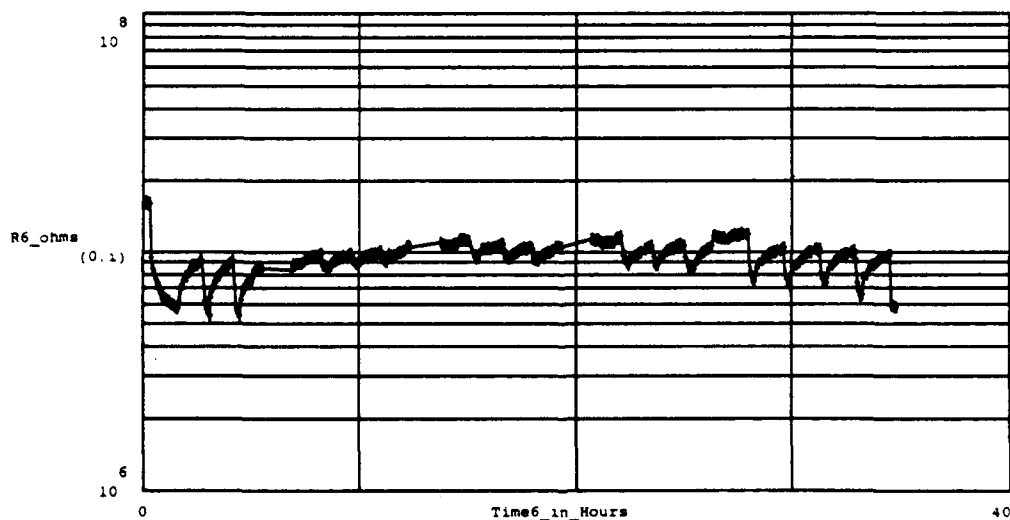


Figure D-6 . DC Resistance Measured Between the Driven-Electrode and Floating-Electrode of the IGE Array, During Series of Purges and Challenge Gas Exposures. The Number of Measurements (at crosses) is 420. The Testing Conditions Included the Following:

IGE Array Number : 6.	Thin-film Material : Cobalt Phthalocyanine.
Thin-film Thickness : 5,400 Angstroms	Test Temperature(s) : Purge & Challenge at 150°C
Purge Gas : Room Air.	Challenge Gas : Nitrogen Dioxide.
Challenge Gas Concentration(s) (in order run) : 1000 ppb, 30 ppb, 50 ppb, 100 ppb, 500 ppb, 1000 ppb.	

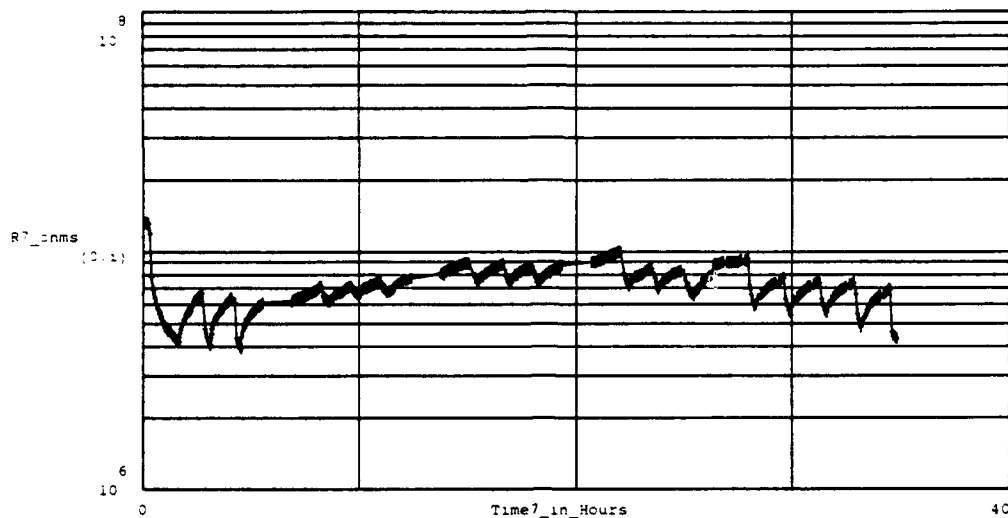


Figure D-7 . DC Resistance Measured Between the Driven-Electrode and Floating-Electrode of the IGE Array, During Series of Purges and Challenge Gas Exposures. The Number of Measurements (at crosses) is 420. The Testing Conditions Included the Following:

IGE Array Number : 7,	Thin-film Material : Cobalt Phthalocyanine,
Thin-film Thickness : 10,500 Angstroms	Test Temperature(s) : Purge & Challenge at 150°C
Purge Gas : Room Air,	Challenge Gas : Nitrogen Dioxide,
Challenge Gas Concentration(s) (in order run) : 1000 ppb, 30 ppb, 50 ppb, 100 ppb, 500 ppb, 1000 ppb.	

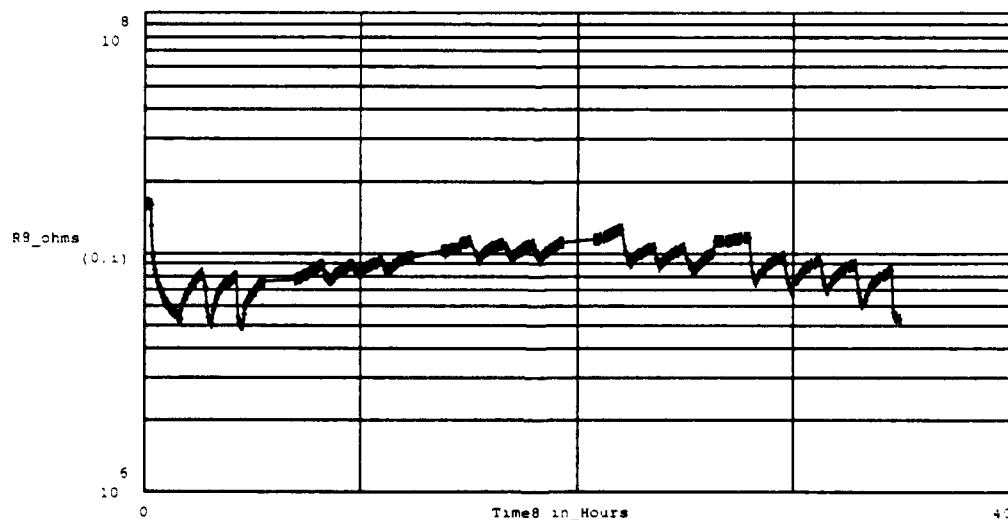


Figure D-8 . DC Resistance Measured Between the Driven-Electrode and Floating-Electrode of the IGE Array, During Series of Purges and Challenge Gas Exposures. The Number of Measurements (at crosses) is 419. The Testing Conditions Included the Following:

IGE Array Number : 8,	Thin-film Material : Cobalt Phthalocyanine,
Thin-film Thickness : 10,500 Angstroms	Test Temperature(s) : Purge & Challenge at 150°C
Purge Gas : Room Air,	Challenge Gas : Nitrogen Dioxide,
Challenge Gas Concentration(s) (in order run) : 1000 ppb, 30 ppb, 50 ppb, 100 ppb, 500 ppb, 1000 ppb.	



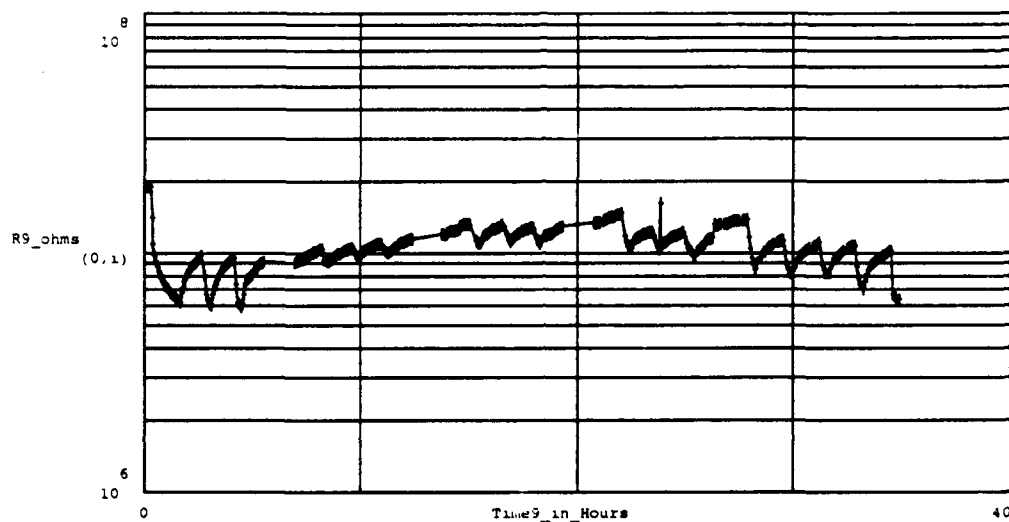


Figure D-9. DC Resistance Measured Between the Driven-Electrode and Floating-Electrode of the IGE Array. During Series of Purges and Challenge Gas Exposures. The Number of Measurements (at crosses) is 419. The Testing Conditions Included the Following:

IGE Array Number : 9.	Thin-film Material : Cobalt Phthalocyanine.
Thin-film Thickness : 10,500 Angstroms	Test Temperature(s) : Purge & Challenge at 150°C
Purge Gas : Room Air.	Challenge Gas : Nitrogen Dioxide.
Challenge Gas Concentration(s) (in order run) : 1000 ppb, 30 ppb, 50 ppb, 100 ppb, 500 ppb, 1000 ppb.	

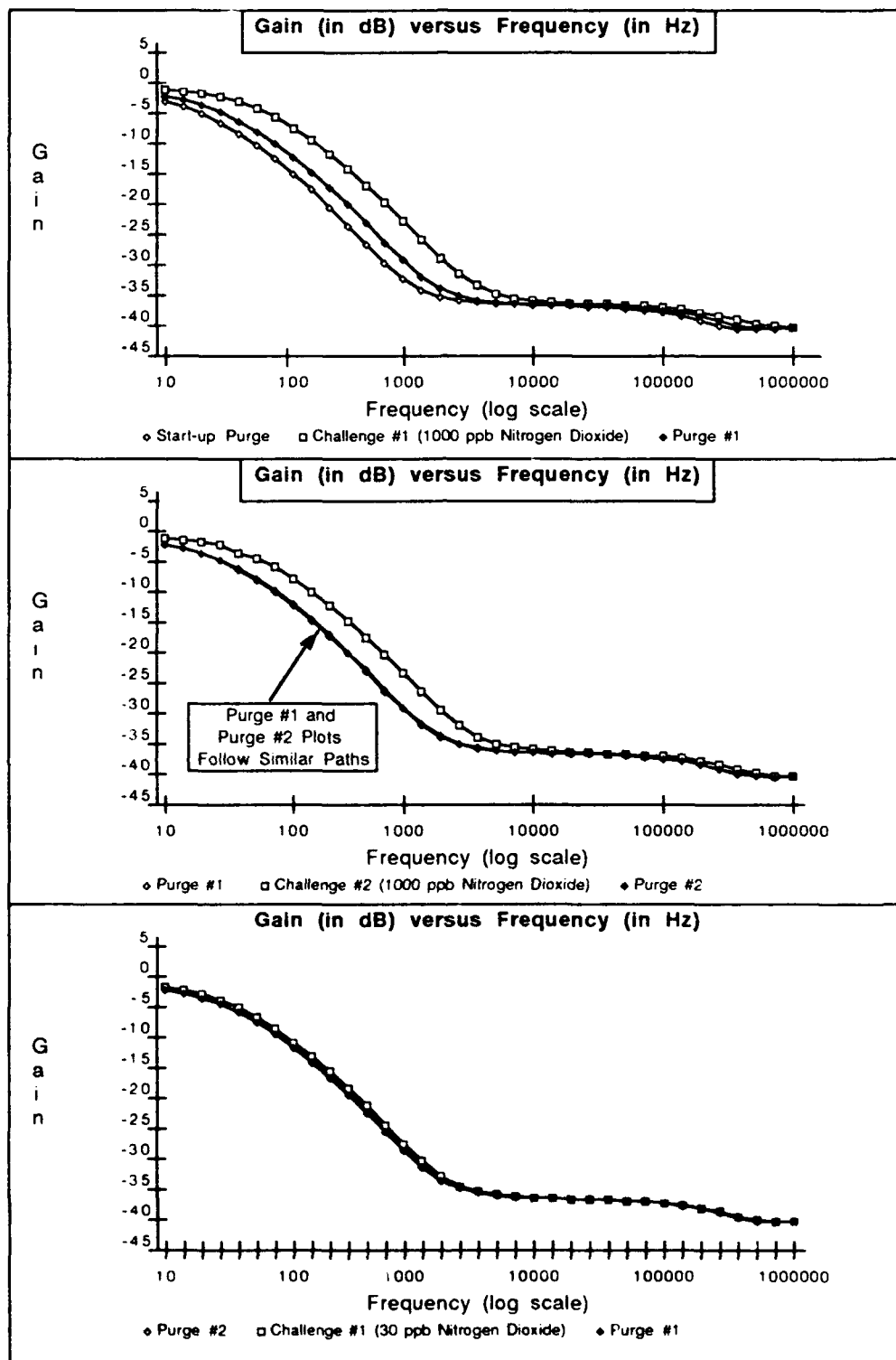


Figure D-10 . Gain versus Frequency Response of IGEFET Microsensor for a Series of Room Air Purges and Challenge Gas Exposures. Testing Conditions: IGE Microsensor Number 1; CoPc Thin-film (2,500 Angstroms Thick); Temperature of 150 degrees Centigrade; Nitrogen Dioxide Challenge Gas (Order of Exposures: 1000 ppb, 30 ppb, 50 ppb, 100 ppb, 500 ppb, 1000 ppb).

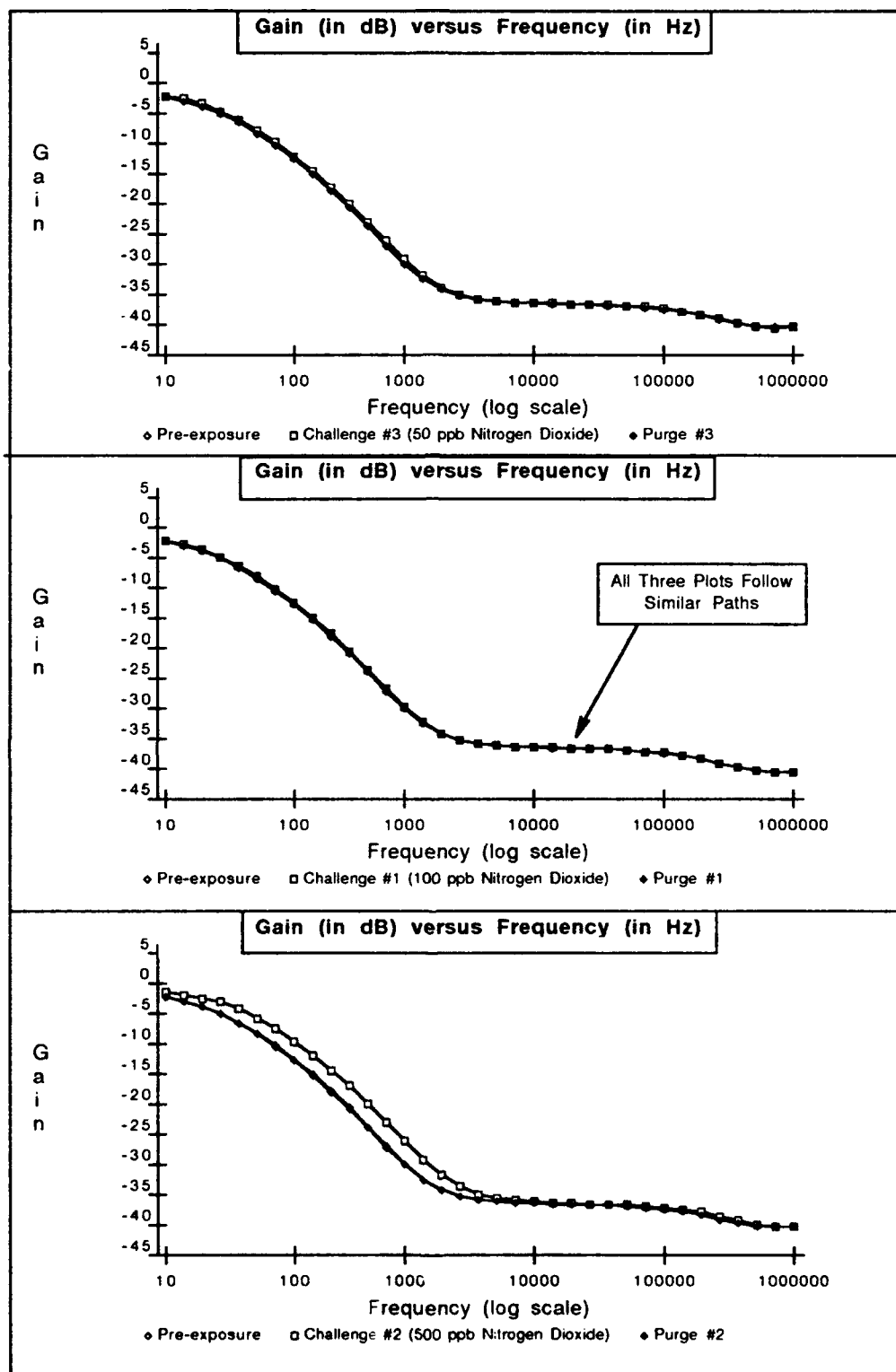


Figure D-11. Gain versus Frequency Response of IGEFET Microsensor for a Series of Room Air Purges and Challenge Gas Exposures. Testing Conditions: IGE Microsensor Number 1C0 Pc Thin-film (2, 500Angstroms Thick); Temperature of 150 degrees Centigrade; Nitrogen Dioxide Challenge Gas (Order of Exposures: 1000 ppb, 30 ppb, 100 ppb, 500 ppb, 1000 ppb).

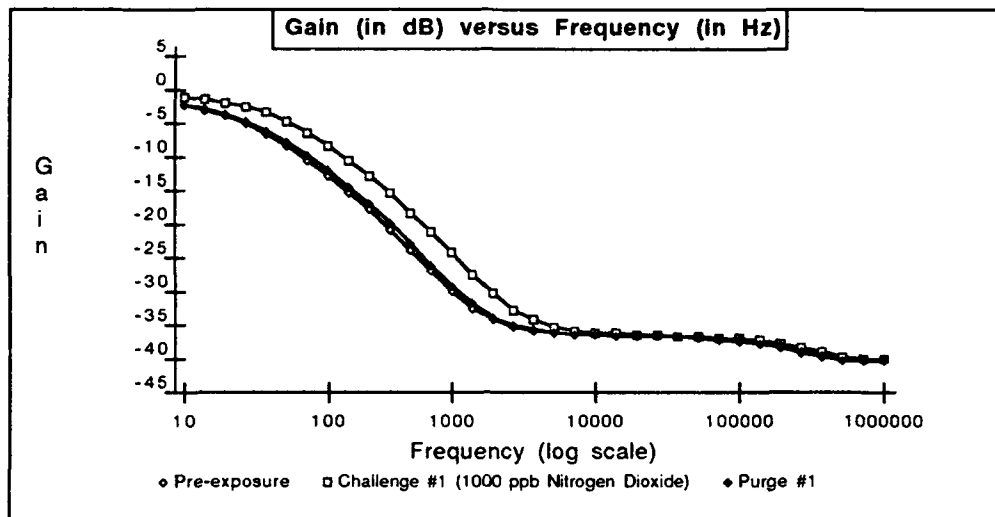


Figure D-12 . Gain versus Frequency Response of IGEFET Microsensor for a Series of Room Air Purges and Challenge Gas Exposures. Testing Conditions: IGE Microsensor Number 1 Co-Pe Thin-film (2500 Angstroms Thick); Temperature of 150 degrees Centigrade; Nitrogen Dioxide Challenge Gas (Order of Exposures: 1000 ppb, 30 ppb, 100 ppb, 500 ppb, 1000 ppb).

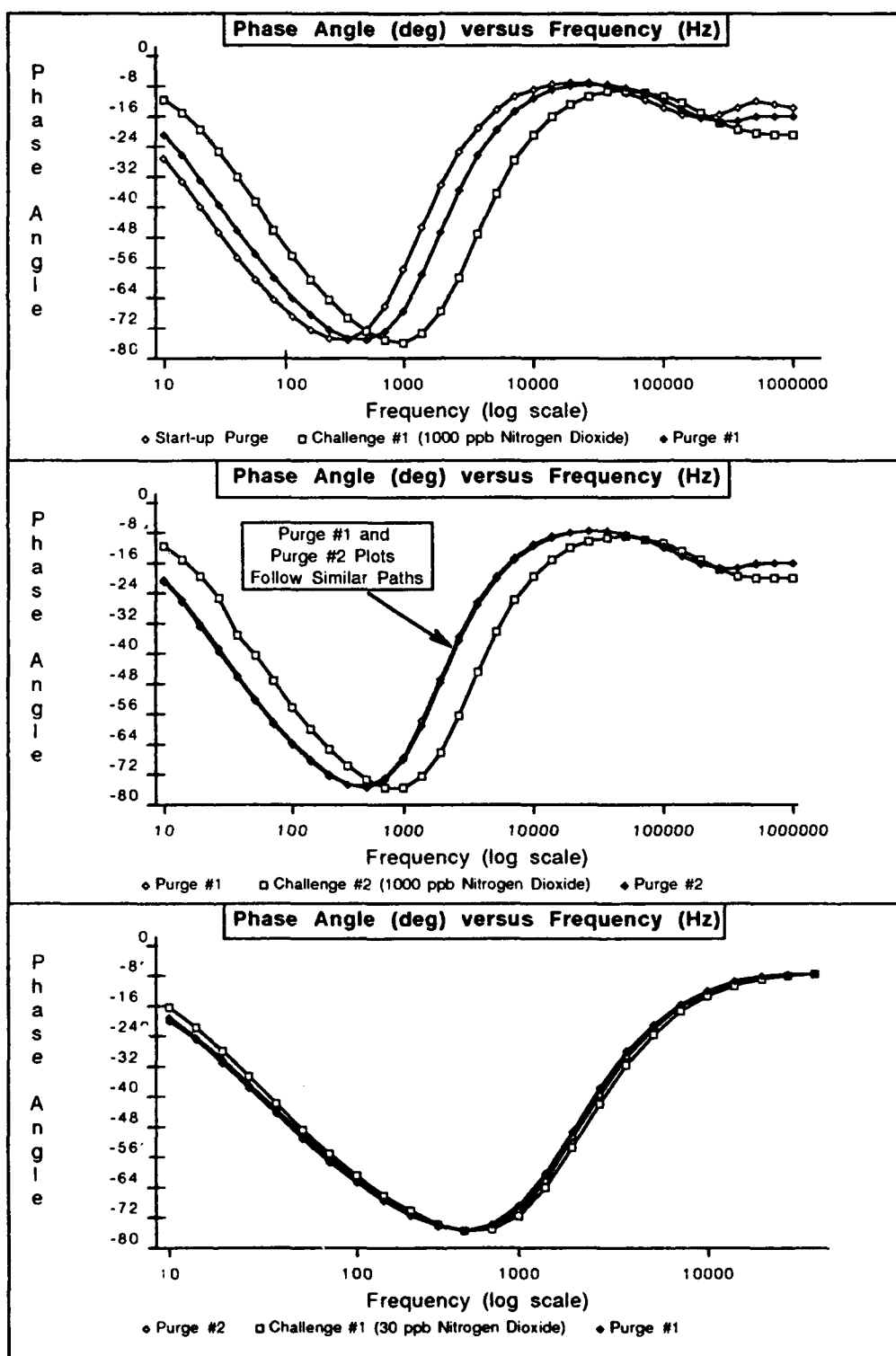


Figure D-13 Phase Angle versus Frequency Response of IGFET Microsensor for a Series of Room Air Purges and Challenge Gas Exposures. Testing Conditions: IGE Microsensor Number 1; CoPc Thin-film (2,500 Angstroms Thick); Temperature of 150 degrees Centigrade; Nitrogen Dioxide Challenge Gas (Order of Exposures: 1000 ppb, 30 ppb, 50 ppb, 100 ppb, 500 ppb, 1000 ppb).

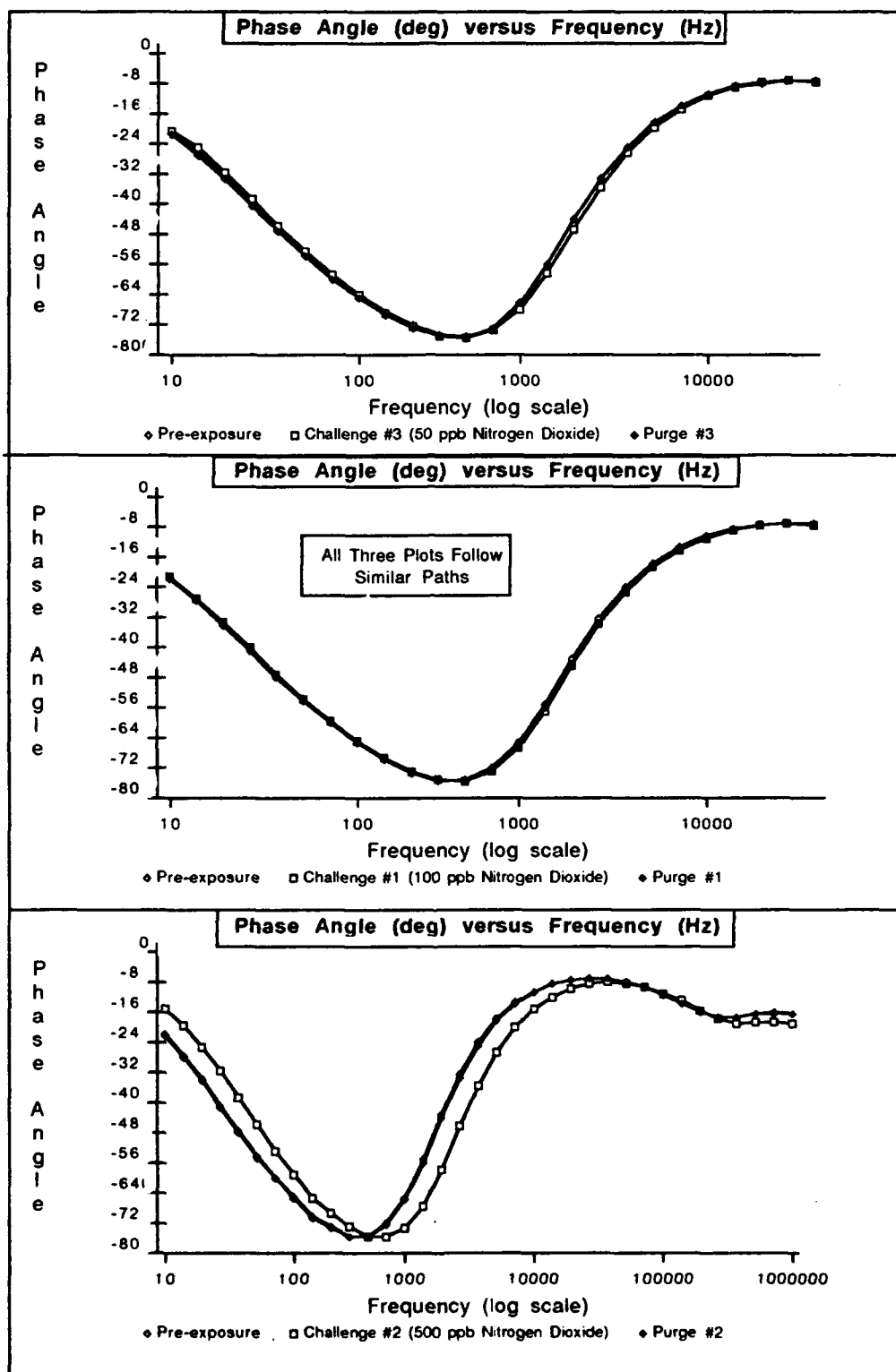


Figure D-14 . Phase Angle versus Frequency Response of IGEFET Microsensor for a Series of Room Air Purges and Challenge Gas Exposures. Testing Conditions: IGE Microsensor Number 1; CoPc Thin-film (2,500 Angstroms Thick); Temperature of 150 degrees Centigrade; Nitrogen Dioxide Challenge Gas (Order of Exposures: 1000 ppb, 30 ppb, 100 ppb, 500 ppb, 1000 ppb).

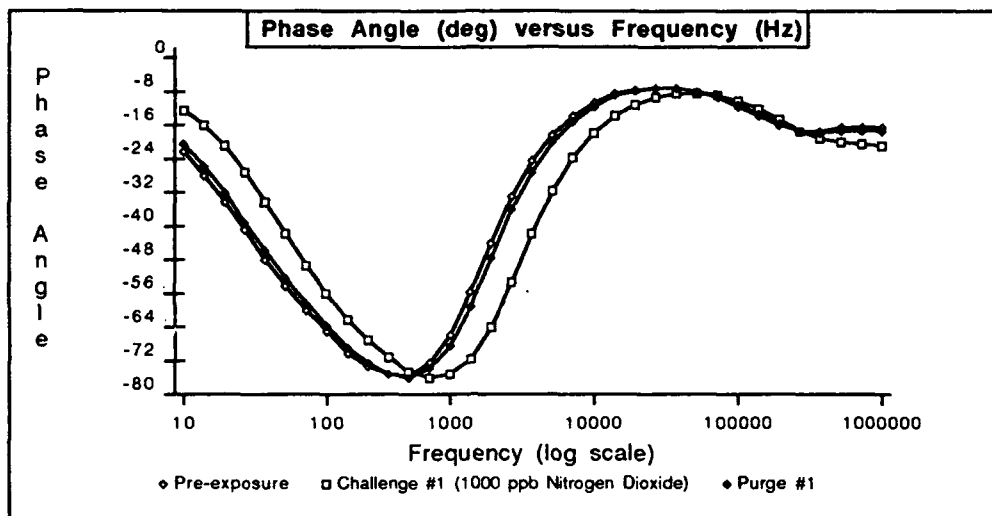


Figure D-15 Phase Angle versus Frequency Response of IGEFET Microsensor for a Series of Room Air Purges and Challenge Gas Exposures. Testing Conditions: IGE Microsensor Number 1; CoPc Thin-film (2,500 Angstroms Thick); Temperature of 150 degrees Centigrade; Nitrogen Dioxide Challenge Gas (Order of Exposures: 1000 ppb, 30 ppb, 100 ppb, 500 ppb, 1000 ppb).

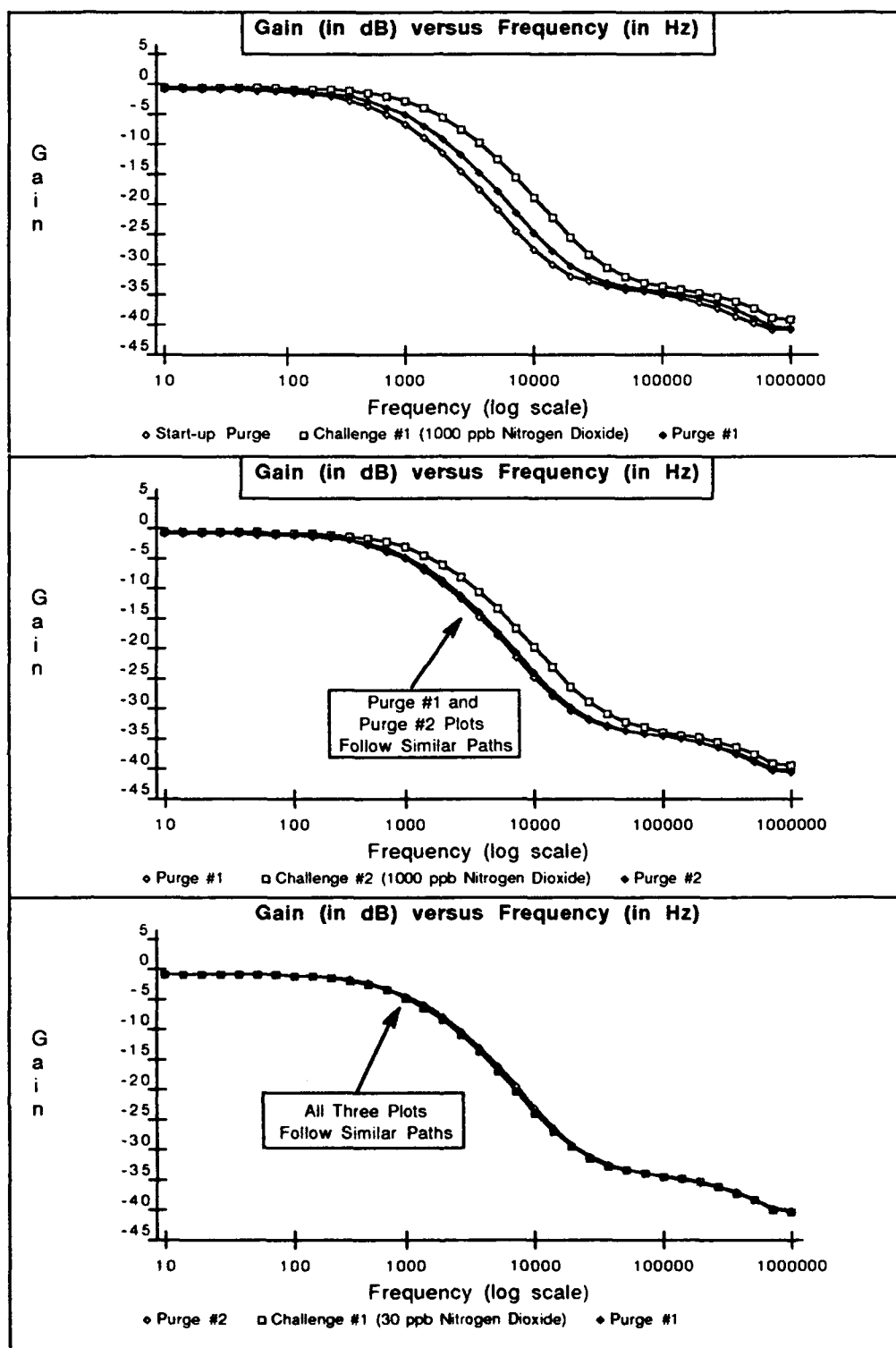


Figure D-16 Gain versus Frequency Response of IGEFET Microsensor for a Series of Room Air Purges and Challenge Gas Exposures. Testing Conditions: IGE Microsensor Number 4; CoPc Thin-film (5,400 Angstroms Thick); Temperature of 150 degrees Centigrade; Nitrogen Dioxide Challenge Gas (Order of Exposures: 1000 ppb, 30 ppb, 50 ppb, 100 ppb, 500 ppb, 1000 ppb).



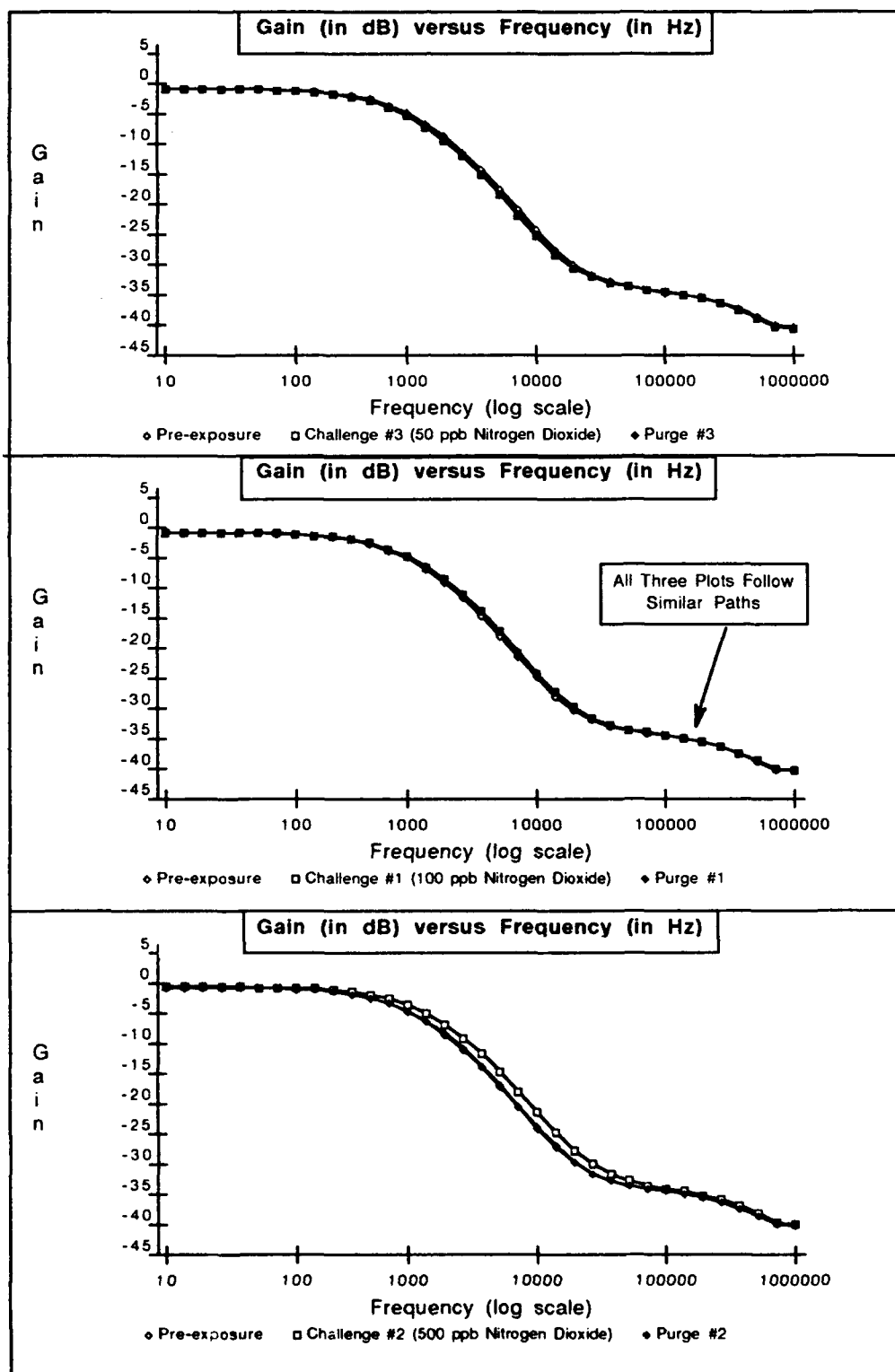


Figure D-17 . Gain versus Frequency Response of IGEFET Microsensor for a Series of Room Air Purges and Challenge Gas Exposures. Testing Conditions: IGE Microsensor Number 4; CoPc Thin-film (5,400 Angstroms Thick); Temperature of 150 degrees Centigrade; Nitrogen Dioxide Challenge Gas (Order of Exposures: 1000 ppb, 30 ppb, 100 ppb, 500 ppb, 1000 ppb).

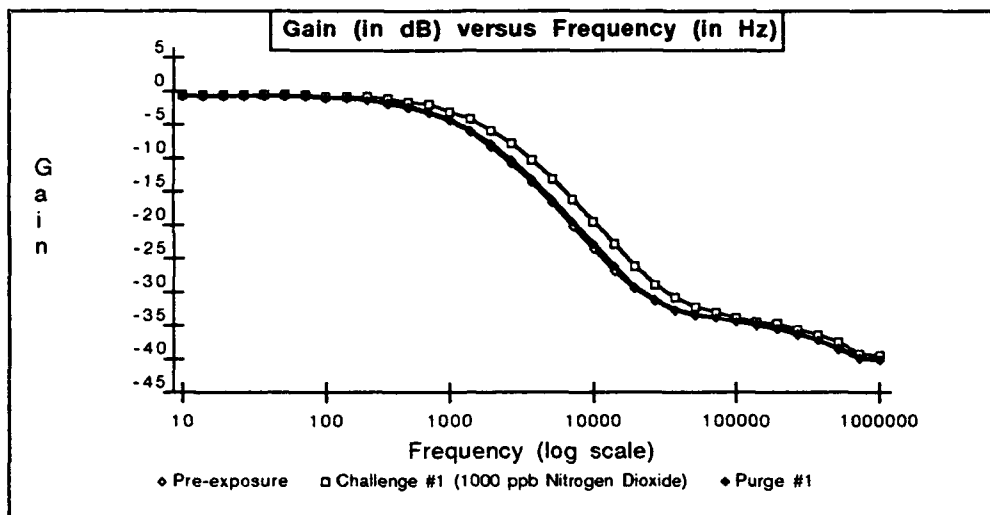


Figure D-18. Gain versus Frequency Response of IGEFET Microsensor for a Series of Room Air Purges and Challenge Gas Exposures. Testing Conditions: IGE Microsensor Number 4; CoPc Thin-film (5,400 Angstroms Thick); Temperature of 150 degrees Centigrade; Nitrogen Dioxide Challenge Gas (Order of Exposures: 1000 ppb, 30 ppb, 100 ppb, 500 ppb, 1000 ppb).

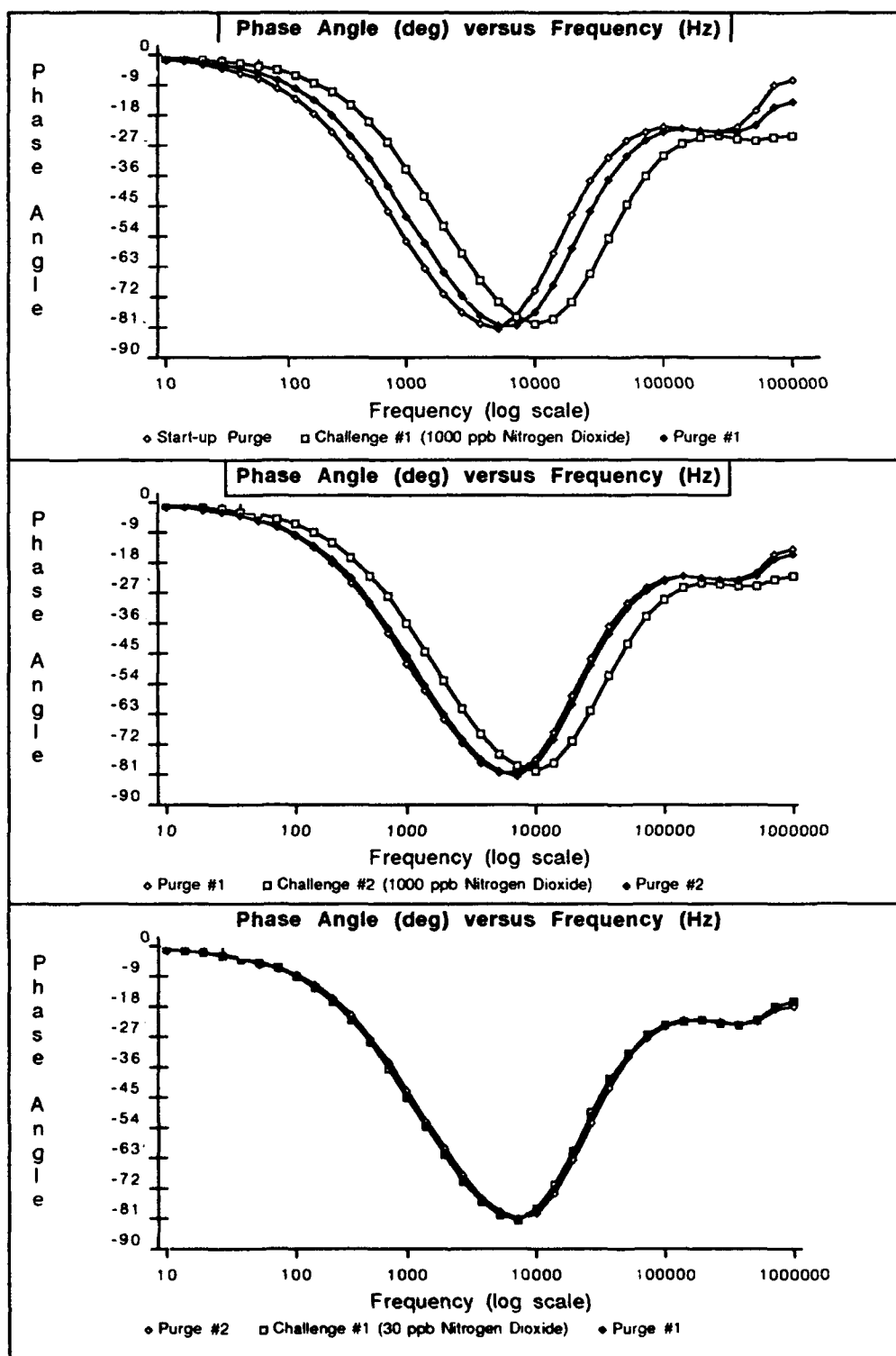


Figure D-19. Phase Angle versus Frequency Response of IGFET Microsensor for a Series of Room Air Purges and Challenge Gas Exposures. Testing Conditions: IGE Microsensor Number 4; CoPc Thin-film (5,400 Angstroms Thick); Temperature of 150 degrees Centigrade; Nitrogen Dioxide Challenge Gas (Order of Exposures: 1000 ppb, 30 ppb, 50 ppb, 100 ppb, 500 ppb, 1000 ppb).

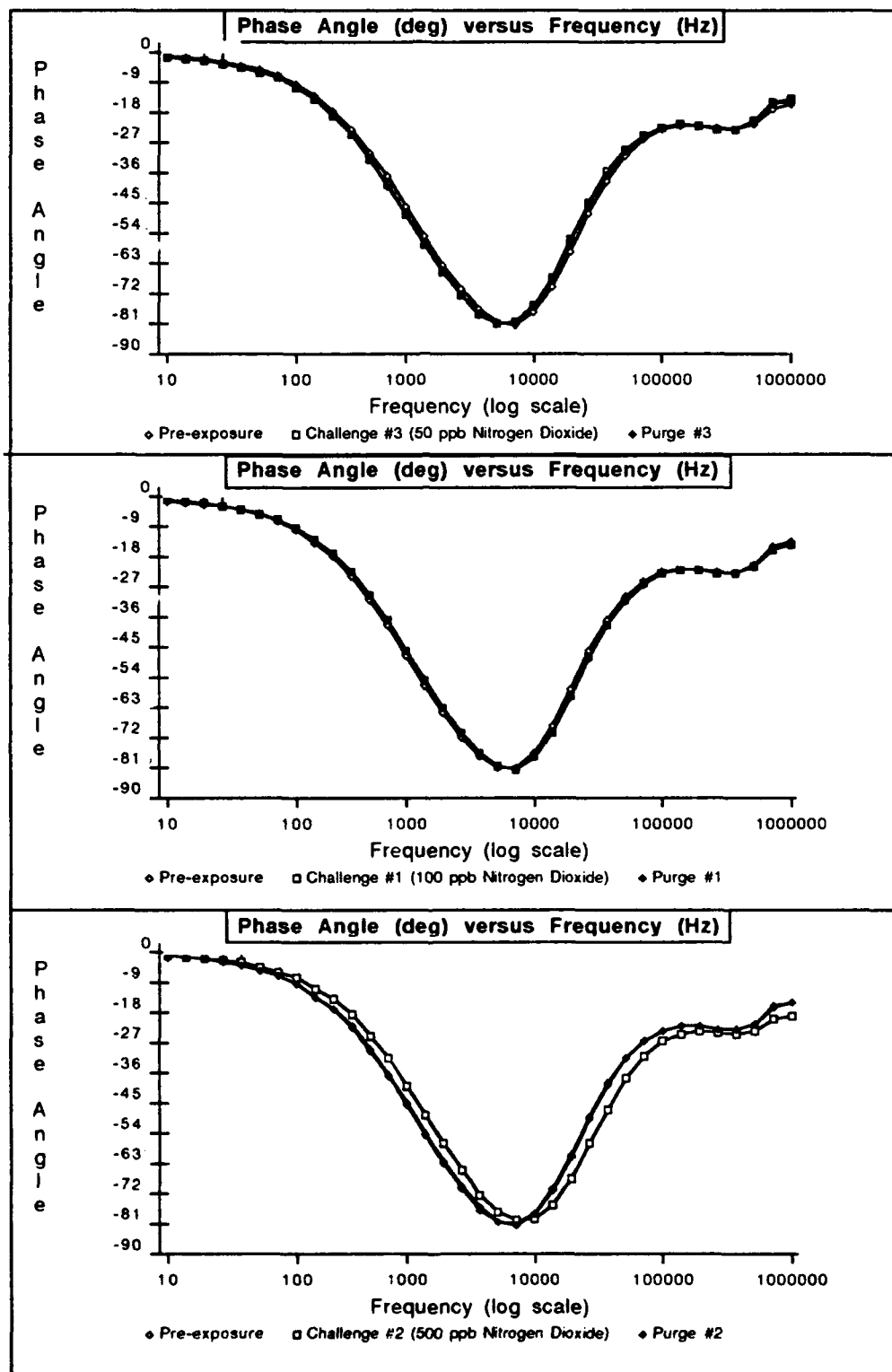


Figure D-20 . Phase Angle versus Frequency Response of IGEFET Microsensor for a Series of Room Air Purges and Challenge Gas Exposures. Testing Conditions: IGE Microsensor Number 4; CoPc Thin-film (5,400 Angstroms Thick); Temperature of 150 degrees Centigrade; Nitrogen Dioxide Challenge Gas (Order of Exposures: 1000 ppb, 30 ppb, 100 ppb, 500 ppb, 1000 ppb).

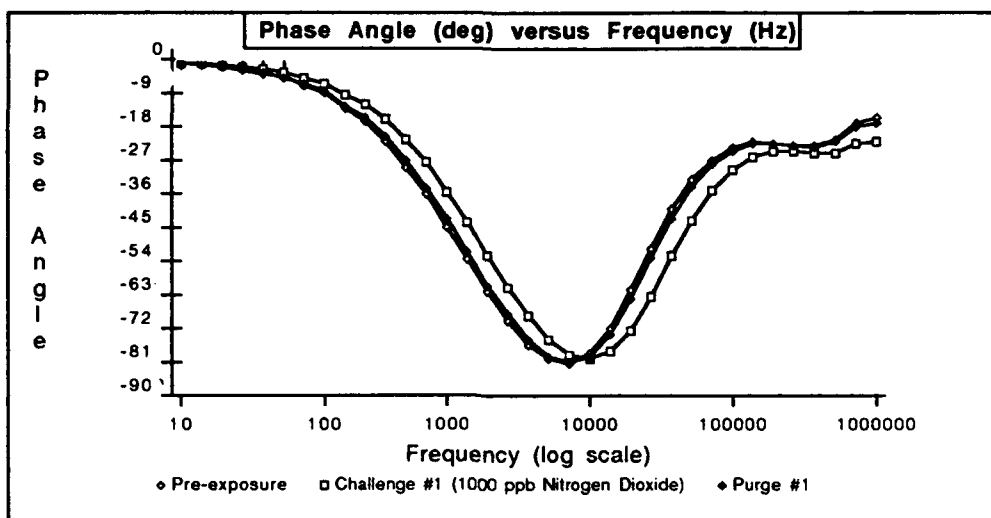


Figure D-21 Phase Angle versus Frequency Response of IGEFET Microsensor for a Series of Room Air Purges and Challenge Gas Exposures. Testing Conditions: IGE Microsensor Number 4; CoPc Thin-film (5,400 Angstroms Thick); Temperature of 150 degrees Centigrade; Nitrogen Dioxide Challenge Gas (Order of Exposures: 1000 ppb, 30 ppb, 100 ppb, 500 ppb, 1000 ppb).

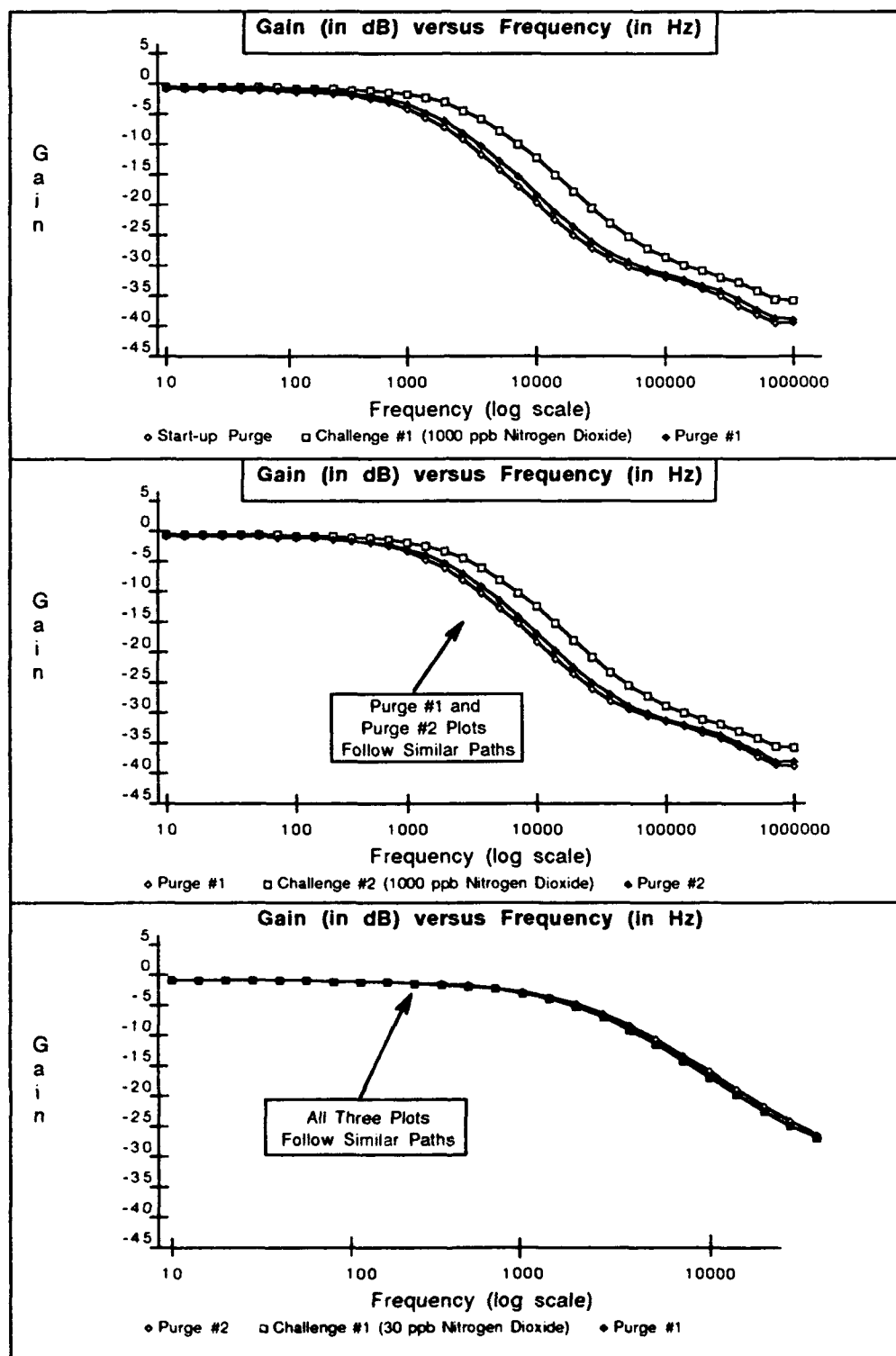


Figure D-22. Gain versus Frequency Response of IGEFET Microsensor for a Series of Room Air Purges and Challenge Gas Exposures. Testing Conditions: IGE Microsensor Number 9; CoPc Thin-film (10,500 Angstroms Thick); Temperature of 150 degrees Centigrade; Nitrogen Dioxide Challenge Gas (Order of Exposures: 1000 ppb, 30 ppb, 50 ppb, 100 ppb, 500 ppb, 1000 ppb).

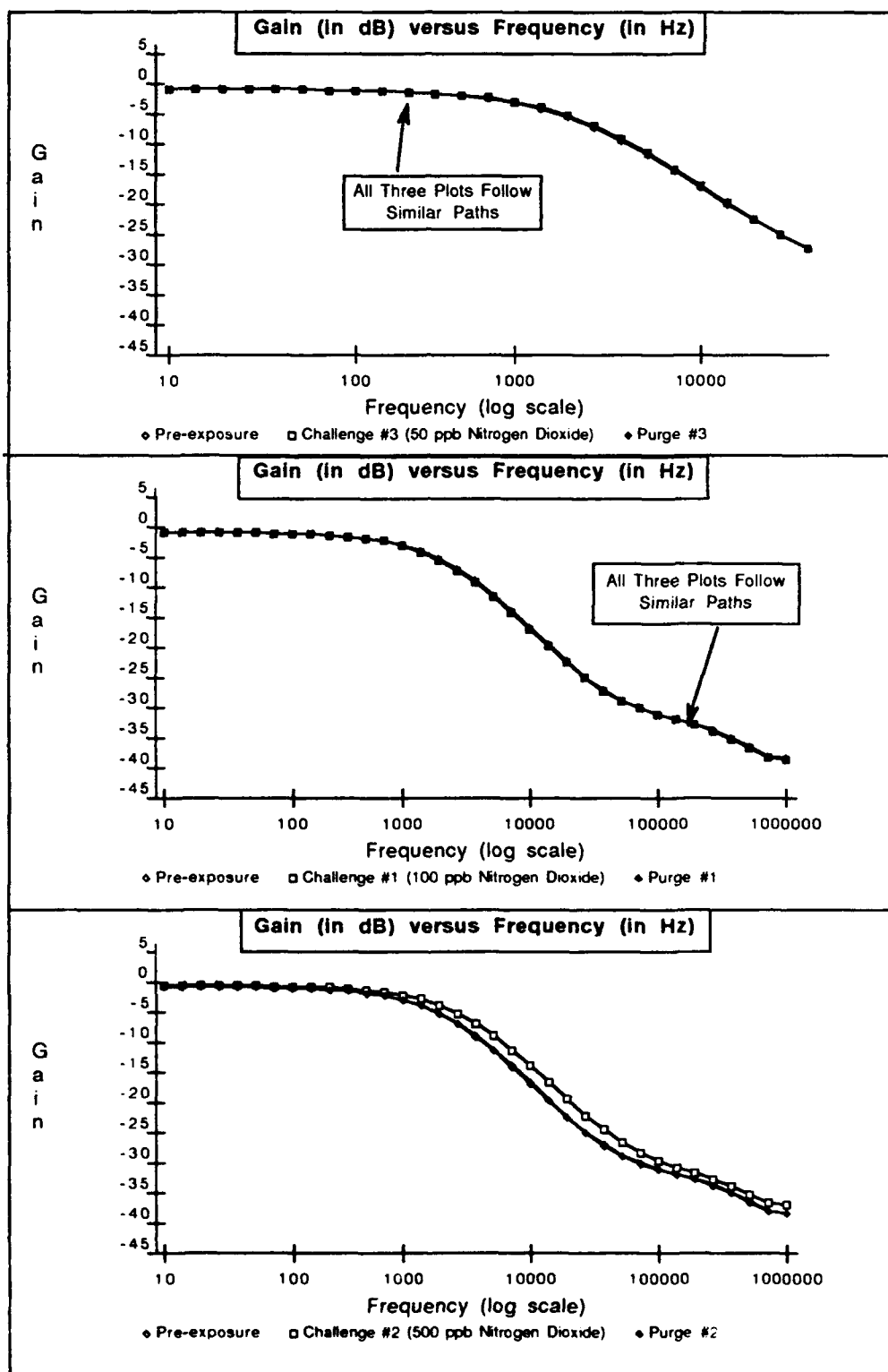


Figure D-23. Gain versus Frequency Response of IGEFET Microsensor for a Series of Room Air Purges and Challenge Gas Exposures. Testing Conditions: IGE Microsensor Number 9; CoPc Thin-film (10,500 Angstroms Thick); Temperature of 150 degrees Centigrade; Nitrogen Dioxide Challenge Gas (Order of Exposures: 1000 ppb, 30 ppb, 100 ppb, 500 ppb, 1000 ppb).

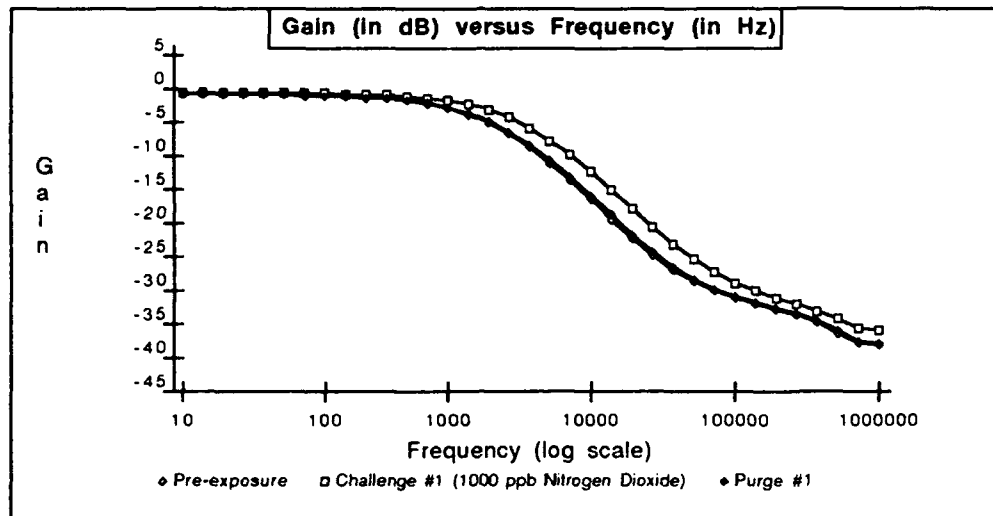


Figure D-24. Gain versus Frequency Response of IGEFET Microsensor for a Series of Room Air Purges and Challenge Gas Exposures. Testing Conditions: IGE Microsensor Number 9; CoPc Thin-film (10,500 Angstroms Thick); Temperature of 150 degrees Centigrade; Nitrogen Dioxide Challenge Gas (Order of Exposures: 1000 ppb, 30 ppb, 100 ppb, 500 ppb, 1000 ppb).



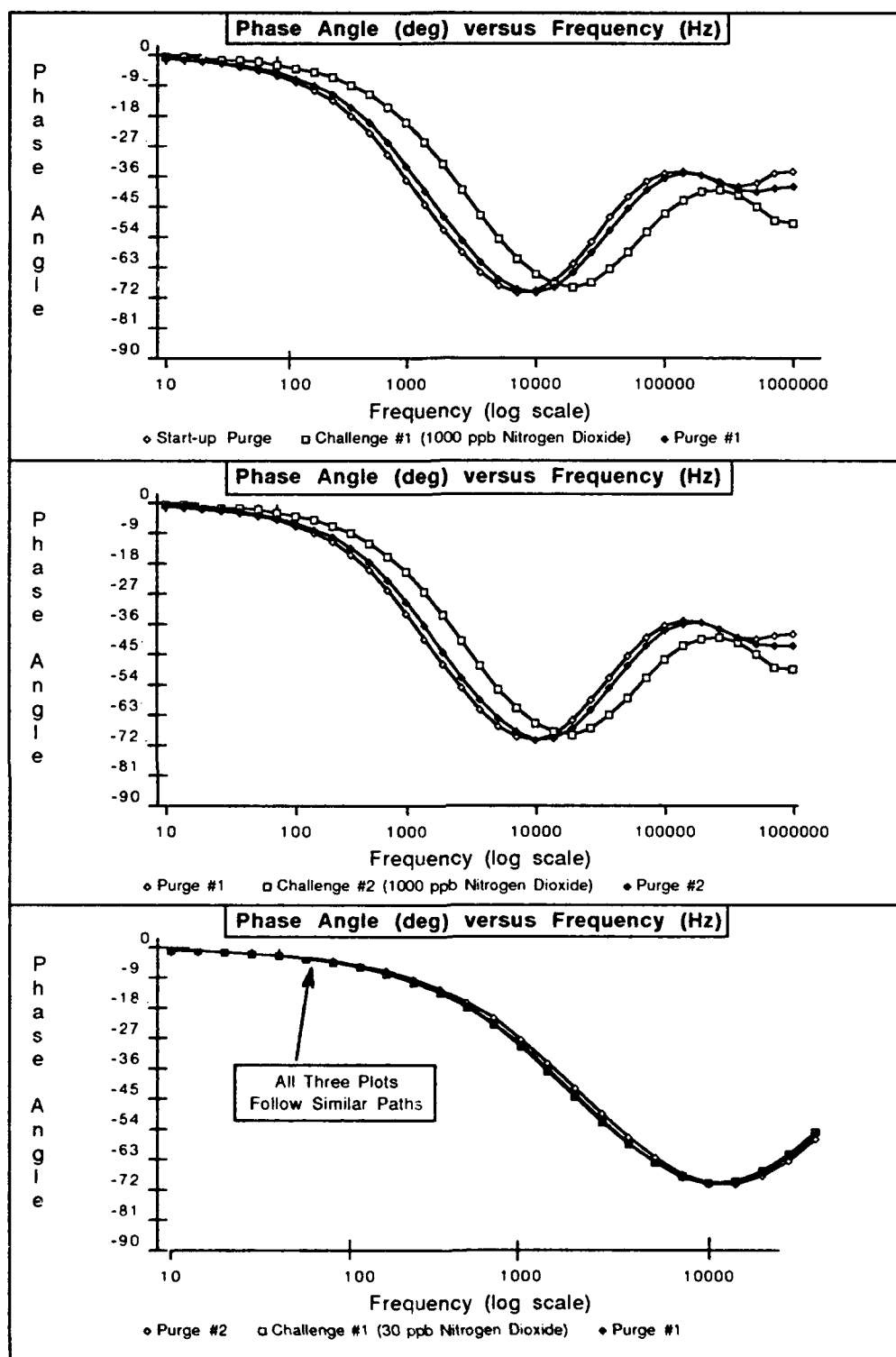


Figure D-25. Phase Angle versus Frequency Response of IGEFET Microsensor for a Series of Room Air Purges and Challenge Gas Exposures. Testing Conditions: IGE Microsensor Number 9; CoPc Thin-film (10,500 Angstroms Thick); Temperature of 150 degrees Centigrade; Nitrogen Dioxide Challenge Gas (Order of Exposures: 1000 ppb, 30 ppb, 50 ppb, 100 ppb, 500 ppb, 1000 ppb).

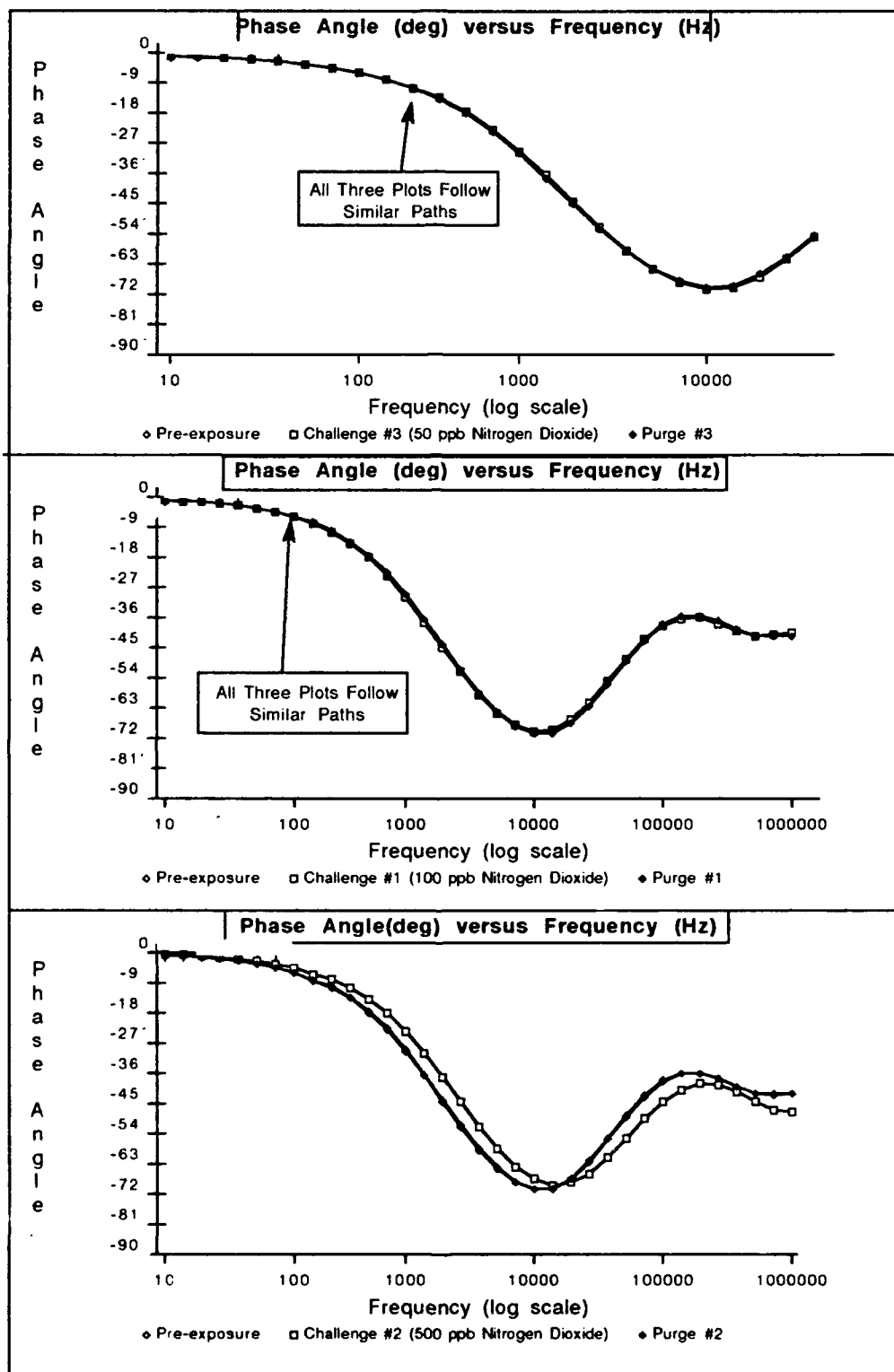


Figure D-26. Phase Angle versus Frequency Response of IGEFET Microsensor for a Series of Room Air Purges and Challenge Gas Exposures. Testing Conditions: IGE Microsensor Number 9; CoPc Thin-film (10,500 Angstroms Thick); Temperature of 150 degrees Centigrade; Nitrogen Dioxide Challenge Gas (Order of Exposures: 1000 ppb, 30 ppb, 100 ppb, 500 ppb, 1000 ppb).

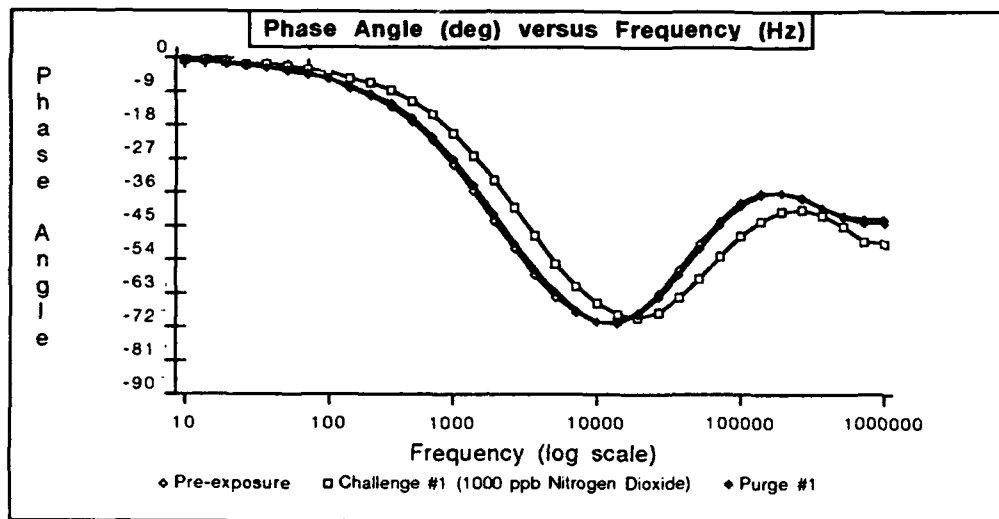


Figure D-27 . Phase Angle versus Frequency Response of IGEFET Microsensor for a Series of Room Air Purges and Challenge Gas Exposures. Testing Conditions: IGE Microsensor Number 9; CoPc Thin-film (10,500 Angstroms Thick); Temperature of 150 degrees Centigrade; Nitrogen Dioxide Challenge Gas (Order of Exposures: 1000 ppb, 30 ppb, 100 ppb, 500 ppb, 1000 ppb).

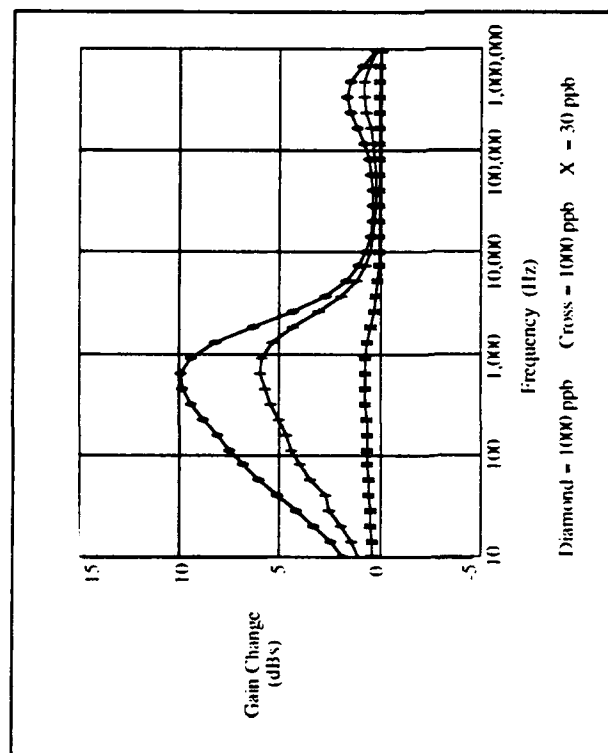


Figure D-28 Change in Gain Transfer Response versus Frequency for CoPc Exposed to Nitrogen Dioxide. The Diamond Plot is the Change from the Start-Up Purge to the End of the 1000 ppb Pre-conditioning Cycle. The Cross Plot is the Change from the Next Purge Cycle to the Second 1000 ppb Exposure. The 'X' Plot is the Change from Purge to 30 ppb Exposure. Testing Conditions: IGI; Microsensor Number 1; CoPc Thin-film (2,500 Angstroms Thick); Temperature of 150 Degree Centigrade; Nitrogen Dioxide Challenge Gas.

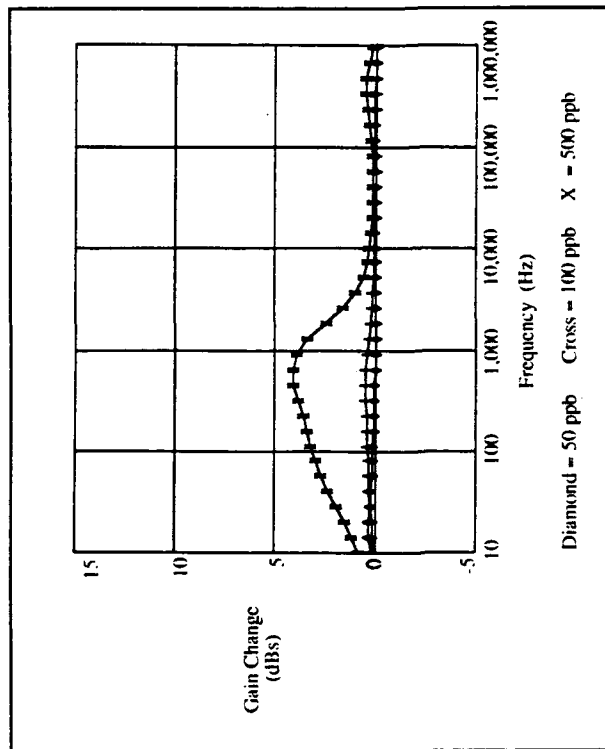


Figure D-29 Change in Gain Transfer Response versus Frequency for CoPc Exposed to Nitrogen Dioxide. The Diamond Plot is the Change from Purge to the End of the 50 ppb Exposure. The Cross Plot is the Change from the Next Purge Cycle to 100 ppb Exposure. The 'X' Plot is the Change from Purge to 500 ppb Exposure. Testing Conditions: IGI; Microsensor Number 1; CoPc Thin-film (2,500 Angstroms Thick); Temperature of 150 Degree Centigrade; Nitrogen Dioxide Challenge Gas.

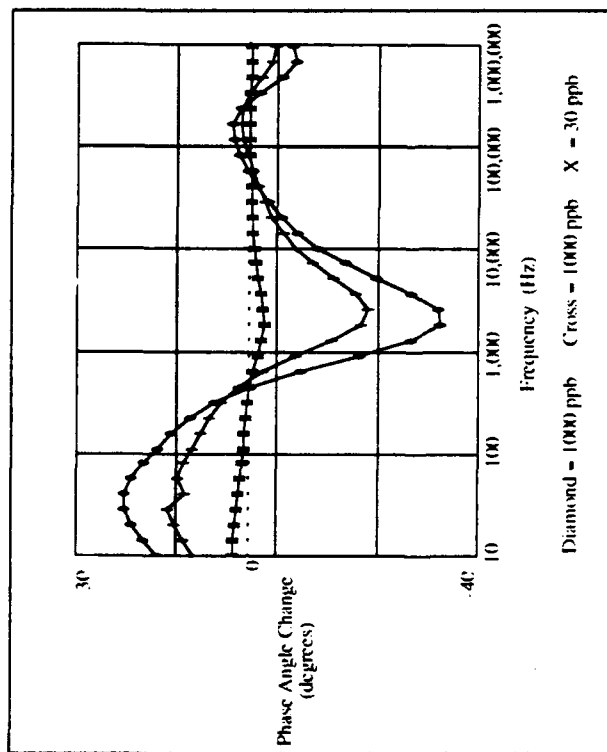


Figure D-30 Change in Phase Angle Transfer Response versus Frequency for CoPc Exposed to Nitrogen Dioxide. The Diamond Plot is the Change from the Start-Up Purge to the End of the 1000 ppb Pre-conditioning Cycle. The Cross Plot is the Change from the Next Purge Cycle to the Second 1000 ppb Exposure. The 'X' Plot is the Change from Purge to 30 ppb Exposure. Testing Conditions: IGE Microsensor Number 1; CoPc Thin-film (2,500 Angstroms Thick); Temperature of 150 Degree Centigrade; Nitrogen Dioxide Challenge Gas.

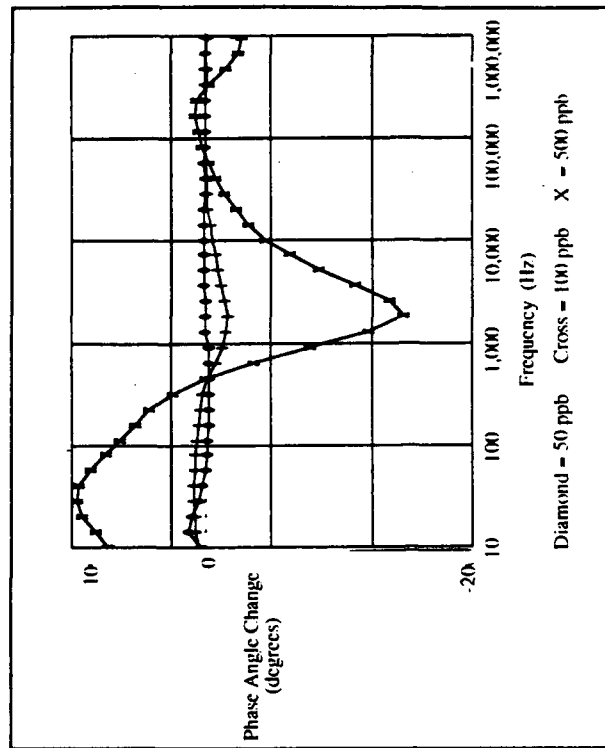


Figure D-31, Change in Phase Angle Transfer Response versus Frequency for CoPc Exposed to Nitrogen Dioxide. The Diamond Plot is the Change from Purge to the End of the 50 ppb Exposure. The Cross Plot is the Change from the Next Purge Cycle to 100 ppb Exposure. The 'X' Plot is the Change from Purge to 500 ppb Exposure. Testing Conditions: IGE Microsensor Number 1; CoPc Thin-film (2,500 Angstroms Thick); Temperature of 150 Degree Centigrade; Nitrogen Dioxide Challenge Gas.

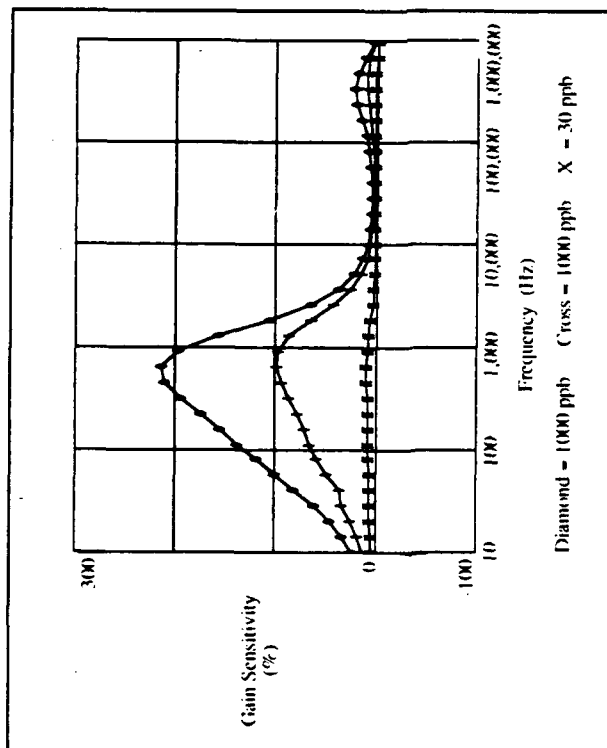


Figure D-32. Percent Change in Gain Transfer Response versus Frequency for CoPe Exposed to Nitrogen Dioxide. The Diamond Plot is the Change from the Start-Up Purge to the End of the 1000 ppb Pre-conditioning Cycle. The Cross Plot is the Change from the Next Purge Cycle to the Second 1000 ppb Exposure. The 'X' Plot is the Change from Purge to 30 ppb Exposure. Testing Conditions: ICI; Microsensor Number 1; CoPe Thin-film (2,500 Angstroms Thick); Temperature of 150 Degree Centigrade; Nitrogen Dioxide Challenge Gas.

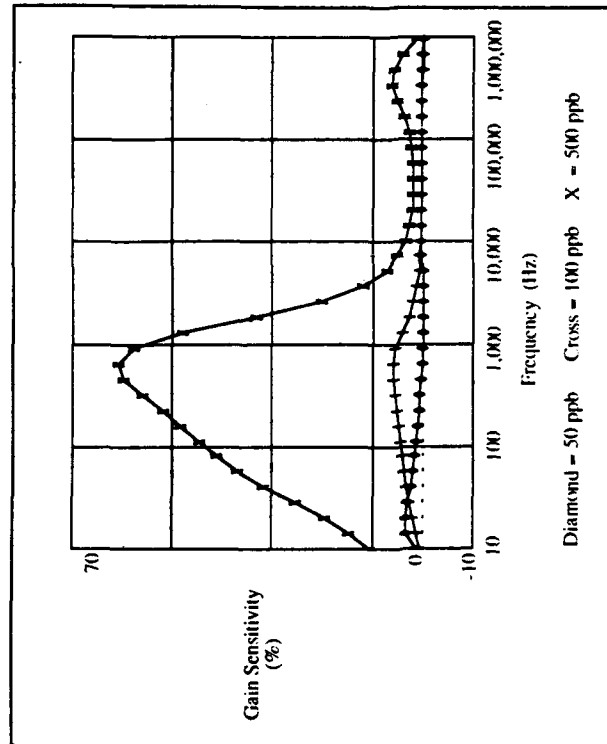


Figure D-33. Percent Change in Gain Transfer Response versus Frequency for CoPe Exposed to Nitrogen Dioxide. The Diamond Plot is the Change from Purge to the End of the 50 ppb Exposure. The Cross Plot is the Change from the Next Purge Cycle to 100 ppb Exposure. The 'X' Plot is the Change from Purge to 500 ppb Exposure. Testing Conditions: ICI; Microsensor Number 1; CoPe Thin-film (2,500 Angstroms Thick); Temperature of 150 Degree Centigrade; Nitrogen Dioxide Challenge Gas.

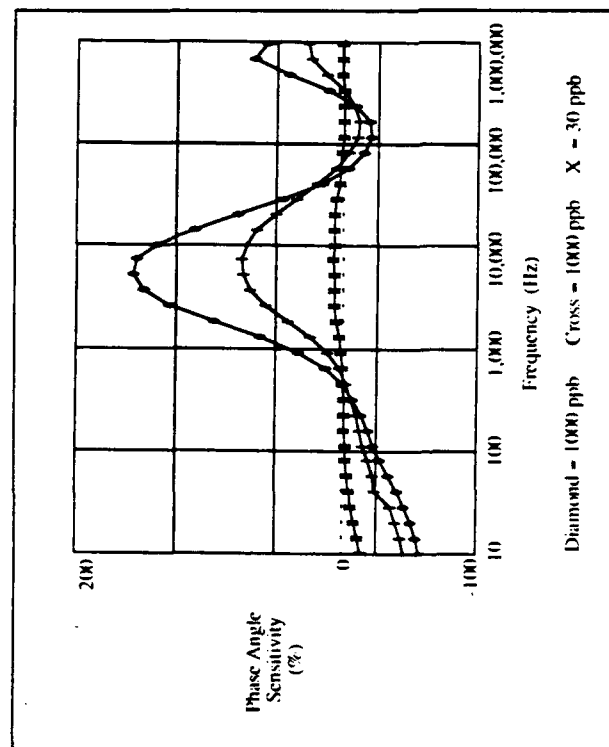


Figure D-34. Percent Change in Phase Angle Transfer Response versus Frequency for Co/Pc Exposed to Nitrogen Dioxide. The Diamond Plot is the Change from the Start-Up Purge to the End of the 1000 ppb Pre-conditioning Cycle. The Cross Plot is the Change from the Next Purge Cycle to the Second 1000 ppb Exposure. The 'X' Plot is the Change from Purge to 30 ppb Exposure. Testing Conditions: IGE Microsensor Number 1; Co/Pc Thin-film (2,500 Angstroms Thick); Temperature of 150 Degree Centigrade; Nitrogen Dioxide Challenge Gas.

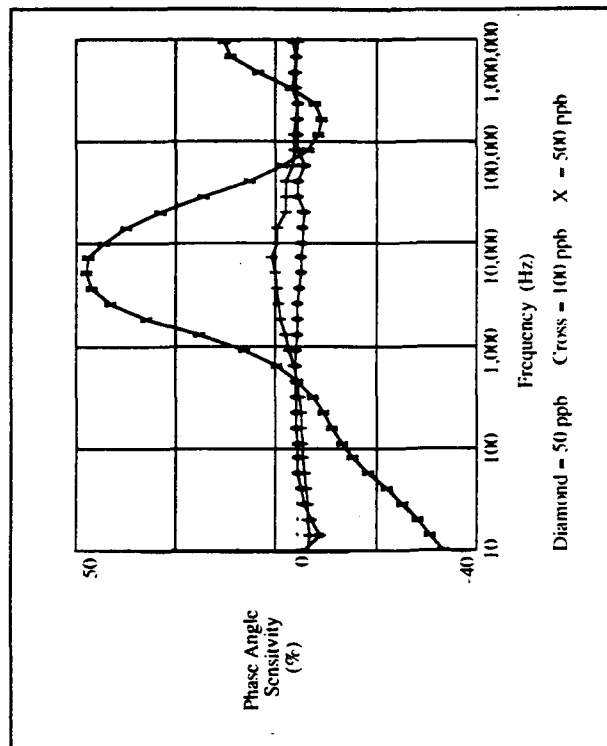


Figure D-35. Percent Change in Phase Angle Transfer Response versus Frequency for Co/Pc Exposed to Nitrogen Dioxide. The Diamond Plot is the Change from Purge to the End of the 50 ppb Exposure. The Cross Plot is the Change from the Next Purge Cycle to 100 ppb Exposure. The 'X' Plot is the Change from Purge to 500 ppb Exposure. Testing Conditions: IGE Microsensor Number 1; Co/Pc Thin-film (2,500 Angstroms Thick); Temperature of 150 Degree Centigrade; Nitrogen Dioxide Challenge Gas.

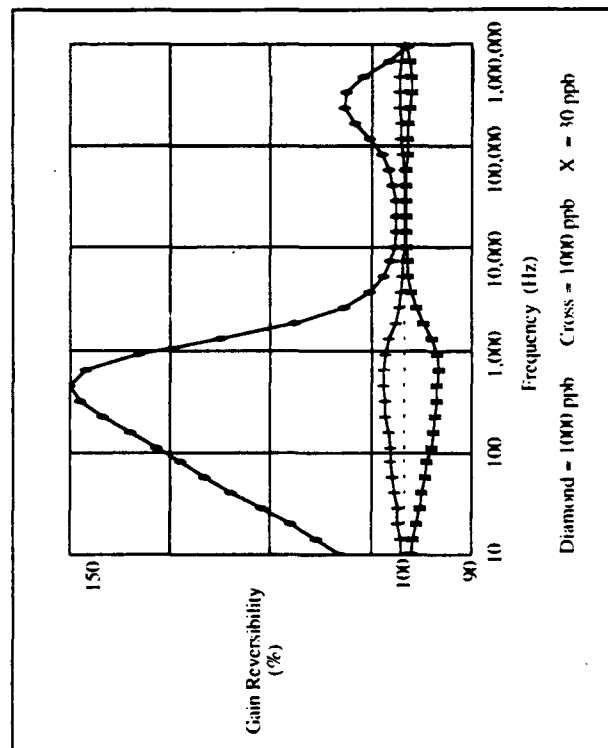


Figure D-36. Reversibility of Gain Transfer Response (Relative to Pre-exposure Purge) versus Frequency for CoPc Exposed to Nitrogen Dioxide. The Diamond Plot is the Change from the Start-Up Purge to the Purge Following the 1000 ppb Pre-conditioning Cycle. The Cross Plot is the Change from the Next Purge Cycle to the Purge Following the Second 1000 ppb Exposure. The 'X' Plot is the Change Between the Purges Before and After a 30 ppb Exposure. Testing Conditions: IGE Microsensor Number 1; CoPc Thin-film (2,500 Angstroms Thick); Temperature of 150 Degree Centigrade; Nitrogen Dioxide Challenge Gas.

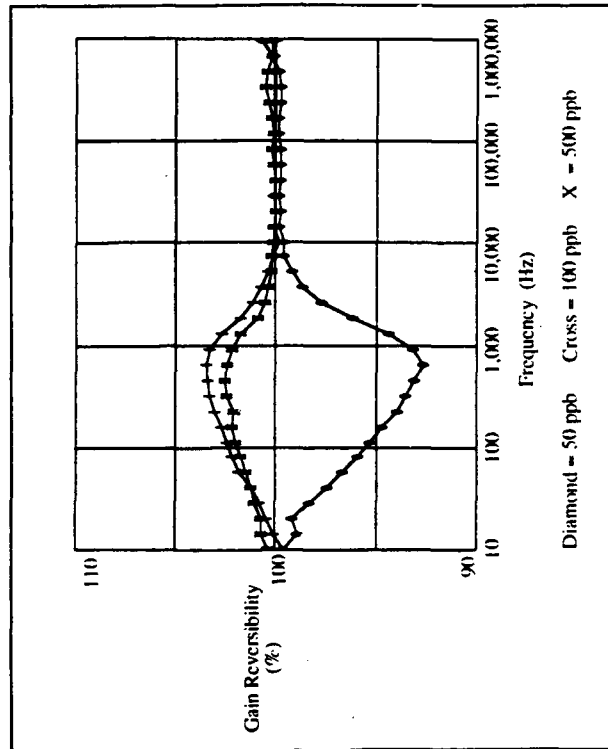


Figure D-37. Reversibility of Gain Transfer Response (Relative to Pre-exposure Purge) versus Frequency for CoPc Exposed to Nitrogen Dioxide. The Diamond Plot is the Change Between the Purges Before and After a 50 ppb Exposure. The Cross Plot is the Change from the Next Purge Cycle to the Purge Following the a 100 ppb Exposure. The 'X' Plot is the Change Between the Purges Before and After a 500 ppb Exposure. Testing Conditions: IGE Microsensor Number 1; CoPc Thin-film (2,500 Angstroms Thick); Temperature of 150 Degree Centigrade; Nitrogen Dioxide Challenge Gas.



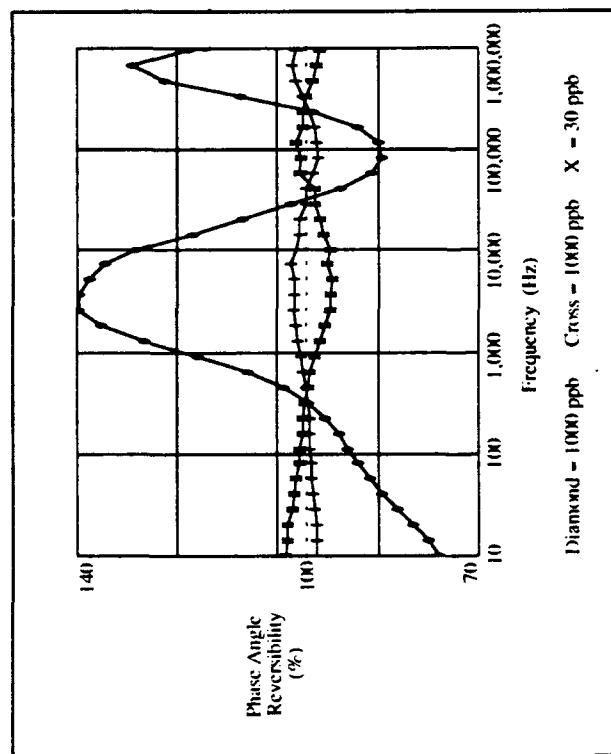


Figure D-38. Reversibility of Phase Angle Transfer Response (Relative to Pre-exposure Purge) versus Frequency for CoPc Exposed to Nitrogen Dioxide. The Diamond Plot is the Change from the Start-Up Purge to the Purge Following the 1000 ppb Pre-conditioning Cycle. The Cross Plot is the Change from the Next Purge Cycle to the Purge Following the Second 1000 ppb Exposure. The 'X' Plot is the Change Between the Purges Before and After a 30 ppb Exposure. Testing Conditions: IGE Microsensor Number 1; CoPc Thin-film (2,500 Angstroms Thick); Temperature of 150 Degree Centigrade; Nitrogen Dioxide Challenge Gas.

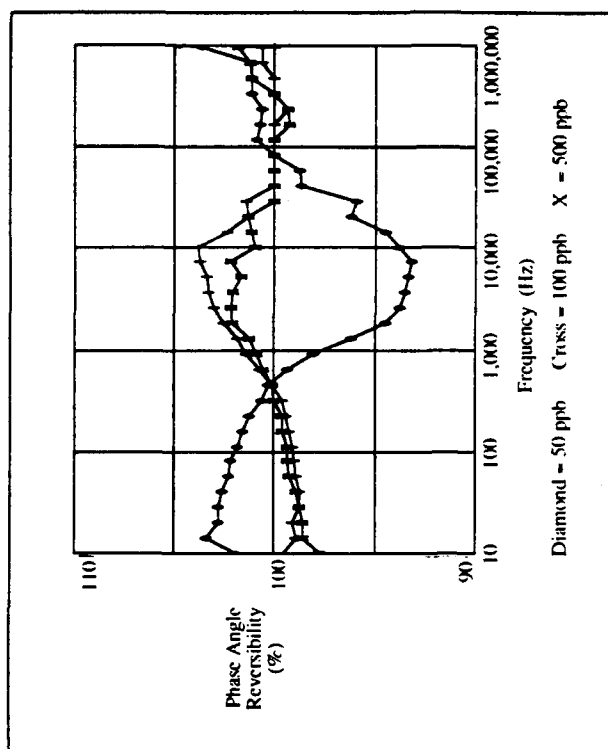


Figure D-39. Reversibility of Phase Angle Transfer Response (Relative to Pre-exposure Purge) versus Frequency for CoPc Exposed to Nitrogen Dioxide. The Diamond Plot is the Change Between the Purges Before and After a 50 ppb Exposure. The Cross Plot is the Change from the Next Purge Cycle to the Purge Following the a 100 ppb Exposure. The 'X' Plot is the Change Between the Purges Before and After a 500 ppb Exposure. Testing Conditions: IGE Microsensor Number 1; CoPc Thin-film (2,500 Angstroms Thick); Temperature of 150 Degree Centigrade; Nitrogen Dioxide Challenge Gas.

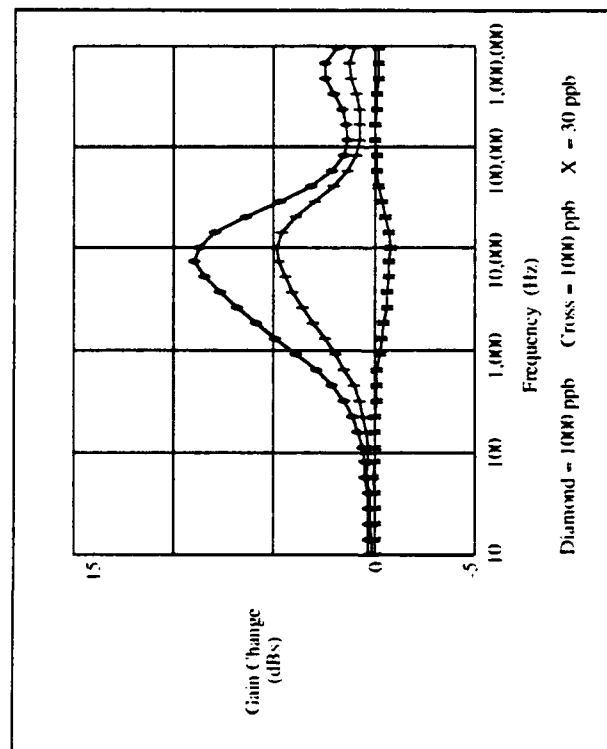


Figure D-40. Change in Gain Transfer Response versus Frequency for CoPc Exposed to Nitrogen Dioxide. The Diamond Plot is the Change from the Start-Up Purge to the End of the 1000 ppb Pre-conditioning Cycle. The Cross Plot is the Change from the Next Purge Cycle to the Second 1000 ppb Exposure. The 'X' Plot is the Change from Purge to 30 ppb Exposure. Testing Conditions: IGIE Microsensor Number 4; CoPc Thin-film (5,400 Angstroms Thick); Temperature of 150 Degree Centigrade; Nitrogen Dioxide Challenge Gas.

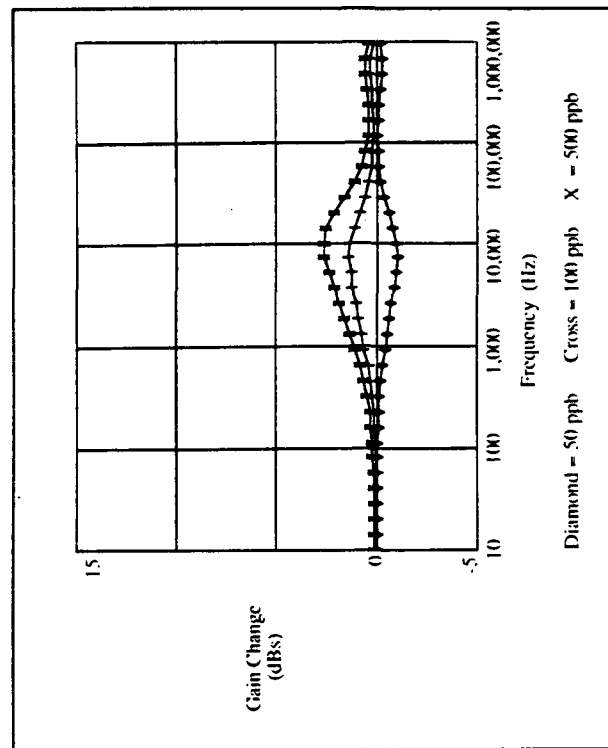


Figure D-41. Change in Gain Transfer Response versus Frequency for CoPc Exposed to Nitrogen Dioxide. The Diamond Plot is the Change from Purge to the End of the 50 ppb Exposure. The Cross Plot is the Change from the Next Purge Cycle to 100 ppb Exposure. The 'X' Plot is the Change from Purge to 500 ppb Exposure. Testing Conditions: IGIE Microsensor Number 4; CoPc Thin-film (5,400 Angstroms Thick); Temperature of 150 Degree Centigrade; Nitrogen Dioxide Challenge Gas.

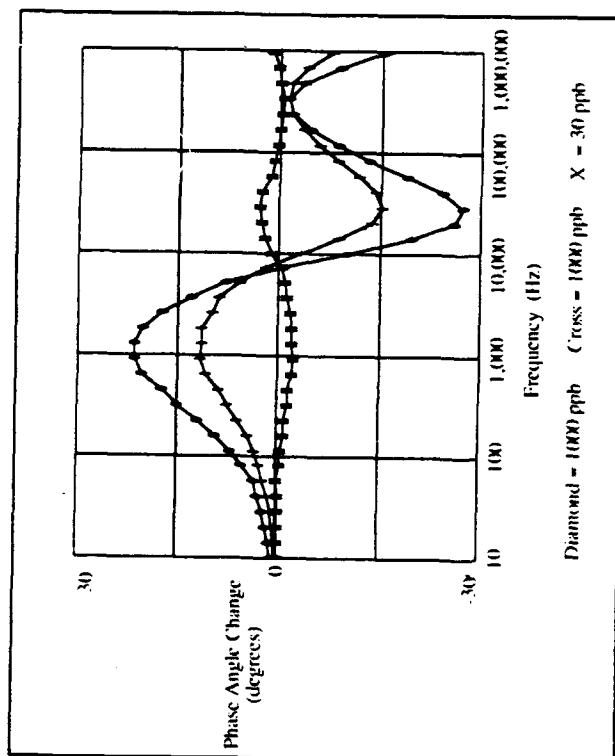


Figure D-42. Change in Phase Angle Transfer Response versus Frequency for Co/Pc Exposed to Nitrogen Dioxide. The Diamond Plot is the Change from the Start-Up Purge to the End of the 1000 ppb Pre-conditioning Cycle. The Cross Plot is the Change from the Next Purge Cycle to the Second 1000 ppb Exposure. The 'X' Plot is the Change from Purge to 30 ppb Exposure. Testing Conditions: IGE Microsensor Number 4; Co/Pc Thin-film (5,400 Angstroms Thick); Temperature of 150 Degree Centigrade; Nitrogen Dioxide Challenge Gas.

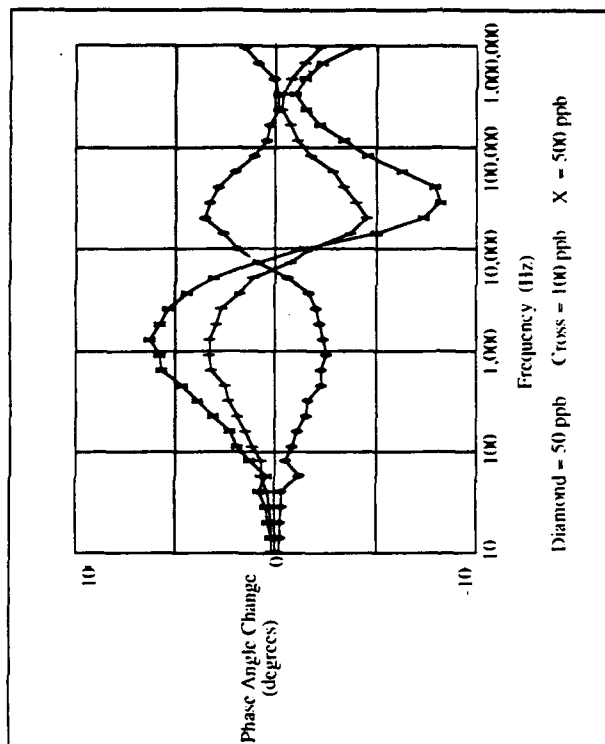


Figure D-43. Change in Phase Angle Transfer Response versus Frequency for Co/Pc Exposed to Nitrogen Dioxide. The Diamond Plot is the Change from Purge to the End of the 50 ppb Exposure. The Cross Plot is the Change from the Next Purge Cycle to 100 ppb Exposure. The 'X' Plot is the Change from Purge to 500 ppb Exposure. Testing Conditions: IGE Microsensor Number 4; Co/Pc Thin-film (5,400 Angstroms Thick); Temperature of 150 Degree Centigrade; Nitrogen Dioxide Challenge Gas.

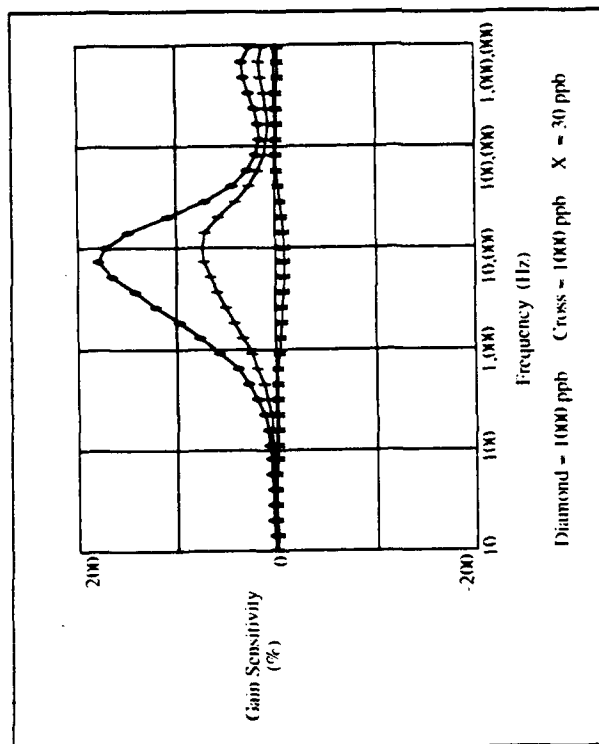


Figure D-44. Percent Change in Gain Transfer Response versus Frequency for CoPc Exposed to Nitrogen Dioxide. The Diamond Plot is the Change from the Start-Up Purge to the End of the 1000 ppb Pre-conditioning Cycle. The Cross Plot is the Change from the Next Purge Cycle to the Second 1000 ppb Exposure. The 'X' Plot is the Change from Purge to 30 ppb Exposure. Testing Conditions: IGE; Microsensor Number 4; CoPc Thin-film (5,400 Angstroms Thick); Temperature of 150 Degree Centigrade; Nitrogen Dioxide Challenge Gas.

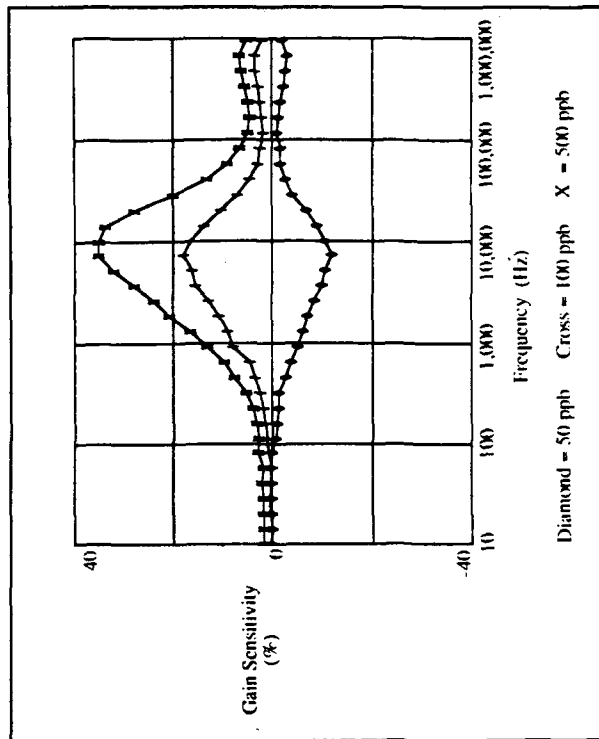


Figure D-45. Percent Change in Gain Transfer Response versus Frequency for CoPc Exposed to Nitrogen Dioxide. The Diamond Plot is the Change from Purge to the End of the 50 ppb Exposure. The Cross Plot is the Change from the Next Purge Cycle to 100 ppb Exposure. The 'X' Plot is the Change from Purge to 500 ppb Exposure. Testing Conditions: IGE; Microsensor Number 4; CoPc Thin-film (5,400 Angstroms Thick); Temperature of 150 Degree Centigrade; Nitrogen Dioxide Challenge Gas.

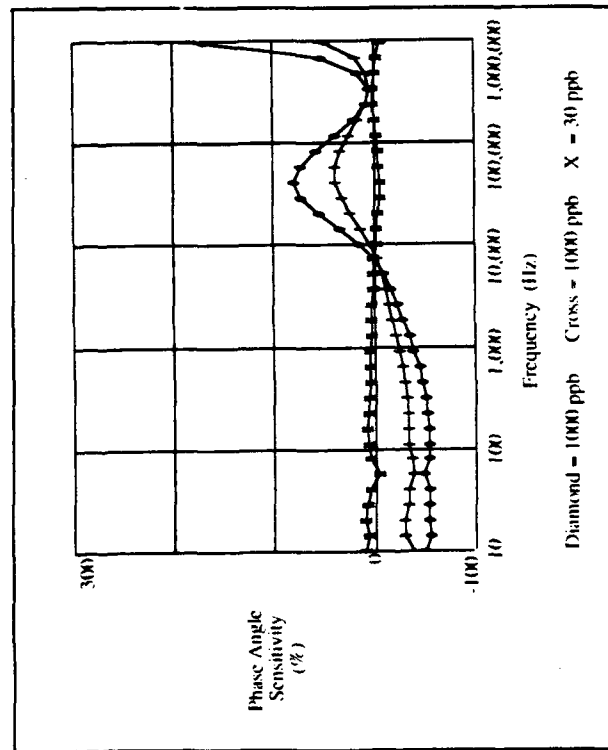


Figure D-46. Percent Change in Phase Angle Transfer Response versus Frequency for CoPc Exposed to Nitrogen Dioxide. The Diamond Plot is the Change from the Start-Up Purge to the End of the 1000 ppb Pre-conditioning Cycle. The Cross Plot is the Change from the Next Purge Cycle to the Second 1000 ppb Exposure. The 'X' Plot is the Change from Purge to 30 ppb Exposure. Testing Conditions: IGE; Microsensor Number 4; CoPc Thin-film (5,400 Angstroms Thick); Temperature of 150 Degree Centigrade; Nitrogen Dioxide Challenge Gas.

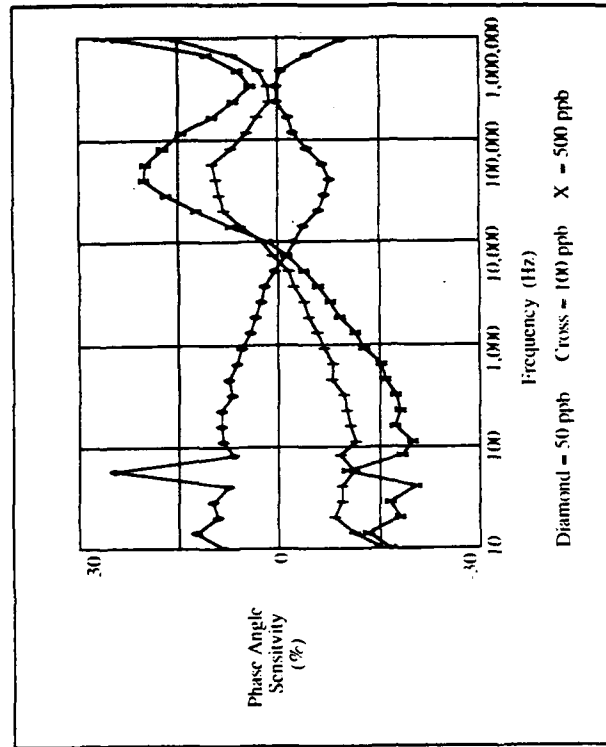


Figure D-47. Percent Change in Phase Angle Transfer Response versus Frequency for CoPc Exposed to Nitrogen Dioxide. The Diamond Plot is the Change from Purge to the End of the 50 ppb Exposure. The Cross Plot is the Change from the Next Purge Cycle to 100 ppb Exposure. The 'X' Plot is the Change from Purge to 500 ppb Exposure. Testing Conditions: IGE; Microsensor Number 4; CoPc Thin-film (5,400 Angstroms Thick); Temperature of 150 Degree Centigrade; Nitrogen Dioxide Challenge Gas.

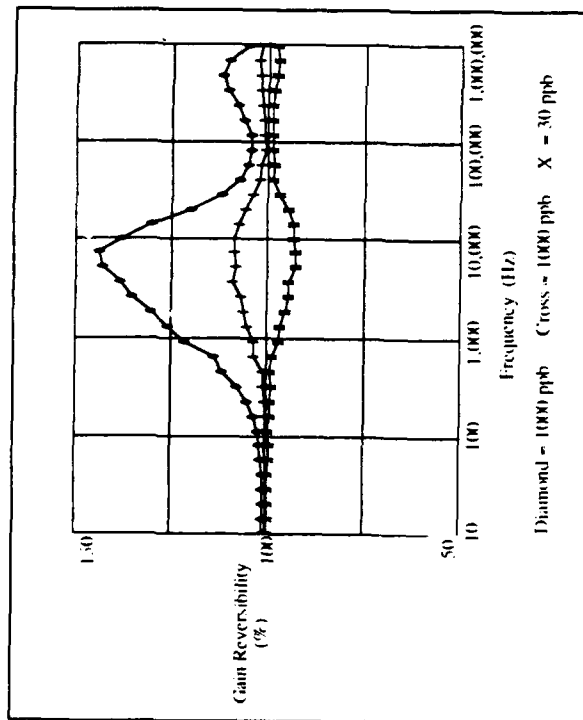


Figure D-48. Reversibility of Gain Transfer Response (Relative to Pre-exposure Purge) versus Frequency for CoPc Exposed to Nitrogen Dioxide. The Diamond Plot is the Change from the Start-Up Purge to the Purge Following the 1000 ppb Pre-conditioning Cycle. The Cross Plot is the Change from the Next Purge Cycle to the Purge Following the Second 1000 ppb Exposure. The 'X' Plot is the Change Between the Purges Before and After a 30 ppb Exposure. Testing Conditions: IGE Microsensor Number 4; CoPc Thin-film (5,400 Angstroms Thick); Temperature of 150 Degree Centigrade; Nitrogen Dioxide Challenge Gas.

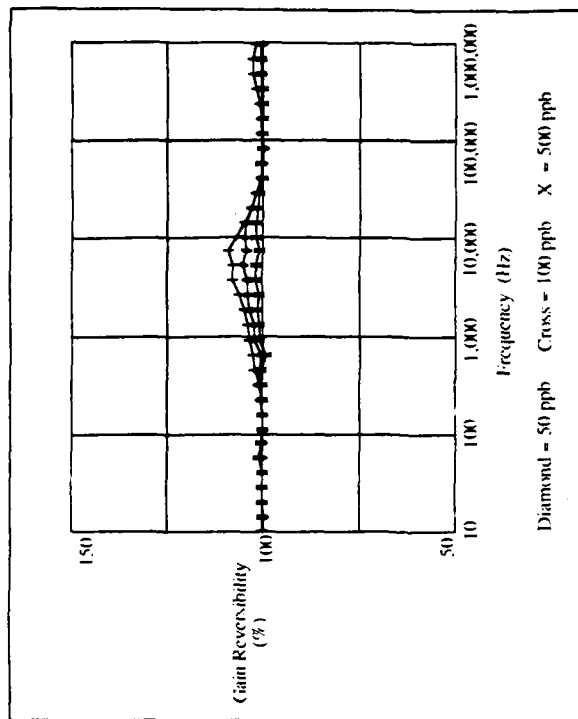


Figure D-49. Reversibility of Gain Transfer Response (Relative to Pre-exposure Purge) versus Frequency for CoPc Exposed to Nitrogen Dioxide. The Diamond Plot is the Change Between the Purges Before and After a 50 ppb Exposure. The Cross Plot is the Change from the Next Purge Cycle to the Purge Following the a 100 ppb Exposure. The 'X' Plot is the Change Between the Purges Before and After a 500 ppb Exposure. Testing Conditions: IGE Microsensor Number 4; CoPc Thin-film (5,400 Angstroms Thick); Temperature of 150 Degree Centigrade; Nitrogen Dioxide Challenge Gas.

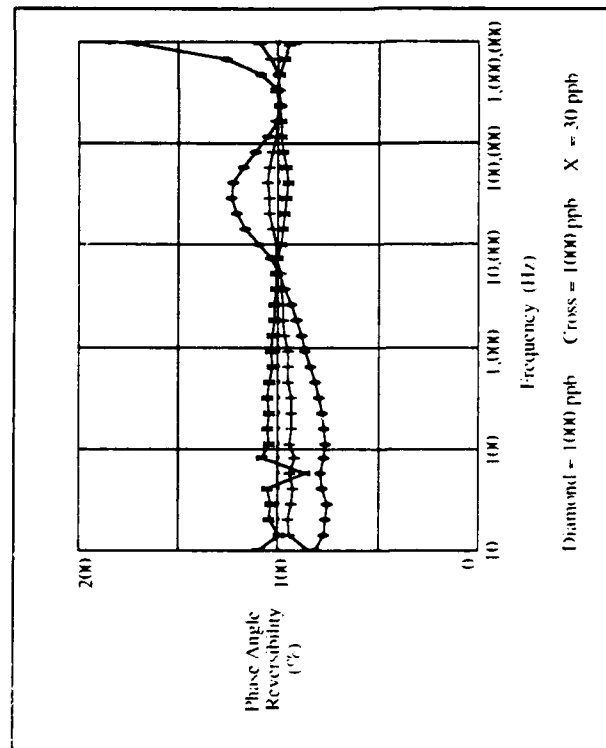


Figure D-50. Reversibility of Phase Angle Transfer Response (Relative to Pre-exposure Purge) versus Frequency for CoPc Exposed to Nitrogen Dioxide. The Diamond Plot is the Change from the Start-Up Purge to the Purge Following the 10000 ppb Pre-conditioning Cycle. The Cross Plot is the Change from the Next Purge Cycle to the Purge Following the Second 10000 ppb Exposure. The 'X' Plot is the Change Between the Purges Before and After a 30 ppb Exposure. Testing Conditions: IGE; Microsensor Number 4; CoPc Thin-film (5,400 Angstroms Thick); Temperature of 150 Degree Centigrade; Nitrogen Dioxide Challenge Gas.

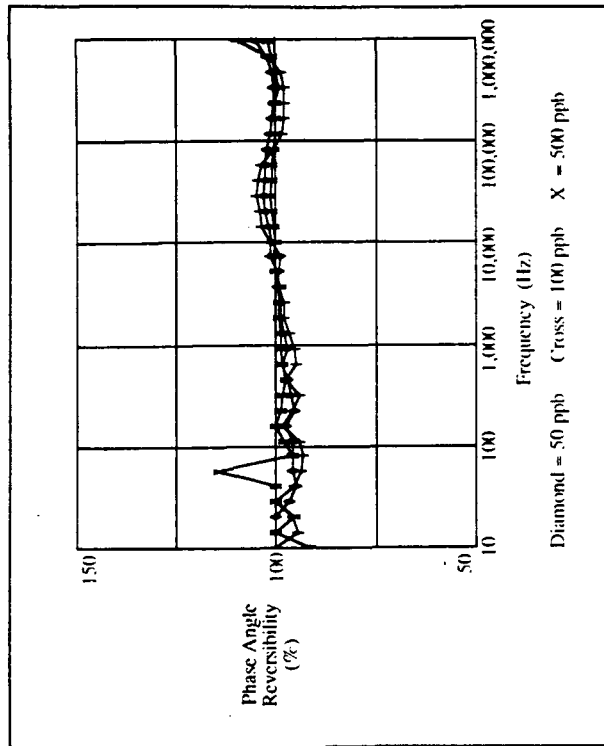


Figure D-51. Reversibility of Phase Angle Transfer Response (Relative to Pre-exposure Purge) versus Frequency for CoPc Exposed to Nitrogen Dioxide. The Diamond Plot is the Change Between the Purges Before and After a 50 ppb Exposure. The Cross Plot is the Change from the Next Purge Cycle to the Purge Following the a 100 ppb Exposure. The 'X' Plot is the Change Between the Purges Before and After a 500 ppb Exposure. Testing Conditions: IGE; Microsensor Number 4; CoPc Thin-film (5,400 Angstroms Thick); Temperature of 150 Degree Centigrade; Nitrogen Dioxide Challenge Gas.

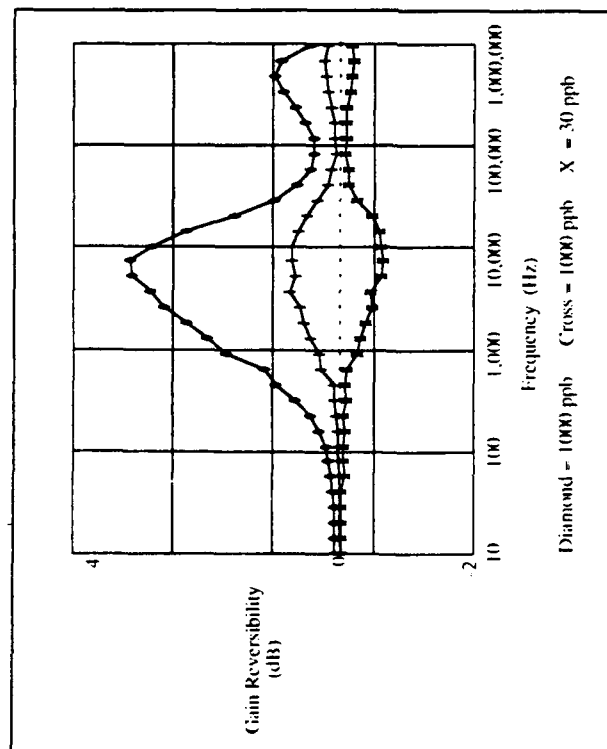


Figure D-52. Reversibility of Gain Transfer CoPc Exposed to Nitrogen Dioxide. The Diamond Plot is the Change from the Start-Up Purge to the Purge Following the 1000 ppb Pre-conditioning Cycle. The Cross Plot is the Change from the Next Purge Cycle to the Purge Following the Second 1000 ppb Exposure. The 'X' Plot is the Change Between the Purges Before and After a 30 ppb Exposure. Testing Conditions: IGE; Microsensor Number 4; CoPc Thin-film (5,400 Angstroms Thick); Temperature of 150 Degree Centigrade; Nitrogen Dioxide Challenge Gas.

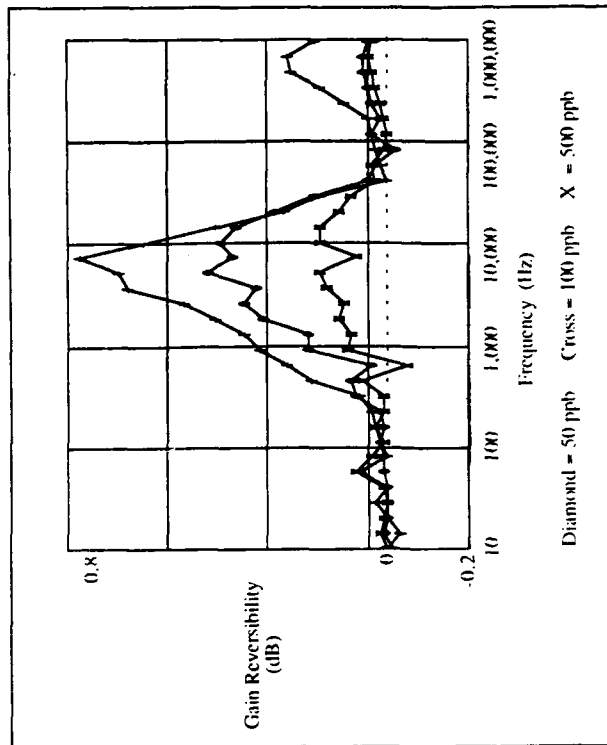


Figure D-53. Reversibility of Gain Transfer Response (Relative to Pre-exposure Purge) versus Frequency for CoPc Exposed to Nitrogen Dioxide. The Diamond Plot is the Change Between the Purges Before and After a 50 ppb Exposure. The Cross Plot is the Change from the Next Purge Cycle to the Purge Following the a 100 ppb Exposure. The 'X' Plot is the Change Between the Purges Before and After a 500 ppb Exposure. Testing Conditions: IGE; Microsensor Number 4; CoPc Thin-film (5,400 Angstroms Thick); Temperature of 150 Degree Centigrade; Nitrogen Dioxide Challenge Gas.



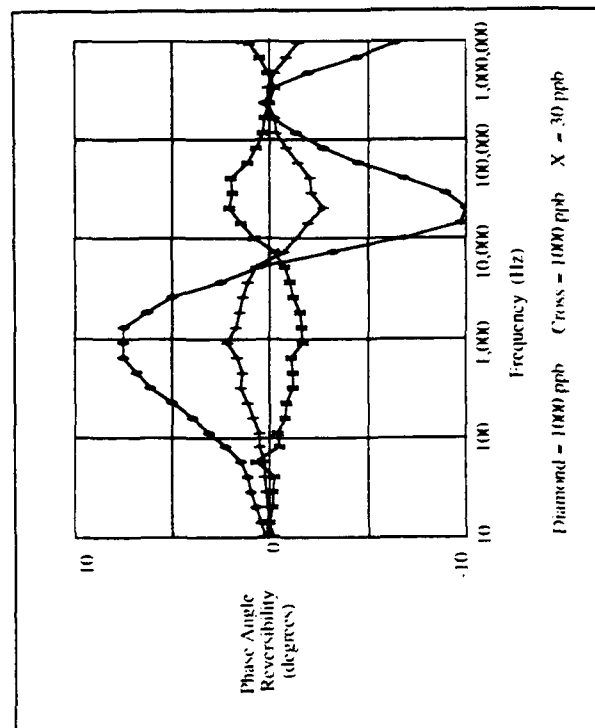


Figure D-54. Reversibility of Phase Angle Transfer Response (Relative to Pre-exposure Purge) versus Frequency for CoPe Exposed to Nitrogen Dioxide. The Diamond Plot is the Change from the Start-Up Purge to the Purge Following the 1000 ppb Pre-conditioning Cycle. The Cross Plot is the Change from the Next Purge Cycle to the Purge Following the Second 1000 ppb Exposure. The 'X' Plot is the Change Between the Purges Before and After a 30 ppb Exposure. Testing Conditions: IGL Microsensor Number 4; CoPe Thin-film (5,400 Angstroms Thick); Temperature of 150 Degree Centigrade; Nitrogen Dioxide Challenge Gas.

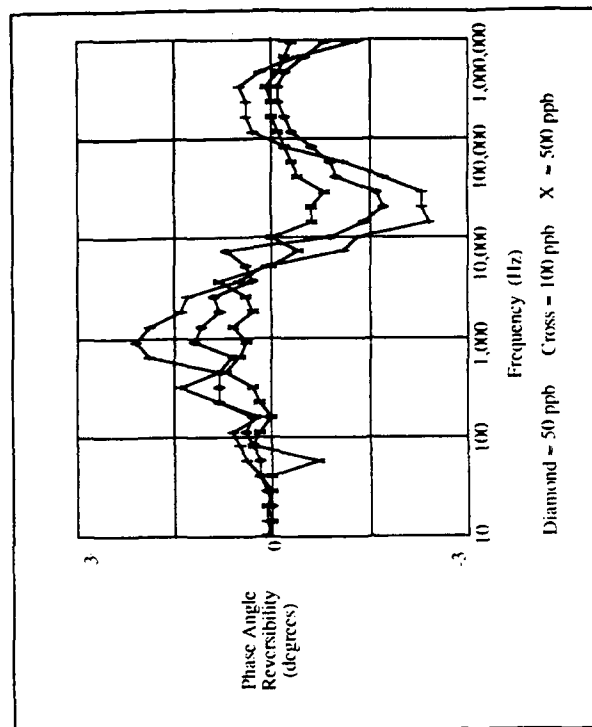


Figure D-55. Reversibility of Phase Angle Transfer Response (Relative to Pre-exposure Purge) versus Frequency for CoPe Exposed to Nitrogen Dioxide. The Diamond Plot is the Change Between the Purges Before and After a 50 ppb Exposure. The Cross Plot is the Change from the Next Purge Cycle to the Purge Following the a 100 ppb Exposure. The 'X' Plot is the Change Between the Purges Before and After a 500 ppb Exposure. Testing Conditions: IGL Microsensor Number 4; CoPe Thin-film (5,400 Angstroms Thick); Temperature of 150 Degree Centigrade; Nitrogen Dioxide Challenge Gas.

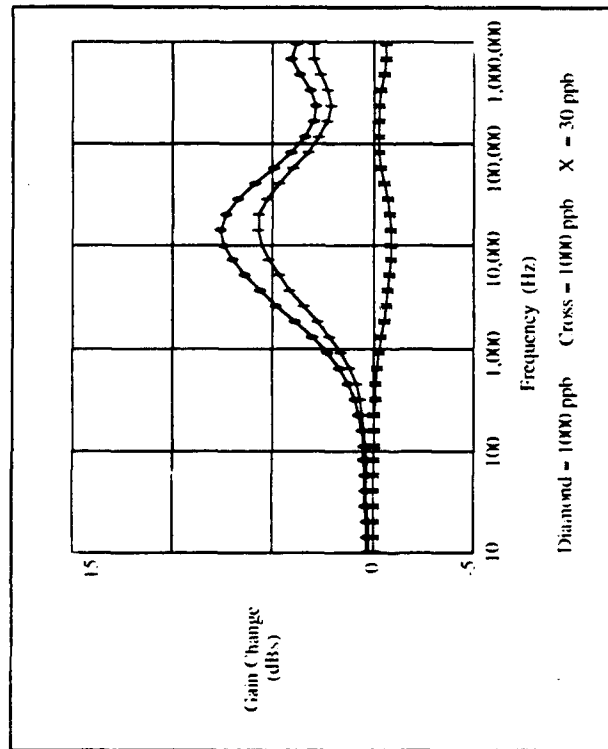


Figure D-56. Change in Gain Transfer Response versus Frequency for Co/Pc Exposed to Nitrogen Dioxide. The Diamond Plot is the Change from the Start-Up Purge to the End of the 1000 ppb Pre-conditioning Cycle. The Cross Plot is the Change from the Next Purge Cycle to the Second 1000 ppb Exposure. The 'X' Plot is the Change from Purge to 30 ppb Exposure. Testing Conditions: IGI; Microsensor Number 9; Co/Pc Thin-film (10,500 Angstroms Thick); Temperature of 150 Degree Centigrade; Nitrogen Dioxide Challenge Gas.

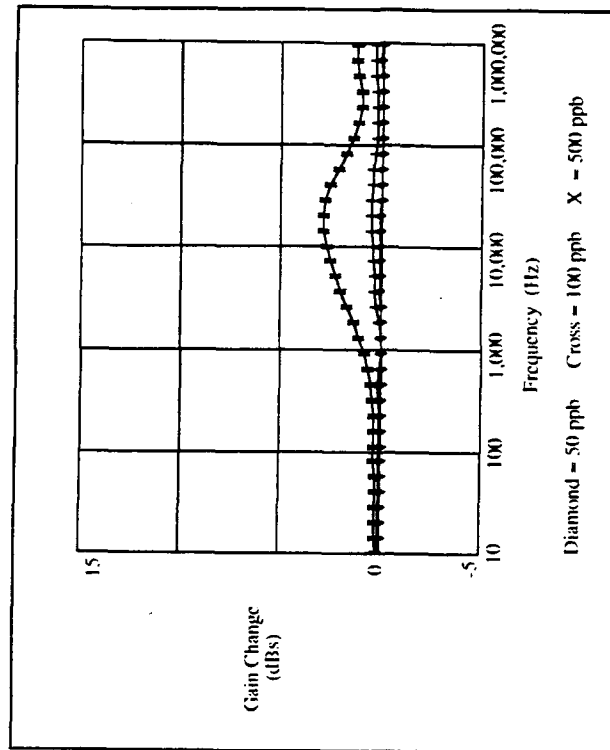


Figure D-57. Change in Gain Transfer Response versus Frequency for Co/Pc Exposed to Nitrogen Dioxide. The Diamond Plot is the Change from Purge to the End of the 50 ppb Exposure. The Cross Plot is the Change from the Next Purge Cycle to 100 ppb Exposure. The 'X' Plot is the Change from Purge to 500 ppb Exposure. Testing Conditions: IGI; Microsensor Number 9; Co/Pc Thin-film (10,500 Angstroms Thick); Temperature of 150 Degree Centigrade; Nitrogen Dioxide Challenge Gas.

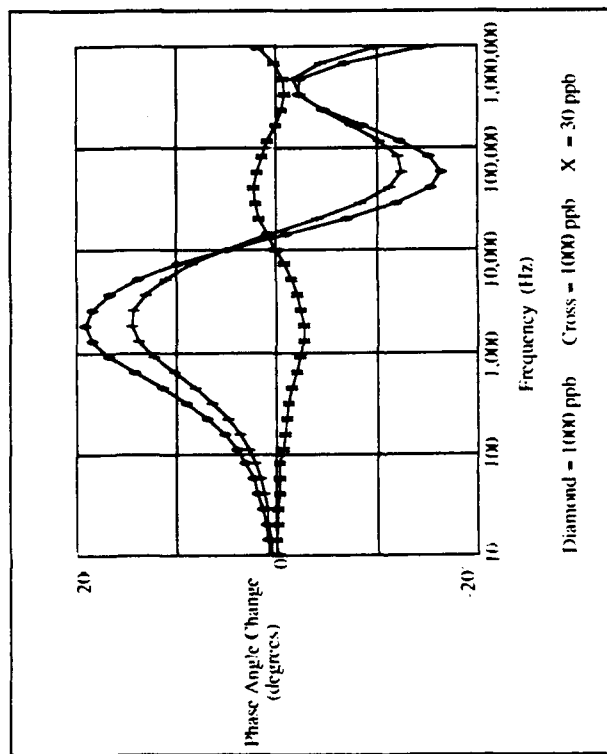


Figure D-58. Change in Phase Angle Transfer Response versus Frequency for CoPc Exposed to Nitrogen Dioxide. The Diamond Plot is the Change from the Start-Up Purge to the End of the 1000 ppb Pre-conditioning Cycle. The Cross Plot is the Change from the Next Purge Cycle to the Second 10000 ppb Exposure. The 'X' Plot is the Change from Purge to 30 ppb Exposure. Testing Conditions: IGI; Microsensor Number 9; CoPc Thin-film (10,500 Angstroms Thick); Temperature of 150 Degree Centigrade; Nitrogen Dioxide Challenge Gas.

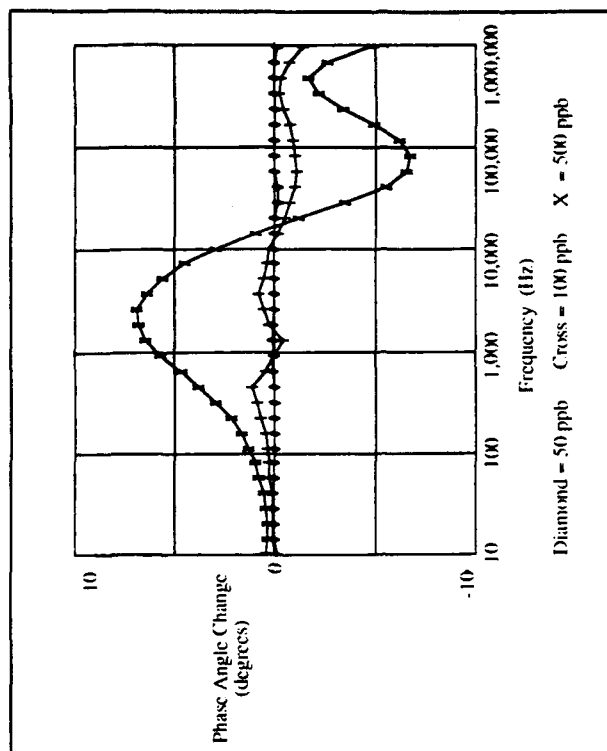


Figure D-59. Change in Phase Angle Transfer Response versus Frequency for CoPc Exposed to Nitrogen Dioxide. The Diamond Plot is the Change from Purge to the End of the 50 ppb Exposure. The Cross Plot is the Change from the Next Purge Cycle to 100 ppb Exposure. The 'X' Plot is the Change from Purge to 500 ppb Exposure. Testing Conditions: IGI; Microsensor Number 9; CoPc Thin-film (10,500 Angstroms Thick); Temperature of 150 Degree Centigrade; Nitrogen Dioxide Challenge Gas.

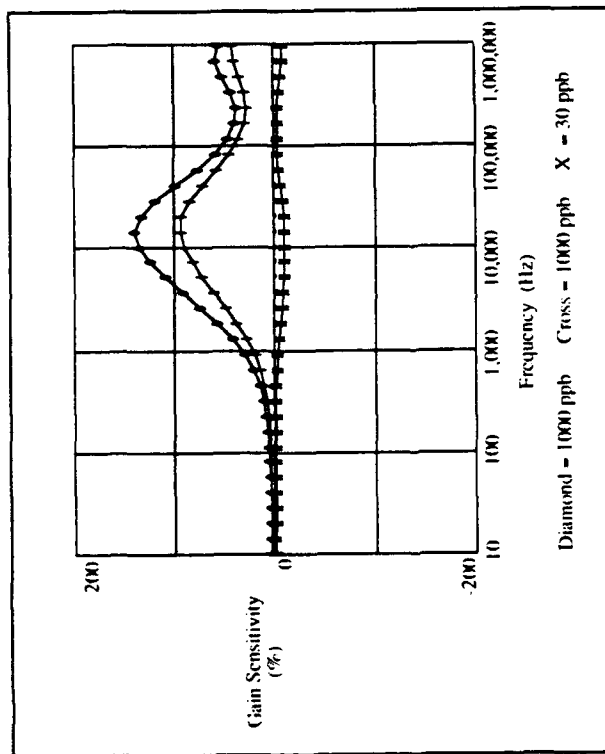


Figure D-60. Percent Change in Gain Transfer Response versus Frequency for CoPc Exposed to Nitrogen Dioxide. The Diamond Plot is the Change from the Start-Up Purge to the End of the 1000 ppb Pre-conditioning Cycle. The Cross Plot is the Change from the Next Purge Cycle to the Second 1000 ppb Exposure. The 'X' Plot is the Change from Purge to 30 ppb Exposure. Testing Conditions: IGE Microsensor Number 9; CoPc Thin-film (10,500 Angstroms Thick); Temperature of 150 Degree Centigrade; Nitrogen Dioxide Challenge Gas.

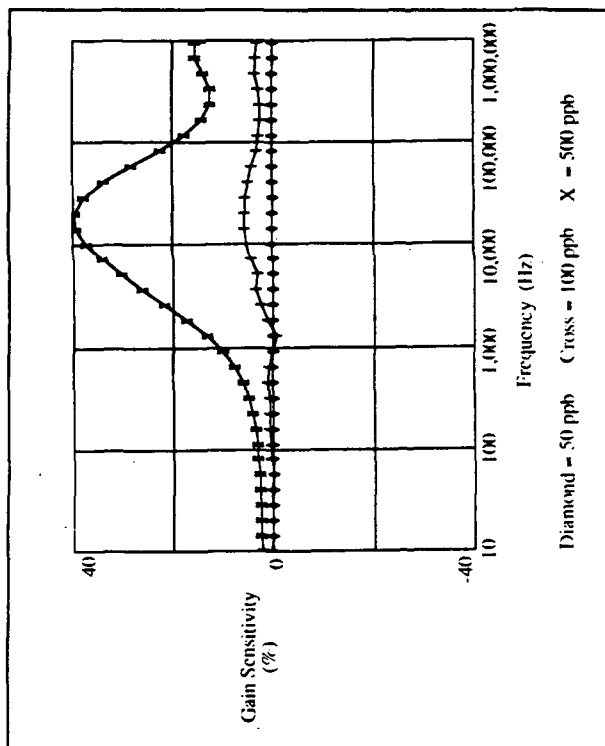


Figure D-61. Percent Change in Gain Transfer Response versus Frequency for CoPc Exposed to Nitrogen Dioxide. The Diamond Plot is the Change from Purge to the End of the 50 ppb Exposure. The Cross Plot is the Change from the Next Purge Cycle to 100 ppb Exposure. The 'X' Plot is the Change from Purge to 500 ppb Exposure. Testing Conditions: IGE Microsensor Number 9; CoPc Thin-film (10,500 Angstroms Thick); Temperature of 150 Degree Centigrade; Nitrogen Dioxide Challenge Gas.

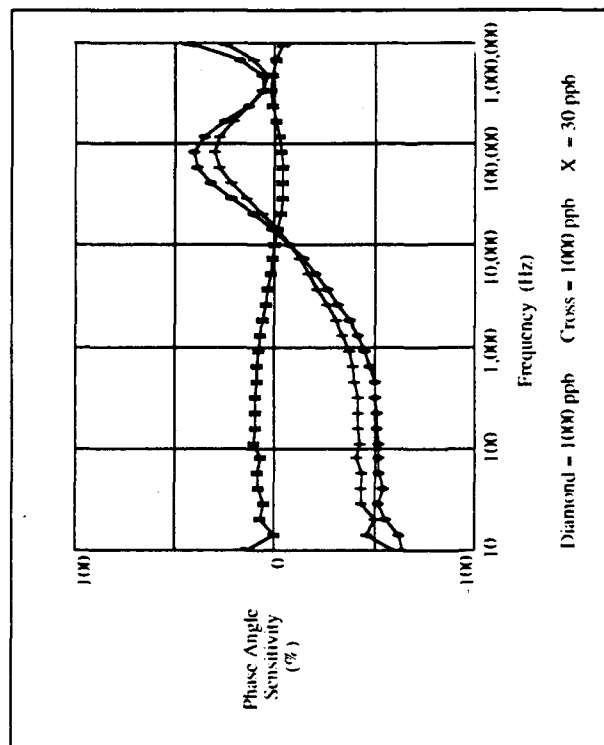


Figure D-62. Percent Change in Phase Angle Transfer Response versus Frequency for CoPc Exposed to Nitrogen Dioxide. The Diamond Plot is the Change from the Start-Up Purge to the End of the 1000 ppb Pre-conditioning Cycle. The Cross Plot is the Change from the Next Purge Cycle to the Second 1000 ppb Exposure. The 'X' Plot is the Change from Purge to 30 ppb Exposure. Testing Conditions: IGI; Microsensor Number 9; CoPc Thin-film (10,500 Angstroms Thick); Temperature of 150 Degree Centigrade; Nitrogen Dioxide Challenge Gas.

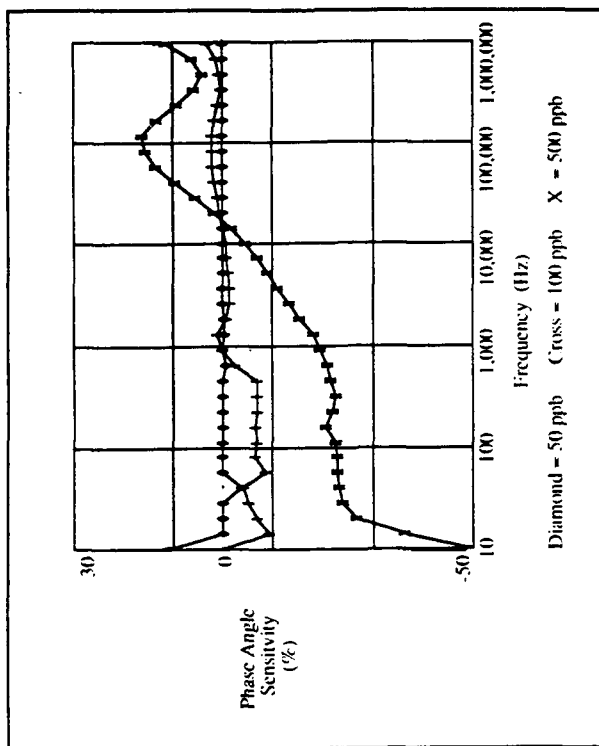


Figure D-63. Percent Change in Phase Angle Transfer Response versus Frequency for CoPc Exposed to Nitrogen Dioxide. The Diamond Plot is the Change from Purge to the End of the 50 ppb Exposure. The Cross Plot is the Change from the Next Purge Cycle to 100 ppb Exposure. The 'X' Plot is the Change from Purge to 500 ppb Exposure. Testing Conditions: IGI; Microsensor Number 9; CoPc Thin-film (10,500 Angstroms Thick); Temperature of 150 Degree Centigrade; Nitrogen Dioxide Challenge Gas.

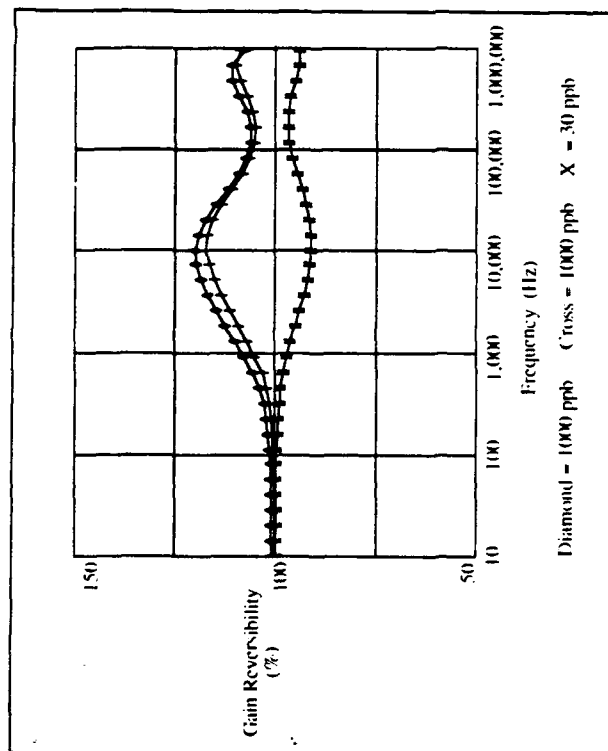


Figure D-64. Reversibility of Gain Transfer Response (Relative to Pre-exposure Purge) versus Frequency for CoPc Exposed to Nitrogen Dioxide. The Diamond Plot is the Change from the Start-Up Purge to the Purge Following the 1000 ppb Pre-conditioning Cycle. The Cross Plot is the Change from the Next Purge Cycle to the Purge Following the Second 1000 ppb Exposure. The 'X' Plot is the Change Between the Purges Before and After a 30 ppb Exposure. Testing Conditions: ICI; Microsensor Number 9; CoPc Thin-film (10,500 Angstroms Thick); Temperature of 150 Degree Centigrade; Nitrogen Dioxide Challenge Gas.

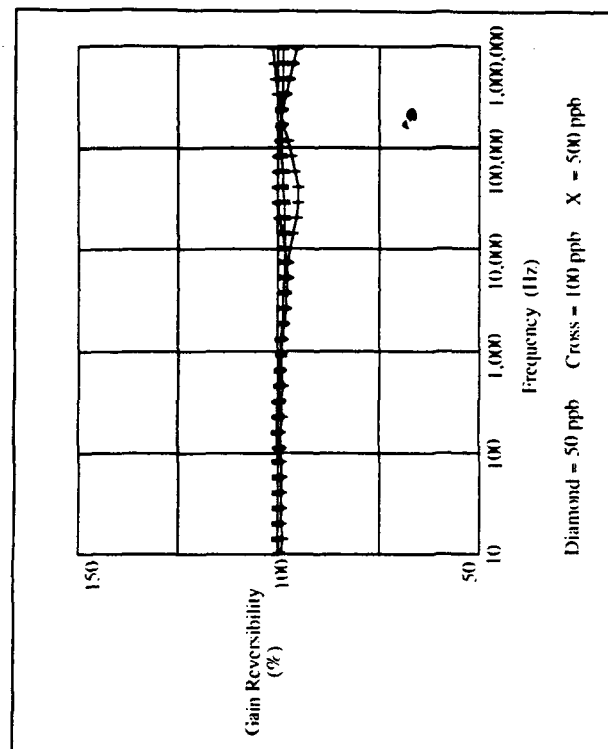


Figure D-65. Reversibility of Gain Transfer Response (Relative to Pre-exposure Purge) versus Frequency for CoPc Exposed to Nitrogen Dioxide. The Diamond Plot is the Change Between the Purges Before and After a 50 ppb Exposure. The Cross Plot is the Change from the Next Purge Cycle to the Purge Following the a 100 ppb Exposure. The 'X' Plot is the Change Between the Purges Before and After a 500 ppb Exposure. Testing Conditions: ICI; Microsensor Number 9; CoPc Thin-film (10,500 Angstroms Thick); Temperature of 150 Degree Centigrade; Nitrogen Dioxide Challenge Gas.

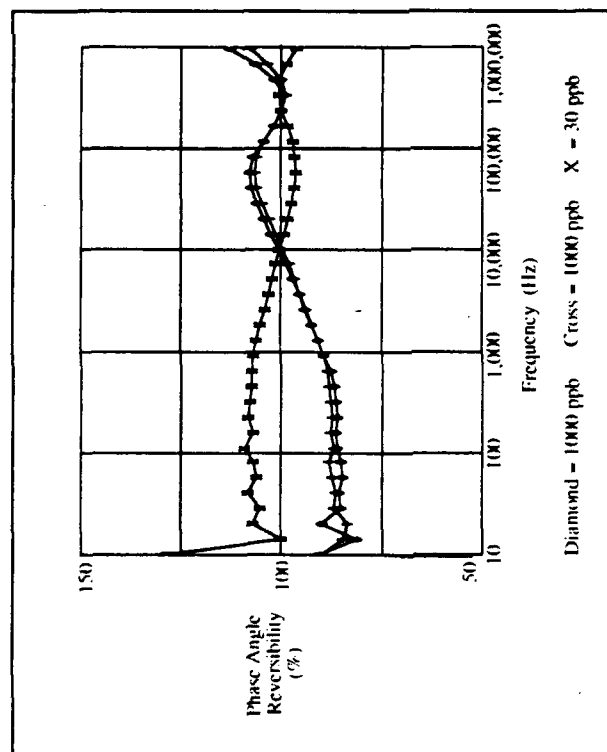


Figure D-66. Reversibility of Phase Angle Transfer Response (Relative to Pre-exposure Purge) versus Frequency for CoPc Exposed to Nitrogen Dioxide. The Diamond Plot is the Change from the Start-Up Purge to the Purge Following the 1000 ppb Pre-conditioning Cycle. The Cross Plot is the Change from the Next Purge Cycle to the Purge Following the Second 1000 ppb Exposure. The 'X' Plot is the Change Between the Purges Before and After a 30 ppb Exposure. Testing Conditions: IGF; Microsensor Number 9; CoPc Thin-film (10,500 Angstroms Thick); Temperature of 150 Degree Centigrade; Nitrogen Dioxide Challenge Gas.

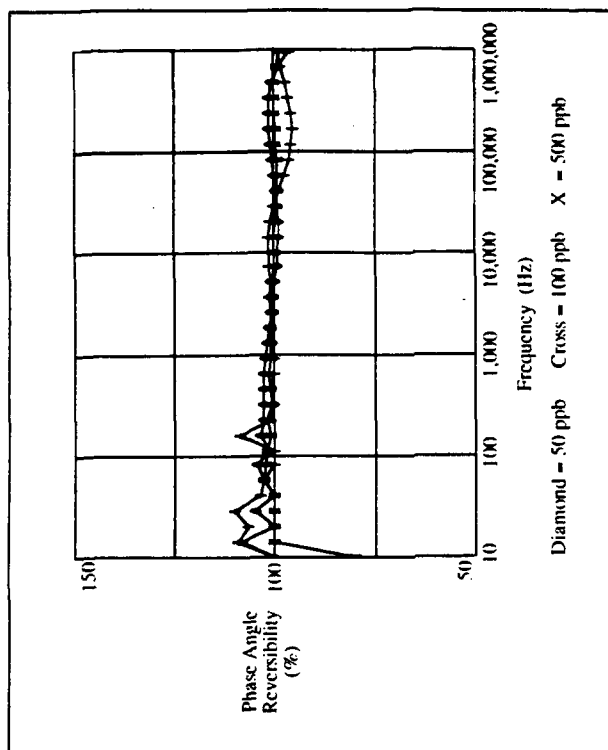


Figure D-67. Reversibility of Phase Angle Transfer Response (Relative to Pre-exposure Purge) versus Frequency for CoPc Exposed to Nitrogen Dioxide. The Diamond Plot is the Change Between the Purges Before and After a 50 ppb Exposure. The Cross Plot is the Change from the Next Purge Cycle to the Purge Following the a 100 ppb Exposure. The 'X' Plot is the Change Between the Purges Before and After a 500 ppb Exposure. Testing Conditions: IGF; Microsensor Number 9; CoPc Thin-film (10,500 Angstroms Thick); Temperature of 150 Degree Centigrade; Nitrogen Dioxide Challenge Gas.

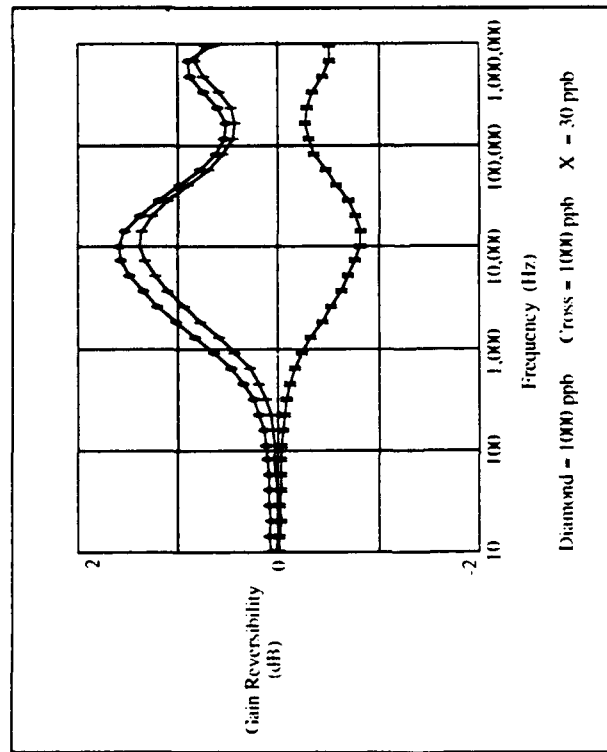


Figure D-68. Reversibility of Gain Transfer Response (Relative to Pre-exposure Purge) versus Frequency for CoPc Exposed to Nitrogen Dioxide. The Diamond Plot is the Change from the Start-Up Purge to the Purge Following the 1000 ppb Pre-conditioning Cycle. The Cross Plot is the Change from the Next Purge Cycle to the Purge Following the Second 1000 ppb Exposure. The 'X' Plot is the Change Between the Purges Before and After a 30 ppb Exposure. Testing Conditions: IGI; Microsensor Number 9; CoPc Thin-film (10,500 Angstroms Thick); Temperature of 150 Degree Centigrade; Nitrogen Dioxide Challenge Gas.

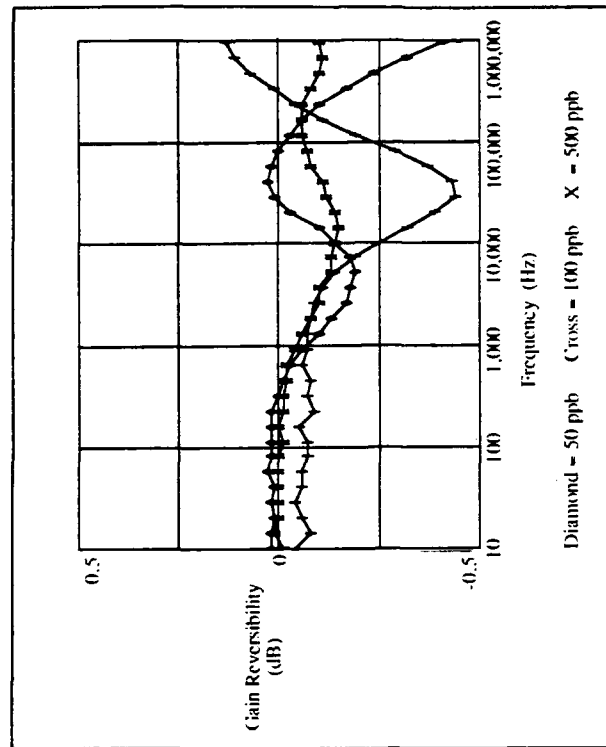


Figure D-69. Reversibility of Gain Transfer Response (Relative to Pre-exposure Purge) versus Frequency for CoPc Exposed to Nitrogen Dioxide. The Diamond Plot is the Change Between the Purges Before and After a 50 ppb Exposure. The Cross Plot is the Change from the Next Purge Cycle to the Purge Following the a 100 ppb Exposure. The 'X' Plot is the Change Between the Purges Before and After a 500 ppb Exposure. Testing Conditions: IGI; Microsensor Number 9; CoPc Thin-film (10,500 Angstroms Thick); Temperature of 150 Degree Centigrade; Nitrogen Dioxide Challenge Gas.



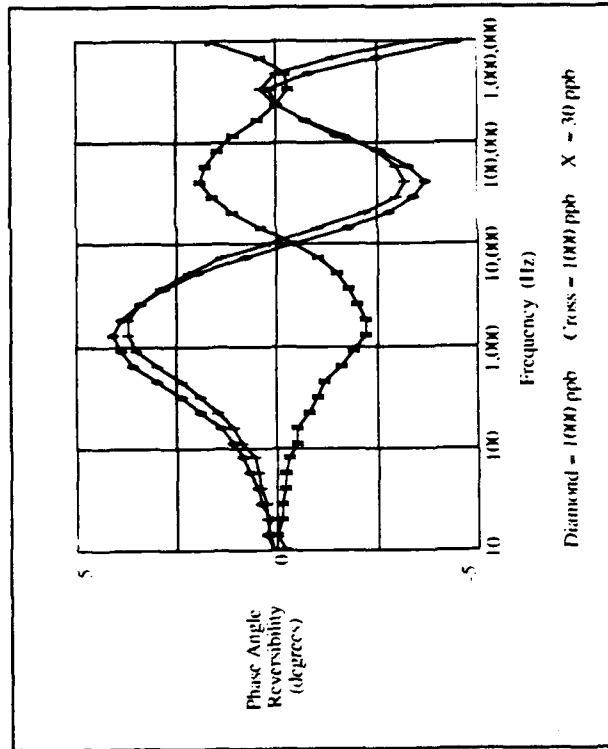


Figure D-70. Reversibility of Phase Angle Transfer Response (Relative to Pre-exposure Purge) versus Frequency for Co/Pc Exposed to Nitrogen Dioxide. The Diamond Plot is the Change from the Start-Up Purge to the Purge Following the 1000 ppb Pre-conditioning Cycle. The Cross Plot is the Change from the Next Purge Cycle to the Purge Following the Second 1000 ppb exposure. The 'X' Plot is the Change Between the Purges Before and After a 30 ppb Exposure. Testing Conditions: IGI Microsensor Number 9; Co/Pc Thin-film (10,500 Angstroms Thick); Temperature of 150 Degree Centigrade; Nitrogen Dioxide Challenge Gas.

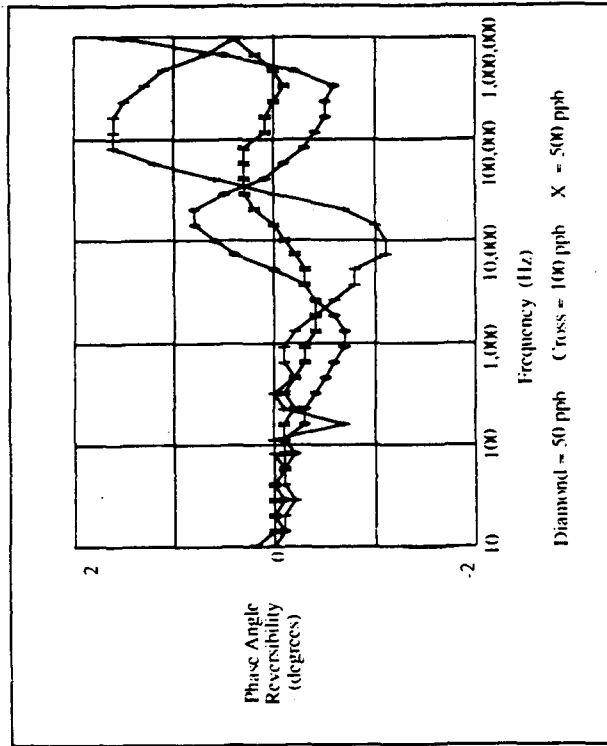


Figure D-71. Reversibility of Phase Angle Transfer Response (Relative to Pre-exposure Purge) versus Frequency for Co/Pc Exposed to Nitrogen Dioxide. The Diamond Plot is the Change Between the Purges Before and After a 50 ppb Exposure. The Cross Plot is the Change from the Next Purge Cycle to the Purge Following the a 100 ppb exposure. The 'X' Plot is the Change Between the Purges Before and After a 500 ppb Exposure. Testing Conditions: IGI Microsensor Number 9; Co/Pc Thin-film (10,500 Angstroms Thick); Temperature of 150 Degree Centigrade; Nitrogen Dioxide Challenge Gas.

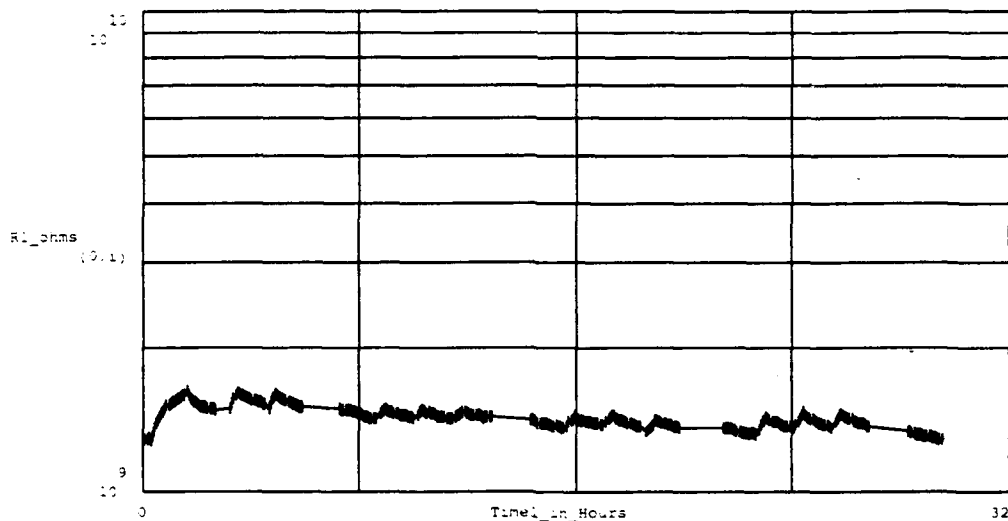


Figure D-72. DC Resistance Measured Between the Driven-Electrode and Floating-Electrode of the IGE Array. During Series of Purges and Challenge Gas Exposures. The Number of Measurements (at crosses) is 338. The Testing Conditions Included the Following:

IGE Array Number : 1.	Thin-film Material : Cobalt Phthalocyanine.
Thin-film Thickness : 2,500 Angstroms	Test Temperature(s) : Purge & Challenge at 150°C
Purge Gas : Room Air.	Challenge Gas : Ammonia.
Challenge Gas Concentration(s) (in order run) : 500 ppm, 16 ppm, 106 ppm, 250 ppm.	

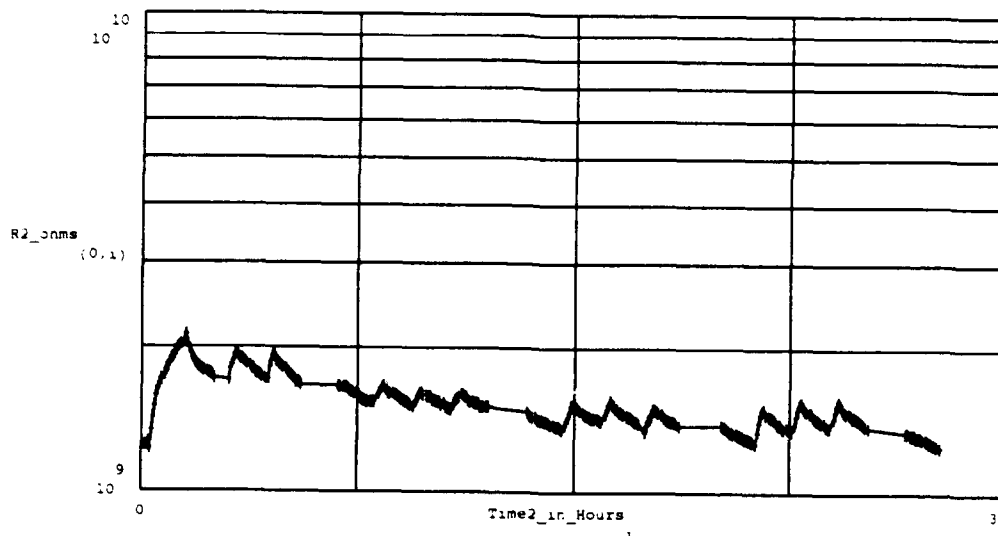


Figure D-73. DC Resistance Measured Between the Driven-Electrode and Floating-Electrode of the IGE Array. During Series of Purges and Challenge Gas Exposures. The Number of Measurements (at crosses) is 338. The Testing Conditions Included the Following:

IGE Array Number : 2.	Thin-film Material : Cobalt Phthalocyanine.
Thin-film Thickness : 2,500 Angstroms	Test Temperature(s) : Purge & Challenge at 150°C
Purge Gas : Room Air.	Challenge Gas : Ammonia.
Challenge Gas Concentration(s) (in order run) : 500 ppm, 16 ppm, 106 ppm, 250 ppm.	

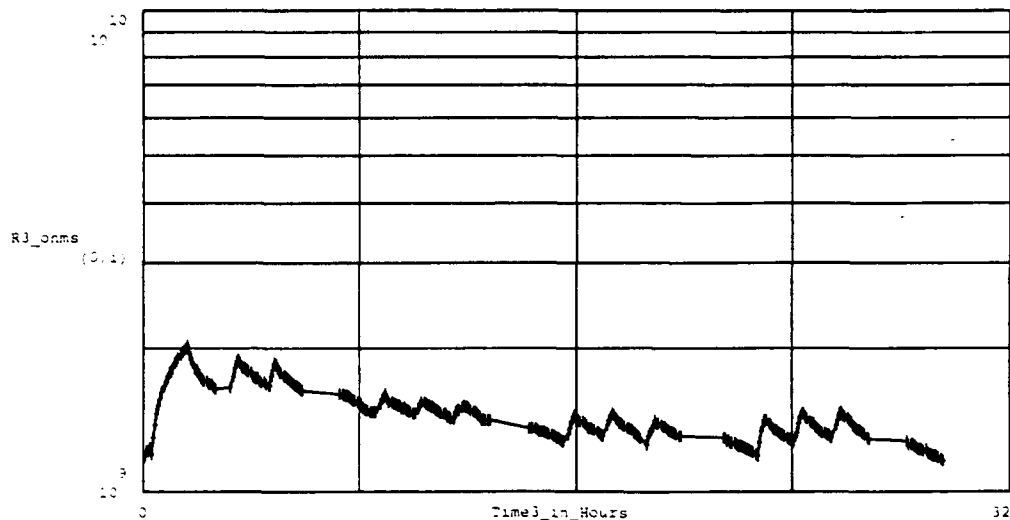


Figure D-74. DC Resistance Measured Between the Driven-Electrode and Floating-Electrode of the IGE Array. During Series of Purges and Challenge Gas Exposures. The Number of Measurements (at crosses) is 338. The Testing Conditions Included the Following:

IGE Array Number : 3,	Thin-film Material : Cobalt Phthalocyanine.
Thin-film Thickness : 2,500 Angstroms	Test Temperature(s) : Purge & Challenge at 150°C
Purge Gas : Room Air,	Challenge Gas : Ammonia,
Challenge Gas Concentration(s) (in order run) : 500 ppm, 16 ppm, 106 ppm, 250 ppm.	

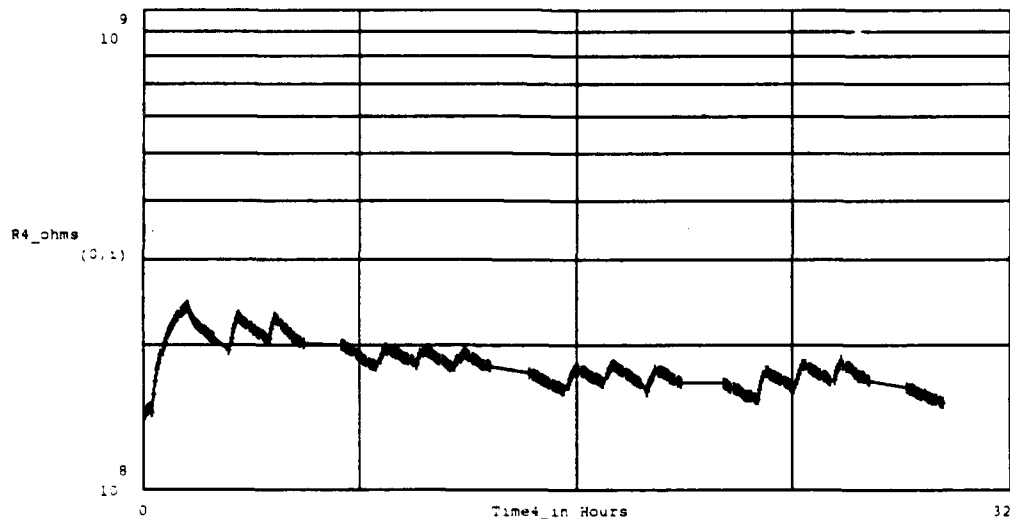


Figure D-75. DC Resistance Measured Between the Driven-Electrode and Floating-Electrode of the IGE Array. During Series of Purges and Challenge Gas Exposures. The Number of Measurements (at crosses) is 338. The Testing Conditions Included the Following:

IGE Array Number : 4,	Thin-film Material : Cobalt Phthalocyanine.
Thin-film Thickness : 5,400 Angstroms	Test Temperature(s) : Purge & Challenge at 150°C
Purge Gas : Room Air,	Challenge Gas : Ammonia,
Challenge Gas Concentration(s) (in order run) : 500 ppm, 16 ppm, 106 ppm, 250 ppm.	

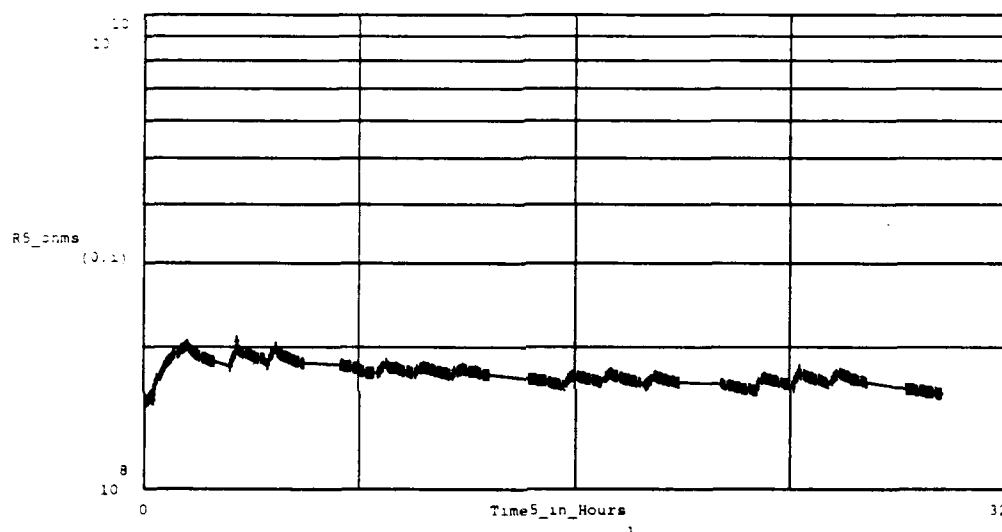


Figure D-76 . DC Resistance Measured Between the Driven-Electrode and Floating-Electrode of the IGE Array. During Series of Purges and Challenge Gas Exposures. The Number of Measurements (at crosses) is 338. The Testing Conditions Included the Following:

IGE Array Number : 5.	Thin-film Material : Cobalt Phthalocyanine.
Thin-film Thickness : 5,400 Angstroms	Test Temperature(s) : Purge & Challenge at 150°C
Purge Gas : Room Air.	Challenge Gas : Ammonia.
Challenge Gas Concentration(s) (in order run) : 500 ppm, 16 ppm, 106 ppm, 250 ppm.	



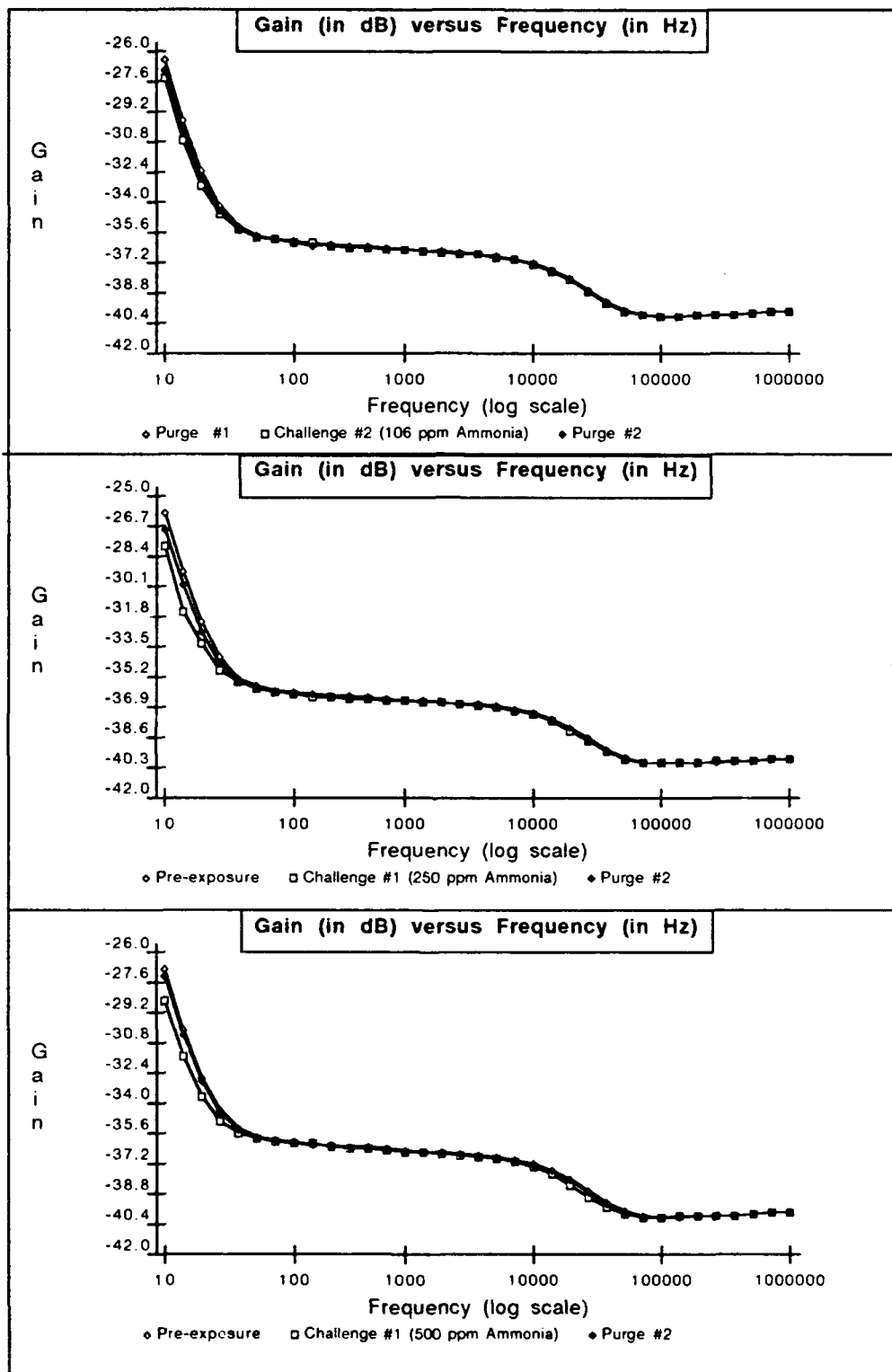


Figure D-78 . Gain versus Frequency Response of IGEFET Microsensor for a Series of Room Air Purges and Challenge Gas Exposures. Testing Conditions: IGE Microsensor Number 1; CoPc Thin-film (2,500 Angstroms Thick); Temperature of 150 degrees Centigrade; Ammonia Challenge Gas (Order of Exposures: 500 ppm, 16 ppm, 106 ppm, 250 ppm, 500 ppm).

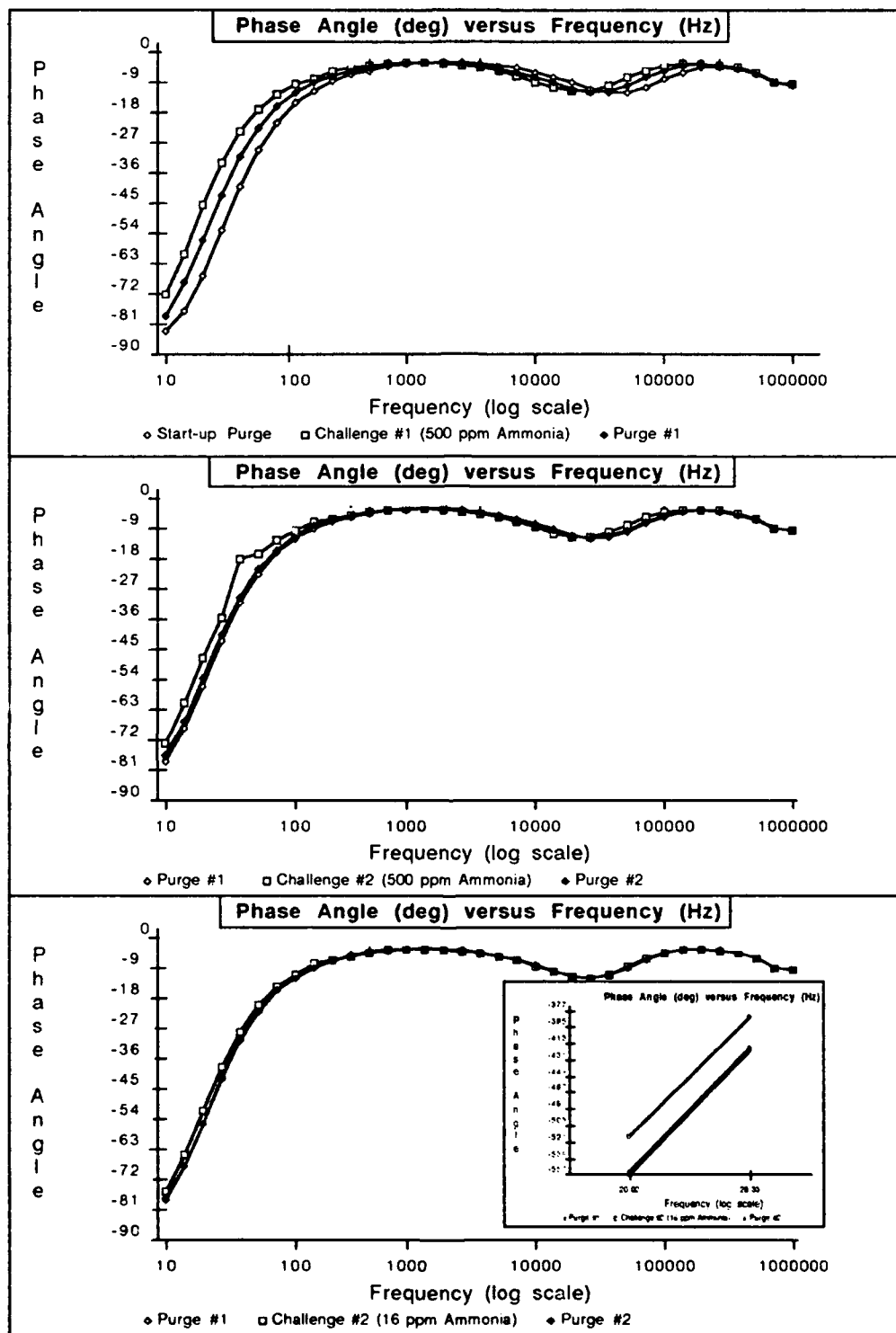


Figure D-79 Phase Angle versus Frequency Response of IGEFET Microsensor for a Series of Room Air Purges and Challenge Gas Exposures. Testing Conditions: IGE Microsensor Number 1; CoPc Thin-film (2,500 Angstroms Thick); Temperature of 150 degrees Centigrade; Ammonia Challenge Gas (Order of Exposures: 500 ppm, 16 ppm, 106 ppm, 250 ppm, 500 ppm).

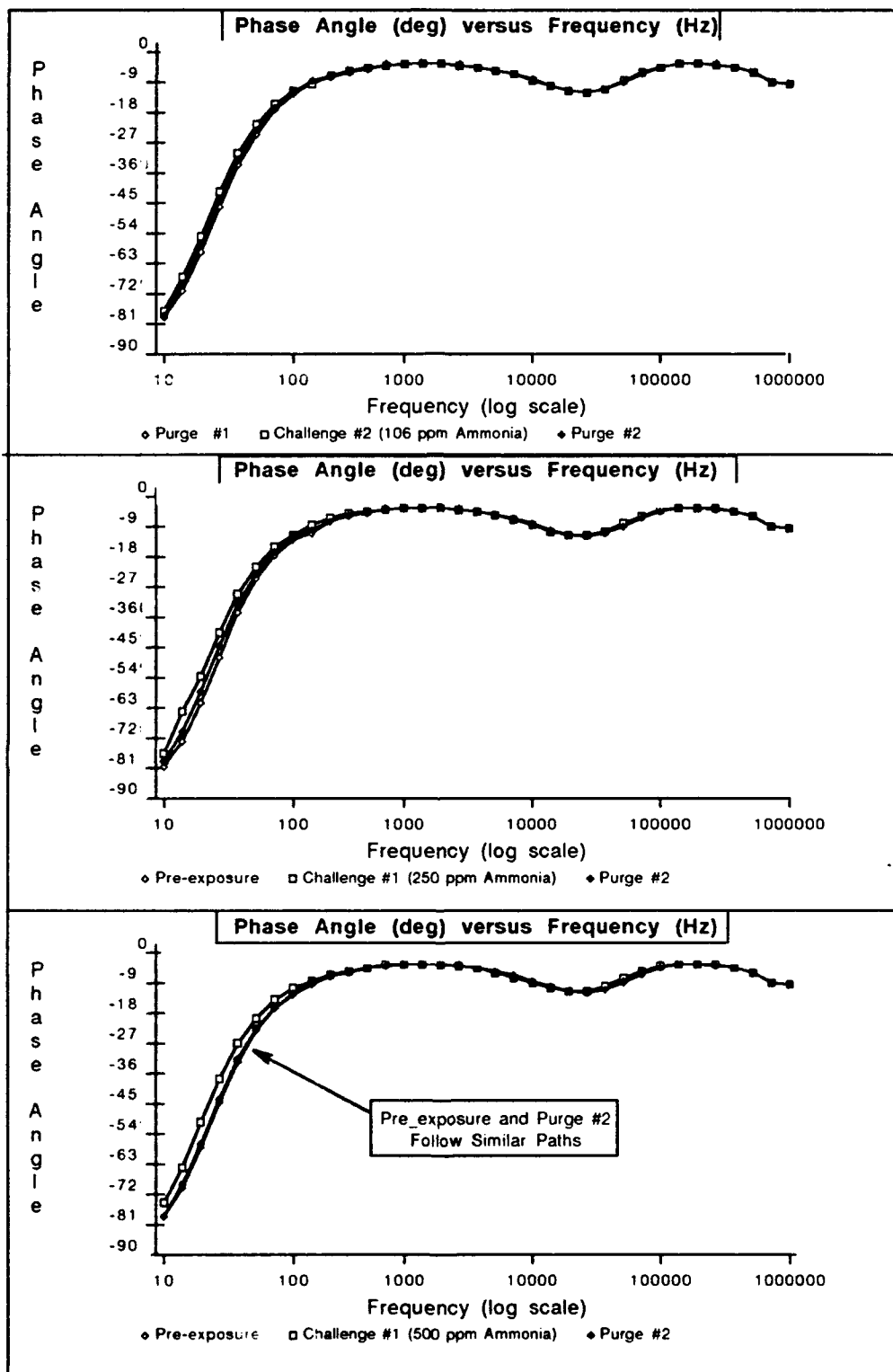


Figure D-80. Phase Angle versus Frequency Response of IGEFET Microsensor for a Series of Room Air Purges and Challenge Gas Exposures. Testing Conditions: IGE Microsensor Number 1; CoPc Thin-film (2,500 Angstroms Thick); Temperature of 150 degrees Centigrade; Ammonia Challenge Gas (Order of Exposures: 500 ppm, 16 ppm, 106 ppm, 250 ppm, 500 ppm).



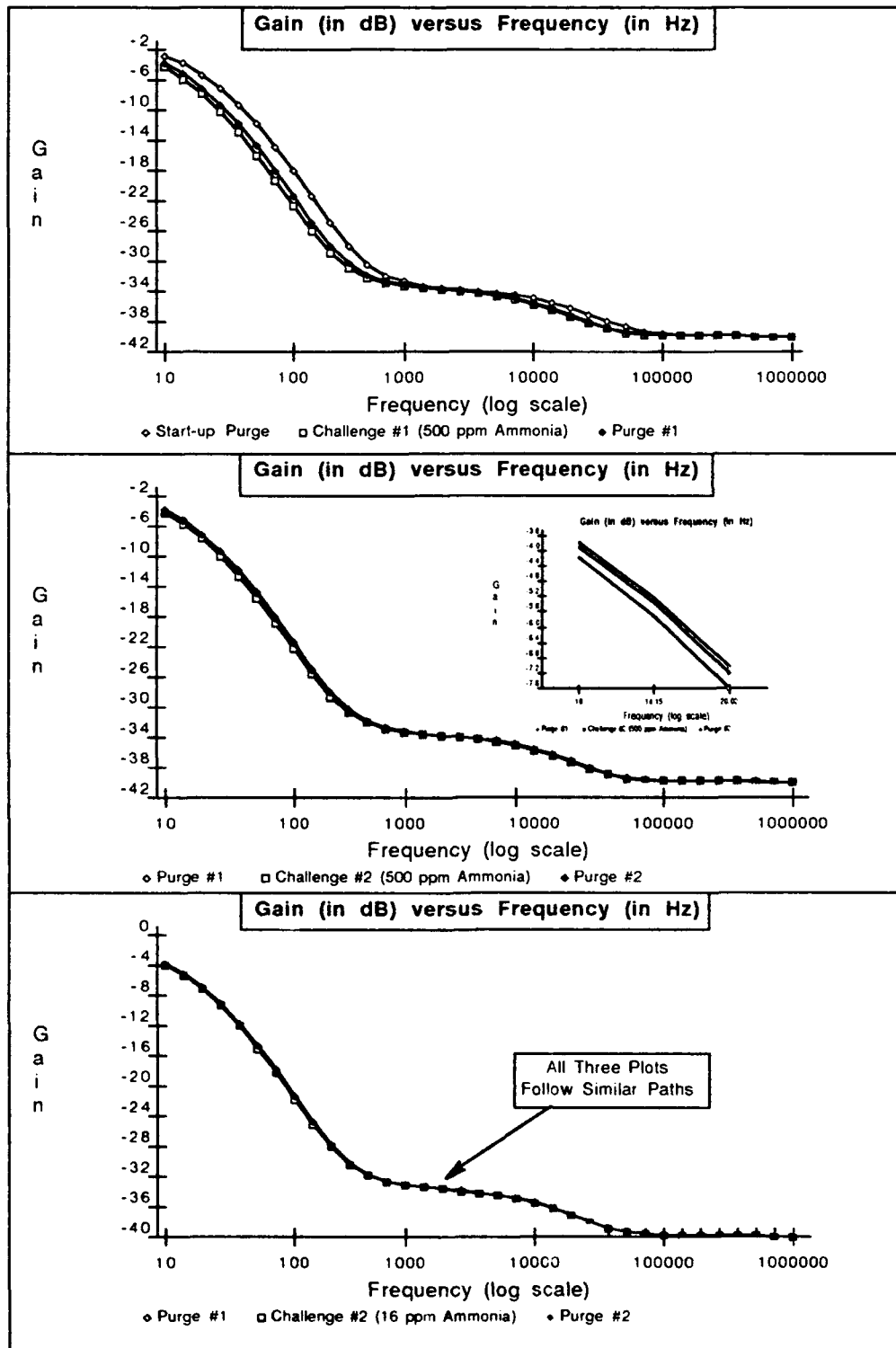


Figure D-81 . Gain versus Frequency Response of IGEFET Microsensor for a Series of Room Air Purges and Challenge Gas Exposures. Testing Conditions: IGE Microsensor Number 4; CoPc Thin-film (5,400 Angstroms Thick); Temperature of 150 degrees Centigrade; Ammonia Challenge Gas (Order of Exposures: 500 ppm, 16 ppm, 106 ppm, . 250 ppm, 500 ppm).

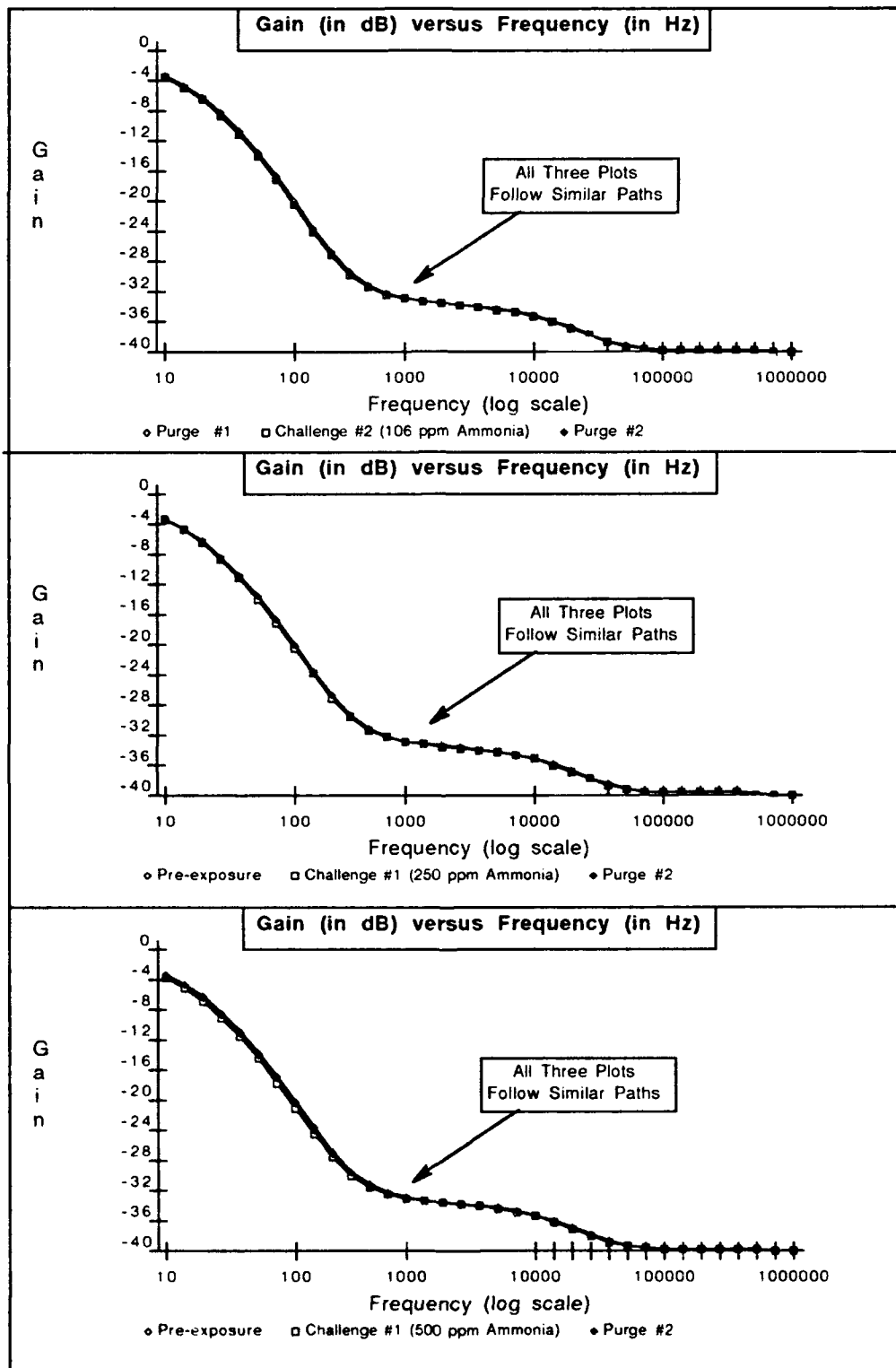


Figure D-82. Gain versus Frequency Response of IGEFET Microsensor for a Series of Room Air Purges and Challenge Gas Exposures. Testing Conditions: IGE Microsensor Number 4; NiPc Thin-film (6,200 Angstroms Thick); Temperature of 150 degrees Centigrade; Ammonia Challenge Gas (Order of Exposures: 500 ppm, 16 ppm, 106 ppm, ., 250 ppm, 500 ppm).

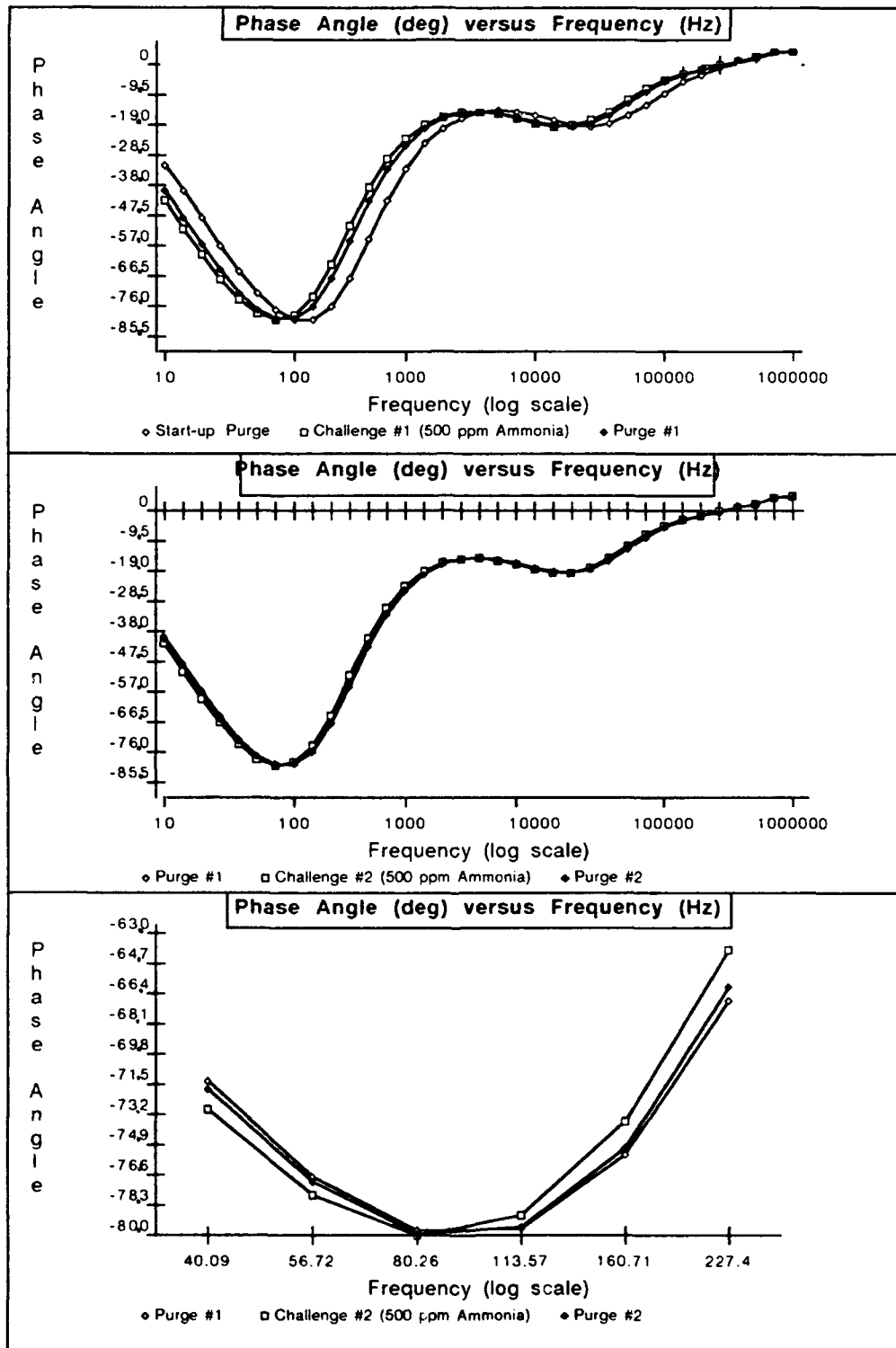


Figure D-83. Phase Angle versus Frequency Response of IGEFET Microsensor for a Series of Room Air Purges and Challenge Gas Exposures. Testing Conditions: IGE Microsensor Number 4; CoPc Thin-film (5,400 Angstroms Thick); Temperature of 150 degrees Centigrade; Ammonia Challenge Gas (Order of Exposures: 500 ppm, 16 ppm, 106 ppm, , 250 ppm, 500 ppm).

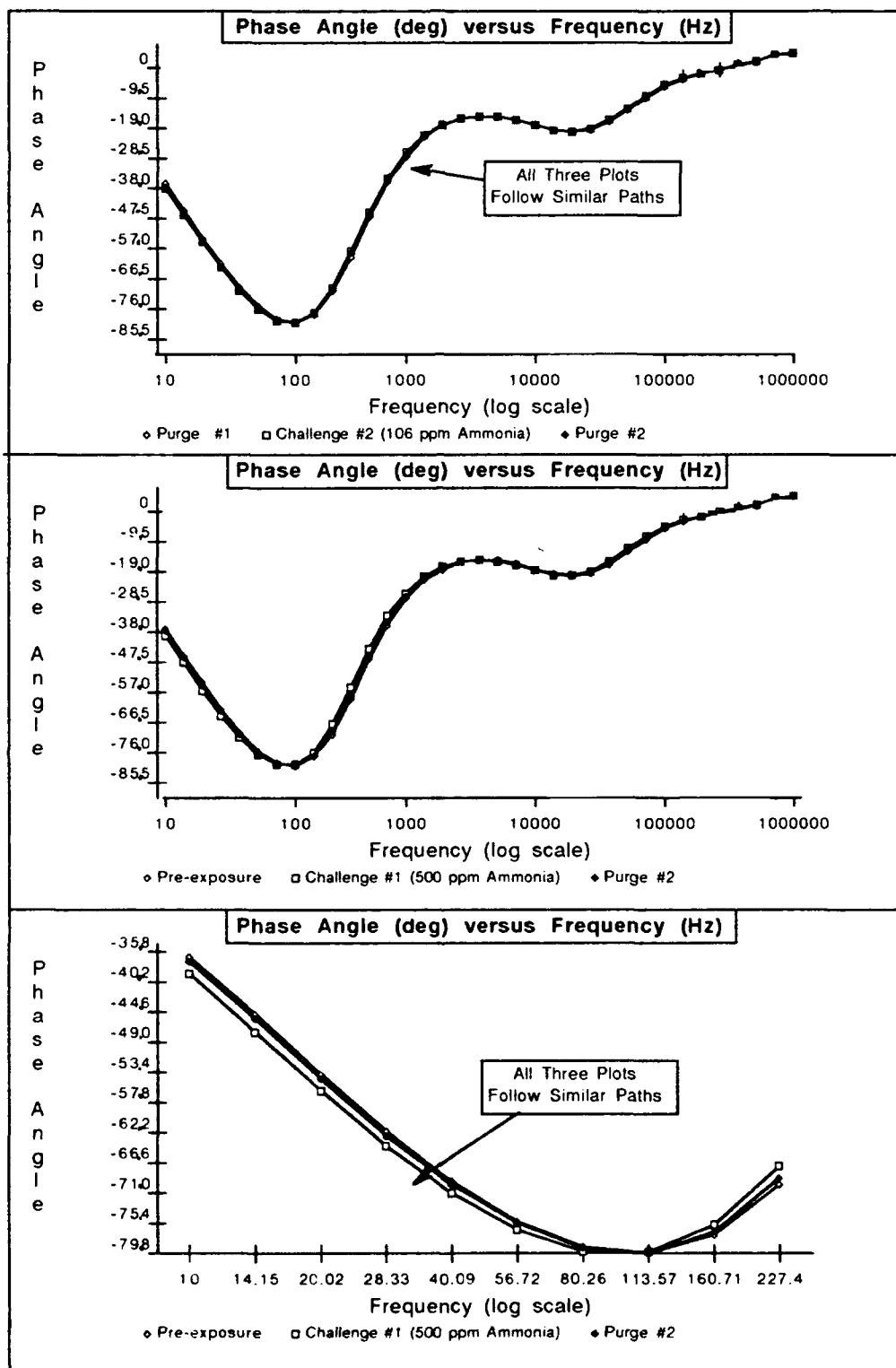


Figure D-84: Phase Angle versus Frequency Response of IGEFET Microsensor for a Series of Room Air Purges and Challenge Gas Exposures. Testing Conditions: IGE Microsensor Number 4; CoPc Thin-film (5,400 Angstroms Thick); Temperature of 150 degrees Centigrade; Ammonia Challenge Gas (Order of Exposures: 500 ppm, 16 ppm, 106 ppm, 250 ppm, 500 ppm)

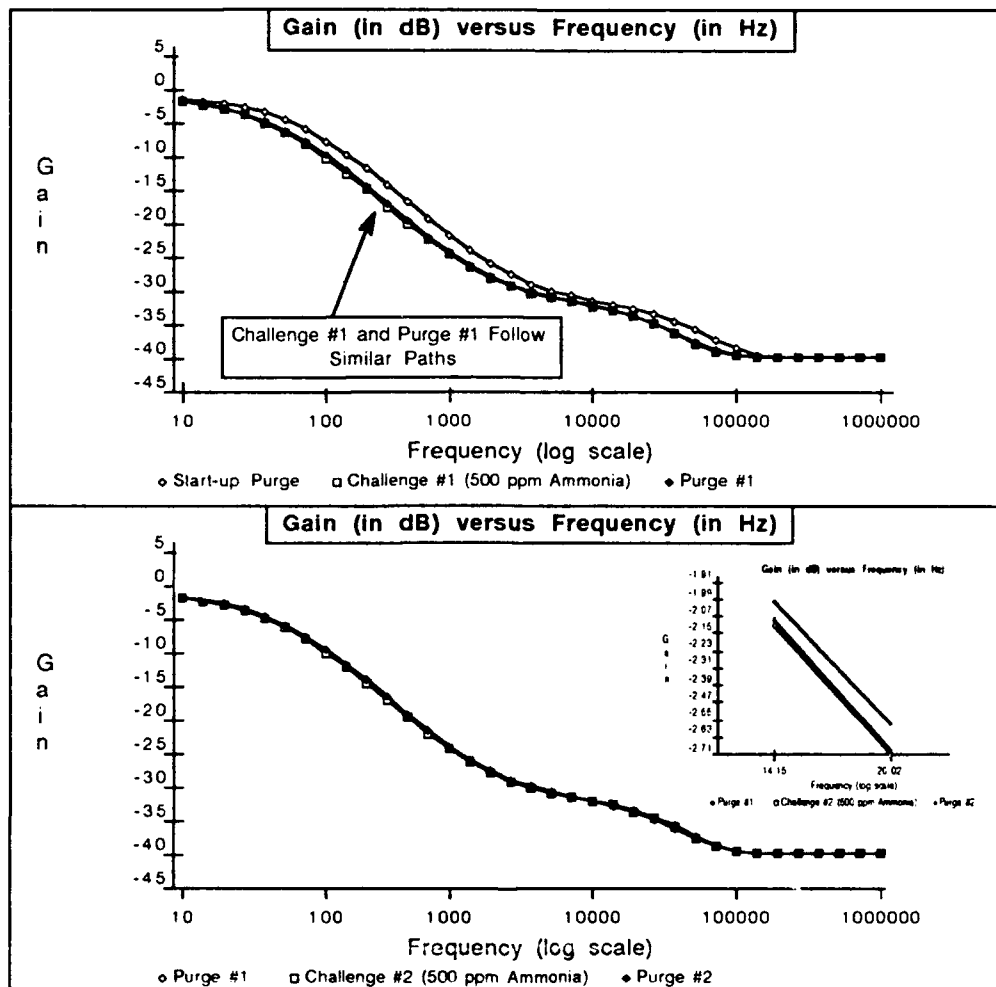


Figure D-85. Gain versus Frequency Response of IGEFET Microsensor for a Series of Room Air Purges and Challenge Gas Exposures. Testing Conditions: IGE Microsensor Number 9; CoPc Thin-film (10,500 Angstroms Thick); Temperature of 150 degrees Centigrade; Ammonia Challenge Gas (Order of Exposures: 500 ppm, 16 ppm, 106 ppm, , 250 ppm, 500 ppm)

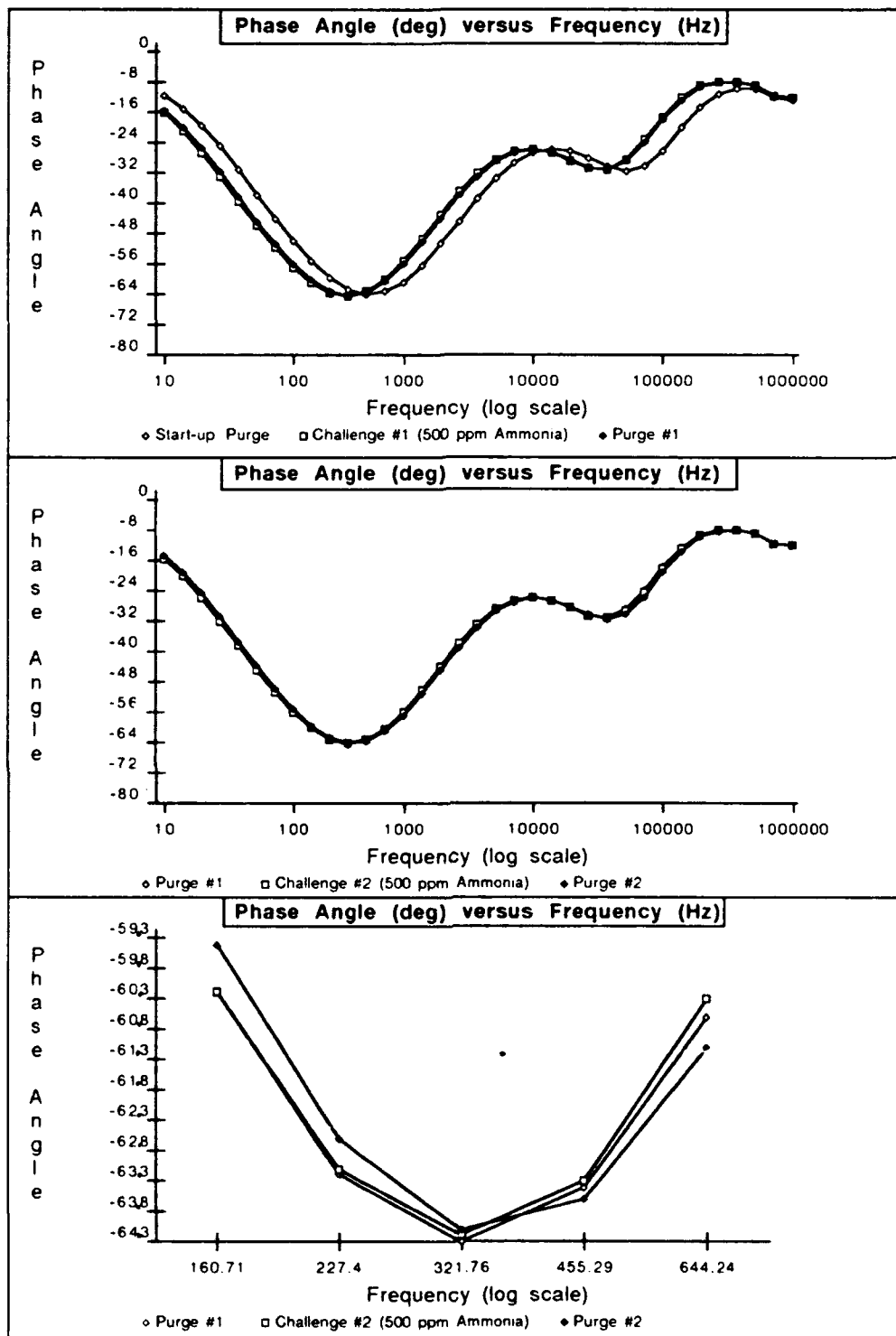


Figure D-86. Phase Angle versus Frequency Response of IGEFET Microsensor for a Series of Room Air Purges and Challenge Gas Exposures. Testing Conditions: IGE Microsensor Number 9; CoPc Thin-film (10,500 Angstroms Thick); Temperature of 150 degrees Centigrade; Ammonia Challenge Gas (Order of Exposures: 500 ppm, 16 ppm, 106 ppm, 250 ppm, 500 ppm).

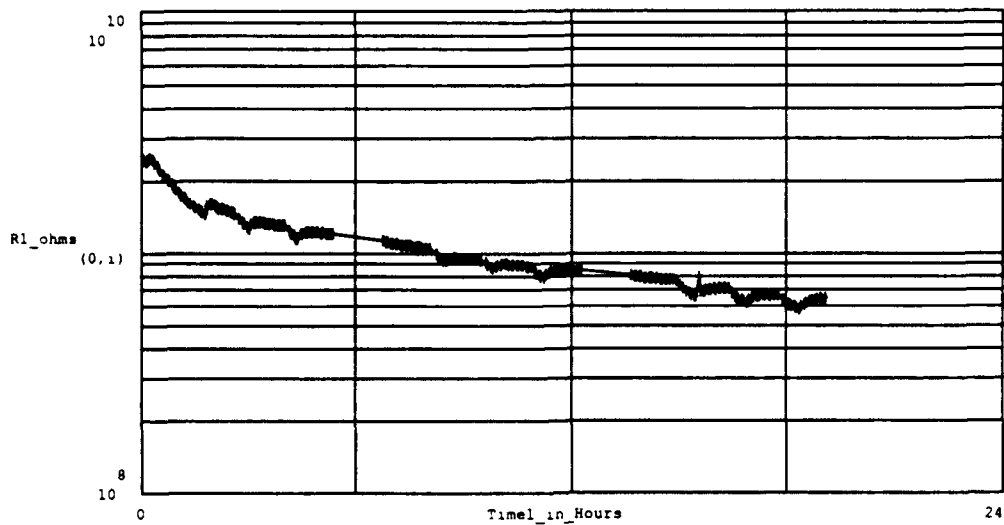


Figure D-57. DC Resistance Measured Between the Driven-Electrode and Floating-Electrode of the IGE Array, During Series of Purges and Challenge Gas Exposures. The Number of Measurements (at crosses) is 237. The Testing Conditions Included the Following:

IGE Array Number : 1,	Thin-film Material : Cobalt Phthalocyanine,
Thin-film Thickness : 2,500 Angstroms	Test Temperature(s) : Purge & Challenge at 150°C
Purge Gas : Room Air,	Challenge Gas : Boron Trifluoride,
Challenge Gas Concentration(s) (in order run) : 24 ppm, 48 ppm.	

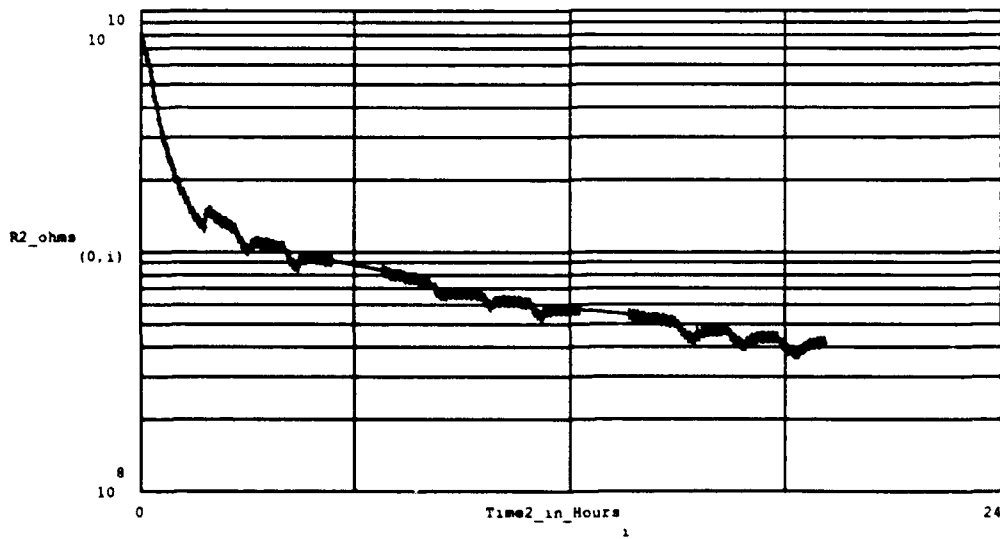


Figure D-58. DC Resistance Measured Between the Driven-Electrode and Floating-Electrode of the IGE Array, During Series of Purges and Challenge Gas Exposures. The Number of Measurements (at crosses) is 237. The Testing Conditions Included the Following:

IGE Array Number : 2,	Thin-film Material : Cobalt Phthalocyanine,
Thin-film Thickness : 2,500 Angstroms	Test Temperature(s) : Purge & Challenge at 150°C
Purge Gas : Room Air,	Challenge Gas : Boron Trifluoride,
Challenge Gas Concentration(s) (in order run) : 24 ppm, 48 ppm.	

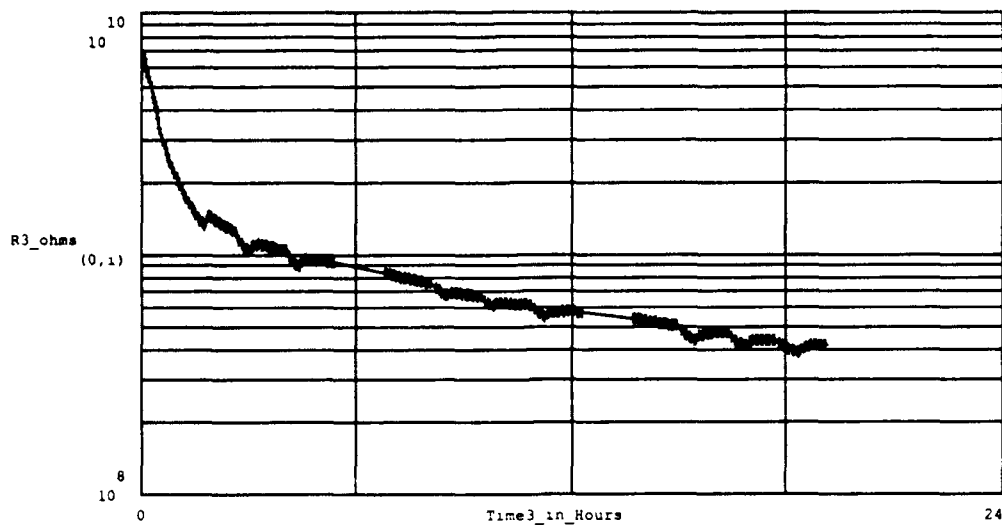


Figure D-59 DC Resistance Measured Between the Driven-Electrode and Floating-Electrode of the IGE Array, During Series of Purges and Challenge Gas Exposures. The Number of Measurements (at crosses) is 237. The Testing Conditions Included the Following:

IGE Array Number : 3,	Thin-film Material : Cobalt Phthalocyanine,
Thin-film Thickness : 2,500 Angstroms	Test Temperature(s) : Purge & Challenge at 150°C
Purge Gas : Room Air,	Challenge Gas : Boron Trifluoride,
Challenge Gas Concentration(s) (in order run) : 24 ppm, 48 ppm.	

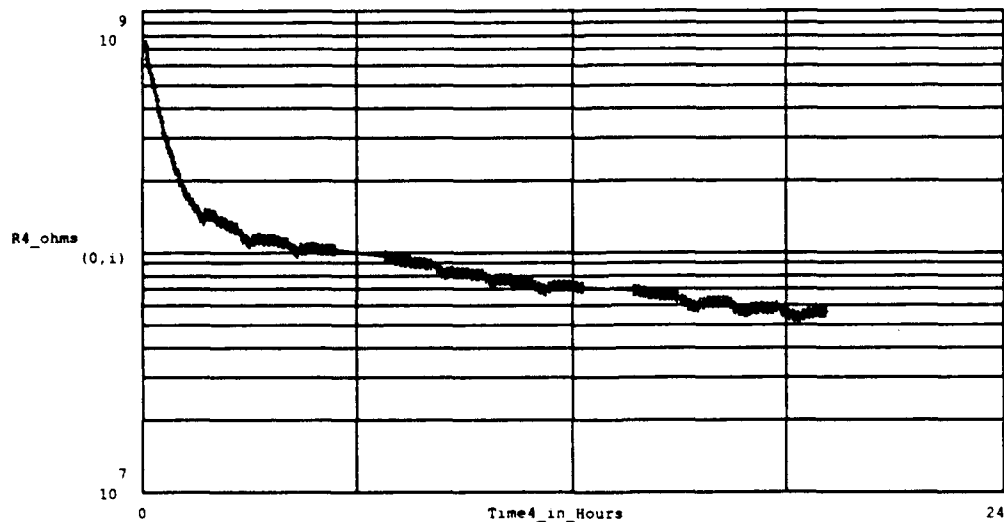


Figure D-60 DC Resistance Measured Between the Driven-Electrode and Floating-Electrode of the IGE Array, During Series of Purges and Challenge Gas Exposures. The Number of Measurements (at crosses) is 237. The Testing Conditions Included the Following:

IGE Array Number : 4,	Thin-film Material : Cobalt Phthalocyanine,
Thin-film Thickness : 5,400 Angstroms	Test Temperature(s) : Purge & Challenge at 150°C
Purge Gas : Room Air,	Challenge Gas : Boron Trifluoride,
Challenge Gas Concentration(s) (in order run) : 24 ppm, 48 ppm.	



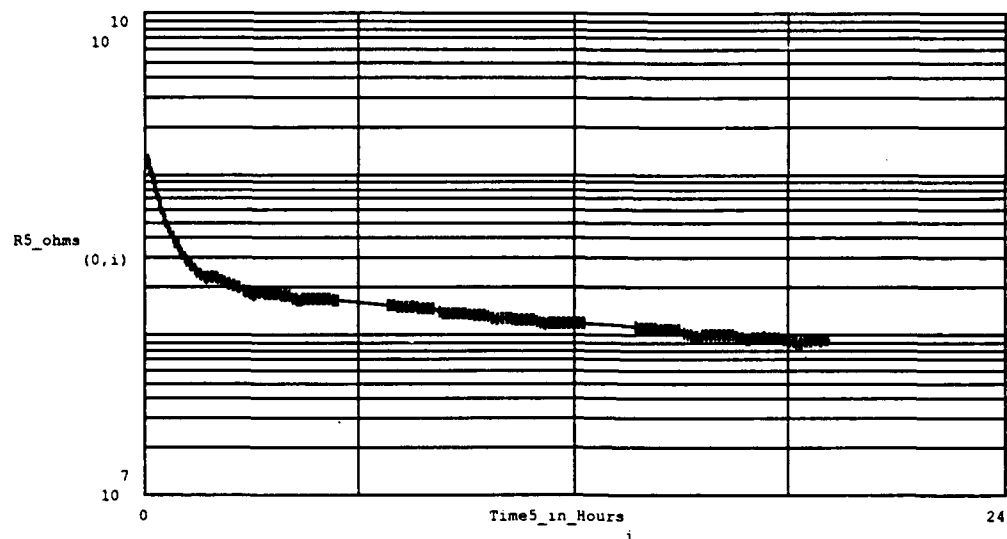


Figure D-91 DC Resistance Measured Between the Driven-Electrode and Floating-Electrode of the IGE Array, During Series of Purges and Challenge Gas Exposures. The Number of Measurements (at crosses) is 237. The Testing Conditions Included the Following:

IGE Array Number : 5,	Thin-film Material : Cobalt Phthalocyanine,
Thin-film Thickness : 5,400 Angstroms	Test Temperature(s) : Purge & Challenge at 150°C
Purge Gas : Room Air,	Challenge Gas : Boron Trifluoride,
Challenge Gas Concentration(s) (in order run) : 24 ppm, 48 ppm.	

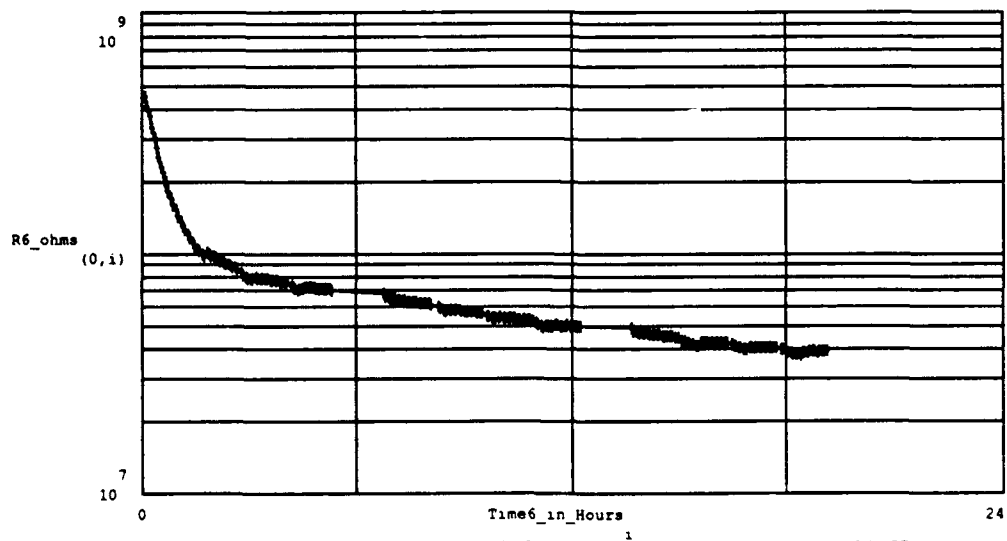


Figure D-92 DC Resistance Measured Between the Driven-Electrode and Floating-Electrode of the IGE Array, During Series of Purges and Challenge Gas Exposures. The Number of Measurements (at crosses) is 237. The Testing Conditions Included the Following:

IGE Array Number : 6,	Thin-film Material : Cobalt Phthalocyanine,
Thin-film Thickness : 10,500 Angstroms	Test Temperature(s) : Purge & Challenge at 150°C
Purge Gas : Room Air,	Challenge Gas : Boron Trifluoride,
Challenge Gas Concentration(s) (in order run) : 24 ppm, 48 ppm.	

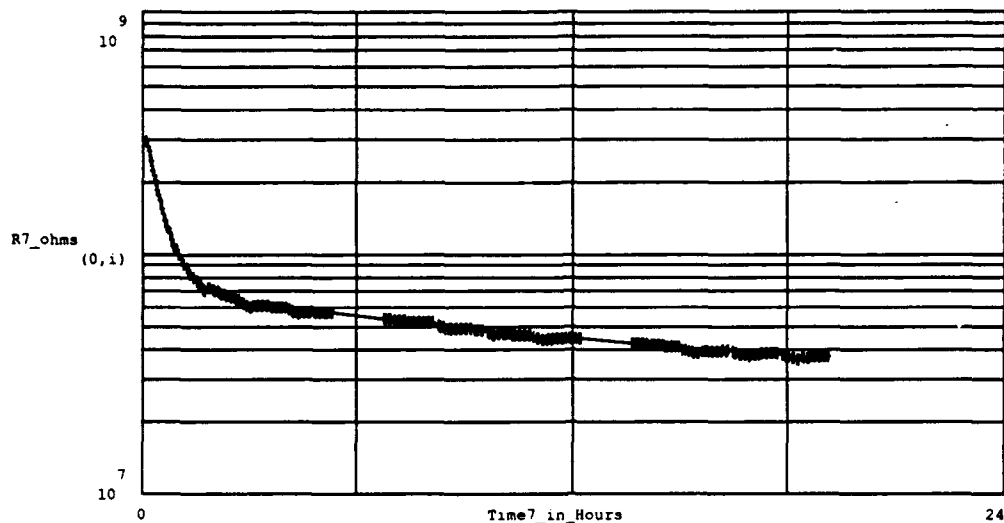


Figure D-93 DC Resistance Measured Between the Driven-Electrode and Floating-Electrode of the IGE Array, During Series of Purges and Challenge Gas Exposures. The Number of Measurements (at crosses) is 237. The Testing Conditions Included the Following:

IGE Array Number : 7,	Thin-film Material : Cobalt Phthalocyanine,
Thin-film Thickness : 10,500 Angstroms	Test Temperature(s) : Purge & Challenge at 150°C
Purge Gas : Room Air,	Challenge Gas : Boron Trifluoride,
Challenge Gas Concentration(s) (in order run) : 24 ppm, 48 ppm.	

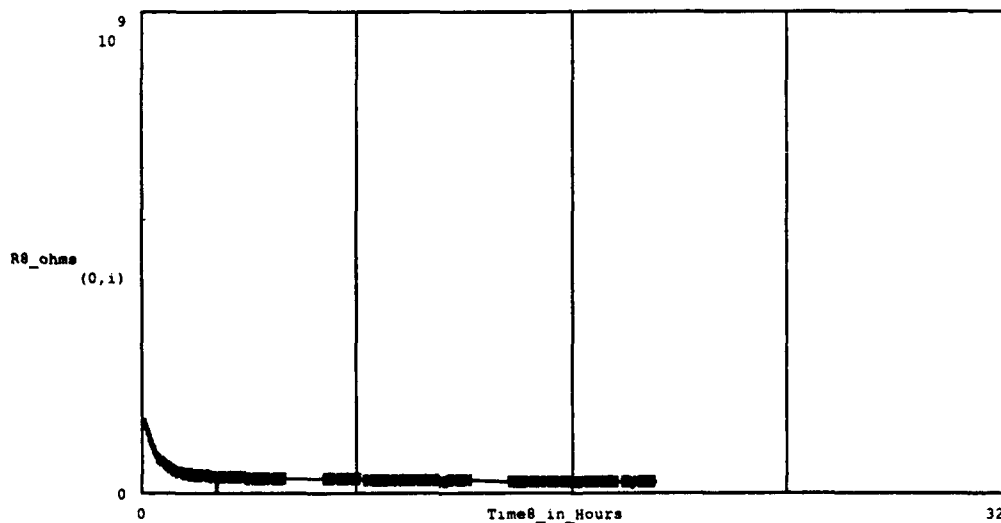


Figure D-94 DC Resistance Measured Between the Driven-Electrode and Floating-Electrode of the IGE Array, During Series of Purges and Challenge Gas Exposures. The Number of Measurements (at crosses) is 237. The Testing Conditions Included the Following:

IGE Array Number : 8,	Thin-film Material : Cobalt Phthalocyanine,
Thin-film Thickness : 10,500 Angstroms	Test Temperature(s) : Purge & Challenge at 150°C
Purge Gas : Room Air,	Challenge Gas : Boron Trifluoride,
Challenge Gas Concentration(s) (in order run) : 24 ppm, 48 ppm.	

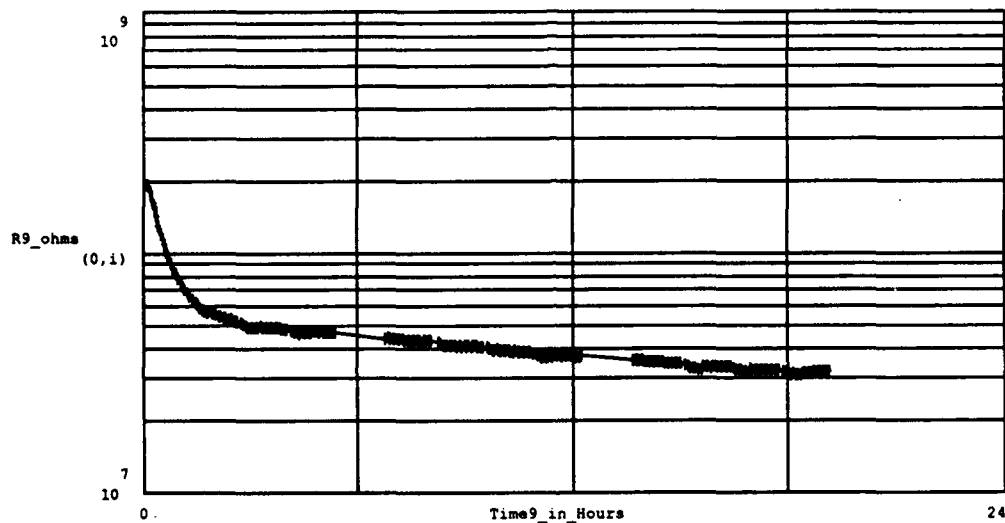


Figure D-95 DC Resistance Measured Between the Driven-Electrode and Floating-Electrode of the IGE Array, During Series of Purges and Challenge Gas Exposures. The Number of Measurements (at crosses) is 237. The Testing Conditions Included the Following:

IGE Array Number : 9,	Thin-film Material : Cobalt Phthalocyanine,
Thin-film Thickness : 10,500 Angstroms	Test Temperature(s) : Purge & Challenge at 150°C
Purge Gas : Room Air,	Challenge Gas : Boron Trifluoride,
Challenge Gas Concentration(s) (in order run) : 24 ppm, 48 ppm.	

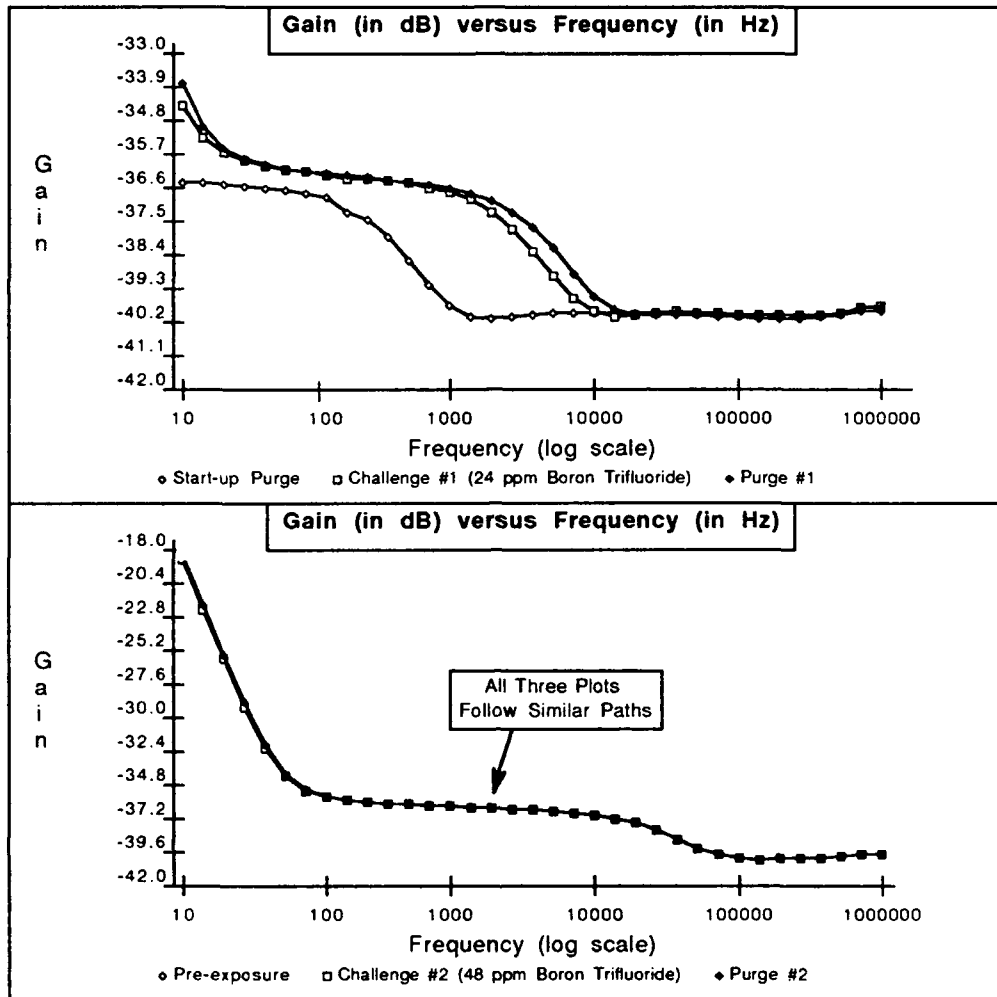


Figure D-96. Gain versus Frequency Response of IGFET Microsensor for a Series of Room Air Purges and Challenge Gas Exposures. Testing Conditions: IGE Microsensor Number 1; CoPc Thin-film (2,500 Angstroms Thick); Temperature of 150 degrees Centigrade; Boron Trifluoride Challenge Gas (Order of Exposures: 24 ppm, 48 ppm).

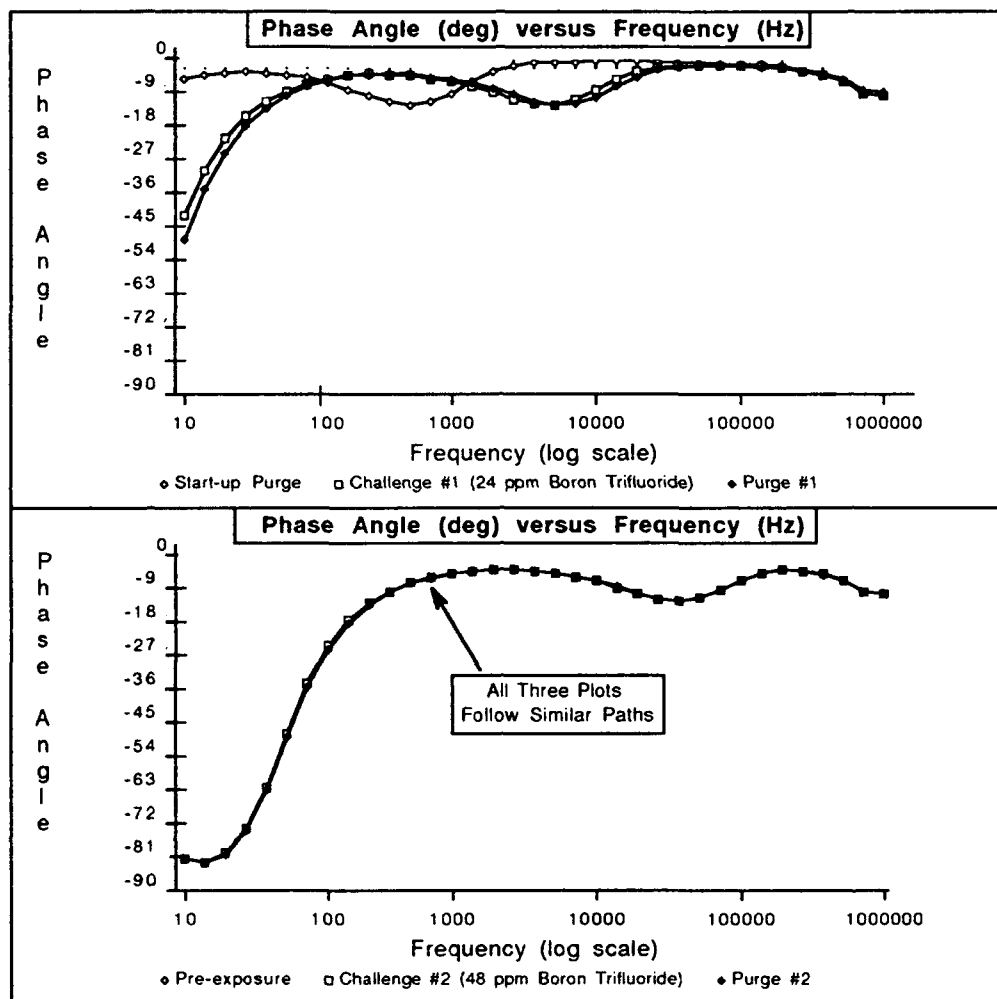


Figure D-97. Phase Angle versus Frequency Response of IGEFET Microsensor for a Series of Room Air Purges and Challenge Gas Exposures. Testing Conditions: IGE Microsensor Number 1; CoPc Thin-film (2,500 Angstroms Thick); Temperature of 150 degrees Centigrade; Boron Trifluoride Challenge Gas (Order of Exposures: 24 ppm, 48 ppm).

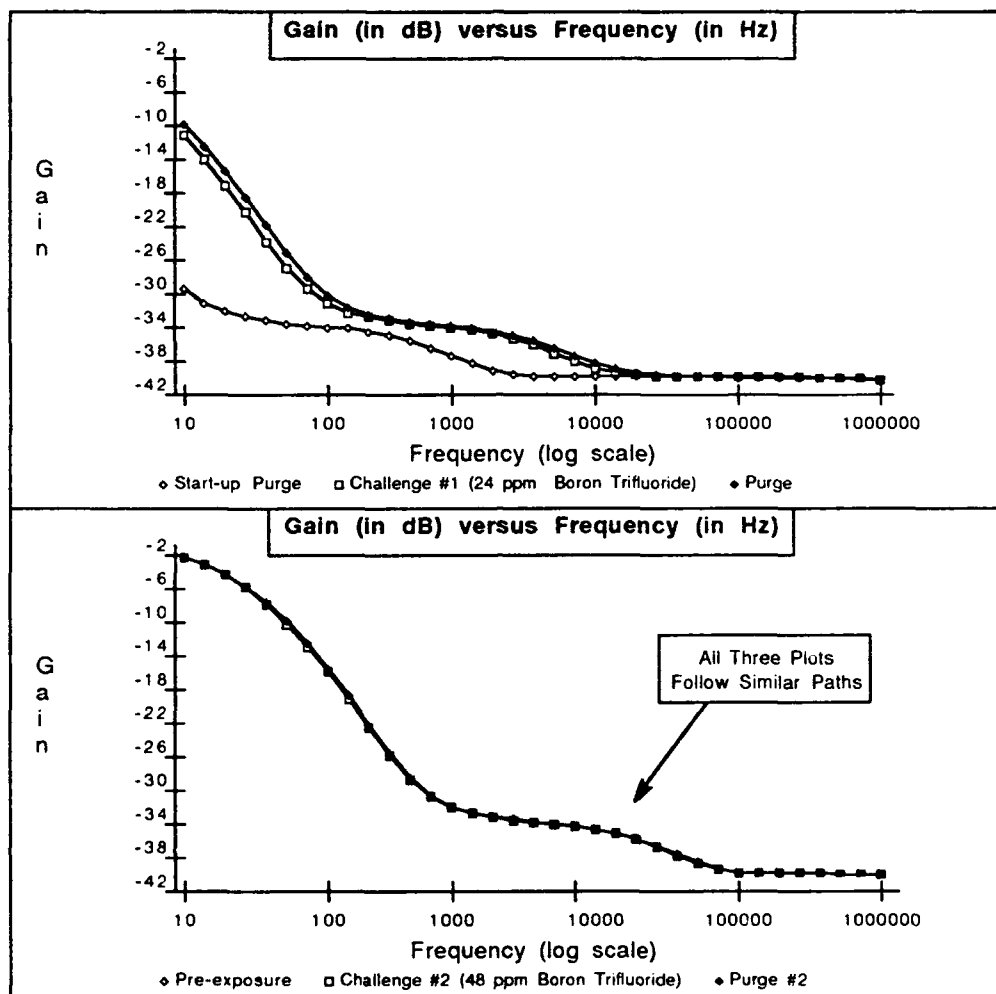


Figure D-98. Gain versus Frequency Response of IGFET Microsensor for a Series of Room Air Purges and Challenge Gas Exposures. Testing Conditions: IGE Microsensor Number 4; CoPc Thin-film (5,400 Angstroms Thick); Temperature of 150 degrees Centigrade; Boron Trifluoride Challenge Gas (Order of Exposures: 24 ppm, 48 ppm).

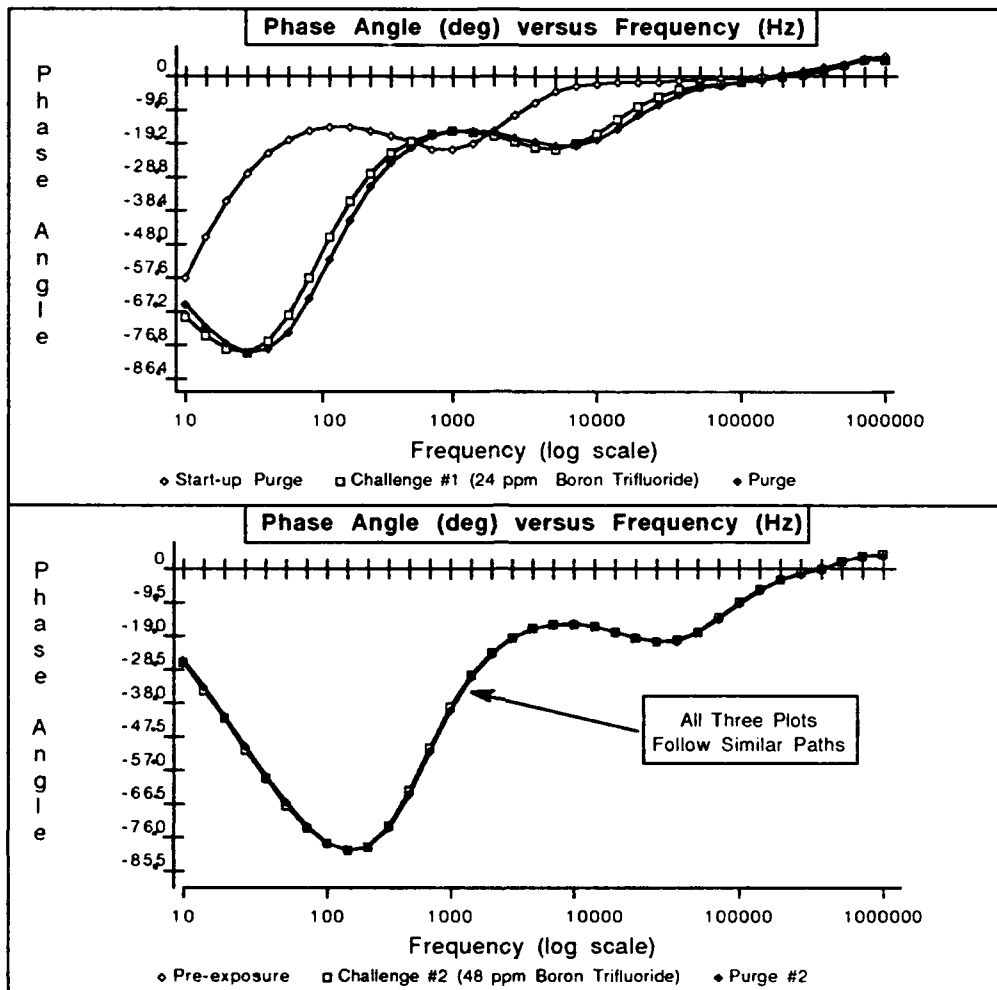


Figure D-99. Phase Angle versus Frequency Response of IGFET Microsensor for a Series of Room Air Purges and Challenge Gas Exposures. Testing Conditions: IGE Microsensor Number 4; CoPc Thin-film (5,400 Angstroms Thick); Temperature of 150 degrees Centigrade; Boron Trifluoride Challenge Gas (Order of Exposures: 24 ppm, 48 ppm).

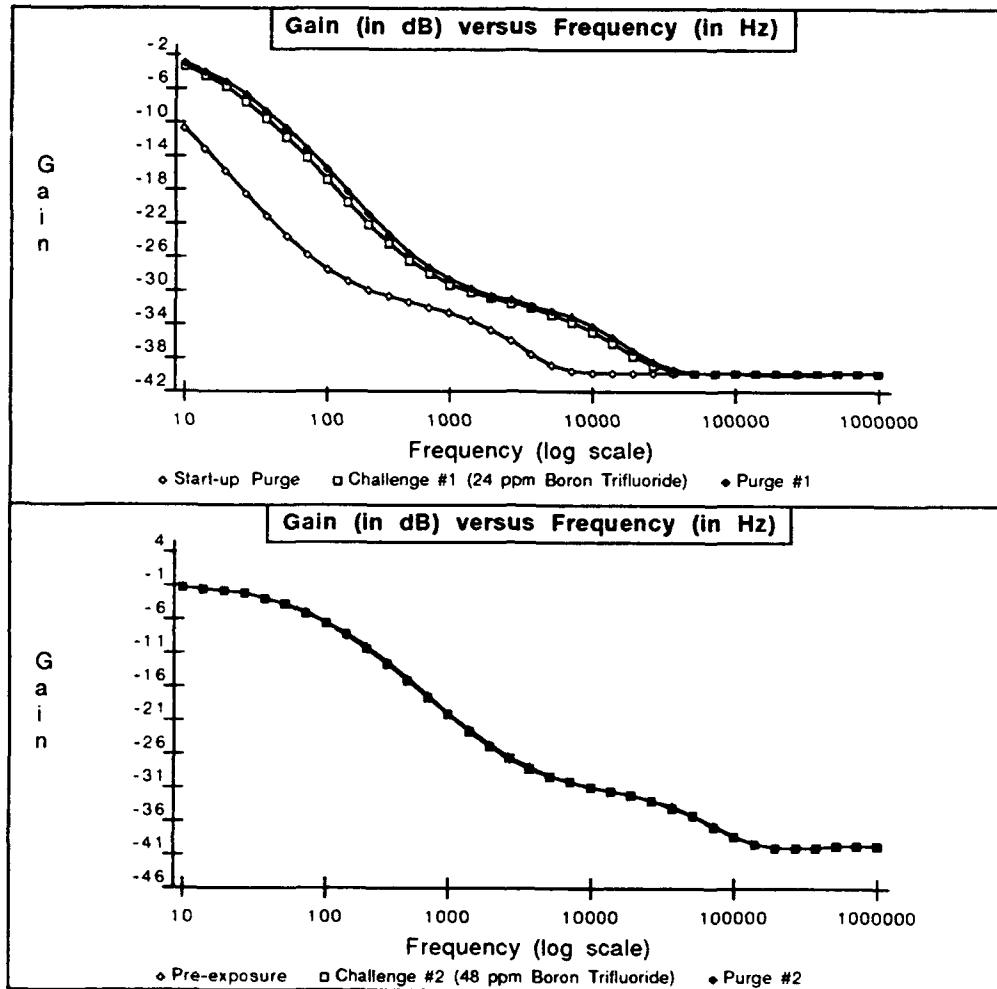
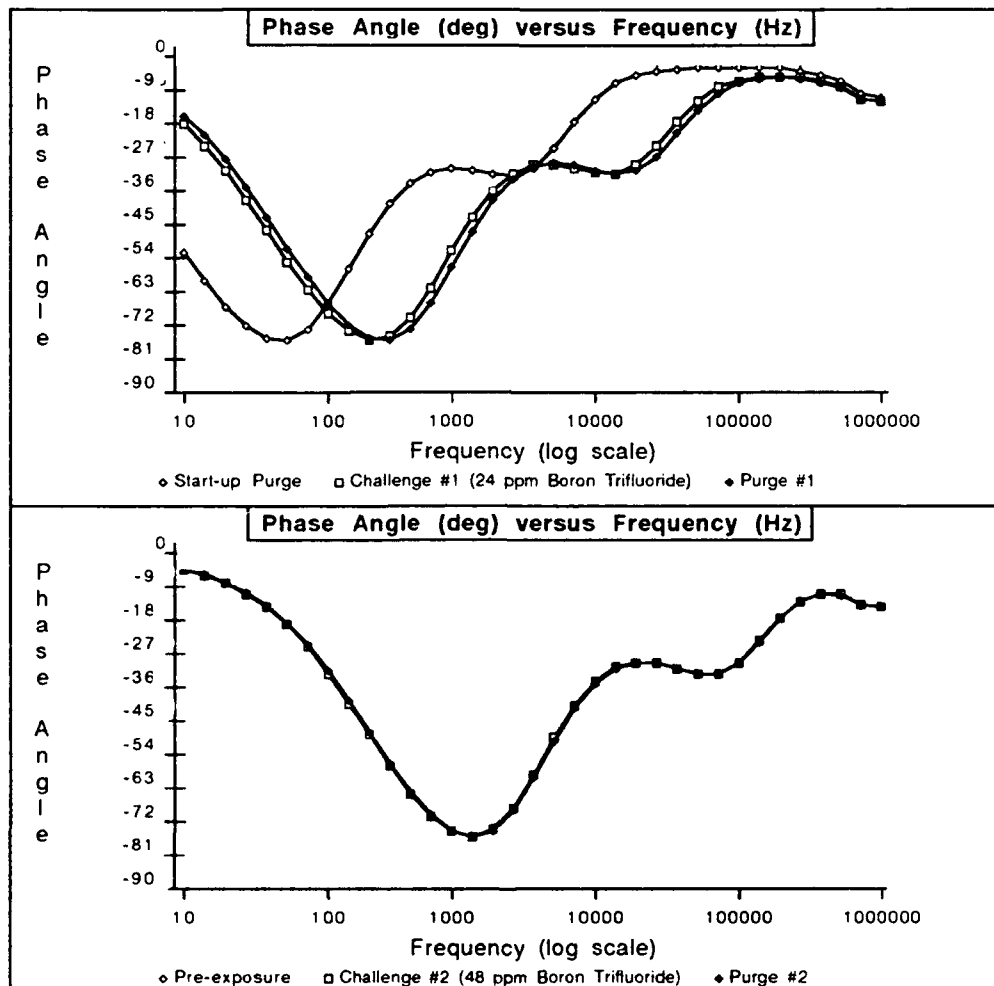


Figure D-100. Gain versus Frequency Response of IGEFET Microsensor for a Series of Room Air Purges and Challenge Gas Exposures. Testing Conditions: IGE Microsensor Number 9; CoPc Thin-film (10,500 Angstroms Thick); Temperature of 150 degrees Centigrade; Ammonia Challenge Gas (Order of Exposures: 24 ppm, 48 ppm).





FigureD-101. Phase Angle versus Frequency Response of IGFET Microsensor for a Series of Room Air Purges and Challenge Gas Exposures. Testing Conditions: IGE Microsensor Number 9; CoPc Thin-film (10,500 Angstroms Thick); Temperature of 150 degrees Centigrade; Ammonia Challenge Gas (Order of Exposures: 24 ppm, 48 ppm).

## *Section 2*

This section summarizes the dc resistance versus time plots for the CoPc films exposed separately to DMMP (Figures D-102 to D-104) and DIMP (Figures D-105 to D-107) at three temperatures: 150°C; 90°C, and 30°C.

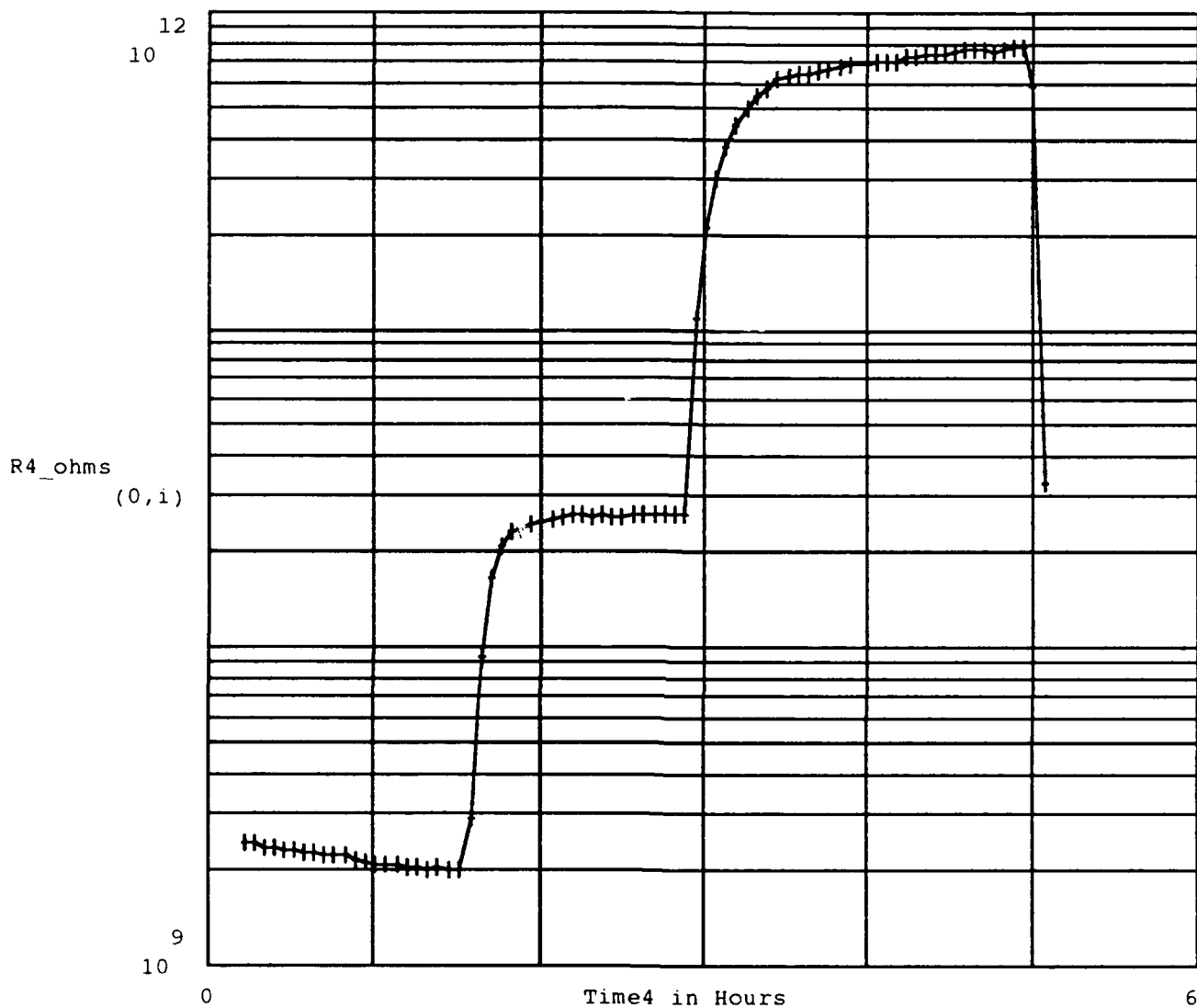


Figure D-102 . DC Resistance Measured Between the Driven-Electrode and Floating-Electrode of the IGE Array, During Series of Purges and Challenge Gas Exposures. The Testing Conditions Included the Following:

IGE Array Number : 4,  
 Thin-film Material : Cobalt Phthalocyanine,  
 Thin-film Thickness : 5200 Angstroms  
 Test Temperature(s) : Initial Purge & Challenge at 150°C, Second Purge  
 & Challenge at 90°C, Third Purge and Challenge at 30°C,  
 Purge Gas : Room Air,  
 Challenge Gas : DMMP,  
 Challenge Gas Concentration(s) (in order run) : 10 ppm.

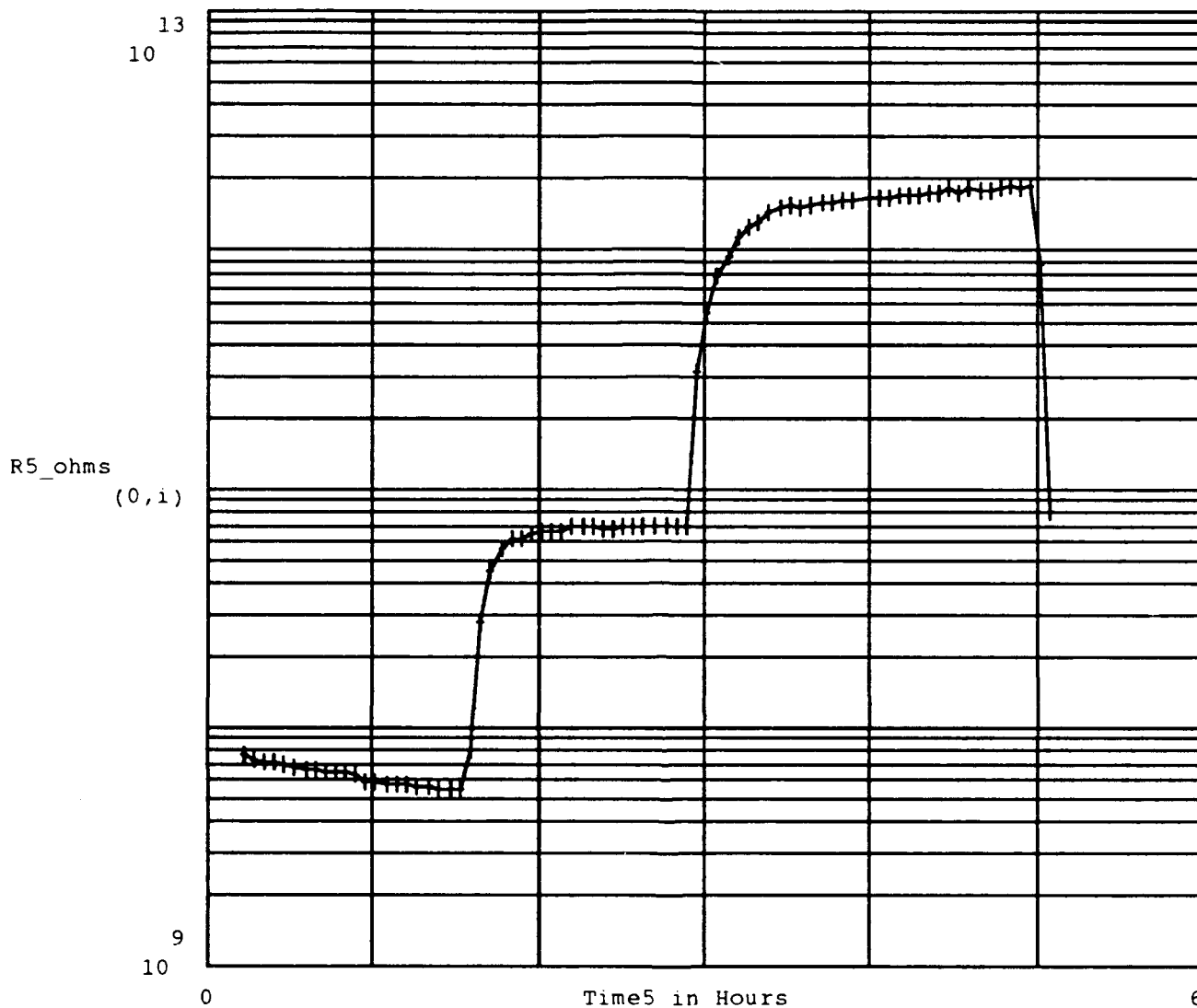


Figure D- 103. DC Resistance Measured Between the Driven-Electrode and Floating-Electrode of the IGE Array, During Series of Purges and Challenge Gas Exposures. The Testing Conditions Included the Following:

IGE Array Number : 5,  
 Thin-film Material : Cobalt Phthalocyanine,  
 Thin-film Thickness : 5200 Angstroms  
 Test Temperature(s) : Initial Purge & Challenge at 150°C, Second Purge  
 & Challenge at 90°C, Third Purge and Challenge at 30°C,  
 Purge Gas : Room Air,  
 Challenge Gas : DMMP,  
 Challenge Gas Concentration(s) (in order run) : 10 ppm.

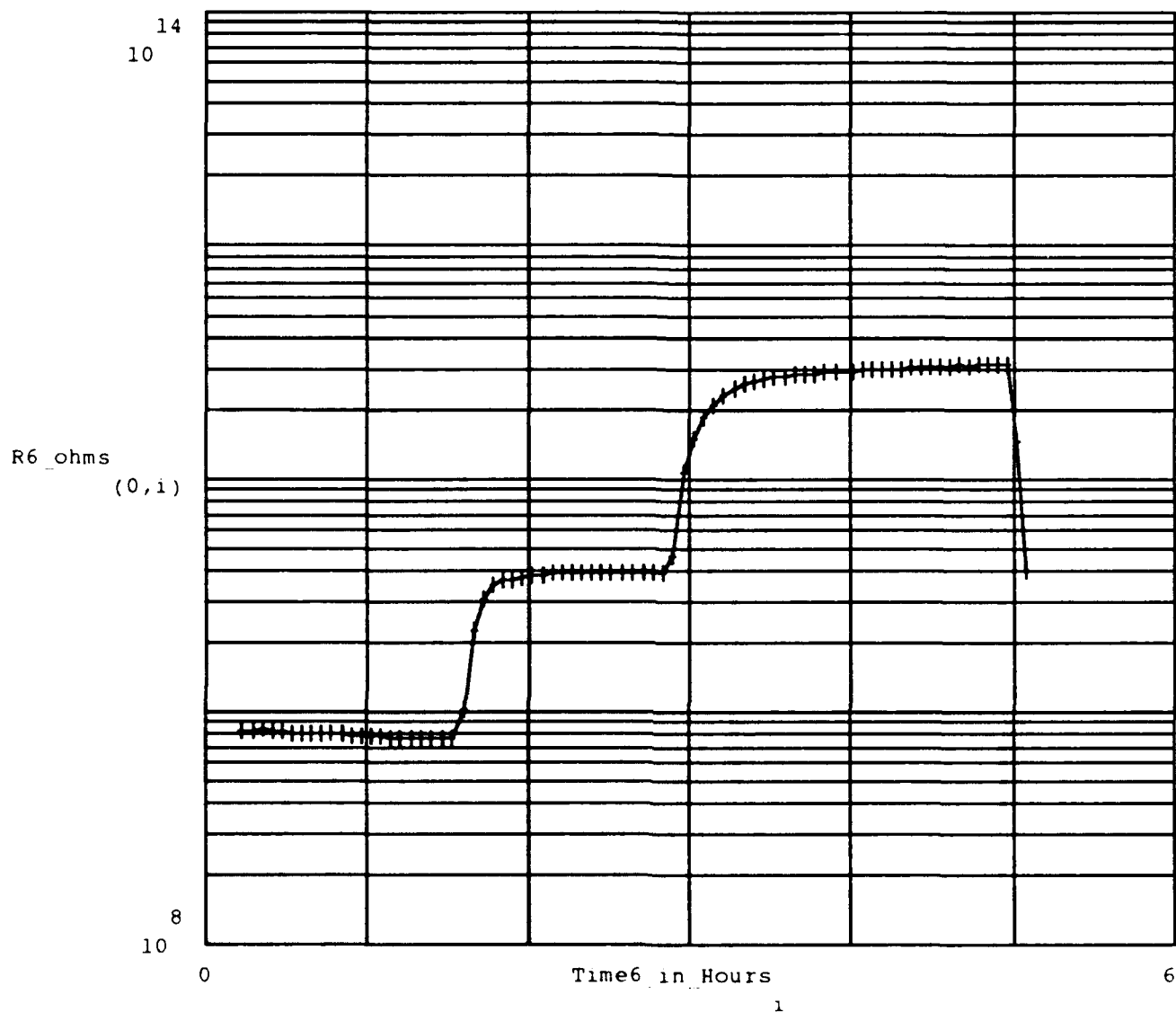


Figure D- 104. DC Resistance Measured Between the Driven-Electrode and Floating-Electrode of the IGE Array, During Series of Purges and Challenge Gas Exposures. The Testing Conditions Included the Following:

IGE Array Number : 6,  
 Thin-film Material : Cobalt Phthalocyanine,  
 Thin-film Thickness : 5200 Angstroms  
 Test Temperature(s) : Initial Purge & Challenge at 150°C, Second Purge  
 & Challenge at 90°C, Third Purge and Challenge at 30°C,  
 Purge Gas : Room Air,  
 Challenge Gas : DMMP,  
 Challenge Gas Concentration(s) (in order run) : 10 ppm.

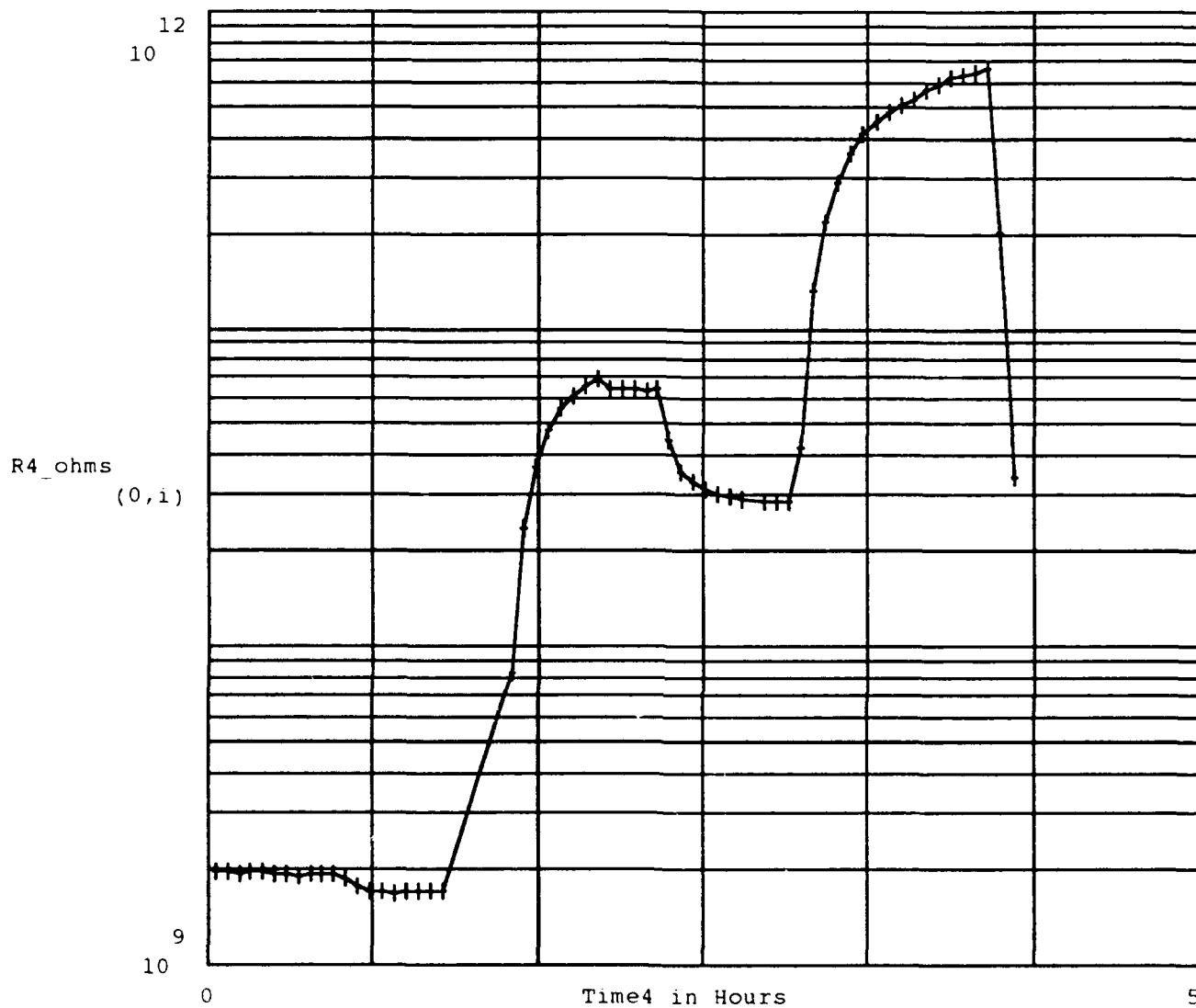


Figure D105 . DC Resistance Measured Between the Driven-Electrode and Floating-Electrode of the IGE Array, During Series of Purges and Challenge Gas Exposures. The Testing Conditions Included the Following:

IGE Array Number : 4,  
 Thin-film Material : Cobalt Phthalocyanine.  
 Thin-film Thickness : 5200 Angstroms  
 Test Temperature(s) : Initial Purge & Challenge at 150°C, Second Purge  
 & Challenge at 90°C, Third Purge and Challenge at 30°C,  
 Purge Gas : Room Air,  
 Challenge Gas : DIMP,  
 Challenge Gas Concentration(s) (in order run) : 3 ppm.

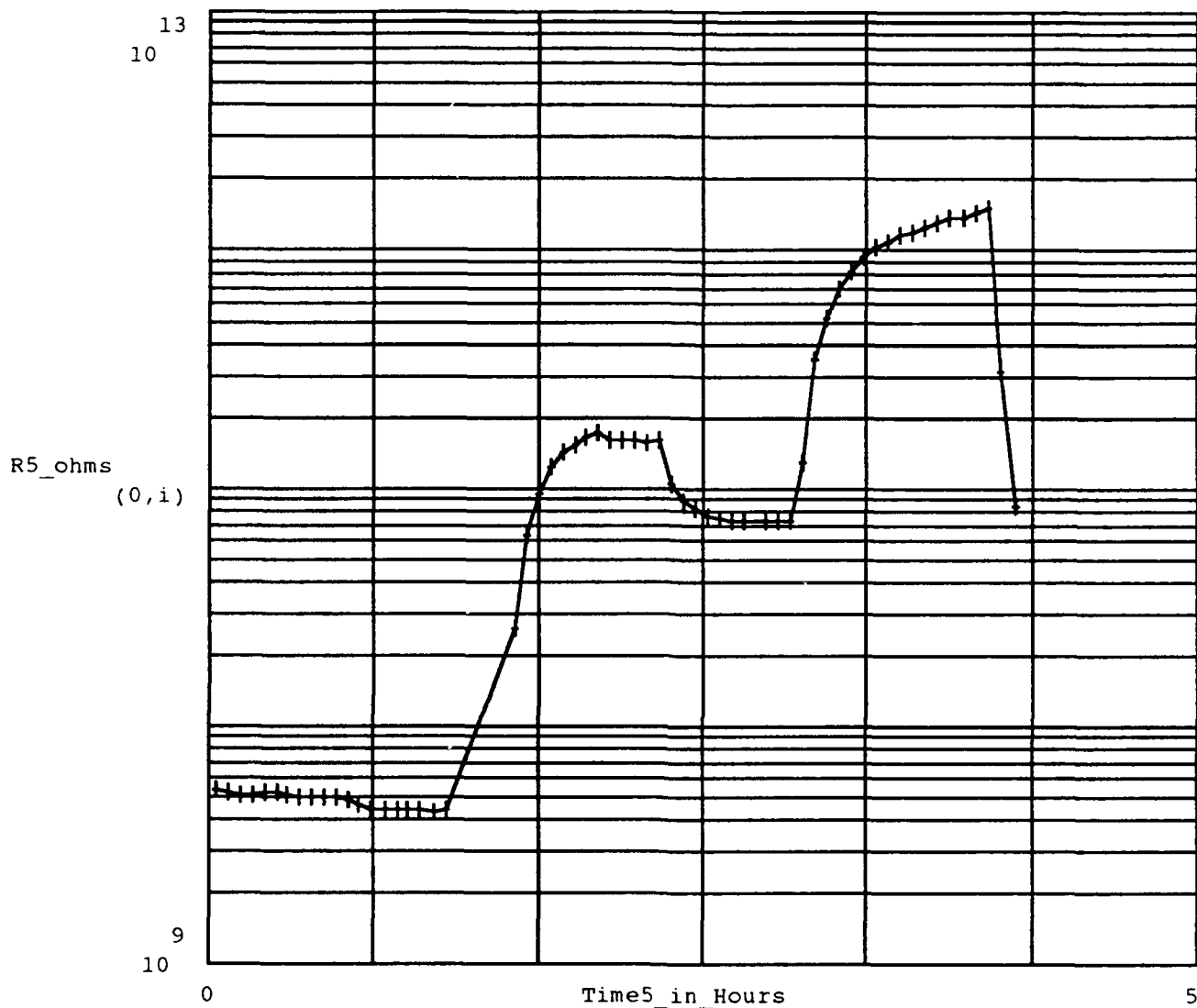


Figure D-106 . DC Resistance Measured Between the Driven-Electrode and Floating-Electrode of the IGE Array, During Series of Purges and Challenge Gas Exposures. The Testing Conditions Included the Following:

IGE Array Number : 5,  
 Thin-film Material : Cobalt Phthalocyanine,  
 Thin-film Thickness : 5200 Angstroms  
 Test Temperature(s) : Initial Purge & Challenge at 150°C, Second Purge  
 & Challenge at 90°C, Third Purge and Challenge at 30°C,  
 Purge Gas : Room Air,  
 Challenge Gas : DIMP,  
 Challenge Gas Concentration(s) (in order run) : 3 ppm.

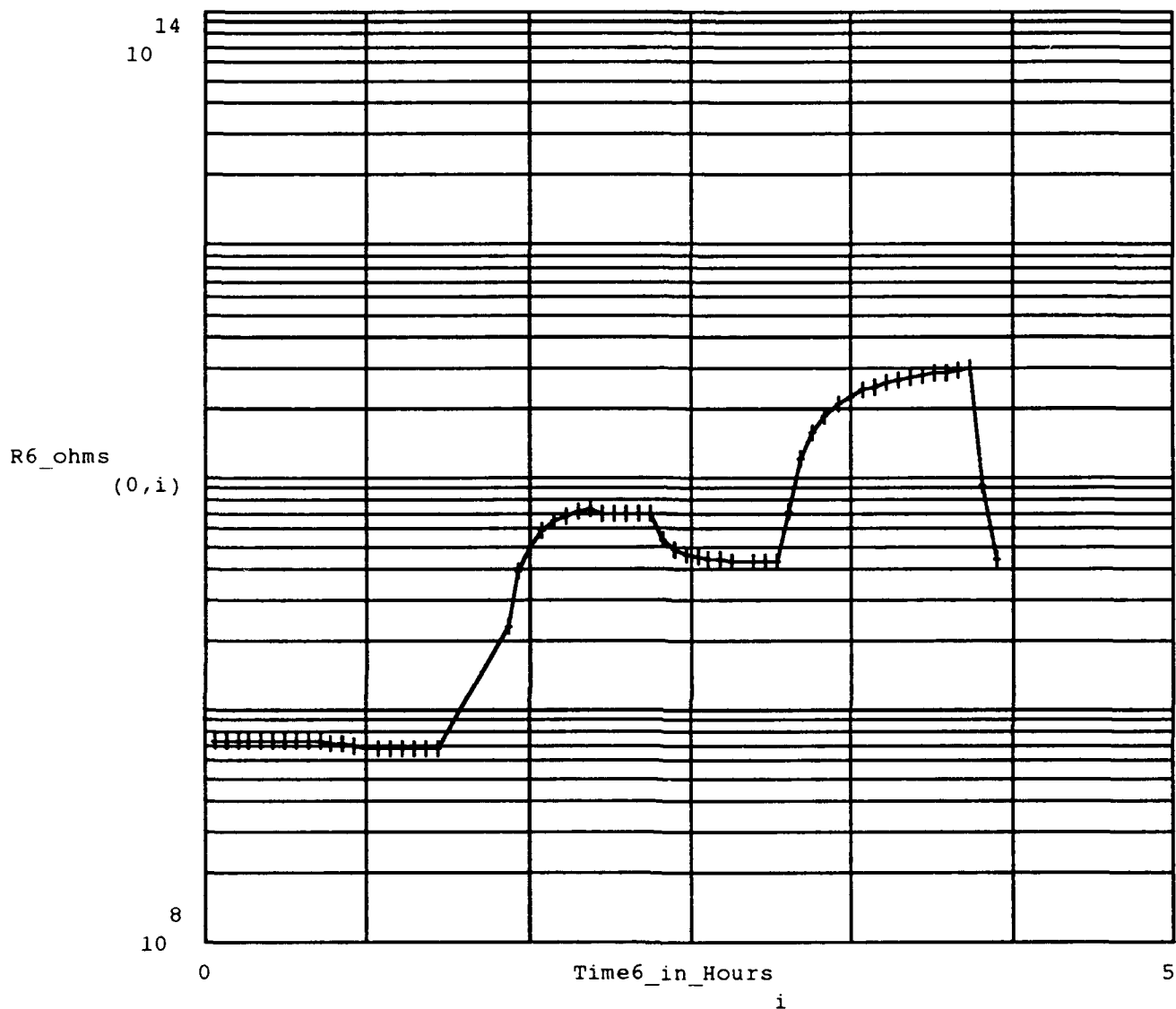


Figure D-107 . DC Resistance Measured Between the Driven-Electrode and Floating-Electrode of the IGE Array, During Series of Purges and Challenge Gas Exposures. The Testing Conditions Included the Following:

IGE Array Number : 6,  
 Thin-film Material : Cobalt Phthalocyanine,  
 Thin-film Thickness : 5200 Angstroms  
 Test Temperature(s) : Initial Purge & Challenge at 150°C, Second Purge  
 & Challenge at 90°C, Third Purge and Challenge at 30°C,  
 Purge Gas : Room Air,  
 Challenge Gas : DIMP,  
 Challenge Gas Concentration(s) (in order run) : 3 ppm.



## *Appendix E: Response of NiPc Thin-Film Coatings.*

This appendix presents a portion of the significant responses to the challenge gases for the NiPc thin-films evaluated during this investigation. The appendix is divided into two sections: Section 1 deals with the responses to challenge gases at 150°C (referred to as the Series II tests in the thesis body); Section 2 presents information concerning DMMP and DIMP challenges to NiPc at temperatures of 150°C, 90°C, and 30°C.

### *Section 1*

Resistance and gain and phase angle transfer function responses for the challenge and purge cycles are provided as:

- NiPc challenged with NO<sub>2</sub> (Figures E-1 to E-21),
  - dc resistance measurements versus time,
  - gain and phase angle measurements versus frequency,
  - sensitivity, and reversibility calculations versus frequency,
- NiPc challenged with NH<sub>3</sub> (Figures E-22 to E-36),
  - dc resistance measurements versus time,
  - gain and phase angle measurements versus frequency,
- NiPc challenged with BF<sub>3</sub> (Figures E-37 to E-51),
  - dc resistance measurements versus time,
  - gain and phase angle measurements versus frequency,

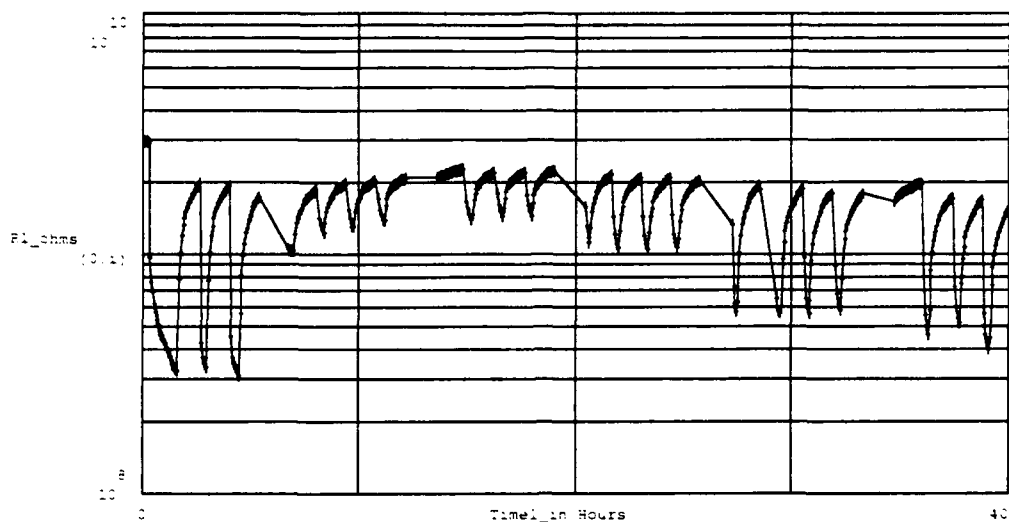


Figure E- 1 : DC Resistance Measured Between the Driven-Electrode and Floating-Electrode of the IGE Array. During Series of Purges and Challenge Gas Exposures. The Number of Measurements Plotted (at crosses) is 479. The Testing Conditions Included the Following:

IGE Array Number : 1.	Thin-film Material : Nickel Phthalocyanine.
Thin-film Thickness : 2,600 Angstroms	Test Temperature(s) : Purge & Challenge at 150°C
Purge Gas : Room Air.	Challenge Gas : NO <sub>2</sub> .
Challenge Gas Concentration(s) (in order run) : 1000 ppb, 30 ppb, 50 ppb, 100 ppb, 500 ppb, 1000 ppb.	

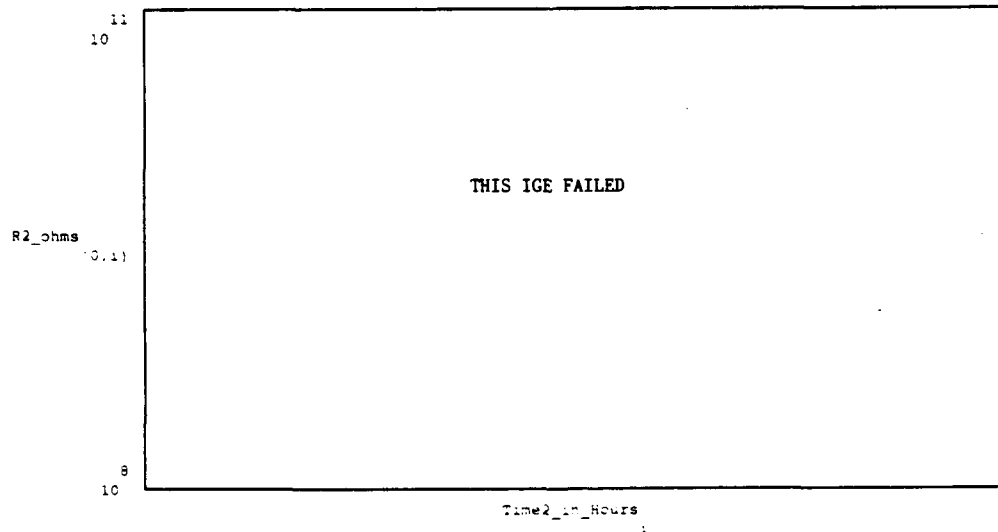


Figure E- 2 : DC Resistance Measured Between the Driven-Electrode and Floating-Electrode of the IGE Array. During Series of Purges and Challenge Gas Exposures. The Number of Measurements Plotted (at crosses) is 479. The Testing Conditions Included the Following:

IGE Array Number : 2.	Thin-film Material : Nickel Phthalocyanine.
Thin-film Thickness : 2,600 Angstroms	Test Temperature(s) : Purge & Challenge at 150°C
Purge Gas : Room Air.	Challenge Gas : NO <sub>2</sub> .
Challenge Gas Concentration(s) (in order run) : 1000 ppb, 30 ppb, 50 ppb, 100 ppb, 500 ppb, 1000 ppb.	

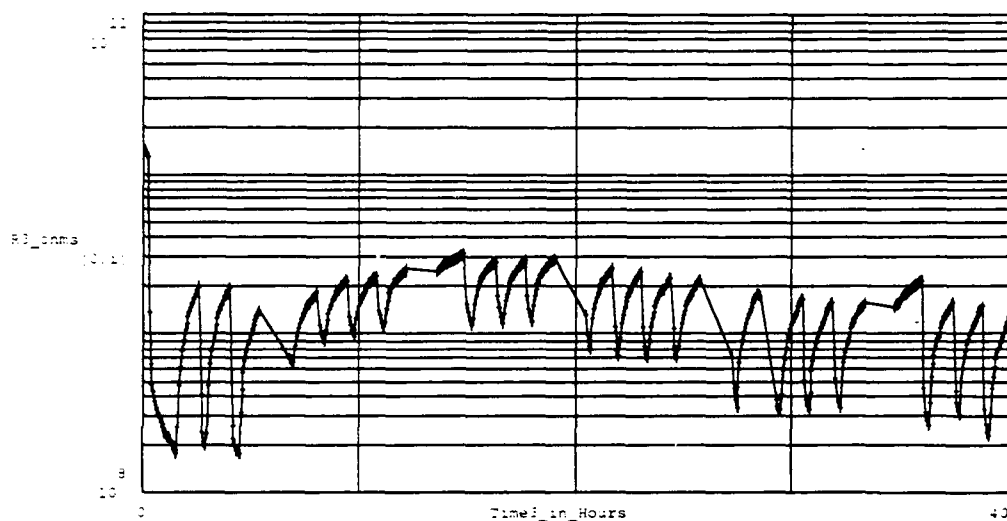


Figure E- 3 . DC Resistance Measured Between the Driven-Electrode and Floating-Electrode of the IGE Array, During Series of Purges and Challenge Gas Exposures. The Number of Measurements Plotted (at crosses) is 479. The Testing Conditions Included the Following:

IGE Array Number : 3,	Thin-film Material : Nickel Phthalocyanine,
Thin-film Thickness : 2,600 Angstroms	Test Temperature(s) : Purge & Challenge at 150°C
Purge Gas : Room Air,	Challenge Gas : NO <sub>2</sub> .
Challenge Gas Concentration(s) (in order run) : 1000 ppb, 30 ppb, 50 ppb, 100 ppb, 500 ppb, 1000 ppb.	

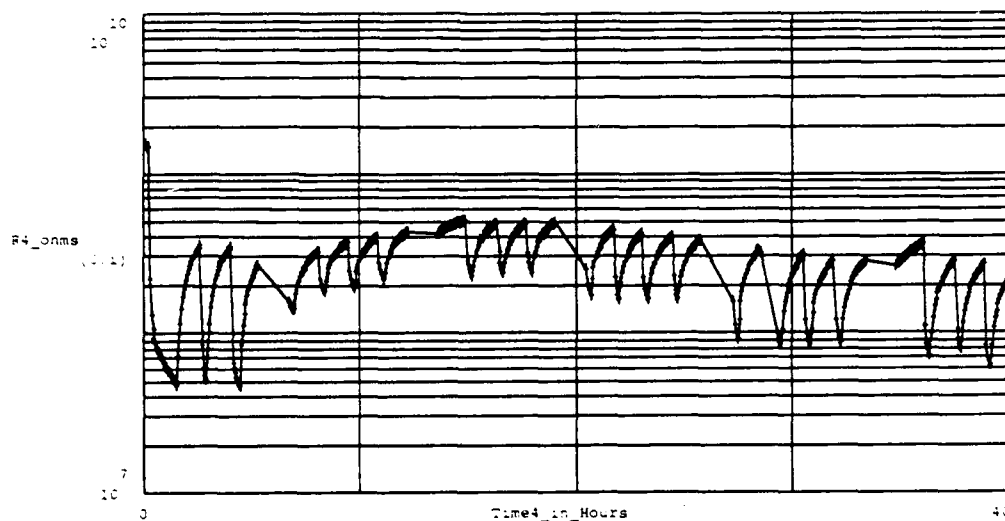


Figure E- 4 . DC Resistance Measured Between the Driven-Electrode and Floating-Electrode of the IGE Array, During Series of Purges and Challenge Gas Exposures. The Number of Measurements Plotted (at crosses) is 479. The Testing Conditions Included the Following:

IGE Array Number : 4,	Thin-film Material : Nickel Phthalocyanine,
Thin-film Thickness : 6,200 Angstroms	Test Temperature(s) : Purge & Challenge at 150°C
Purge Gas : Room Air,	Challenge Gas : NO <sub>2</sub> .
Challenge Gas Concentration(s) (in order run) : 1000 ppb, 30 ppb, 50 ppb, 100 ppb, 500 ppb, 1000 ppb.	

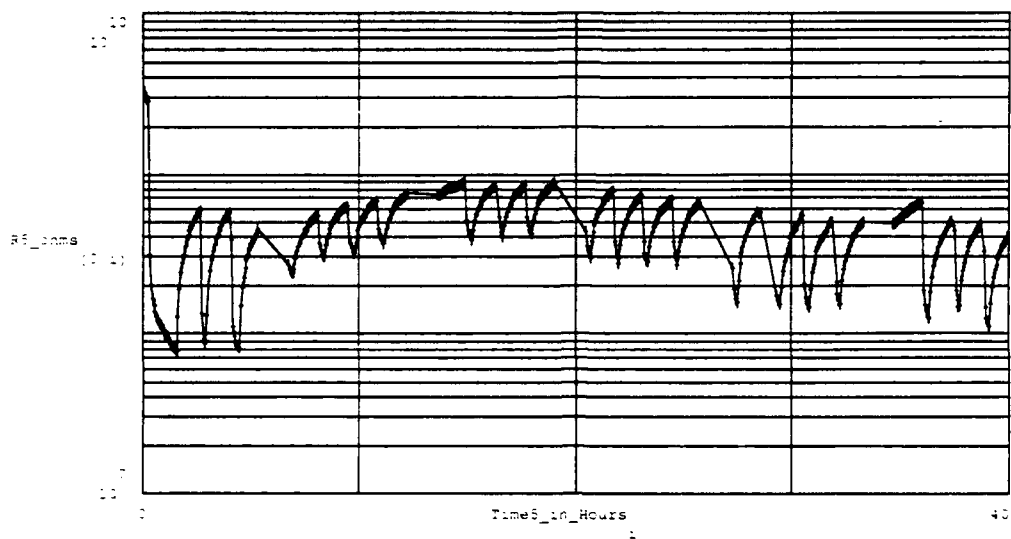


Figure E- 5 . DC Resistance Measured Between the Driven-Electrode and Floating-Electrode of the IGE Array, During Series of Purges and Challenge Gas Exposures. The Number of Measurements Plotted (at crosses) is 479. The Testing Conditions Included the Following:

IGE Array Number : 5.	Thin-film Material : Nickel Phthalocyanine.
Thin-film Thickness : 6,200 Angstroms	Test Temperature(s) : Purge & Challenge at 150°C
Purge Gas : Room Air.	Challenge Gas : NO <sub>2</sub> .
Challenge Gas Concentration(s) (in order run) : 1000 ppb, 30 ppb, 50 ppb, 100 ppb, 500 ppb, 1000 ppb.	

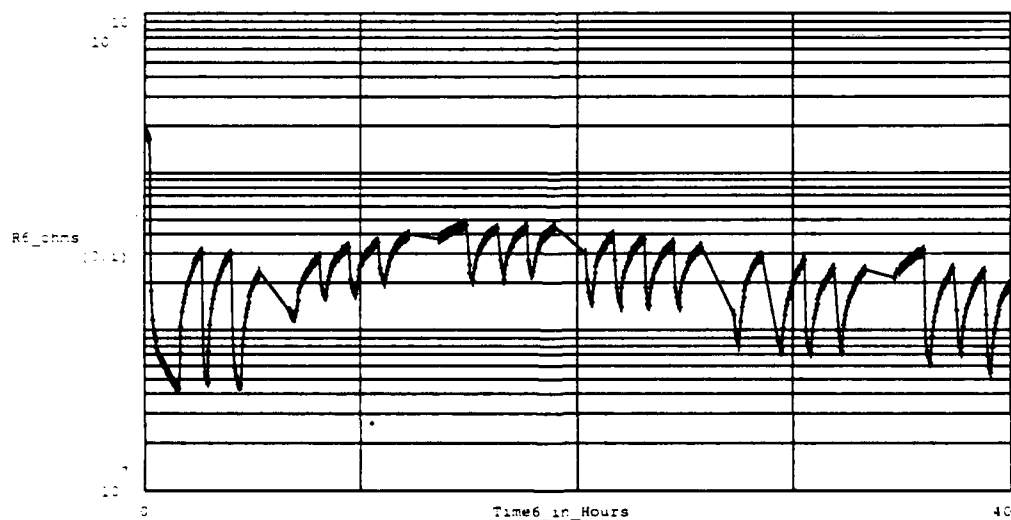


Figure E- 6 . DC Resistance Measured Between the Driven-Electrode and Floating-Electrode of the IGE Array, During Series of Purges and Challenge Gas Exposures. The Number of Measurements Plotted (at crosses) is 479. The Testing Conditions Included the Following:

IGE Array Number : 6.	Thin-film Material : Nickel Phthalocyanine.
Thin-film Thickness : 6,200 Angstroms	Test Temperature(s) : Purge & Challenge at 150°C
Purge Gas : Room Air.	Challenge Gas : NO <sub>2</sub> .
Challenge Gas Concentration(s) (in order run) : 1000 ppb, 30 ppb, 50 ppb, 100 ppb, 500 ppb, 1000 ppb.	

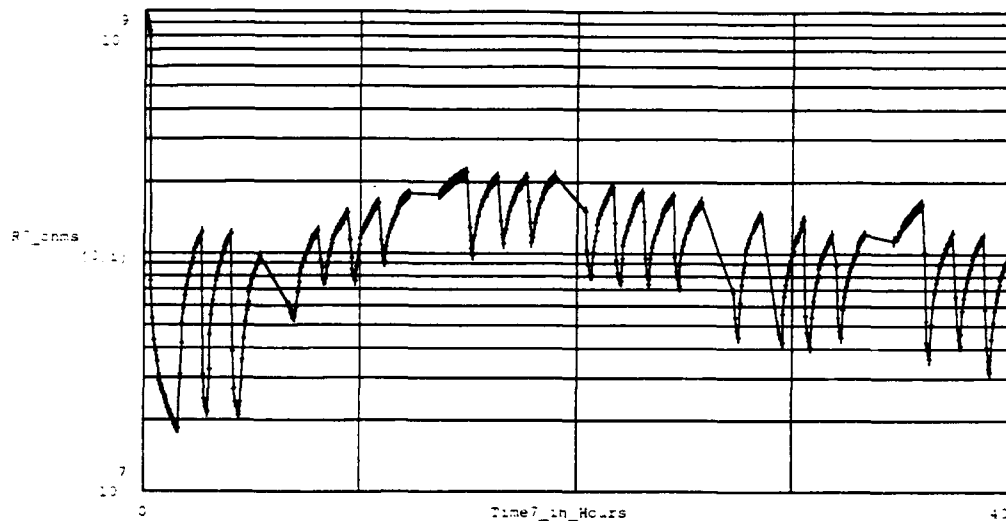


Figure E- 7 . DC Resistance Measured Between the Driven-Electrode and Floating-Electrode of the IGE Array, During Series of Purges and Challenge Gas Exposures. The Number of Measurements Plotted (at crosses) is 479. The Testing Conditions Included the Following:

IGE Array Number : 7,	Thin-film Material : Nickel Phthalocyanine,
Thin-film Thickness : 12,500 Angstroms	Test Temperature(s) : Purge & Challenge at 150°C
Purge Gas : Room Air.	Challenge Gas : NO <sub>2</sub> .
Challenge Gas Concentration(s) (in order run) : 1000 ppb, 30 ppb, 50 ppb, 100 ppb, 500 ppb, 1000 ppb.	

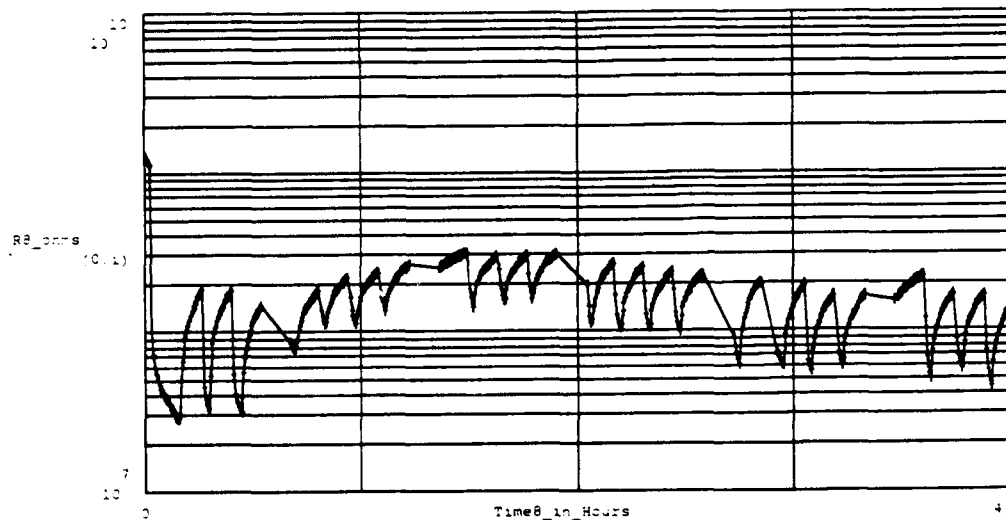


Figure E- 8 . DC Resistance Measured Between the Driven-Electrode and Floating-Electrode of the IGE Array, During Series of Purges and Challenge Gas Exposures. The Number of Measurements Plotted (at crosses) is 479. The Testing Conditions Included the Following:

IGE Array Number : 8,	Thin-film Material : Nickel Phthalocyanine,
Thin-film Thickness : 12,500 Angstroms	Test Temperature(s) : Purge & Challenge at 150°C
Purge Gas : Room Air.	Challenge Gas : NO <sub>2</sub> .
Challenge Gas Concentration(s) (in order run) : 1000 ppb, 30 ppb, 50 ppb, 100 ppb, 500 ppb, 1000 ppb.	

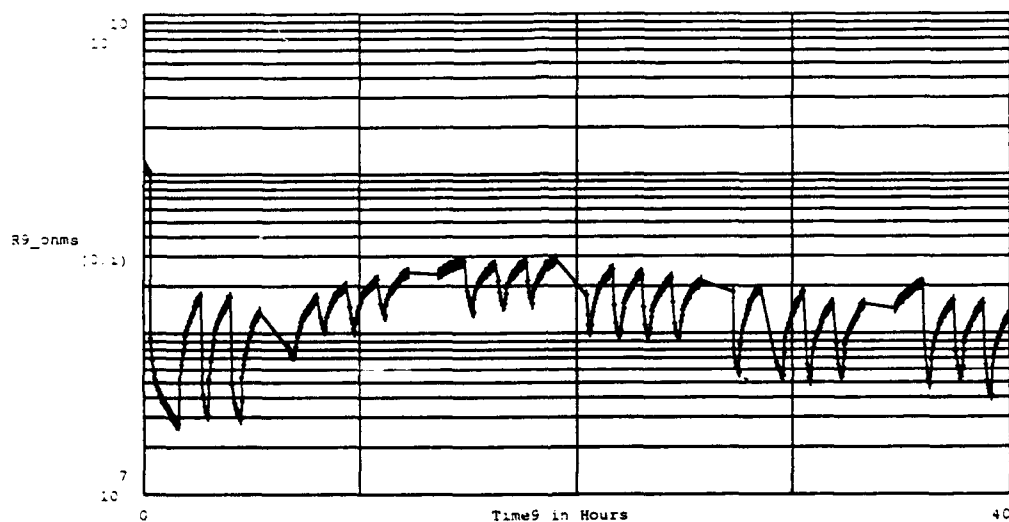
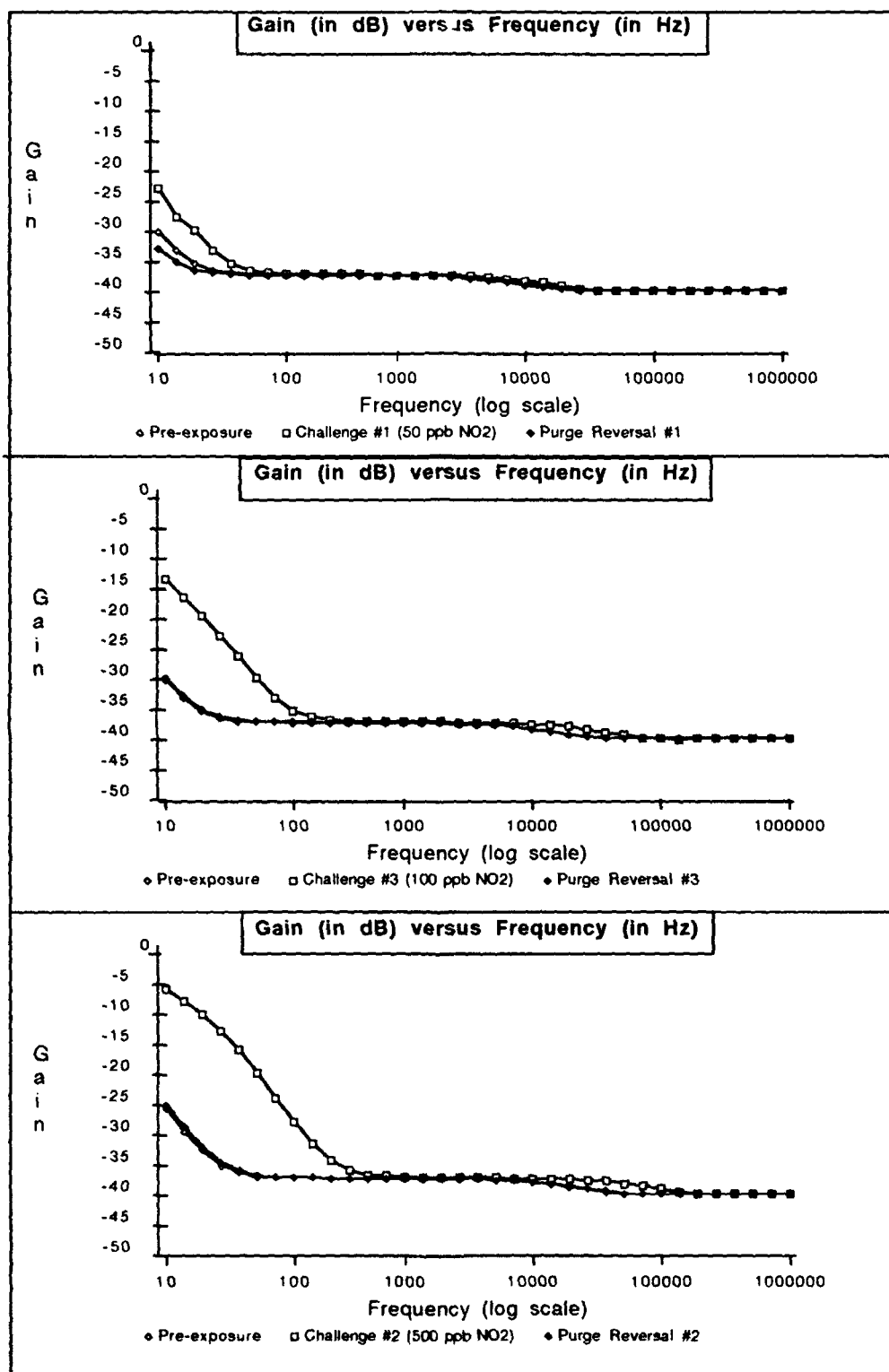


Figure E-9 . DC Resistance Measured Between the Driven-Electrode and Floating-Electrode of the IGE Array. During Series of Purges and Challenge Gas Exposures. The Number of Measurements Plotted (at crosses) is 479. The Testing Conditions Included the Following:

IGE Array Number : 9.	Thin-film Material : Nickel Phthalocyanine.
Thin-film Thickness : 12,500 Angstroms	Test Temperature(s) : Purge & Challenge at 150°C
Purge Gas : Room Air.	Challenge Gas : NO <sub>2</sub> .
Challenge Gas Concentration(s) (in order run) : 1000 ppb, 30 ppb, 50 ppb, 100 ppb, 500 ppb, 1000 ppb.	





FigureE-11 . Gain versus Frequency Response of IGEFET Microsensor for a Series of Room Air Purges and Challenge Gas Exposures. Testing Conditions: IGE Microsensor Number 1; NiPc Thin-film (2,600 Angstroms Thick); Temperature of 150 degrees Centigrade; Nitrogen Dioxide Challenge Gas (Order of Exposures: 1000 ppb, 30 ppb, 50 ppb, 100 ppb, 500 ppb, 1000 ppb).



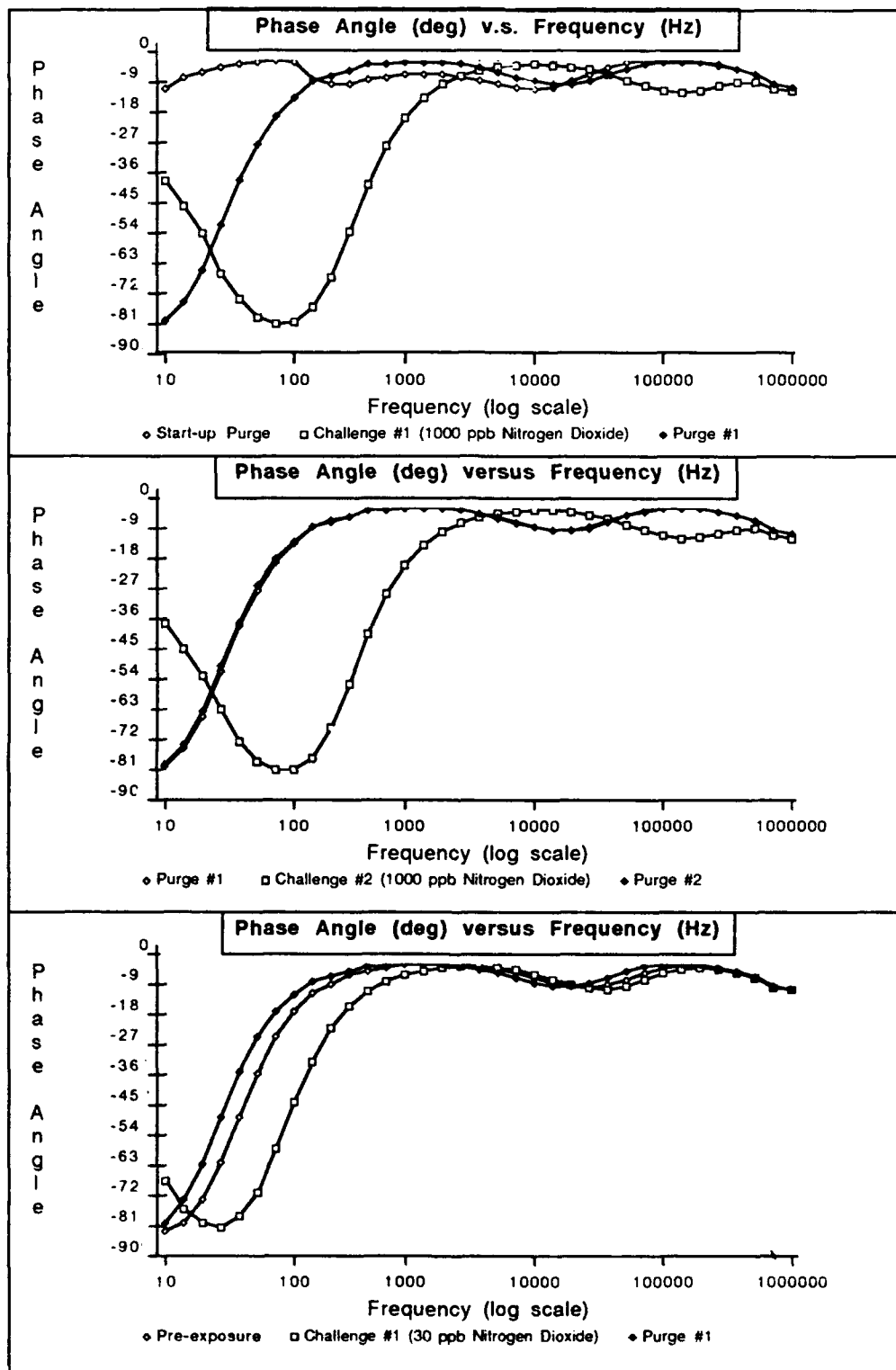


Figure E-12 Phase Angle versus Frequency Response of IGFET Microsensor for a Series of Room Air Purges and Challenge Gas Exposures. Testing Conditions: IGE Microsensor Number 1; NiPc Thin-film (2,600 Angstroms Thick); Temperature of 150 degrees Centigrade; Nitrogen Dioxide Challenge Gas (Order of Exposures: 1000 ppb, 30 ppb, 50 ppb, 100 ppb, 500 ppb, 1000 ppb).

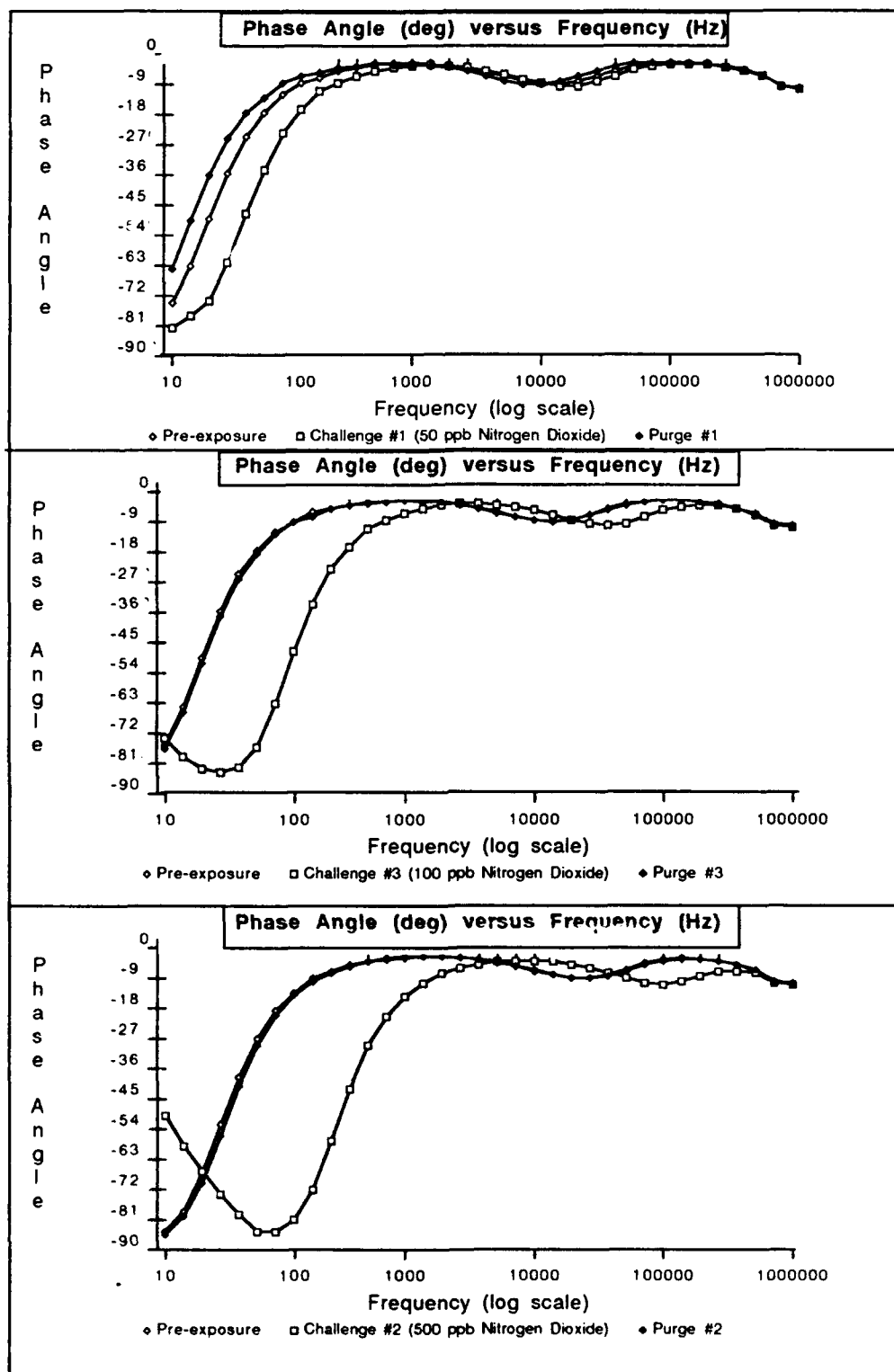


Figure E-13. Phase Angle versus Frequency Response of IGEFET Microsensor for a Series of Room Air Purges and Challenge Gas Exposures. Testing Conditions: IGE Microsensor Number 1; NiPc Thin-film (2,600 Angstroms Thick); Temperature of 150 degrees Centigrade; Nitrogen Dioxide Challenge Gas (Order of Exposures: 1000 ppb, 30 ppb, 50 ppb, 100 ppb, 500 ppb, 1000 ppb).



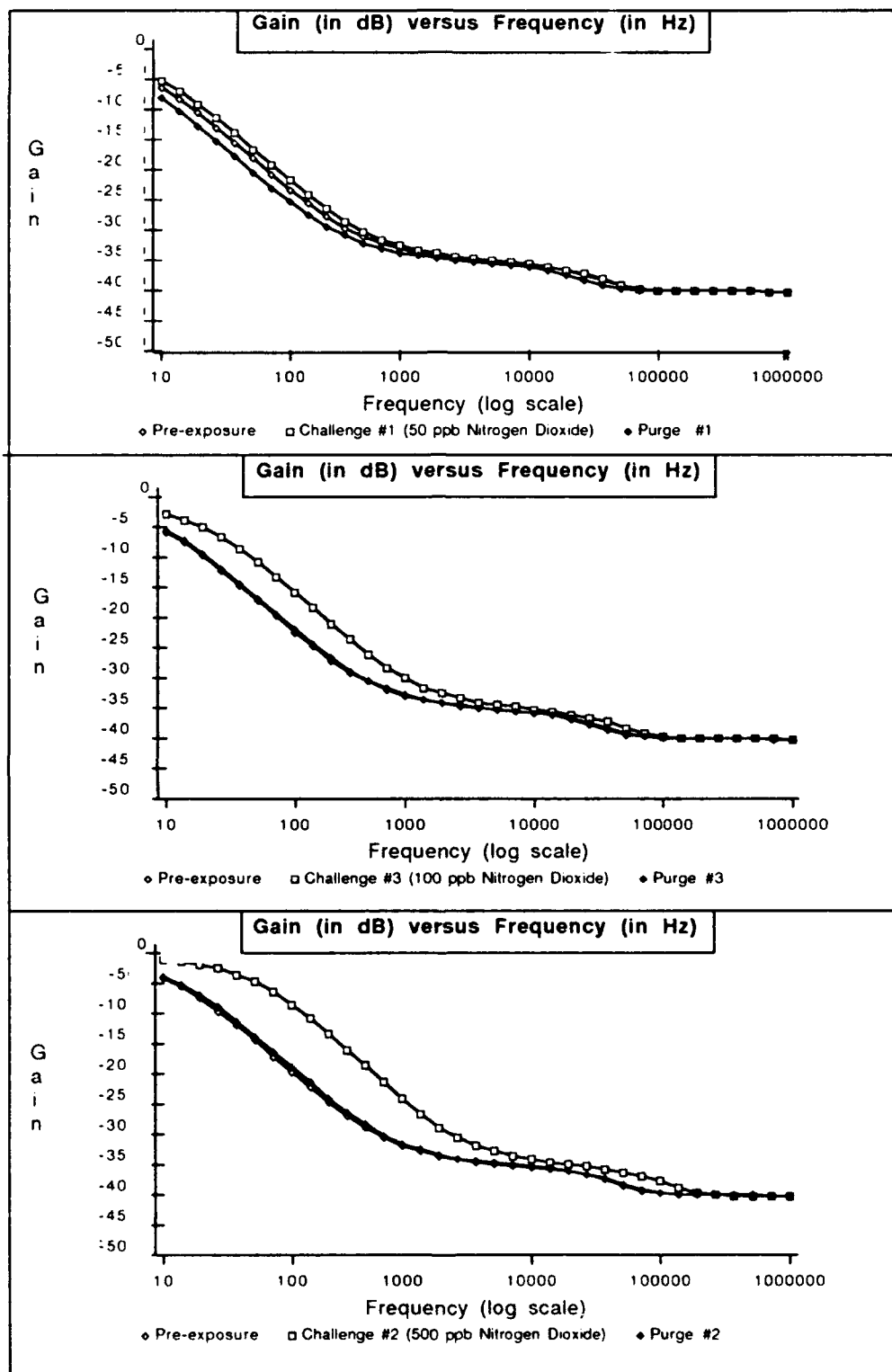


Figure E-15. Gain versus Frequency Response of IGEFET Microsensor for a Series of Room Air Purges and Challenge Gas Exposures. Testing Conditions: IGE Microsensor Number 4; NiPc Thin-film (6,200 Angstroms Thick); Temperature of 150 degrees Centigrade; Nitrogen Dioxide Challenge Gas (Order of Exposures: 1000 ppb, 30 ppb, 50 ppb, 100 ppb, 500 ppb, 1000 ppb).

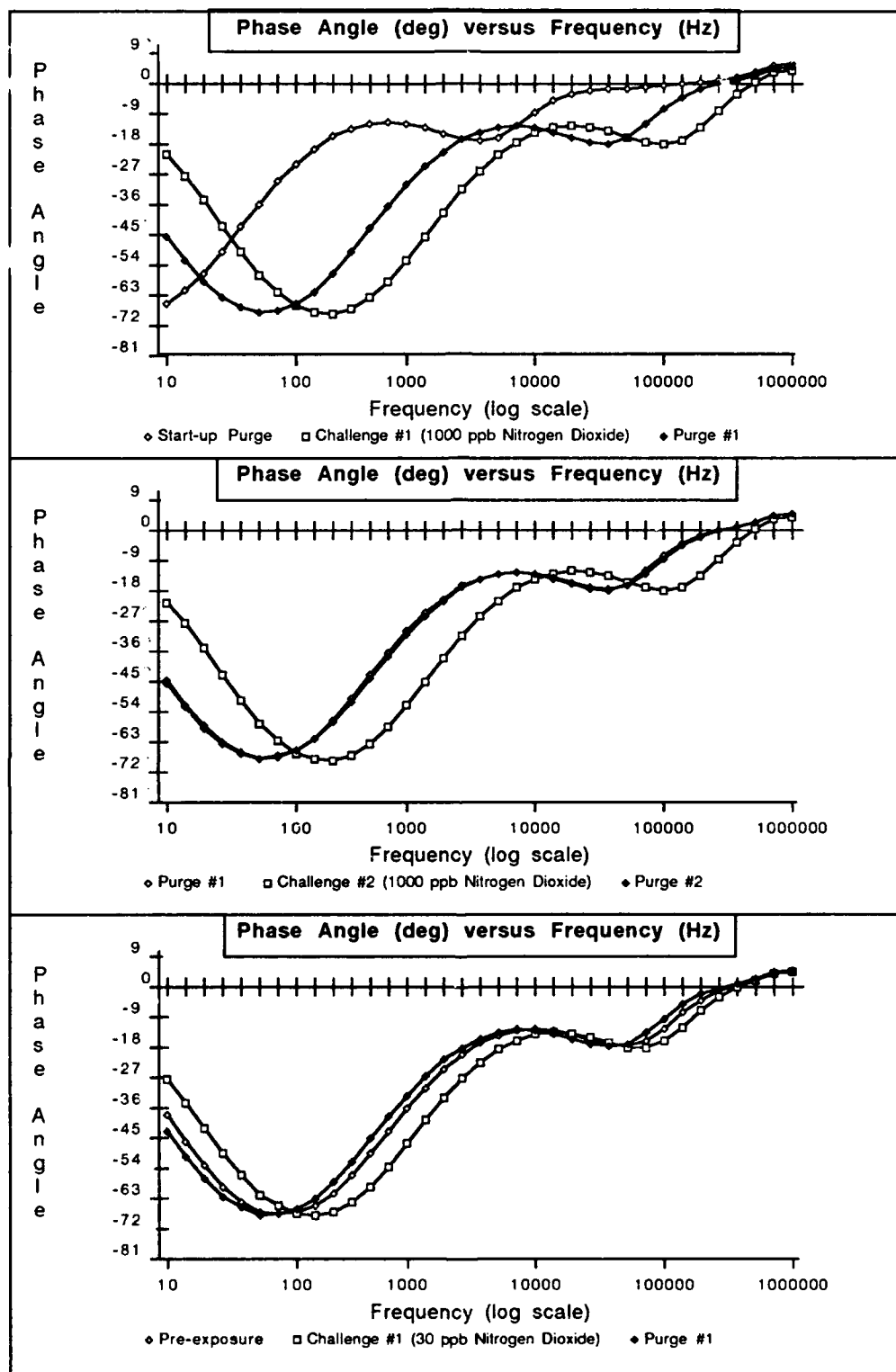


Figure E-16 Phase Angle versus Frequency Response of IGEFET Microsensor for a Series of Room Air Purges and Challenge Gas Exposures. Testing Conditions: IGE Microsensor Number 4; NiPc Thin-film (6,200 Angstroms Thick); Temperature of 150 degrees Centigrade; Nitrogen Dioxide Challenge Gas (Order of Exposures: 1000 ppb, 30 ppb, 50 ppb, 100 ppb, 500 ppb, 1000 ppb).

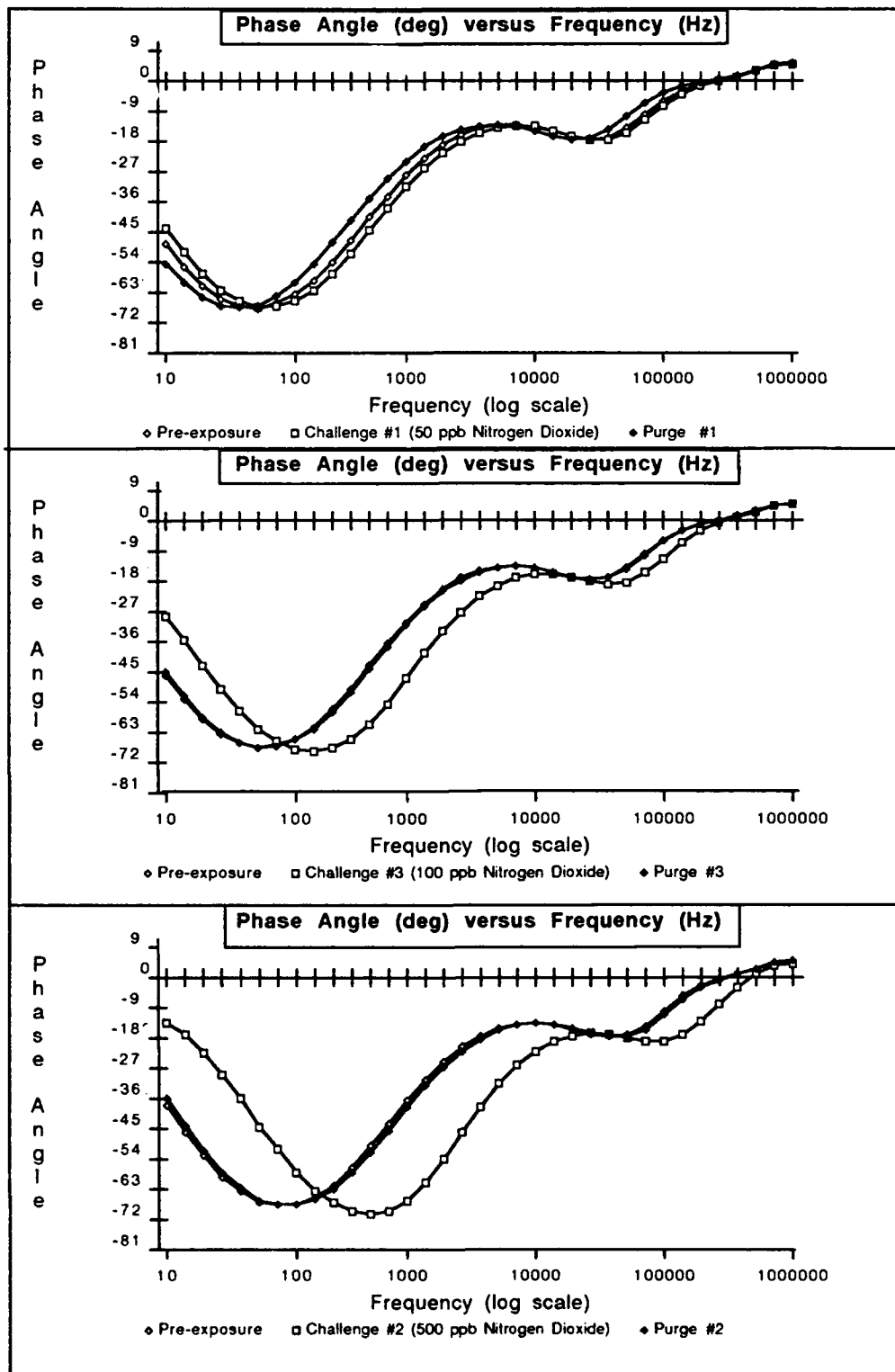


Figure E-17. Phase Angle versus Frequency Response of IGEFET Microsensor for a Series of Room Air Purges and Challenge Gas Exposures. Testing Conditions: IGE Microsensor Number 4; NiPc Thin-film (6,200 Angstroms Thick); Temperature of 150 degrees Centigrade; Nitrogen Dioxide Challenge Gas (Order of Exposures: 1000 ppb, 30 ppb, 50 ppb, 500 ppb, 1000 ppb).

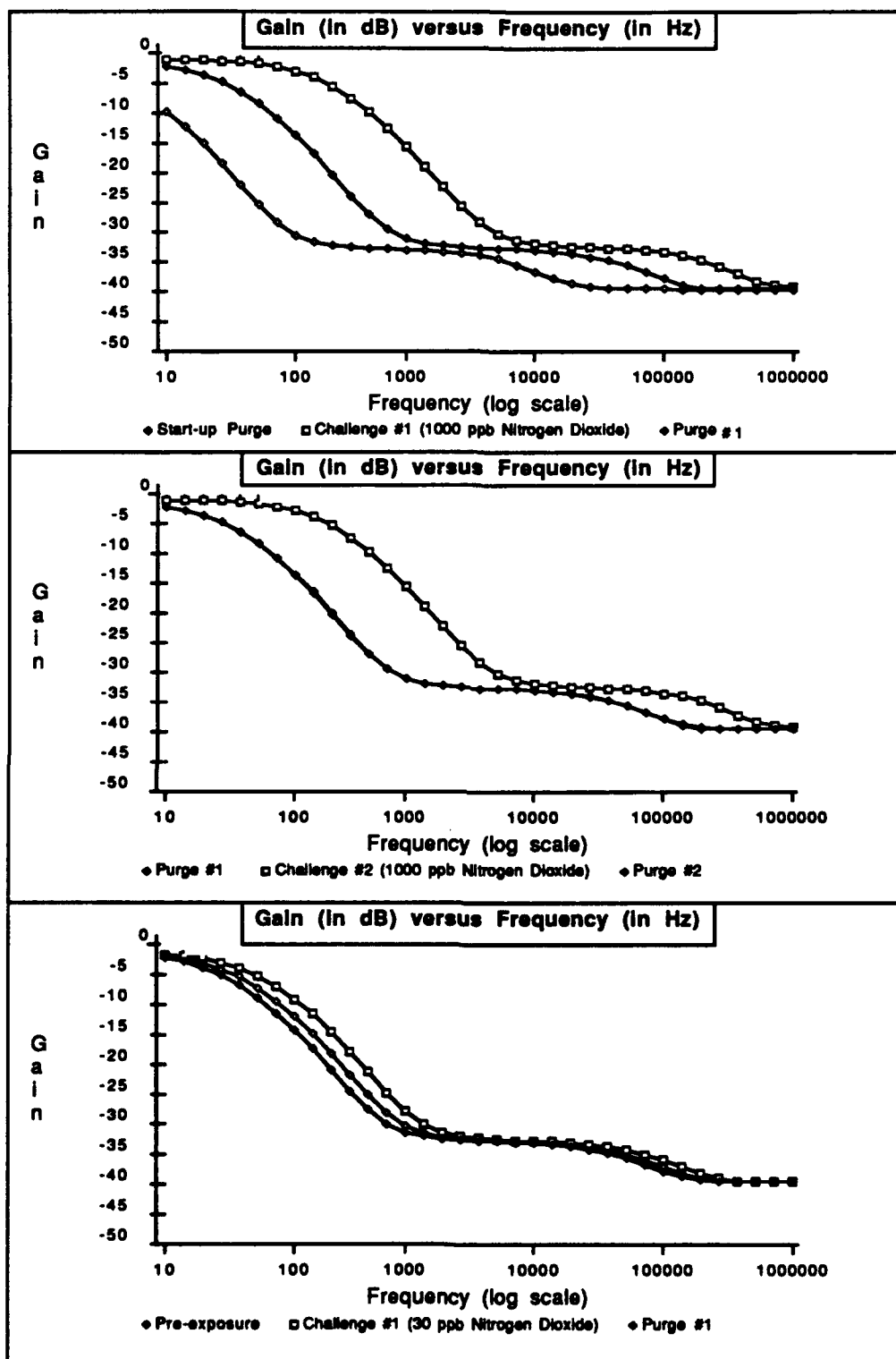


Figure E-18 . Gain versus Frequency Response of IGEFET Microsensor for a Series of Room Air Purges and Challenge Gas Exposures. Testing Conditions: IGE Microsensor Number 9; NiPc Thin-film (12,500 Angstroms Thick); Temperature of 150 degrees Centigrade; Nitrogen Dioxide Challenge Gas (Order of Exposures: 1000 ppb, 30 ppb, 50 ppb, 100 ppb, 500 ppb, 1000 ppb).

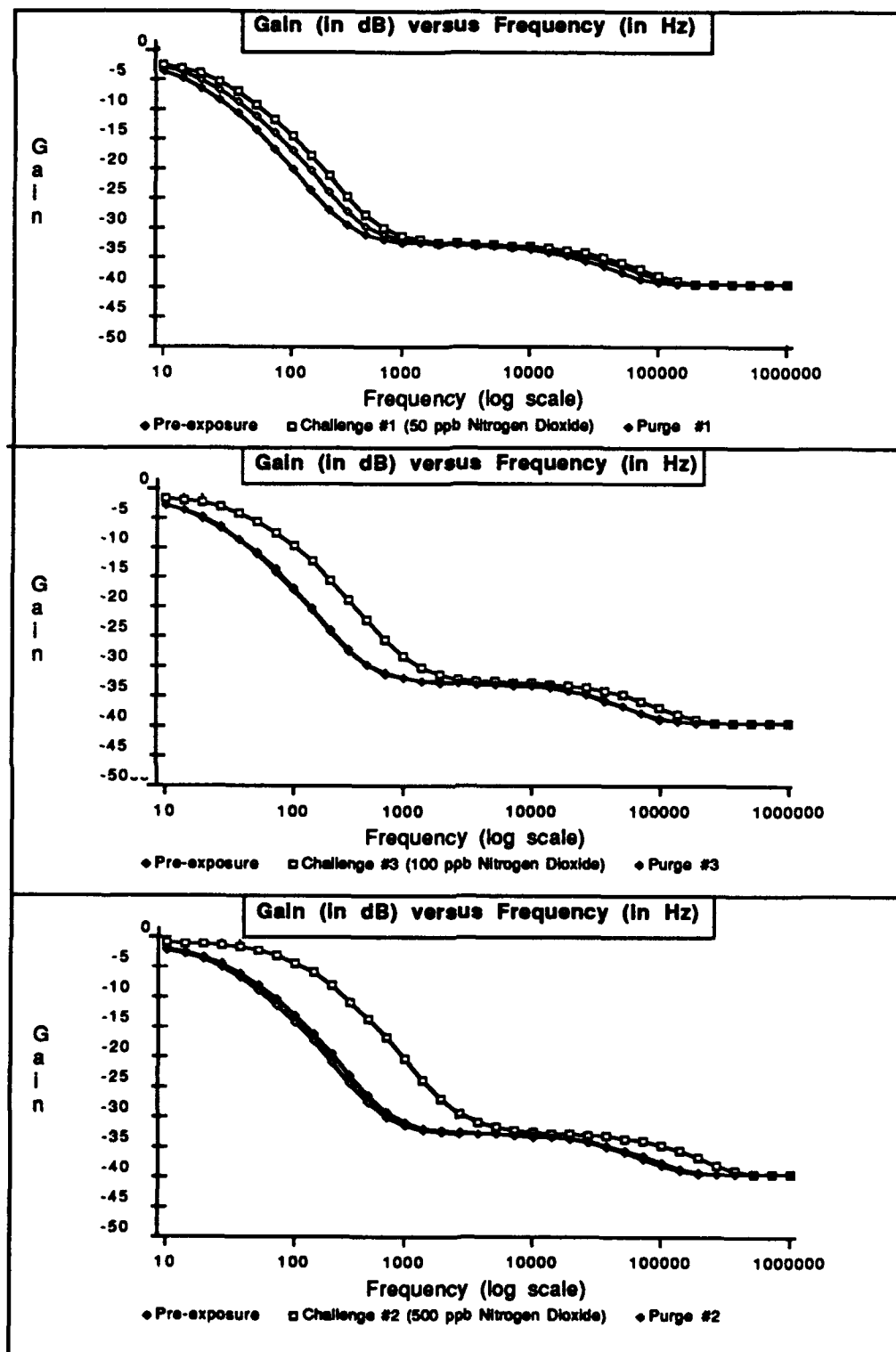


Figure E-19. Gain versus Frequency Response of IGEFET Microsensor for a Series of Room Air Purges and Challenge Gas Exposures. Testing Conditions: IGE Microsensor Number 9; NiPc Thin-film (12,500 Angstroms Thick); Temperature of 150 degrees Centigrade; Nitrogen Dioxide Challenge Gas (Order of Exposures: 1000 ppb, 30 ppb, 50 ppb, 100 ppb, 500 ppb, 1000 ppb).



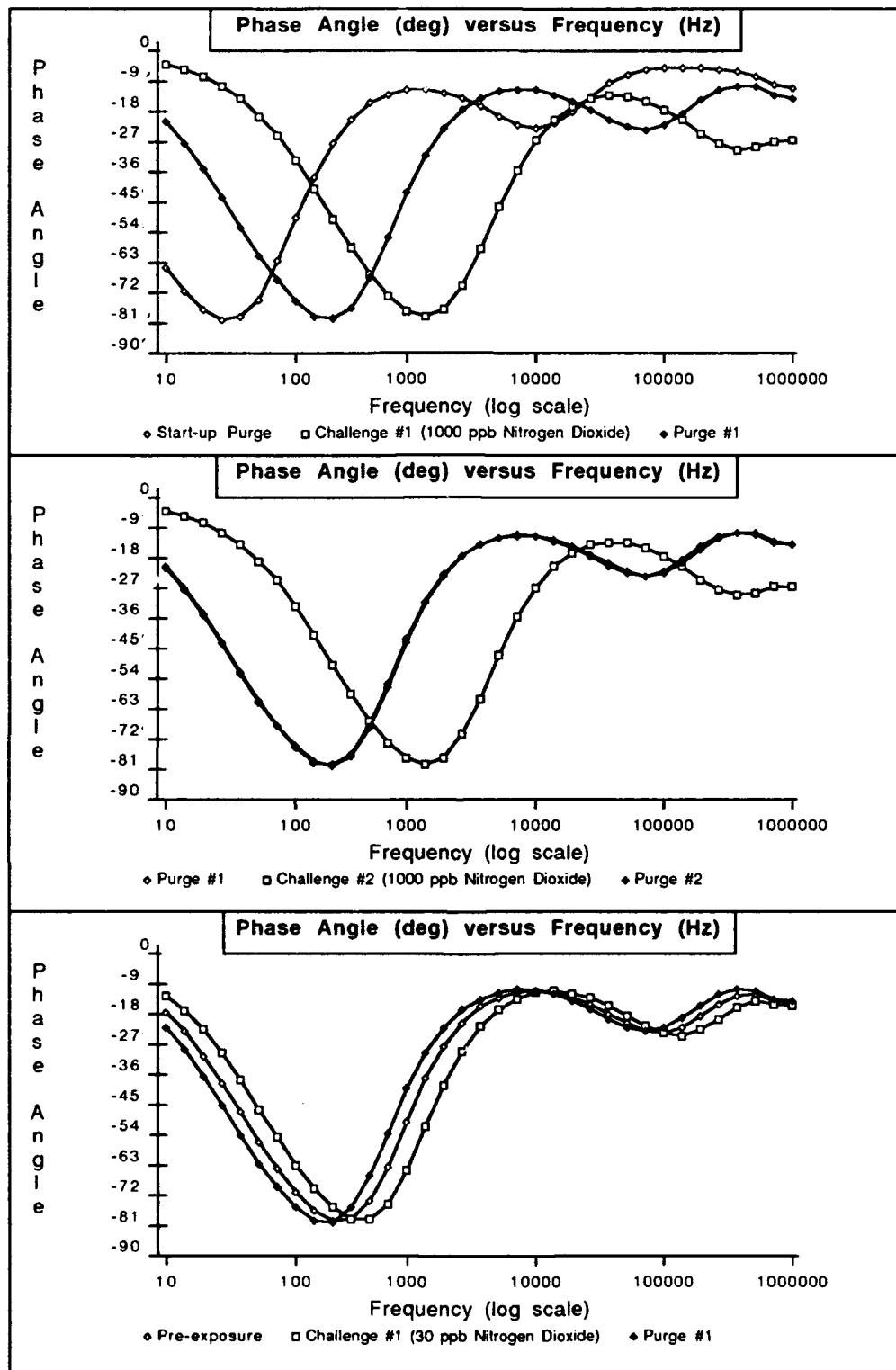


Figure E-20 . Phase Angle versus Frequency Response of IGEFET Microsensor for a Series of Room Air Purges and Challenge Gas Exposures. Testing Conditions: IGE Microsensor Number 9; NiPc Thin-film (12,500 Angstroms Thick); Temperature of 150 degrees Centigrade; Nitrogen Dioxide Challenge Gas (Order of Exposures: 1000 ppb, 30 ppb, 50 ppb, 100 ppb, 500 ppb, 1000 ppb).

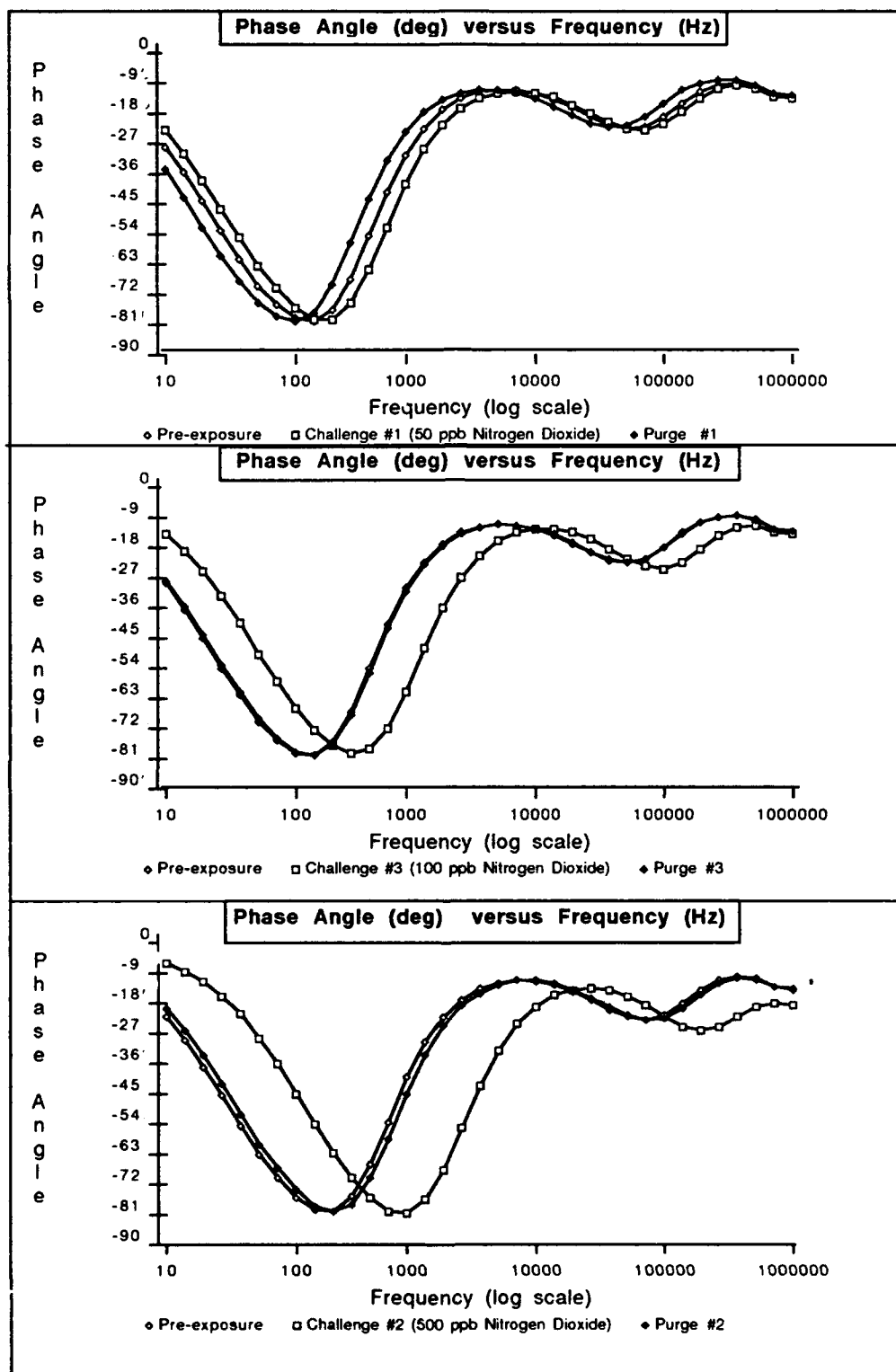


Figure E-21 . Phase Angle versus Frequency Response of IGEFET Microsensor for a Series of Room Air Purges and Challenge Gas Exposures. Testing Conditions: IGE Microsensor Number 9; NiPc Thin-film (12,500 Angstroms Thick); Temperature of 150 degrees Centigrade; Nitrogen Dioxide Challenge Gas (Order of Exposures: 1000 ppb, 30 ppb, 50 ppb, 100 ppb, 500 ppb, 1000 ppb).

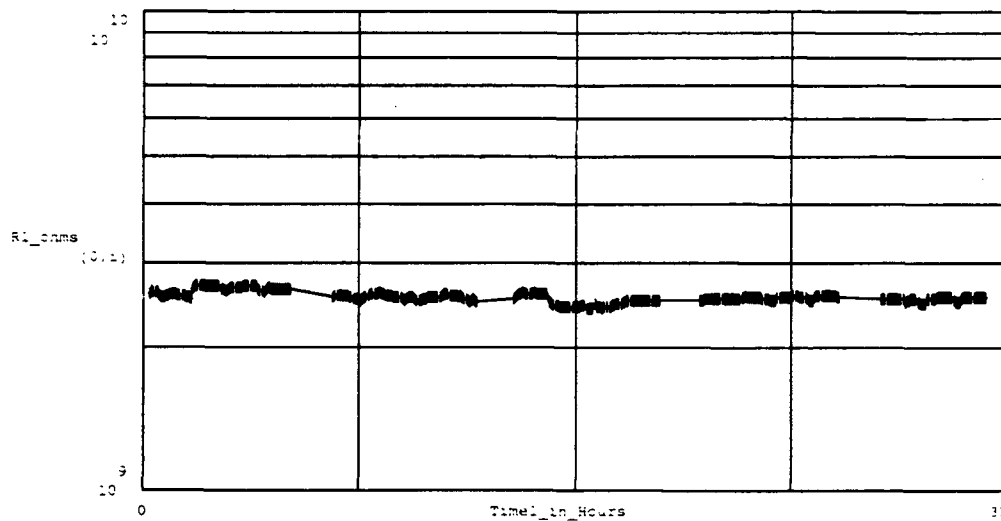


Figure E-22 . DC Resistance Measured Between the Driven-Electrode and Floating-Electrode of the IGE Array, During Series of Purges and Challenge Gas Exposures. The Number of Measurements (at crosses) is 376. The Testing Conditions Included the Following:

IGE Array Number : 1.	Thin-film Material : Nickel Phthalocyanine.
Thin-film Thickness : 2,600 Angstroms	Test Temperature(s) : Purge & Challenge at 150°C
Purge Gas : Room Air.	Challenge Gas : NH <sub>3</sub> .
Challenge Gas Concentration(s) (in order run) : 500 ppm, 16 ppm, 106 ppm, 250 ppm, 500 ppm.	

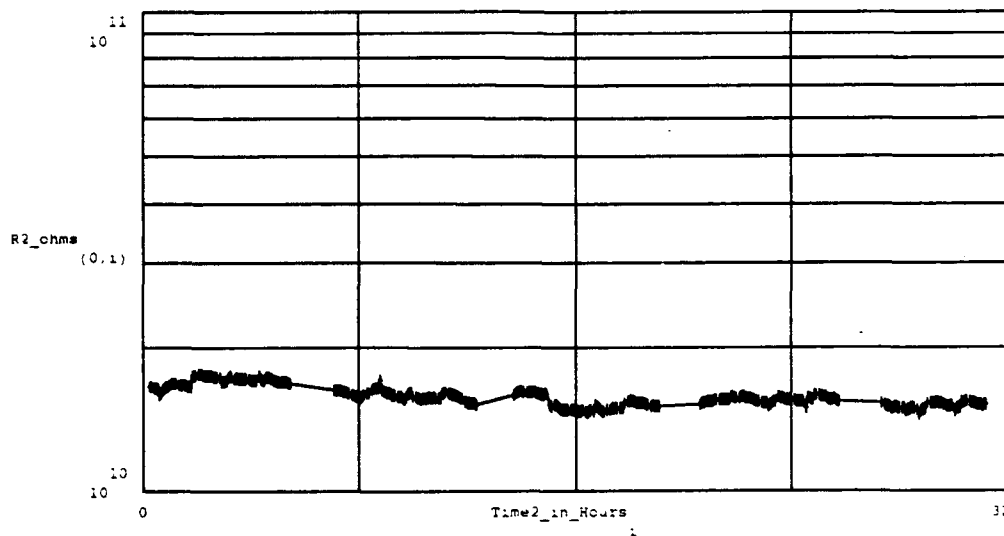


Figure E- 23 . DC Resistance Measured Between the Driven-Electrode and Floating-Electrode of the IGE Array, During Series of Purges and Challenge Gas Exposures. The Number of Measurements (at crosses) is 376. The Testing Conditions Included the Following:

IGE Array Number : 2.	Thin-film Material : Nickel Phthalocyanine.
Thin-film Thickness : 2,600 Angstroms	Test Temperature(s) : Purge & Challenge at 150°C
Purge Gas : Room Air.	Challenge Gas : NH <sub>3</sub> .
Challenge Gas Concentration(s) (in order run) : 500 ppm, 16 ppm, 106 ppm, 250 ppm, 500 ppm.	

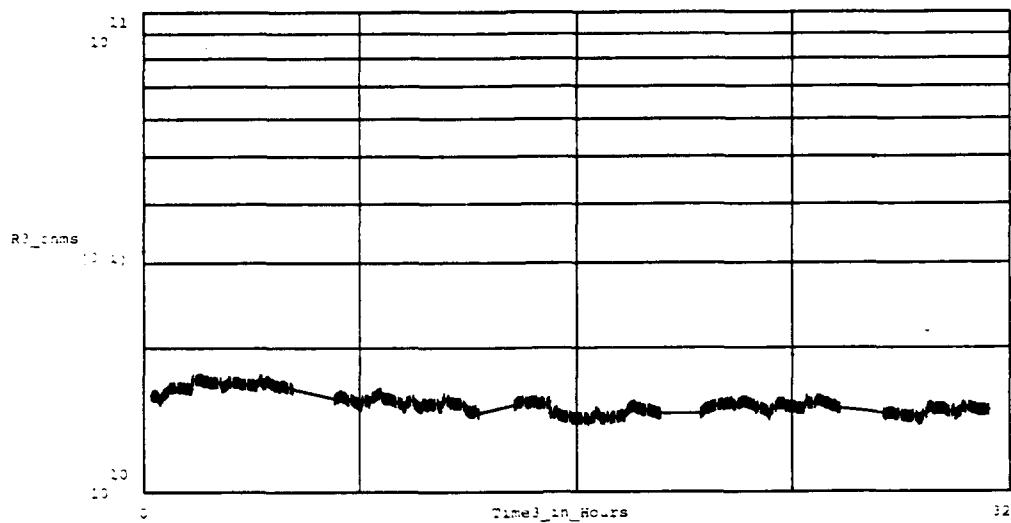


Figure E-24 . DC Resistance Measured Between the Driven-Electrode and Floating-Electrode of the IGE Array. During Series of Purges and Challenge Gas Exposures. The Number of Measurements (at crosses) is 376. The Testing Conditions Included the Following:

IGE Array Number : 3.	Thin-film Material : Nickel Phthalocyanine.
Thin-film Thickness : 2,600 Angstroms	Test Temperature(s) : Purge & Challenge at 150°C
Purge Gas : Room Air.	Challenge Gas : NH <sub>3</sub> .
Challenge Gas Concentration(s) (in order run) : 500 ppm, 16 ppm, 106 ppm, 250 ppm, 500 ppm..	

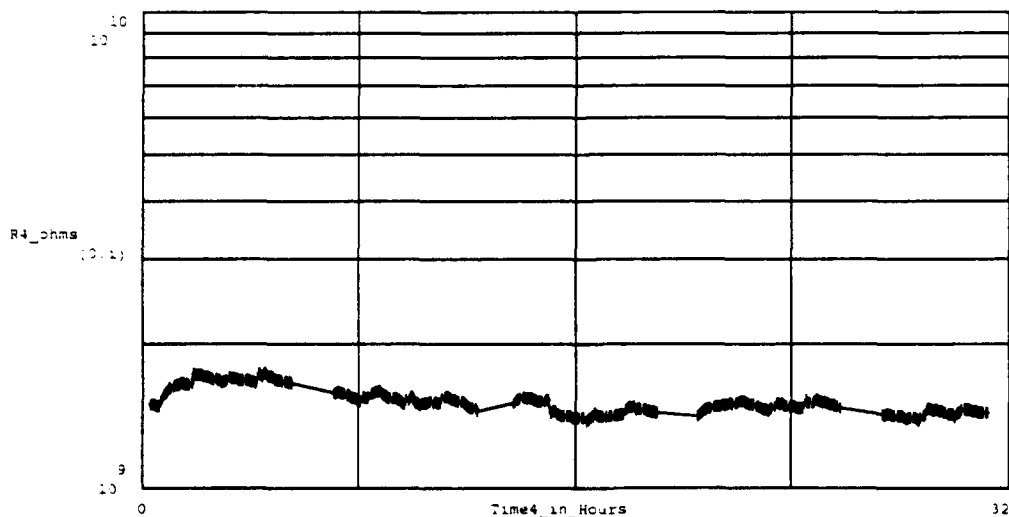


Figure E- 25 . DC Resistance Measured Between the Driven-Electrode and Floating-Electrode of the IGE Array. During Series of Purges and Challenge Gas Exposures. The Number of Measurements (at crosses) is 376. The Testing Conditions Included the Following:

IGE Array Number : 4.	Thin-film Material : Nickel Phthalocyanine.
Thin-film Thickness : 6,200 Angstroms	Test Temperature(s) : Purge & Challenge at 150°C
Purge Gas : Room Air.	Challenge Gas : NH <sub>3</sub> .
Challenge Gas Concentration(s) (in order run) : 500 ppm, 16 ppm, 106 ppm, 250 ppm, 500 ppm.	

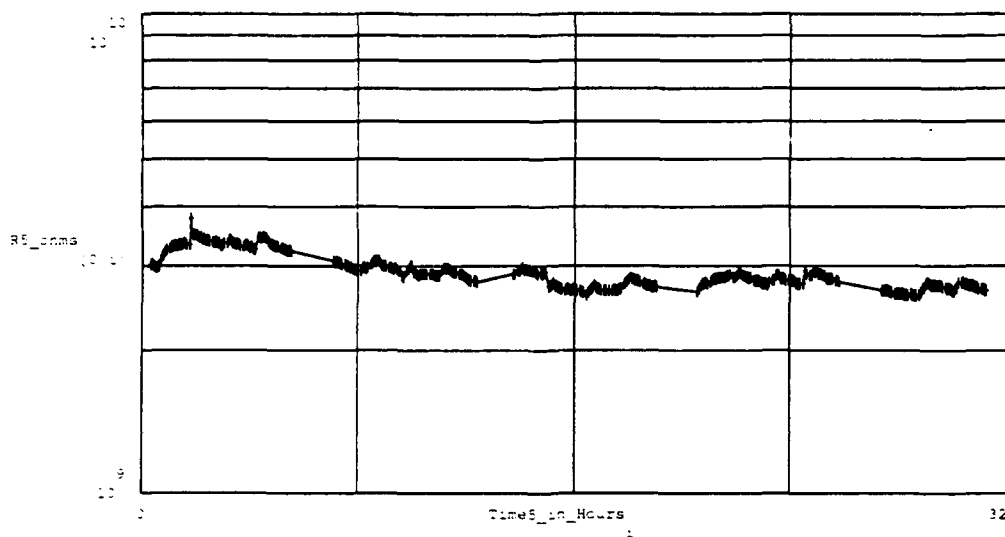


Figure E-26 . DC Resistance Measured Between the Driven-Electrode and Floating-Electrode of the IGE Array, During Series of Purges and Challenge Gas Exposures. The Number of Measurements (at crosses) is 376. The Testing Conditions Included the Following:

IGE Array Number : 5.	Thin-film Material : Nickel Phthalocyanine.
Thin-film Thickness : 6,200 Angstroms	Test Temperature(s) : Purge & Challenge at 150°C
Purge Gas : Room Air.	Challenge Gas : NH <sub>3</sub> .
Challenge Gas Concentration(s) (in order run) : 500 ppm, 16 ppm, 106 ppm, 250 ppm, 500 ppm.	

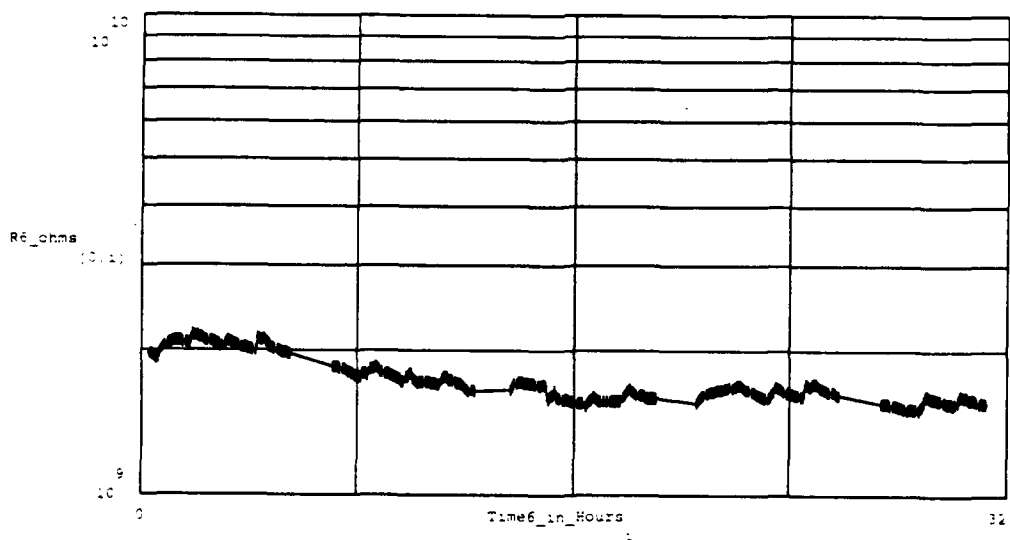


Figure E-27 . DC Resistance Measured Between the Driven-Electrode and Floating-Electrode of the IGE Array, During Series of Purges and Challenge Gas Exposures. The Number of Measurements (at crosses) is 376. The Testing Conditions Included the Following:

IGE Array Number : 6.	Thin-film Material : Nickel Phthalocyanine.
Thin-film Thickness : 6,200 Angstroms	Test Temperature(s) : Purge & Challenge at 150°C
Purge Gas : Room Air.	Challenge Gas : NH <sub>3</sub> .
Challenge Gas Concentration(s) (in order run) : 500 ppm, 16 ppm, 106 ppm, 250 ppm, 500 ppm.	

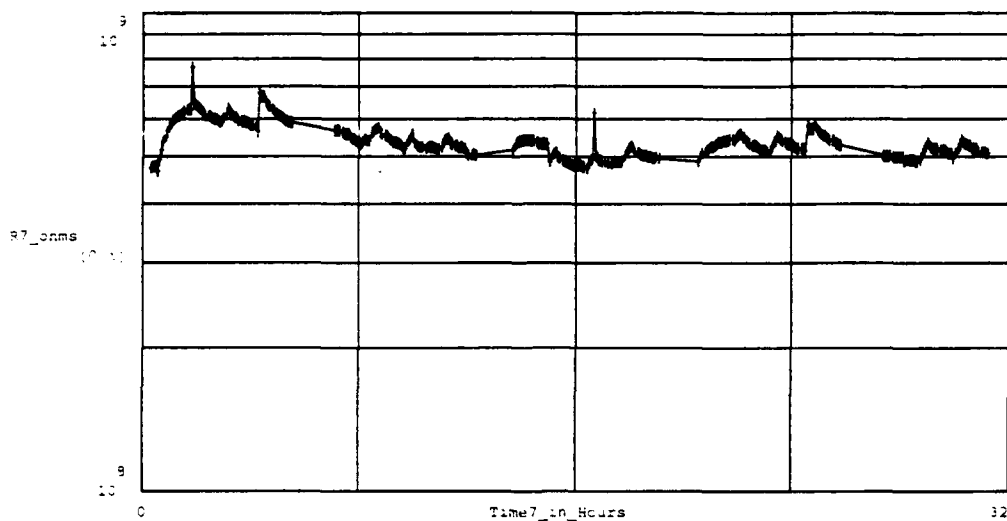


Figure E-28 . DC Resistance Measured Between the Driven-Electrode and Floating-Electrode of the IGE Array, During Series of Purges and Challenge Gas Exposures. The Number of Measurements (at crosses) is 376. The Testing Conditions Included the Following:

IGE Array Number : 7,	Thin-film Material : Nickel Phthalocyanine.
Thin-film Thickness : 12,500 Angstroms	Test Temperature(s) : Purge & Challenge at 150°C
Purge Gas : Room Air.	Challenge Gas : NH <sub>3</sub> .
Challenge Gas Concentration(s) (in order run) : 500 ppm, 16 ppm, 106 ppm, 250 ppm, 500 ppm.	

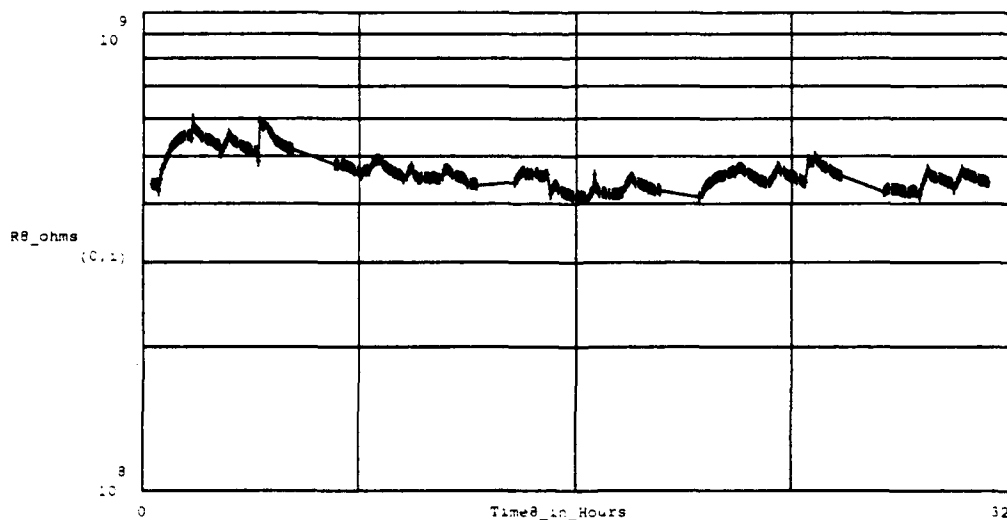


Figure E-29 . DC Resistance Measured Between the Driven-Electrode and Floating-Electrode of the IGE Array, During Series of Purges and Challenge Gas Exposures. The Number of Measurements (at crosses) is 376. The Testing Conditions Included the Following:

IGE Array Number : 8,	Thin-film Material : Nickel Phthalocyanine.
Thin-film Thickness : 12,500 Angstroms	Test Temperature(s) : Purge & Challenge at 150°C
Purge Gas : Room Air.	Challenge Gas : NH <sub>3</sub> .
Challenge Gas Concentration(s) (in order run) : 500 ppm, 16 ppm, 106 ppm, 250 ppm, 500 ppm.	

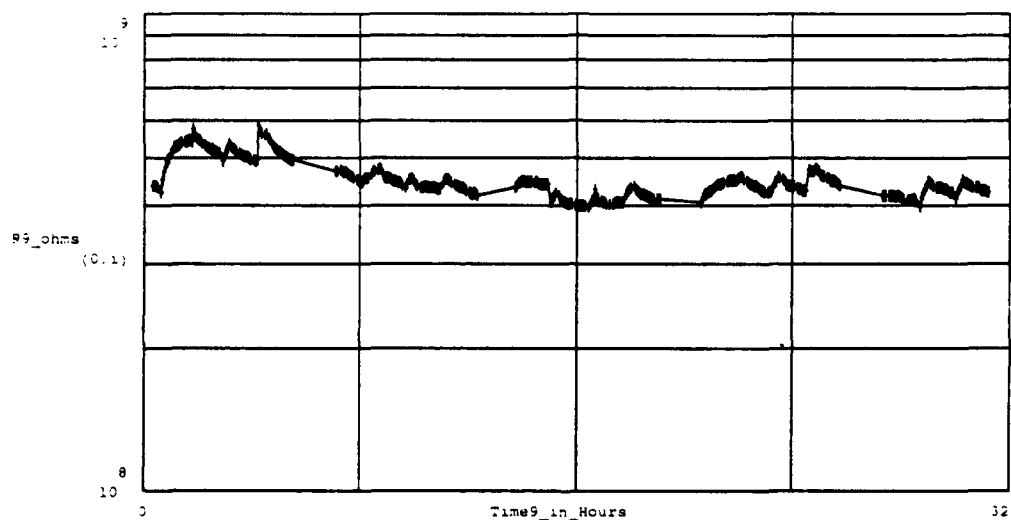


Figure E-30 . DC Resistance Measured Between the Driven-Electrode and Floating-Electrode of the IGE Array. During Series of Purges and Challenge Gas Exposures. The Number of Measurements (at crosses) is 376. The Testing Conditions Included the Following:

IGE Array Number : 9.	Thin-film Material : Nickel Phthalocyanine.
Thin-film Thickness : 12,500 Angstroms	Test Temperature(s) : Purge & Challenge at 150°C
Purge Gas : Room Air.	Challenge Gas : NH <sub>3</sub> .
Challenge Gas Concentration(s) (in order run) : 500 ppm, 16 ppm, 106 ppm, 250 ppm, 500 ppm.	

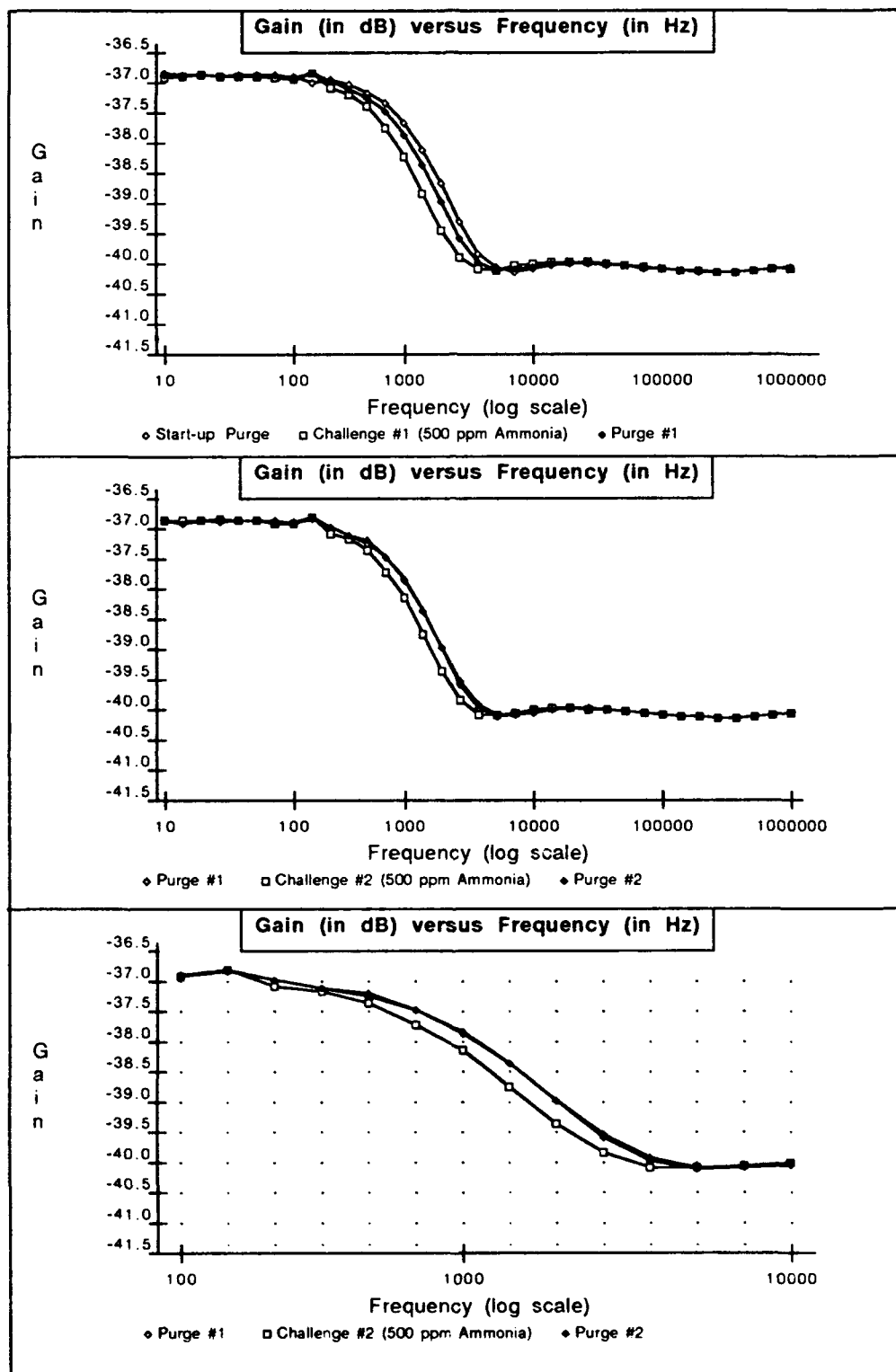


Figure E-31 . Gain versus Frequency Response of IGEFET Microsensor for a Series of Room Air Purges and Challenge Gas Exposures. Testing Conditions: IGE Microsensor Number 1; NiPc Thin-film (2,600 Angstroms Thick); Temperature of 150 degrees Centigrade; Ammonia Challenge Gas (All Exposures:500 ppm).



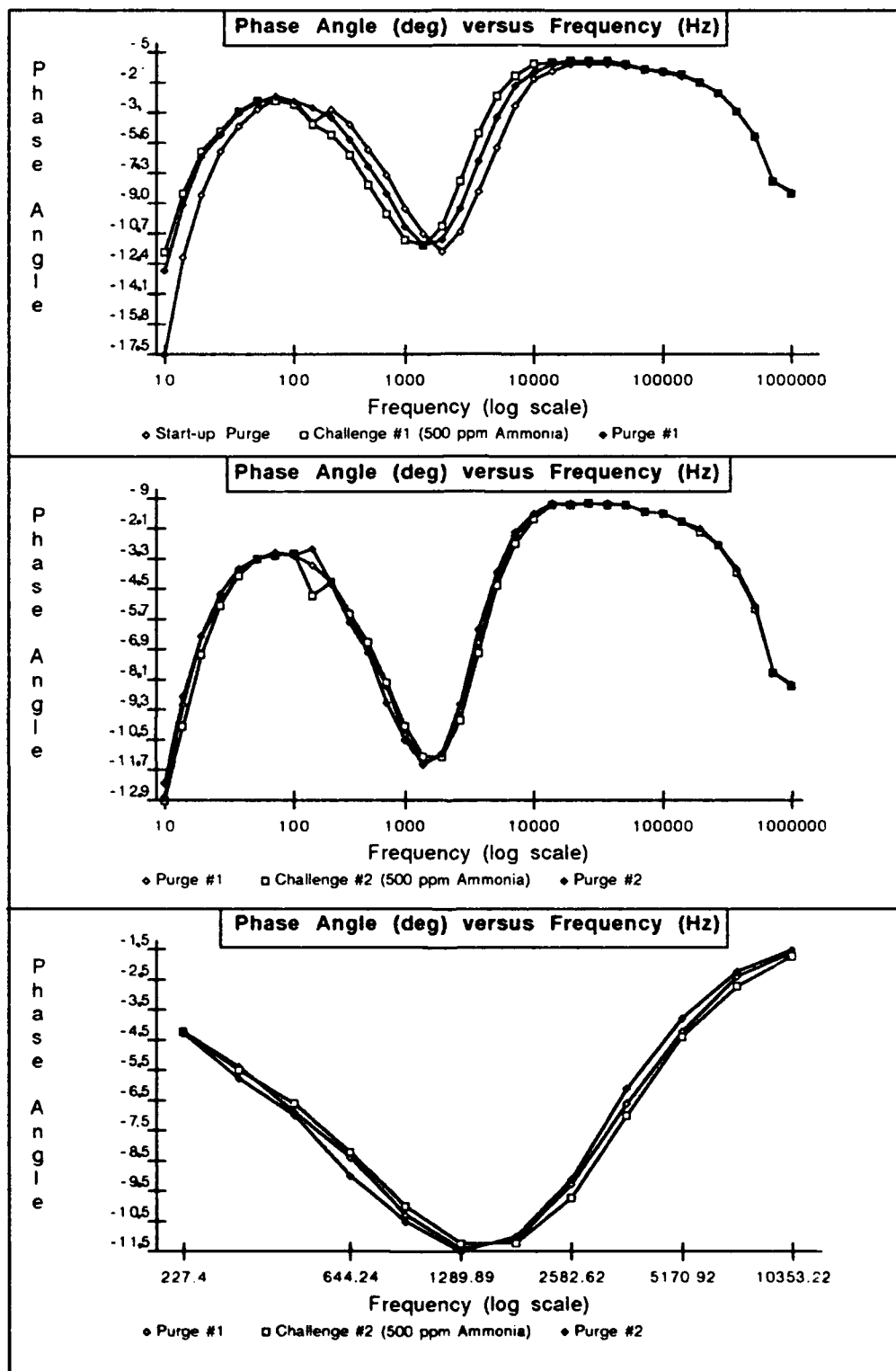


Figure E-32. Phase Angle versus Frequency Response of IGEFET Microsensor for a Series of Room Air Purges and Challenge Gas Exposures. Testing Conditions: IGE Microsensor Number 1; NiPc Thin-film (2,600 Angstroms Thick); Temperature of 150 degrees Centigrade; Ammonia Challenge Gas (All Exposures:500 ppm).

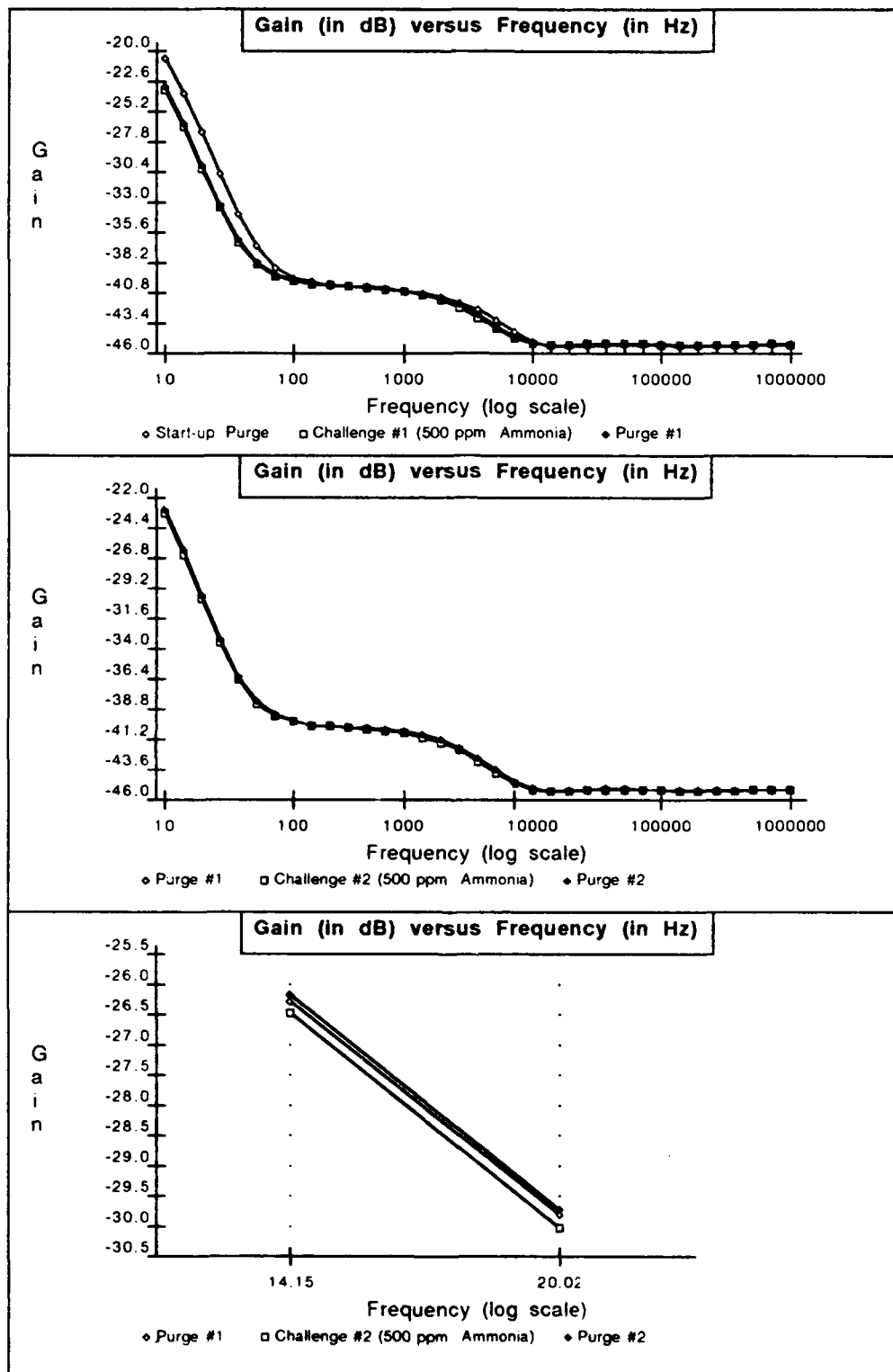


Figure E-33 Gain versus Frequency Response of IGEFET Microsensor for a Series of Room Air Purges and Challenge Gas Exposures. Testing Conditions: IGE Microsensor Number 4; NiPc Thin-film (6,200 Angstroms Thick); Temperature of 150 degrees Centigrade; Ammonia Challenge Gas (All Exposures:500 ppm).

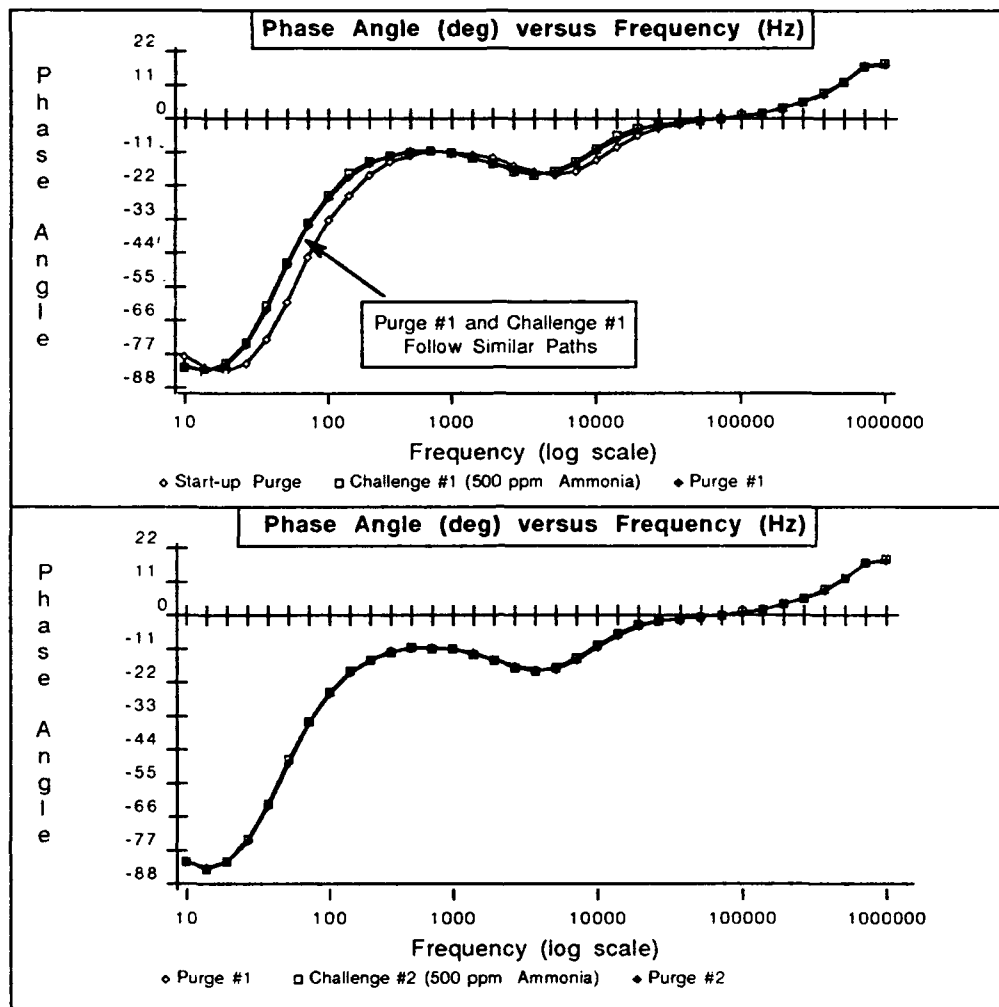


Figure E-34. Gain versus Frequency Response of IGEFET Microsensor for a Series of Room Air Purges and Challenge Gas Exposures. Testing Conditions: IGE Microsensor Number 4; NiPc Thin-film (6,200 Angstroms Thick); Temperature of 150 degrees Centigrade; Ammonia Challenge Gas (All Exposures:500 ppm).



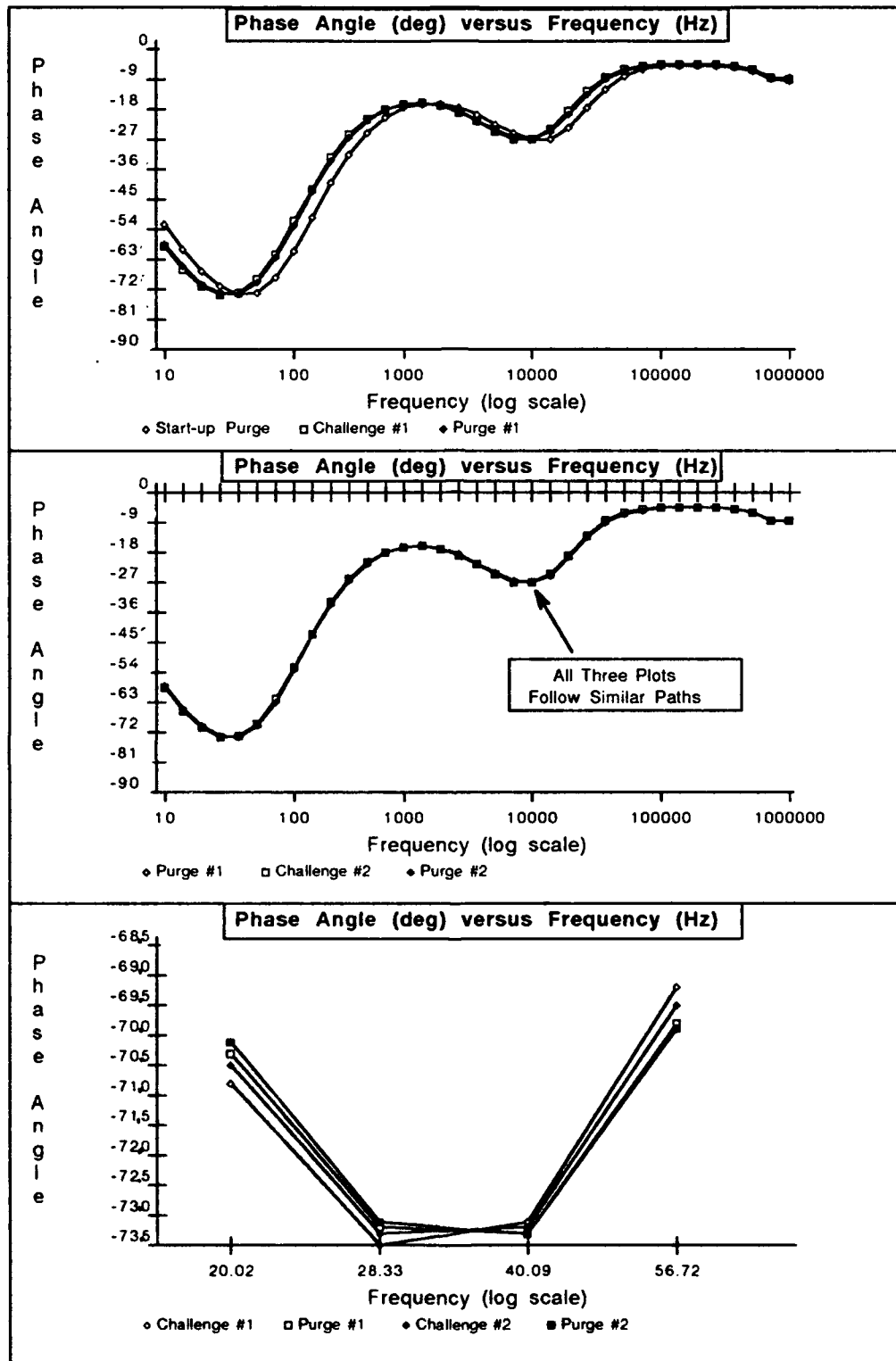


Figure E-36 . Phase Angle versus Frequency Response of IGEFET Microsensor for a Series of Room Air Purges and Challenge Gas Exposures. Testing Conditions: IGE Microsensor Number 8; NiPc Thin-film (12,500 Angstroms Thick); Temperature of 150 degrees Centigrade; Ammonia Challenge Gas (All Exposures: 500 ppm).

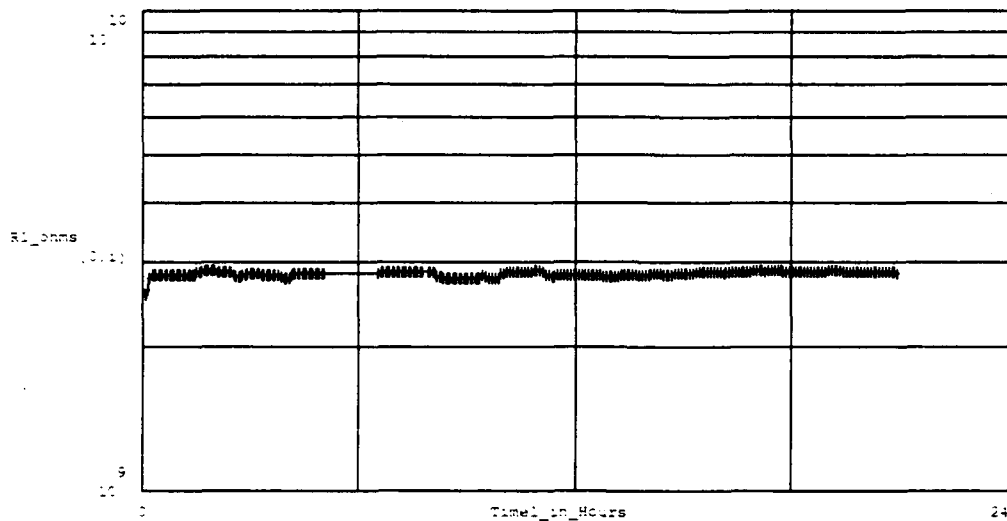


Figure E- 37 . DC Resistance Measured Between the Driven-Electrode and Floating-Electrode of the IGE Array, During Series of Purges and Challenge Gas Exposures. The Number of Measurements (at crosses) is 262. The Testing Conditions Included the Following:

IGE Array Number : 1, Thin-film Material : Nickel Phthalocyanine,  
 Thin-film Thickness : 2,600 Angstroms Test Temperature(s) : Purge & Challenge at 150°C  
 Purge Gas : Room Air. Challenge Gas : BF<sub>3</sub>.  
 Challenge Gas Concentration(s) (in order run) : 105 ppm, 24 ppm.

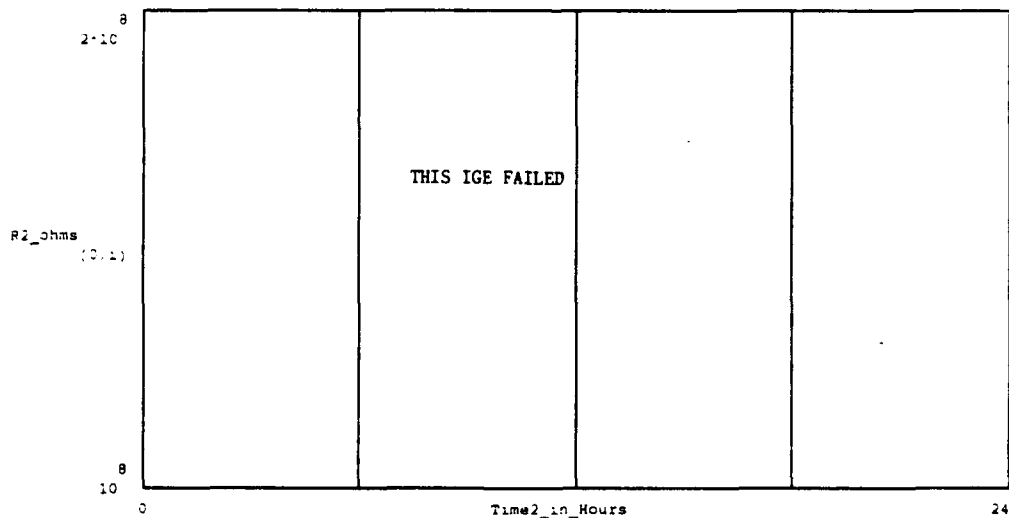


Figure E- 38. DC Resistance Measured Between the Driven-Electrode and Floating-Electrode of the IGE Array, During Series of Purges and Challenge Gas Exposures. The Number of Measurements (at crosses) is 262. The Testing Conditions Included the Following:

IGE Array Number : 2, Thin-film Material : Nickel Phthalocyanine,  
 Thin-film Thickness : 2,600 Angstroms Test Temperature(s) : Purge & Challenge at 150°C  
 Purge Gas : Room Air. Challenge Gas : BF<sub>3</sub>.  
 Challenge Gas Concentration(s) (in order run) : 105 ppm, 24 ppm.

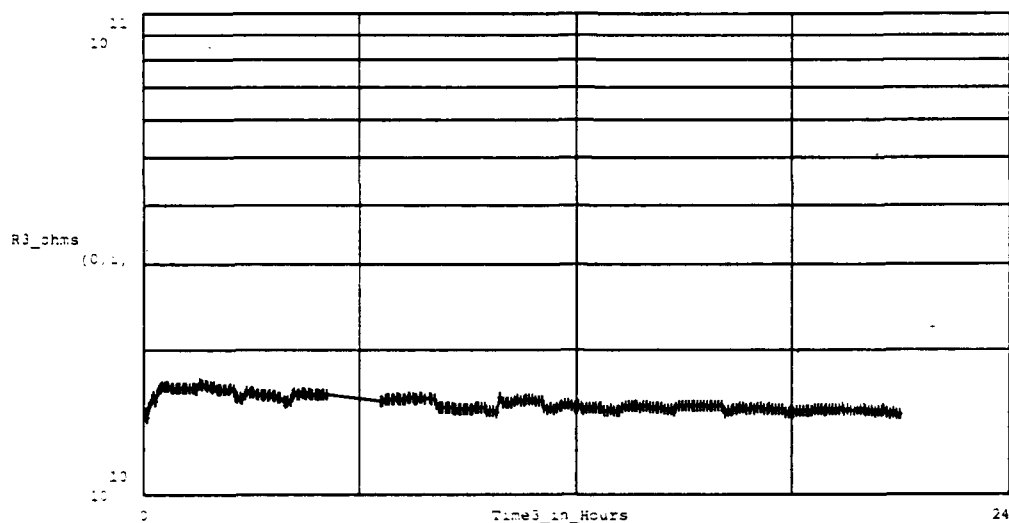


Figure E- 39 . DC Resistance Measured Between the Driven-Electrode and Floating-Electrode of the IGE Array, During Series of Purges and Challenge Gas Exposures. The Number of Measurements (at crosses) is 262. The Testing Conditions Included the Following:

IGE Array Number : 3.	Thin-film Material : Nickel Phthalocyanine.
Thin-film Thickness : 2.600 Angstroms	Test Temperature(s) : Purge & Challenge at 150°C
Purge Gas : Room Air.	Challenge Gas : BF <sub>3</sub> .
Challenge Gas Concentration(s) (in order run) : 105 ppm, 24 ppm.	

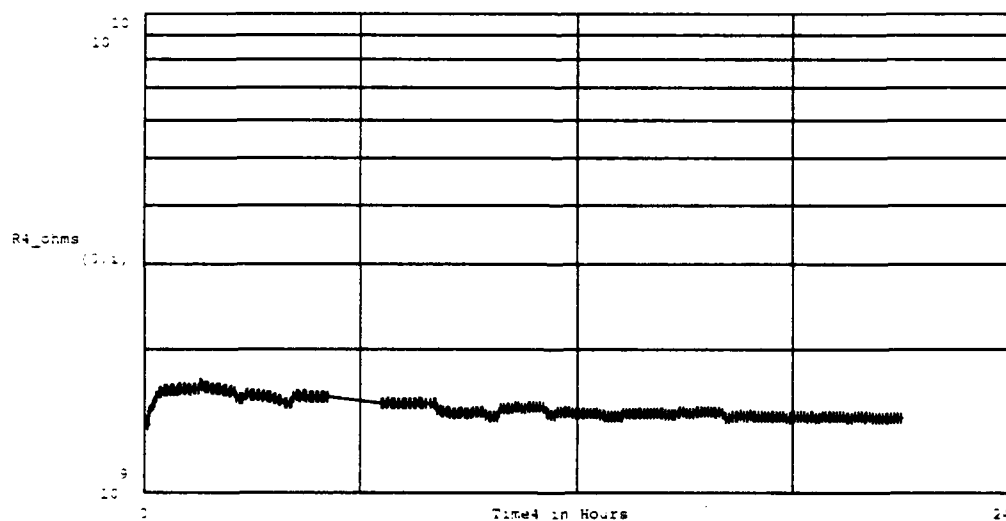


Figure E- 40 . DC Resistance Measured Between the Driven-Electrode and Floating-Electrode of the IGE Array, During Series of Purges and Challenge Gas Exposures. The Number of Measurements (at crosses) is 262. The Testing Conditions Included the Following:

IGE Array Number : 4.	Thin-film Material : Nickel Phthalocyanine.
Thin-film Thickness : 6.200 Angstroms	Test Temperature(s) : Purge & Challenge at 150°C
Purge Gas : Room Air.	Challenge Gas : BF <sub>3</sub> .
Challenge Gas Concentration(s) (in order run) : 105 ppm, 24 ppm.	

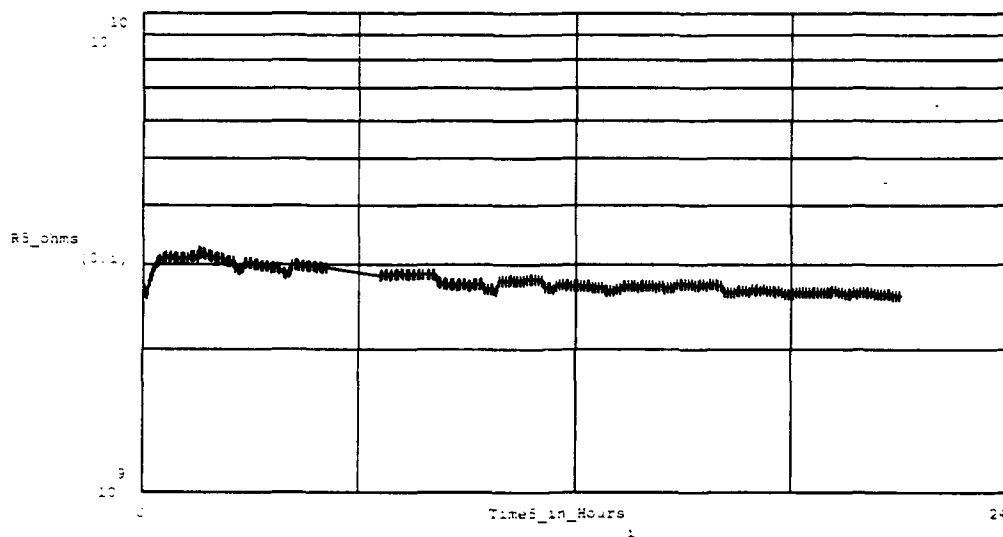


Figure E- 41 . DC Resistance Measured Between the Driven-Electrode and Floating-Electrode of the IGE Array, During Series of Purges and Challenge Gas Exposures. The Number of Measurements (at crosses) is 262. The Testing Conditions Included the Following:

IGE Array Number : 5.	Thin-film Material : Nickel Phthalocyanine.
Thin-film Thickness : 6,200 Angstroms	Test Temperature(s) : Purge & Challenge at 150°C
Purge Gas : Room Air.	Challenge Gas : BF <sub>3</sub> .
Challenge Gas Concentration(s) (in order run) : 105 ppm, 24 ppm.	

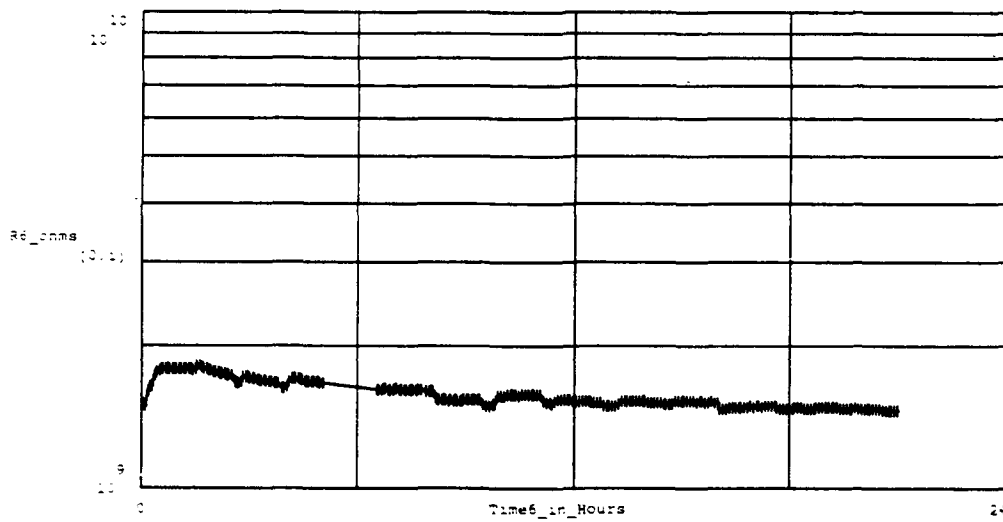


Figure E- 42 . DC Resistance Measured Between the Driven-Electrode and Floating-Electrode of the IGE Array, During Series of Purges and Challenge Gas Exposures. The Number of Measurements (at crosses) is 262. The Testing Conditions Included the Following:

IGE Array Number : 6.	Thin-film Material : Nickel Phthalocyanine.
Thin-film Thickness : 6,200 Angstroms	Test Temperature(s) : Purge & Challenge at 150°C
Purge Gas : Room Air.	Challenge Gas : BF <sub>3</sub> .
Challenge Gas Concentration(s) (in order run) : 105 ppm, 24 ppm.	



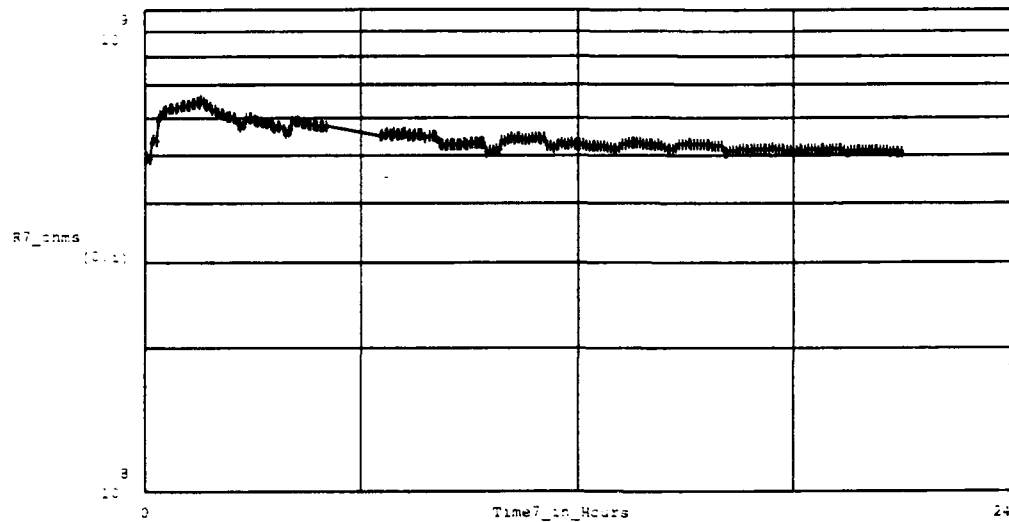


Figure E- 43 . DC Resistance Measured Between the Driven-Electrode and Floating-Electrode of the IGE Array. During Series of Purges and Challenge Gas Exposures. The Number of Measurements (at crosses) is 262. The Testing Conditions Included the Following:

IGE Array Number : 7,	Thin-film Material : Nickel Phthalocyanine,
Thin-film Thickness : 12,500 Angstroms	Test Temperature(s) : Purge & Challenge at 150°C
Purge Gas : Room Air,	Challenge Gas : BF <sub>3</sub> ,
Challenge Gas Concentration(s) (in order run) : 105 ppm, 24 ppm.	

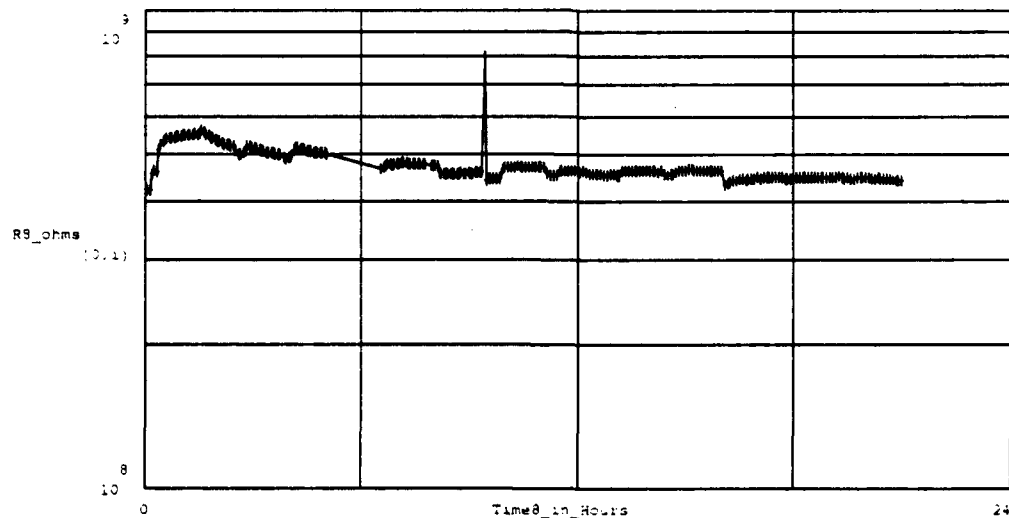


Figure E- 44 . DC Resistance Measured Between the Driven-Electrode and Floating-Electrode of the IGE Array. During Series of Purges and Challenge Gas Exposures. The Number of Measurements (at crosses) is 262. The Testing Conditions Included the Following:

IGE Array Number : 8,	Thin-film Material : Nickel Phthalocyanine,
Thin-film Thickness : 12,500 Angstroms	Test Temperature(s) : Purge & Challenge at 150°C
Purge Gas : Room Air,	Challenge Gas : BF <sub>3</sub> ,
Challenge Gas Concentration(s) (in order run) : 105 ppm, 24 ppm.	

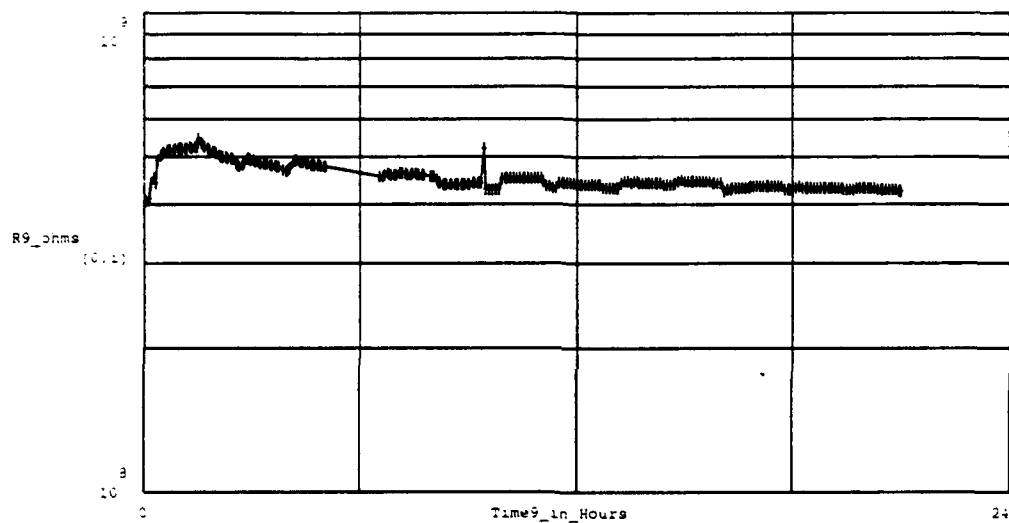


Figure E- 45. DC Resistance Measured Between the Driven-Electrode and Floating-Electrode of the IGE Array. During Series of Purges and Challenge Gas Exposures. The Number of Measurements (at crosses) is 262. The Testing Conditions Included the Following:

IGE Array Number : 9.	Thin-film Material : Nickel Phthalocyanine.
Thin-film Thickness : 12,500 Angstroms	Test Temperature(s) : Purge & Challenge at 150°C
Purge Gas : Room Air.	Challenge Gas : BF <sub>3</sub> .
Challenge Gas Concentration(s) (in order run) : 105 ppm, 24 ppm.	

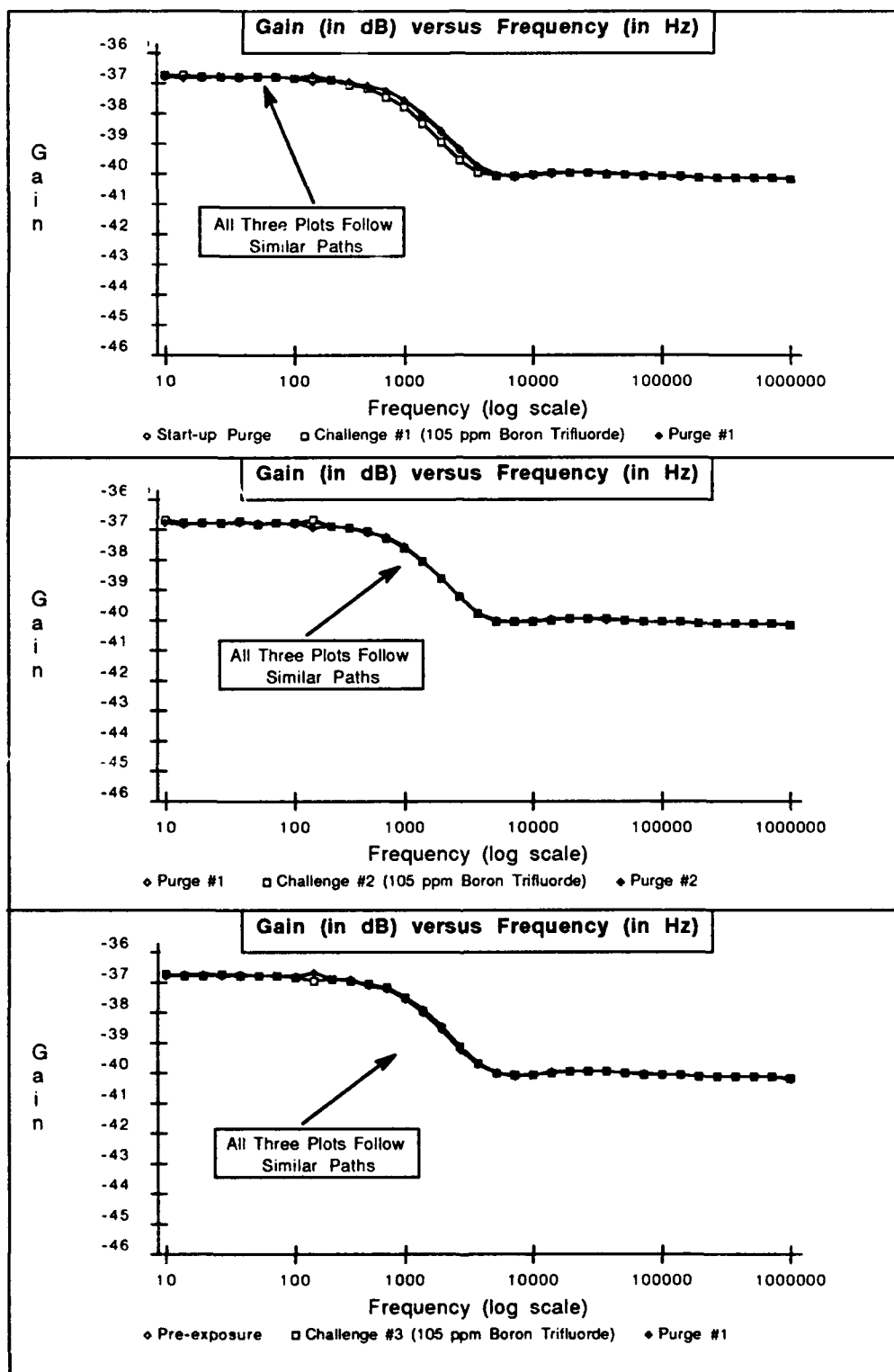


Figure E-46 . Gain versus Frequency Response of IGEFET Microsensor for a Series of Room Air Purges and Challenge Gas Exposures. Testing Conditions: IGE Microsensor Number 1; NiPc Thin-film (2,600 Angstroms Thick); Temperature of 150 degrees Centigrade; Boron Trifluoride Challenge Gas (All Exposures: 105 ppm).

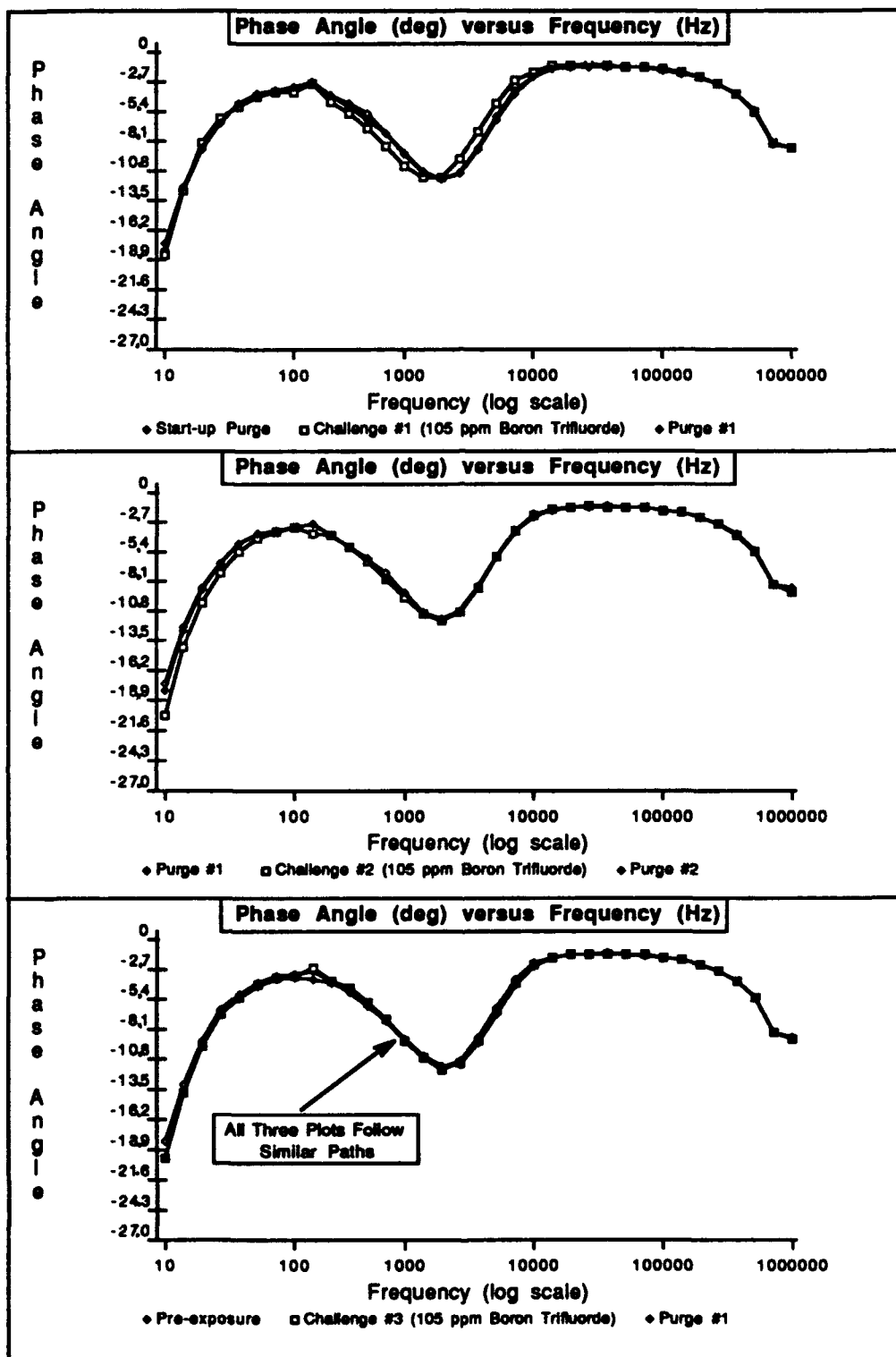


Figure E-47. Phase Angle versus Frequency Response of IGEFET Microsensor for a Series of Room Air Purges and Challenge Gas Exposures. Testing Conditions: IGE Microsensor Number 1; NiPc Thin-film (2,600 Angstroms Thick); Temperature of 150 degrees Centigrade; Boron Trifluoride Challenge Gas (All Exposures: 105 ppm).

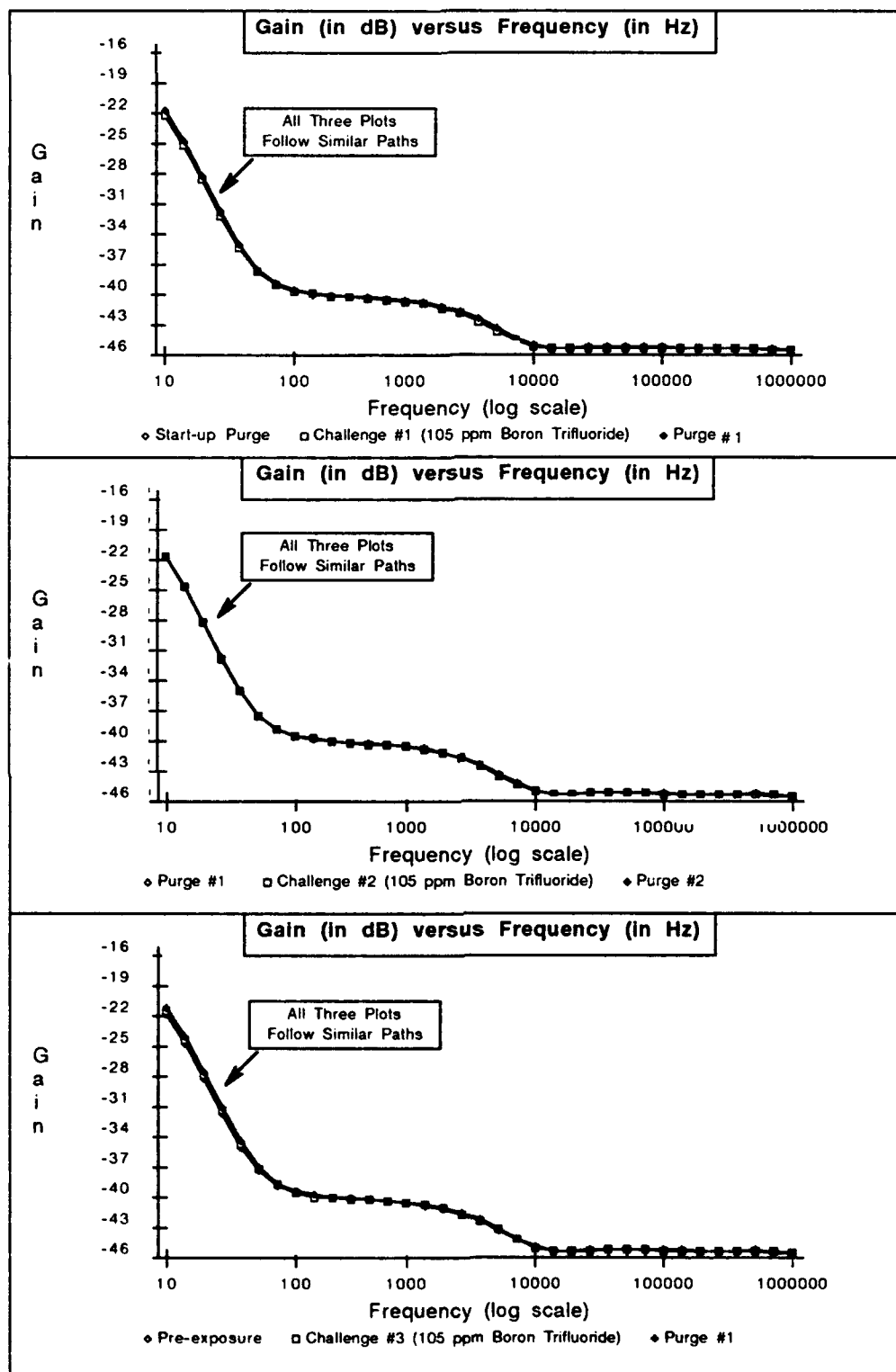


Figure E-48. Gain versus Frequency Response of IGEFET Microsensor for a Series of Room Air Purges and Challenge Gas Exposures. Testing Conditions: IGE Microsensor Number 4; NiPc Thin-film (6,200 Angstroms Thick); Temperature of 150 degrees Centigrade; Boron Trifluoride Challenge Gas (All Exposures: 105 ppm).

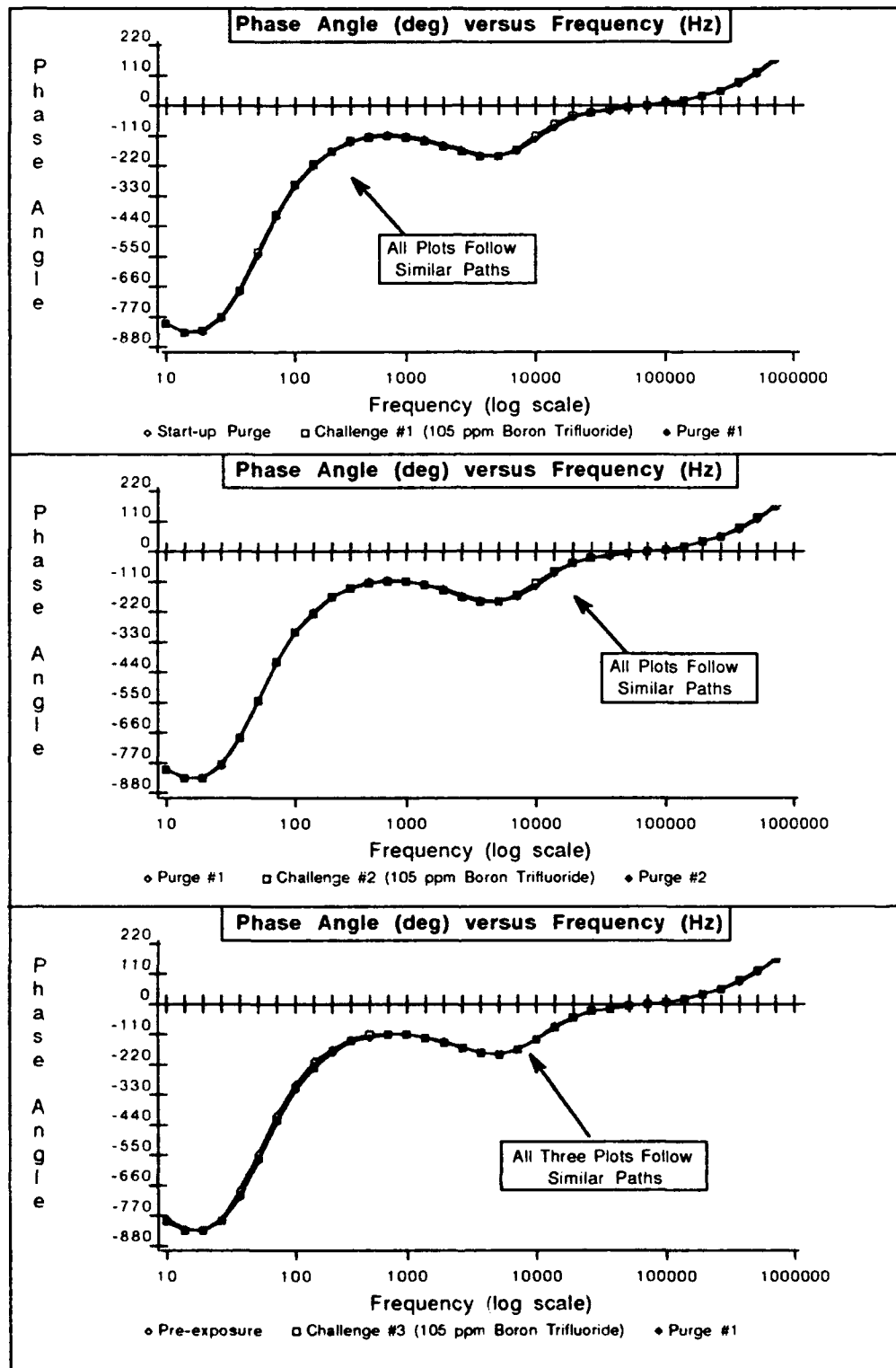


Figure E-49. Phase Angle versus Frequency Response of IGEFET Microsensor for a Series of Room Air Purges and Challenge Gas Exposures. Testing Conditions: IGE Microsensor Number 4; NiPc Thin-film (6,200 Angstroms Thick); Temperature of 150 degrees Centigrade; Boron Trifluoride Challenge Gas (All Exposures: 105 ppm).

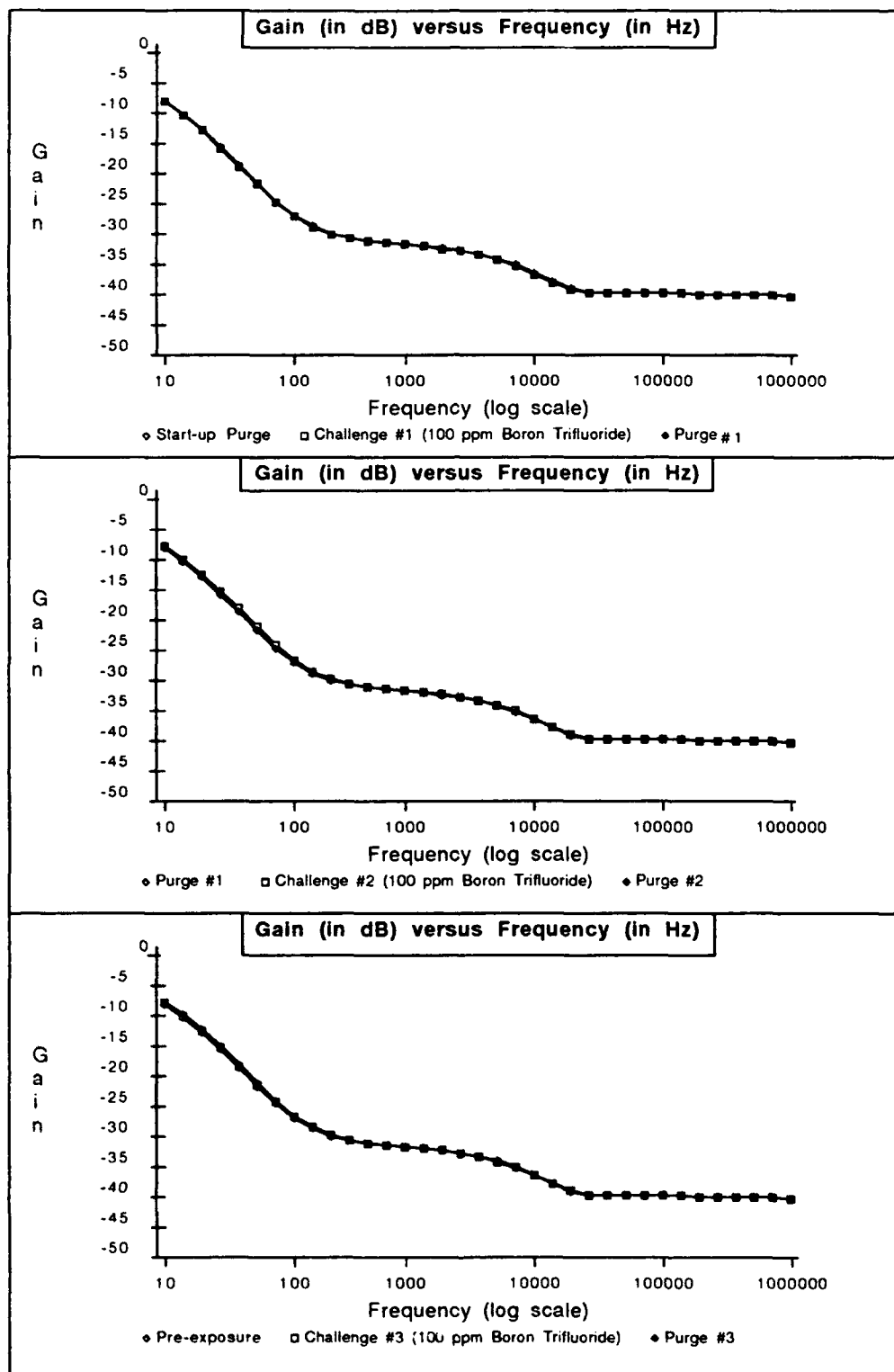


Figure E-50 . Gain versus Frequency Response of IGEFET Microsensor for a Series of Room Air Purges and Challenge Gas Exposures. Testing Conditions: IGE Microsensor Number 8; NiPc Thin-film (12,500 Angstroms Thick); Temperature of 150 degrees Centigrade; Boron Trifluoride Challenge Gas (All Exposures: 100 ppm).

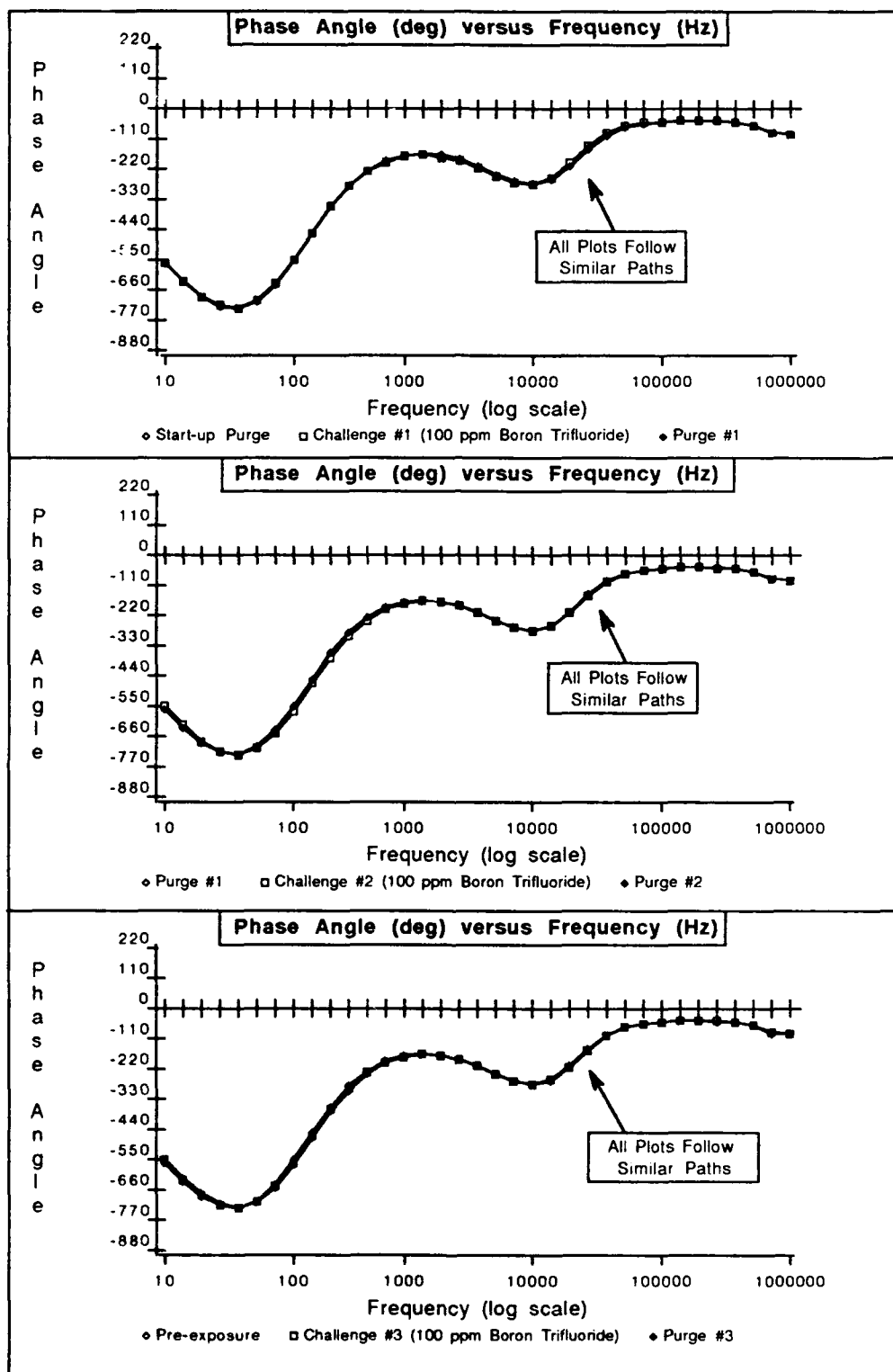


Figure E-51 . Phase Angle versus Frequency Response of IGEFET Microsensor for a Series of Room Air Purges and Challenge Gas Exposures. Testing Conditions: IGE Microsensor Number 8; NiPc Thin-film (12,500 Angstroms Thick); Temperature of 150 degrees Centigrade; Boron Trifluoride Challenge Gas (All Exposures: 105 ppm).



## *Section 2*

This section summarizes dc resistance versus time plots for the NiPc films exposed separately to DMMP (Figures E-52 to E-54) and DIMP (Figures E-55 to E-57) at three temperatures: 150°C, 90°C, and 30°C.

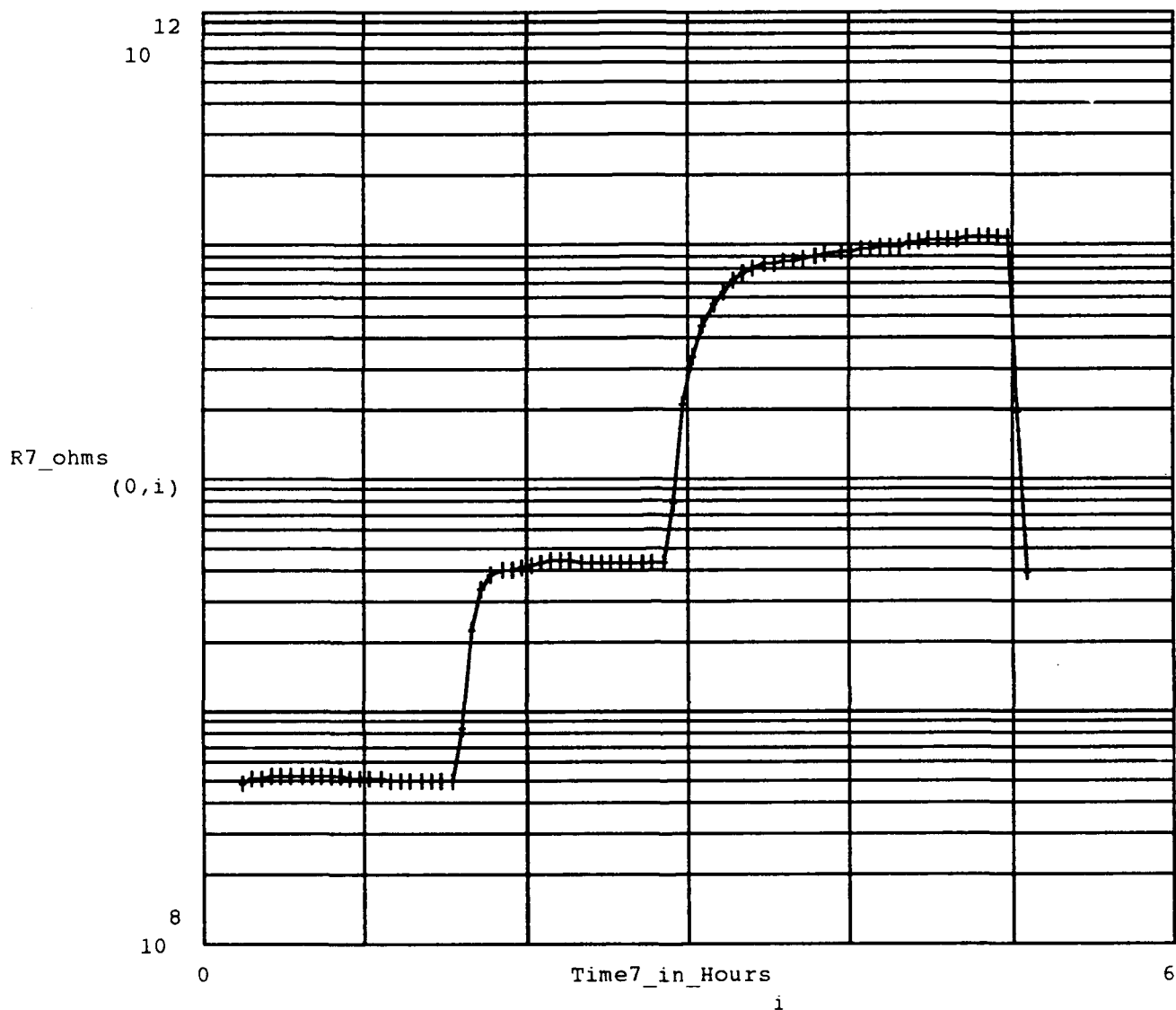


Figure E-52 . DC Resistance Measured Between the Driven-Electrode and Floating-Electrode of the IGE Array, During Series of Purges and Challenge Gas Exposures. The Testing Conditions Included the Following:

IGE Array Number : 7,  
 Thin-film Material : Nickel Phthalocyanine,  
 Thin-film Thickness : 6800 Angstroms  
 Test Temperature(s) : Initial Purge & Challenge at 150°C, Second Purge  
 & Challenge at 90°C, Third Purge and Challenge at 30°C,  
 Purge Gas : Room Air,  
 Challenge Gas : DMMP,  
 Challenge Gas Concentration(s) (in order run) : 10 ppm.

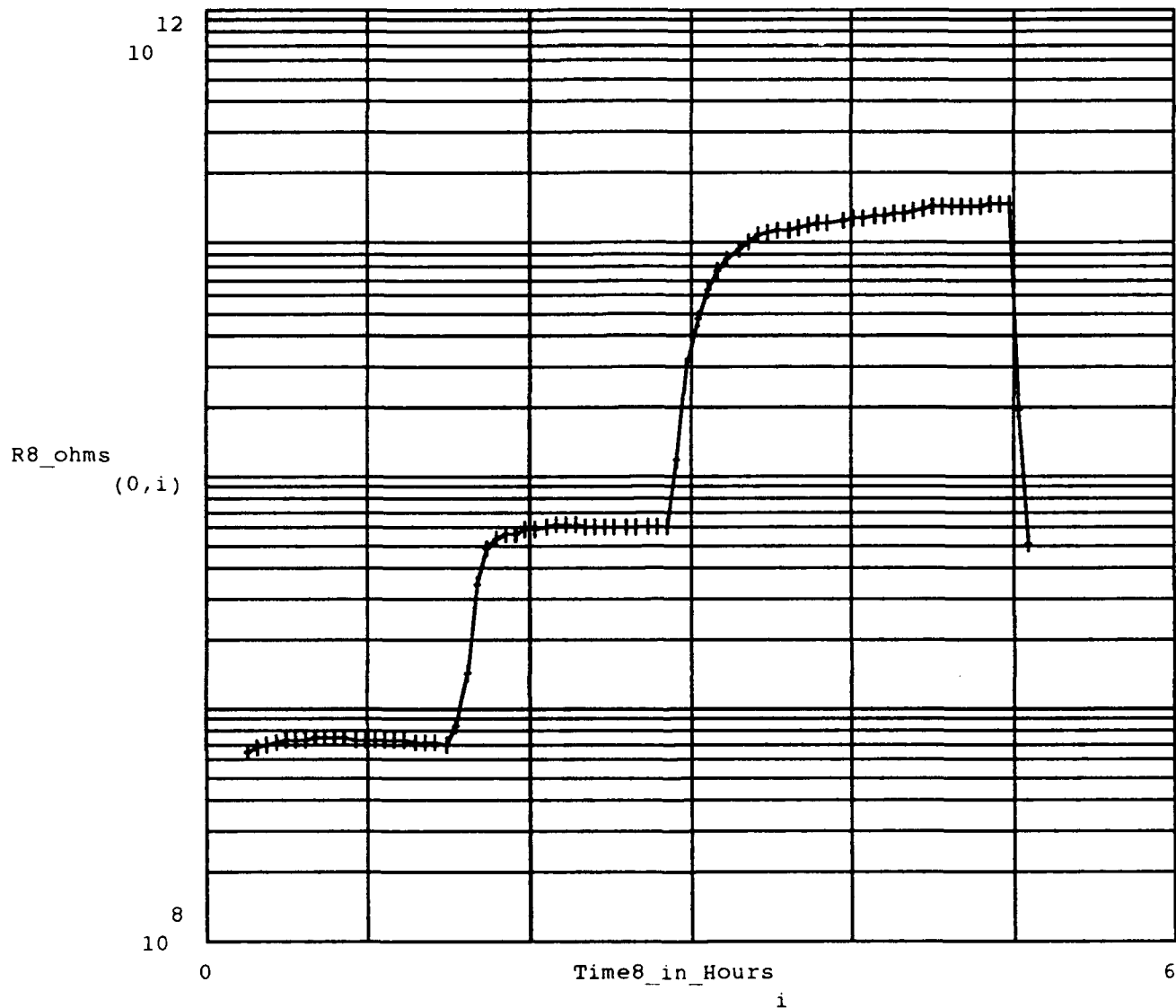


Figure E- 53 . DC Resistance Measured Between the Driven-Electrode and Floating-Electrode of the IGE Array, During Series of Purges and Challenge Gas Exposures. The Testing Conditions Included the Following:

IGE Array Number : 8,  
 Thin-film Material : Nickel Phthalocyanine,  
 Thin-film Thickness : 6800 Angstroms  
 Test Temperature(s) : Initial Purge & Challenge at 150°C, Second Purge  
 & Challenge at 90°C, Third Purge and Challenge at 30°C,  
 Purge Gas : Room Air,  
 Challenge Gas : DMMP,  
 Challenge Gas Concentration(s) (in order run) : 10 ppm.

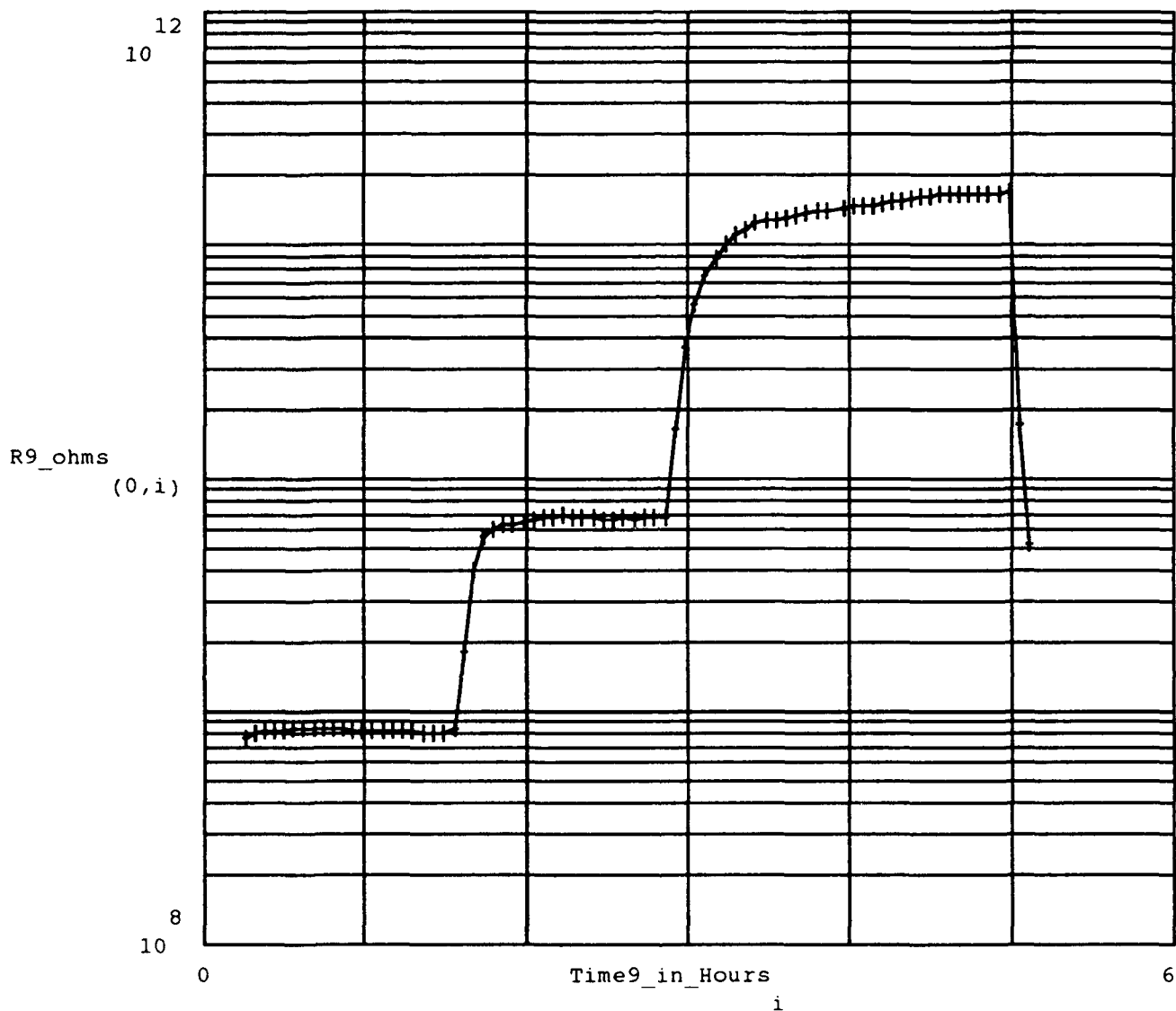


Figure E- 54 . DC Resistance Measured Between the Driven-Electrode and Floating-Electrode of the IGE Array, During Series of Purges and Challenge Gas Exposures. The Testing Conditions Included the Following:

IGE Array Number : 9,  
 Thin-film Material : Nickel Phthalocyanine,  
 Thin-film Thickness : 6800 Angstroms  
 Test Temperature(s) : Initial Purge & Challenge at 150°C, Second Purge  
 & Challenge at 90°C, Third Purge and Challenge at 30°C,  
 Purge Gas : Room Air,  
 Challenge Gas : DMMP,  
 Challenge Gas Concentration(s) (in order run) : 10 ppm.

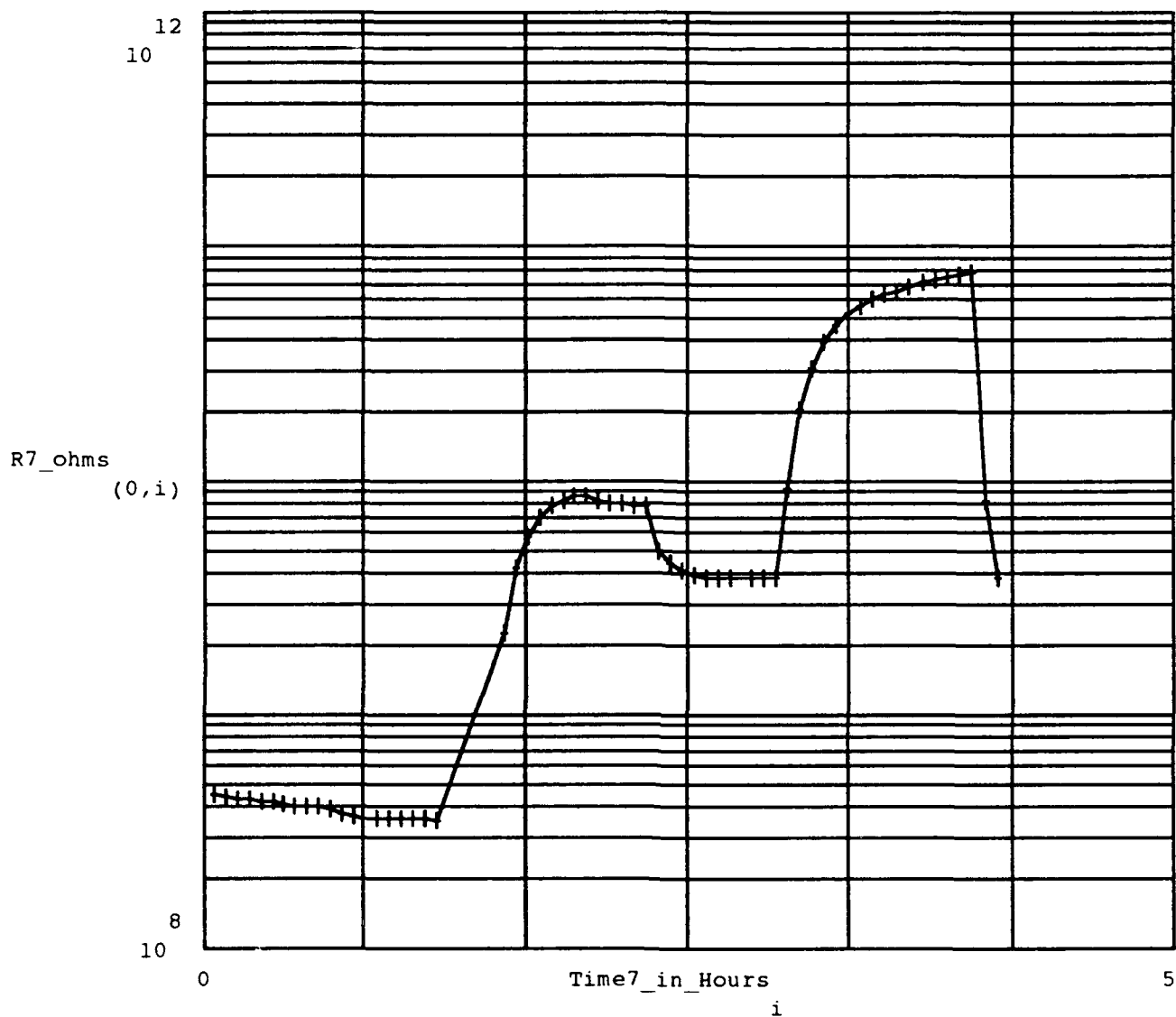


Figure E- 55 . DC Resistance Measured Between the Driven-Electrode and Floating-Electrode of the IGE Array, During Series of Purges and Challenge Gas Exposures. The Testing Conditions Included the Following:

IGE Array Number : 7,  
 Thin-film Material : Nickel Phthalocyanine,  
 Thin-film Thickness : 6800 Angstroms  
 Test Temperature(s) : Initial Purge & Challenge at 150°C, Second Purge  
 & Challenge at 90°C, Third Purge and Challenge at 30°C.  
 Purge Gas : Room Air,  
 Challenge Gas : DIMP,  
 Challenge Gas Concentration(s) (in order run) : 3 ppm.

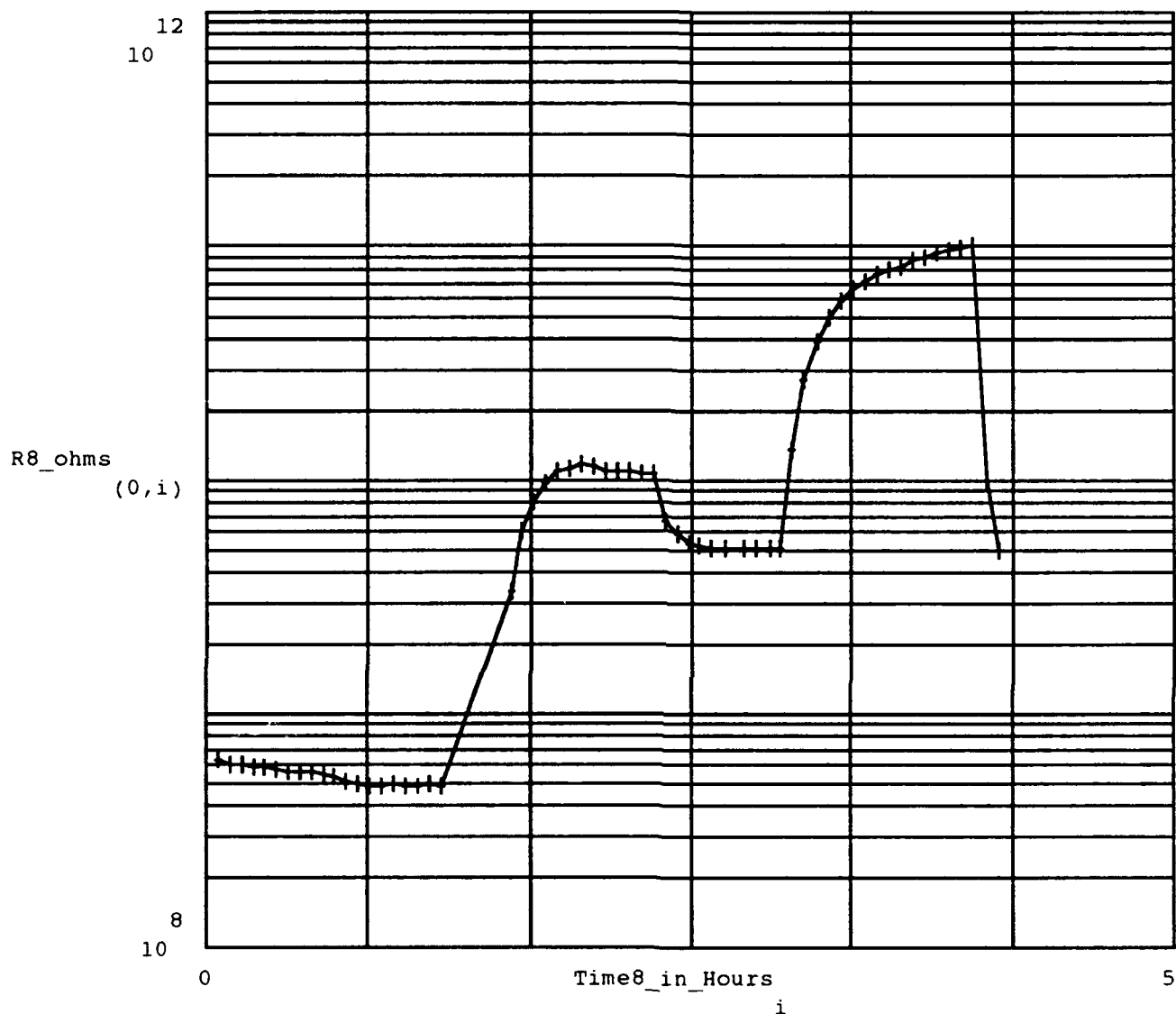


Figure E- 56 . DC Resistance Measured Between the Driven-Electrode and Floating-Electrode of the IGE Array, During Series of Purges and Challenge Gas Exposures. The Testing Conditions Included the Following:

IGE Array Number : 8,  
 Thin-film Material : Nickel Phthalocyanine,  
 Thin-film Thickness : 6800 Angstroms  
 Test Temperature(s) : Initial Purge & Challenge at 150°C, Second Purge  
 & Challenge at 90°C, Third Purge and Challenge at 30°C,  
 Purge Gas : Room Air,  
 Challenge Gas : DIMP,  
 Challenge Gas Concentration(s) (in order run) : 3 ppm.

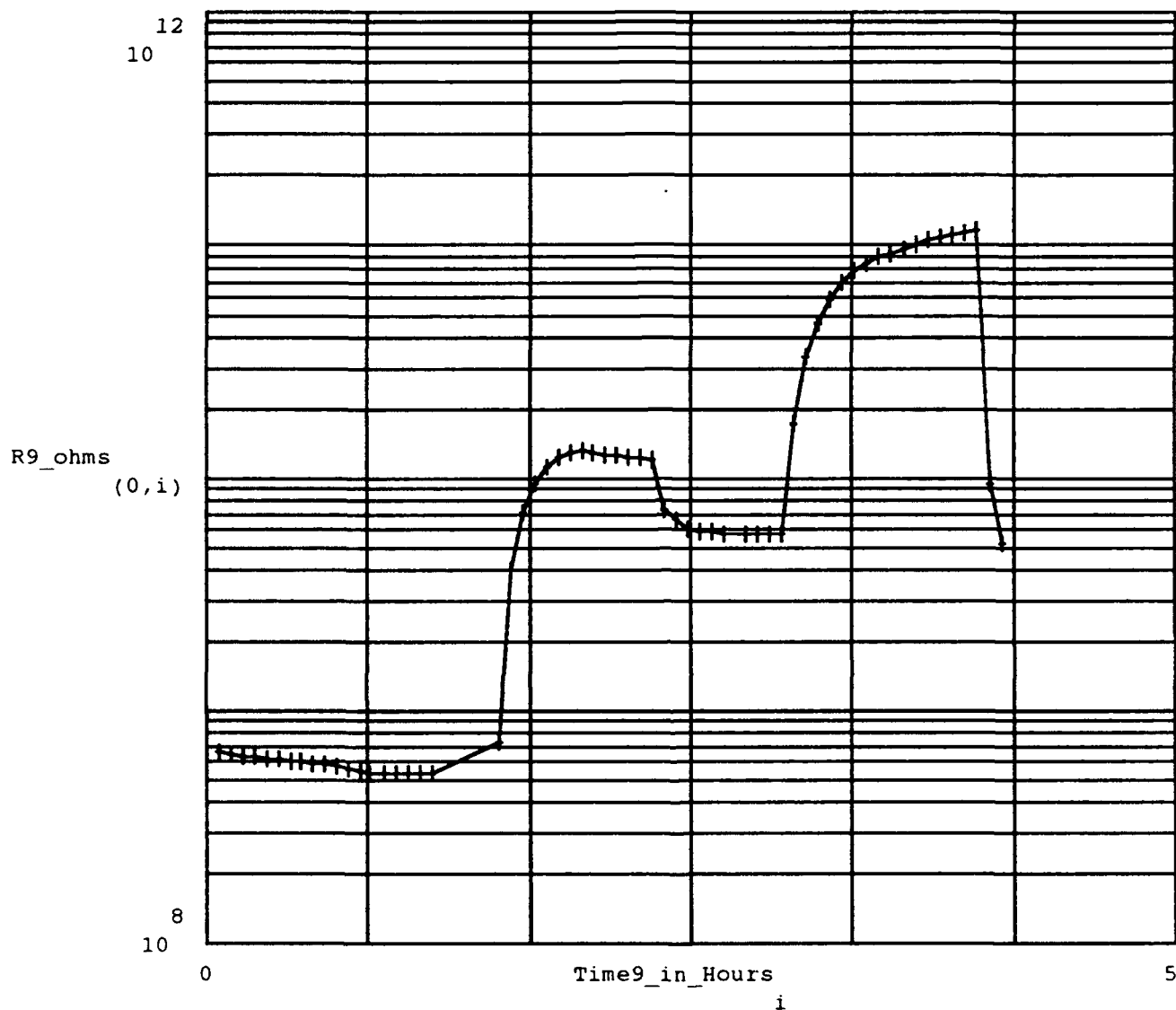


Figure E- 57 . DC Resistance Measured Between the Driven-Electrode and Floating-Electrode of the IGE Array, During Series of Purges and Challenge Gas Exposures. The Testing Conditions Included the Following:

IGE Array Number : 9,  
 Thin-film Material : Nickel Phthalocyanine,  
 Thin-film Thickness : 6800 Angstroms  
 Test Temperature(s) : Initial Purge & Challenge at 150°C, Second Purge  
 & Challenge at 90°C, Third Purge and Challenge at 30°C,  
 Purge Gas : Room Air,  
 Challenge Gas : DIMP,  
 Challenge Gas Concentration(s) (in order run) : 3 ppm.

## Bibliography

1. Beaudet, R. A. *et al.* Test and Evaluation Plan for Chemical Defense Detectors I. Generic Test Plan." U.S. Army Research Office, Human Systems Division. Contract # DAA G29-81-0100-TCN 84-511 (May 1985) (AD-B140-977) LIMITED DISTRIBUTION.
2. Butler, M.,A. "Optical Fiber Hydrogen Sensor." *Appl. Phys. Lett.* 45 (10), 1007-1009, (1984).
3. Cranny, A. W. J. and J. K. Atkinson. "A Comparision of Thick- and Thin-film Gas Sensitive Organic Semiconductor Compounds," *Sensors and Actuators B4*: 169-174 (1991).
4. Gray, Paul E. and C. L. Searle. *Electronic Principles: Physics, Models and Circuits*. New York: John Wiley & Sons, 1969.
5. Hamann, C. *et al.* "Lead Phthalocyanine Thin Films for NO<sub>2</sub> Sensors," *Sensors and Actuators, B4*: 73-78 (1991).
6. Hufault, John R. *Op Amp Network Design*. New York: John Wiley & Sons, Inc., 1986.
7. Jenkins, Capt Thomas. *Evaluation of Doped Phthalocyanine Polymers for Use with a Chemically-Sensitive Field-Effect Transistor*. MS Thesis, AFIT/GE/ENG/88D-18. Department of Electrical and Computer Engineering, Air Force Institute of Technology (AU), Wright-Patterson AFB OH, (4 December 1988) (AD-A215-662).
8. -----, Personal interview and correspondence. Department of Electrical and Computer Engineering, Air Force Institute of Technology (AU), Wright-Patterson AFB OH, 24 October 1991.
9. Jiri, Janata. *Principles of Chemcial Sensors*. Second Edition. New York: Plenum Publishing Corp., 1989.
10. Keithley Instruments, Inc. *Model 617 Programmable Electrometer Instruction Manual*. Document Number 617-901-01, Rev. C., Keithley Instruments, Inc. Cleveland, OH, June 1986.



11. Kolesar, Maj Edward S., Jr. *Electronic Detection of Low Concentrations of Organophosphorus Compounds with a Solid State Device Utilizing Supported Copper and Cuprous Oxide Island Films*. Ph.D Dissertation, University of Texas, Austin, TX, (May) 1985 (AD-A158-181).
12. -----, "Thesis Performance Handout and Potential Research Topics." Unpublished Handout for Prospective Thesis Students. Department of Electrical and Computer Engineering, Air Force Institute of Technology (AU), Wright-Patterson AFB OH, (June 1989).
13. -----, "Detection of Gaseous Organophosphorus Compounds Using a Supported Copper+ Cuprous Oxide Island Film." *Proceedings of the IEEE National Aerospace and Electronics Conference-(NAECON)*, Dayton, OH, 23-27 May 1988.
14. ----- and Capt John M. Wiseman. "Interdigitated Gate Electrode Field Effect Transistor for the Selective Detection of Nitrogen Dioxide and Diisopropyl Methylphosphonate." *Analytical Chemistry*, 61; 2355-2361 (1989).
15. Kolesar, Edward S. Jr. "Sensor for Detecting Chemicals," *U. S. Patent Number 4,906,440* (6 March 1990).
16. Lezoff, C. C., and A. B. P. Lever. *Phthalocyanines: Properties and Applications*. New York: VCH Publishers, Inc., 1989.
17. Lucklum, R. *et al.* "Quartz Microbalance Sensors for Gas Detection," *Sensors and Actuators B4*: 499-504 (1991).
18. Murday, J. *et al.* "Performance Limits of Chemical Microsensor Technology." *Proceedings of the 1986 U. S. Army Chemical Research, Development, and Engineering Center Scientific Conference on Chemical Defense Research*, Vol. 1, (18-21 November 1986) (AD-B113-947) LIMITED DISTRIBUTION.
19. Roberts, John D. *et al.* *Organic Chemistry: Methane to Macromolecules*. Menlo Park, California: W. A. Benjamin, Inc. (1971).

20. Roberts, G. G. and B. Holcroft. "The Properties of Conducting Langmuir-Blodgett Films: A Study Using Acoustometric Devices," *Thin Solid Films*, 160: 53-60 (1988)
21. Schielde E. and G. Guilbault. "Piezoelectric Detectors for Organophosphorous Compounds and Pesticides," *Analytical Chemistry*, 44: 1764-1768 (September 1972).
22. Shin, Capt Jenny. *Evaluation of Chemically-Sensitive Field-Effect Transistors for the Detection of Organophosphorus Compounds*. MS Thesis, AFIT/GE/ENG/89D-47. Department of Electrical and Computer Engineering, Air Force Institute of Technology (AU), Wright-Patterson AFB OH, (5 December 1989) (AD-A215-536).
23. Sorum, C. H., *Fundamentals of General Chemistry*. Englewood Cliffs, New Jersey: Prentice-Hall, Inc. (1964).
24. Temofonte, T. A., and K. F. Schoch. "Phthalocyanine Semiconductor Sensors for Room-Temperature ppb Level Detection of Toxic Gases." *J. Appl. Phys.* 65(3), 1350-1355, (1 February 1989).
25. Wilson, Alan *et al.* "A MicroSensor-Controlled Nitrogen Dioxide Sensing System," *Sensors and Actuators B4*: 409-504 (1991).
26. Wiseman, Capt John M. *Investigation of the Impedance Modulation of Thin Films With a Chemically-Sensitive Field-Effect Transistor*. MS Thesis, AFIT/GE/ENG/88D-661. Department of Electrical and Computer Engineering, Air Force Institute of Technology (AU), Wright-Patterson AFB OH, (5 December 1988) (AD-A202-766).